ELSEVIER

Tetrahedron

Tetrahedron Vol. 61, No. 43, 2005

Contents

REPORT

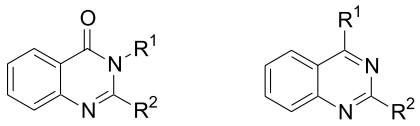

1 **2**

Synthetic methods for the construction of the 4(3*H*)-quinazolinone **1** and quinazoline **2** skeletons, with a particular emphasis on the 2-substituted and 2,4-disubstituted analogues, are reviewed. The report contains 127 references.

ARTICLES

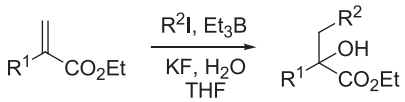

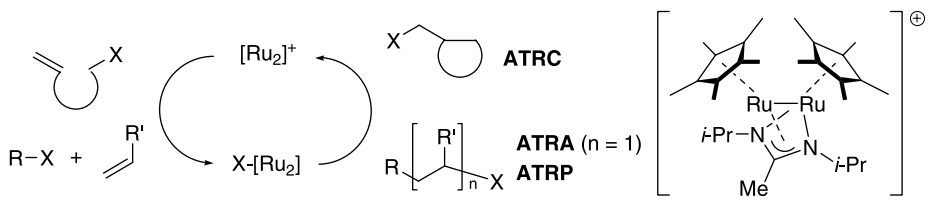

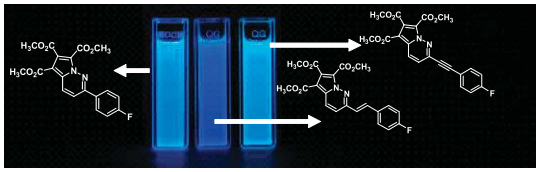

Three different classes of new pyrrolopyridazines were made as potential blue organic luminophors. Their optical and electrochemical properties were compared. One of the luminophors 2-(4-fluorophenyl)pyrrolo[1,2-*b*]pyridazine-5,6,7-tricarboxylic acid trimethyl ester (**2**) showed a relative quantum yield as high as 0.9 and compound **8** in the vinyl bridged pyrrolopyridazine series has been characterized by its X-ray crystal structure analysis.

The reaction of indole with (1*H*-indol-3-yl)(alkyl) methanol was efficiently catalyzed by ceric ammonium nitrate (CAN) under ultrasonic irradiation to afford the unsymmetrical bisindolylalkane in good to excellent yields.

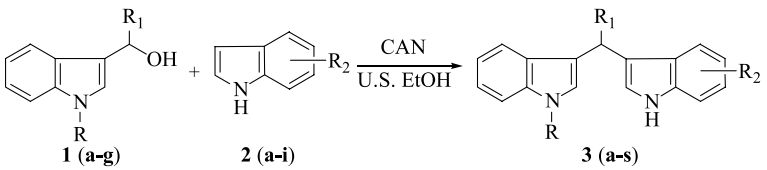

R= H, Ts
R_1= Ph, *n*-Nonanyl, *n*-Octanyl, *n*-Hexanyl, *n*-Butanyl
R_2= CH_3, H, BnO, Ts

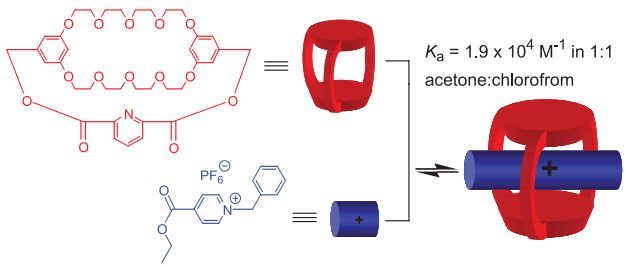

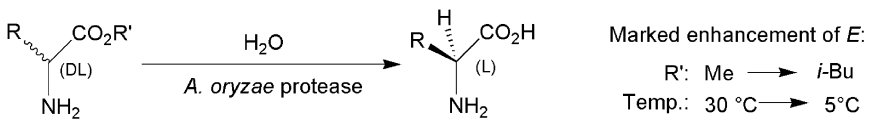

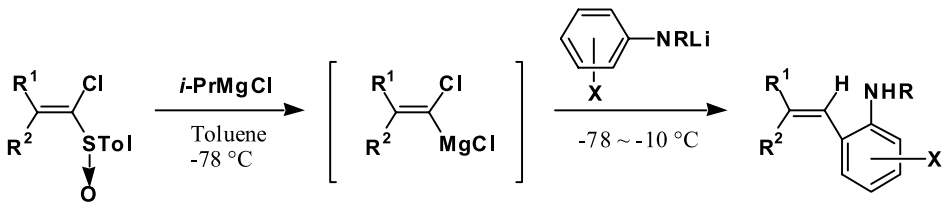

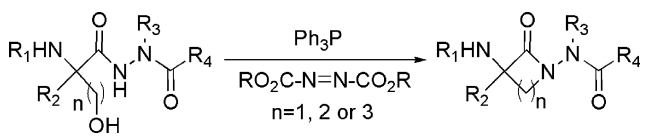

Resveratrol was treated with several kinds of peroxidases and inorganic reagents so as to prepare ε-viniferin. Thallium(III) nitrate in methanol gave (±)-ε-viniferin in good yield. On the other hand, peroxidases did not lead to ε-viniferin.

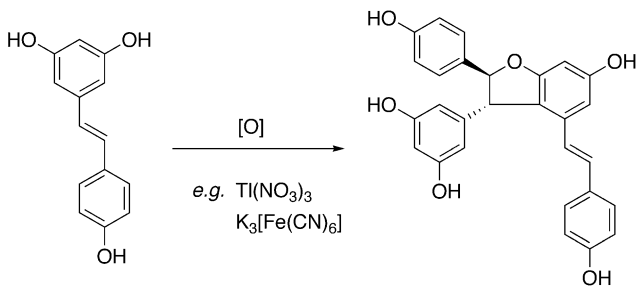

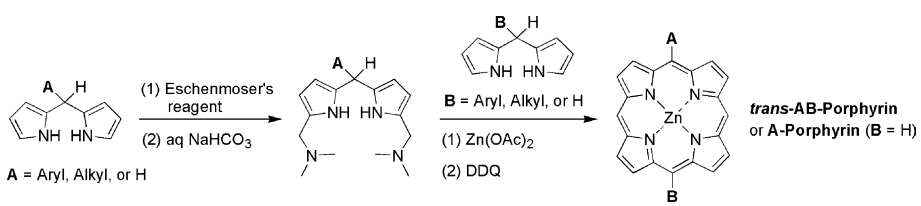

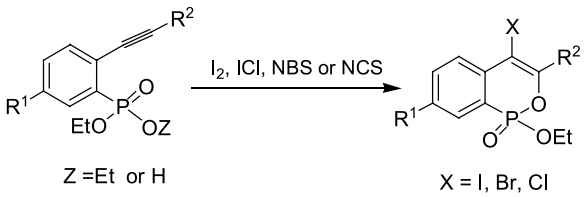

Z =Et or H

X = I, Br, Cl

Ligands **1**–**3** are able to act as cation and anion sensors. Their fluorescent and electrochemical properties are studied. The influence that biphenyl conformation has on these properties is considered. The X-ray single crystal structure of one of the described ligands has been determined.

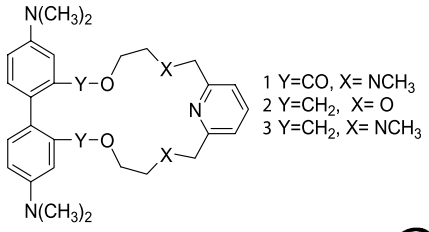

1 Y=CO, X= NCH_3
2 Y=CH_2, X= O
3 Y=CH_2, X= NCH_3

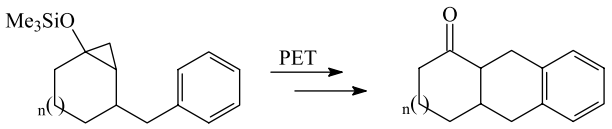

n = 1, 2

n = 1, 2

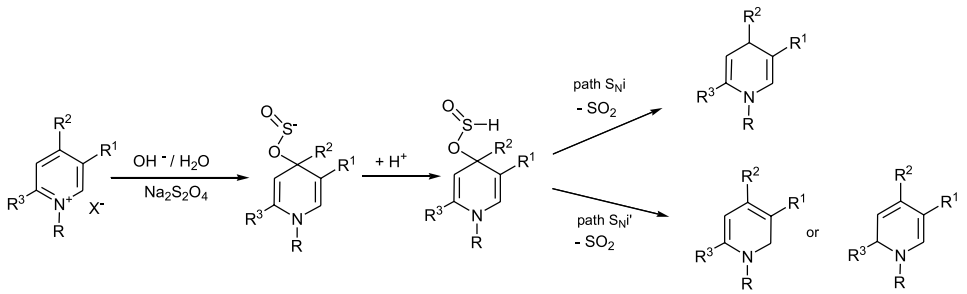

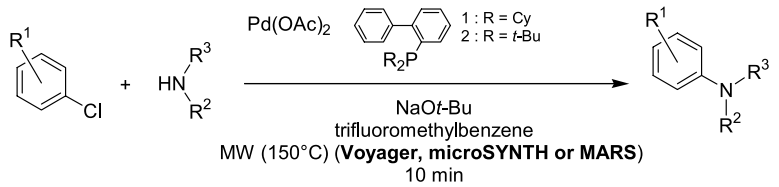

Reactions of guaiazulene (**1**) with heteroaromatic-carbaldehydes [i.e., 2-furaldehyde (**2**), thiophene-2-carbaldehyde (**3**) and pyrrole-2-carbaldehyde (**4**)] in methanol in the presence of hexafluorophosphoric acid at 25 °C for 30 min under aerobic conditions give the corresponding methylium hexafluorophosphates **5**, **6** and **7**, respectively, in 93, 98 and 85% isolated yields. The title studies are reported.

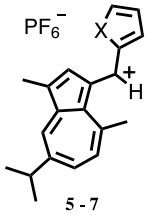

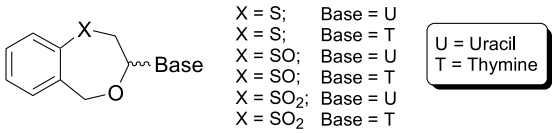

OTHER CONTENTS

*Corresponding author
ⓘ+ Supplementary data available via ScienceDirect

Indexed/Abstracted in: AGRICOLA, Beilstein, BIOSIS Previews, CAB Abstracts, Chemical Abstracts, Chemical Engineering and Biotechnology Abstracts, Current Biotechnology Abstracts, Current Contents: Life Sciences, Current Contents: Physical, Chemical and Earth Sciences, Current Contents Search, Derwent Drug File, Ei Compendex, EMBASE/Excerpta Medica, Medline, PASCAL, Research Alert, Science Citation Index, SciSearch

ELSEVIER

ISSN 0040-4020

Available online at www.sciencedirect.com
SCIENCE DIRECT
Tetrahedron
Tetrahedron 61 (2005) 10153–10202

Tetrahedron report number 737

Synthesis of quinazolinones and quinazolines

David J. Connolly, Declan Cusack, Timothy P. O'Sullivan and Patrick J. Guiry*

Centre for Synthesis and Chemical Biology, Department of Chemistry, Conway Institute of Biomolecular and Biomedical Sciences, University College Dublin, Belfield, Dublin 4, Ireland

Received 30 June 2005

Available online 9 August 2005

Contents

Keywords: Quinazolinones; Quinazolines; Luotonins; Rutaecarpine.
* Corresponding author. Tel.: +353 1 7166782; fax: +353 1 7162127; e-mail: p.guiry@ucd.ie

doi:10.1016/j.tet.2005.07.010

1. Introduction

Heterocyclic chemistry comprises at least half of all organic chemistry research worldwide. In particular, heterocyclic structures form the basis of many pharmaceutical, agrochemical and veterinary products. 4(3*H*)-Quinazolinones **1** and related quinazolines **2** are classes of fused heterocycles that are of considerable interest because of the diverse range of their biological properties, for example, anticancer, diuretic, anti-inflammatory, anticonvulsant and antihypertensive activities.[1–4]

Many of the literature synthetic methods for elaboration of this simple ring structure are, however, time consuming, tedious and often low yielding.[5–8]

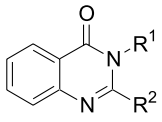

1

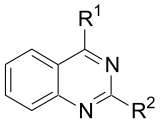

2

In this review, which covers the literature up to the end of 2004, we describe the new and improved methods for the construction of the 4(3*H*)-quinazolinone and quinazoline skeletons, with a particular emphasis on the 2-substituted and 2,4-disubstituted analogues. Some of these procedures have clear technical advantages over older methods in terms of yield and versatility, but do not employ new chemistry in the construction of the ring systems. The use of combinatorial synthesis, microwave-enhanced processes and new catalytic methodologies in the preparation of these heterocycles is a clear indication that significant advancement has been made in recent years.

The syntheses of both quinazolinones and quinazolines will be classified into the following five categories, based on the substitution patterns of the ring system:

- 2-Substituted-4(3*H*)-quinazolinones and -quinazolines (Section 2).
- 3-Substituted-4(3*H*)-quinazolinones (Section 3).
- 4-Substituted-quinazolines (Section 4).
- 2,3-Disubstituted-4(3*H*)-quinazolinones (Section 5).
- 2,4-Disubstituted-4(3*H*)-quinazolinones and quinazolines (Section 6).

Within each subclassification, the methods will be described, where possible, beginning with the most recent developments in the construction of these important heterocycles.

2. 2-Substituted-4(3*H*)-quinazolinones and -quinazolines

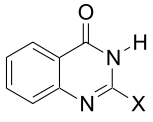

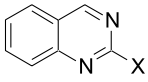

2.1. Amidation and cyclisation of 2-aminobenzoic acid derivatives

The most common approach involves amidation of 2-aminobenzonitrile, 2-aminobenzoic acid and 2-aminobenzamide. As an example, the reaction of 2-aminobenzonitrile **3** (X=H) with 3-phenyl-acryloyl chloride **4** followed by oxidative ring closure under basic conditions produced 2-styryl-4(3*H*)-quinazolinone **6** (X=H) in 29% yield, Scheme 1.[9–12]

This procedure is tolerant of a wide range of substitution patterns on the benzene ring and, in most cases, the amide intermediates **5** can be isolated in good yields. The overall yields to these 2-styryl-quinazolinones **6**, however, varied between 4 and 61%.[13]

A modification of this protocol was reported by Bandgar, whereby a urea–hydrogen peroxide adduct was utilised with potassium carbonate to yield 2-substituted quinazolinones possessing varied substitution patterns in the starting material in yields ranging from 86 to 98%.[14] This

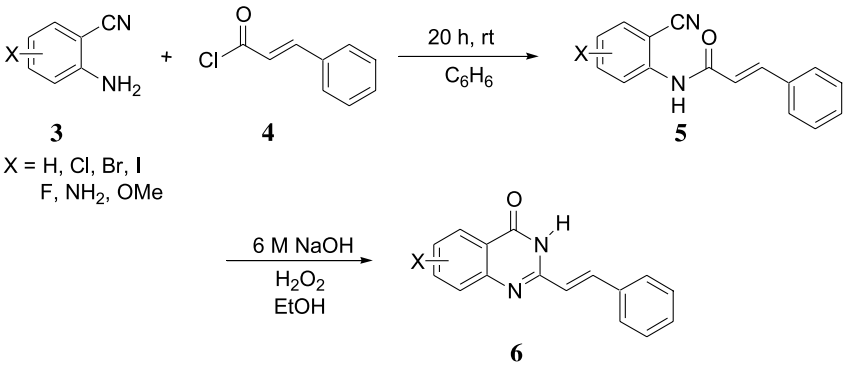

Scheme 1.

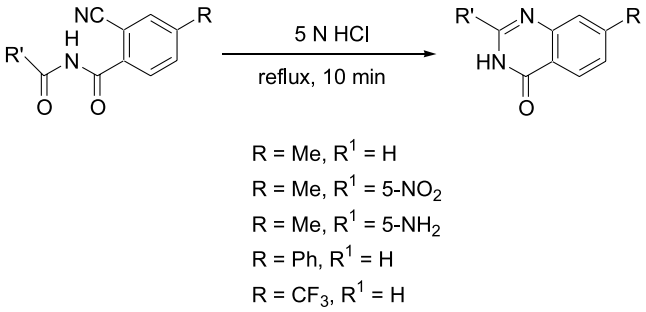

Scheme 2.

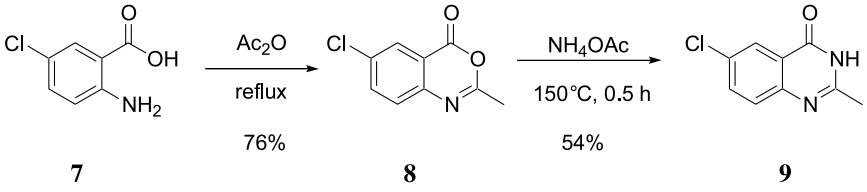

Scheme 3.

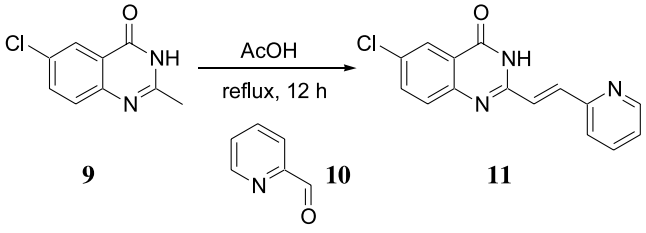

Scheme 4.

methodology was also used to synthesise 2-hydroxymethylquinazolin-4(3*H*)-one in good yields by Batvetsias.[15]

Showell has reported that a range of 2-substituted quinazolin-4(3*H*)-one derivatives could be synthesised under acidic conditions.[16] The advantages of this methodology include short reaction times and high yields, Scheme 2.

Another procedure employed by Jiang et al. involved the treatment of 5-chloroanthranilic acid **7** with acetic anhydride to afford the benzoxazinone **8** in 76% yield, Scheme 3.[13] Stirring with ammonium acetate at an elevated temperature afforded 6-chloro-2-methylquinazolin-4(3*H*)-one **9** in 54% yield. In addition, intermediate **8** could also be treated with a primary amine to introduce an *N*3-substituent.[17,18]

6-Chloro-2-methylquinazolin-4(3*H*)-one **9** could also be used to gain entry to other heteroaromatic analogues.[13] For example, **9** was refluxed for 12 h in glacial acetic acid with pyridine-2-carbaldehyde **10** to give 6-chloro-2-(2-pyridin-2yl-vinyl)-quinazolin-4(3*H*)-one **11** in 68% yield, Scheme 4. These 2-styrylquinazolin-4(3*H*)-one analogues have growth-inhibitory activity against leukaemia cells. Lee et al. used a similar synthesis to access a range of 2-aryl-quinazolinones that were active against a panel of tumour cell lines.[19]

Rad-Moghadam and Mohseni recently published a route to 2-substituted quinazolin-4(3*H*)-ones under microwave conditions.[20] This protocol involves the condensation of anthranilic acid **12**, ammonium acetate and the orthoesters **13**, which gives access to the 2-substituted-4(3*H*)-quinazolinone **14**, Scheme 5.

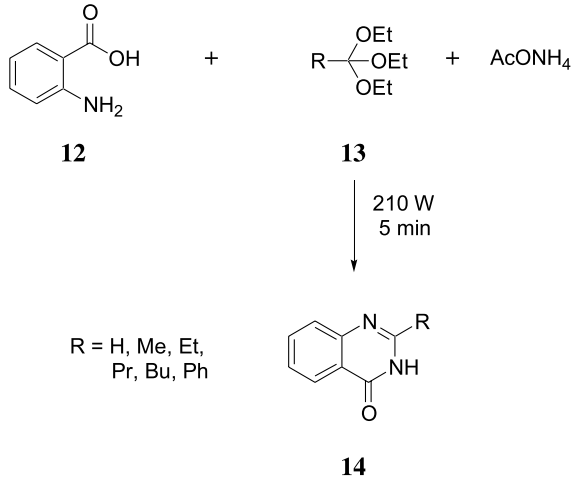

Scheme 5.

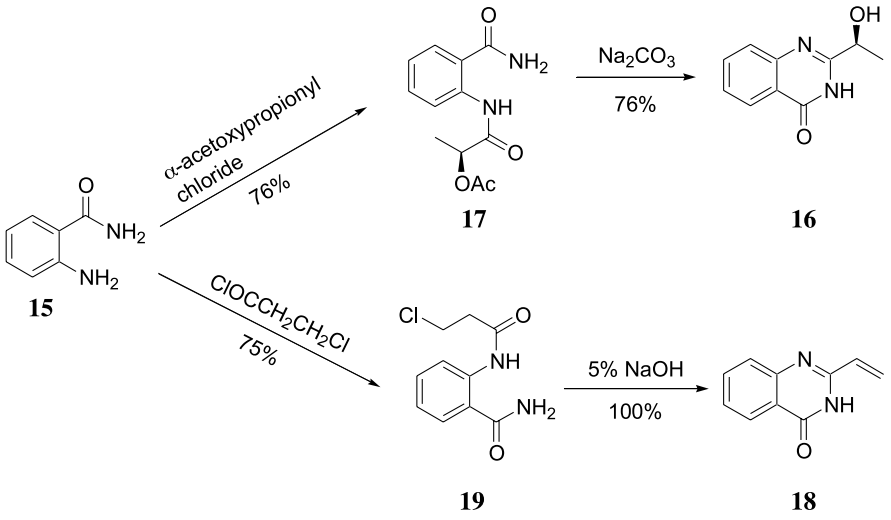

Scheme 6.

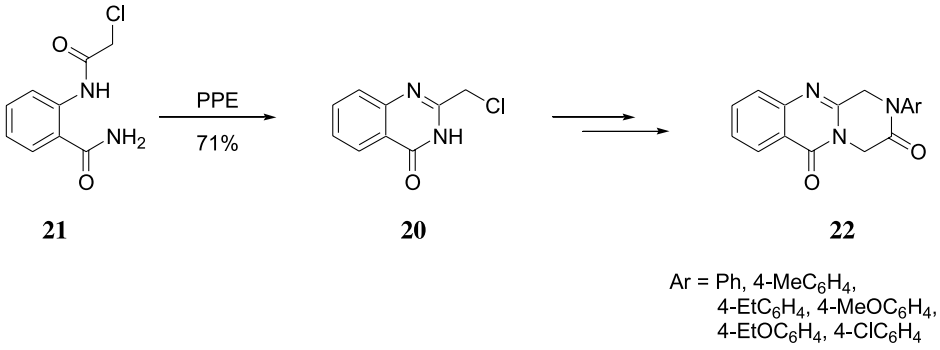

Scheme 7.

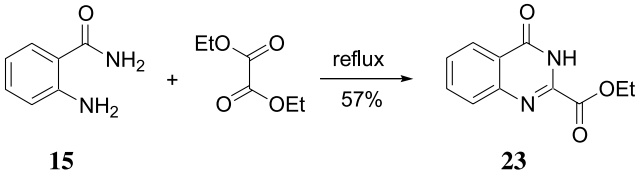

Scheme 8.

These reactions were solvent free and were completed in a short time (5 min), giving high yields (77–83%). The use of ammonium acetate negates the requirement to prepare anhydrous ammonia. Condensation can also be achieved using more traditional reflux conditions in an ethanolic solution, giving higher yields, but with longer reaction times.

The condensation of amides of anthranilamide **15** can be traced back to 1887, when Körner reported that treatment of an *N*-benzoylorthoanilamide with aqueous potassium hydroxide yielded 2-phenylquinazolin-4(3*H*)-one.[21] More recently, Bergman has utilised this methodology in the total synthesis of chrysogine **16** via **17** and to produce 2-vinyl-quinazolin-4(3*H*)-one **18** from **19**, Scheme 6.[22,23] It has also been used by chemists at the Fujisawa Pharmaceutical Company in the synthesis of a series of 2-substituted-4(3*H*)-quinazolinone inhibitors of poly(ADP-ribose)polymerase.[24]

Reddy and Nagaraju reported the use of polyphosphate ethyl ester (PPE) to achieve the synthesis of 2-chloromethyl-quinazolin-4(3*H*)-one **20** in 71% yield from **21**, Scheme 7.[25] This compound was manipulated further to give 2-aryl-2*H*-pyrazino[2,1-*b*]quinazoline-3,6(1*H*,4*H*)-diones **22**.

The synthesis of 2-carboethoxy-quinazoline-4(3*H*)-one **23** has been reported by Baker and Almaula in 1962 from anthranilamide **15** and diethyl oxalate, Scheme 8.[26]

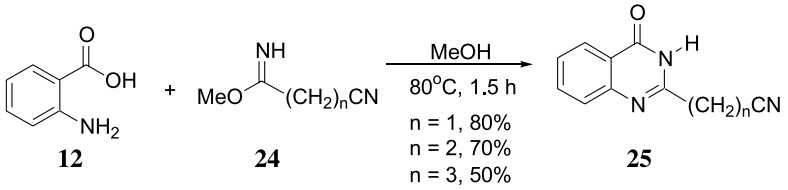

Scheme 9.

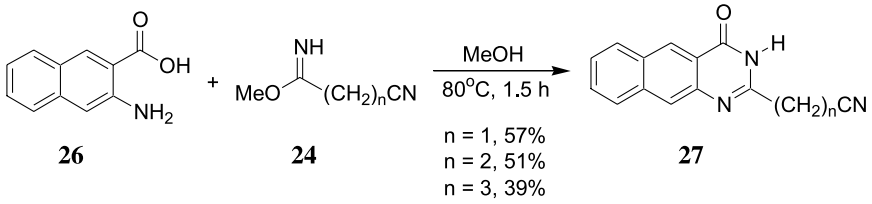

Scheme 10.

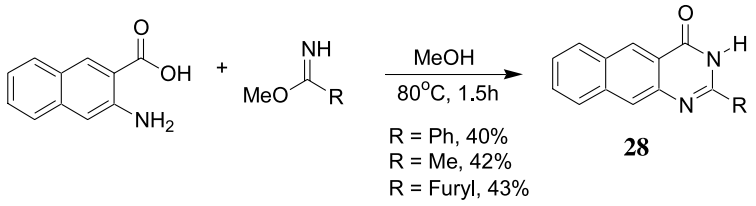

Scheme 11.

Johne and von Manfred Süsse have reported conditions under which **23** can be either *O*-alkylated or *N*-alkylated.[27] Analogues and derivatives of this compound have been used in the study of potential anthelmintics,[28] anti-allergic agents[29] and antitubercular agents.[30]

2.2. Condensation of imidates with 2-aminobenzoic acid

The reaction of imidates **24** and anthranilic acid **12** was reported in the early 1960s by Ried et al.[31–33] A related approach was employed by Hennequin et al. for the preparation of a series of quinazoline antifolate thymidylate synthase inhibitors.[34] The two components were condensed in methanol at 80 °C to afford the desired quinazolinones **25** in good yields, Scheme 9.

The reaction of imidates **24** with 3-amino-3-naphthalene-2-carboxylic acid **26** was also investigated and produced the corresponding benzo-fused quinazolinones **27** in moderate to good yields, Scheme 10.

In addition, the latter procedure was employed to introduce 2-alkyl and 2-aryl substituents on the benzo-fused quinazolinones **28**, with yields ranging from 40–43%, Scheme 11.

Connolly and Guiry extended this methodology to synthesise a series of 2-aryl- and 2-alkylquinazolinones.[35] The necessary imidates **31a–g** were preformed by reacting the corresponding nitriles **29a–f** and were formed as their hydrochloride salts **30a–f**, an exception being the 2-pyridyl imidate **31g**, which was formed in situ by a base-catalysed reaction. The generation of the imidate hydrochloride salts gave excellent yields in all cases, Scheme 12, Table 1.

Prior to condensation with anthranilic acid, the imidate salts were converted into the corresponding imidates **31a–g** by reaction with one equivalent of base. The condensation reaction afforded the quinazolinones **32a–g** in satisfactory to good yields, Scheme 13, Table 2.

2.3. 2-Alkylthio-quinazolinone synthesis via thiocyanates

Gruner and co-workers developed a novel route to 2-alkylthio-quinazolines by heating a suspension of

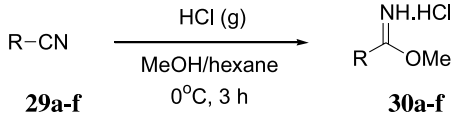

Scheme 12.

Table 1. Synthesis of imidate salts **30a–f** from nitriles **29a–f**

Nitrile **29**	R	Yield of **30** (%)
a	Me	75
b	Bn	97
c	Cy	96
d	Ph	62
e	*i*-Pr	98
f	*t*-Bu	85
g	2-Pyridyl	97[a]

[a] Imidate formed by base-catalysed route.

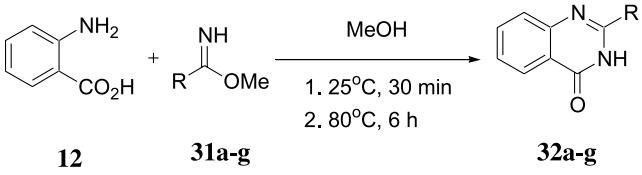

Scheme 13.

Table 2. Condensation of imidiate esters **31a–g** to form quinazolinones **32a–g**

Imidate ester **31**	R	Yield of **32** (%)
a	Me	42[a]
b	Bn	65[b]
c	Cy	44[c]
d	Ph	46[c]
e	*i*-Pr	47[c]
f	*t*-Bu	56[d]
g	2-Pyridyl	70[a]

[a] 0 °C.
[b] After initial 30 min reaction.
[c] Precipitated at 25 °C.
[d] Upon addition of water.

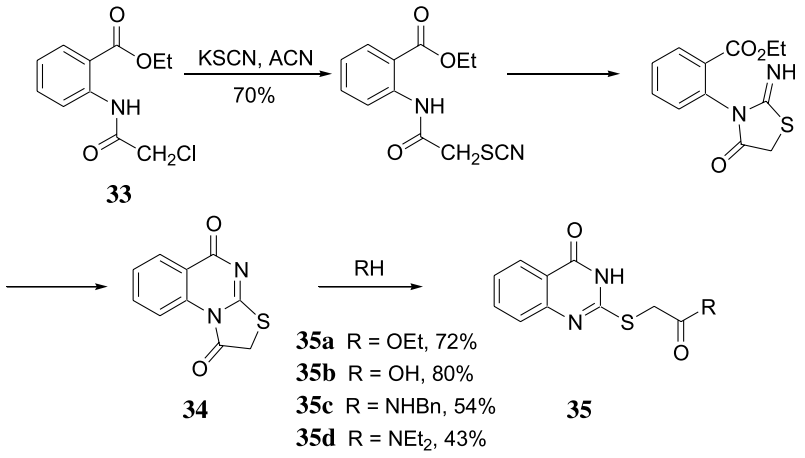

Scheme 14.

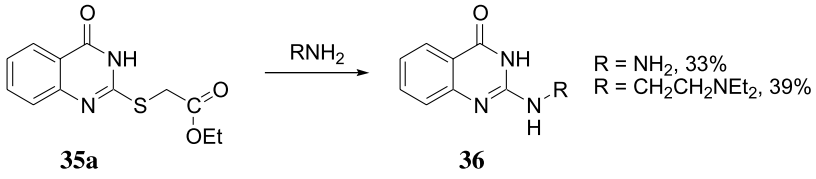

Scheme 15.

N-chloroacetyl-anthranilic acid ethyl ester **33** with potassium thiocyanate in acetonitrile (ACN).[36] It was discovered that the alcohol or amine employed as the solvent reacted with the thiazolo[3,2-*a*]quinazoline-1,5-dione intermediate **34** to furnish the corresponding 4-oxo-3,4-dihydroquinazolines **35a–d** in 43–72% yield, Scheme 14.

Treatment of product **35a** with primary amines afforded 2-amino-4-oxo-3,4-dihydroquinazolines **36** in acceptable yields (33–39%) by elimination of the thioacetic acid moiety, Scheme 15.

2.4. Triazolines to quinazolines

Erba et al. employed a three-component reaction to form 2-alkylquinazolines from the reaction of amidines with ammonia.[37] In the first step, an aldehyde is reacted with morpholine and, subsequently, with an aryl azide to afford the triazolines **37** in acceptable yields, Scheme 16.

On exposure to a saturated ethanolic solution of ammonia in a sealed vessel at 150 °C or, alternatively, in ammonium acetate in boiling toluene, the triazolines **37** were converted

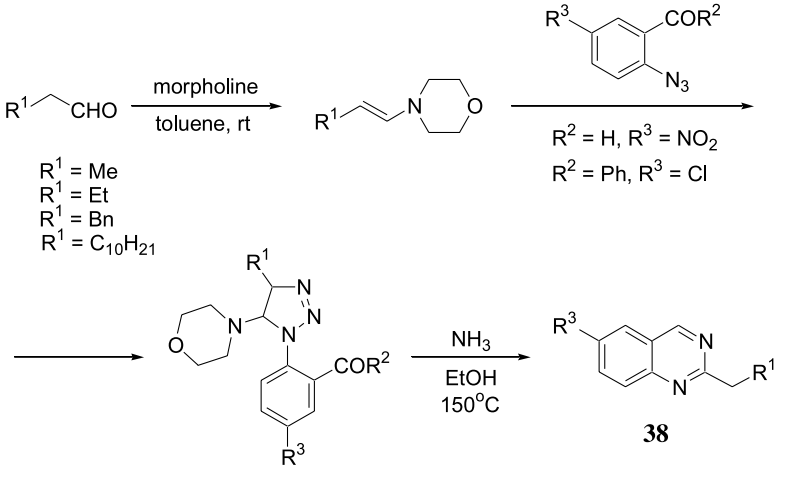

37a R_1 = Et, R^2 = H, R^3 = NO_2
37b R_1 = Me, R^2 = H, R^3 = NO_2
37c R_1 = Bn, R^2 = H, R^3 = NO_2
37d R_1 = $C_{10}H_{21}$, R^2 = H, R^3 = NO_2

Scheme 16.

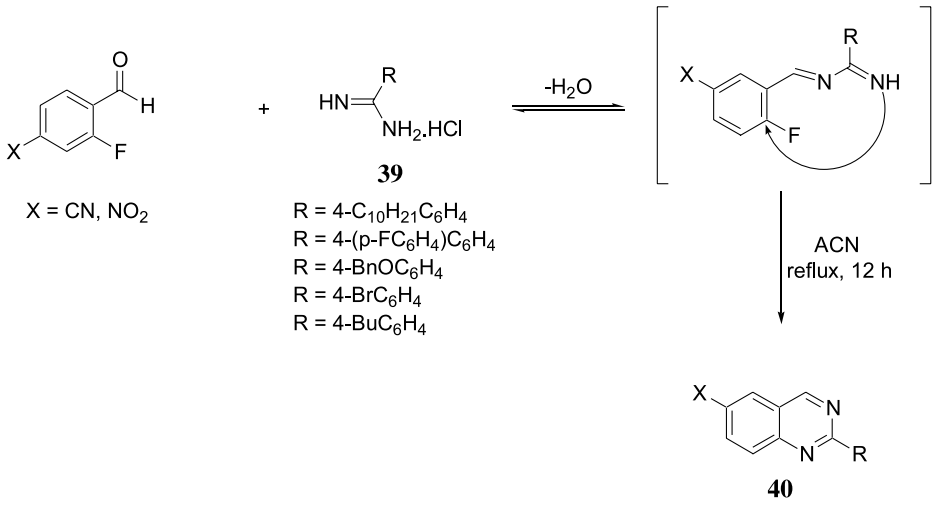

39

40

Scheme 17.

Table 3. Synthesis of quinazoline derivatives **40** from amidines and 2-fluorobenzaldehyde

Entry	Product **40**	Yield (%)
1	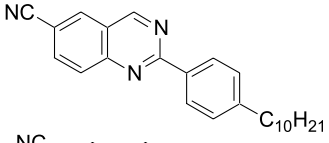	62
2	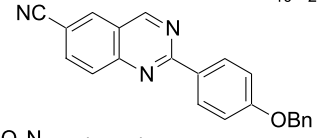	57
3	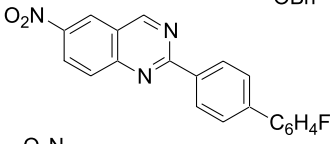	55
4	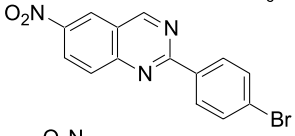	69
5	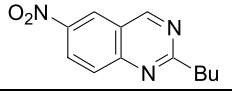	67

into the desired quinazoline products **38** in approximately 30 min. The ring-closure step worked well for the triazolines **37a** and **37b**, affording the 2-alkyquinazolines in 92 and 95% yield, respectively. In comparison, the triazolines **37c** and **37d** only gave moderate yields of 38 and 37%.

Overall, this procedure is characterised by the use of readily available starting materials for the synthesis of 2-substituted-quinazolines that bear electron-withdrawing groups.

2.5. Reaction of amidines with 2-fluorobenzaldehyde

Kotsuki et al. developed a condensation of cyano- and nitro-activated *o*-fluorobenzaldehydes with amidines **39** to give a variety of quinazoline derivatives **40** in good yields.[38] This method involves tandem imine formation with the aldehyde function and an intramolecular nucleophilic aromatic substitution at the fluorine-substituted carbon centre, Scheme 17. The reaction is carried out in refluxing acetonitrile with potassium carbonate in the presence of powdered molecular sieves, and the crude product is purified by chromatography.

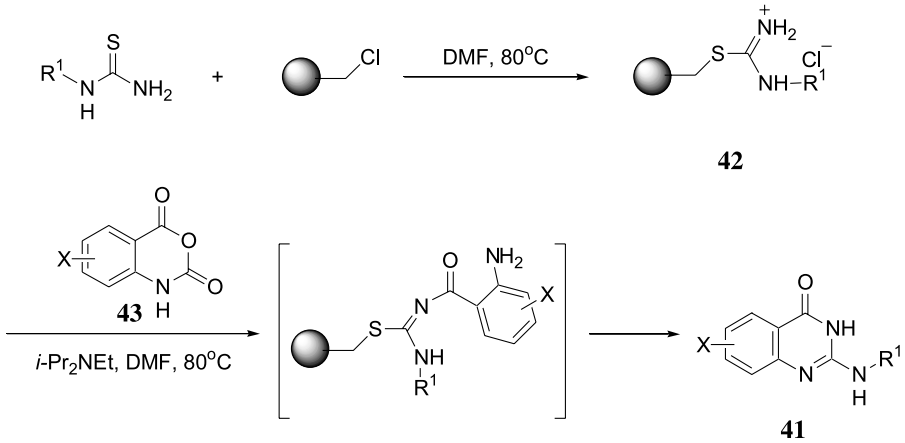

42

43

41

Scheme 18.

Table 4. Synthesis of 2-amino-quinazolinones **41** from resin-bound isothioureas

Entry	Product **41**	Yield (%)[a]	Purity (%)[b]
1	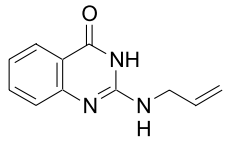	65	93 (100)
2	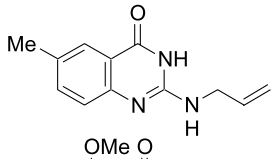	67	97 (100)
3	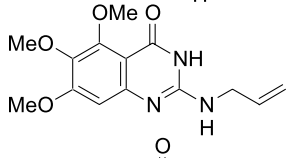	64	98 (100)
4	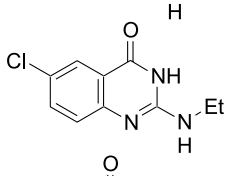	88	97 (100)
5	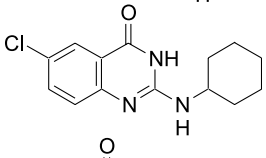	88	94 (100)
6	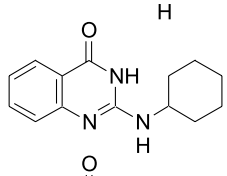	81	100 (100)
7	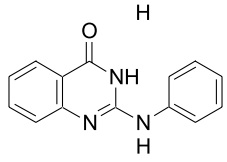	53	84 (90)
8	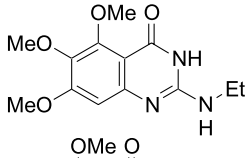	80	95 (10)
9	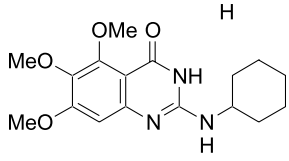	60	94 (100)

[a] Based on amount of isatoic anhydride used.
[b] Determined by HPLC using both UV (254 nm) and ELSD detectors; numbers in brackets are from ELSD detector.

The general applicability of this procedure is apparent, Table 3, and a variety of quinazoline derivatives were obtained in moderate to good yields using both aromatic and aliphatic amidines.

2.6. Synthesis of 2-amino-quinazolinones from resin-bound isothioureas

A concise and efficient solid-phase synthesis of 2-amino-quinazolin-4(3*H*)-ones **41** was reported by Yang and Kaplau, involving the reaction of polymer-bound isothioureas **42** with isatoic anhydride derivatives **43** with good yields and excellent purity, Scheme 18, Table 4.[39]

The required thiourea is efficiently loaded onto a chloromethylated polystyrene resin in DMF at 80 °C to form the polymer-bound isothiourea. Unlike most solid-phase methods that require a large excess of reagents to force the reactions to completion, this method proceeds well with a stoichiometric amount of isatoic anhydride. A feature of this approach is that the thiol generated remains attached to the solid support, providing a more practical and environmentally friendly synthesis of 2-amino-quinazolin-4(3*H*)-ones.

2.7. Hetero-Diels–Alder synthesis of 2-substituted-quinazolinones

The synthesis of 2-substituted-quinazolinones by the cyclisation of 1-aryl-4-dimethylamino-2-phenyl-1,3-diaza-1,3-butadienes **44** and phenyl isocyanate was reported by Croce et al.[40] The reaction was carried out under an atmosphere of nitrogen in toluene at reflux temperature, to furnish the desired products **45** in good yields, Scheme 19.

The presence of the electron-rich dimethylamino group on the diene destabilises the cycloaddition adduct, facilitating the elimination of the *N*,*N*-dimethyl-*N*′-phenylformamidine **46** as a side product.

2.8. Reaction of nitriles with lithiated 2-aminobenzamides

Couture and co-workers have developed a novel procedure for the synthesis of 2-aryl- and 2-alkylquinazolin-4(3*H*)-ones **47** by the reaction of lithium 2-(diethylaminocarbonyl)anilide **48** with the appropriate aryl or aliphatic nitrile.[41] This route is highly efficient when aryl and heteroaryl nitriles are used. In the case of alkyl nitriles,

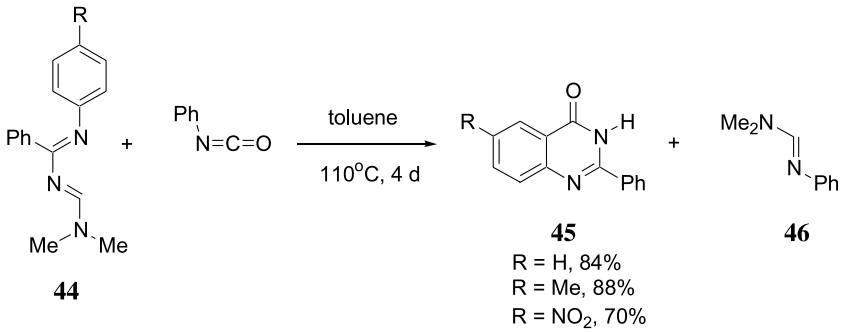

44

45
R = H, 84%
R = Me, 88%
R = NO_2, 70%

46

Scheme 19.

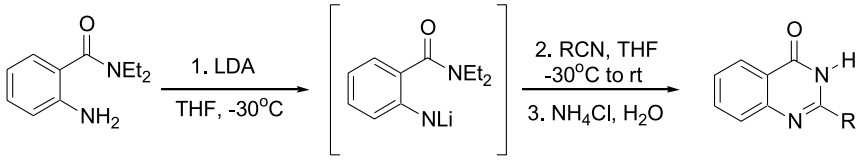

Scheme 20.

Table 5. Reaction of nitriles with lithiated 2-aminobenzamides to form 2-aryl- and 2-alkylquinazolin-4(3*H*)-ones **47**

Entry	2-Substituent (R)	Yield (%)
1		75
2		48
3		63
4	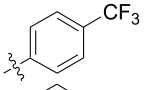	43
5	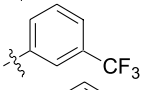	45
6	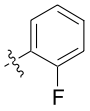	15
7	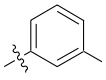	55
8	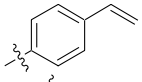	72
9		52
10		37

which possess acidic α-protons, good conversions are still obtained, considering that reaction with the lithium intermediate **48** is a possible side reaction, Scheme 20, Table 5.

Although the yields are modest in some cases, these are outweighed by the simplicity and generality of the process, which represents a convenient route to 2-aryl- and 2-alkylquinazolin-4(3*H*)-ones.

2.9. Reaction of methyl anthranilate with carbonimidates

Garratt et al. have developed the use of one-carbon compounds as synthetic intermediates in the synthesis of 2-aminoquinazolin-4(3*H*)-ones.[42] As an example, the reaction of diphenyl cyano-carbonimidate **49** with methyl anthranilate **50** treated with sodium hydride in dioxane afforded the *o*-phenylisourea **51** in 50% yield after 16 h at room temperature, Scheme 21. Addition of **51** to a saturated solution of the appropriate amine afforded the 3-substituted-4-oxo-3,4-dihydro-1*H*-ylidene-cyanamides **52**.

The cyano group was hydrolysed with hydrochloric acid followed by treatment with sodium hydroxide to yield the 2-aminoquinazolin-4(3*H*)-one derivatives **53** in good yields.

2.10. Condensation of anthranilate esters with guanidine

The amino-quinazolin-4(3*H*)-one **54** was developed by Hess et al.[43] It was prepared in moderate yield from the corresponding methyl anthranilate **50** with excess guanidine **55** in the presence of sodium ethoxide in ethanol, Scheme 22.

2-Chloro-quinazolin-4(3*H*)-one **56** could similarly be formed by alkaline hydrolysis of the corresponding 2,4-dichloroquinazoline at room temperature, which allowed the effects of varying the 2-substituents on the biological activity to be explored. For example, on heating diethylamine and the 2-chloro-quinazolin-4(3*H*)-one **56** for 5 h at

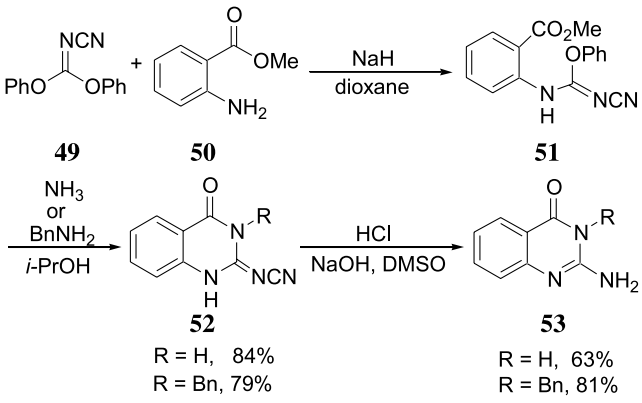

Scheme 21.

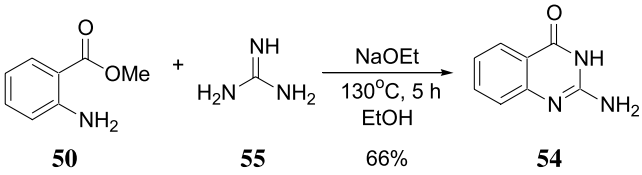

Scheme 22.

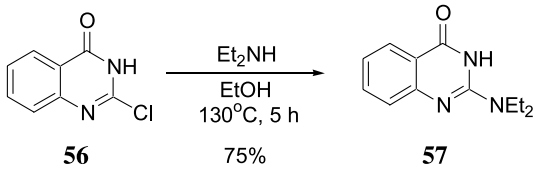

Scheme 23.

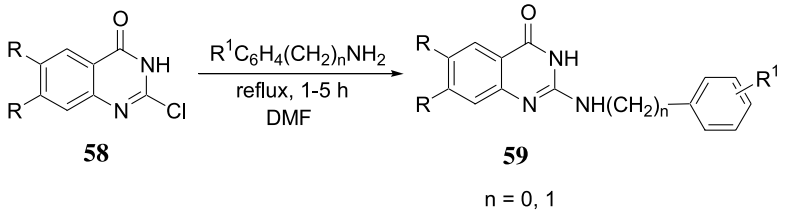

Scheme 24.

Table 6. Synthesis of aldose reductase pharmacophores **59**

Entry	R	R^1	*n*	Yield (%)
1	H	H	1	83
2	H	H	0	65
3	H	4′-OH	0	83
4	H	4′-CO_2H	0	89
5	H	4′-SO_3Na	0	57
6	H	3′-OH, 4′-CO_2H	0	72
7	OMe	H	1	87
8	OMe	H	0	86
9	OMe	4′-CO_2H	0	56

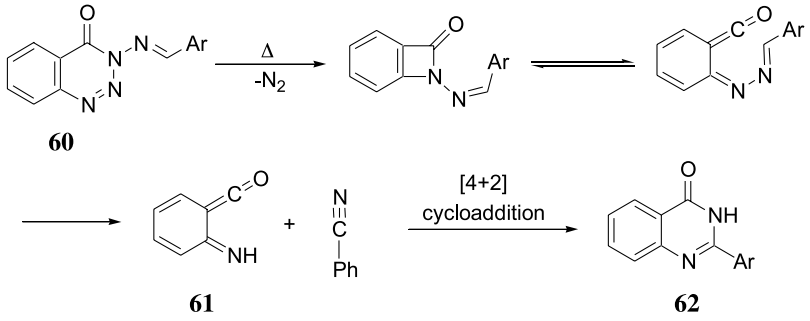

Scheme 25.

130 °C, the desired product **57** was obtained in 75% yield, Scheme 23.

Millen et al. also applied this procedure in their study of key pharmacophores **59** of aldose reductase, prepared from **58**, Scheme 24.[44]

The yields of **59** ranged from 56 to 87% depending on the substitution pattern, Table 6.

2.11. 2-Arylquinazolinones from benzotriazin-4-ones

Smalley and co-workers prepared a range of quinazolin-4(3*H*)-ones by the thermolysis of 3-arylideneamino-1,2,3-benzotriazin-4-ones **60** in paraffin oil at 300 °C, Scheme 25.[45] During the thermolysis process, a 1,3-hydrogen shift occurs with subsequent loss of aryl cyanide, which engages in a [4+2] cycloaddition with the imino-ketene **61**, leading to 2-aryl-quinazolinone **62** formation. This procedure tolerates a variety of 2-aryl substituents and the yields of **62** obtained ranged from 56 to 71%, Table 7.

2.12. Direct condensation of aldehydes and anthranilamide and its derivatives

Abdel-Jalil et al. reported that the condensation of aryl, alkyl and heteroaryl aldehydes in refluxing ethanol in the presence of $CuCl_2$ generates a Schiff base intermediate **63**, which is, in turn, converted into the 2-substituted quinazolinones **64a–g** in excellent yields, Scheme 26, Table 8.[46]

In a one-pot procedure, the aldehyde, anthranilamide and 3 equiv of $CuCl_2$ are refluxed in ethanol for 2–3 h. After purification by chromatography, the 2-substituted quinazolinones **64a–g** are isolated in 71–88% yield.

Although the preparation of 4-substituted-4(3*H*)-

Table 7. Synthesis of arylquinazolinones **62** from benzotriazin-4-ones

Entry	Ar	Yield (%)
1	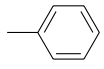	56
2	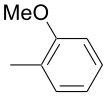	58
3	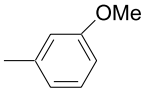	67
4	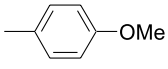	71
5	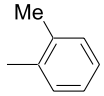	58
6	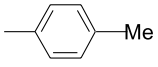	58
7	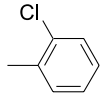	47
8	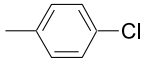	64
9	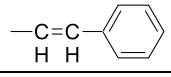	58

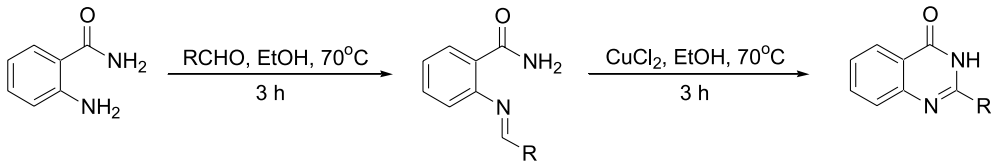

63 64a-g

Scheme 26.

Table 8. Condensation of aldehydes and anthranilamide to form quinazolinones **64a–g**

Product	R	Yield (%)[a,b]
64a	Me	82
64b	Bu	88
64c	Ph	84
64d	*p*-ClC_6H_4	79
64e	*p*-$MeOC_6H_4$	85
64f	2-Thiophenyl	81
64g	2-Furyl	86

[a] Reaction times vary.
[b] All reactions listed carried out in ethanol.

quinazolinones has been reported before via condensation of an aldehyde employing $NaHSO_3$[47] or DDQ,[48] this method has the advantage of a lower temperature, which may prevent decomposition products from forming.

3. 3-Substituted-4-quinazolines

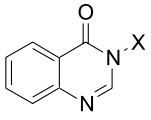

3.1. Vilsmeier reagent in quinazolinone synthesis

A novel dimerisation reaction to furnish 3-substituted-4(3*H*)-quinazolinones in high yield was developed by Perumal et al. by treating 5-substituted-2-aminobenzoic acid derivatives **65** with the Vilsmeier reagent **66**, Scheme 27.[49] This novel reaction occurred between 80 and 90 °C when two differently substituted acids were reacted with a combination of DMF and $POCl_3$. It was found that no dimeric product was obtained after heating the reaction mixture at 60 °C, even for prolonged periods of time, prompting a study into the effect of the addition of amines to the reaction mixture at low temperature. No reaction occurred when a mixture of **65** and primary amine was treated with the Vilsmeier reagent **66** at room temperature. It was found, however, that, if the Vilsmeier reagent was added at 0 °C to **65** followed by the addition of the suitably substituted primary amine at room temperature, the corresponding quinazolinones were obtained in low yield.

It was proposed that the chloromethyleniminium salt **66** formed from DMF and $POCl_3$ reacts with the benzoic acid **65** to give the corresponding acid chloride **67**, which, at high temperature (Scheme 27, Route B), then reacts with a molecule of 2-aminobenzoyl chloride. The diacid chloride **68** that is produced undergoes spontaneous cyclisation followed by migration of the dimethylamino group to give the product quinazoline **69** in good yields, Table 9.

When an external amine is added to the reaction mixture at low temperature an alternative reaction pathway occurs (Scheme 27, Route A). The added amine reacts with the acid chloride **67** with subsequent loss of HCl followed by cyclisation to produce the intermediate **70**, which then expels a dimethylamino group to afford the appropriately substituted quinazolinone **71**.

4. 4-Substituted quinazolines

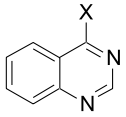

4.1. Derivatisation of 4(3*H*)-quinazolinones

The introduction of chlorine at the 4-position in the quinazolinone skeleton can be achieved through the use of $POCl_3$[50] or thionyl chloride.[51,52] An alternative to using $POCl_3$ was reported by Sugimoto et al.[53] This involves chlorination with a phosphonium salt of *N*-chlorosuccinimide **72a**, Scheme 28. Treatment of the quinazolinone with this salt in refluxing dioxane for 4 h furnished 4-chloroquinazoline in 73% yield.

Bromination with the analogous phosphonium salt **72b** produced the 4-bromoquinazoline in 1 and 5% yield, depending on the reaction time. The poor yield is proposed to be due to the unstable nature of the product.

4-Chloroquinazolines, for example, compound **73**, are important synthetic intermediates as they can be derivatised further through nucleophilic attack at the C-4 position. This is illustrated in the synthesis of **74**, an intermediate in the synthesis of AX7593, a quinazoline-derived photoaffinity probe for epithelial growth factor receptor (EGFR), Scheme 29.[54]

A thiomethyl substituent can also be used to activate the 4-position towards nucleophilic substitution.[55] The formation of a thiomethyl ether is achieved in two steps by treating the corresponding quinazolinone **75** with Lawesson's reagent (P_2S_5) to yield a quinazolinethione **76**, Scheme 30. Subsequent lithiation and methylation lead to the formation of the thioether **77**, which can then be treated with a nucleophile to give the 4-substituted quinazoline **78**.

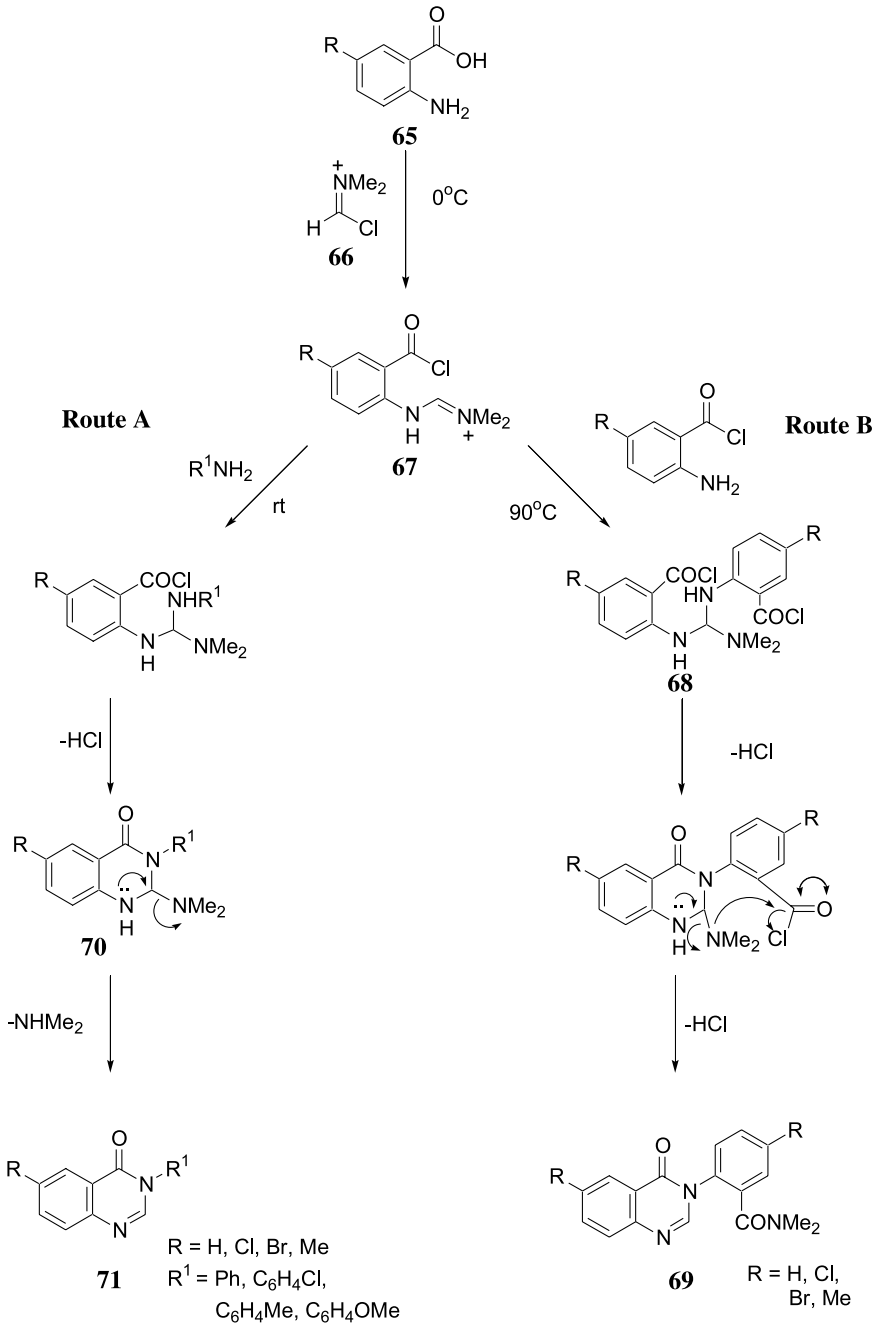

Scheme 27.

Table 9. Synthesis of quinazoline **69** using the Vilsmeier reagent

Entry	R in **69**	Yield (%)
1	H	83
2	Cl	82
3	Br	86
4	Me	50

4.2. Reaction of anilines with 2-aminobenzonitrile

Recently, there has been a renewed interest in 4-arylamino-quinazolines, owing to reports of their high biological activity as potential antitumour agents.[56] The amidines **79** are readily synthesised from the reaction of 2-aminobenzo-nitrile with anilines and anhydrous aluminium chloride,

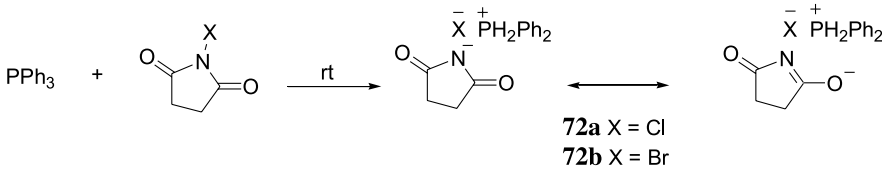

Scheme 28.

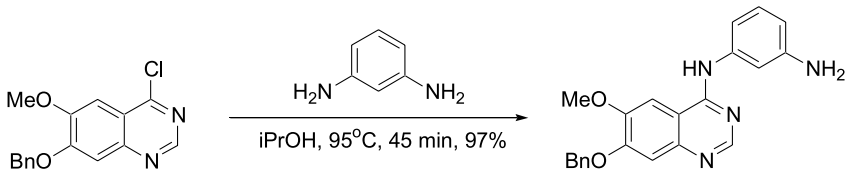

73 74

Scheme 29.

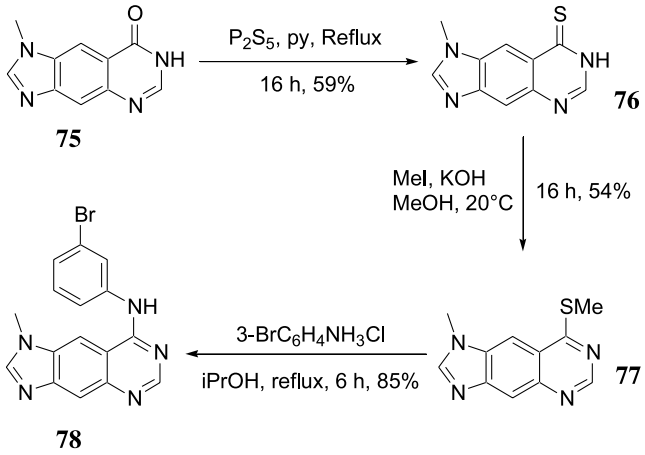

Scheme 30.

Scheme 31.[57,58] It was found that an optimal yield of amidines **79** was obtained using an excess of the required aniline and aluminium chloride. The formation of these amidines is, however, limited by the aromatic substitution pattern on the aniline. No reaction was observed with 3,4-dichloroaniline or with nitroanilines, possibly due to the reduced nucleophilicity of the amino group in each case.

Scheme 31.

The 2-amino-*N*-arylbenzamides **79** furnished the 4-arylaminoquinazolines **80** in good yields (70–92%) when heated with 85% formic acid, although the reaction can only be applied to the synthesis of 2-unsubstituted 4-arylaminoquinazolines, Scheme 32, Table 10. This route was later modified to enable the preparation of 2-aryl-4-aminoquinazolines and will be detailed later in this review.

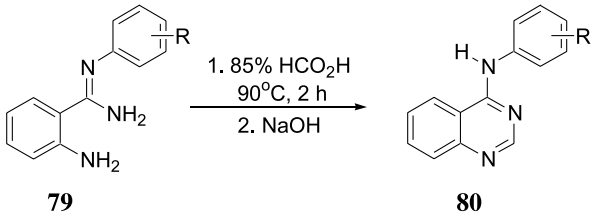

79 80

Scheme 32.

Table 10. Reaction of anilines with 2-aminobenzonitrile to form 4-arylaminoquinazolines **80**

R	Yield (%)	R	Yield (%)
H	82	3-I	92
2-Me	70	4-Me	84
2-Br	73	4-Cl	92
3-Me	84	4-Br	91
3-Cl	90	3,4-$(Me)_2$	83
3-Br	92	3,4-$(Cl)_2$	92

In May 2003, the US Food and Drug Administration (FDA) approved the first epidermal growth factor receptor inhibitor, Iressa, for the treatment of lung cancer, further highlighting the importance of the 4-anilinoquinazolines in medicine, Scheme 33.[59]

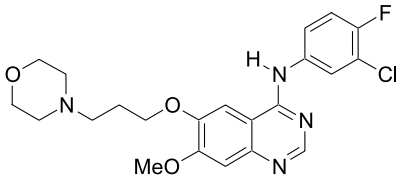

Iressa

Scheme 33.

4.3. Reaction of anilines with 2-amidinobenzonitriles

Tsou et al. reported an efficient method for the synthesis of 4-anilinoquinazolines. 5-Nitroanthranilonitrile **81** was condensed with DMF acetal to yield **82**.[60] Heating this compound with 3-bromoaniline in acetic acid yielded the desired quinazoline **83** in excellent yield, Scheme 34.

An advantage of this approach is the formation of the quinazoline ring and the incorporation of the 4-anilino group in the one step.

Yoon et al. reported the reaction of *N*,*N*-dimethylamidinobenzamide **84** with benzylamine **85** to give 4-aminoquinazoline **86** under the conditions of microwave (MW) irradiation, Scheme 35.[61]

4.4. Palladium-mediated approach

Watanabe et al. have developed a novel palladium complex-catalysed synthesis of quinazoline derivatives by employing an intermolecular reductive *N*-heterocyclisation.[62] A palladium complex of $PdCl_2(PPh_3)_2$ with $MoCl_5$ showed high catalytic activity for the *N*-heterocyclisation of

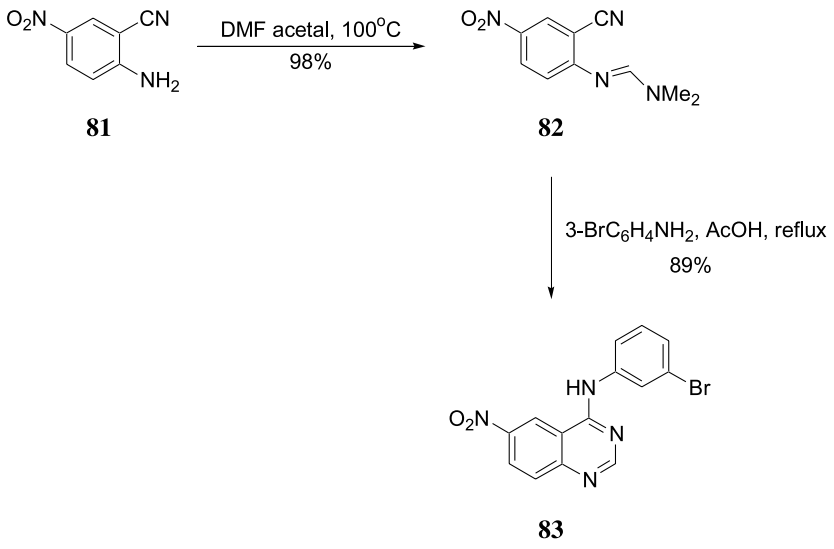

81 82 83

Scheme 34.

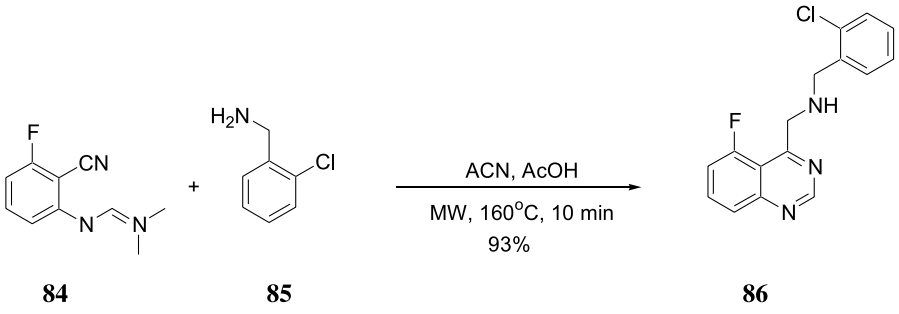

84 85 86

Scheme 35.

2-nitrophenyl ketones **87** with formamide **88** to afford the corresponding 4-substituted quinazolines **89**, Scheme 36.

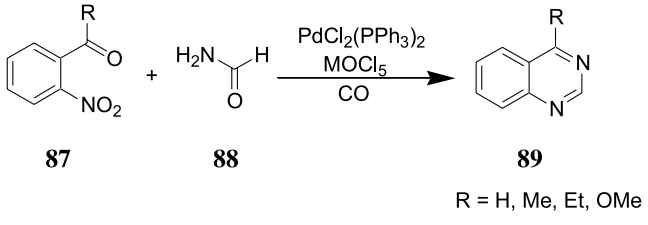

87 88 89

Scheme 36.

In the absence of the palladium complex, 2-nitrobenzaldehyde **90** reacted with formamide to give the corresponding *N*-[1-formylamino-1-(2-nitro-phenyl)-methyl]-formamide **91**, Scheme 37.

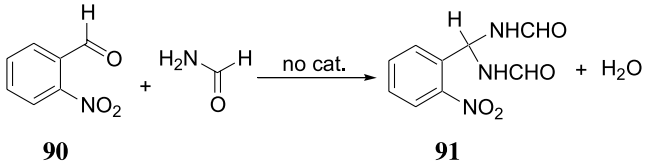

90 91

Scheme 37.

When formamide **91** was treated in the presence of the catalyst under CO pressure at 100 °C for 16 h, the quinazoline **92** was produced in 29% yield, Scheme 38. This suggests that *N*-[1-formylamino-1-(2-nitro-phenyl)-methyl]-formamide is a possible intermediate in the reductive *N*-heterocyclisation.

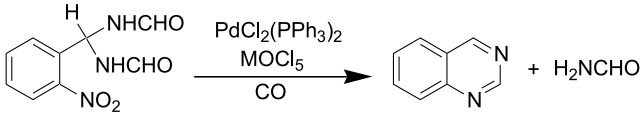

91 92

Scheme 38.

The suggested mechanism for this process begins with the carbonyl group of the 2-nitrophenyl ketone **87** condensing with the formamide **88** to give the corresponding bisamide **93**, Scheme 39. A nitrene intermediate **94** is generated by deoxygenation of the nitro group with carbon monoxide. It is proposed that the Lewis acidic $MoCl_5$ coordinates to the oxygen atoms of the nitro group, weakening the N–O bond and thereby facilitating the deoxygenation process. An intramolecular nucleophilic addition of the nitrene to the carbonyl group of the bisamide follows to generate the metallacyclic intermediate **95**, which subsequently undergoes decarboxylation. Finally, the reductive elimination of

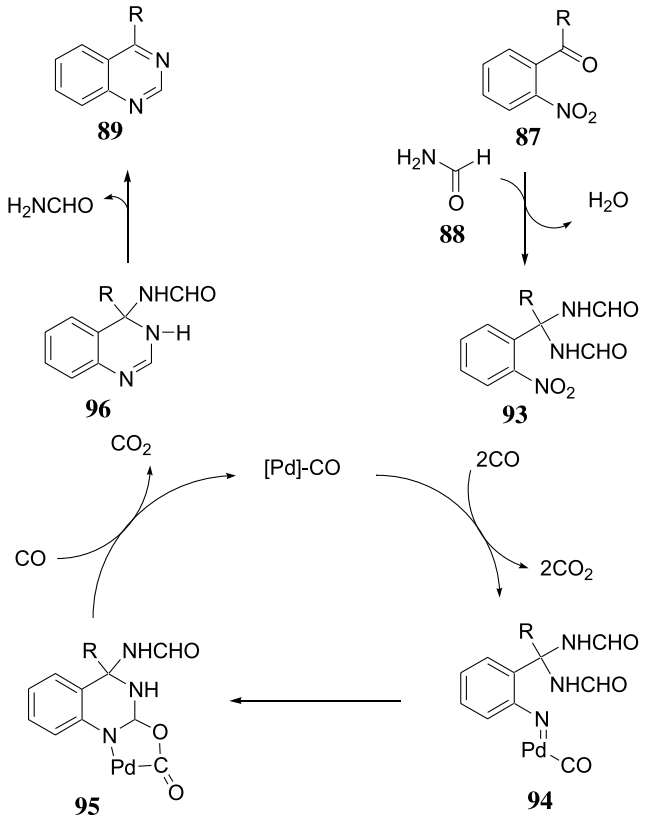

Scheme 39.

the 3,4-dihydro-4-(*N*-formylamino)quinazoline **96** regenerates the active catalyst and dehydroamidation of **96** furnishes the desired quinazoline **89**.

This novel route to biologically important compounds represents the first transition-metal-complex-catalysed intermolecular reductive *N*-heterocyclisation and offers a new synthetic method for preparing quinazoline derivatives, albeit in moderate yields (19–44%), Table 11.

Table 11. Reductive *N*-heterocyclisation of 2-nitrophenyl ketones **87** to form quinazoline derivatives **89**

Entry	Substrate **87**	Product **89**	Yield (%)
1	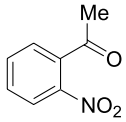	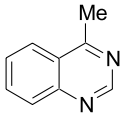	44
2	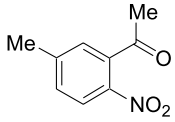	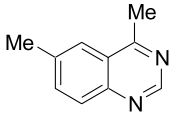	44
3	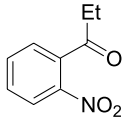	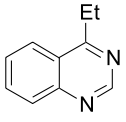	19
4	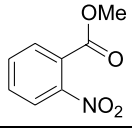	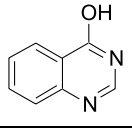	40

5. 2,3-Disubstituted-4(3*H*)-quinazolines

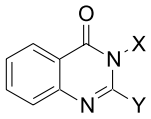

5.1. Combinatorial approach to quinazolinones

Houghten et al. developed a novel, traceless and chemoselective approach for the solid-phase synthesis of 2-arylamino-substituted quinazolinones with the possibility of manipulation at three positions.[63] Starting from the *p*-methyl benzhydryl amine (MBHA) resin **97**, a specific *o*-nitrobenzoic acid was attached and the aromatic nitro group was then reduced with tin(II) chloride to furnish the required *o*-aniline **98**, Scheme 40. The resin was dried and subsequently reacted with an appropriate aryl isothiocyanate and the resin-bound thiourea **99** was reacted with Mukaiyama's reagent (2-chloro-1-methylpyridinium iodide). A primary amine was added at room temperature to generate the corresponding guanidine **100** and the desired 2-amino-substituted quinazoline was obtained via an intramolecular cyclisation. This was followed by cleavage from the resin using hydrofluoric acid at 0 °C for 1.5 h to give the product quinazoline **101** in good yield and purity, Table 12.

This method demonstrates a traceless approach for the parallel solid-phase synthesis of *o*-arylamino-substituted quinazolines from common materials such as 2-nitrobenzoic acid derivatives (R^1), aryl isocyanates (R^2) and amines (R^3).

The literature on solid-phase approaches to quinazolines and quinazolinones has recently been reviewed by Vögtle and Marzinzik.[64]

5.2. Intramolecular coupling of azides to carbonyl groups

A mild and efficient route for the synthesis of fused [2,1-*b*] quinazolinones was reported by Kamal and co-workers.[65] The procedure employs an intermolecular azido-reductive cyclisation in the preparation of the pyrrolo[2,1-*b*]quinazolinone ring system **102**, Scheme 41, Table 13. This was exploited in the synthesis of deoxyvasicinone, a precursor for vasicinone, a known bronchodilater.[66]

The $FeCl_3$/NaI combination had not previously been investigated for the reduction of the azide functionality and the role of NaI could be attributed to the in situ formation of FeI_3. In addition, the use of excess NaI appears to be crucial for high conversions. This new reductive cyclisation method affords an alternative route towards the preparation of these pharmacologically important fused quinazolinones **102** in high yields (85–97%).

The synthesis of optically active *l*-vasicinone, a known pyrrolo[2,1-*b*]-quinazolinone alkaloid, was undertaken by Eguchi et al. employing the intramolecular aza-Wittig reaction as the key step in the construction of the quinazolinone ring skeleton, Scheme 42.[67]

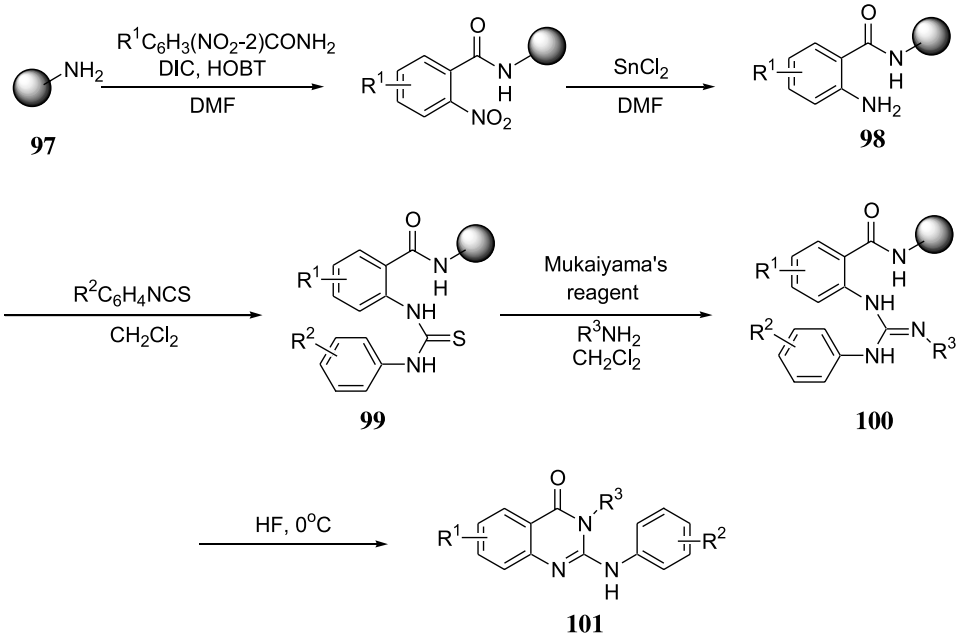

Scheme 40.

Table 12. Combinatorial production of quinazolines **101**

Entry	R^1	R^2	R^3	Yield of **101** (%)[a]
1	H	2-Cl, 4-NO_2	*i*-Bu	86
2	H	4-NO_2	$(Me)_2CHCH_2CH_2CH_2$	89
3	H	2,3-Cl	*i*-Bu	83
4	H	3-Cl	*i*-Bu	91
5	H	4-CN	*i*-Bu	88
6	H	H	*i*-Bu	86
7	H	4-NO_2	$PhCH_2CH_2CH_2$	85
8	H	4-NO_2	$Me(CH_2)_4CH_2$	88
9	5-MeO	4-NO_2	$(Me)_2CHCH_2CH_2CH_2$	85
10	5-Pyridyl	3,5-Cl	$Me(CH_2)_2CH_2$	86
11	5-Pyridyl	4-NO_2	$Me(CH_2)_2CH_2$	88

[a] Based on weight of crude material (relative to the initial loading of the resin).

The synthesis of *l*-vasicinone was initiated by protection of the chiral synthon, (3*S*)-3-hydroxy-γ-lactam with *tert*-butyldimethylsilyl chloride, followed by condensation with *o*-azidobenzoyl chloride **103** using sodium hydride in tetrahydrofuran. The intermediate **104** was treated with tri-*n*-butylphosphine, which, in turn, initiated the tandem Staudinger-intramolecular aza-Wittig reaction, furnishing *o-tert*-butyldimethylsilyl vasicinone **105** in 76% yield. Finally, deprotection of the silyl ether by tetra-*n*-butylammonium fluoride (TBAF) enabled the preparation of *l*-vasicinone in 52% overall yield with a 97% ee.

Recently Hernández et al. reported the use of an Eguchi aza-Wittig reaction to fashion the 2,3-disubstituted quinazolinone skeleton in the course of a synthesis of analogues of *N*-acetylardeemin, a multidrug resistance reversal agent.[68]

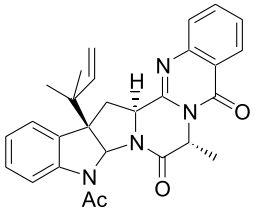

N-acetylardeemin

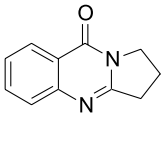

deoxyvasicinone

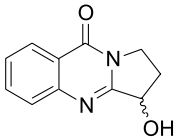

vasicinone

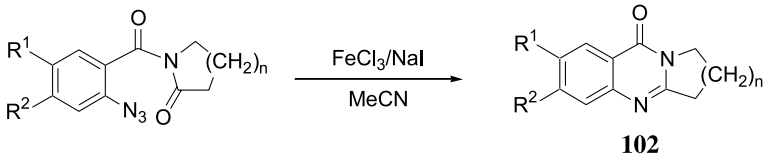

Scheme 41.

Table 13. Synthesis of quinazolinones **102** via intermolecular azido-reductive cyclisation

Entry	R^1	R^2	*n*	Yield of **102** (%)
1	H	H	1	97
2	Me	H	1	97
3	H	Cl	1	96
4	H	H	2	88
5	Me	H	2	87
6	H	Cl	2	85
7	H	H	3	95
8	Me	H	3	94
9	H	Cl	3	96

5.3. Formation of pyrrole-based quinazolinones from benzodiazepines

The medicinal research of Fabis et al. showed that the aromatic system of pyrrolo[2,1-*c*][1,4]benzodiazopine was reactive towards nucleophiles, leading to the formation of quinazolines as rearrangement products.[69] Heating the 2-hydroxypyrrolo[2,1-*c*][1,4]benzodiazepine with thionyl chloride **106** in the presence of pyridine gave the 11-chloropyrrolo[2,1-*c*][1,4]benzodiazepine **107** in 70% yield, Scheme 43. This represents a straightforward method for the synthesis of aromatic pyrrolo[2,1-*c*][1,4]benzodiazepines. It

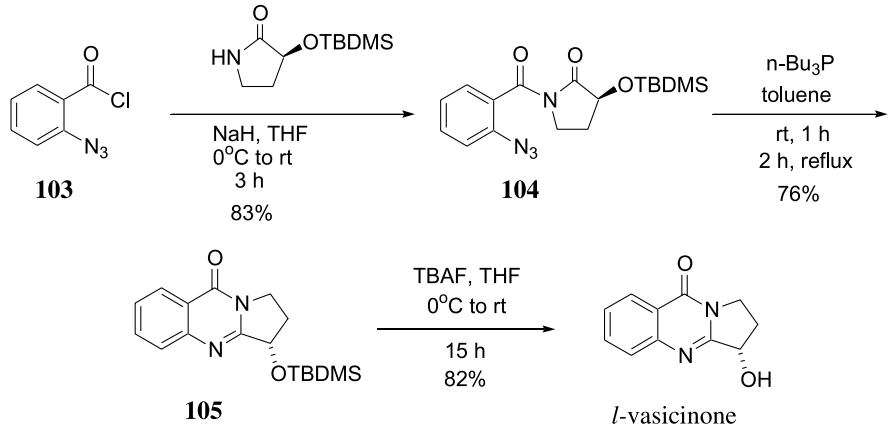

Scheme 42.

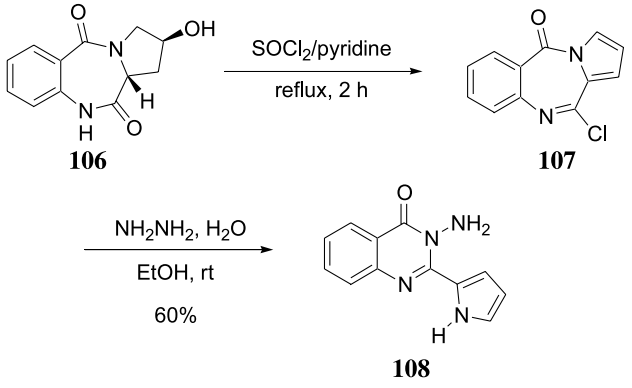

Scheme 43.

became apparent that the double reactivity of such compounds at the carbonylpyrrole bond and at the chloroimine moiety would be useful in accessing the quinazolinone skeleton. This was exemplified by the addition of hydrazine to furnish the desired 3-amino-2-(1*H*-pyrrol-2-yl)-4(3*H*)-quinazolinone **108** in a respectable 60% yield.

5.4. Formation of 2,3-disubstituted quinazolinones from benzoxazepinediones

Uskokovic et al. reported the synthesis of 2-(α-hydroxyalkyl)-3-*N*-methylquinazolinones **109** from 4,1-benzoxazepine-2,5(1*H*,3*H*)-diones **110**.[70] Commencing with

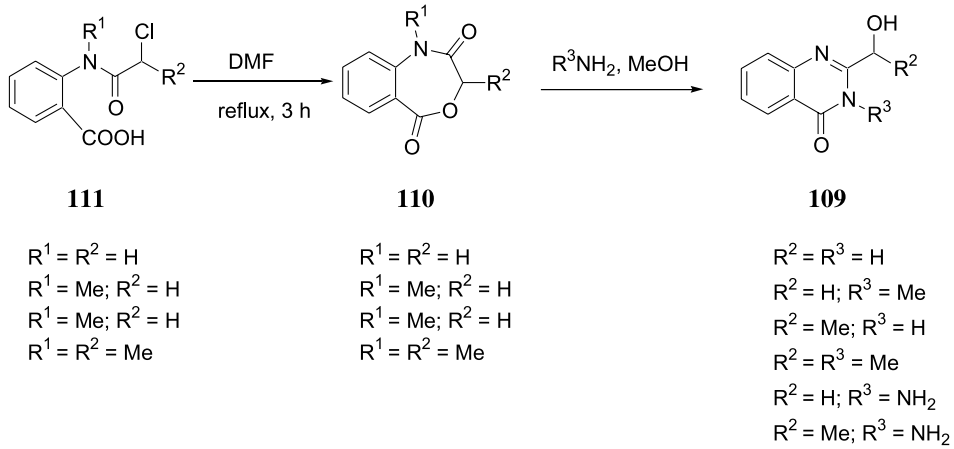

Scheme 44.

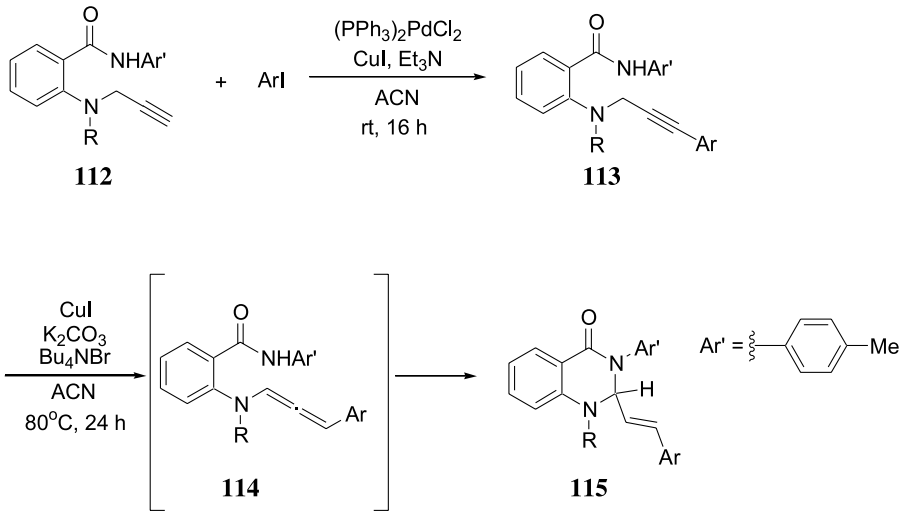

Scheme 45.

Table 14. Synthesis of quinazolinones **115** via copper-catalysed cyclisation

Entry	R	Ar	Disubstituted alkynes **113** (%)	Quinazolinones **115** (%)
1	Me	2-MeC_6H_4	76	67
2	Me	2-Thienyl	75	61
3	Me	2,4-Dimethoxypyrimidin-5-yl	79	65
4	Me	2-$MeCO_2C_6H_4$	90	69
5	Bn	2-MeC_6H_4	72	63
6	Bn	2-Thienyl	73	67
7	Bn	2,4-Dimethoxypyrimidin-5-yl	91	62
8	Bn	2-$MeCO_2C_6H_4$	89	61

anthranilic acid, amidation proceeds in excellent yield, Scheme 44. Ring closure of **111** to form the benzoxazepines was achieved by heating to reflux in DMF for 3 h, giving **110** in acceptable yield. The formation of **109** was achieved in methanolic solution in the presence of methylamine over 1 week.

5.5. Quinazolinones via copper-catalysed cyclisation

Kundu and Chaudhuri developed a novel copper-catalysed heteroannulation to (*E*)-2-(2-arylvinyl)quinazolinones from alkynes.[71] A series of 2-[*N*-alkyl(benzyl)-*N*-(prop-2′-ynyl] aminobenzamides **112** reacted with aryl iodides under palladium–copper catalysis to yield the disubstituted alkynes **113**. The alkynes subsequently underwent a highly regio- and stereoselective cyclisation in the presence of CuI, K_2CO_3 and *n*-Bu_4NBr in acetonitrile to furnish the required quinazolinones in good yields, Scheme 45, Table 14. The conversion of the alkynyl-aminobenzamides into the disubstituted alkynes occurred via a Sonogashira–Hagihara coupling, followed by a rearrangement to the allene intermediates **114**. The amide nitrogen partakes in nucleophilic attack on the terminal carbon of the allene with concomitant ring closure to give the substituted quinazoline derivatives **115** with predominant *E*-stereochemistry at the vinylic group.

This is the first reported synthesis of quinazolinones employing a copper-catalysed cyclisation. The method is very mild, requires inexpensive starting materials and is experimentally undemanding.

5.6. Synthesis of fluorinated quinazolinones

Smith et al. have developed a one-step synthesis of 4(3*H*)-quinazolinones **116** by employing 2-fluoro-substituted benzoyl chlorides **117** and 2-amino-*N*-heterocycles **118** in a cyclocondensation, Scheme 46.[72] The quinazolinone precipitates immediately after treatment of a dichloromethane solution containing the required heterocycle and diisopropylethylamine with the acyl chloride at room temperature. The yields are, however, low to moderate, and in most cases, the major products are the corresponding amides **119**, Scheme 46, Table 15.

The experimental results reveal that, as the number of fluorines on the benzoyl chloride decreases, the isolated yields of the cyclised product also decrease. The introduction of a nitro group at the 5-position enables the ring closure to occur more efficiently, due to the ability of the *p*-nitro group to promote the nucleophilic aromatic substitution reaction. The most plausible mechanism for quinazolinone formation is initial nucleophilic attack of the ring nitrogen on the benzoyl chloride followed by

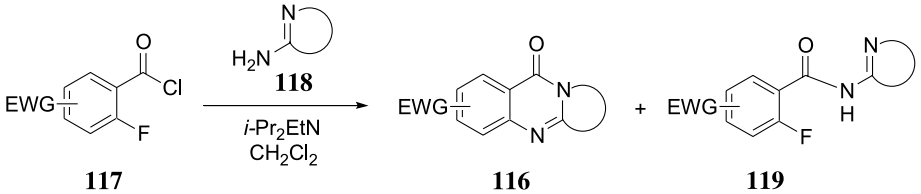

Scheme 46.

Table 15. Reaction of acyl chlorides **117** with 2-amino-*N*-heterocycles **118** to form fluorinated quinazolinones **116**

Entry	Acyl chloride **117**	2-Amino-*N*-heterocycle **118**	Yield of **116** (%)
1	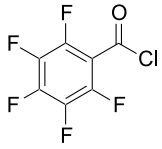	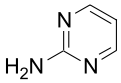	40
2	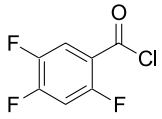	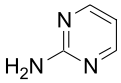	12
3	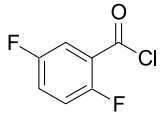	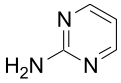	9
4	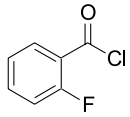	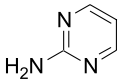	3
5	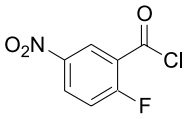	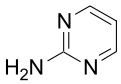	36
6	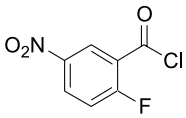	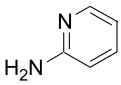	40
7	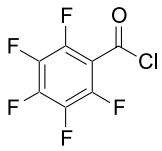	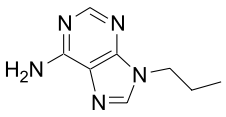	10
8	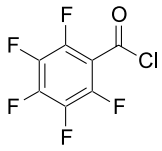	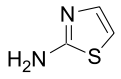	20
9	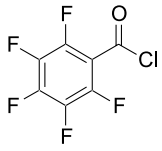	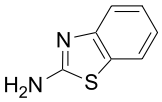	30

intramolecular nucleophilic substitution of the 2-fluoro substituent. This proposed mechanism is supported by the fact that the ring nitrogen is the most nucleophilic atom in 2-aminopyrimidine.[73]

5.7. 2,3-Disubstituted quinazolinones via benzoxazinones and benzoxazadiones

Benzoxazinones and benzoxazadiones are common intermediates in the synthesis of 2,3-disubstituted quinazolinones. Párkányi and Schmidt[74] prepared 2,3-disubstituted-quinazolines from chloro-substituted anthranilic acids and acetic anhydride in a study similar to the work of Jiang et al. described in Section 2.1.[13] The intermediate (4*H*)-3,1-benzoxazinones such as **120** were then reacted with amino-substituted thiazoles **121a** and a 1,3,4-thiadiazole derivative **121b** to afford the desired products **122** and **123** in moderate to good yields, Scheme 47, Table 16.

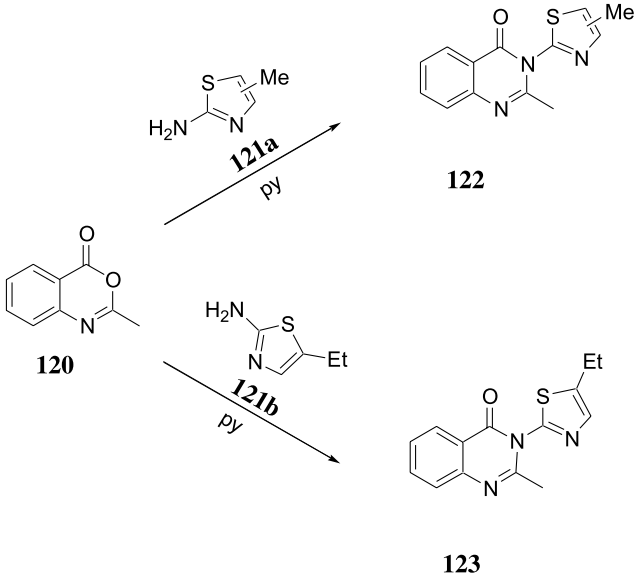

Scheme 47.

Table 16. Synthesis of quinazolinones **122** and **123**

Entry	Substituents	Yield (%)
1	5-Cl-3-(5-MT)	55
2	6-Cl-3-(5-MT)	42
3	7-Cl-3-(5-MT)	29
4	6,8-Cl_2-3-(5-MT)	39
5	7-Cl-3-(4-MT)	47
6	6,8-Cl_2-3-(4-MT)	51
7	7-Cl-3-(5-ETD)	52
8	6,8-Cl_2-3-(5-ETD)	38

5-MT=5-methylthiazol-2-yl, 4-MT=4-methylthiazol-2-yl, 5-ETD=5-ethyl-1,3,4-thiadiazol-2-yl.

A similar approach was taken by Kumar et al. in their synthesis of the novel 2,3-disubstituted quinazolinone **125** from **120** and **124**, Scheme 48.[75]

It is possible to introduce an acyclic *N*-substituent using this method as demonstrated by Zhou et al. for a range of sulfonamides **128** (88 in total) from **126** and **127** with a variety of substitution patterns, Scheme 49, Table 17.[76]

During the course of investigating this reaction, some open-chain product **129** was isolated, Scheme 50. In order to test the hypothesis that this reaction proceeded via an open-chain intermediate, equivalent amounts of **130** and benzenesulfonylhydrazide **131** were dissolved in anhydrous DMF. The mixture was stirred at room temperature for 22 h, affording **129** and 5% of the cyclised product **132**. Heating this mixture subsequently furnished **132** in 78% yield following chromatographic purification, supporting the idea of an acyclic intermediate.

Xue et al. reported the optimisation of Grimmel's conditions for generating C_2,N_3-disubstituted-4-quinazolinones.[77,78] Using Grimmel's methodology, *N*-acetylanthranilic acids

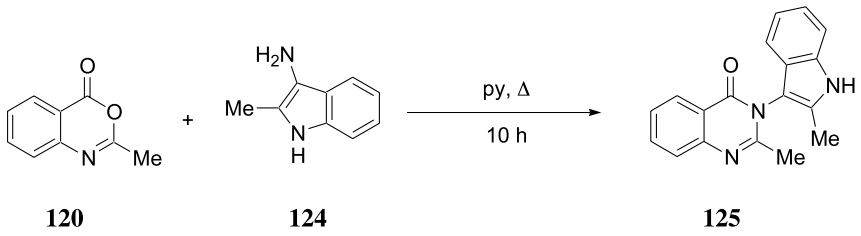

120 **124** **125**

Scheme 48.

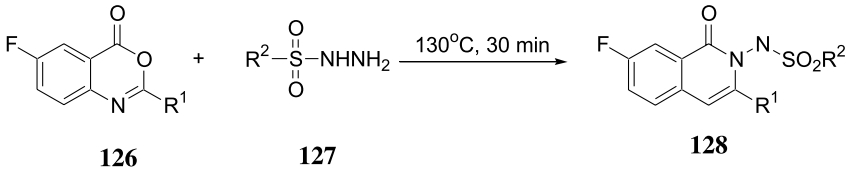

126 **127** **128**

Scheme 49.

Table 17. Synthesis of 3-sulfonamide-substituted quinazolines **128**[a]

Entry	R^2	R^1 (% yield)[b]			
		Phenethyl	Bn	Ph	2-Thiophene-methylene
1	4-CO_2H-Ph	98	81	67	99
2	4-NHCOMe-Ph	99	94	58	99
3	4-OCF_3-Ph	96	90	81	74
4	3,4-Di-Cl-Ph	83	85	40	29
5	4-CF_3-Ph	90	92	87	45
6	4-CN-Ph	90	88	51	73
7	4-Cl-Ph	90	90	68	49
8	Bn	82	96	45	79
9	3-NO_2-4-Cl-Ph	92	89	55	24
10	3-CO_2H-Ph	99	98	98	83
11	5′-(*N*-Thiophen-2-yl-methyl-benzamide)	83	72	37	51
12	4-*i*-Pr-Ph	86	76	64	32
13	4-OMe-Ph	85	90	73	71
14	3,4-Di-F-Ph	92	89	98	75
15	2-Cl-Ph	95	70	60	80
16	3,4-Di-OMe-Ph	86	69	90	63
17	3,5-Di-Cl-Ph	95	92	53	50
18	4-F-Ph	95	98	99	78
19	4-NO_2-Ph	95	81	99	97
20	4-*t*-Bu	92	82	44	50
21	2,4-Di-Cl-5-Me-Ph	57	17	26	<5
22	2,4-Di-Cl-Ph	<5	8	15	52

[a] All of the products <90% pure by ELSD were purified by reverse-phase HPLC in automated fashion using Waters MS-triggered purification system using ACN and H_2O as eluting solvent.
[b] The yields are estimated by HPLC (ELSD) from LC-MS results of the reaction mixture before HPLC purification.

such as **133** are heated with anilines in toluene or xylene in the presence of dehydrating agents such as phosphorous trichloride, phosphorous oxychloride or thionyl chloride to yield **134**, Scheme 51.

In Grimmel's original paper, no trace of **135** was observed when *N*-acetoxyacetylanthranilic acid and aniline were refluxed together in the presence of 0.34 equiv of PCl_3, Scheme 52.

When the same methodology was applied to *o*-chloroaniline **136** and carboxylic acid **137**, however, a small amount of **138** (10%) was observed. Subsequent experimentation led to the isolation of **139**, which was proposed as being a

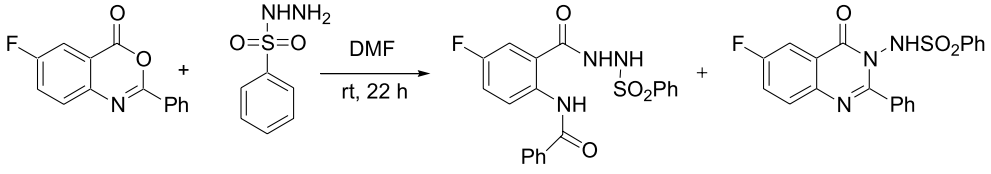

130 **131** **129** **132**

Scheme 50.

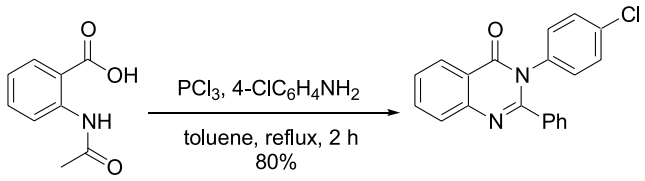

133 134

Scheme 51.

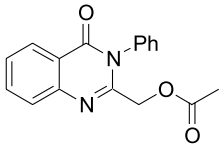

135

Scheme 52.

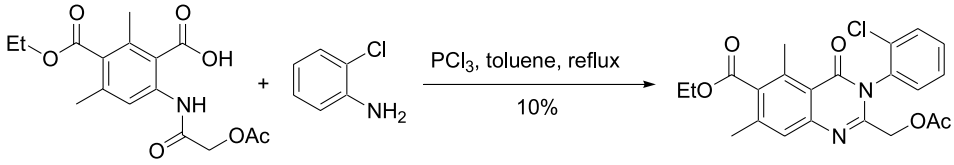

137 136 138

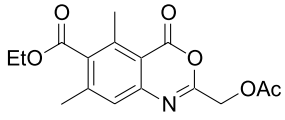

139

Scheme 53.

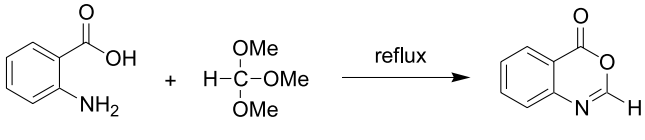

12 140

Scheme 54.

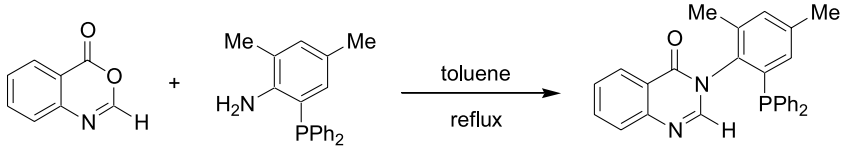

141

Scheme 55.

plausible intermediate in the formation of the quinazolinone product, Scheme 53.

By changing both the solvent and the temperature used, yields from 87 to 98% for a range of quinazolinones were obtained in polar aprotic solvents.

Virgil and Dai reported the synthesis of 2-hetero-substituted atropisomeric quinazolinone phosphine ligands in good yields.[79] The synthesis of the 2-unsubstituted ligand was initiated by the formation of (4*H*)-3,1-benzoxazin-4-one **140** via the condensation of anthranilic acid **12** with trimethyl orthoester, Scheme 54.

After removal of the excess orthoester, the crude product was mixed with aminophosphine in toluene and subsequently heated to reflux for 6 h to afford the quinazolinone **141** in 88% yield, Scheme 55.

By direct lithiation of the 2-unsubstituted quinazolinone system **141** it was possible to carry out a range of electrophilic substitutions, Scheme 56. Electrophiles such as chlorodiphenylphosphine, solid sulfur and dimethyl disulfide were added at −78 °C to furnish a new series of quinazolinone-based ligands. This concise one-pot synthesis allows efficient access to a new class of P–S and P–P chelate atropisomeric ligands **142**.

An earlier procedure implemented by Virgil and co-workers focused on the synthesis of monodentate atropisomeric ligands for asymmetric catalysis. This was based on the reaction of phosphoanilines **143** with *N*-acetyl anthranilic acid **144** and employed benzenesulfonyl chloride as the coupling agent, Scheme 57.[80]

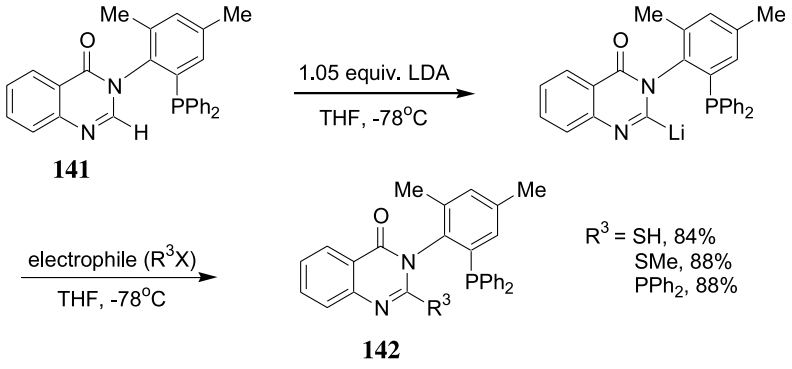

Scheme 56.

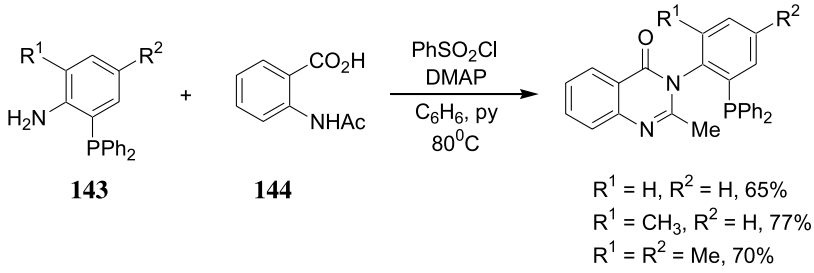

Scheme 57.

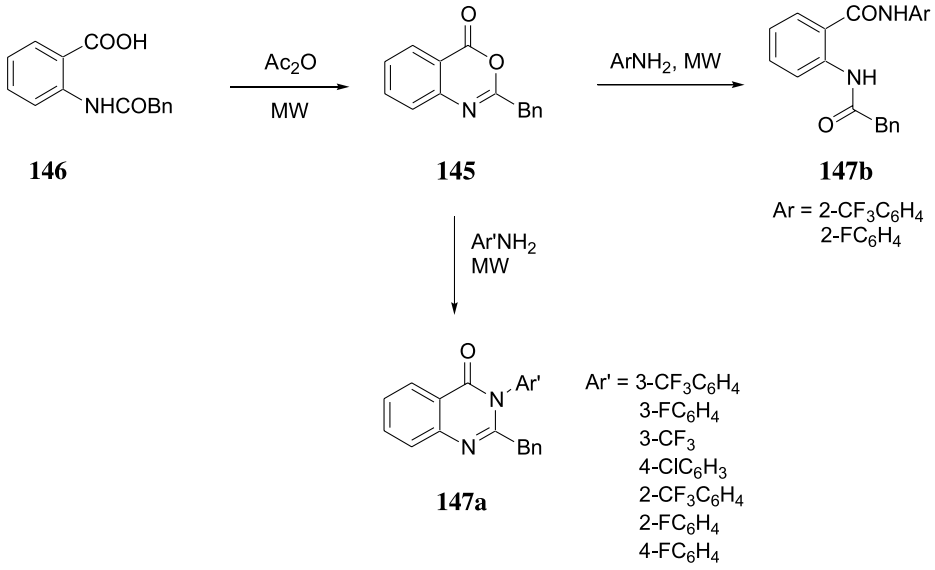

Scheme 58.

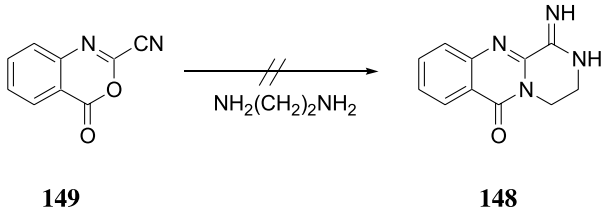

Scheme 59.

Both of these methods allow access to the desired quinazolinones in good yields and the method is amenable to efficient scale up.[81]

Dandia et al. reported the synthesis of fluorinated 2,3-disubstituted quinazoline-4(3*H*)ones **147** under microwave conditions.[82] The intermediate benzoxazin-4-one **145** was synthesised in situ by reacting the anthranilamide derivative **146** with acetic anhydride, Scheme 58. *meta*- and *para*-substituted anilines gave 2,3-disubstituted quinazolinone

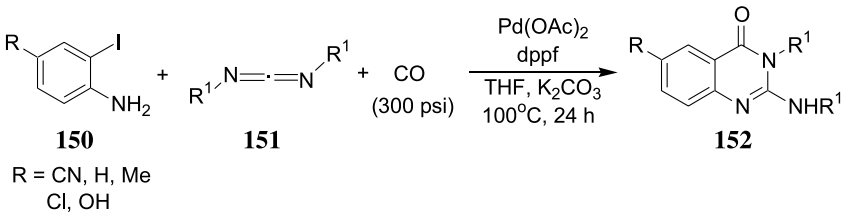

Scheme 60.

Table 18. Synthesis of 2-amino-4(3*H*)-quinazolinones **152** from iodoanilines **150** and carbodiimides **151**

Entry	R	R^1	Isolated yield of **152** (%)[a]
1	H	4-ClC_6H_4	75
2	H	4-BrC_6H_4	73
3	H	Cy	0
4	H	Ph	64
5	H	4-MeC_6H_4	0

[a] Purified by silica gel chromatography.

products **147a** in good yield, whereas *ortho*-substituted anilines produced only **147b**.

Proceeding via a benzoxazine does not, however, guarantee that a 2,3-disubstituted quinazolinone will be obtained. de Fatima Pereira et al. disclosed that efforts to produce **148** via **149** failed, Scheme 59.[83]

In spite of these limitations, it is clear from the numerous examples cited that this is an important intermediate in the synthesis of 2,3-disubstituted quinazolinones and provides access to unusual substitution patterns in the final products.

5.8. Quinazolinone derivatives via palladium-catalysed cyclocarbonylation

Larksarp and Alper developed a palladium acetate/diphenylphosphinoferrocene (dppf) catalyst system for the cyclocarbonylation of *o*-iodoanilines **150** with heterocumulenes **151** to afford the corresponding 4(3*H*)-quinazolinone derivatives **152**, Scheme 60.[84] Carbodiimides and ketenimines were employed in this convenient synthesis and the reactions were conducted at 100 °C for 24 h under carbon monoxide pressure, Table 18.

2-Amino-4(3*H*)-quinazolinones were accessed in moderate to good yields by employing carbodiimide **151** under the conditions described. The reaction was found to tolerate both nitrile and hydroxyl functional groups on the *o*-iodoanilines. Only starting material was, however, recovered when carbodiimides bearing electron-donating substituents were used.

A possible mechanism for the palladium-catalysed cyclocarbonylation reaction of *o*-iodoanilines with carbodiimides is outlined in Scheme 61. The initial reaction of the *o*-iodoanilines **150** with carbodiimides **151** produces a guanidine intermediate **153**, followed by oxidative addition

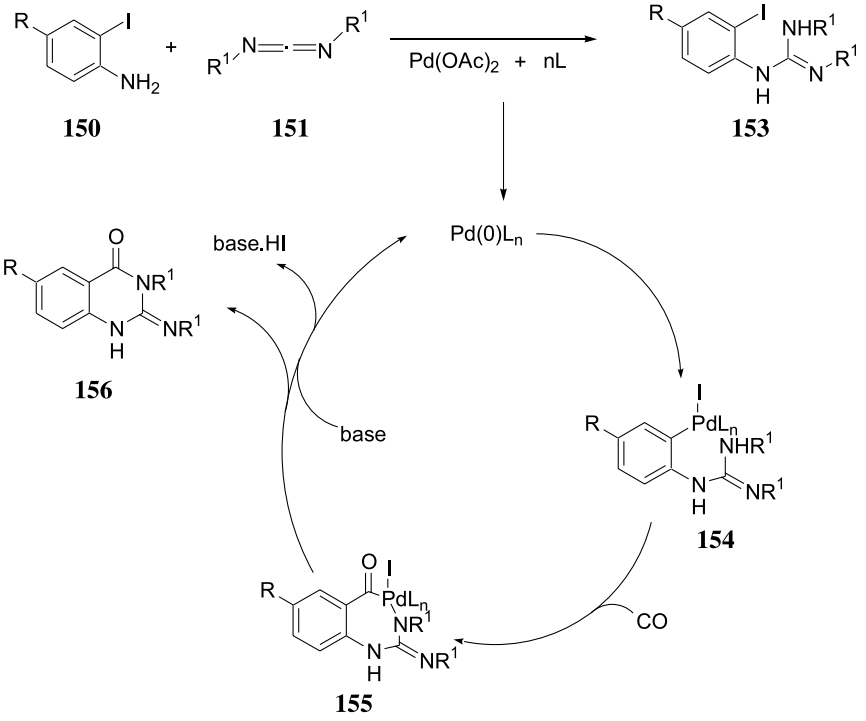

Scheme 61.

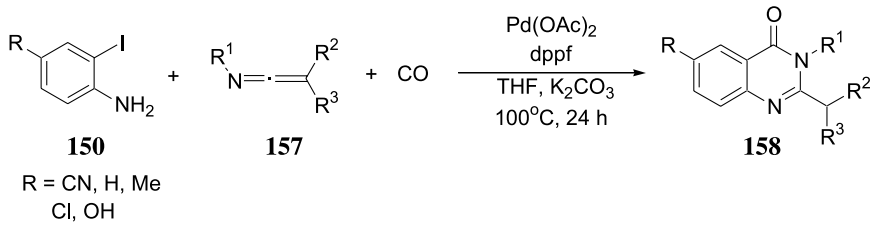

Scheme 62.

Table 19. Syntheis of 2-alkyl-4(3*H*)-quinazolinones **158** from ketenimines **157**

Entry	R	$R^1N{=}C{=}C(R)^2(R)^3$	Isolated yield of **158** (%)[a]
1	H	PhN=C=C(Me)(CO_2Et)	98
2	H	^{n}BuN=C=C(Me)(CO_2Et)	72
3	H	PhN=C=C(Me)(COPh)	95
4	H	PhN=C=C(CO_2Et)$_2$	71
5	Cl	*p*-TolylN=C=C(Ph)$_2$	0

[a] Purified by chromatography.

of the palladium catalyst into the C–I bond to give **154**. There is also the possibility of coordination between the NHR^1 moiety and palladium in the aroylpalladium intermediate **155**, and subsequent reductive elimination would result in the formation of the desired quinazoline derivative. The 4(3*H*)-quinazolinone-2-imine intermediate **156** formed rearranges to give the more stable 2-amino-4(3*H*)-quinazolinone **152**.

A further extension of this methodology used ketenimines **157** rather than carbodiimides in the reaction with *o*-iodoanilines **150** and CO, Scheme 62. An equimolar amount of the ketenimine was employed under a carbon monoxide pressure of 300 psi using $Pd(OAc)_2$ and dppf catalysis to afford the 2-alkyl-4(3*H*)-quinazolinones **158** in good to excellent yields, Table 19.

The success of the reaction was, however, dependent on the substitution pattern of the ketenimine employed and ketenimines substituted with multiple aromatic groups did not react with *o*-iodoaniline.

The mechanism of the reaction proceeds in a similar manner to that described for carbodiimides. It is now possible, however, to form two amidine intermediates from the reaction of *o*-iodoaniline with the ketenimine, Scheme 63.

By a process of oxidative addition and carbonyl insertion, intermediate **159** is formed, Scheme 63. This is followed by subsequent coordination of the amine to palladium with reductive elimination to afford **160**. This intermediate rearranges to give the more stable 2-alkyl-4(3*H*)-quinazolinone **161**. An alternative route to this compound may involve oxidative addition and carbonyl insertion to afford **162** followed by a base-catalysed intramolecular cyclisation.

5.9. Bis(imidoyl)chlorides for quinazoline formation

The reaction of anthranilic acids **163** with oxalic acid-bis(imidoyl)chlorides **164** to prepare quinazolinones **165** was detailed by Langer and Döring.[85] From their studies, moderate to good yields were achieved with reaction times of 3 days at 60 °C, Scheme 64, Table 20.

The functionalised anthranilic acid **163** reacts as a dinucleophile with the bis(imidoyl)chloride **164** to generate a seven-membered ring and cleavage of the corresponding lactone **166** forms the intermediate **167**. An intramolecular prototropic shift followed by nucleophilic attack of the

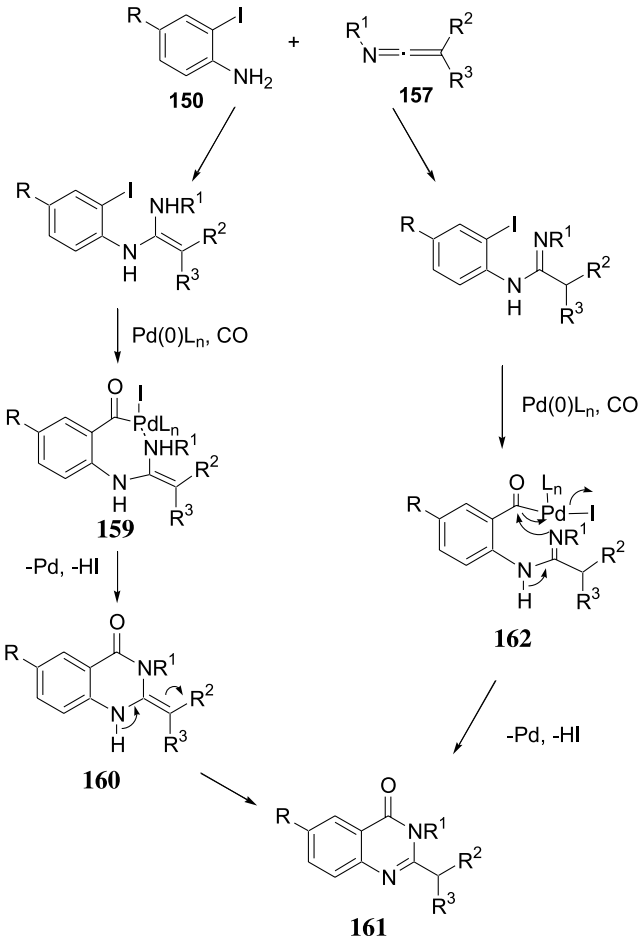

Scheme 63.

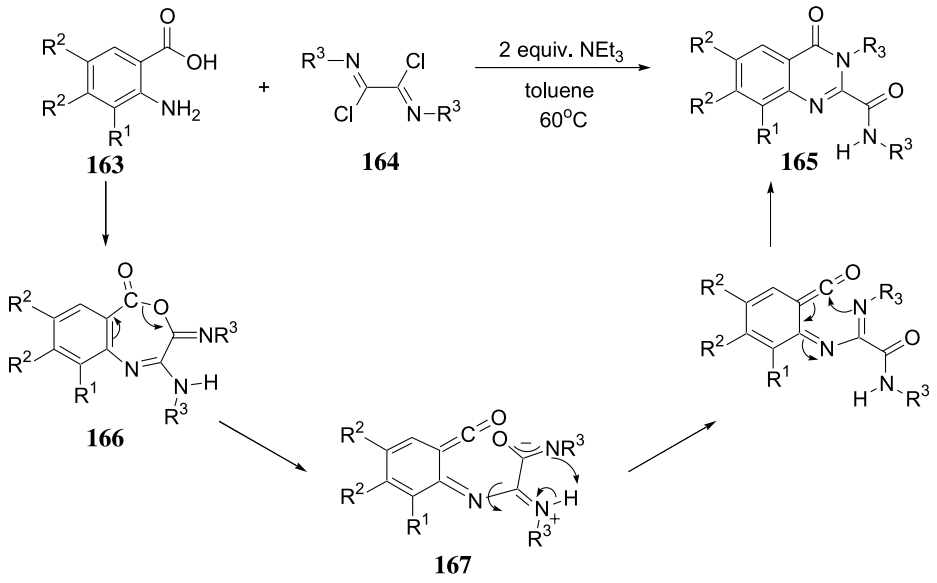

Scheme 64.

Table 20. Reaction of anthranilic acids with bis(imidoyl)chlorides to form quinazolinones **165**

Entry	R^1	R^2	R^3	Yield of **165** (%)
1	H	H	Ph	62
2	H	H	4-(Me)C_6H_4	60
3	Me	H	4-(Me)C_6H_4	45
4	H	OMe	4-(Me)C_6H_4	50
5	Me	H	4-(MeO)C_6H_4	61
6	H	OMe	4-(MeO)C_6H_4	68
7	H	H	4-(Bu^t)C_6H_4	42

amidine nitrogen on the ketene yields the quinazolinone skeleton **165**. Interestingly, the regioselective cyclisation proceeded to give the more thermodynamically stable six-membered ring by reaction of the more nucleophilic amidine nitrogen.

In an effort to improve the chemical yield, an ester derivative of the anthranilic acid **168** was employed. A complex reaction mixture was, however, obtained in the stoichiometric reaction of the anthranilic ester with the bis(phenylimidoyl)chloride **164**. An interesting reaction occurred when 2 equiv of the ester **168** were used, as this

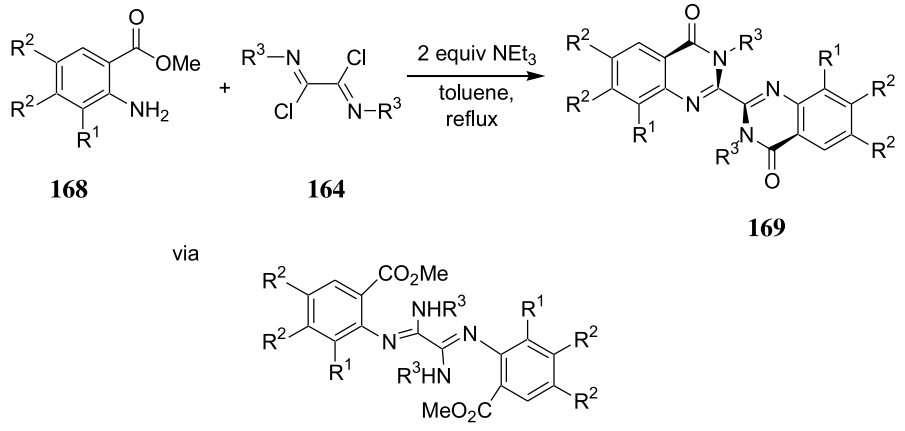

Scheme 65.

Table 21. Reaction of anthranilic acid esters with bis(imidoyl)chlorides to form 2,2′-bis-quinazolin-4-ones **169**

Entry	R^1	R^2	R^3	Yield of **169** (%)
1	H	H	Ph	32
2	H	OMe	Ph	40
3	H	H	4-(Me)C_6H_4	38
4	H	H	4-(MeO)C_6H_4	41
5	Me	H	4-(MeO)C_6H_4	53
6	H	OMe	4-(MeO)C_6H_4	60

resulted in the formation of the 2,2′-bis-quinazolin-4-ones **169** in reasonable yields after extended reaction times in refluxing toluene, Scheme 65, Table 21.

The formation of 2,2′-bis-quinazolin-4-ones **169** was rationalised by the condensation of two molecules of the anthranilic ester with the bis(imidoyl)chloride, with the ensuing two-fold cyclisation by attack of the amidine nitrogen atoms on the ester groups. Due to steric interaction between the R^3 aryl groups and the quinazolin-4-one rings,

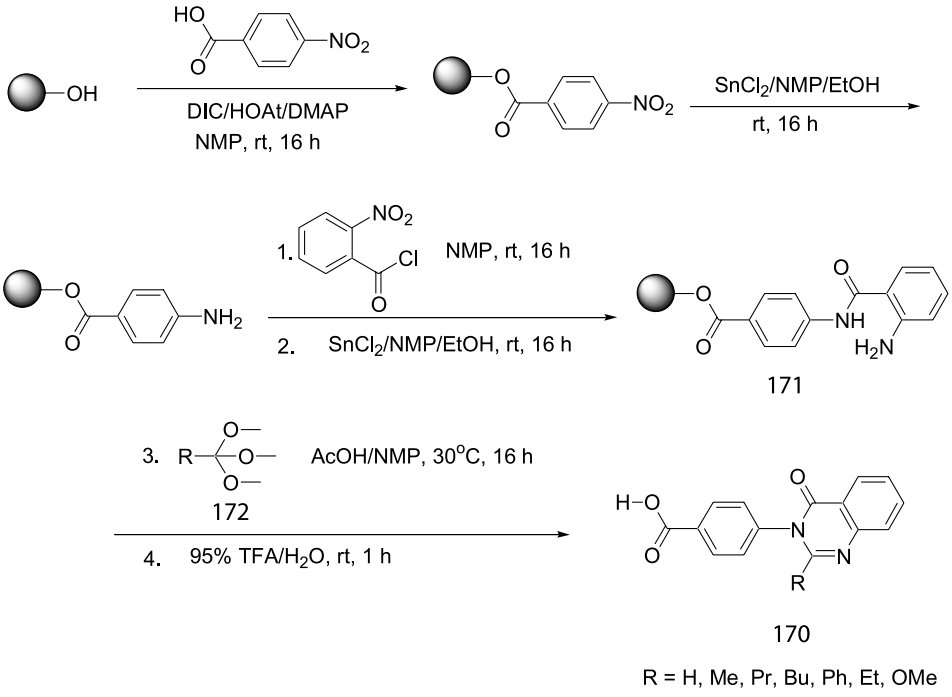

Scheme 66.

the rotation around the central carbon–carbon bond is severely restricted.

This procedure represents an efficient synthesis of the biologically relevant quinazolin-4-ones and also enables a new type of dimeric *N*-heterocyclic system to be prepared.

5.10. Reaction of polymer-bound anthranilamides with orthoformates

Makino et al. synthesised a series of quinazolinones **170** by cyclocondensation of anthranilamides **171** on solid supports with a variety of orthoformates **172**, Scheme 66.[86] The reactions proceeded smoothly under mildly acidic conditions and the products obtained exhibited excellent purity.

In this procedure, implemented by Makino, a surface-grafted polymer, Synphase™ Lanterns, with a long-chain hydroxymethyl phenoxy linker was employed. Since the reaction with carboxylic acids did not proceed smoothly on the solid phase, orthoformates were applied as carboxylic acid equivalents in the cyclocondensation. The reaction proceeded well with acetic acid and *N*-methyl-pyrrolidone (NMP). This strategy worked for both alkyl and aryl orthoformates with yields of around 70% based on theoretical loading weights of the target molecules. An advantageous feature of this method is that molecules with functional groups such as alkenes can be synthesised without problems under the mildly acidic conditions employed. Although the route is limited by the commercial availability of the orthoformates, it is superior to the solid-phase synthesis reported by Zhang et al.[87]

In Zhang's procedure, reagents with a lower oxidation state than orthoformates were employed. An oxidation step was, however, required and the products obtained were not of high purity, Scheme 67. This method is effective for the preparation of 2-alkyl- and 2-aryl-3-substituted-quinazolinones **173**, but it is not applicable to the synthesis of molecules that are susceptible to oxidation.

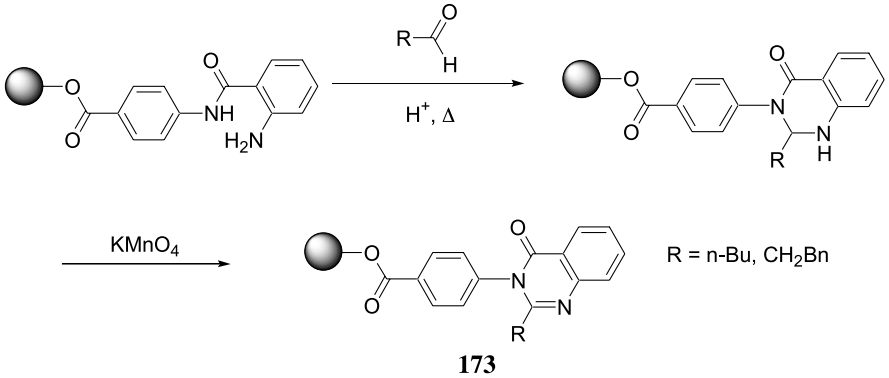

Scheme 67.

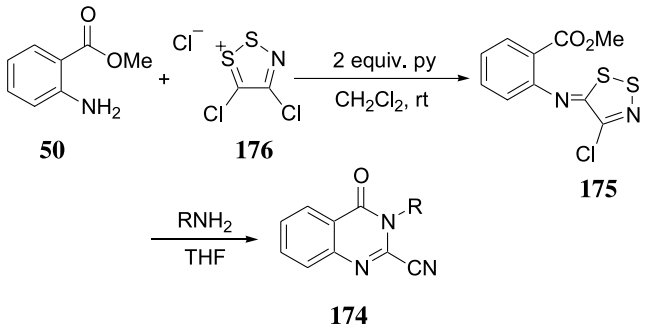

Scheme 68.

Table 22. Preparation of 3-substituted 2-cyano-quinazolinones **174** using Appel's salt

Entry	Amine (R)	Time (h)	Yield of **174** (%)
1	Me	1	73
2	Et	1	81
3	*i*-Pr	4	74
4	*n*-Me$(CH_2)_3CH_2$	1	67
5	Bn	24	63
6	NH_2	2	60

5.11. Preparation of 2,3-disubstituted quinazolinones using Appel's salt

Kim et al. developed a facile synthesis of 3-substituted 2-cyano-4(3*H*)-quinazolinones **174** by the reaction of primary alkylamines with intermediate **175**.[88] The latter was prepared in 50% yield by the reaction of methyl anthranilate **50** with 4,5-dichloro-1,2,3-dithiazolium chloride (Appel's salt) **176** in the presence of pyridine, Scheme 68. The 3-alkyl-2-cyano-4(3*H*)-quinazolinones **174** were furnished in moderate to good yields, Table 22.

The cyano group of the 3-methyl-2-cyano-4(3*H*)quinazolinone **174** (R=Me) can be readily displaced by various nucleophiles to give the corresponding 2-substituted analogues in good to excellent yields. This allows a rapid and efficient synthesis of new quinazoline systems and the results obtained are summarised in Scheme 69.

de Fatima Pereira reported the synthesis of novel 1-imino-2, 3-dihydro-1*H*-pyrazino[2,1,-*b*]quinazoline-5-ones in acceptable yield in a two-step process, Scheme 70.[83] Commencing with a methyl anthranilate **177**, Appel's salt **176** condenses with the amino group. In a second condensation step, 1,2-diaminoethane condenses with **178** to give either **179** or **180**, Table 23.

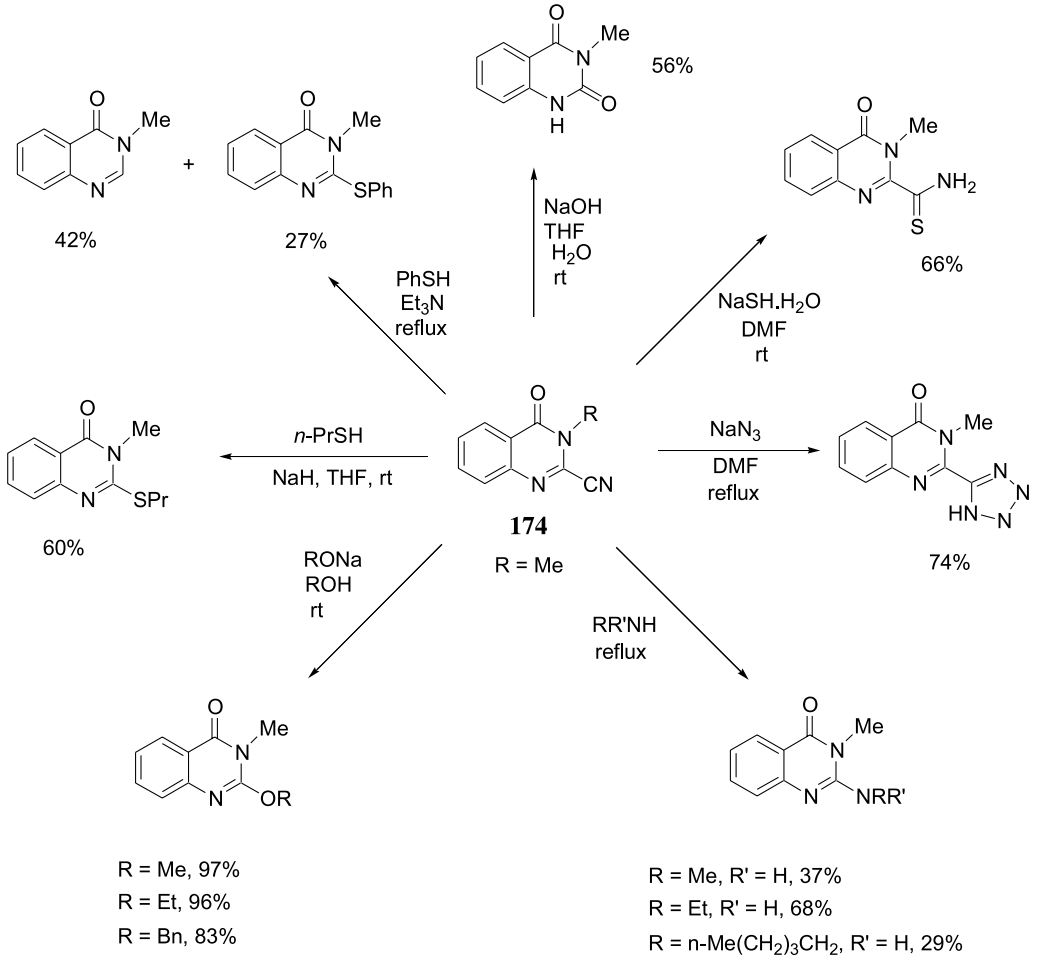

Scheme 69.

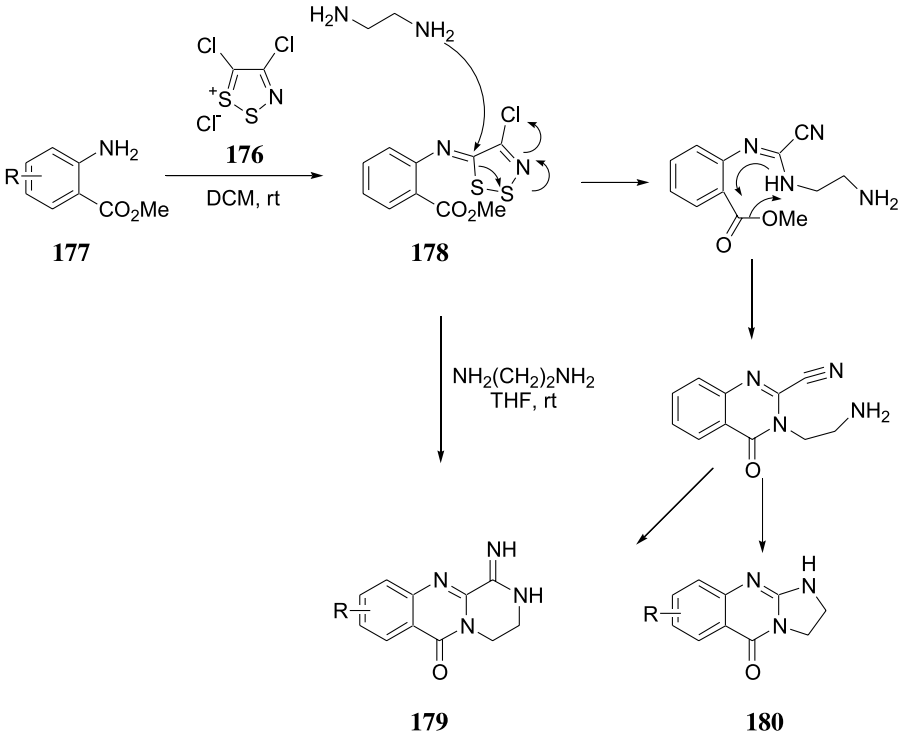

Scheme 70.

Table 23. Synthesis of quinazolines **179** and **180**

177	Diamine (equiv)	Yield of **178** (%)	Yield of **179** (%)	Yield of **180** (%)
R=H	1	98	54	8
R=H	3	—	56	18
R=Br	1	98	74	17
R=Br	3	—	4	28
R=4-Cl	1	71	61	22
R=4-Cl	3	—	8	57
R=4,5-diOMe	1	99	—	—
R=4,5-diOMe	3	—	62	—

5.12. Reaction of resin-bound aldehydes with anthranilamides

In a solid-phase synthesis of quinazolinones by Zhang et al., polymer-supported anthranilamide precursors and aldehydes were combined under acidic conditions to furnish the quinazolinone **181** and 1,2-dihydro-quinazolinone **182** skeletons, Scheme 71.[87] Subsequent dehydrogenation was effected using potassium permanganate. The desired products were obtained in acceptable yields and purities after cleavage with trifluoroacetic acid and additional diversity at the 3-position was possible by employing an amino acid-derivatised polymer support.

An advantage of this approach is that the anthranilamide-derivatised Wang resins **183** could be derived from either nitrobenzoic acids **184** or isatoic anhydrides **185**, allowing a range of aromatic substitution patterns to be accessed, Figure 1.

5.13. Chemoselective lithiation of quinazolinone derivatives

Smith et al. reported the preparation of 3-(acylamino)-2-unsubstituted and 3-amino-2-substituted quinazolinone systems **186** and their subsequent lithiation, Scheme 72.[89]

The required 3-(pivaloylamino)- and 3-(acetylamino)-4(3*H*)-quinazolinones **186a** and **186b** were prepared as outlined in Scheme 72. For example, the former compound was prepared in 85% yield from the reaction of pivaloyl chloride with 3-amino-quinazolinone. Subsequent treatment with alkyllithium reagents promoted nucleophilic attack at the imine bond, giving the corresponding 1,2-addition product **187**, rather than lithiation at the 2-position, Scheme 73, Route A.

The reactions were complete within a 5 min period and very good yields of the addition products were achieved, Table 24, Route A. It was later discovered that chemoselective lithiation at the 2-position of 3-(pivaloylamino)- and 3-(acylamino)-4(3*H*)-quinazolinones **186a** and **186b** was possible using lithium diisopropylamide at low temperature to furnish a range of 2-substituted products **188**, Scheme 73, Table 24, Route B.

This direct lithiation is a facile, practical and regioselective process, enabling the synthesis of a range of derivatives including those that are not easily accessed by other routes. The ease of removal of the acylamino group affords the 3-amino analogues **189** under basic or acidic conditions, Scheme 74.

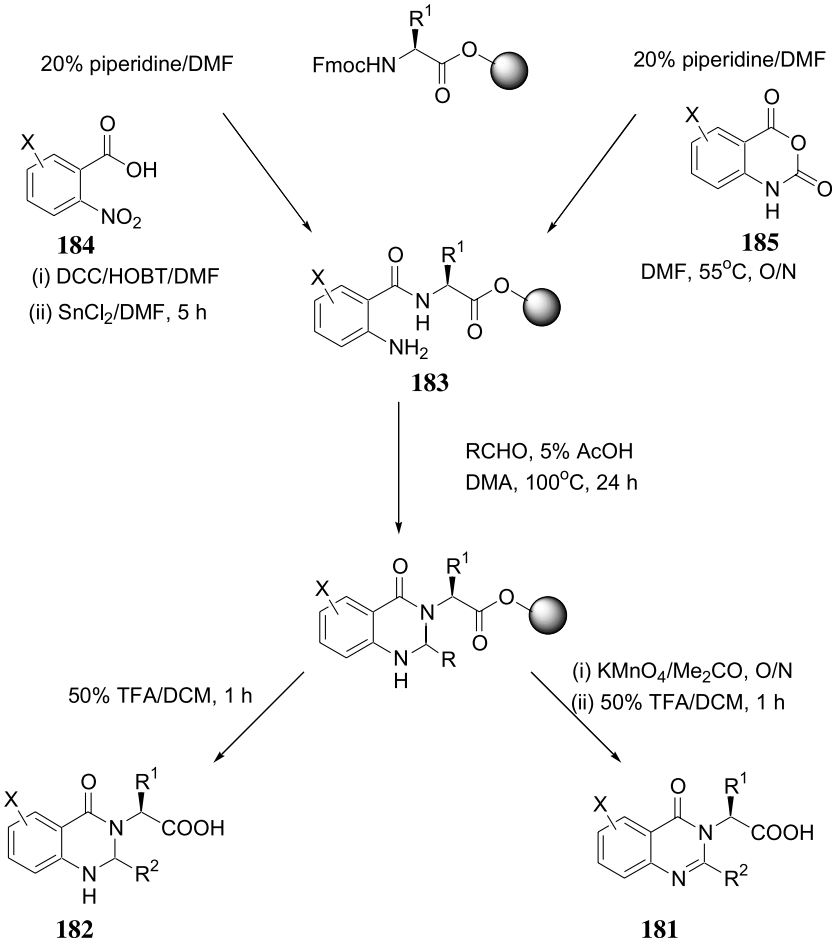

Scheme 71.

A subsequent discovery showed that 3-amino-2-methyl-4(3*H*)-quinazolinones **190** could be lithiated readily using 2.2 equiv of *n*-butyllithium at low temperature in THF and then quenched by a series of electrophiles in high yield.[90] Interestingly, attack by the *n*-BuLi at the carbonyl group or the imine functionality of the quinazolinone ring did not occur, Scheme 75, Route A.

Based on the success observed using alkyllithiums, the methodology was transferred to the 3-amino-2-ethyl-4(3*H*)-quinazolinones **191**, although only low yields of the desired products were obtained. Increased yields were achieved, however, by the use of lithium diisopropylamide at low temperature, Scheme 75, Route B. These simple procedures provide aminoquinazolinone derivatives that were only previously available with difficulty. This new approach obviates the need for protecting groups and allows direct access to quinazolinones bearing the amino functionality.

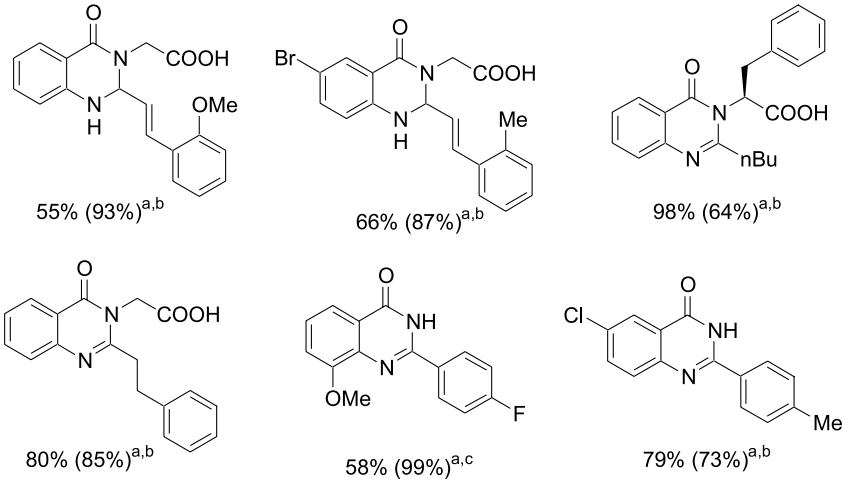

Figure 1. (a) Crude yield (numbers in brackets refer to HPLC purity). (b) Isatoic anhydride route. (c) *o*-Nitrobenzoic acid route.

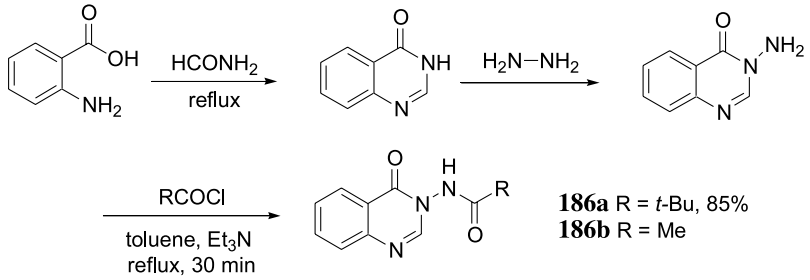

Scheme 72.

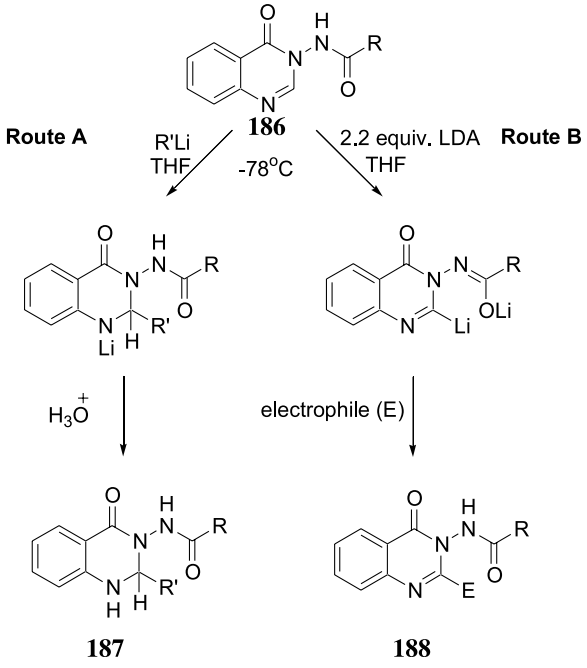

Scheme 73.

Table 24, Route A. Synthesis of quinazolines **187**

Product	R	R′	Yield of **187** (%)
1	*t*-Bu	*n*-Bu	96
2	*t*-Bu	*t*-Bu	98
3	*t*-Bu	Me	90
4	Me	*n*-Bu	82
5	Me	*t*-Bu	84
6	Me	Me	70

Table 24, Route B. Synthesis of quinazolines **188**

Product	R	E	Yield of **188** (%)
1	*t*-Bu	$(Ph)_2C(OH)$	85
2	*t*-Bu	Me	89
3	Me	$(Ph)_2C(OH)$	80
4	Me	D	79
5	Me	PhC(OH)(Me)	80

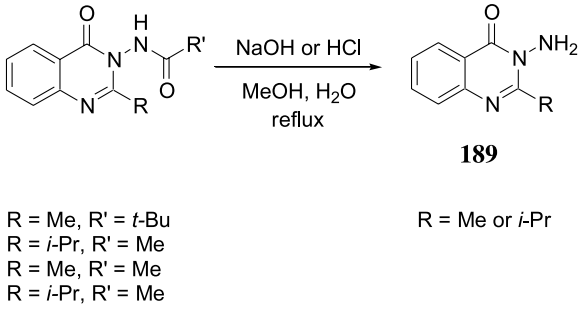

Scheme 74.

5.14. Quinazolinone formation using 1-acetyl-1-methylhydrazine

Peet et al. demonstrated that 2,3-disubstituted-4(3*H*)-quinazolinones such as **192** could be prepared from the cyclisation of 2-amino-benzoic acid *N*-acetyl-*N*-methyl-hydrazide **193** under acidic conditions.[91] The latter compound was obtained from the reaction of *o*-nitrobenzoyl chloride **194** with 1-acetyl-1-methylhydrazine **195** to give the corresponding substitution product **196** in 64% yield, followed by catalytic reduction of the nitro group using 10% Pd/C. This aniline intermediate **193** was also prepared by the use of isatoic anhydride **185** (X=H) and 1-acetyl-1-methylhydrazine **195**, albeit in lower yield, Scheme 76.

A suggested mechanism for the cyclisation of the diacylhydrazine **193** involves the initial transfer of the acetyl moiety to the aromatic amino functionality and the resulting 2-[*o*-(acetylamino)benzoyl]-1-methyl hydrazine **197** then rearranges and dehydrates to form 2-methyl-3-(methylamino)-4(3*H*)-quinazolinone **192**, Scheme 77.

The cyclisation furnished the desired product in a respectable 78% yield and this procedure represents a simple and efficient synthesis of 2,3-disubstituted quinazolinones.

5.15. Approaches to luotonins and rutaecarpine

Luotonins A–F **198**–**203** were isolated from the aerial parts of *Peganum nigellastrum*, a plant that has traditionally been used in Chinese medicine, Scheme 78.[92] Due to its potent biological activity, luotonin A **198**, (which has an IC_{50} value of 1.8 μg/ml against murine leukaemia P-388) has been the target of numerous syntheses.

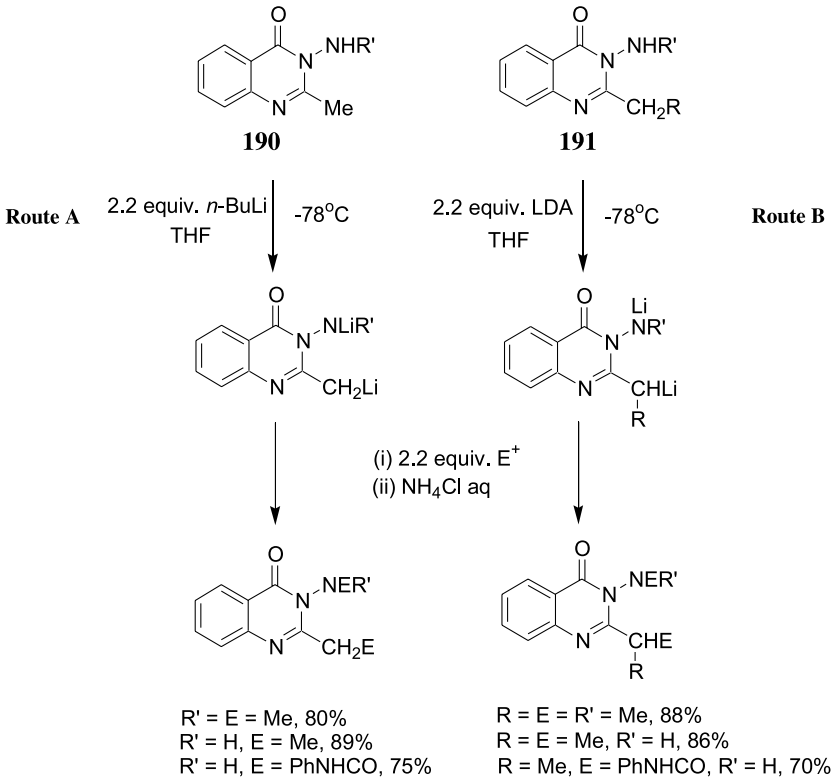

Scheme 75.

A number of naturally occurring 2,3-disubstituted quinazolinones exist that possess a high biological activity. Among these, vasicinone (vide supra, Section 5.2), luotonins **198**–**203** and rutaecarpine **204** have received much attention from the synthetic community. Indeed, synthetic approaches to some of these molecules published before 2003 have been reviewed recently by Bergman.[93] In this section, we will survey the routes to these important alkaloids, which have been published subsequently.

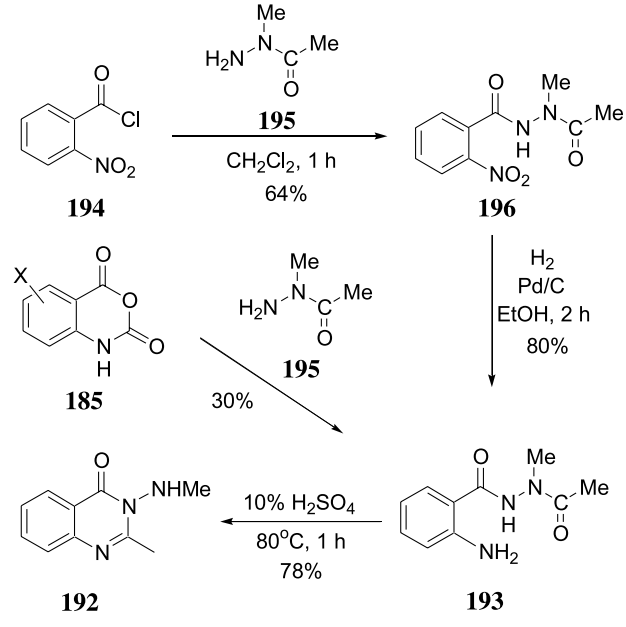

Scheme 76.

Harayma et al. have reported a simple convergent synthesis of luotonin A.[94] Rings A, B, D and E are present in the starting materials. The route commences with the alkylation of **205** by **206** under basic conditions to give **207**, Scheme 79. Completion of the synthesis is achieved by intramolecular palladium-assisted coupling to generate ring C.

This process was optimised by using tricyclohexylphosphine and potassium acetate, furnishing luotonin A in 86% yield. Even in the absence of the phosphine ligand, the reaction proceeded in 61% yield.

This synthetic methodology was extended to synthesise rutaecarpine **204** from **208**, Scheme 80.

Mhaske and Argade have published a general high-yielding route to luotonins A, B and F with the key step being a regioselective lithiation, which allows the construction of the C ring in these compounds.[95] LDA, *s*-BuLi, *t*-BuLi and *n*-BuLi were tested in the presence and absence of TMEDA over a temperature range from 0 to −78 °C. The reactivity of mesityllithium at −20 °C with **209**, however, produced **210**. Dilithiated species **210** could be further elaborated to give **211**, an important intermediate in the synthesis of luotonin A **198**, Scheme 81. Similarly **210** could be reacted with DMF to furnish aldehyde **212**, a common precursor to both luotonin B **199** and luotonin E **200**.

This is a high-yielding route and could be potentially useful for the generation of analogues, as well as a range of other natural and synthetic polycyclic compounds.

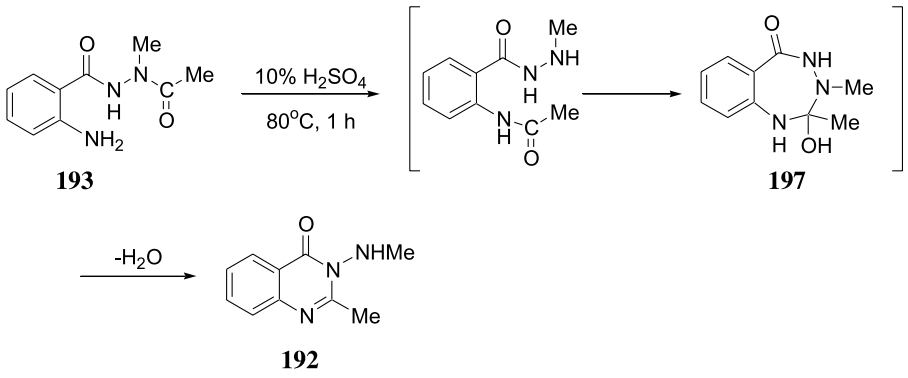

Scheme 77.

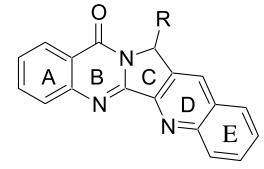

luotonin A **198** R = H
luotonin B **199** R = OH
luotonin E **200** R = OMe

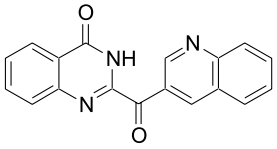

luotonin F **201**

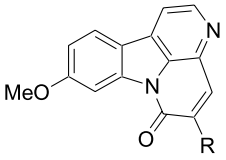

luotonin C **202** R = Me
luotonin D **203** R = Et

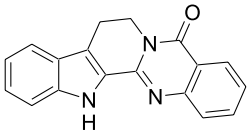

rutaecarpine **204**

Scheme 78.

Lee et al. reported the condensation of **213** based on the observation that *N*-arylbenzimino chlorides condense with anthranilic acid.[96] In this case, pretreatment with gaseous or concentrated hydrochloric acid improves the yield of the reaction. In terms of strategy, this route follows Ganesan's synthesis of luotonin A **198**, with **213** being the key intermediate used to construct rings D and E, Scheme 82.[97]

Using this simple procedure, it was also possible to synthesise, among other molecules, the antibiotic, trypanthrine **214**, via ozonolysis of the olefin **215**, which was prepared from substrate **216**, Scheme 83. A similar process was employed for the synthesis of rutaecarpine **204**, Table 25.

The Povarov reaction is an important method for the construction of tetrahydroquinolines in a multicomponent fashion, Scheme 84.[98] It may be viewed as either a concerted Hetero-Diels–Alder reaction or a stepwise Mannich process. This reaction may be carried out in either protic or Lewis acidic conditions. Oxidation of the tetrahydroquinoline ring furnishes a quinoline. Both intra- and intermolecular Povarov cyclisations have been used to synthesise luotonin A.

Twin and Batey have disclosed a convenient route to luotonin A by use of an intramolecular Povarov reaction.[99]

In a method developed by Mazurkiewicz, propargylamine was added to **217** to afford **218**, which is subsequently converted into its amide derivative **219**, Scheme 85.[100] Intermediate **219** undergoes cyclisation–dehydration in the presence of Hünig's base, triphenylphosphine and iodine to form **220** in excellent yield. Compound **220** then rearranges on treatment with piperidine and silica gel to produce the advanced intermediate **221**.

Hydrolysis of **221**, followed by Dess-Martin periodinane-mediated oxidation to aldehyde **222**, Scheme 85, allows for the formation of imine **223**, Scheme 86, which then

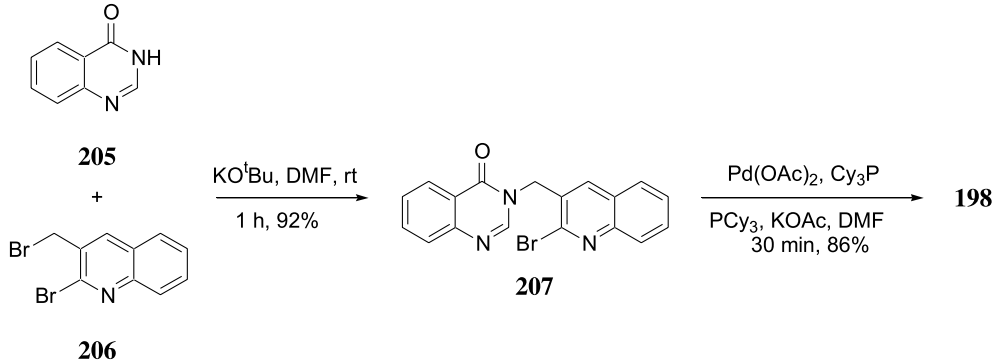

Scheme 79.

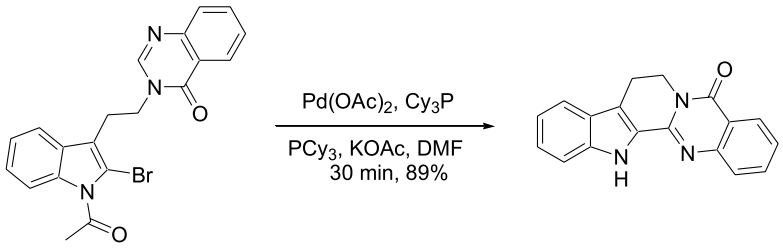

208 204

Scheme 80.

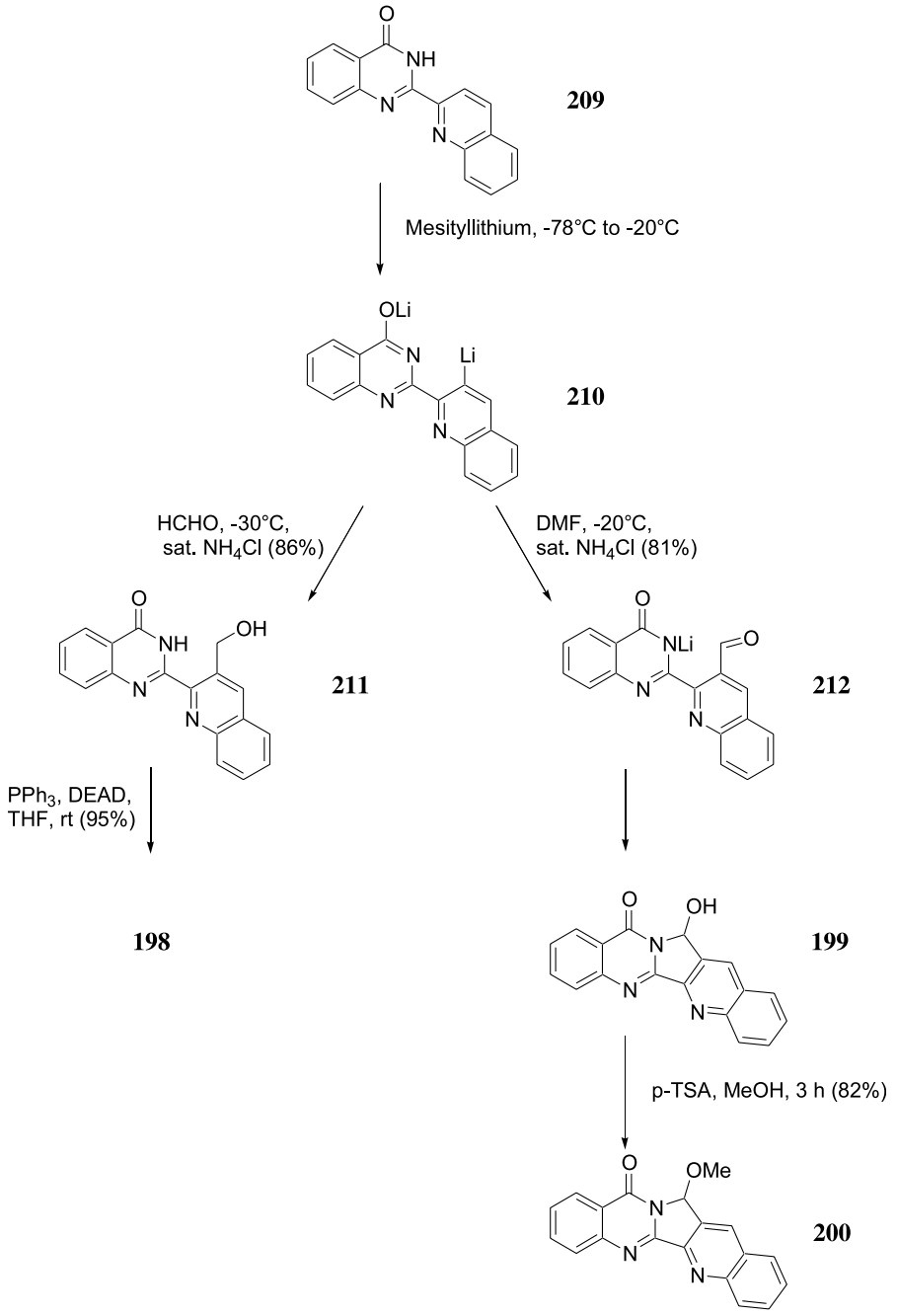

Scheme 81.

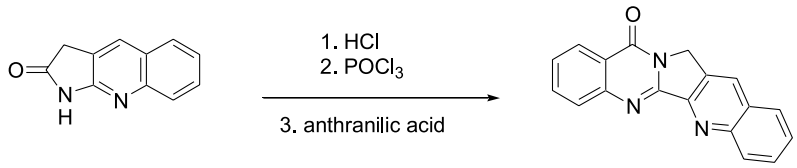

213 198

Scheme 82.

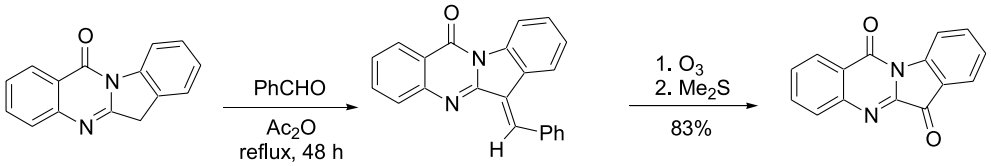

216 215 214

Scheme 83.

Table 25. Synthesis of 2,3-polymethylene-4(3*H*)-quinazolinones and related alkaloids

Entry	Substrate	Product[a]	Yield (%)[b]
1		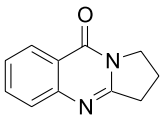	88
2		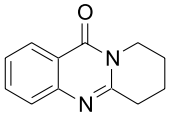	92
3	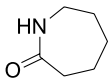	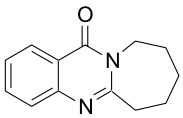	95
4	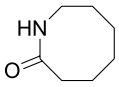	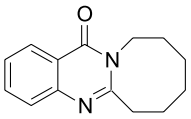	90
5	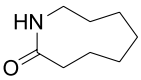	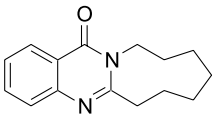	85
6	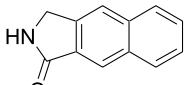	**198**	88
7	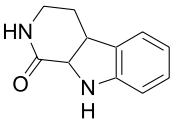	**204**	92

[a] Spectral data of the products match previously reported data.
[b] Isolated, but unoptimised yield.

undergoes Povarov cyclisation in an inverse-electron-demand Hetero-Diels–Alder reaction and is subsequently oxidised to yield luotonin A.

As in the previous examples outlined in this section, the mild conditions used make this a suitable synthetic method for the synthesis of analogues for QSAR studies.

Osborne and Stevenson reported an intermolecular Povarov cyclisation to achieve the formal total synthesis of luotonin A.[101] *N*-Acetyl-2-azetine **224**, a compound readily available in gram quantities from cheap starting materials, was reacted with **225** in the presence of a Lewis acid catalyst to afford quinoline **226** in 78% yield following the addition of HCl to an acetonitrile solution, Scheme 87. Subsequent treatment of **226** with sodium ethoxide in ethanol gave rise to the lactam **213**, which, as mentioned previously, can be converted into luotonin A using 2-sulfinylaminobenzoyl chloride.[97]

Chavan and Sivappa published an efficient route to the related alkaloid rutaecarpine **204**, Scheme 88.[102] Generation of the indole is achieved by use of the Fischer indole synthesis, as previously disclosed by Kokosi et al.[103] The synthesis of *N*-aryl hydrazone **227**, an important intermediate in the synthesis of rutaecarpine, was obtained by employing a Dieckmann cyclisation of ester **228**. This route allowed easier access to **229** and, hence, rutaecarpine **204**.

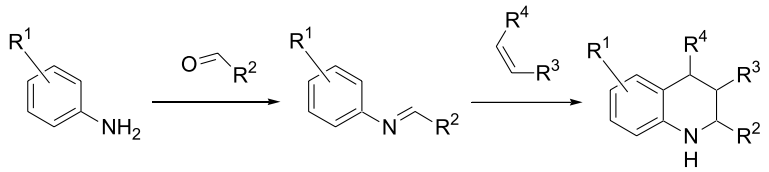

Scheme 84.

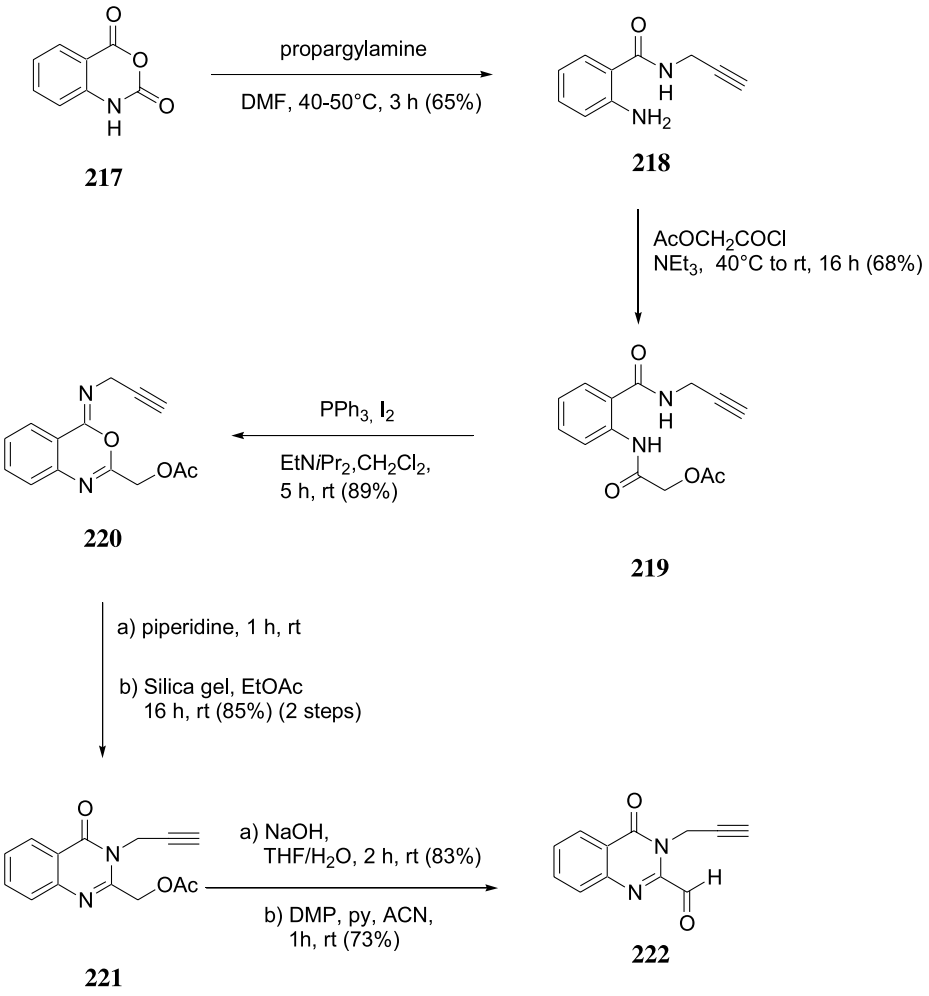

Scheme 85.

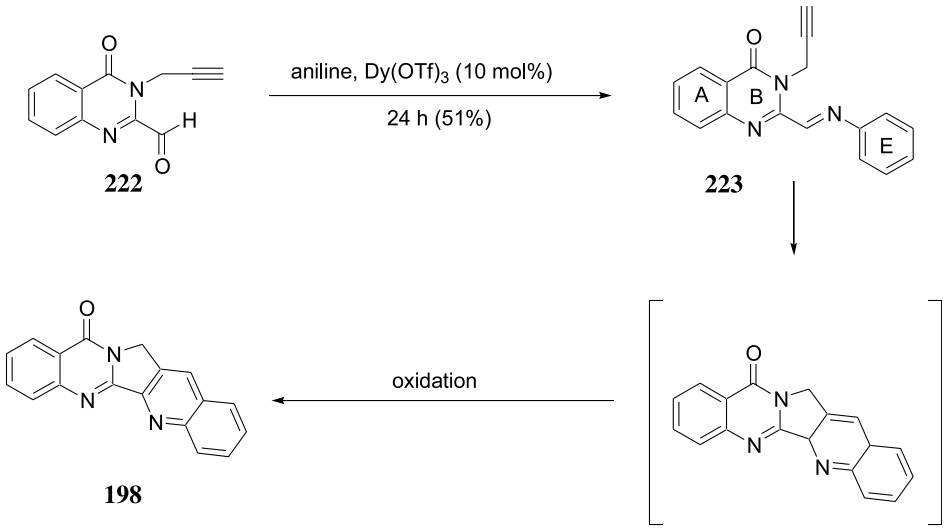

Scheme 86.

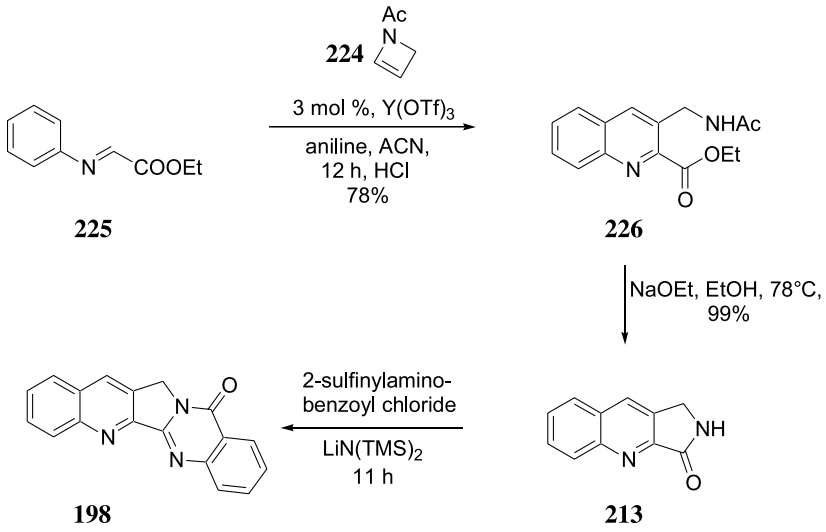

Scheme 87.

6. 2,4-Disubstituted-4(3*H*)-quinazolinones and -quinazolines

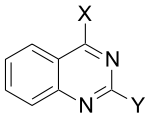

6.1. Polymer-supported synthesis of 2,4-diaminoquinazolines

The solid-phase synthesis reported by Wilson enabled the preparation of 2,4-diaminoquinazolines **229** in good yields and purities.[104] This was accomplished using an acyl isothiocyanate resin **230** with functionalised 2-aminobenzonitriles **231** and amines **232** as the key building blocks in the synthesis, Scheme 89.

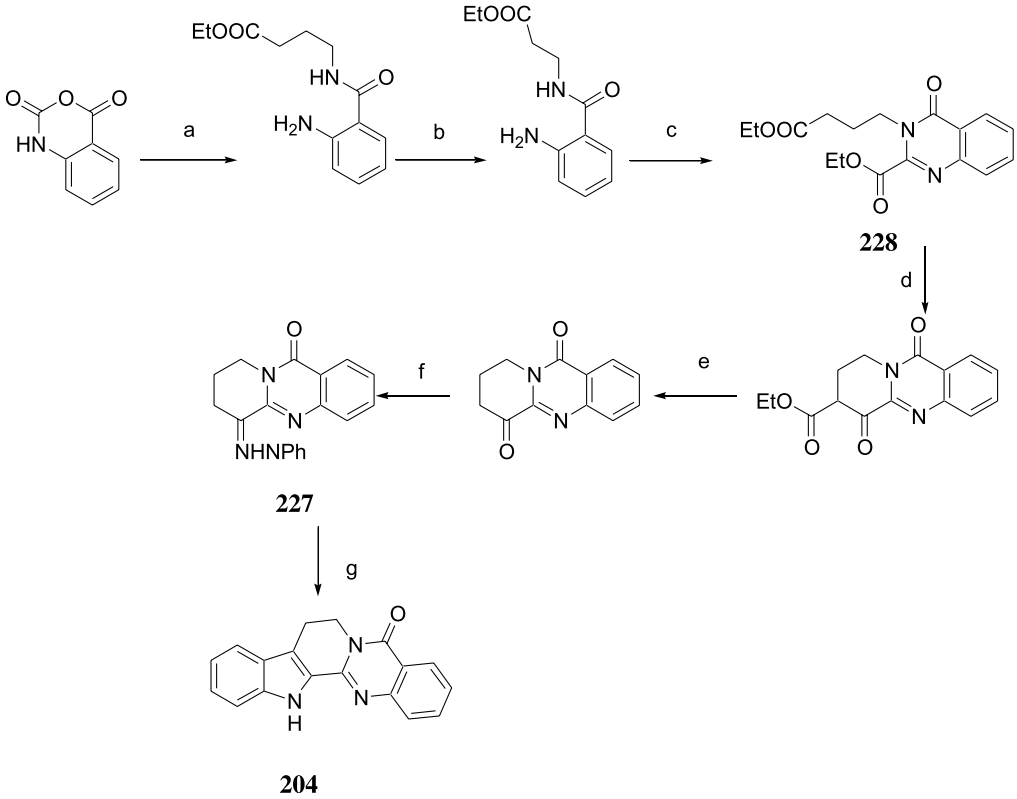

Scheme 88. (a) Ethyl γ-aminobutyrate. HCl, DMF, NEt_3, DMAP (cat.), 96%; (b) Ethyl oxalyl chloride, DCM, k_2CO_3, 98%; (c) PCl_3, xylene, reflux, 2 h, 80%; (d) NaH, DMF, 80%, 6 N HCl, reflux, 81%; (e) $PhNHNH_2$; (f) PPA, 180 °C.

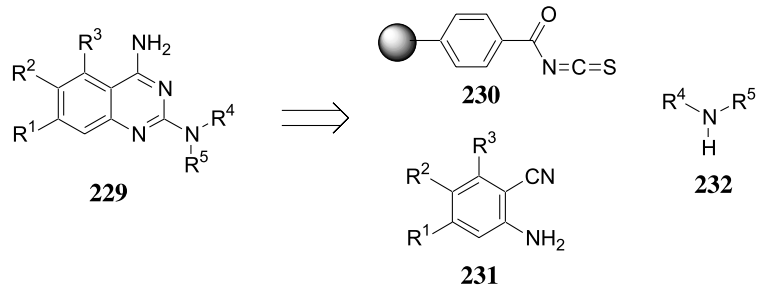

Scheme 89.

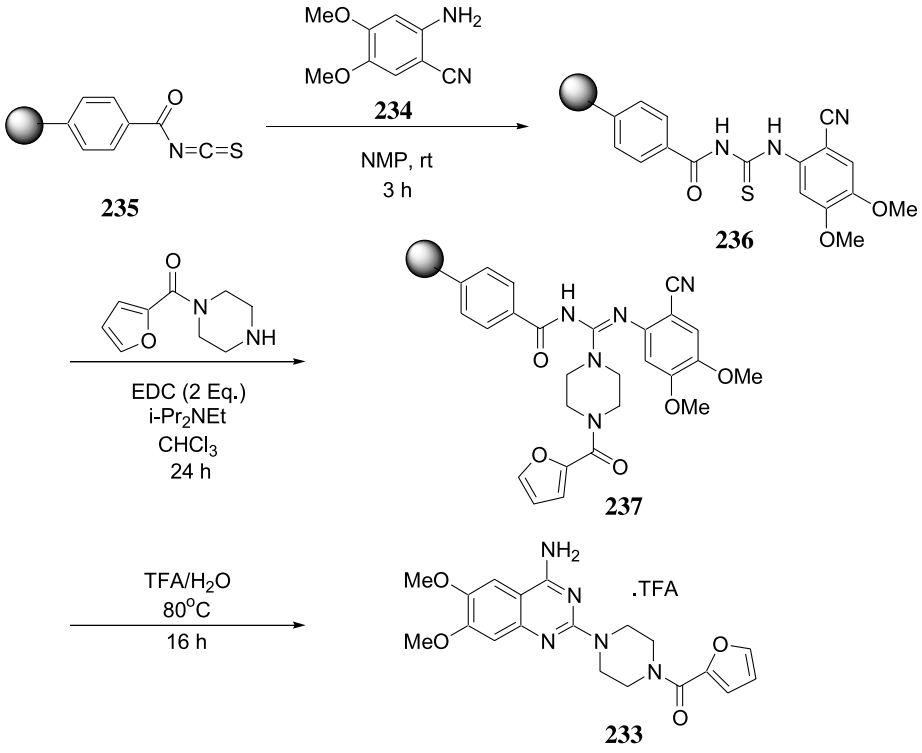

Scheme 90.

This approach enabled the synthesis of the α-1 antagonist prazosin **233** in good yield and purity, Scheme 90. Using prazosin **233** as an example, the reaction of 2-amino-4,5-dimethoxybenzonitrile **234** dissolved in *N*-methylpyrrolidinone with the acyl isothiocyanate resin **235** produced the intermediate **236**. This was followed by the addition of the appropriate amine, in this case, 1-(2-furoyl)-piperazine, in the presence of EDC to furnish the resin-bound guanidine **237**. The optimal ring-closure and cleavage conditions employed trifluoroacetic acid and water at 80 °C to afford prazosin **233** in 70% yield.

The scope and generality of this method were later harnessed to synthesise a range of other analogues, Table 26.

A variety of 2-aminobenzonitriles were tolerated, allowing alkyl, alkoxy and halogen groups to be incorporated into the quinazoline structure. In addition, a series of secondary amines were successfully employed. In the case of the primary amine, *t*-BuNH$_2$ (entry 7), the *tert*-butyl group was not present in the quinazoline product and was probably lost during the resin cleavage. Surprisingly, in comparison with the ammonia example (entry 6), *t*-BuNH$_2$ provided the 2,4-diaminoquinazoline of higher yield and purity.

This traceless linker approach has enabled access to a small library of 2,4-disubstituted quinazolines, which exhibit a wide range of pharmacology.[105,106] This new method provides a useful alternative to the widely employed procedure involving the sequential chlorine displacement from 2,4-dichloroquinazoline (Section 6.8).

6.2. Reaction of 2-amino-*N*-arylbenzamides with benzaldehydes

As discussed in Section 4.2, Szczepankiewicz et al.[57,58] modified their procedure so that the 2-amino-*N*-arylbenzamides **238** employed could be reacted with benzaldehyde or its ring-substituted derivatives to afford the 2-aryl-4-arylimino-(1*H*)-2,3-dihydroquinazolines **239**, Scheme 91.

Table 26. Polymer-supported synthesis of 2,4-diaminoquinazolines

Entry	Product	Yield (%)	Purity (%)
	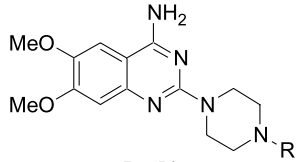		
1	R=Ph	74	89
2	R=Me	74	93
	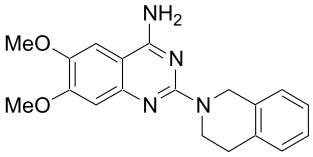		
3		45	92
	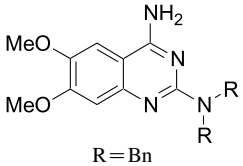		
4	R=Bn	65	91
5	R=Me	38	89
6	R=H (from NH_3)	24	74
7	R=H (from *t*-BuNH_2)	76	98
	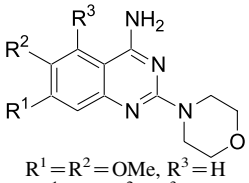		
8	$R^1=R^2=$OMe, $R^3=$H	55	94
9	$R^1=$Cl, $R^2=R^3=$H	47	94

Treatment of these dihydroquinazoline derivatives **239** with potassium permanganate afforded the corresponding aromatic quinazolines **240** in reasonable yield. For example, 2-(2-phenyl)- and 2-(2-methylethyl)-4-phenylaminoquinazoline were prepared in 62 and 53% yields, respectively.

This methodology was extended to synthesise 4-arylquinazolines **241a–o** with a secondary amino function at the 2-position by reacting guanidines **242** and benzaldehydes **243**, Scheme 92, Table 27.

6.3. Baeyer–Villiger oxidation of 3-arylimino-2-indolinones

The rearrangement of 4-imino-(1*H*,4*H*)-3,1-benzoxazin-2-ones to 2,4-quinazolinediones via an isocyanate carboxamide intermediate was reported by Azizian et al.[107] This procedure involves the reaction of 3-arylimino-2-indolinones **244** with *m*-chloroperbenzoic acid at 0 °C to afford the corresponding benzoxazinone intermediate **245**, Scheme 93. The expected 3-aryl-2,4(1*H*,3*H*)-quinazolinediones **246** were formed, along with related carbamate derivatives **247**, which could be converted into the quinazolinediones **246** by refluxing in methanol.

A possible mechanism may involve rearrangement of the Baeyer–Villiger oxidation product to an isocyanate carboxamide intermediate **248**, which can cyclise spontaneously to give the required product **246**. Alternatively, methanol could attack the isocyanate to generate the carbamate derivative **247**. The generality of this one-pot procedure has enabled the synthesis of a range of quinazolinediones under mild conditions in high yields, Table 28.

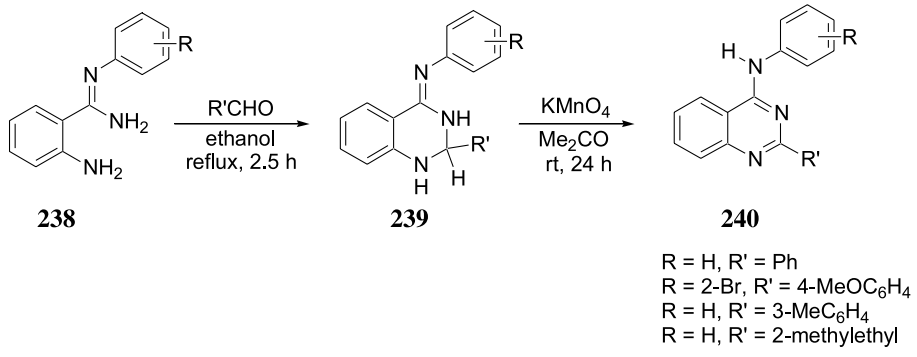

Scheme 91.

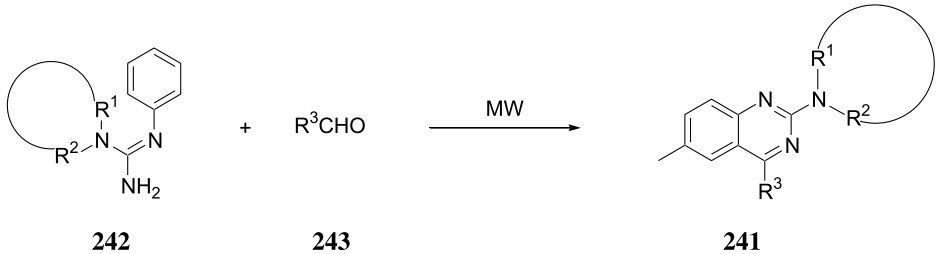

Scheme 92.

Table 27. Reaction of guanidines **242** and benzaldehydes **243** to form **241a–o**

Compound	R^1–R^2	R^3	Yield (%)
241a	$(CH_2)_2$–O–$(CH_2)_2$	–Ph	78
241b	$(CH_2)_2$–O–$(CH_2)_2$	*p*-O_2N–C_6H_4	81
241c	$(CH_2)_2$–O–$(CH_2)_2$	*p*-MeO–C_6H_4	83
241d	$(CH_2)_2$–O–$(CH_2)_2$	*p*-$(Me)_2N$–C_6H_4	72
241e	$(CH_2)_2$–O–$(CH_2)_2$	*p*-Cl–C_6H_4	78
241f	–$(CH_2)_4$–	–Ph	80
241g	–$(CH_2)_4$–	*p*-O_2N–C_6H_4	83
241h	–$(CH_2)_4$–	*p*-MeO–C_6H_4	84
241i	–$(CH_2)_4$–	*p*-$(Me)_2N$–C_6H_4	74
241j	–$(CH_2)_4$–	*p*-Cl–C_6H_4	77
241k	–$(CH_2)_5$–	–Ph	80
241l	–$(CH_2)_5$–	*p*-O_2N–C_6H_4	84
241m	–$(CH_2)_5$–	*p*-MeO–C_6H_4	78
241n	–$(CH_2)_5$–	*p*-$(Me)_2N$–C_6H_4	73
241o	–$(CH_2)_5$–	*p*-Cl–C_6H_4	78

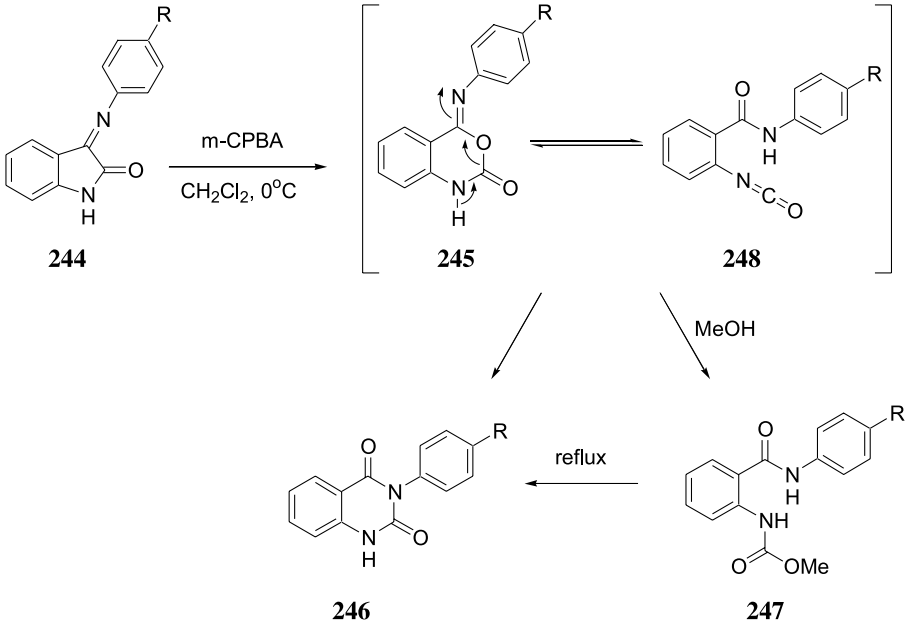

Scheme 93.

Table 28. Synthesis of quinazolinediones **246** via Baeyer–Villiger oxidation of 3-arylimino-2-indolinones

Entry	R	Yield of **246** (%)[a]
1	H	80
2	Me	93
3	Cl	82
4	Br	83

[a] All products recrystallised from methanol.

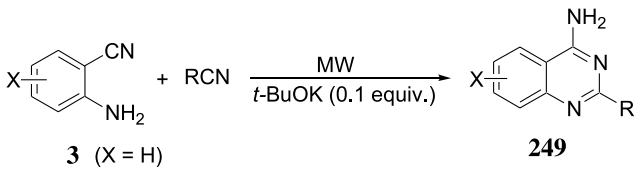

Scheme 94.

6.4. 2-Substituted-4-aminoquinazolines by microwave irradiation

Seijas et al. reported a microwave-promoted synthesis of 4-aminoquinazolines **249** by reacting cyanoaromatic compounds with anthranilonitrile **3** (X=H) in a domestic microwave oven, Scheme 94.[108] As an example, anthranilonitrile, 2-thiophenenitrile and potassium *tert*-butoxide were added to a test tube and heated for 1 min to afford 4-amino-2-(2-thiophenyl)-quinazoline in 90% yield, Table 29. It was found that this method was superior to the traditional methods of synthesis for this class of compound. As a comparison, 4-amino-2-benzylquinazoline was prepared in 73% yield after 3 min by microwave irradiation, whereas the same compound was obtained in only 40% yield after refluxing for 48 h in isopropanol.

A dramatic reduction in reaction time, the absence of solvents and the use of only a catalytic amount of base are appealing features of this approach.

Table 29. Synthesis of 2-substituted-4-aminoquinazolines **249** by microwave irradiation

Entry	2-Substituent (R)	Time (min)	Yield of **249** (%)[a]
1	2-$NH_2C_6H_4$	1	82
2	Ph	2	93
3	4-$MeOC_6H_4$	1	76
4	3-CNC_6H_4	2	85
5	2-Thiophenyl	1.5	90
6	2-Furanyl	1.5	84
7	4-Pyridyl	2	91
8	3-Pyridyl	0.5	79
9	2-Pyridyl	1.5	85
10	Bn	3	73

[a] All yields are from products purified by crystallisation.

of DBU under mild conditions was developed by Mizuno et al.[109] Carbon dioxide reacts with 2-aminobenzonitriles **234** in the presence of the suitable base to generate the carbamate salts **251**. This is followed by nucleophilic cyclisation with attack of the carbamate oxygen on the nitrile functionality. A rearrangement then occurs to afford the intermediate **252**, which is protonated to yield the desired 2,4-dihydroxyquinazoline **250**, Scheme 95.

This experimentally convenient procedure can be used to prepare the unsubstituted 2,4-dihydroxyquinazoline in high yield and purity. Excellent yields (90–97%) were also obtained in the presence of both methoxy- and nitro-substituted 2-aminobenzonitriles.

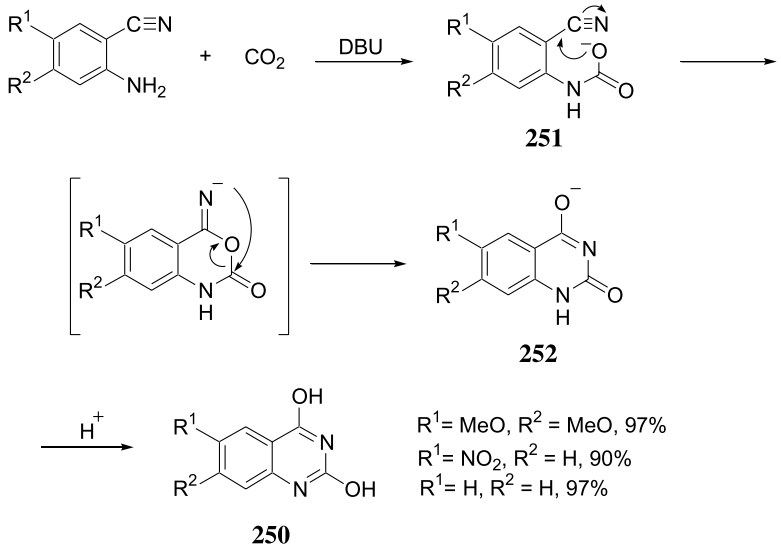

Scheme 95.

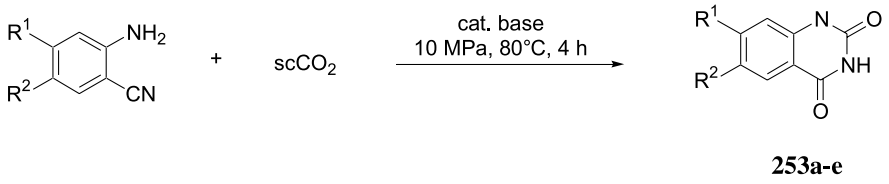

Scheme 96.

6.5. Synthesis of 2,4-dihydroxyquinazolines

The synthesis of 2,4-dihydroxyquinazolines **250** using 2-aminobenzonitriles and carbon dioxide in the presence

Table 30. Synthesis of 2,4-dihydroxyquinazolines **253a–e** in $scCO_2$

Product	R^1	R^2	Base	Yield (%)
253a	H	H	DBU (0.1 equiv)	91
253a	H	H	Et_3N (0.1 equiv)	70
253b	OMe	OMe	DBU (0.1 equiv)	97
253c	H	Cl	DBU (0.1 equiv)	54
253c	H	Cl	DBU (0.2 equiv)	96
253c	H	Cl	NEt_3	86
253d	Cl	H	DBU (0.1 equiv)	64
253d	Cl	H	DBU (0.2 equiv)	67
253e	H	NO_2	DBU (0.1 equiv)	0
253e	H	NO_2	DBU (0.5 equiv)	20

The same group has recently reported the use of supercritical carbon dioxide ($scCO_2$) instead of DMF and DMSO to carry out this type of transformation on an extended range of substituted 2-aminobenzonitriles **253a–e**, Scheme 96, Table 30.[110] Good to excellent yields were obtained and the use of supercritical carbon dioxide as solvent obviates the need for toxic organic solvents.

6.6. Quinazoline formation by thermal ring contraction

Sashida et al. studied the thermolysis of 5-methoxy- and 5-diethylamino-(3*H*)-1,4-benzodiazepines to give 4-methoxy- and 4-diethylaminoquinazolines by a ring contraction mechanism, Scheme 97.[111]

On heating the 5-methoxy-(3*H*)-1,4-benzodiazepines **254** in diphenyl ether at 160–170 °C for 6 h, the

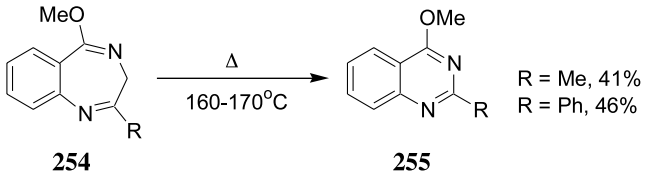

Scheme 97.

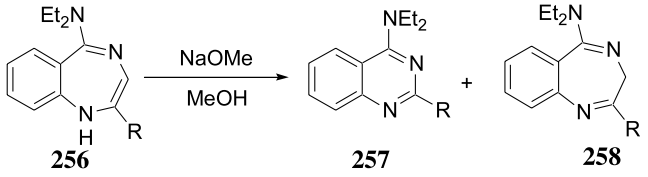

	257	258
R = Me	34%	-
R = Ph	29%	28%

Scheme 98.

4-methoxyquinazolines **255** were furnished as the sole products in moderate yields (41–46%). Similarly, 5-diethylamino-(3*H*)-1,4-benzodiazepines **256** were treated with sodium methoxide at room temperature to give the corresponding 4-diethylaminoquinazolines **257** in acceptable yields, Scheme 98.

The behaviour of the 2-phenyl derivative **256** (R=Ph) differed from its 2-methyl analogue **256** (R=Me) as an approximate 1:1 mixture of the benzodiazepine **258** (R=Ph) and the expected quinazoline **257** (R=Ph) was obtained. An increase in the chemical yield to ca. 60% was observed on refluxing the 2-phenyl-benzodiazepine **258** (R=Ph) in xylene or by further treatment with sodium methoxide.

A possible mechanism to account for the products obtained involves a thermal electrocyclisation to produce aziridine-type compounds **259**, Scheme 99. These undergo ring opening to give the corresponding *N*-ylides **260** and subsequent fission of the N–C bond yields the required quinazolines **261**.

6.7. Preparation of fluorine-containing pyridoquinazolines

Okada employed 5,7-bis-(trifluoroacetyl)-8-quinaolylamine **262** as a convenient building block for the synthesis of quinoline-fused quinazolines bearing a trifluoromethyl functionality.[112] The C-2 substituent in each case was derived from the corresponding aldehyde and aqueous ammonia was used as the *N*-3 source in a straightforward synthesis of the desired compounds, Scheme 100, Table 31.

The benzaldehyde derivatives reacted with the quinoline starting material to afford 2-aryl-1,2-

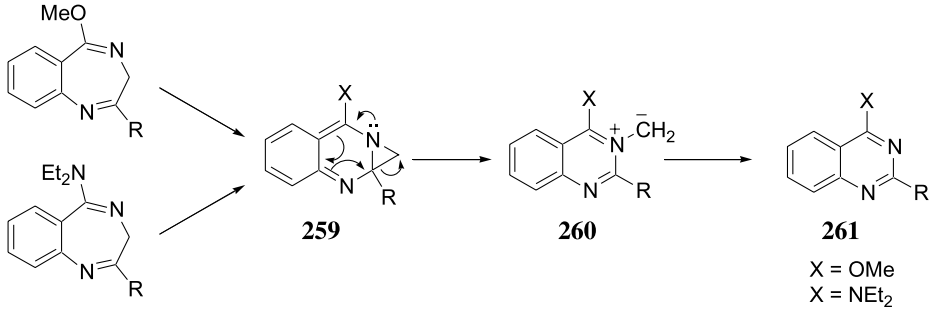

Scheme 99.

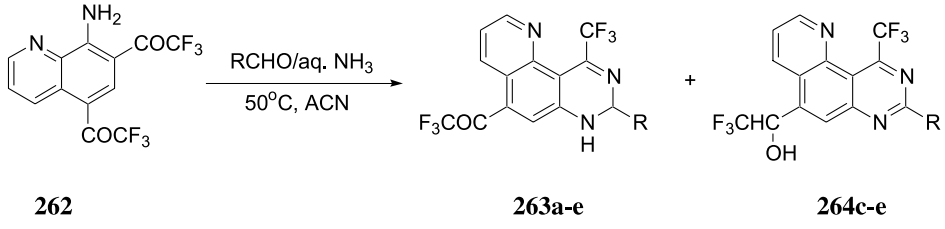

Scheme 100.

Table 31. Condensation of 5,7-bis-(trifluoroacetyl)-8-quinaolylamine **262** with aldehydes to form **263a–e** and **264c–e**

Entry	R	RCHO (equiv)	Time (h)	Product	Isolated yield (%)
1	Et	3	24	**263a**	62
2	*i*-Pr	5	72	**263b**	87
3	*p*-$MeOC_6H_4$	5	24	**263c**	84
4	*p*-$MeOC_6H_4$	5	48	**263c/264c**	71/23
5	Ph	5	24	**263d**	88
6	Ph	5	48	**264d/264d**	71/18
7	*p*-ClC_6H_4	5	24	**263e**	60
8	*p*-ClC_6H_4	5	96	**263e/264e**	50/46

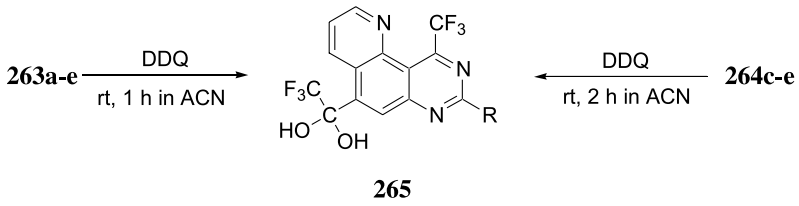

Scheme 101.

dihydropyridoquinazolines **263** in 60–88% yields with recovery of the unreacted substrate. It was noted that prolonged heating (48–96 h) resulted in the formation of the unexpected 2-aryl-α,4-bis(trifluoromethyl)-pyrido[3,2-*h*]quinazoline-6-methanols **264c–e** in 18–46% yield. Treatment of the quinazoline products **263a–e** with DDQ at room temperature for 1 h furnished the fluorine-containing pyrido[3,2-*h*]quinazolines **265** in 85–95% yield, Scheme 101. The alcohols **264c–e** could also be converted in excellent yields (82–94%) by oxidation into the quinazoline derivatives **265** using DDQ. This route enables access to products that are not easily obtained by other methods.

6.8. Reactivity of 2,4-dichloroquinazolines

Strekowski et al. reported that the reaction of organolithium reagents with 2,4-dichloroquinazoline **266** was regioselective, resulting in predominant substitution at the 4-position, Scheme 102.[113]

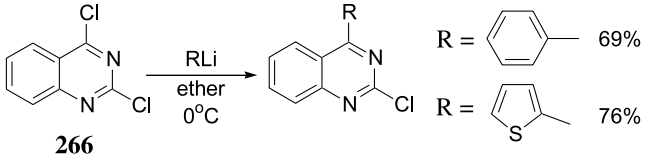

Scheme 102.

The reaction of 4-chloroquinazoline **267** with phenyllithium resulted in the formation of 2-[(benzylidene)amino]benzonitrile **268** as the minor product and 2-[diphenylmethyl)-amino]benzonitrile **269** as the major product, Scheme 103.

This indicates that the addition of a lithium reagent to the unsubstituted 2-position is favoured over substitution at the 4-chloro substituent. Similarly, the reaction of 2-chloro-4-phenyl-quinazoline **270** with 1 equiv of phenyllithium gave a complicated mixture of products, Scheme 104. The expected 2,4-diphenylquinazoline was not formed, possibly as a result of ring opening of the pyrimidine ring system.

The 2-chloro substituent can, however, be replaced by both alkoxides and amines to give the corresponding 2,4-disubstituted quinazolines in 60–80% yields. Indeed, this substitution can be carried out selectively depending on the conditions.

2,4-Dichoroquinazolines may be synthesised by chlorinating a quinazoline-2,4-dione using phosphorous oxychloride or thionyl chloride. Regiospecific substitution can be achieved by simply treating with a nucleophile. Substitution at the 4-position can be achieved by treating 2,4-dichloroquinazoline with a nucleophile. This is illustrated in the course of several syntheses.

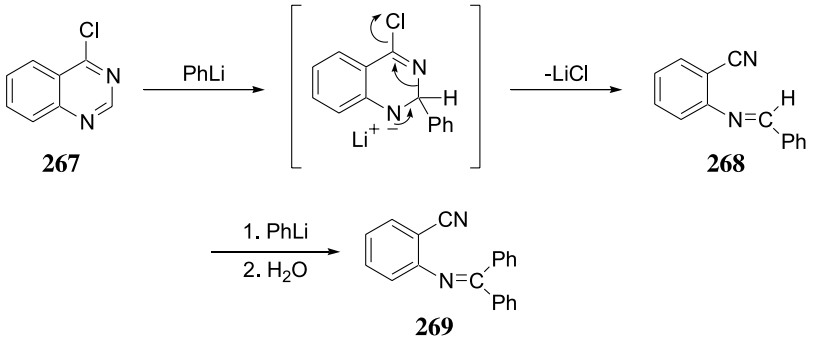

Scheme 103.

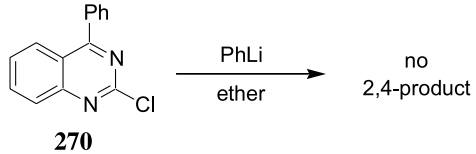

Scheme 104.

Lee et al. exploited the differential reactivity of 2,4-dichloroquinazoline derivatives **271** as part of their structure–activity relationship studies of phosphodiesterase inhibitors.[114] The 6-substituted quinazoline-2,4-diones **272** were readily prepared from the anthranilamides **273a** by treatment with phosgene, Scheme 105. Alternatively, the reaction of anthranilic acids **273b**

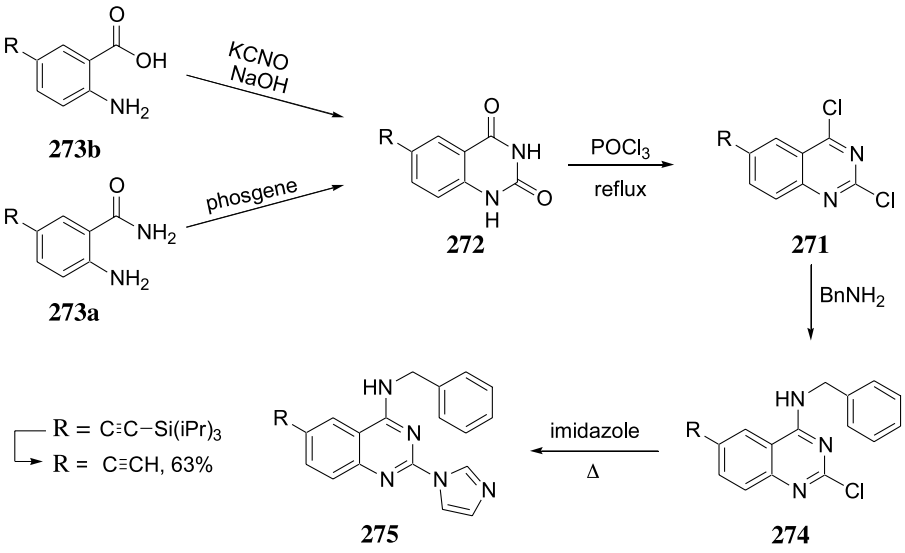

Scheme 105.

and potassium cyanate followed by ring cyclisation could be employed.

In the light of commercial interest in quinazoline antihypertensive agents, a similar procedure for the synthesis of kilogram quantities of the substituted quinazoline-2,4-dione was developed by Hammen and Allen.[115]

The substituted 2,4-dichloroquinazoline was prepared in excellent yield by refluxing the 6-substituted quinazoline-2,4-dione **272** in phosphorus oxychloride. Replacement of the 4-chloro group by a primary amine such as benzylamine afforded the desired intermediate **274**. An imidazole group was subsequently introduced at the 2-position to furnish the required 2,4-diaminoquinazoline **275** in 63% yield. It was found that the 4-benzylamino fragment imparted a greater activity than the 4-anilino series in the study of PDE inhibitors. In addition, the 2-position imidazolyl substituents gave a slightly higher potency than the corresponding 2-pyridyl analogues. This method demonstrates how assisted drug design technology can identify potentially causal relationships between structural fragments and biological activity.

A series of quinazolines was prepared in order to evaluate their usefulness as a possible treatment for obstructive pulmonary disease such as asthma.[116]

Protection of the aminophenol starting material was required in order to allow the efficient alkylation of the hydroxyl functionality, Scheme 106. Deprotection and subsequent reaction with the isocyanate afforded intermediate **276**. It was found that the yield from the cyclisation reaction with phosphorus oxychloride was dependent on the nature of the 6- and 7-substituents (80% for **277a–c** and 10% for **277d**).

A Stille coupling resulted in exclusive reaction at the 4-chloro substituent in 2,4-dichloroquinazoline derivatives **278**, since this position is the most electrophilic, Scheme 107.

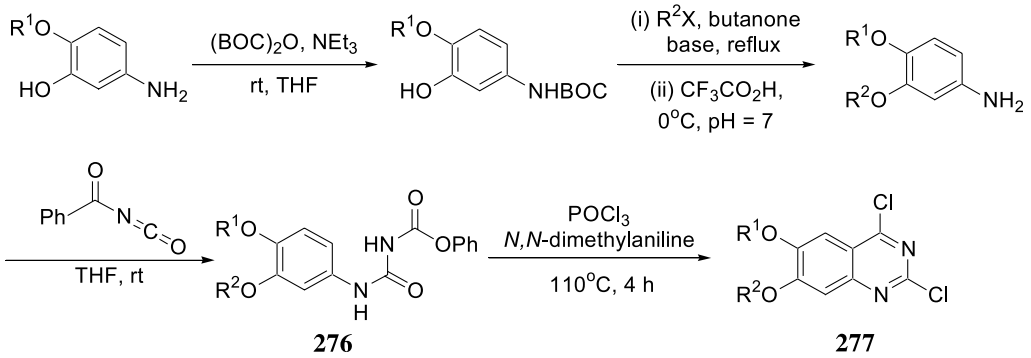

a R^1= Me, R^2 = CH_2Ph
b R^1= Me, R^2 = CH_2CO_2Et
c R^1= H, R^2 = CH_2CO_2Et
d R^1= R^2 = CH_2CO_2Et

Scheme 106.

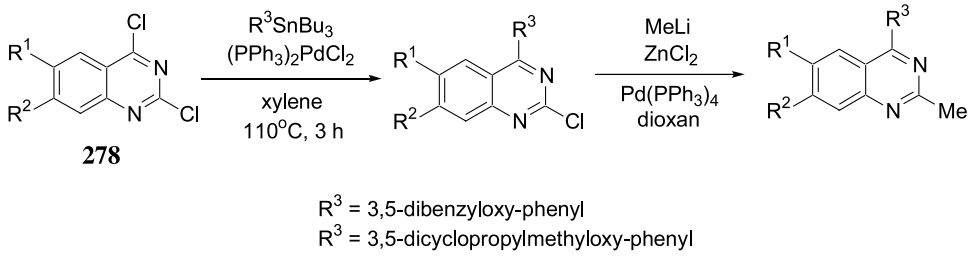

Scheme 107.

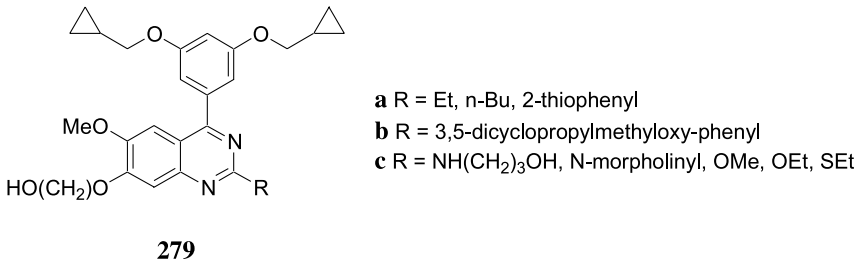

Scheme 108.

Lastly, substitution at the remaining 2-position by both organotin and organozinc reagents was possible using similar cross-coupling methodology, producing **279a** and **279b**. Alcohols, thiols or amines in the presence of sodium hydroxide could also be used to replace the 2-chloro substituent, to produce **279c** in yields of 50–90%, Scheme 108.

By exploiting the inherent reactivity of 2,4-dichloroquinazoline, it was possible to access a large number of biologically relevant products.

This reactivity may also be exploited for the elaboration of 2,4-quinazolines. Undheim et al. investigated the use of trialkylalanes in palladium-catalysed alkylations, with emphasis on the selectivity for carbo-substitution in 2,4-dichloroquinazoline **266**.[117] The mechanism of this process involves oxidative addition at the more electrophilic 4-position of the quinazoline moiety to the palladium(II) complex. Transfer of an alkyl group from aluminium to the palladium template occurs and subsequent reductive elimination furnishes the alkylated product, Scheme 109.

Reaction at the 4-position can be effected with trimethylalane and tri-isobutylalane and tetrakis(triphenylphosphine) palladium as catalyst. After 24 h at reflux, the monoalkylated products **280** (R=Me or *i*-Bu) were obtained in good yields (63 and 76%). Addition of another equivalent of the appropriate alane enabled further substitution at the 2-position, with yields varying from 63–80%. This method complements the existing procedures involving organostannanes, organozinc and organomagnesium reagents for carbo-substitution, allowing regioselective modification of biologically important quinazolines.

More recently, Weber et al. have exploited this reactivity at the 4-position, while producing a solid-phase library of 2-substitued quinazolinones.[118,119]

6.9. Chlorination of quinazoline-2,4-dione in the presence of cyclic amines

Yoshida et al. have developed a convenient synthetic route to 2-(4-allylpiperazin-1-yl)-4-chloroquinazoline **281**, a key intermediate in the preparation of 2-(4-allylpiperazin-1-yl)-4-pentyl-oxyquinazoline, a compound, which is potentially useful in the treatment of dementia, Scheme 110.[120] The reaction of quinazoline-2,4-dione **253a** with 1,4-diallylpiperazine and 1,4-dimethylpiperazine produced the products in 64 and 74% yield, respectively.

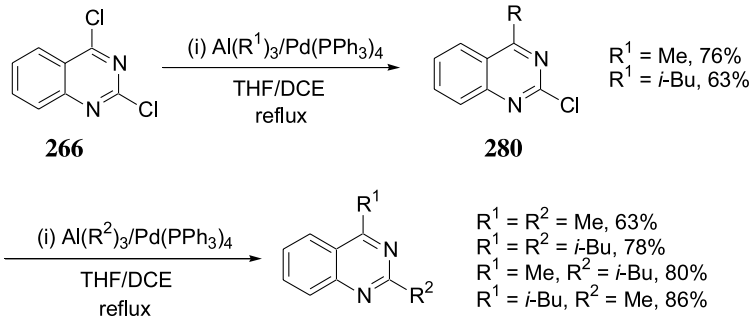

Scheme 109.

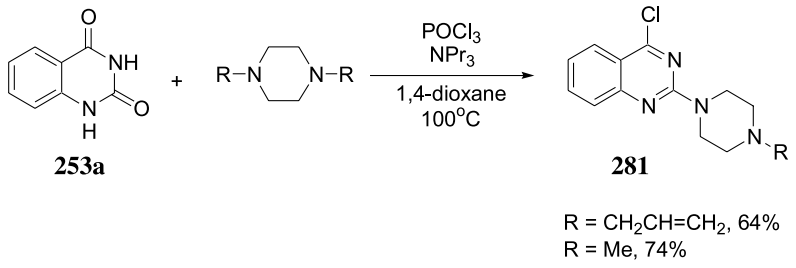

Scheme 110.

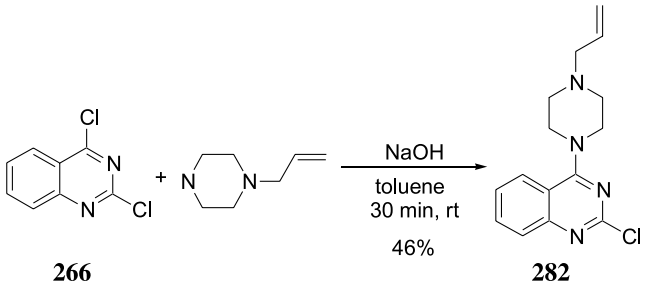

Scheme 111.

The above reaction shows that tertiary amines react selectively at the 2-position of the quinazolinedione in the presence of phosphorus oxychloride.[121] As previously noted, however, the 4-position of 2,4-dichloroquinazoline **266** is more reactive than the 2-position for nucleophilic attack by primary or secondary amines.[5] This was further demonstrated by the reaction of 1-allylpiperazine and 2,4-dichloroquinazoline in the presence of aqueous sodium hydroxide. The reaction was complete after 30 min at room temperature and furnished 4-(4-allyl-piperazin-1-yl)-2-chloro-quinazoline **282** in 46% yield after recrystallisation, Scheme 111.

An investigation into the reaction of 2,4-quinazolinedione **253a** with phosphorus oxychloride revealed that the *N*-methylpyrrolidine base reacted with intermediate **283** to form a quaternary ammonium salt, Scheme 112.[122] Under the reaction conditions employed, this ammonium salt degraded to form 2-(4-chloro-*N*-methylbutylamino)-4(3*H*)-quinazolinone **284** in 78% yield. Further reaction to facilitate chlorination at the 4-position was also possible, furnishing the product **285** in 87% yield. Interestingly, when a bulky alkylamine base such as *N*-*sec*-butyl- or *N*-*tert*-butylpyrrolidine was examined, only 2,4-dichloroquinazoline **266** was isolated. This indicates that the product ratio depends on the bulkiness, rather than the basicity, of the alkylamine used.

An earlier study revealed that tri-*n*-propylamine, the base commonly employed in conjunction with phosphorus oxychloride, was sufficiently bulky to enable smooth conversion of the quinazolinedione into the 2,4-dichloro species. When triethylamine was substituted, however, 4-chloro-2-diethylaminoquinazoline was obtained as the product.[123] This procedure represents a facile synthesis of 2-(*N*-alkyl-4-chlorobutyl amino)-4-chloroquinazolines, which are amenable to further elaboration at the 2- and 4-positions.

6.10. Synthesis of 2,4-diaminoquinazolines

Zielinski et al. reported a method to enable the synthesis of 2,4-diaminoquinazolines by reacting chloroamidines with dialkylcyanamides. Phenyl isocyanate derivatives with electron-donating and -withdrawing groups were reacted with *N*,*N*-diethylamine to prepare the substituted urea compounds. The subsequent chlorination was facilitated with the use of phosphorus pentachloride. For example, 2-(*N*,*N*-diethylamino)-4-(*N*,*N*-dimethylamino)quinazoline **286a** was prepared in 79% yield from the cyclisation of the intermediate **287** (R^1=H), which was obtained from the reaction of *N*,*N*-dimethylcyanamide **288** (R^1=H) with chloroamidine **289**, Scheme 113.[124]

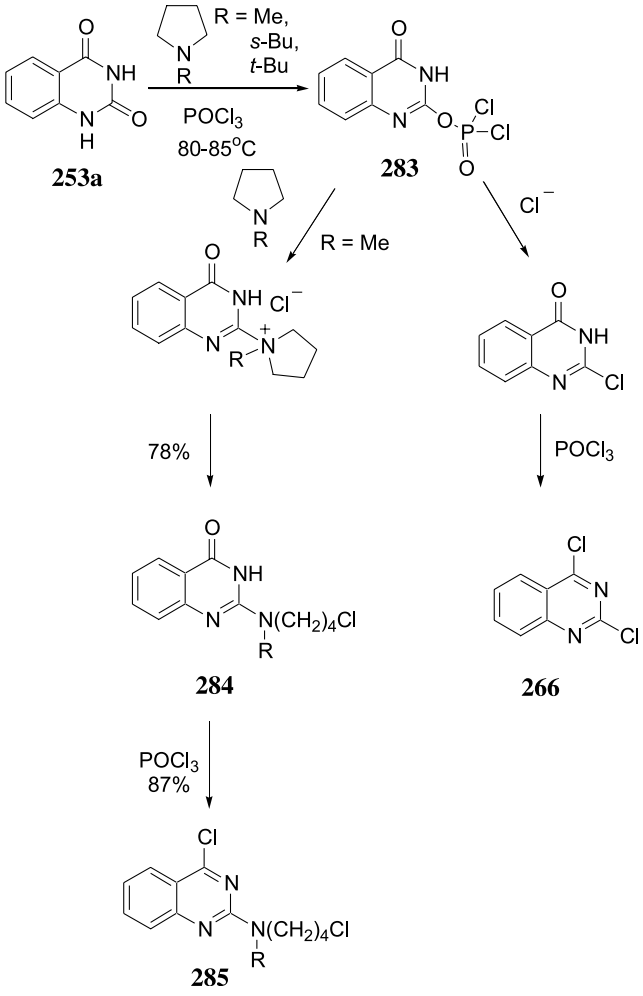

Scheme 112.

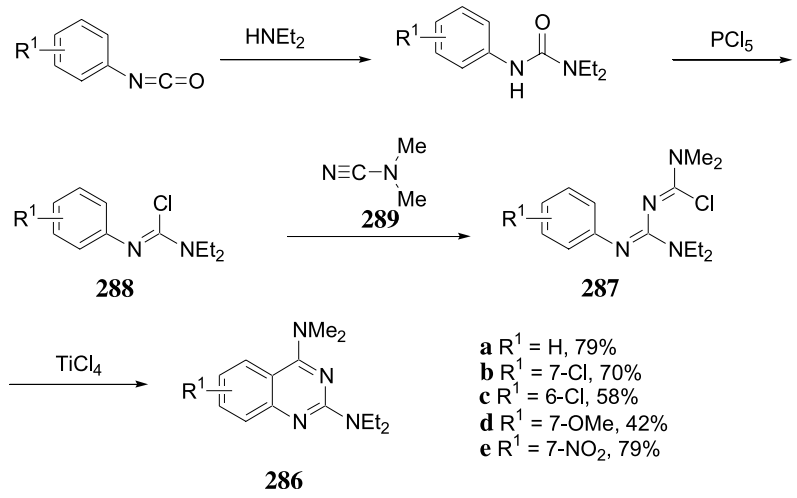

Scheme 113.

The use of other nitriles such as acetonitrile, benzonitrile, phenylacetonitrile and cyanamide did not afford the required quinazoline derivatives. This synthetically useful procedure, however, tolerated a range of substituents on the phenyl isocyanate starting material to give the appropriately substituted products. Unfortunately, purification of the quinazoline from these reaction mixtures was difficult in some cases, therefore reducing the isolated yield.

6.11. Rearrangement of triazolines to 2-alkyl-4-arylaminoquinazolines

Erba and Sporchia reported a synthesis of 2-alkyl-4-arylaminoquinazolines **290** by the condensation of arylamines with amidines **291**, Scheme 114.[125] As discussed in Section 2.4, these amidines could be formed by a thermal rearrangement of the triazolines **292**.

The reaction of primary arylamines and *N*-(2-cyanophenyl) amidines **291** was subsequently investigated and two condensations were developed, namely Route A, which involved refluxing the arylamine and the amidine in an organic acid, or Route B, heating the amidine with an equimolar amount of arylamine hydrochloride without any solvent in a sealed tube. Similar results were obtained with each procedure, but high temperatures and the presence of an acid, either an organic acid or its amine salt, were necessary for the successful completion of the reaction. This thermal rearrangement is the method of choice for a straightforward synthesis of functionalised amidines, which can be used to prepare 2-alkyl-4-arylaminoquinazolines in moderate to good yields (30–65%).

6.12. Access to quinazoline derivatives using Grignard reagents

The research of Bergman et al. demonstrated that 2-aminobenzonitrile reacted with Grignard reagents and the resulting intermediate **293** was useful in accessing a variety of important quinazoline derivatives, Scheme 115.[126,127]

Cyclisation of the intermediate **293** after reaction with acid chlorides, anhydrides and formates produced the respective quinazolines in moderate to good yields. 2-Aminobenzonitrile in ether was added dropwise to an ethereal solution of the required organomagnesium reagent. As an example, the reaction of the intermediate **293** (R=Ph) with benzoyl chloride and subsequent cyclisation furnished 2,4-diphenylquinazoline in 80% yield. This general approach for the synthesis of 2,4-disubstituted quinazolines is highly flexible and is a useful addition to the existing procedures.

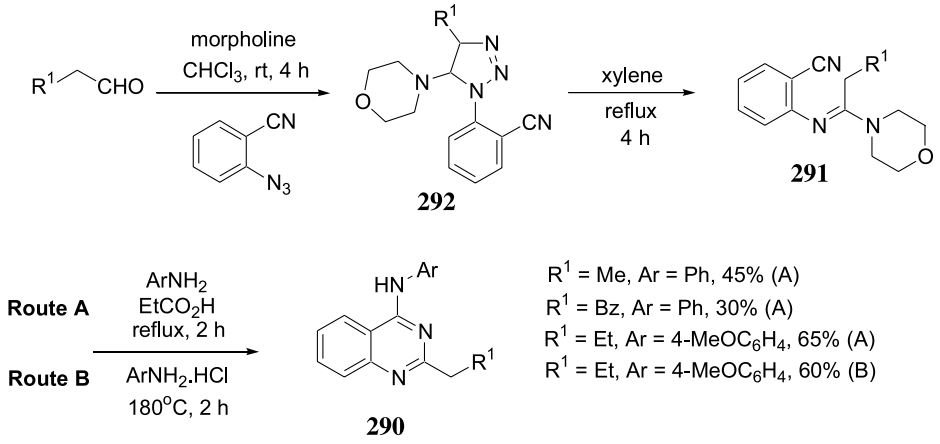

Scheme 114.

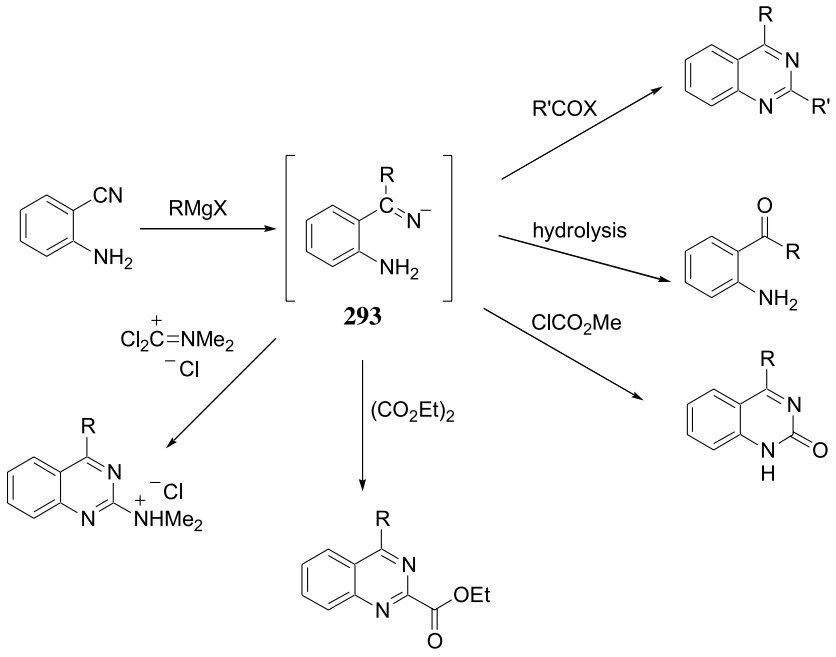

Scheme 115.

7. Conclusions

Given the advances in synthetic methodology and technology in recent years and the continued interest in the quinazoline skeleton in medicinal chemistry and drug development, the development of efficient and reliable methods for the construction of these molecules will ensure that this is an active and important area of research in heterocyclic chemistry.

Acknowledgements

D.J.C. acknowledges financial support from Enterprise Ireland (BR/99/238 & SC/2002/349) and Schering Plough (Avondale) Company. D.C. and T.O.'S acknowledge financial support from the Centre for Synthesis and Chemical Biology (CSCB), which was funded by the Higher Education Authority's Programme for Research in Third-Level Institutions (PRTLI).

References and notes

1. Chan, J. H.; Hong, J. S.; Kuyper, L. F.; Jones, M. L.; Baccanari, D. P.; Tansik, R. L.; Boytos, C. M.; Rudolph, S. K.; Brown, A. D. *J. Heterocycl. Chem.* **1997**, *34*, 145.
2. Gackenheimer, S. L.; Schaus, J. M.; Gehlert, D. R. *J. Pharmacol. Exp. Ther.* **1996**, *732*, 113.
3. Dempcy, R. O.; Skibo, E. B. *Biochemistry* **1991**, *30*, 8480.
4. Nordisk-Droge. 18113; Patent, N. A. Ed.; Nordisk Droge- and Kemi-Kalieforretning AIS: Netherlands, 1965.
5. Armarego, W. L. F. *Fused Pyrimidines, Part 1: Quinazolines*; Interscience: New York, 1967.
6. Undheim, K.; Benneche, T. In *Comprehensive Heterocyclic Chemistry II*, *Vol. 6*; Pergamon: Oxford, 1998.
7. Gilchrist, T. L. *J. Chem. Soc., Perkin Trans. 1* **2001**, 2491–2515.
8. Gilchrist, T. L. *J. Chem. Soc., Perkin Trans. 1* **1999**, 2849–2866.
9. Bogert, M. T.; Hand, W. F. *J. Am. Chem. Soc.* **1902**, *24*, 1031.
10. Bogert, M. T.; Hand, W. F. *J. Am. Chem. Soc.* **1903**, *25*, 935.
11. Taylor, E. C.; Knopf, R. J.; Borror, A. L. *J. Am. Chem. Soc.* **1960**, *82*, 3152.
12. Irwin, W. J.; Wibberly, D. G. *J. Chem. Soc., Chem. Commun.* **1965**, 4240.
13. Jiang, J. B.; Hesson, D. P.; Dusak, B. A.; Dexter, D. L.; Kang, G. L.; Hamel, E. *J. Med. Chem.* **1990**, *33*, 1721–1728.
14. Bandgar, B. P. *Synth. Commun.* **1997**, *27*, 2065–2068.
15. Batvetsias, V. *Synth. Commun.* **1998**, *28*, 4547–4559.
16. Showell, G. A. *Synth. Commun.* **1980**, *10*, 241–243.
17. Zentmyer, D. T.; Wagner, E. C. *J. Org. Chem.* **1949**, *14*, 967.
18. Errede, L. A.; McBrady, J. J.; Oien, H. T. *J. Org. Chem.* **1977**, *42*, 656.
19. Xia, Y.; Yang, Z.-Y.; Hour, M.-J.; Kyo, S.-C.; Xia, P.; Bastow, K. F.; Nakanishi, Y.; Nampoothiri, P.; Hackl, T.; Hamel, E.; Lee, K.-H. *Bioorg. Med. Chem. Lett.* **2001**, *11*, 1193–1196.
20. Rad-Moghadam, K.; Mohseni, M. *J. Chem. Res. (S)* **2003**, 487.
21. Körner, M. *J. Prakt. Chem.* **1887**, *36*, 155.
22. Bergman, J.; Brynolf, A. *Tetrahedron Lett.* **1990**, *46*, 1295–1310.
23. Witt, A.; Bergman, J. *Tetrahedron* **2000**, *56*, 7245–7253.
24. Hattori, K. *J. Med. Chem.* **2004**, *47*, 4151–4154.
25. Reddy, P. S. N.; Nagaraju, C. *Synth. Commun.* **1991**, *21*, 173–181.
26. Baker, B. R.; Almaula, P. I. *J. Org. Chem.* **1962**, *27*, 4672.
27. von Manfred Süsse, F. A.; Johne, S. *Helv. Chem. Acta* **1986**, *69*, 1017.
28. Rastoogi, R.; Sharma, S. *Indian J. Chem., Sect. B* **1982**, *21*, 744–746.
29. Sellstedt, J. H.; Guinosso, C. J.; Begany, A. J.; Bell, S. C.; Rosenthale, M. *J. Med. Chem.* **1975**, *18*, 926.

30. Joshi, V.; Chaudhari, R. P. *Indian J. Chem., Sect. B* **1987**, *26*, 602.
31. Ried, W.; Stephan, W. *Chem. Ber.* **1963**, *96*, 1218.
32. Ried, W.; Stephan, W. *Chem. Ber.* **1962**, *95*, 3042.
33. Ried, W.; Sinharray, A. *Chem. Ber.* **1963**, *96*, 3306.
34. Hennequin, L. F.; Boyle, F. T.; Wardleworth, J. M.; Marsham, P. R.; Kimbell, R.; Juckman, A. L. *J. Med. Chem.* **1996**, 39.
35. Connolly, D. J.; Guiry, P. J. *Synlett* **2001**, *11*, 1707.
36. Gruner, M.; Rehwald, M.; Eckert, K.; Gewald, K. *Heterocycles* **2000**, *53*, 2363.
37. Erba, E.; Pocor, D.; Valk, M. J. *J. Chem. Soc., Perkin Trans. 1* **1999**, 421.
38. Kotsuki, H.; Sakai, H.; Morimoto, H.; Suenaga, H. *Synlett* **1999**, *12*, 1993.
39. Yang, R.-Y.; Kaplau, A. *Tetrahedron Lett.* **2000**, *41*, 7005–7008.
40. Croce, P. D.; Ferracioli, R.; La Rosa, C. *Heterocycles* **1997**, *45*, 1309.
41. Couture, A.; Cornet, H.; Grandclaudon, P. *Synthesis* **1991**, 1609–1610.
42. Garratt, P. J.; Hobbs, C. J.; Wrigglesworth, R. *J. Org. Chem.* **1989**, *54*, 1062.
43. Hess, H.-J.; Cronin, T. H.; Scriabine, A. *J. Med. Chem.* **1968**, *11*, 130–138.
44. De Ruiter, J.; Brubaker, A. N.; Millen, J.; Riley, T. N. *J. Med. Chem.* **1986**, *29*, 625.
45. McC. Paterson, T.; Smalley, R. K.; Suschitzky, H. *Synthesis* **1975**, 187–189.
46. Abdel-Jalil, R. J.; Völter, W.; Saeed, M. *Tetrahedron Lett.* **2004**, *45*, 3475–3476.
47. Lopez, S. E.; Rosales, M. E.; Urdaneta, N.; Gody, M. V.; Charris, J. E. *J. Chem. Res. (S)* **2000**, 229–259.
48. Deepthi, K. S.; Reddy, D. S.; Reddy, P. P.; Reddy, P. S. N. *Indian J. Chem., Sect. B* **2000**, *39*, 220–222.
49. Majo, V. J.; Perumal, P. T. *Tetrahedron Lett.* **1996**, *37*, 5015.
50. Alexandre, F.-R.; Berecibar, A.; Wrigglesworth, R.; Bessen, T. *Tetrahedron* **2003**, *59*, 1413–1419.
51. Rewcastle, G. W.; Palmer, B. D.; Bridges, A. J. *J. Med. Chem.* **1996**, *39*, 918–928.
52. Tobe, M.; Isobe, Y.; Tomizawa, H.; Nagasaki, T.; Takahashi, H.; Fukazawa, T.; Hayashi, H. *Bioorg. Med. Chem.* **2003**, *11*, 383–391.
53. Sugimoto, O.; Mori, M.; Moriya, K.; Tanji, K. *Helv. Chem. Acta* **2001**, *84*, 1112.
54. Shreder, K. R.; Wong, M. S.; Nomanbhoy, T.; Leventhal, P. S.; Fuller, S. R. *Org. Lett.* **2004**, *6*, 3715–3718.
55. Rewcastle, G. W.; Palmer, B. D.; Bridges, A. J.; Hollis Showalter, H. D.; Sun, L.; Nelson, J.; McMichael, A.; Kraker, A. J.; Fry, D. W.; Denny, W. A. *J. Med. Chem.* **1996**, *39*, 918–928.
56. Traxler, T. M.; Furet, P.; Mett, H.; Buchdunger, E.; Meyer, J.; Lydon, N. *J. Med. Chem.* **1996**, *29*, 918–928.
57. Szczepankiewicz, W.; Suwinski, J.; Bujok, R. *Tetrahedron* **2000**, *56*, 9343.
58. Szczepankiewicz, W.; Suwinski, J. *Tetrahedron Lett.* **1998**, *39*, 1785.
59. Barker, A. J.; Gibson, K. H.; Grundy, W.; Godfrey, A. A.; Barlow, J. J.; Healy, M. P.; Woodburn, J. R.; Ashton, S. E.; Curry, B. J.; Scarlett, L.; Henthorn, L.; Richards, L. *Bioorg. Med. Chem. Lett.* **2001**, *11*, 1911.
60. Tsou, H.-R.; Mamuya, N.; Johnson, B. D.; Reich, M. F.; Gruber, B. C.; Ye, F.; Nilakantan, R.; Shen, R.; Discafari, C.; DeBlanc, R.; Davis, R.; Koehn, F. E.; Greenberger, L. M.; Wang, Y. F.; Wissner, A. *J. Med. Chem.* **2001**, *44*, 2719–2734.
61. Yoon, D. S.; Han, Y.; Stark, T. M.; Haber, J. C.; Gregg, B. T.; Stankovich, S. B. *Org. Lett.* **2004**, *6*, 4775–4778.
62. Akazome, M.; Yamamoto, J.; Kondo, T.; Watanabe, Y. *J. Organomet. Chem.* **1995**, *494*, 229.
63. Yu, Y.; Ostresh, J. M.; Houghten, R. A. *J. Org. Chem.* **2002**, *67*, 5831.
64. Vögtle, M. M.; Marzinzik, A. L. *QSAR Combinatorial Chem.* **2004**, *23*, 440–459.
65. Kamal, A.; Ramana, K. V.; Ankati, H. B.; Ramana, A. V. *Tetrahedron Lett.* **2002**, *43*, 6861.
66. Amin, A. H.; Mehta, D. R. *Nature* **1959**, *183*, 1317.
67. Eguchi, S.; Suzuki, J.; Okawa, T.; Matsushita, Y. *J. Org. Chem.* **1996**, *61*, 7316.
68. Hernández, F.; Morales, V.; Buenadicha, F. L.; Söllhuber, M.; Avendaño, C. *Tetrahedron: Asymmetry* **2004**, *15*, 3045–3058.
69. Fabis, F.; Santos, J. S. O.; Fouchet-Jolivet, S.; Rault, S. *Tetrahedron Lett.* **2002**, *43*, 6861.
70. Uskokovic, M.; Iacobelli, J.; Toome, V.; Wenner, W. *J. Org. Chem.* **1964**, *29*, 582.
71. Kundu, N. G.; Chaudhuri, G. *Tetrahedron Lett.* **2001**, *42*, 2883.
72. Deetz, M. J.; Malerich, J. P.; Beatty, A. M.; Smith, B. C. *Tetrahedron Lett.* **2001**, *42*, 1851.
73. Brown, D. J. *The Pyrimidines*; Wiley Interscience: New York, 1994.
74. Párkányi, C. J.; Schmidt, D. S. *J. Heterocycl. Chem.* **2000**, *37*, 725.
75. Kumar, A.; Sharma, S.; Archana; Bajaj, K.; Sharma, S.; Panwar, H.; Singh, T.; Srivastaia, V. K. *Bioorg. Med. Chem.* **2003**, *11*, 5293–5299.
76. Zhou, Y.; Murphy, D. E.; Sun, Z.; Gregor, V. E. *Tetrahedron Lett.* **2004**, *45*, 8049–8051.
77. Xue, S.; McKenna, J.; Shieh, W.-C.; Repic, O. *J. Org. Chem.* **2004**, *69*, 6474–6477.
78. Grimmel, H. W.; Guenther, A.; Morgan, J. F. *J. Am. Chem. Soc.* **1946**, *68*, 539.
79. Dai, X.; Virgil, S. *Tetrahedron: Asymmetry* **1999**, *40*, 1245.
80. Dai, X.; Wong, A.; Virgil, S. *J. Org. Chem.* **1998**, *63*, 2597.
81. Dai, X.; Virgil, S. *Tetrahedron Lett.* **1999**, *40*, 1245.
82. Dandia, A.; Singh, R.; Sarawgi, P. *J. Fluorine Chem.* **2004**, *125*, 1835–1840.
83. de Fatima Pereira, M.; Alexandre, R.; Thièry, V.; Besson, T. *Tetrahedron Lett.* **2004**, *45*, 3097–3099.
84. Larksarp, C.; Alper, H. *J. Org. Chem.* **2000**, *65*, 2773.
85. Wuckelt, J.; Döring, M.; Beckert, R.; Langer, P. *Synlett* **1999**, *7*, 1100.
86. Makino, S.; Suzuki, N.; Nakanishi, E.; Takahashi, T. *Synlett* **2000**, *11*, 1670.
87. Mayer, J. P.; Lewis, G. S.; Curtis, M. J.; Zhang, J. *Tetrahedron Lett.* **1997**, *38*, 8445.
88. Lee, H.-S.; Chang, Y.-G.; Kim, K. *J. Heterocycl. Chem.* **1996**, *61*, 659.
89. Smith, K.; El-Hiti, G. A.; Abbdel-Megeed, M. F.; Abdo, A. *J. Org. Chem.* **1996**, *61*, 647.
90. Smith, K.; El-Hiti, G. A.; Abbdel-Megeed, M. F.; Abdo, A. *J. Org. Chem.* **1996**, *61*, 656.
91. Peet, N. P.; Sunder, S.; Cregge, R. J. *J. Org. Chem.* **1976**, *41*, 2733.
92. Xiao, X.-H.; Qou, G.-L.; Wang, H.-L.; Lui, L.-S.; Zheng,

Y.-L.; Jia, Z.-J.; Dreng, Z.-B. *Chin. J. Pharmacol. Toxicol.* **1988**, 232–234.
93. Witt, A.; Bergman, J. *Curr. Org. Chem.* **2003**, *7*, 659–677.
94. Harayama, T.; Hori, A.; Serban, G.; Morikami, Y.; Matsumoto, T.; Abe, H.; Takeuchi, Y. *Tetrahedron* **2004**, *60*, 10645.
95. Mhaske, S. B.; Argade, N. P. *J. Org. Chem.* **2004**, *69*, 4563–4566.
96. Lee, E. S.; Park, J.-G.; Jahng, Y. *Tetrahedron Lett.* **2003**, *44*, 1883–1886.
97. Wang, H.; Ganesan, A. *Tetrahedron Lett.* **1998**, *39*, 9097–9098.
98. Povarov, L. S. *Russ. Chem. Rev.* **1967**, *36*, 656–670.
99. Twin, H.; Batey, R. A. *Org. Lett.* **2004**, *6*, 4913–4916.
100. Mazurkiewicz, R. *Monatsh. Chem.* **1989**, *120*, 973–980.
101. Osborne, D.; Stevenson, P. J. *Tetrahedron Lett.* **2002**, *43*, 5469–5470.
102. Chavan, S. P.; Sivappa, R. *Tetrahedron Lett.* **2004**, *45*, 997–999.
103. Kokosi, J.; Hermecz, I.; Szasz, G.; Meszaros, Z. *Tetrahedron Lett.* **1981**, *22*, 4861.
104. Wilson, L. J. *Org. Lett.* **2001**, *4*, 585.
105. Patane, M. A.; Scott, A. L.; Broten, T. P.; Chang, R. S. L.; Ransom, R. W.; Disalvo, J.; Forray, C.; Bock, M. G. *J. Med. Chem.* **1998**, *41*, 1205.
106. Werbel, L. M.; Elslager, E. F.; Newton, L. S. *J. Heterocycl. Chem.* **1987**, *24*, 345.
107. Azizian, J.; Mehrdad, M.; Jadidi, K.; Sarrafi, Y. *Tetrahedron Lett.* **2000**, *41*, 5265.
108. Seijas, J. A.; Vázquez-Tato, M. P.; Martínez, M. M. *Tetrahedron Lett.* **2000**, *41*, 2215.
109. Mizuno, T.; Okamoto, N.; Ito, T.; Miyata, T. *Tetrahedron Lett.* **2000**, *41*, 1051.
110. Mizuno, T.; Iwai, T.; Ishino, Y. *Tetrahedron Lett.* **2004**, *45*, 7073–7075.
111. Kaname, M.; Tsuchiya, T.; Sashida, H. *Heterocycles* **1999**, *51*, 2407.
112. Okada, E.; Tsukushi, N. *Heterocycles* **1999**, *51*, 1999.
113. Harden, D. B.; Mokrosz, M. J.; Strekowski, L. *J. Org. Chem.* **1998**, *53*, 413.
114. Lee, S. J.; Konishi, Y.; Yu, D. T.; Miskowski, T. A.; Riviello, C. M.; Macina, O. T.; Frierson, M. R.; Kondo, K.; Sugitani, M.; Sircar, J. C.; Blazejewski, K. M. *J. Med. Chem.* **1995**, *38*, 3547.
115. Hammen, P.; Allen, P. D. *J. Heterocycl. Chem.* **1987**, *24*, 1701.
116. Charpiot, B.; Brun, J.; Donze, I.; Naef, R.; Stefani, M.; Mueller, T. *Bioorg. Med. Chem. Lett.* **1998**, *8*, 1999.
117. Mangalagiu, I.; Benneche, T.; Undheim, K. *Tetrahedron Lett.* **1996**, *37*, 1309–1312.
118. Weber, C.; Bielik, A.; Szendrei, G. I.; Greiner, I. *Tetrahedron Lett.* **2002**, *43*, 2971–2974.
119. Weber, C.; Demeter, A.; Szendrei, G. I.; Greiner, I. *Tetrahedron Lett.* **2003**, *44*, 7533–7536.
120. Yoshida, K.; Tanaka, T.; Ohtaka, H. *J. Chem. Soc., Perkin Trans. 1* **1991**, 1279.
121. Miki, H. *Chem. Pharm. Bull.* **1982**, *30*, 1947.
122. Miki, H. *Heterocycles* **1982**, *1*, 15.
123. Miki, H. *Heterocycles* **1982**, *1*, 7.
124. Zielinski, W.; Kudelko, A.; Holt, E. M. *Heterocycles* **1998**, *48*, 319.
125. Erba, E.; Sporchia, D. *J. Chem. Soc., Perkin Trans. 1* **1997**, 3021.
126. Bergman, J.; Brynolf, A.; Elman, B.; Vuorinen, E. *Tetrahedron* **1986**, *42*, 3697.
127. Wiklund, P.; Bergman, J. *J. Org. Biomol. Chem.* **2003**, *1*, 367–372.

Biographical sketch

David Connolly studied at University College Dublin receiving his Honours BSc degree in Chemistry in 1999. Working in the group of Professor Pat Guiry, he completed his PhD in 2003 where he researched the synthesis and resolution of axially chiral P,N-ligands and their application in asymmetric catalysis. During his PhD he also worked with Dr John Brown at Oxford University (Rh-catalysed hydroboration) as a Marie-Curie Training Fellow. He is currently employed in the pharmaceutical industry with Bristol-Myers Squibb in Dublin.

Tim O'Sullivan was born in County Kerry, Ireland. He studied at the University of Limerick receiving his Honours BSc degree in Industrial Chemistry in 1997. He subsequently obtained a PhD under the guidance of Professor Lewis Mander at the Australian National University focussing on the total synthesis of diterpenoids. He returned to Ireland to work as a postdoctoral fellow with Dr Mary Meegan in the Department of Pharmaceutical Chemistry, Trinity College Dublin. He is currently employed as a senior postdoctoral fellow at the Centre for Synthesis and Chemical Biology, University College Dublin in the research group of Professor Pat Guiry and is involved in the synthesis of novel Lipoxin analogues.

Declan Cusack was born in Dublin, Ireland in 1981. He studied medicinal chemistry at Trinity College, Dublin, graduating with first class honours in 1999. At present, he is studying for a PhD in the area of organic synthesis and asymmetric catalysis under the supervision of Professor Pat Guiry.

Pat Guiry was born in County Tipperary, Ireland and graduated with an Honours BSc degree in Chemistry from University College Dublin in 1986. He stayed at University College Dublin for his PhD working under the supervision of Professor Dervilla Donnelly on the application of aryllead triacetates to the synthesis of natural products. During his PhD, he also worked in Marseille in 1988 under the supervision of Dr. Jean-Pierre Finet (Cu-catalysed N-arylation) and at Texas A&M in 1989 with Professor Sir Derek Barton (mechanistic studies of arylation/phenol arylation). He received his PhD degree in 1990 and moved to the group of Dr. John Brown FRS at the Dyson Perrins Laboratory, Oxford University for postdoctoral studies in the area of asymmetric catalysis. During this three year stay, he was appointed in 1991 as a Tutorial Fellow at Wadham College Oxford and in 1992 as College Lecturer/Director of Studies at St Hughs College Oxford. He returned to University College Dublin as a College Lecturer in 1993 where he started his independent research. His research interests are the design and preparation of chiral ligands and their application in a broad range of asymmetric catalytic transformations. He was a visiting researcher in the group of Professor Andreas Pfaltz at the Max Planck Institut für Kohlenforschung at Mülheim an der Ruhr (Germany) in 1996. He was the recipient of a President's Research Award in 1996 and a President's Teaching Award in 2000 from University College Dublin. He was promoted to Senior Lecturer in 2002 and to Professor in 2003. He was the Merck Frosst Visiting Professor at the University of Toronto in early 2004. He was appointed as the Chief Executive of the Conway Institute of Biomolecular and Biomedical Sciences at University College Dublin in 2004. A keen tennis player, he represented Ireland in 2005 in the Trabert Cup (ITF World Team Competition) in Perth where he was team captain.

Available online at www.sciencedirect.com
SCIENCE DIRECT
Tetrahedron 61 (2005) 10203–10215
Tetrahedron

Radical-mediated hydroxyalkylation of α,β-unsaturated esters

Tomoko Yajima, Chiaki Saito and Hajime Nagano*

Department of Chemistry, Faculty of Science, Ochanomizu University, Otsuka, Bunkyo-ku, Tokyo 112-8610, Japan

Received 21 July 2005; revised 9 August 2005; accepted 11 August 2005

Abstract—The radical-mediated hydroxyalkylation of α,β-unsaturated esters with alkyl iodides, trialkylborane, water and KF in THF gave the corresponding α-hydroxy esters. The synthetic advantage of the method was demonstrated by a short-step total synthesis of (±)-tanikolide.

1. Introduction

Radical additions have become a very useful synthetic tool because of the many advantages over ionic reactions, and much attention has been paid to the development of efficient carbon–carbon bond-forming reactions.[1] Frequently used methodologies of alkyl radical addition to alkenes are hydroalkylation with tributyltin hydride (the tin hydride method), allylalkylation with allyltributyltin (the fragmentation method), and haloalkylation via halogen atom transfer (the Kharasch type method). If concomitant introduction of alkyl and hydroxyl moieties to α-methylene esters is possible by one-pot reaction, the reaction is referred to as hydroxyalkylation and such a method would provide a novel route to α-hydroxy esters being useful building blocks in organic synthesis and structural motifs in a variety of biologically active natural products.[2] To our knowledge, however, a few reports have described the radical-mediated hydroxyalkylation of α-methylene esters.[3]

During the investigation of chelation-controlled diastereoselective alkyl radical addition to α-methylene-γ-oxycarboxylic acid esters **I** yielding ester **II**,[4] we have observed the formation of hydroxytrifluoromethylation[5] products **III** when CF_3I was used as the radical precursor (Scheme 1).[6] We continued the study to broaden the reaction scope and here report the radical-mediated hydroxyalkylation of α,β-unsaturated esters using various alkyl iodides and Et_3B in the presence of KF and H_2O.

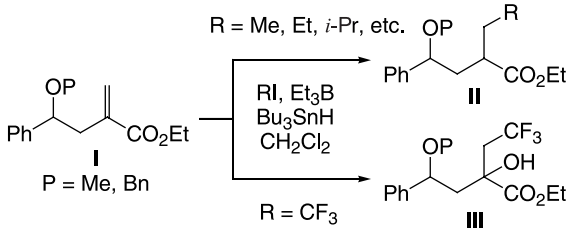

Scheme 1.

2. Results and discussion

2.1. Hydroxyalkylation

Initially, we examined the radical reaction of ethyl 2-phenethylpropenoate (**1**) with CF_3I. Table 1 shows representative results of the radical reaction under selected conditions. Following the procedure for the alkyl radical addition,[4] **1** was treated with CF_3I (gaseous, ca. 6 equiv) in the presence of Et_3B (1 equiv) and *n*-Bu_3SnH (3 equiv) in anhydrous CH_2Cl_2 at room temperature for 6 h. Work-up with KF and H_2O[7] gave hydroxytrifluoromethylated ester **2** in 30% isolated yield (entry 1). Neither hydrotrifluoromethylated ester **3** nor iodotrifluoromethylated ester **4** was observed. As *n*-Bu_3SnH did not act as a hydrogen donor, we next performed the reaction in the presence of H_2O (4 equiv) and KF (30 equiv), but without the tin reagent. The reaction gave **2** in 50% isolated and 90% conversion yields (entry 2), but gave a lower yield without KF[8] (entry 3). The reaction performed without the additives gave a complex mixture, and alcohol **2** was isolated in 20% yield (entry 4). The reaction was probably contaminated by H_2O during the bubbling of CF_3I gas at −30 °C. The use of THF as solvent enhanced the yield of **2**, although the reaction was not completed (75% isolated and 95% conversion yields, entry 5). Further enhancement of yield was not observed

Keywords: Hydroxyalkylation; α,β-Unsaturated esters; α-Hydroxy esters; Radical reaction; Tanikolide.
* Corresponding author. Tel.: +81 3 5978 5348; fax: +81 3 5978 5715; e-mail: nagano@cc.ocha.ac.jp

0040–4020/$ - see front matter © 2005 Elsevier Ltd. All rights reserved.
doi:10.1016/j.tet.2005.08.039

Table 1. Hydroxytrifluoromethylation of **1** with CF_3I[a]

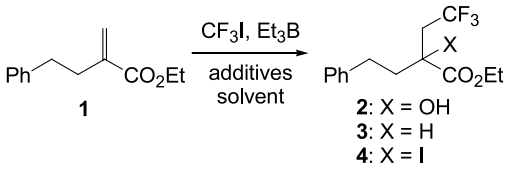

Entry	Additives (equiv)	Solvent	Yield of **2** (%)[b]
1[c]	*n*-Bu_3SnH (3)	CH_2Cl_2	30
2	H_2O (4), KF (30)	CH_2Cl_2	50 (90)
3	H_2O (4)	CH_2Cl_2	25
4	—	CH_2Cl_2	20
5	H_2O (4), KF (30)	THF	75 (95)
6	H_2O (4), K_2CO_3 (10)	THF	46 (53)
7	H_2O (4), KCl (30)	THF	48

[a] Compound **1** was allowed to react with CF_3I (gaseous, ca. 6 equiv) in the presence of Et_3B (1 equiv) and additives in the solvent (10 mL/mmol) at −30 °C and the reaction mixture was stirred at room temperature for 6 h under N_2 atmosphere.
[b] Isolated yield. Conversion yield in parenthesis.
[c] After the reaction was completed, the reaction mixture was stirred with KF and H_2O at room temperature for additional 3 h (Ref. 7).

even in the presence of 2.0 equiv of triethylborane. K_2CO_3[9] and KCl were less effective than KF (entries 6 and 7). The reaction in the presence of KI, KOH, Na_2CO_3 or $CaCO_3$ gave the alcohol **2** in lower yield (ca. 20%). No reaction took place in the absence of the radical initiator Et_3B.

We subsequently applied the best reaction conditions (Table 1, entry 5) to the reactions of various α,β-unsaturated carbonyl compounds with CF_3I (Table 2). The reactions of methyl, isopropyl and phenyl esters **5**, **7** and **9** were investigated, but the yields were lower than ethyl ester **1** (Table 2, entry 1 vs Table 1, entry 5). α-Methylene amide **11** and α-methylene-γ-lactone **13** also gave the corresponding hydroxytrifluoromethylated products **12** and **14**, respectively, although the yields were lower (entries 2 and 3). The reaction of ethyl 2-hexylpropenoate (**15**) afforded the corresponding hydroxytrifluoromethylation product **16** in 70% yield (entry 4). α-Methylene esters **17**, **19**, **21** and **23** with an additional electron-withdrawing methoxy (or ethoxy) carbonyl group also reacted with CF_3 radical to give **18**, **20**, **22** and **24**, respectively (entry 5). Nonterminal

Table 2. Hydroxytrifluoromethylation of electron deficient alkenes with CF_3I[a]

Entry	Substrate	Product	Yield (%)[a]	d.r.
1	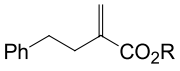 **5** (R = Me) **7** (R = *i*-Pr) **9** (R = Ph)	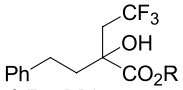 **6** (R = Me) **8** (R = *i*-Pr) **10** (R = Ph)	**6**: 43 (81) **8**: 38 (70) **10**: 26 (43)	
2	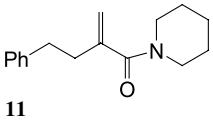 **11**	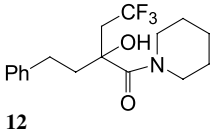 **12**	14 (26)	
3	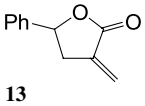 **13**	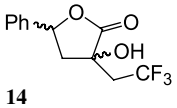 **14**	25 (36)	60:40[b]
4	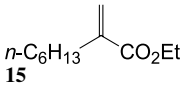 **15**	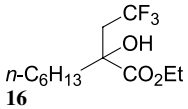 **16**	70 (80)	
5	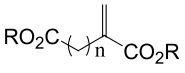 **17** (R = Me, *n* = 1) **19** (R = Et, *n* = 1) **21** (R = Et, *n* = 2) **23** (R = Et, *n* = 3)	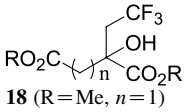 **18** (R = Me, *n* = 1) **20** (R = Et, *n* = 1) **22** (R = Et, *n* = 2) **24** (R = Et, *n* = 3)	**18**: 22 (54) **20**: 33 (59) **22**: 47 (77) **24**: 46 (73)	
6[c]	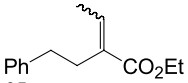 **25**	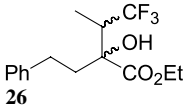 **26**	40 (91)	60:40[b]
7	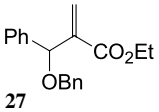 **27**	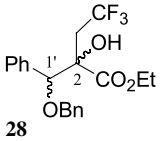 **28**	39 (78)	89:11[d]

Table 2 (*continued*)

Entry	Substrate	Product	Yield (%)[a]	d.r.
8	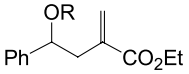	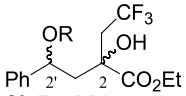		
	29 (R=Me) **31** (R=Bn)	**30** (R=Me) **32** (R=Bn)	**30**: 76 (80) **32**: 62 (82)	60:40[e]
9	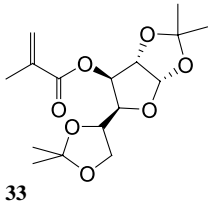	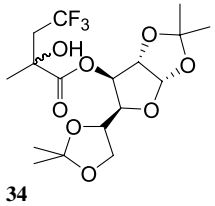	51	50:50
	33	**34**		
10	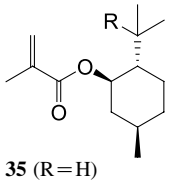	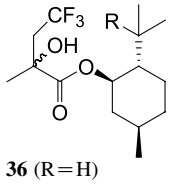		
	35 (R=H) **37** (R=Ph)	**36** (R=H) **38** (R=Ph)	**36**: 36 (50) **38**: 62 (82)	50:50 56:44[b]

Reaction conditions: the substrate was allowed to react with CF_3I (gaseous, ca. 6 equiv) in the presence of Et_3B (1 equiv) and additives in the solvent (10 mL/mmol) at −30 °C and the reaction mixture was stirred at room temperature for 6 h under N_2 atmosphere.
[a] Isolated yield. Conversion yield in parenthesis.
[b] The relative configurations of the products were not determined.
[c] The *E*/*Z* ratio of **25**=2.6:1.
[d] The stereochemistry of the major diastereomer of **28** was (2*R**,1′*R**).
[e] The stereochemistry of the major diastereomer of **30** and **32** was (2*R**,2′*R**). (see Ref. 11).

alkene **25** underwent hydroxytrifluoromethylation to give **26** despite the fact that the radical addition reactions of nonterminal alkenes are in general sluggish (entry 6).[10]

The stereochemical outcome of hydroxytrifluoromethylation was examined in entries 7–10. The reaction of β-benzyloxy-α-methylenecarboxylic acid ester **27** gave hydroxytrifluoromethylated esters **28**[11] in 76% yield with good 1,2-asymmetric induction; (2*R**,1′*R**)-**28**:(2*S**,1′*R**)-**28**=89:11 (entry 7). The reaction of γ-methoxy-α-methylenecarboxylic acid ester **29**[4b,d] afforded hydroxytrifluoromethylated esters **30**[12] in 76% yield, but with poor diastereoselectivity; (2*R**,2′*R**)-**30**:(2*S**,2′*R**)-**30**=60:40 (entry 8). The success in chelation-controlled 1,3-asymmetric induction in alkyl radical addition to α-methylene-γ-oxycarboxylic acid esters[4] prompted us to apply the chelation control to the hydroxytrifluoromethylation reaction. However, addition of Lewis acid $MgBr_2 \cdot OEt_2$, which gave good diastereoselectivites in alkyl radical addition to **29**,[4] was not effective for the hydroxytrifluoromethylation because of the presence of H_2O as Lewis base. The use of $La(OTf)_3$, which is known to coordinate with carbonyl oxygen even in H_2O,[13] instead of $MgBr_2 \cdot OEt_2$ did not improve the diastereoselectivity.[14] The reaction of γ-benzyloxy-α-methylenecarboxylic acid ester **31**[4b,d] also gave hydroxytrifluoromethylated esters **32**[12] in good yield, but with poor diastereoselectivity (entry 8).

The chiral auxiliary-contorolled reactions of glucose derivative **33**, menthol derivative **35** and phenylmenthol derivative **37** were then attempted (entries 9 and 10). The reactions proceeded in moderate yields, but with no diastereoselectivities. The diastereomers of **34**, **36** and **38** were easily separable by silica gel column chromatography, respectively.

The optimized reaction conditions were further applied to the reactions with various alkyl iodides (Table 3). Reactions of **1** with perfluoroalkyl iodides were tested and the corresponding alcohols **39**–**41** were obtained, respectively (entries 1–3). The yield was affected by the number of

Table 3. Hydroxyalkylation of **1** with RI[a]

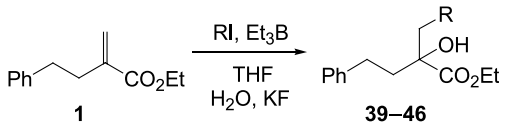

1 **39–46**

Entry	RI	Product	Yield[b]
1	C_2F_5I	**39** (R=C_2F_5)	59 (92)
2	$C_6F_{13}I$	**40** (R=C_6F_{13})	68 (93)
3	*i*-C_3F_7I	**41** (R=*i*-C_3F_7)	35 (88)
4	ICH_2CN	—	nr
5	ICH_2CO_2Et	**42** (R=CH_2CO_2Et)	75 (95)
6	CH_2ClI	**43** (R=CH_2Cl)	22 (69)
7	CH_2I_2	**44** (R=CH_2I)	30 (67)
8	EtI	**45** (R=Et)	18 (33)
9	MeI	**45** (R=Et)	16 (40)
10	*i*-PrI	**45** (R=Et)	7 (13)
		46 (R=*i*-Pr)	9 (16)

[a] Compound **1** was allowed to react with iodide (3 equiv) in the presence of Et_3B (1 equiv), KF and H_2O in THF (10 mL/mmol) at 0 °C and the reaction mixture was stirred for 6 h under N_2 atmosphere.
[b] Isolated yield. Conversion yield in parenthesis.

fluorine atom attached to the radical carbon: $CF_3\cdot > CF_3CF_2\cdot$, $C_5F_{11}CF_2\cdot > i\text{-}(CF_3)_2CF\cdot$.

Entries 4–9 show the results of monosubstituted methyl radical additions in the order of group electronegativity of the substituents.[15] Iodoacetonitrile yielding a highly electron deficient radical was not suitable for the reaction and the starting material was recovered (entry 4). The results suggest that radicals with highly electron-withdrawing substituents (low SOMOs) were not add to electron-deficient α-methylene ester **1** (low LUMO). In entry 5, the electron-deficient radical derived from ethyl iodoacetate gave alcohol **42** in 75% isolated and 95% conversion yields. The reaction with ethyl bromoacetate, however, did not afford the alcohol. These results suggest the reaction contains a halogen-transfer step[16] because the bromine-atom transfer reaction is slower than the iodine-atom transfer reaction.[17] The reaction of alkyl radicals containing a halogen atom such as Cl or I also proceeded (entries 6 and 7).[18] The reaction with ethyl iodide gave hydroxyethylation product **45** in 16% yield (entry 8). Low yields in entries 6–8 may also depend on the low halogen-transfer ability of the iodides. The use of methyl iodide, however, gave hydroxyethylation product **45** in 16% yield instead of the expected hydroxymethylation product (entry 9).[19] Compound **45** was probably formed by the reaction of ethyl radical generated from triethylborane. However, in the absence of methyl iodide, the reaction did not proceed. Methyl iodide may play a role in an iodine-atom transfer step. Addition of I_2, ICH_2CN or $n\text{-}Bu_3SnI$ as an I-donor did not affect the yield. The reaction with isopropyl iodide gave hydroxyisopropylated ester **46** in 9% yield accompanied by hydroxyethylated ester **45** in 7% yield (entry 10).

The above results indicate that (1) the reaction proceeded in a radical manner; (2) the hydroxyl group in the products originated from H_2O and (3) the reaction contains a halogen-transfer step. To confirm the fact that the hydroxyl group in the product originated from H_2O, a labeled experiment using $H_2^{18}O$ was performed. As expected, the reaction of **1** with CF_3I in the presence of $H_2^{18}O$ gave ^{18}O-labeled alcohol **2** (HRMS calcd for $C_{14}H_{17}F_3{}^{16}O_2{}^{18}O$ [M^+] 292.1240, found 292.1215). The unlabeled alcohol **2** was not transformed into ^{18}O labeled **2** under radical reaction conditions in the presence of $H_2^{18}O$. Furthermore, the reaction of **1** with CF_3I was performed in the presence of 2 equiv of molecular oxygen[20] to give hydroperoxide **47** in 45% yield (Scheme 2) together with **2** (30% yield; cf. entry 4 in Table 1).

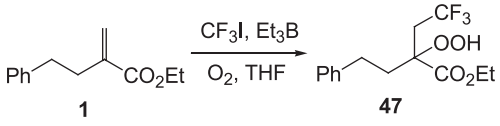

Scheme 2.

A possible reaction pathway for the formation of hydroxyalkylation products is shown in Scheme 3. The addition of an alkyl radical to electron deficient alkene **A** gives radical intermediate **B**. Subsequent iodine-atom transfer reaction may give α-iodo ester **C**,[21] which is then hydrolyzed with

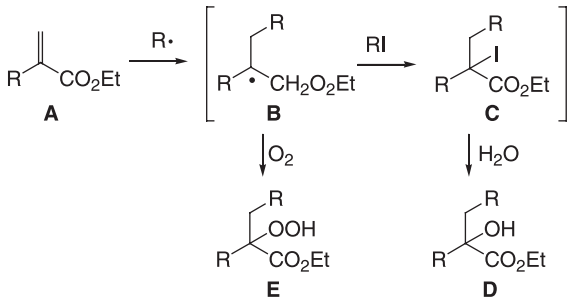

Scheme 3. Possible reaction pathway.

H_2O to give hydroxyalkylated product **D**. The reaction of radical intermediate **B** with molecular oxygen gives hydroperoxide **E**.

The results suggest the reaction proceeds through α-iodo esters, although these intermediates were unstable[21b] under the reaction condition and were not detected in the reaction mixtures. In this case, further radical reactions of the α-iodo esters were suppressed because of their rapid hydrolysis with H_2O. In order to verify the rapid hydrolysis, diethyl 2-iodo-2,4-dimethylpentanedioate (**48**) and ethyl 2-iodo-2-methylpentanoate (**50**) were allowed to react with KF and H_2O in THF (Scheme 4).[22,23] The hydrolysis of iodide **48**, which bears an electron-withdrawing ethoxycarbonyl group β to the quaternary carbon atom, was completed within 6 h and the corresponding *tert*-alcohol **49** was yielded quantitatively. However, the hydrolysis of iodide **50** took 9 h for the conversion to the corresponding alcohol **51**. KF was found to accelerate the hydrolysis of α-iodo esters and without it the hydrolysis was sluggish.

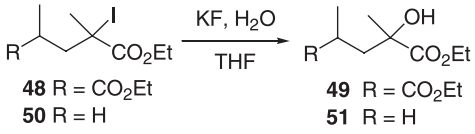

Scheme 4.

2.2. Synthesis of (±)-tanikolide

(*R*)-(+)-Tanikolide is a brine-shrimp toxic and antifungal metabolite newly isolated from the marine cyanobacterium *Lyngbya majuscule* collected from Tanikeli Island, Madagascar.[24] Recently, several syntheses of both racemic

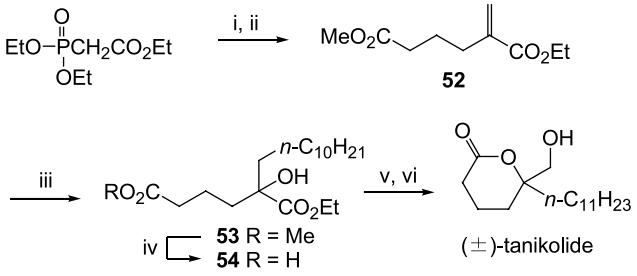

Scheme 5. Reagents and conditions: (i) NaH, DMSO, $Br(CH_2)_3CO_2Me$, 60 °C, 2 h; (ii) HCHO, THF, K_2CO_3, 80 °C, 75% for two steps; (iii) $B(n\text{-}C_{10}H_{21})_3$, $n\text{-}C_{10}H_{21}I$, THF, KF, H_2O, 0 °C, 8 h, 43%; (iv) LiOH, THF, H_2O, 0 °C to rt, 4 h; 1 mol/L HCl (to pH 1), rt, 80%; (v) $NaBH_4$, $CaCl_2$, KOH, EtOH, 24 h; 1 mol/L HCl (to pH 1), 0 °C; (vi) *p*-TsOH, benzene, rt, 3 h, 67% for two steps from **54**.

and (+)-tanikolide have appeared in the literature.[25] To demonstrate the synthetic advantage of our hydroxyalkylation reaction, a short-step total synthesis of (±)-tanikolide was carried out (Scheme 5).

Our synthesis commenced with the alkylation of triethyl phosphonoacetate with methyl 4-bromobutanoate. The alkylation proceeded smoothly using NaH as the base in DMSO at 60 °C. The Horner–Wadsworth–Emmons reaction of the alkylated phosphonoacetate was performed using aqueous formaldehyde and potassium carbonate in THF to yield **52** in 75% yield for two steps. The key hydroxydecylation step was then performed. The use of triethylborane as a radical initiator gave hydroxyethylation product in 11% yield without detection of hydroxydecylation product **53**. The use of tridecylborane[26] yielded desired product **53** in 18% isolated and 90% conversion yields. The use of 2.0 equiv of tridecylborane gave hydroxydecylation product **53** in 43% yield. The selective saponification of the methoxycarbonyl group of **53** with LiOH generated monoester **54** in 80% yield. Finally, the reduction of monoester **54** with $NaBH_4/CaCl_2/KOH$ reduction system,[25d] followed by the lactonization with *p*-TsOH, gave (±)-tanikolide (67% for two steps). The spectroscopic data of the synthetic tanikolide were in accord with those reported previously.[24,25]

3. Conclusion

We have developed a new method of radical hydroxyalkylation of α,β-unsaturated esters using alkyl iodides and trialkylborane in the presence of KF and H_2O. The synthetic advantage of the method was demonstrated by the short-step total synthesis of (±)-tanikolide.

4. Experimental

4.1. General

^{1}H NMR spectra were recorded on a JEOL GSX-270 (270 MHz) or GSX-400 (400 MHz) spectrometer with $CDCl_3$ as the solvent and tetramethylsilane as an internal standard. ^{13}C NMR spectra were recorded on the instruments operating at 67.9 or 100.5 MHz with $CDCl_3$ as the solvent and internal standard (δ 77.0). IR spectra were taken on a SHIMADZU FTIR-8700 spectrometer. Mass spectra (EI^+) were obtained on a JEOL JMS-700 mass spectrometer. Precoated Merck Kieselgel 60 F_{254} and Kanto silica gel 60 (spherical neutral) were used for thin layer chromatography and flash chromatography, respectively.

For the preparation of **29** and **31**, see Ref. 4d. Substrates **21**,[27] **27**,[28] **33**,[29] **35**[30], and **37**[31] were prepared according to the literature procedures. Substrates **17** and **19** were purchased from TCI Japan. Iodides **48** and **50** were prepared following the procedures reported in the literature.[22,23]

4.1.1. Ethyl 2-phenethyl-2-propenoate 1. To a suspension of NaH (220 mg of a 60% dispersion in mineral oil, 5.5 mmol) in DMSO (5 mL) was added triethyl phosphonoacetate (0.99 mL, 5.0 mmol) at room temperature and the mixture was stirred for 30 min. (2-Iodoethyl)benzene (905 mg, 5.0 mmol) was then added dropwise. The reaction mixture was heated at 60 °C for 2 h. The reaction was quenched with H_2O and the aqueous layer was extracted with ethyl acetate three times. The combined oraganic layers were dried over sodium sulfate and the extract was evaporated. To a solution of the residue in THF (5 mL) were added aqueous potassium carbonate (1 g dissolved in 2.5 mL of H_2O) and aqueous formaldehyde (37%, 5 mL) and the mixture was heated at 80 °C for 2 h. The product was extracted with ethyl acetate, and the organic layer was dried over sodium sulfate and evaporated. The residue was chromatographed on silica gel to give **1** (673 mg, 66%). Colorless oil; ^{1}H NMR (400 MHz) δ 1.32 (t, J=7.2 Hz, 3H, OCH_2CH_3), 2.61 (t, J=7.2 Hz, 2H, CH_2), 2.79 (t, J=7.2 Hz, 2H, CH_2), 4.22, (q, J=7.2 Hz, 2H, OCH_2CH_3), 5.50 (s, 1H, C=C*H*H), 6.15 (s, 1H, C=CH*H*), 7.18 (m, 3H, arom), 7.28 (m, 2H, arom); ^{13}C NMR (100 MHz) δ 14.3, 34.0, 35.0, 60.7, 125.0, 125.8, 128.2, 128.4, 140.0, 141.3, 167.0; IR (neat, cm^{-1}) 2931, 1716, 1631, 1497, 1454, 1396, 1257, 1184, 1134, 1029, 945, 818, 748, 698; MS *m*/*z* 204 (M^+, 16%), 158 (23), 130 (33), 91 (100); HRMS calcd for $C_{13}H_{16}O_2$ [M^+] 204.1150, found 204.1139.

4.1.2. Methyl 2-phenethyl-2-propenoate 5. The hydrolysis of ester **1** (1.02 g, 5 mmol) with 2.0 equiv of sodium hydroxide in refluxing ethanol gave 2-phenethyl-2-propenoic acid (761 mg, 86%). To a solution of the carboxylic acid (52 mg, 0.3 mmol) and triphenylphosphine (236 mg, 0.9 mmol) in THF (1.5 mL) were added methanol (18 μL, 0.45 mmol) and diisopropyl azodicarboxylate (59 μL, 0.3 mmol). The mixture was stirred at room temperature for 5 h. After evaporation of the solvent, the residue was chromatographed on silica gel to give methyl ester **5** (48 mg, 84%). Colorless oil; ^{1}H NMR (400 MHz) δ 2.62 (t, J=6.8 Hz, 2H, CH_2), 2.79 (t, J=6.8 Hz, 2H, CH_2), 3.76 (s, 3H, CH_3), 5.50 (s, 1H, C=C*H*H), 6.15 (s, 1H, C=CH*H*), 7.18 (m, 3H, arom), 7.28 (m, 2H, arom); ^{13}C NMR (100 MHz) δ 33.9, 34.9, 51.8, 125.3, 125.8, 128.2, 128.4, 139.7, 141.2, 167.4; IR (neat, cm^{-1}) 2951, 1720, 1632, 1439, 1199, 1138, 945, 698; MS *m*/*z* 190 (M^+, 14%), 158 (15), 130 (30), 91 (100); HRMS calcd for $C_{12}H_{14}O_2$ [M^+] 190.0994, found 190.0975.

4.1.3. Isopropyl 2-phenethyl-2-propenoate 7. Compound **7** was prepared following the procedure described for **5** except for the use of 2-propanol instead of methanol (84%). Colorless oil; ^{1}H NMR (400 MHz, $CDCl_3$) δ 1.26 (d, J=6.3 Hz, 6H, $CH_3\times2$), 2.61 (t, J=9.3 Hz, 2H, CH_2), 2.78 (t, J=9.3 Hz, 2H, CH_2), 5.09 (septet, J=6.3 Hz, 1H, CH), 5.47 (s, 1H, C=C*H*H), 6.13 (s, 1H, C=CH*H*), 7.17–7.31 (m, 5H, arom); ^{13}C NMR (100 MHz, $CDCl_3$) δ 21.9, 34.0, 35.0, 68.0, 124.7, 125.8, 128.2, 128.4, 140.4, 141.4, 166.5; IR (neat, cm^{-1}) 2982, 1712, 1258, 1107, 748, 698; MS *m*/*z* 218 (M^+, 4%), 176 (26), 130 (25), 91 (100); HRMS calcd for $C_{14}H_{18}O_2$ [M^+] 218.1307, found 218.1298.

4.1.4. Phenyl 2-phenethyl-2-propenoate 9. To a solution of 2-phenethyl-2-propenoic acid (176 mg, 1.0 mmol) and dicyclohexylcarbodiimide (247 mg, 1.2 mmol) in CH_2Cl_2 (2 mL) was added phenol (188 mg, 2.0 mmol). The mixture was stirred at room temperature for 2 days. The reaction was quenched with 0.5 mol/L HCl aqueous solution and the

product was extracted with ethyl acetate. The organic layer was washed with aqueous $NaHCO_3$ and dried over sodium sulfate. After evaporation of the solvent, the residue was chromatographed on silica gel to give phenyl ester **9** (183 mg, 76%). Colorless oil; ^{1}H NMR (400 MHz, $CDCl_3$) δ 2.73 (t, J=7.3 Hz, 2H, CH_2), 2.88 (t, J=7.3 Hz, 2H, CH_2), 5.69 (s, 1H, C=C*H*H), 6.39 (s, 1H, C=CH*H*), 7.11 (d, J=7.6 Hz, 2H, arom), 7.18–7.37 (m, 6H, arom), 7.39 (t, J=8.3 Hz, 2H, arom); ^{13}C NMR (100 MHz, $CDCl_3$) δ 34.0, 35.0, 121.5, 125.7, 125.9, 127.1, 128.3, 128.4, 129.3, 139.3, 141.1, 150.7, 165.4; IR (neat, cm^{-1}) 2928, 1732, 1492, 1195, 1165, 1111, 748, 691; MS *m/z* 252 (M^+, 3%), 209 (100), 131 (32), 91 (35); HRMS calcd for $C_{17}H_{16}O_2$ [M^+] 252.1150, found 252.1155.

4.1.5. 2-Methylene-4-phenyl-1-piperidino-1-butanone 11. To a solution of 2-phenethyl-2-propenoic acid (88 mg, 0.5 mmol) in CH_2Cl_2 (2 mL) was added triethylamine (0.1 mL, 0.75 mmol). To the reaction mixture cooled to 0 °C, was added pivaloyl chloride (92 μL, 0.75 mmol) and the mixture was stirred at the temperature for 1 h. To the reaction mixture was added a solution of piperidine (74 μL, 0.75 mmol), triethylamine (1 mL) and 4-dimethylaminopyridine (49 mg, 0.4 mmol) in CH_2Cl_2 (2 mL) at 0 °C and the mixture was stirred at room temperature for 6 h. The reaction was quenched with aqueous ammonium chloride and the aqueous layer was extracted with ethyl acetate. The organic layer was dried over sodium sulfate. After evaporation of the solvent, the residue was chromatographed on silica gel to give amide **11** (107 mg, 88%). Colorless oil; ^{1}H NMR (400 MHz, $CDCl_3$) δ 1.43–1.65 (m, 6H, piperidinyl), 2.61 (t, J=8.7 Hz, 2H, CH_2), 2.80 (t, J=8.7 Hz, 2H, CH_2), 3.41 (br, 2H, piperidinyl), 3.59 (br, 2H, piperidinyl), 5.05 (s, 1H, C=C*H*H), 5.17 (s, 1H, C=CH*H*), 7.16–7.30 (m, 5H, arom); ^{13}C NMR (100 MHz, $CDCl_3$) δ 24.6, 25.7, 26.6, 33.7, 35.8, 42.4, 48.0, 114.0, 125.9, 128.2 (2C), 141.0, 144.3, 170.3; IR (neat, cm^{-1}) 2936, 2855, 1616, 1439, 698; MS *m/z* 243 (M^+, 80%), 228 (10), 152 (100), 138 (33); HRMS calcd for $C_{16}H_{21}NO$ [M^+] 243.1623, found 243.1614.

4.1.6. Ethyl 2-hexylpropenoate 15. Compound **15** was prepared following the procedure described for **1** except for the use of hexyl iodide instead of (2-iodoethyl)benzene (58%). Pale yellow oil; ^{1}H NMR (270 MHz) δ 0.89 (t, J=7.0 Hz, 3H, CH_3), 1.30 (t, J=7.0 Hz, 3H, OCH_2CH_3), 1.22–1.50 (m, 8H), 2.29 (m, 2H), 4.20 (q, J=7.0 Hz, 2H, OCH_2CH_3), 5.50 (s, 1H, C=C*H*H), 6.11 (s, 1H, C=CH*H*); ^{13}C NMR (67.8 MHz) δ 14.2, 14.3, 22.7, 28.4, 29.0, 31.7, 31.9, 60.5, 124.0, 141.0, 167.2; IR (neat, cm^{-1}) 2928, 2858, 1720, 1184, 1153, 1030, 941; MS *m/z* 184 (M^+, 15%), 139 (39), 115 (100), 102 (69), 87 (66); HRMS calcd for $C_{11}H_{20}O_2$ [M^+] 184.1464, found 184.1463.

4.1.7. Diethyl 2-methylenehexanedioate 23. Compound **23** was prepared following the procedure described for **1** except for the use of ethyl 4-bromobutanoate instead of (2-iodoethyl)benzene (75%). Colorless oil; ^{1}H NMR (400 MHz) δ 1.26 (t, J=7.2 Hz, 3H, OCH_2CH_3), 1.31 (t, J=7.2 Hz, 3H, OCH_2CH_3), 1.82 (quintet, J=7.6 Hz, 2H, $CH_2CH_2CH_2$) 2.33 (t, J=7.6 Hz, 2H, $CH_2CH_2CH_2$), 2.37 (t, J=7.6 Hz, 2H, $CH_2CH_2CH_2$), 4.13 (q, J=7.2 Hz, 2H, OCH_2CH_3), 4.23 (q, J=7.2 Hz, 2H, OCH_2CH_3), 5.55 (s, 1H, C=CH*H*), 6.18 (s, 1H, C=CH*H*); ^{13}C NMR (67.8 MHz) δ 14.2, 14.3, 23.6, 31.2, 33.6, 60.3, 60.6, 125.0, 139.8, 166.9, 173.2; IR (neat, cm^{-1}) 2982, 1732, 1632, 1373, 1180, 1138, 1030, 945, 818; MS *m/z* 169 (M^+-CO_2Et, 100%), 140 (94), 112 (73), 95 (56), 67 (85); HRMS calcd for $C_9H_{13}O_3$ [M^+-OEt] 169.0865, found 169.0869.

4.1.8. Ethyl 2-phenethyl-2-butenoates 25. Compound **15** was prepared following the procedure described for **1** except for the use of acetaldehyde instead of formaldehyde (64%). MS *m/z* 218 (M^+, 14%), 172 (51), 91 (100); HRMS calcd for $C_{14}H_{18}O_2$ [M^+] 218.1306, found 218.1300. *Major (E) isomer*. Colorless oil; ^{1}H NMR (270 MHz) δ 1.30 (t, J=7.0 Hz, 3H, OCH_2CH_3), 1.62 (d, J=7.3 Hz, 3H, CH_3), 2.61 (m, 2H, CH_2CH_2), 2.68 (m, 2H, CH_2CH_2), 4.19 (q, J=7.0 Hz, 2H, OCH_2CH_3), 6.86 (q, J=7.3 Hz, 1H, C=CH), 6.82–7.29 (m, 5H, arom);^{13}C NMR (67.8 MHz) δ 14.0, 14.4, 28.8, 35.2, 60.3, 125.7, 128.1, 128.4, 132.3, 137.8, 141.7, 167.5. *Minor (Z) isomer*. Colorless oil; ^{1}H NMR (270 MHz) δ 1.32 (t, J=7.0 Hz, 3H, OCH_2CH_3), 1.95 (d, J=7.3 Hz, 3H, CH_3), 2.61 (m, 2H, CH_2CH_2), 2.68 (m, 2H, CH_2CH_2), 4.23 (q, J=7.0 Hz, 2H, OCH_2CH_3), 5.94 (q, J=7.3 Hz, 1H, C=CH), 6.82–7.29 (m, 5H, arom); ^{13}C NMR (67.8 MHz) δ 14.4, 15.7, 35.8, 36.8, 60.0, 125.7, 128.1, 128.4, 132.1, 137.0, 141.6, 167.7.

4.1.9. Diethyl 2-iodo-2,4-dimethylpentanedioate 48. Pale yellow oil; MS *m/z* 297 (M^+-OEt, 20%), 215 (42), 169 (56), 142 (25), 113 (100); HRMS calcd for $C_9H_{14}IO_3$ [M^+-OEt] 296.9988, found 297.0033. *Major diasteromer*. ^{1}H NMR (400 MHz) δ 1.25 (d, J=7.2 Hz, 3H, CH_3), 1.24–1.32 (m, 6H, $OCH_2CH_3\times2$), 2.04 (s, 3H, CH_3), 2.26 (dd, J=2.7, 14.9 Hz, 1H, C*H*H), 2.54 (dd, J=8.8, 14.9 Hz, 1H, CH*H*), 2.66 (m, 1H, CH), 4.10–4.25 (m, 4H, $OCH_2CH_3\times2$); ^{13}C NMR (100 MHz) δ 13.7, 14.2, 19.5, 30.0, 39.1, 39.4, 47.0, 60.7, 62.0, 172.4, 175.8. *Minor diasteromer*. ^{1}H NMR (400 MHz) δ 1.18 (d, J=7.2 Hz, 3H, CH_3), 1.24–1.32 (m, 6H, $OCH_2CH_3\times2$), 2.02 (s, 3H, CH_3), 2.37 (m, 1H, CH), 2.45 (m, 1H, C*H*H), 2.81 (dd, J=8.3, 14.4 Hz, 1H, CH*H*), 4.10–4.25 (m, 4H, $OCH_2CH_3\times2$); ^{13}C NMR (100 MHz) δ 13.7, 14.2, 19.1, 30.1, 38.6, 41.3, 47.9, 60.8, 62.0, 172.5, 175.8.

4.1.10. Diethyl 2-hydroxy-2,4-dimethylpentanedioate 49. IR (neat, cm^{-1}) 3498, 2985, 2939, 1747, 1458, 1381, 1308, 1199, 1107, 1061, 1030, 964. *Less polar major diastereomer*. Colorless oil; ^{1}H NMR (400 MHz) δ 1.19 (d, J=7.1 Hz, 3H, CH_3), 1.25 (t, J=7.3 Hz, 3H, OCH_2CH_3), 1.30 (t, J=7.3 Hz, 3H, OCH_2CH_3), 1.41 (s, 3H, CH_3), 1.70 (dd, J=3.9, 12.4 Hz, 1H, C*H*H), 2.31 (dd, J=9.1, 12.4 Hz, 1H, CH*H*), 2.65 (ddt, J=3.9, 9.1, 7.1 Hz, 1H, CH), 3.22 (s, 1H, OH), 4.09 (m, 2H, OCH_2CH_3), 4.18 (dq, J=10.8, 7.3 Hz, 1H, $OCHHCH_3$), 4.22 (dq, J=10.8, 7.3 Hz, 1H, $OCHHCH_3$); ^{13}C NMR (100 MHz) δ 14.1, 14.2, 19.1, 26.1, 35.1, 43.1, 60.4, 62.0, 73.5, 176.5, 176.6; MS *m/z* 187 (M^+-OEt, 7%), 159 (17), 113 (100); HRMS calcd for $C_9H_{15}O_4$ [M^+-OEt] 187.0970, found 187.0932. *More polar minor diasteromer*. Colorless oil; ^{1}H NMR (400 MHz) δ 1.13 (d, J=7.1 Hz, 3H, CH_3), 1.26 (t, J=7.3 Hz, 3H, OCH_2CH_3), 1.31 (t, J=7.3 Hz, 3H, OCH_2CH_3), 1.39 (s, 3H, CH_3), 1.85 (dd, J=4.4, 14.4 Hz, 1H, C*H*H), 2.31 (dd, J=9.2, 14.4 Hz, 1H, CH*H*), 2.48 (ddt, J=4.4, 9.2,

7.1 Hz, 1H, CH), 3.33 (s, 1H, OH), 4.13 (q, J=7.3 Hz, 2H, OCH_2CH$_3$), 4.25 (q, J=7.3 Hz, 2H, OCH_2CH$_3$); ^{13}C NMR (100 MHz) δ 14.1, 14.2, 18.5, 27.0, 36.0, 43.2, 60.4, 62.0, 74.0, 176.7, 176.8; MS m/z 187 (M^+-OEt, 7%), 159 (17), 113 (100); HRMS calcd for $C_9H_{15}O_4$ [M^+-OEt] 187.0970, found 187.0932.

4.1.11. Ethyl 2-iodo-2-methylpentanoate 50. Pale yellow oil; ^{1}H NMR (400 MHz) δ 0.97 (t, J=7.3 Hz, 3H, CH$_3$), 1.27 (m, 1H, CHH), 1.29 (t, J=7.3 Hz, 3H, OCH$_2$CH_3), 1.47 (m, 1H, CHH), 2.03 (s, 3H, CH$_3$), 2.05 (ddd, J=4.8, 11.6, 14.0 Hz, 1H, CHH), 2.14 (ddd, J=5.2, 12.0, 14.0 Hz, 1H, CHH), 4.23 (q, J=7.3 Hz, 2H, OCH_2CH$_3$); ^{13}C NMR (67.8 MHz) δ 13.8, 13.9, 20.9, 30.3, 41.5, 46.8, 61.8, 172.8; MS m/z 270 (M^+, 1%), 197 (10), 143 (72), 115 (50), 69 (100); $C_8H_{15}IO_2$ [M^+] 270.0117, found 270.0081.

4.1.12. Ethyl 2-hydroxy-2-methylpentanoate 51. Colorless oil; ^{1}H NMR (400 MHz) δ 0.91 (t, J=7.2 Hz, 3H, CH$_3$), 1.16 (m, 1H, CHH), 1.30 (t, J=7.2 Hz, 3H, OCH$_2$CH_3), 1.39 (s, 3H, CH$_3$), 1.47 (m, 1H, CHH), 1.62 (ddd, J=4.4, 11.6, 13.4 Hz, 1H, CHH), 1.73 (ddd, J=5.2, 12.0, 13.4 Hz, 1H, CHH), 3.16 (s, 1H, OH), 4.23 (q, J=7.2 Hz, 2H, OCH_2CH$_3$); ^{13}C NMR (67.8 MHz) δ 14.3, 14.4, 17.1, 26.2, 42.4, 61.8, 74.5, 177.2.

4.2. Radical reactions

General procedure for the hydroxytrifluoromethylation. To a solution of α-methylene ester (0.15 mmol) in THF (1.5 mL) were added KF (200 mg) and H_2O (11 μL, 4 equiv). To the suspension cooled to −30 °C were added trifluoromethyl iodide (gaseous, ca. 3 equiv) and triethylborane (1.06 mol/mL in hexane; 0.15 mmol, 1 equiv). The mixture was stirred at room temperature for 6 h. After filtration, the solvent was evaporated in vacuo. The residue was purified by flash chromatography on silica gel to give the product.

General procedure for the hydroxyalkylation with alkyl iodides other than trifluoromethyl iodide. To a solution of α-methylene ester (0.15 mmol) in THF (1.5 mL) were added KF (200 mg) and H_2O (11 μL, 4 equiv). To the suspension cooled to 0 °C were added alkyl iodide (0.45 mmol, 3 equiv) and triethylborane (1.06 mol/mL in hexane; 0.15 mmol, 1 equiv). The mixture was stirred at 0 °C for 6 h. After filtration, the solvent was evaporated in vacuo. The residue was purified by flash chromatography on silica gel to give the product.

4.2.1. Ethyl 4,4,4-trifluoro-2-hydroxy-2-phenethylbutanoate 2. Colorless oil; ^{1}H NMR (400 MHz) δ 1.32 (t, J=7.2 Hz, 3H, OCH$_2$CH_3), 2.04 (ddd, J=5.6, 12.0, 13.6 Hz, 1H, CHH), 2.05 (ddd, J=5.6, 12.0, 13.6 Hz, 1H, CHH), 2.49 (ddd, J=5.6, 11.2, 13.6 Hz, 1H, CHH), 2.58 (dq, J=15.2, 10.4 Hz, 1H, CF$_3$CHH), 2.68 (dq, J=15.2, 10.4 Hz, 1H, CF$_3$CHH), 2.81 (ddd, J=5.6, 11.2, 13.6 Hz, 1H, CHH), 3.61 (s, 1H, OH), 4.27 (m, 2H, OCH_2CH$_3$), 7.15–7.30 (m, 5H, arom); ^{13}C NMR (100 MHz) δ 14.1, 29.3, 41.5, 42.3 (q, J_{C-F}=27.3 Hz, CF$_3$CH_2), 62.8, 73.3 (q, J_{C-F}=2.8 Hz, CF$_3$CH$_2$C), 125.2 (q, J_{C-F}=276.2 Hz, CF$_3$), 126.1, 128.3, 128.4, 140.6, 174.1; IR (neat, cm^{-1}) 3514, 3028, 1736, 1605, 1497, 1454, 1369, 1273, 1242, 1196, 1134, 1076, 1014, 895, 702; MS m/z 290 (M^+, 3%), 217 (10), 186 (100); HRMS calcd for $C_{14}H_{17}F_3O_3$ [M^+] 290.1130, found 290.1158.

4.2.2. Methyl 4,4,4-trifluoro-2-hydroxy-2-phenethylbutanoate 6. Colorless oil; ^{1}H NMR (400 MHz) δ 2.03 (m, 2H, CH$_2$), 2.42 (ddd, J=5.9, 11.7, 13.7 Hz, 1H, CHH), 2.59 (dq, J=15.1, 10.2 Hz, 1H, CF$_3$CHH), 2.63 (dq, J=15.1, 10.2 Hz, 1H, CF$_3$CHH), 2.82 (ddd, J=5.9, 10.7, 13.7 Hz, 1H, CHH), 3.57 (s, 1H, OH), 3.79 (s, 3H, Me), 7.14–7.30 (m, 5H, arom); ^{13}C NMR (100 MHz) δ 29.3, 41.4, 42.6 (q, J_{C-F}=27.3 Hz, CF$_3$CH_2), 53.4, 73.5 (q, J_{C-F}=1.8 Hz, CF$_3$CH$_2$C), 125.1 (q, J_{C-F}=276.2 Hz, CF$_3$), 126.1, 128.3, 128.4, 140.5, 174.6; IR (neat, cm^{-1}) 3524, 2959, 1736, 1458, 1273, 1130; MS m/z 276 (M^+, 3%), 217 (10), 172 (100), 91 (72); HRMS calcd for $C_{13}H_{15}F_3O_3$ [M^+] 276.0973, found 276.0955.

4.2.3. Isopropyl 4,4,4-trifluoro-2-hydroxy-2-phenethylbutanoate 8. Colorless oil; ^{1}H NMR (400 MHz) δ 1.31 (d, J=6.3 Hz, 3H, CH$_3$), 1.32 (d, J=6.3 Hz, 3H, CH$_3$), 2.01 (m, 2H, CH$_2$), 2.39 (ddd, J=6.0, 12.3, 13.2 Hz, 1H, CHH), 2.55 (dq, J=15.2, 10.8 Hz, 1H, CF$_3$CHH), 2.67 (dq, J=15.2, 10.8 Hz, 1H, CF$_3$CHH), 2.79 (ddd, J=6.0, 10.7, 13.2 Hz, 1H, CHH), 3.62 (s, 1H, OH), 5.14 (sep, J=6.3 Hz, 1H, CH), 7.13–7.30 (m, 5H, arom); ^{13}C NMR (100 MHz) δ 21.5, 21.9, 29.4, 42.0, 42.5 (q, J_{C-F}=27.3 Hz, CF$_3$CH_2), 71.0, 73.3, 125.2 (q, J_{C-F}=276.2 Hz, CF$_3$), 126.4, 128.3, 128.5, 140.7, 173.6; IR (neat, cm^{-1}) 3512, 2986, 1732, 1377, 1273, 1200, 1134, 1103, 698; MS m/z 217 (M^+-CO$_2i$-Pr, 10%), 158 (15), 158 (15), 105 (23), 91 (100); HRMS calcd for $C_{11}H_{12}F_3O$ [M^+-CO$_2i$-Pr] 217.0841, found 217.0840.

4.2.4. Phenyl 4,4,4-trifluoro-2-hydroxy-2-phenethylbutanoate 10. Colorless oil; ^{1}H NMR (400 MHz) δ 2.16 (ddd, J=4.9, 12.2, 13.7 Hz, 1H, CHH), 2.28 (ddd, J=4.9, 13.7, 13.7 Hz, 1H, CHH), 2.61 (ddd, J=5.2, 13.2, 13.2 Hz, 1H, CHH), 2.73 (dq, J=15.2, 10.4 Hz, 1H, CF$_3$CHH), 2.89 (dq, J=15.2, 10.4 Hz, 1H, CF$_3$CHH), 2.94 (m, 1H, CHH), 3.56 (s, 1H, OH), 7.07 (d, J=7.6 Hz, 2H, arom), 7.21–7.33 (m, 6H, arom), 7.43 (t, J=7.2 Hz, 2H, arom); ^{13}C NMR (100 MHz) δ 29.5, 41.8, 42.7 (q, J_{C-F}=27.3 Hz, CF$_3$CH_2), 73.8 (q, J_{C-F}=2.7 Hz, CF$_3$CH$_2$C), 120.9, 122.5 (q, J_{C-F}=276.2 Hz, CF$_3$), 126.3, 126.6, 128.3, 128.7, 129.7, 140.4, 150.0, 173.0; IR (neat, cm^{-1}) 3511, 1759, 1493, 1269, 1192, 1165, 1126, 748, 698; MS m/z 217 (M^+-CO$_2$Ph, 2%), 133 (10), 105 (21), 94 (87), 91 (100); HRMS calcd for $C_{11}H_{12}F_3O$ [M^+-CO$_2$Ph] 217.0841, found 217.0831.

4.2.5. 4,4,4-Trifluoro-2-hydroxy-2-phenethyl-1-piperidino-1-butanone 12. Colorless oil; ^{1}H NMR (400 MHz) δ 1.57–1.77 (m, 6H, piperidine), 2.10 (m, 2H, CH$_2$), 2.41 (ddd, J=6.0, 11.2, 13.6 Hz, 1H, CHH), 2.62 (dq, J=16.0, 10.4 Hz, 1H, CF$_3$CHH), 2.67 (dq, J=16.0, 10.4 Hz, 1H, CF$_3$CHH), 2.86 (ddd, J=6.0, 11.2, 14.0 Hz, 1H, CHH), 3.55 (br, 4H, piperidine), 5.41 (s, 1H, OH), 7.15–7.33 (m, 5H, arom); ^{13}C NMR (100 MHz) δ 24.3, 25.4, 25.8, 29.6, 41.3, 43.1 (q, J_{C-F}=27.5 Hz, CF$_3$CH_2), 72.9, 125.3 (q, J_{C-F}=277.2 Hz, CF$_3$), 126.0, 128.3, 128.4, 141.0, 170.4; IR (neat, cm^{-1}) 3344, 2939, 2858, 1627, 1454, 1269, 1126, 698. MS m/z 329 (M^+, 1%), 225 (69), 113 (28), 112 (38), 91

(100); HRMS calcd for $C_{17}H_{22}F_3NO_2$ [M^+] 329.1603, found 329.1593.

4.2.6. 3-Hydroxy-5-phenyl-3-(2,2,2-trifluoroethyl)tetrahydrofuran-2-ones 14. Colorless oil; IR (neat, cm^{-1}) 3433, 1778, 1379, 1333, 1261, 1194, 1142, 1016, 961, 700; MS *m/z* 260 (M^+, 4%), 217 (10), 216 (89), 133 (56), 105 (100); HRMS calcd for $C_{12}H_{11}F_3O_3$ [M^+] 260.0660, found 260.0669. *Major diastereomer*. ^{1}H NMR (270 MHz) δ 2.68 (dq, J=16.8, 10.8 Hz, 1H, CF_3CHH), 2.51 (dd, J=8.9, 14.0 Hz, 1H, C*H*H), 2.72 (dq, J=16.8, 10.8 Hz, 1H, CF_3CHH), 2.91 (s, 1H, OH), 3.05 (dd, J=6.5, 14.0 Hz, 1H, CH*H*), 5.45 (dd, J=6.5, 8.9 Hz, 1H, C*H*Ph), 7.14–7.32 (m, 5H, arom); ^{13}C NMR (100 MHz) δ 40.2 (q, J_{C-F}=28.2 Hz, CF_3CH_2), 42.4, 73.1, 78.3, 124.8 (q, J_{C-F}=277.0 Hz, CF_3), 125.7, 128.8, 129.0, 137.5, 176.5. *Minor diastereomer*. ^{1}H NMR (270 MHz) δ 2.29 (dd, J=10.0, 13.8 Hz, 1H, C*H*H), 2.52 (dq, J=16.6, 10.0 Hz, 1H, CF_3CHH), 2.55 (s, 1H, OH), 2.85 (m, 1H, CF_3CHH), 2.88 (dd, J=5.1, 13.8 Hz, 1H, CH*H*), 5.73 (dd, J=5.1, 10.0 Hz, 1H, C*H*Ph), 7.14–7.32 (m, 5H, arom); ^{13}C NMR (100 MHz) δ 39.9 (q, J_{C-F}=27.4 Hz, CF_3CH_2), 43.5, 73.5 (q, J_{C-F}=2.4 Hz, CF_3CH_2C), 79.9, 125.2 (q, J_{C-F}=277.0 Hz, CF_3), 125.4, 125.7, 128.8, 137.4, 175.2.

4.2.7. Ethyl 2-hydroxy-2-(2,2,2-trifluoroethyl)octanoate 16. Colorless oil; ^{1}H NMR (270 MHz) δ 0.87 (m, 3H, CH_3), 1.08 (m, 1H), 1.29 (m, 6H), 1.31 (t, J=7.3 Hz, 3H, OCH_2CH_3), 1.43 (m, 1H), 1.68 (m, 2H), 2.56 (dq, J=14.9, 10.5 Hz, 1H, CF_3CHH), 2.63 (dq, J=14.9, 10.5 Hz, 1H, CF_3CHH), 3.48 (s, 1H, OH), 4.29 (q, J=7.3 Hz, 2H, OCH_2CH_3); ^{13}C NMR (67.8 MHz) δ 14.06, 14.09, 22.5, 28.9, 29.1, 31.6, 39.9, 42.4 (q, J_{C-F}=26.8 Hz, CF_3CH_2), 62.6, 73.6 (q, J_{C-F}=2.2 Hz, CF_3CH_2C), 125.3 (q, J_{C-F}=278.3 Hz, CF_3), 174.3; IR (neat, cm^{-1}) 3487, 2959, 2932, 2860, 2349, 1738, 1454, 1369, 1261, 1198, 1146, 1103, 1018. MS *m/z* 225 (M^+-OEt, 18%), 197 (100), 179 (56); HRMS calcd for $C_{10}H_{16}F_3O_2$ [M^+-OEt] 225.1103, found 225.1099.

4.2.8. Dimethyl 2-hydroxy-2-(2,2,2-trifluoroethyl) butanedioate 18. Colorless oil; ^{1}H NMR (270 MHz) δ 2.63 (q, J=5.3 Hz, 2H, CH_2CF_3), 2.79 (d, J=10.9 Hz, 1H, C*H*H), 2.95 (d, J=10.9 Hz, 1H, CH*H*), 3.71 (s, 3H, CH_3), 3.86 (s, 3H, CH_3), 3.95 (s, 1H, OH); ^{13}C NMR (100 MHz) δ 42.2 (q, J_{C-F}=27.5 Hz, CF_3CH_2), 43.2, 52.2, 53.6, 71.8 (q, J_{C-F}=2.7 Hz, CF_3CH_2C), 124.7 (q, J_{C-F}=276.8 Hz, CF_3), 169.9, 173.1; IR (neat, cm^{-1}) 3498, 2959, 1751, 1732, 1447, 1146, 1126, 964; MS *m/z* 185 (M^+-CO_2Me, 100%), 153 (93), 111 (75); HRMS calcd for $C_6H_8F_3O_3$ [M^+-CO_2Me] 185.0425, found 185.0397.

4.2.9. Diethyl 2-hydroxy-2-(2,2,2-trifluoroethyl)butanedioate 20. Colorless oil; ^{1}H NMR (270 MHz) δ 1.26 (t, J=6.8 Hz, 3H, OCH_2CH_3), 1.32 (t, J=6.8 Hz, 3H, OCH_2CH_3), 2.63 (q, J=5.3 Hz, 2H, CH_2CF_3), 2.75 (d, J=15.6 Hz, 1H, C*H*H), 2.93 (d, J=15.6 Hz, 1H, CH*H*), 3.97 (s, 1H, OH), 4.15 (q, J=6.8 Hz, 2H, OCH_2CH_3), 4.31 (q, J=6.8 Hz, 2H, OCH_2CH_3); ^{13}C NMR (100 MHz) δ 13.9, 14.1, 42.2 (q, J_{C-F}=28.2 Hz, CF_3CH_2), 43.5, 61.2, 62.9, 71.8 (q, J_{C-F}=2.3 Hz, CF_3CH_2C), 122.6 (q, J_{C-F}=265 Hz, CF_3), 169.4, 172.7; IR (neat, cm^{-1}) 3502, 2986, 1740, 1373, 1200, 1165, 1138; MS *m/z* 199 (M^+-CO_2Et, 76%), 153 (100), 111 (46); HRMS calcd for $C_7H_{10}F_3O_3$ [M^+-CO_2Et] 199.0582, found 199.0592.

4.2.10. Diethyl 2-hydroxy-2-(2,2,2-trifluoroethyl) pentanedioate 22. Colorless oil; ^{1}H NMR (270 MHz) δ 1.25 (t, J=7.2 Hz, 3H, OCH_2CH_3), 1.32 (t, J=7.2 Hz, 3H, OCH_2CH_3), 2.08 (m, 2H, CH_2CF_3), 2.20 (ddd, J=5.4, 9.7, 15.6 Hz, 1H, C*H*H), 2.49 (ddd, J=6.8, 9.7, 15.6 Hz, 1H, C*H*H), 2.55 (dq, J=15.1, 10.2 Hz, 1H, CF_3CHH), 2.69 (dq, J=15.1, 10.2 Hz, 1H, CF_3CHH), 3.57 (s, 1H, OH), 4.15 (q, J=7.2 Hz, 2H, OCH_2CH_3), 4.27 (dq, J=10.8, 7.2 Hz, 1H, $OCHHCH_3$), 4.32 (dq, J=10.8, 7.2 Hz, 1H, $OCHHCH_3$); ^{13}C NMR (100 MHz) δ 14.0, 14.2, 28.2, 34.5, 42.4 (q, J_{C-F}=27.2 Hz, CF_3CH_2), 60.7, 63.0, 72.8 (q, J_{C-F}=2.5 Hz, CF_3CH_2C), 125.0 (q, J_{C-F}=275 Hz, CF_3), 172.5, 173.8; IR (neat, cm^{-1}) 3500, 1986, 1736, 1373, 1273, 1242, 1192, 1134, 1018; MS *m/z* 241 (M^+-OEt, 13%), 213 (32), 167 (100); HRMS calcd for $C_9H_{12}F_3O_4$ [M^+-OEt] 241.0687, found 241.0697.

4.2.11. Diethyl 2-hydroxy-2-(2,2,2-trifluoroethyl)hexanedioate 24. Colorless oil; ^{1}H NMR (270 MHz) δ1.25 (t, J=7.2 Hz, 3H, OCH_2CH_3), 1.32 (t, J=7.2 Hz, 3H, OCH_2CH_3), 1.81 (m, 2H, $CH_2CH_2CF_3$), 2.30 (m, 4H, $CH_2\times2$), 2.54 (dq, 1H, J=15.2, 10.4 Hz, CF_3CHH), 2.66 (dq, 1H, J=15.2, 10.4 Hz, CF_3CHH), 3.51 (s, 1H, OH), 4.12 (q, J=7.2 Hz, 2H, OCH_2CH_3), 4.29 (dq, J=10.6, 7.2 Hz, 1H, $OCHHCH_3$), 4.31 (dq, J=10.6, 7.2 Hz, 1H, $OCHHCH_3$); ^{13}C NMR (100 MHz) δ 14.1, 14.3, 18.5, 33.8, 39.0, 42.3 (q, J_{C-F}=26.4 Hz, CF_3CH_2), 60.4, 62.8, 73.8 (q, J_{C-F}=2.5 Hz, CF_3CH_2C), 125.2 (q, J_{C-F}=274 Hz, CF_3), 172.7, 174.1; IR (neat, cm^{-1}) 3499, 2986, 1732, 1373, 1261, 1188, 1134, 1026; MS *m/z* 255 (M^+-OEt, 20%), 227 (33), 181 (100), 153 (52); HRMS calcd for $C_{10}H_{14}F_3O_4$ [M^+-OEt] 255.0844, found 255.0859.

4.2.12. Ethyl 4,4,4-trifluoro-2-hydroxy-3-methyl-2-phenethylbutanoates 26. Colorless oil; IR (neat, cm^{-1}) 3530, 2988, 1732, 1450, 1254, 1188, 1134, 1011, 746; MS *m/z* 304 (M^+, 62%), 231 (100), 200 (97), 172 (96), 152 (95), 133 (92); HRMS calcd for $C_{15}H_{19}F_3O_3$ [M^+] 304.1287, found 304.1325. *Major diastereomer*. ^{1}H NMR (400 MHz) δ 1.16 (d, J=7.2 Hz, 3H, CH_3), 1.34 (t, J=7.2 Hz, 3H, OCH_2CH_3), 2.14 (ddd, J=5.6, 13.6, 13.6 Hz, 1H, C*H*H), 2.20 (ddd, J=4.6, 13.2, 13.2 Hz, 1H, CH*H*), 2.32 (ddd, J=5.6, 13.6, 13.6 Hz, 1H, C*H*H), 2.66 (m, 1H, CF_3CH), 2.81 (ddd, J=4.6, 13.2, 13.2 Hz, 1H, CH*H*), 3.62 (s, 1H, OH), 4.27 (q, J=7.2 Hz, 2H, OCH_2CH_3), 7.15–7.30 (m, 5H, arom); ^{13}C NMR (100 MHz) δ 9.9, 14.2, 30.2, 38.9, 45.2 (q, J_{C-F}=24.7 Hz, CF_3CH_2), 62.8, 77.0, 127.0 (q, J_{C-F}=275.5 Hz, CF_3), 126.0, 128.3, 128.4, 140.9, 174.2. *Minor diastereomer*. ^{1}H NMR (400 MHz) δ 1.27 (d, J=7.2 Hz, 3H, CH_3), 1.36 (t, J=7.2 Hz, 3H, OCH_2CH_3), 1.89 (ddd, J=5.2, 12.8, 12.8 Hz, 1H, C*H*H), 2.07 (ddd, J=4.8, 13.2, 13.2 Hz, 1H, CH*H*), 2.28 (ddd, J=5.2, 12.8, 12.8 Hz, 1H, C*H*H), 2.73 (m, 1H, CF_3CH), 2.76 (ddd, J=4.8, 13.2, 13.2 Hz, 1H, CH*H*), 3.43 (s, 1H, OH), 4.29 (q, J=7.2 Hz, 2H, OCH_2CH_3), 7.14–7.32 (m, 5H, arom); ^{13}C NMR (100 MHz) δ 8.2, 14.2, 29.5, 39.1, 45.1 (q, J_{C-F}=24.1 Hz, CF_3CH_2), 62.7, 75.6, 126.8 (q, J_{C-F}=275.5 Hz, CF_3), 126.1, 128.3, 128.4, 140.9, 174.8.

4.2.13. Ethyl 2-(benzyloxyphenylmethyl)-4,4,4-trifluoro-2-hydroxybutyrate 28. Colorless oil; MS *m/z* 258 (M^+ − OH–OBn, 6%), 197 (65), 91 (100); HRMS calcd for $C_{13}H_{13}F_3O_2$ [M^+ − OH–OBn] 258.0868, found 258.0847. *Major diasteromer*. ^{1}H NMR (400 MHz) δ 1.23 (t, J=6.8 Hz, 3H, CH_3), 2.60 (dq, J=15.2, 10.4 Hz, 1H, CF_3CHH), 2.60, (ddq, J=0.8, 15.2, 10.4 Hz, 1H, CF_3CHH), 3.63 (d, J=0.8 Hz, 1H, OH), 4.13 (dq, J=10.0, 6.8 Hz, 1H, $OCHHCH_3$), 4.14 (d, J=12.4 Hz, 1H, Bn), 4.30 (dq, J=10.0, 6.8 Hz, 1H, $OCHHCH_3$), 4.45 (s, 1H, CH), 4.49 (d, J=12.4 Hz, 1H, Bn), 7.09–7.45 (m, 10H, arom); ^{13}C NMR (100 MHz) δ 14.0, 39.1 (q, J_{C-F}=28.2 Hz, CF_3CH_2), 62.7, 70.5, 76.4 (q, J_{C-F}=3.2 Hz, $CF_3CH_2CH_2$), 83.5, 125.3, (q, J_{C-F}=233.4 Hz, CF_3), 127.8, 128.0, 128.3, 128.4, 129.0, 129.1, 134.7, 137.0, 172.6. Minor diasteromer. ^{1}H NMR (400 MHz) δ 1.18 (t, J=6.8 Hz, 3H, CH_3), 2.60 (m, 1H, CF_3CHH), 3.12, (dq, J=15.6, 10.8 Hz, 1H, CF_3CHH), 3.33 (s, 1H, OH), 4.18 (m, 2H, OCH_2CH_3), 4.20 (d, J=12.4 Hz, 1H, Bn), 4.43 (s, 1H, CH), 4.57 (d, J=12.4 Hz, 1H, Bn), 7.09–7.45 (m, 10H, arom).

4.2.14. Ethyl 4,4,4-trifluoro-2-hydroxy-2-(2-methoxy-2-phenylethyl)butanoates 30. *Less polar major diastereomer* (2*R*,2′*R**). Clear cubic crystal; mp 86 °C (from hexane/diethyl ether, 10:1); ^{1}H NMR (270 MHz) δ 1.36 (t, J=7.0 Hz, 3H, OCH_2CH_3), 1.86 (dd, J=2.2, 14.3 Hz, 1H, CHH), 2.28 (dd, J=10.8, 14.3 Hz, 1H, CHH), 2.45 (dq, J=15.1, 10.3 Hz, 1H, CF_3CHH), 2.66 (dq, J=15.1, 10.3 Hz, 1H, CF_3CHH), 3.07 (s, 3H, OCH_3), 3.93 (s, 1H, OH), 4.29 (m, 1H, $OCHHCH_3$), 4.30 (m, 1H, $OCHHCH_3$), 4.41 (dd, J=1.9, 10.5 Hz, 1H, CH), 7.25–7.37 (m, 5H, arom); ^{13}C NMR (67.8 MHz) δ 14.0, 43.0 (q, J_{C-F}=26.8 Hz, CF_3CH_2), 48.3, 56.7, 62.5, 71.2 (q, J_{C-F}=2.2 Hz, CF_3CH_2C), 78.2, 125.1 (q, J_{C-F}=269.4 Hz, CF_3), 126.2, 127.7, 128.4, 141.3, 174.2; IR (KBr, cm^{-1}) 3500, 2964, 1734, 1454, 1273, 1194, 1134, 1015, 961, 920, 895, 827, 750; MS *m/z* 320 (M^+, 1%), 289 (35), 257 (86), 215 (100); HRMS calcd for $C_{15}H_{19}F_3O_4$ [M^+] 320.1235, found 320.1209. Crystallographic data have been deposited at the Cambridge Crystallographic Data Center (CCDC). CCDC reference number 195916. *More polar minor diastereomer* (2*S**,2′*R**) Colorless oil; ^{1}H NMR (270 MHz) δ 1.33 (t, J=7.0 Hz, 3H, OCH_2CH_3), 2.01 (dd, J=3.2, 14.6 Hz, 1H, CHH), 2.19 (dd, J=9.7, 14.6 Hz, 1H, CHH), 2.68 (m, 2H, CF_3CH_2), 3.19 (s, 3H, OCH_3), 4.24 (m, 2H, OCH_2CH_3), 4.32 (dd, J=3.2, 9.7 Hz, 1H, CH), 4.73 (s, 1H, OH), 7.24–7.39 (m, 5H, arom); ^{13}C NMR (67.8 MHz) δ 14.2, 42.5 (q, J_{C-F}=27.4 Hz, CF_3CH_2), 47.0, 56.4, 62.1, 74.1 (q, J_{C-F}=2.2 Hz, CF_3CH_2C), 81.4, 125.2 (q, J_{C-F}=277.8 Hz, CF_3), 126.3, 128.1, 128.6, 140.2, 173.6; IR (neat, cm^{-1}) 3500, 2951, 1738, 1456, 1367, 1271, 1234, 1190, 1138, 1099, 1024, 853, 760, 702; MS *m/z* 320 (M^+, 1%), 289 (35), 257 (86), 215 (100); HRMS calcd for $C_{15}H_{19}F_3O_4$ [M^+] 320.1235, found 320.1250.

4.2.15. Ethyl 2-(2-benzyloxy-2-phenylethyl)-4,4,4-trifluoro-2-hydroxybutanoates 32. *Less polar major diastereomer* (2*R**,2′*R**). Colorless oil; ^{1}H NMR (270 MHz) δ 1.11 (t, J=7.3 Hz, 3H, OCH_2CH_3), 1.90 (dd, J=2.2, 14.3 Hz, 1H, CHH), 2.38 (dd, J=10.5, 14.3 Hz, 1H, CHH), 2.42 (dq, J=14.9, 10.3 Hz, 1H, CF_3CHH), 2.61 (dq, J=14.9, 10.3 Hz, 1H, CF_3CHH), 3.79 (dq, J=10.3, 7.0 Hz, 1H, $OCHHCH_3$), 3.94 (s, 1H, OH), 4.01 (dq, J=10.3, 7.0 Hz, 1H, $OCHHCH_3$), 4.13 (d, J=10.5 Hz, 1H, $OCHHPh$), 4.28 (d, J=10.5 Hz, 1H, $OCHHPh$), 4.68 (dd, J=2.2, 10.5 Hz, 1H, CH), 7.25–7.37 (m, 10H, arom); ^{13}C NMR (67.8 MHz) δ 13.7, 43.1 (q, J_{C-F}=27.3 Hz, CF_3CH_2), 48.0, 62.3, 70.9, 71.4 (q, J_{C-F}=2.8 Hz, CF_3CH_2C), 76.2, 125.1 (q, J_{C-F}=277.2 Hz, CF_3), 126.4, 127.6, 127.8, 128.0, 128.4, 128.6, 137.6, 141.4, 174.2; IR (neat, cm^{-1}) 3487, 2964, 1732, 1360, 1306, 1271, 1198, 1232, 1163, 1140, 1094, 1024, 754, 700; MS *m/z* 305 (M^+ − Bn, 24%), 244 (31), 215 (89), 186 (100); HRMS calcd for $C_{14}H_{16}F_3O_4$ [M^+ − Bn] 305.1001, found 305.0989. *More polar minor diastereomer* (2*S**,2′*R**). Colorless oil; ^{1}H NMR (270 MHz) δ 1.30 (t, J=7.0 Hz, 3H, OCH_2CH_3), 2.06 (dd, J=3.2, 14.6 Hz, 1H, CHH), 2.27 (dd, J=10.3, 14.6 Hz, 1H, CHH), 2.67 (q, J=10.3 Hz, 2H, CF_3CH_2), 4.20 (m, 2H, OCH_2CH_3), 4.24 (d, J=10.6 Hz, 1H, $OCHHPh$), 4.35 (d, J=10.6 Hz, 1H, $OCHHPh$), 4.54 (dd, J=3.2, 10.3 Hz, 1H, CH), 4.67 (s, 1H, OH), 7.25–7.37 (m, 10H, arom); ^{13}C NMR (67.8 MHz) δ 14.1, 44.8 (q, J_{C-F}=27.3 Hz, CF_3CH_2), 47.0, 62.1, 71.0, 74.1 (q, J_{C-F}=2.8 Hz, CF_3CH_2C), 79.4, 125.1 (q, J_{C-F}=277.2 Hz, CF_3), 126.6, 128.0, 128.2, 128.3, 128.5, 128.8, 137.0, 140.5, 173.7; IR (neat, cm^{-1}) 3514, 2978, 2858, 1732, 1456, 1371, 1271, 1141, 1093, 1024, 748, 700; MS *m/z* 305 (M^+ − Bn, 9%), 244 (11), 215 (24), 186 (100); HRMS calcd for $C_{14}H_{16}F_3O_4$ [M^+ − Bn] 305.1001, found 305.0989.

4.2.16. 1,2:5,6-Di-*O*-isopropylidene-D-glucosyl 4,4,4-trifluoro-2-hydroxy-2-methylbutanoate 34. IR (neat, cm^{-1}) 3472, 2989, 1740, 1373, 1188, 1153, 1026, 849, 733; MS *m/z* 399 (M^+ − CH_3, 23%), 127 (35), 101 (100); HRMS calcd for $C_{16}H_{22}F_3O_8$ [M^+ − Me] 399.1266, found 399.1284. *Less polar diastereomer*. Colorless oil; ^{1}H NMR (400 MHz) δ 1.28 (s, 3H, CH_3), 1.32 (s, 3H, CH_3), 1.39 (s, 3H, CH_3), 1.50 (s, 3H, CH_3), 1.53 (s, 3H, CH_3), 2.59 (dq, J=15.1, 10.2 Hz, 1H, CF_3CHH), 2.69 (dq, J=15.1, 10.2 Hz, 1H, CF_3CHH), 3.98 (m, 1H, OCH), 4.17 (m, 3H, OCH, OCH_2), 4.49 (d, J=4.0 Hz, 1H, OCH), 5.34 (d, J=4.0 Hz, 1H, OCH), 5.86 (d, J=4.0 Hz, 1H, OCH); ^{13}C NMR (100 MHz) δ 25.2, 26.2, 26.7, 26.8, 27.3, 42.8 (q, J_{C-F}=27.3 Hz, CF_3CH_2), 67.9, 71.1 (q, J_{C-F}=2.8 Hz, CF_3CH_2C), 72.3, 78.2, 80.0, 82.4, 105.1, 109.5, 112.6, 125.1 (q, J_{C-F}=301.8 Hz, CF_3), 173.7. *More polar diastereomer*. Colorless oil; ^{1}H NMR (400 MHz) δ 1.29 (s, 3H, CH_3), 1.32 (s, 3H, CH_3), 1.40 (s, 3H, CH_3), 1.51 (s, 3H, CH_3), 1.53 (s, 3H, CH_3), 2.57 (dq, J=10.2, 15.2 Hz, 1H, CF_3CHH), 2.73 (dq, J=10.2, 15.2 Hz, 1H, CF_3CHH), 3.99 (m, 1H, OCH), 4.17 (m, 3H, OCH, OCH_2), 4.49 (d, J=4.0 Hz, 1H, OCH), 5.27 (d, J=4.0 Hz, 1H, OCH), 5.89 (d, J=4.0 Hz, 1H, OCH); ^{13}C NMR (100 MHz) δ 24.9, 26.3, 26.7, 26.8, 31.6, 42.9 (q, J_{C-F}=27.4 Hz, CF_3CH_2), 67.8, 71.4 (q, J_{C-F}=2.8 Hz, CF_3CH_2C), 72.3, 78.4, 80.0, 83.0, 105.0, 109.6, 112.6, 125.3 (q, J_{C-F}=298.0 Hz, CF_3), 173.6.

4.2.17. (1*R*,2*S*,5*R*)-5-Methyl-2-(1-methylethyl)cyclohexyl 4,4,4-trifluoro-2-hydroxy-2-methylbutanoate 36. Colorless oil; IR (neat, cm^{-1}) 3504, 2959, 2874, 1732, 1458, 1369, 1304, 1192, 1150, 1076, 949; MS *m/z* 227 (M^+ − CH_2CF_3, 6%), 139 (53), 83 (100); HRMS calcd for $C_{13}H_{23}O_3$ [M^+ − CH_2CF_3] 227.1648, found 227.1594. *Less polar diastereomer*. Colorless oil; ^{1}H NMR (400 MHz) δ 0.75 (d, J=6.8 Hz, 3H, CH_3), 0.91 (d, J=6.0 Hz, 3H, CH_3), 0.92 (d, J=6.0 Hz, 3H, CH_3), 0.96–1.09 (m, 4H), 1.47 (s, 3H, CH_3), 1.49 (m, 1H), 1.81 (m, 2H), 1.85

(m, 1H), 2.02 (m, 1H), 2.51 (dq, J=14.8, 10.4 Hz, 1H, CF_3CHH), 2.66 (dq, J=14.8, 10.4 Hz, 1H, CF_3CHH), 3.46 (s, 1H, OH), 4.74 (dt, J=4.4, 9.6 Hz, 1H, OCH); ^{13}C NMR (100 MHz) δ 15.9, 21.1, 22.1, 23.1, 26.2, 27.4, 31.4, 34.2, 40.1, 42.6 (q, J_{C-F}=28.0 Hz, CF_3CH_2), 46.9, 71.1, 77.3, 125.0 (q, J_{C-F}=285.1 Hz, CF_3), 174.4. *More polar diastereomer*. Colorless oil; ^{1}H NMR (400 MHz) δ 0.74 (d, J=6.8 Hz, 3H, CH_3), 0.90 (d, J=6.0 Hz, 3H, CH_3), 0.92 (d, J=6.0 Hz, 3H, CH_3), 0.96–1.09 (m, 4H), 1.46 (s, 3H, CH_3), 1.49 (m, 1H), 1.73 (m, 2H), 1.85 (m, 1H), 2.02 (m, 1H), 2.56 (dq, J=14.8, 10.4 Hz, 1H, CF_3CHH), 2.72 (dq, J=14.8, 10.4 Hz, 1H, CF_3CHH), 3.50 (s, 1H, OH), 4.78 (dt, J=4.4, 9.6 Hz, 1H, OCH); ^{13}C NMR (100 MHz) δ 15.7, 20.9, 22.1, 23.0, 26.0, 27.4, 31.5, 34.2, 40.3, 42.8 (q, J_{C-F}=28.0 Hz, CF_3CH_2), 47.0, 71.1, 77.3, 125.0 (q, J_{C-F}=285.1 Hz, CF_3), 174.5.

4.2.18. (1*R*,2*S*,5*R*)-5-Methyl-2-(1-methyl-1-phenylethyl) cyclohexyl 4,4,4-trifluoro-2-hydroxy-2-methylbutanoate 38. IR (neat, cm^{-1}) 3502, 2959, 1728, 1188, 1153, 702; MS *m*/*z* 267 ($M^+-C(CH_3)_2Ph$, 3%), 214 (10), 119 (100); HRMS calcd for $C_{12}H_{18}F_3O_3$ [$M^+-C(CH_3)_2Ph$] 267.1208, found 267.1239. *Less polar diastereomer*. Colorless oil; ^{1}H NMR (400 MHz) δ 0.90 (d, J=6.3 Hz, 3H, CH_3), 0.99 (m, 2H, CH_2), 1.16 (s, 3H, CH_3), 1.19 (m, 1H), 1.22 (s, 3H, CH_3), 1.30 (s, 3H, CH_3), 1.50 (m, 1H), 1.71 (m, 1H), 1.82 (m, 1H), 1.97 (m, 1H), 2.11 (dq, J=15.1, 10.7 Hz, 1H, CF_3CHH), 2.20 (s, 1H, OH), 2.26 (dq, J=15.1, 10.7 Hz, 1H, CF_3CHH), 2.27 (m, 1H), 4.83 (dt, J=4.4, 10.3 Hz, 1H, OCH), 7.26 (m, 2H, arom), 7.33 (m, 3H, arom); ^{13}C NMR (100 MHz) δ 21.8, 23.8, 26.5, 26.6, 29.6, 31.3, 34.6, 39.5, 40.7, 42.0 (q, J_{C-F}=27.4 Hz, CF_3CH_2), 49.2, 71.4 (q, J_{C-F}=2.7 Hz, CF_3CH_2C), 77.9, 125.1, 125.2, 126.8 (q, J_{C-F}=298.1 Hz, CF_3), 128.3, 151.9, 173.3. *More polar diastereomer*. Colorless oil; ^{1}H NMR (400 MHz) δ 0.89 (d, J=6.4 Hz, 3H, CH_3), 0.97 (m, 2H, CH_2), 1.14 (m, 1H), 1.17 (s, 3H, CH_3), 1.22 (s, 3H, CH_3), 1.31 (s, 3H, CH_3), 1.49 (m, 1H), 1.69 (m, 2H), 1.98 (m, 1H), 2.21 (m, 1H), 2.29 (dq, J=15.1, 10.7 Hz, 1H, CF_3CHH), 2.40 (dq, J=15.1, 10.7 Hz, 1H, CF_3CHH), 2.65 (s, 1H, OH), 4.87 (dt, J=4.4, 10.3 Hz, 1H, OCH), 7.19 (m, 2H, arom), 7.30 (m, 3H, arom); ^{13}C NMR (100 MHz) δ 21.8, 25.5, 26.4, 26.9, 28.3, 31.4, 34.5, 39.7, 40.8, 42.1 (q, J_{C-F}=27.3 Hz, CF_3CH_2), 49.5, 71.3 (q, J_{C-F}=2.7 Hz, CF_3CH_2C), 78.2, 125.2, 125.4, 126.7 (q, J_{C-F}=320.9 Hz, CF_3), 128.2, 151.3, 173.8.

4.2.19. Ethyl 4,4,5,5,5-pentafluoro-2-hydroxy-2-phenethylpentanoate 39. Colorless oil; ^{1}H NMR (400 MHz) δ 1.31 (t, J=6.8 Hz, 3H, OCH_2CH_3), 2.07 (m, 2H, CH_2), 2.44 (m, 1H, C*H*H), 2.57 (m, 1H, C*H*H), 2.66 (m, 1H, CH*H*), 2.81 (ddd, 1H, J=5.8, 10.7, 13.6 Hz, CH*H*), 3.63 (s, 1H, OH), 4.21 (dq, J=10.7, 6.8 Hz, 1H, OC*H*HCH$_3$), 4.30 (dq, J=10.7, 6.8 Hz, 1H, OCH*H*CH$_3$), 7.14–7.30 (m, 5H, arom); ^{13}C NMR (100 MHz) δ 14.1, 29.3, 38.1 (t, J_{C-F}=19.2 Hz, CF_2CH_2), 42.0, 62.8, 73.4 (t, J_{C-F}=1.8 Hz, CF_2CH_2C), 126.1, 128.3, 128.4, 140.6, 174.2; IR (neat, cm^{-1}) 3524, 2986, 1740, 1238, 1196, 1146, 702; MS *m*/*z* 340 (M^+, 3%), 267 (11), 236 (100), 208 (53), 91 (63); HRMS calcd for $C_{15}H_{17}F_5O_3$ [M^+] 340.1098, found 340.1107.

4.2.20. Ethyl 4,4,5,5,6,6,7,7,8,8,9,9,9-tridecafluoro-2-hydroxy-2-phenethylnonanoate 40. Colorless oil; ^{1}H NMR (400 MHz) δ 1.31 (t, J=6.8 Hz, 3H, OCH_2CH_3), 2.06 (m, 2H, CH_2), 2.44 (ddd, J=6.4, 9.8, 12.0 Hz, 1H, C*H*H), 2.55 (m, 1H, C*H*H), 2.71 (m, 1H, CH*H*), 2.82 (m, 1H, CH*H*), 3.87 (s, 1H, OH), 4.22 (dq, J=10.8, 6.8 Hz, 1H, OC*H*HCH$_3$), 4.31 (dq, J=10.8, 6.8 Hz, 1H, OCH*H*CH$_3$), 7.15–7.30 (m, 5H, arom); ^{13}C NMR (100 MHz) δ 14.0, 29.2, 39.0 (t, J_{C-F}=20.1 Hz, CF_2CH_2), 42.1, 62.8, 73.6, 126.1, 128.3, 128.4, 140.5, 174.2; IR (neat, cm^{-1}) 3526, 2932, 2986, 1736, 1331, 1196, 1138, 1018, 748, 698; MS *m*/*z* 467 (M^+-CO_2Et, 3%), 436 (26), 408 (14), 361 (2), 91 (7), 58 (100); HRMS calcd for $C_{16}H_{12}F_{13}O$ [M^+-CO_2Et] 467.0681, found 467.0665.

4.2.21. Ethyl 4,5,5,5-tetrafluoro-2-hydroxy-2-phenethyl-4-trifluoromethylnonanoate 41. Colorless oil; ^{1}H NMR (400 MHz) δ 1.31 (t, J=7.2 Hz, 3H, OCH_2CH_3), 2.05 (m, 2H, CH_2), 2.41 (ddd, J=6.0, 6.0, 13.6 Hz, 1H, C*H*H), 2.52 (dd, J=15.6, 24.4 Hz, 1H, CFC*H*H), 2.73 (dd, 1H, J=8.2, 15.6 Hz, CFC*H*H), 2.81 (ddd, J=5.6, 5.6, 13.6 Hz, 1H, C*H*H), 3.63 (s, 1H, OH), 4.24 (dq, J=13.2, 7.2 Hz, 1H, OC*H*HCH$_3$), 4.25 (dq, J=13.2, 7.2 Hz, 1H, OCH*H*CH$_3$), 7.14–7.30 (m, 5H, arom); ^{13}C NMR (100 MHz) δ 14.0, 29.3, 36.6 (d, J_{C-F}=20.1 Hz, $CFCH_2$), 42.1, 62.9, 73.5 (d, J_{C-F}=3.7 Hz, $CFCH_2CH_2$), 126.1, 128.3, 128.4, 140.5, 174.0; IR (neat, cm^{-1}) 3530, 2932, 1740, 1231, 1188, 1161, 1130, 698; MS *m*/*z* 390 (M^+, 3%), 317 (13), 286 (100), 258 (45), 91 (51); HRMS calcd for $C_{16}H_{17}F_7O_3$ [M^+] 390.1066, found 390.1083.

4.2.22. Diethyl 2-hydroxy-2-phenylethylpentanedioate 42. Colorless oil; ^{1}H NMR (400 MHz) δ 1.25 (t, J=7.2 Hz, 3H, OCH_2CH_3), 1.30 (t, J=7.2 Hz, 3H, OCH_2CH_3), 1.98 (ddd, J=5.6, 12.0, 14.0 Hz, 1H, C*H*H), 2.05 (m, 1H, CH*H*), 2.08 (m, 2H, CH_2), 2.21 (ddd, J=5.6, 9.6, 15.6 Hz, 1H, C*H*H), 2.43 (ddd, J=5.2, 12.0, 14.0 Hz, 1H, C*H*H), 2.47 (ddd, J=6.0, 9.6, 15.6 Hz, 1H, C*H*H), 2.80 (ddd, J=5.2, 12.0, 14.0 Hz, 1H, C*H*H), 3.45 (s, 1H, OH), 4.12 (q, J=7.2 Hz, 2H, OCH_2CH_3), 4.20 (q, J=7.2 Hz, 2H, OCH_2CH_3), 7.17 (m, 3H, arom), 7.27 (m, 2H, arom); ^{13}C NMR (100 MHz) δ 14.2, 14.3, 28.9, 30.0, 34.1, 40.9, 60.5, 62.2, 76.2, 125.8, 128.2, 128.3, 128.4, 173.1, 175.9; IR (neat, cm^{-1}) 3510, 2982, 2936, 1732, 1454, 1373, 1245, 1188, 1118, 1026, 702; MS *m*/*z* 263 (M^+-OEt, 8%), 235 (43), 204 (90), 189 (100), 158 (82); HRMS calcd for $C_{15}H_{19}O_4$ [M^+-OEt] 263.1283, found 263.1237.

4.2.23. Ethyl 4-chrolo-2-hydroxy-2-phenethylbutanoate 43. Colorless oil; ^{1}H NMR (400 MHz) δ 1.32 (t, J=7.4 Hz, 3H, OCH_2CH_3), 1.96 (ddd, J=5.4 12.2, 13.7 Hz, 1H, C*H*H), 2.08 (ddd, J=5.4, 13.7, 13.7 Hz, 1H, CH*H*), 2.21 (ddd, J=4.9, 7.8, 13.7 Hz, 1H, C*H*H), 2.30 (m, 1H, CH*H*), 2.41 (ddd, J=4.9, 11.7, 11.7 Hz, 1H, C*H*H), 2.78 (ddd, J=4.9, 11.7, 11.7 Hz, 1H, CH*H*), 3.51 (s, 1H, OH), 3.56 (m, 1H, CH*H*), 3.62 (ddd, J=4.9, 8.7, 11.7 Hz, 1H, CH*H*), 4.23 (q, J=7.4 Hz, 2H, OCH_2CH_3), 7.15–7.30 (m, 5H, arom); ^{13}C NMR (100 MHz) δ 14.3, 29.7, 39.4, 41.4, 41.8, 62.5, 75.4, 126.0, 128.3, 128.4, 141.0, 175.7; IR (neat, cm^{-1}) 3531, 2932, 1732, 1454, 1246, 4496, 745, 698; MS *m*/*z* 199 (M^+-CO_2Et, 11%), 197 (33), 168 (24), 166 (70), 168 (24), 105 (12), 91 (100); HRMS calcd for $C_{11}H_{14}ClO$ [M^+-CO_2Et] 197.0734, found 197.0713.

4.2.24. Ethyl 2-hydroxy-4-iodo-2-phenethylbutanoate 44. Colorless oil; ^{1}H NMR (400 MHz) δ 1.32 (t, J=7.3 Hz,

3H, OCH_2CH_3), 1.96 (ddd, J=4.9, 11.2, 13.7 Hz, 1H, C*H*H), 2.03 (ddd, J=5.3, 11.2, 13.7 Hz, 1H, CH*H*), 2.37 (m, 3H, CH_2, C*H*H), 2.77 (ddd, J=5.3, 11.2, 13.7 Hz, 1H, C*H*H), 2.98 (ddd, J=5.9, 9.8, 11.7 Hz, 1H, CH*H*), 3.25 (ddd, J=4.9, 9.8, 11.7 Hz, 1H, CH*H*), 3.44 (s, 1H, OH), 4.22 (q, J=7.3 Hz, 2H, OCH_2CH_3), 7.14–7.29 (m, 5H, arom); ^{13}C NMR (100 MHz) δ −2.9, 14.3, 29.8, 40.7, 43.8, 62.5, 77.8, 126.0, 128.3, 128.4, 141.0, 175.3; IR (neat, cm^{-1}) 3445, 2928, 1728, 1454, 1246, 1188, 1018, 748, 698; MS *m*/*z* 289 ($M^+ - CO_2Et$, 7%), 258 (24), 105 (22), 91 (100); HRMS calcd for $C_{11}H_{14}IO$ [$M^+ - CO_2Et$] 289.0090, found 289.0107.

4.2.25. Ethyl 2-hydroxy-2-phenethylpentanoate 45. Colorless oil; ^{1}H NMR (400 MHz). δ 0.90 (t, J=7.3 Hz, 3H, CH_3), 1.13 (m, 1H, C*H*H), 1.30 (t, J=6.8 Hz, 3H, OCH_2CH_3), 1.51 (m, 1H, CH*H*), 1.66 (ddd, J=5.2, 11.7, 13.6 Hz, 1H, C*H*H), 1.73 (ddd, J=5.2, 13.6, 13.6 Hz, 1H, CH*H*), 1.97 (ddd, J=5.6, 11.7, 14.0 Hz, 1H, C*H*H), 2.05 (ddd, J=5.6, 14.0, 14.0 Hz, 1H, CH*H*), 2.41 (ddd, J=5.3, 11.7, 11.7 Hz, 1H, C*H*H), 2.80 (ddd, J=5.3, 11.7, 13.6 Hz, 1H, CH*H*), 3.33 (s, 1H, OH), 4.20 (m, 2H, OCH_2CH_3), 7.15–7.29 (m, 5H, arom); ^{13}C NMR (100 MHz) δ 14.3, 14.4, 16.9, 30.1, 41.1, 41.7, 61.9, 77.1, 125.8, 128.3, 128.4, 141.7, 176.6; IR (neat, cm^{-1}) 3517, 2959, 1724, 1454, 1267, 1184, 698. MS *m*/*z* 177 ($M^+ - CO_2Et$, 66%), 146 (63), 91 (100); HRMS calcd for $C_{12}H_{17}O$ [$M^+ - CO_2Et$] 177.1279, found 177.1270.

4.2.26. Ethyl 2-hydroxy-4-methyl-2-phenethylpentanoate 46. Colorless oil; ^{1}H NMR (400 MHz) δ 0.84 (d, J=6.8 Hz, 3H, CH_3), 0.95 (d, J=6.8 Hz, 3H, CH_3), 1.31 (t, J=7.3 Hz, 3H, OCH_2CH_3), 1.68 (m, 2H, C*H*H, CH), 1.78 (m, 1H, CH*H*), 1.94 (ddd, J=5.4, 11.7, 13.2 Hz, 1H, C*H*H), 2.02 (ddd, J=5.4, 11.7, 13.2 Hz, 1H, CH*H*), 2.38 (ddd, J=5.4, 11.7, 13.2 Hz, 1H, C*H*H), 2.78 (ddd, J=5.4, 11.7, 13.2 Hz, 1H, CH*H*), 3.34 (s, 1H, OH), 4.21 (q, J=6.8 Hz, 2H, OCH_2CH_3), 7.15–7.31 (m, 5H, arom); ^{13}C NMR (100 MHz) δ 14.3, 23.3, 24.3, 24.5, 29.9, 42.3, 47.8, 61.9, 77.2, 125.8, 128.2, 128.3, 141.6, 177.1; IR (neat, cm^{-1}) 3524, 2959, 1720, 1454, 1227, 1184, 748, 698; MS *m*/*z* 191 ($M^+ - CO_2Et$, 41%), 160 (40), 91 (100); HRMS calcd for $C_{13}H_{19}O$ [$M^+ - CO_2Et$] 191.1436, found 191.1433.

4.2.27. Ethyl 4,4,4-trifluoro-2-hydroperoxy-2-phenethylbutanoate 47. Colorless oil; ^{1}H NMR (400 MHz) δ 1.33 (t, J=7.2 Hz, 3H, OCH_2CH_3), 2.17 (ddd, J=5.2, 12.0, 14.4 Hz, 1H, C*H*H), 2.27 (ddd, J=5.2, 12.0, 14.4 Hz, 1H, CH*H*), 2.61 (ddd, J=5.2, 12.0, 13.6 Hz, 1H, C*H*H), 2.71 (ddd, J=5.2, 12.0, 13.6 Hz, 1H, CH*H*), 2.77 (dq, J=15.6, 11.2 Hz, 1H, CF_3CHH), 2.96 (dq, J=15.6, 11.2 Hz, 1H, CF_3CHH), 4.28 (m, 2H, OCH_2CH_3), 7.15–7.30 (m, 5H, arom) 9.10 (s, 1H, OOH); ^{13}C NMR (100 MHz) δ 14.2, 29.7, 35.9, 36.8 (q, J_{C-F}=29.2 Hz, CF_3CH_2), 62.4, 84.9 (q, J_{C-F}=1.8 Hz, CF_3CH_2C), 125.0 (q, J_{C-F}=276.2 Hz, CF_3), 126.3, 128.2, 128.5, 140.3, 171.0; IR (neat, cm^{-1}) 3422, 2939, 1736, 1454, 1373, 1265, 1184, 1142, 1049, 864, 702; MS *m*/*z* 306 (M^+, 1%), 186 (19), 91 (100); HRMS calcd for $C_{14}H_{17}F_3O_4$ [M^+] 306.1079, found 306.1074.

4.3. Total synthesis of (±)-tanikolide

4.3.1. 1-Ethyl 6-methyl 2-methylenehexanedioate 52. Compound **52** was prepared following the procedure described for **1** except for the use of methyl 4-bromobutanoate instead of (2-iodoethyl)benzene (75%). Colorless oil; ^{1}H NMR (400 MHz) δ 1.26 (t, J=7.2 Hz, 3H, OCH_2CH_3), 1.30 (t, J=7.4 Hz, 3H, OCH_2CH_3) 1.83 (quintet, J=7.4 Hz, 2H, $CH_2CH_2CH_2$) 2.34 (m, 4H, $CH_2CH_2CH_2$), 3.67 (s, 3H, CH_3), 4.21 (q, J=7.4 Hz, 2H, OCH_2CH_3), 5.55 (s, 1H, C=CH*H*), 6.17 (s, 1H, C=CH*H*); ^{13}C NMR (67.8 MHz) δ 14.2, 23.6, 31.2, 33.4, 51.5, 60.6, 125.0, 139.8, 166.8, 173.6; IR (neat, cm^{-1}) 2982, 2955, 1716, 1632, 1439, 1369, 1180, 1138, 1026, 949; MS *m*/*z* 169 (M^+ − OMe, 40%), 155 (45), 154 (76), 126 (80), 67 (100); HRMS calcd for $C_9H_{13}O_3$ [M^+ − OMe] 169.0865, found 169.0883.

4.3.2. 1-Ethyl 6-methyl 2-hydroxy-2-undecylhexanedioate 53. Compound **53** was prepared following the general procedure of hydroxyalkyration (43%). Colorless oil; ^{1}H NMR (400 MHz) δ 0.88 (t, J=6.8 Hz, 3H, CH_3), 1.25 (m, 16H, CH_2×8), 1.31 (t, J=7.8 Hz, 3H, OCH_2CH_3), 1.46 (m, 2H, CH_2), 1.64 (m, 4H, CH_2×2), 1.78 (m, 2H, CH_2), 2.31 (m, 2H, CH_2), 3.24 (s, 1H, OH), 3.66 (s, 3H, OCH_3), 4.25 (q, J=7.8 Hz, 2H, OCH_2CH_3); ^{13}C NMR (100 MHz) δ 14.2, 14.3, 19.3, 22.7, 23.4, 29.4, 29.5, 29.5, 29.6, 29.7, 29.7, 32.0, 34.0, 38.6, 39.3, 51.5, 61.9, 77.1, 173.6, 176.5; IR (neat, cm^{-1}) 3528, 2924, 2855, 1728, 1462, 1180, 1022. MS *m*/*z* 271 ($M^+ - CH_2CH_2CO_2Me$, 18%), 253 (100), 225 (58); HRMS calcd for $C_{16}H_{31}O_3$ [$M^+ - CH_2CH_2CO_2Me$] 271.2273, found 271.2284.

4.3.3. 1-Ethyl 6-hydrogen 2-hydroxy-2-undecylhexanedioate 54. To a solution of diester **53** (30 mg, 0.08 mmol) in THF (0.5 mL) were added $LiOH \cdot H_2O$ (5 mg, 0.12 mmol) and H_2O (0.5 mL) at 0 °C. The reaction mixture was allowed to stand at room temperature for 20 h and then acidified with 1 mol/L HCl to attain pH 1. The mixture was extracted with ethyl acetate, and the organic layer was dried over anhydrous sodium sulfate and evaporated. The residue was chromatographed on silica gel to give monoester **54** (22 mg, 80%). Colorless oil; ^{1}H NMR (400 MHz) δ 0.88 (t, J=6.8 Hz, 3H, CH_3), 1.25 (m, 16H, CH_2×8), 1.30 (t, J=7.2 Hz, 3H, OCH_2CH_3), 1.46 (m, 2H, CH_2), 1.65 (m, 4H, CH_2×2), 1.79 (m, 2H, CH_2), 2.35 (m, 2H, CH_2), 4.25 (q, J=7.2 Hz, 2H, OCH_2CH_3); ^{13}C NMR (100 MHz) δ 14.2, 14.3, 19.0, 22.7, 23.4, 29.4, 29.5, 29.6, 29.6, 29.7, 29.7, 32.0, 33.8, 38.4, 39.4, 61.9, 77.2, 176.5, 178.5; IR (neat, cm^{-1}) 3532, 2920, 2847, 1721, 1697, 1466, 1180; MS *m*/*z* 271 ($M^+ - CH_2CH_2CO_2H$, 22%), 253 (100), 225 (68); HRMS calcd for $C_{16}H_{31}O_3$ [$M^+ - CH_2CH_2CO_2H$] 271.2273, found 271.2294.

4.3.4. (±)-Tanikolide. To a solution of **54** (50 mg, 0.15 mmol) in ethanol (3 mL) were added a solution of KOH (34 mg, 0.6 mmol) in ethanol (0.6 mL) and $CaCl_2$ (133 mg, 1.2 mmol) in ethanol (0.6 mL). The mixture was cooled to 0 °C, and then a suspension of $NaBH_4$ (46 mg, 1.2 mmol) in ethanol (0.5 mL) was added. The mixture was allowed to stand at room temperature for 17 h, and then acidified with 1 mol/L HCl at 0 °C to attain pH 1. After evaporation of ethanol, the residue was extracted with CH_2Cl_2 for three times. The combined organic layers were dried over sodium sulfate and the extract was evaporated. To a solution of the residue in benzene (3 mL) was added

p-toluenesulfonic acid monohydrate (19 mg, 0.1 mmol) and the mixture was stirred at room temperature for 3 h. After evaporation of the solvent, the residue was chromatographed on silica gel to give (±)-tanikolide (28 mg, 67%). Colorless oil; ^{1}H NMR (400 MHz) δ 0.88 (t, J=6.8 Hz, 3H, CH_3), 1.25 (m, 18H, $CH_2\times9$), 1.61–1.97 (m, 6H, $CH_2\times3$), 2.48 (m, 2H, CH_2), 3.55 (d, J=11.6 Hz, 1H, C*H*HOH), 3.66 (d, J=11.6 Hz, 1H, CH*H*OH); ^{13}C NMR (100 MHz) δ 14.3, 16.8, 22.8, 23.6, 26.7, 29.4, 29.55, 29.63, 29.69, 29.71, 29.9, 30.1, 32.0, 36.6, 67.6, 86.4, 171.3; IR (neat, cm^{-1}) 3419, 2925, 2853, 1732, 1243, 1048; MS *m*/*z* 253 (M^+-CH_2OH, 100%), 225 (86), 129 (27); HRMS calcd for $C_{16}H_{29}O_2$ [M^+-CH_2OH] 253.2167, found 253.2162.

Acknowledgements

This work was supported by a Grant-in-Aid from the Ministry of Education, Science, Sports, and Culture, Japan (No. 12740397). We are also grateful to F-Tech, Inc., for a generous supply of tirfluoromethyl iodide.

References and notes

1. For books, see: (a) Fossey, J.; Lefort, D.; Sorba, J. *Free Radicals in Organic Chemistry*; Wiley: Masson, 1995. (b) Renaud, P.; Sibi, M. P. *Radicals in Organic Synthesis*, *Vols. 1–2*; VCH: Weinheim, 2001. (c) Zard, S. Z. *Radical Reactions in Organic Synthesis*; Oxford University Press: Oxford, 2003.
2. For books, see: (a) Coppola, G. M.; Schuster, H. F. *Hydroxy acids in Enantioselective Synthesis*; VCH: Weinheim, 1997. (b) Hanessian, S. *Total Synthesis of Natural Products. The Chiron Approach*; Pergamon: New York, 1983; Chapter 2.
3. (a) Punniyamurthy, T.; Bhatia, B.; Iqbal, J. *J. Org. Chem.* **1994**, *59*, 850–853. (b) Iwahama, T.; Sakaguchi, S.; Ishii, Y. *J. Chem. Soc.* **2000**, 613–614. (c) Hirano, K.; Iwahama, T.; Sakaguchi, S.; Ishii, Y. *J. Chem. Soc.* **2000**, 2457–2458. (d) Hara, T.; Iwahama, T.; Sakaguchi, S.; Ishii, Y. *J. Org. Chem.* **2001**, *66*, 6425–6431.
4. (a) Nagano, H.; Toi, S.; Yajima, T. *Synlett* **1999**, 53–54. (b) Nagano, H.; Hirasawa, T.; Yajima, T. *Synlett* **2000**, 1073–1075. (c) Nagano, H.; Matsuda, M.; Yajima, T. *J. Chem. Soc., Perkin Trans. 1* **2001**, 174–182. (d) Nagano, H.; Toi, S.; Hirasawa, T.; Matsuda, M.; Hirasawa, S.; Yajima, T. *J. Chem. Soc., Perkin Trans. 1* **2002**, 2525–2538. (e) Nagano, H.; Ohkouchi, H.; Yajima, T. *Tetrahedron* **2003**, *59*, 3649–3663.
5. The hydroxytrifluoromethylation of α,β-unsaturated esters via carbocation intermediates by electrooxidation, see: Uneyama, K.; Watanabe, S.; Tokunaga, Y.; Kitagawa, K.; Sato, Y. *Bull. Chem. Soc. Jpn.* **1992**, *54*, 1976–1981.
6. A part of the results in this article has been reported as a preliminary letter: Yajima, T.; Nagano, H.; Saito, C. *Tetrahedron Lett.* **2003**, *44*, 7027–7029.
7. Leibner, J. E.; Jacobus, J. *J. Org. Chem.* **1979**, *44*, 449–550.
8. *O*-Alkylation of PhOH with alkyl halide in the presence of KF, see: (a) Clark, J. H.; Miller, J. M. *J. Chem. Soc., Chem. Commun.* **1976**, 229–230. (b) Clark, J. H.; Holland, H. L.; Miller, J. M. *Tetrahedron Lett.* **1976**, *38*, 3361–3364. (c) Clark, J. H.; Miller, J. M. *J. Am. Chem. Soc.* **1977**, *99*, 498–504.
9. Transformations of halides to the corresponding alcohols using aqueous carbonate has been reported: (a) Smith, J. G.; Dibble, P. W.; Sandborn, R. E. *J. Org. Chem.* **1986**, *51*, 3762–3768. (b) Ji, J.; Zhang, C.; Lu, X. *J. Org. Chem.* **1995**, *60*, 1160–1169.
10. Giese, B. *Angew. Chem., Int. Ed. Engl.* **1983**, *22*, 753–764.
11. The relative configuration of **28** was tentatively assigned as follows: compound **28** was transformed into ethyl 4,4,4-trifluoro-2-hydroxy-2-(hydroxyphenylmethyl)butanoate by the hydrogenolysis of the benzyl group over Pd/C. The relative configuration of ethyl 4,4,4-trifluoro-2-hydroxy-2-(hydroxyphenylmethyl)butanoate was determined by comparing the chemical shift values of ^{1}H and ^{13}C NMR spectra with those of methyl 2,3-dihydroxy-2-methyl-3-phenypropanoate. Heathcock, C. H.; Pirrung, M. C.; Young, S. D.; Hagen, J. P.; Jarvi, E. T.; Badertscher, U.; Marki, H. P.; Montgomery, S. H. *J. Am. Chem. Soc.* **1984**, *106*, 8161–8164. Spectral data of ethyl 4,4,4-trifluoro-2-hydroxy-2-(hydroxyphenylmethyl)-butanoates. *Major diasteromer*. Colorless oil; ^{1}H NMR (400 MHz) δ 1.33 (t, J=7.3 Hz, 3H, CH_3), 2.19 (dq, J=15.2, 10.2 Hz, 1H, CF_3CHH), 2.64, (dq, J=15.2, 10.2 Hz, 1H, CF_3CHH), 2.77 (br, 1H, OH), 2.78 (s, 1H, OH), 4.35 (m, 2H, OCH_2CH_3), 4.76 (d, J=5.4 Hz, 1H, CH), 7.37 (m, 5H, arom); ^{13}C NMR (100 MHz) δ 14.0, 39.0 (q, J_{C-F}=27.5 Hz, CF_3CH_2), 63.2, 76.5, 78.0, 125.2, (q, J_{C-F}=250 Hz, CF_3), 127.7, 128.4, 128.9, 137.6, 172.9; IR (neat, cm^{-1}) 3396, 2985, 1733, 1373, 1241, 1138, 702; MS *m*/*z* 258 ($M^+-OH\times2$, 7%), 201 (27), 186 (100), 111 (44); HRMS calcd for $C_{13}H_{13}F_3O_2$ [$M^+-OH\times2$] 258.0868, found 258.0884. *Minor diasteromer*. Colorless oil; ^{1}H NMR (400 MHz) δ 1.19 (t, J=7.3 Hz, 3H, CH_3), 2.83 (dq, J=14.9, 10.3 Hz, 1H, CF_3CHH), 3.12, (dq, J=14.9, 10.3 Hz, 1H, CF_3CHH), 2.90 (d, J=8.8 Hz, 1H, OH), 3.50 (s, 1H, OH), 4.06, (dq, J=10.0, 7.3 Hz, 1H, $OCHHCH_3$), 4.14, (dq, J=10.0, 7.3 Hz, 1H, $OCHHCH_3$), 4.68 (d, J=8.8 Hz, 1H, CH), 7.27 (m, 5H, arom); ^{13}C NMR (100 MHz) δ 13.9, 39.3 (q, J_{C-F}=27.5 Hz, CF_3CH_2), 62.9, 77.0, 77.2, 125.0 (q, J_{C-F}=250.2 Hz, CF_3), 127.0, 128.2, 128.8, 137.5, 171.7; IR (neat, cm^{-1}) 3479, 2986, 1733, 1372, 1241, 1139, 701; MS *m*/*z* 258 ($M^+-OH\times2$, 2%), 219 (2), 111 (28), 84 (100); HRMS calcd for $C_{13}H_{13}F_3O_2$ [$M^+-OH\times2$] 258.0868, found 258.0852.
12. The relative configuration of (2*R**,2′*R**)-**30** was determined by X-ray analysis. *Crystal data* for (2*R**,2′*R**)-**30**: $C_{15}H_{19}F_3O_4$, M=320.30, monoclinic, space group $P2_1/n$, α=18.265(7), β=6.7669(15), c=12.870(3) Å, β=99.15(2)°, V=1570.5(8) Å^3, Z=4, μ=1.037 mm^{-1}, T=293 K, R_{int}=0.1937; 4693 reflections were collected and 2839 independent reflections were used. R_1=0.0946, wR_2=0.2362 ($I>2\sigma(I)$ observed data); R_1=0.1264, wR_2=0.3036 (all data). CCDC reference number 195916. The relative configurations of **32** were determined by comparing the chemical shift values in ^{1}H and ^{13}C NMR spectra with those of **30**.
13. Kobayashi, S.; Hachiya, I. *J. Org. Chem.* **1994**, *59*, 3590–3596.
14. (a) Nagano, H.; Kuno, Y. *J. Chem. Soc., Chem. Commun.* **1994**, 987–988. (b) Nagano, H.; Kuno, Y.; Omori, Y.; Iguchi, M. *J. Chem. Soc., Perkin Trans. 1* **1996**, 389–394. (c) Sibi, M. P.; Ji, J.; Sausker, J. B.; Jasperse, C. P. *J. Am. Chem. Soc.* **1999**, *121*, 7517–7526.
15. (a) Inamoto, N.; Masuda, S. *Chem. Lett.* **1982**, 1003–1006. (b) Boyd, R. J.; Boyd, S. L. *J. Am. Chem. Soc.* **1992**, *114*,

1652–1655. (c) Suresh, C. H.; Koga, N. *J. Am. Chem. Soc.* **2002**, *124*, 1790–1797.
16. (a) Kharasch, M. S.; Jensen, E. V.; Urry, W. H. *Science* **1945**, *102*, 128. (b) Kharasch, M. S.; Skell, P. S.; Fisher, P. *J. Am. Chem. Soc.* **1948**, *70*, 1055–1059. (c) Schiesser, C. H.; Wild, L. M. *Tetrahedron* **1996**, *52*, 13265–13314.
17. Curran, D. P.; Bosch, E.; Kaplan, J.; Newcomb, M. *J. Org. Chem.* **1989**, *54*, 1826–1831.
18. Iodide **44** was not hydrolyzed under the reaction condition.
19. (a) Miyabe, H.; Ueda, M.; Yoshioka, N.; Naito, T. *Synlett* **1999**, 465–467. (b) Miyabe, H.; Ueda, M.; Yoshioka, N.; Yamakawa, K.; Naito, T. *Tetrahedron* **2000**, *56*, 2413–2420.
20. The conversion of halides to alcohols, via peroxyl radical intermediates, with oxygen and Et_3B, see: Kihara, N.; Ollivier, C.; Renaud, P. *Org. Lett.* **1999**, *9*, 1419–1422 and references cited therein.
21. For radical-mediated iodoperfluoroalkylation reaction of α-methylene esters, see: (a) Kamigata, N.; Fukushima, T.; Terakawa, Y.; Yoshida, M.; Iyoda, M. *J. Chem. Soc., Perkin Trans. 1* **1991**, 627–633. (b) Qui, Z.-M.; Burton, D. J. *J. Org. Chem.* **1995**, *60*, 3465–3472 and references cited therein.
22. Hayen, A.; Koch, R.; Saak, W.; Haase, D.; Metzger, J. O. *J. Am. Chem. Soc.* **2000**, *122*, 12458–12468.
23. Harpp, D. N.; Bao, L. Q.; Black, C. J.; Gleason, J. G.; Smith, R. A. *J. Org. Chem.* **1975**, *40*, 3420–3427.
24. Singh, I. P.; Milligan, K. E.; Gerwick, W. H. *J. Nat. Prod.* **1999**, *62*, 1333–1335.
25. For the synthesis of (±)-tanikolide, see: (a) Chang, M.-Y.; Lin, C.-L.; Chen, S.-T. *J. Chin. Chem. Soc.* **2001**, *48*, 787–794. (b) Krauss, J. *Nat. Prod. Lett.* **2001**, *15*, 393–399. (c) Zhang, R.; Wang, Z.; Wei, F.; Huang, Y. *Synth. Commun.* **2002**, *32*, 2187–2194. (d) Zhai, H.; Chen, Q.; Zhao, J.; Luo, S.; Jia, X. *Tetrahedron Lett.* **2003**, *44*, 2893–2894. For the synthesis of (+)-tanikolide, see: (e) Koumbis, A. E.; Dieti, K. M.; Vikentiou, G.; Gallos, J. K. *Tetrahedron Lett.* **2003**, *44*, 2513–2516. (f) Ohgiya, T.; Nishiyama, S. *Tetrahedron Lett.* **2004**, *45*, 8273–8275. (g) Arasaki, H.; Iwata, M.; Makida, M.; Masaki, Y. *Chem. Pharm. Bull.* **2004**, *51*, 848–852. (h) Schomaker, J. M.; Borhan, B. *Org. Biomol. Chem.* **2004**, *2*, 621–624. (i) Chen, Q.; Deng, H.; Zhao, J.; Lu, Y.; He, M.; Zhai, H. *Tetrahedron* **2005**, *61*, 8390–8393 and references cited therein.
26. Kabalka, G. W.; Sastry, K. A. R.; McCollum, G. W.; Yoshioka, H. *J. Org. Chem.* **1981**, *46*, 4296–4298.
27. Kagan, J.; Tolentino, L.; Ettlinger, M. G. *J. Org. Chem.* **1975**, *40*, 3085–3093.
28. Yajima, T.; Okada, K.; Nagano, H. *Tetrahedron* **2004**, *60*, 5683–5693.
29. Torsell, K. B. G.; Hazell, A. C.; Hazell, R. G. *Tetrahedron* **1985**, *41*, 5569–5575.
30. Thijs, L.; Keltjens, R.; Ettema, G. J. B. U.S. Patent 2003073742, 2003; *Chem. Abstr.* **2003**, *138*, 321017.
31. Meth-Cohn, O.; Moore, C.; Taljaard, H. C. *J. Chem. Soc., Perkin Trans. 1* **1988**, 2663–2674.

Available online at www.sciencedirect.com
SCIENCE DIRECT
Tetrahedron
Tetrahedron 61 (2005) 10216–10226

Atom-transfer radical reactions catalyzed by a coordinatively unsaturated diruthenium amidinate, $[(\eta^5\text{-}C_5Me_5)Ru(\mu_2\text{-}i\text{-}PrN{=}C(Me)Ni\text{-}Pr)Ru(\eta^5\text{-}C_5Me_5)]^+$

Yukihiro Motoyama, Shiori Hanada, Shota Niibayashi, Kazuya Shimamoto, Naoki Takaoka and Hideo Nagashima*

Institute for Materials Chemistry and Engineering, Graduate School of Engineering Science, Kyushu University, Kasuga, Fukuoka 816-8580, Japan

Received 9 July 2005; revised 10 August 2005; accepted 11 August 2005

Available online 31 August 2005

Abstract—Atom-transfer radical cyclization (ATRC) and addition (ATRA) catalyzed by a coordinatively unsaturated diruthenium amidinate complex **4**, $[(\eta^5\text{-}C_5Me_5)Ru(\mu_2\text{-}i\text{-}PrN{=}C(Me)Ni\text{-}Pr)Ru(\eta^5\text{-}C_5Me_5)]^+$, are investigated, and their features are compared with those of atom-transfer radical polymerization (ATRP). As an example of ATRC, a cationic diruthenium amidinate **4** is found to exhibit excellent catalytic reactivity for the cyclization of *N*-allyl α-halogenated acetamides including an alkaloid skeleton at ambient temperature. A catalytic species generated in situ from a halide complex, $(\eta^5\text{-}C_5Me_5)Ru(\mu_2\text{-}i\text{-}PrN{=}C(Me)Ni\text{-}Pr)Ru(\eta^5\text{-}C_5Me_5)(X)$ [X=Cl, Br] and sodium salts of weakly coordinating anions such as $NaPF_6$ and $NaBPh_4$ also shows high catalytic activity; this actually provides a solution for a problematic instability of **4** as the practical catalyst. The in situ-generated catalyst species **4** is also active towards the intermolecular ATRA of α,α,γ-trichlorinated γ-lactam with alkenes at rt to afford the corresponding α-alkylated γ-lactams in moderate yields. Examination of ATRP of methyl methacrylate (MMA) showed that both the isolated **4** [Y=PF_6] and in situ-generated **4** [Y=PF_6] are effective for the polymerization of MMA in the presence of 2-bromoisobutylate as the initiator. Use of the isolated catalyst results in controlled polymerization at initial stage of the reaction; in contrast, the polymerization with in situ-generated catalyst produces poly(MMA) with wide molecular weight distribution. The isolated catalyst **4** is powerful for the activation of a C–Br bond of macromolecule initiators; $BrCMe_2CO_2[O(CH_2)_4]_n\text{-}n\text{-}Bu$ (M_n=3800; M_w/M_n=1.2) initiated ATRP of MMA even at 25 °C to afford the poly(THF)–poly(MMA) block copolymer of M_n=26,000 and M_w/M_n=1.2 with the aid of **4**. The roles of the coordinatively unsaturated ruthenium species for these reactions are discussed.

1. Introduction

Atom-transfer radical reaction (ATRR) has now become one of the most important carbon–carbon bond-forming reactions, which is utilized for synthetic organic chemistry and polymer synthesis.[1] Atom transfer radical addition (ATRA) has long been known as a typical carbon–carbon bond forming reactions involving radical intermediates, and catalysis of certain metal salts and complexes are investigated since the report by Asscher and Vofsci in 1961.[2] Our discovery of copper-catalyzed cyclizations of allyl trichloroacetates and *N*-allyltrichloroacetamides[3a] offered a research field of transition metal-catalyzed atom-transfer radical cyclization (ATRC), which have afforded unique synthetic methods for carbo- and heterocycles including macrolide and alkaloid skeletons.[4] Elaborations to extend ATRA to polymerization, that is, transition metal-catalyzed atom-transfer radical polymerization (ATRP), by Matasjewsky and Sawamoto have provided methods for well-controlled radical polymerization,[5] and numerous studies using ATRP have been published in recent several years.[6] From the organometallic point-of-view, it should be noted that requirement of high reaction temperatures is a general disadvantage of ATRR, especially in the reactions involving activation of less reactive carbon–halogen bonds. This could be solved by development of efficient catalysts, and success of CuCl(bipyridine) catalyst system, which was reported for an efficient catalyst for ATRC in 1989[3c] and for ATRP in 1995,[5b] suggests that investigation to seek for new and efficient catalyst for ATRR is still important.

In this paper, we wish to report our studies to develop new catalysts for ATRR, in which coordinatively unsaturated

Keywords: Amidinate; Coordinatively unsaturated complex; Polymerization; Radical Cyclization; Ruthenium.
* Corresponding author. Tel./fax: +81 92 583 7819; e-mail: nagasima@cm.kyushu-u.ac.jp

0040–4020/$ - see front matter © 2005 Elsevier Ltd. All rights reserved.
doi:10.1016/j.tet.2005.08.037

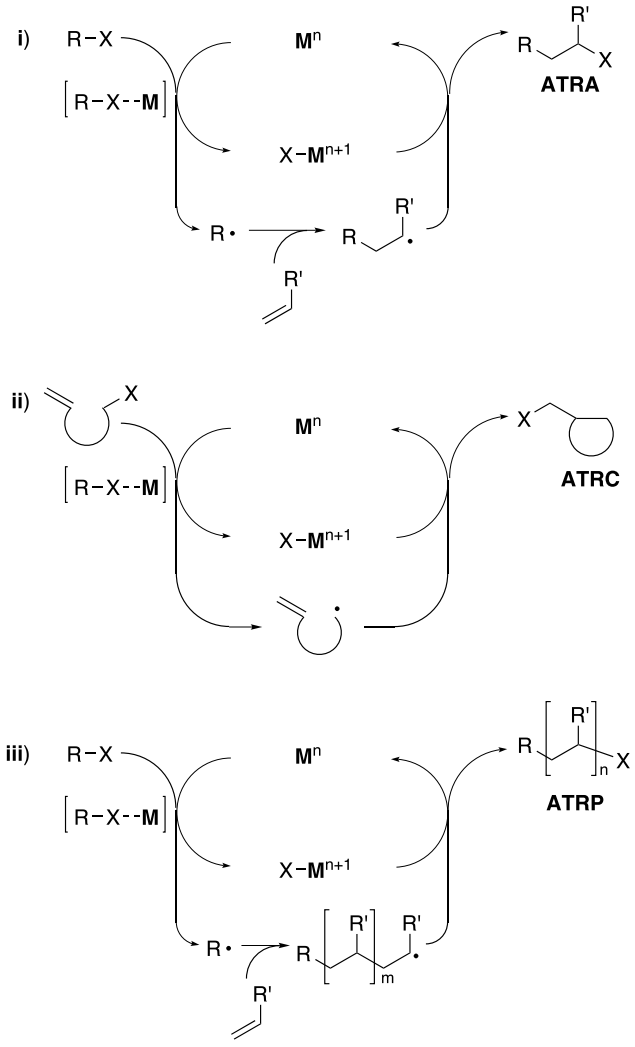

Scheme 1. Atom-transfer radical reactions with transition metal complex: (i) ATRA; (ii) ATRC; (iii) ATRP.

organometallic species with appropriate redox potentials act as efficient catalysts. ATRR is generally explained by the schemes shown in Scheme 1. The atom-transfer reaction of organic halides (R–X) with transition metals (**M**) proceeds via the redox mechanism involving a [R–X···**M**] complex as an intermediary species, and the formal oxidation state of the metal species is increased by one, and **M**–X is formed by the halogen abstraction.[7] In the [R–X···**M**] complex, **M** has to be coordinatively unsaturated, and thus, use of isolated coordinatively unsaturated complexes as the catalyst could facilitate the production of [R–X···**M**], which subsequently undergoes atom transfer process to produce the radical species ($R^{\bullet}$) to initiate the reaction. If the **M** has appropriate redox potential, the catalytic cycle illustrated in Scheme 1 could be successfully operated.

As part of our studies in this line, we have recently developed two ruthenium amidinates, (η^5-C_5Me_5)Ru(amidinate) **1** having 16 valence electrons and (η^5-C_5Me_5)-Ru(amidinate)Cl **2** bearing 17 valence electrons [amidinate = *i*-Pr–N=C(Me)N*i*-Pr].[8] Actually, these complexes **1** and **2** behaved as efficient catalysts for the cyclization of *N*-allyl- and *N*-vinyltrichloroacetamides.[8c] Despite the potential utility of the ruthenium amidinates **1** and **2** for this type of cyclization, it was problematic that these complexes are sensitive to air and moisture and difficult to handle. To overcome this instability problem of the catalyst, we were interested in isolable coordinatively unsaturated diruthenium amidinate **4** bearing 34 valence electrons to ATRR, which can be facilely generated in situ from air- and moisture stable diruthenium amidinates **3**.[9] Scope of these diruthenium amidinates as catalysts for ATRC and ATRA is described in relation to the low-temperature activation of organic halides and stereochemical outcomes of the reactions, and their performance is compared with that for ATRP[10] (Chart 1).

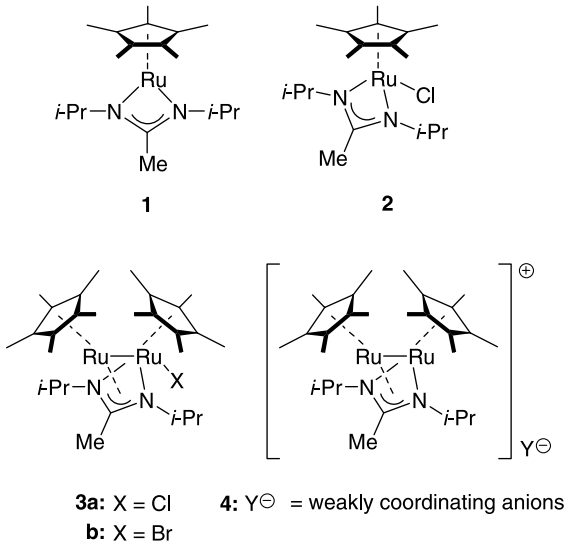

Chart 1.

2. Results and discussion

2.1. Redox potential of diruthenium amidinate complexes 3 and 4

As reported previously, the neutral diruthenium amidinates (**3a**: X=Cl, **3b**: X=Br) can be prepared from 2 equiv of lithium *N*,*N*′-diisopropylacetamidinate and [(η^5-C_5Me_5)-RuX]$_4$ in THF at ambient temperature.[9a] The characteristic feature of the neutral diruthenium amidinates **3** is that a halide ligand on **3** reversibly dissociates in dichloromethane forming coordinatively unsatulated [(η^5-C_5Me_5)Ru(μ_2-*i*-PrN=C(Me)N*i*-Pr)Ru(η^5-C_5Me_5)]$^+$(X^-) complex **4**, where X=Cl or Br. Interestingly, such dissociation of halides could not be observed in THF or aromatic solvents such as benzene or toluene.[9b] The isolable cationic complexes **4** with weakly coordinating anions can be easily synthesized by treatment of **3** with silver or sodium salts of the corresponding anions in dichloromethane as dark purple solids, and their coordinatively unsaturated structures were determined by X-ray diffraction.[9b] Cyclic voltammograms of **3a** (X=Cl) and **4** [Y=BF_4] in THF showed a quasi-reversible one electron oxidation wave (**3a**: E_{pa} = −0.02 V, E_{pc} = −0.08 V; **4**: E_{pa} = −0.002 V, E_{pc} = −0.05 V vs Ag/Ag^+ at the scan rate of 0.1 V/s) due to the Ru^{II}/Ru^{III} oxidation process.

It is known that CuCl/bipyridine catalyst stably exists as a chlorine-bridged dimer, however, it dissociates to a

coordinatively unsaturated monomer with 16 valence electrons, which initiates ATRR.[11] As reported earlier, the monoruthenium amidinate, **1** is also a 16-electron complex, being active for ATRR, too.[8c] The redox potentials for CuCl/bipyridine in THF is $E_{pa}=+0.03$ V, $E_{pc}=-0.13$ V [Cu^{I}/Cu^{II}], whereas that of **1** is $E_{pa}=-0.32$ V, $E_{pc}=-0.46$ V [Ru^{II}/Ru^{III}]; $E_{pa}=+0.53$ V [Ru^{III}/Ru^{IV}]. The coordinatively unsaturated nature and the redox potential close to CuCl/bipyridine suggested that the cationic diruthenium amidinate **4**, which showed coordinatively unsaturation and have redox potential similar to CuCl(bipy), is a good candidate for new catalysts of ATRR; **4** could form the [R–X···$\mathbf{Ru^{II}_2}$] intermediate in contact with organic halides, and subsequent electron transfer from the ruthenium species to the organic halides leads to the formation of R˙ and Ru_2–X.

2.2. Atom-transfer radical cyclization

As we expected, the reaction of *N*-allyl-*N*-benzyltrichloroacetamide **5a** catalyzed by the isolated **4** [Y=$B(C_6F_5)_4$] was proved to proceed smoothly at 25 °C to afford **6a** in 94% yield within 30 min (Table 1, entry 1). The reaction of **5a** was also catalyzed by 10 mol% of **3a** (X=Cl), though it was slower than that with **4** (entry 2). Coordinatively unsaturated species **4** reversibly formed from air stable **3** in CH_2Cl_2 should be the active catalyst species. Generation of **4** was assisted by addition of silver or sodium salts of weakly coordinating anions (Y^-) to the reaction with **3**; in fact, the color of the reaction mixture gradually turns from brown to dark purple. Thus, the catalytic cyclizations of **5a** with a 1:1 molar ratio of **3a** and AgY (Y=BF_4 and PF_6) were accomplished within 1 h to form the corresponding lactam in high yields (entries 3 and 4). Sodium salts of weakly coordinating anions were more effective as the activator of **3** than the silver salts; cyclization of **5a** was complete within 30 min to give the cyclized product **6a** in quantitative yield (entries 5 and 6). The choice of solvents is crucial for the efficient generation of the active species, which affected the chemical yield of the product (entries 7–9). Dichloromethane is the best solvent so far; the rate of cyclization was remarkably slow in benzene due to the low solubility of the sodium salts, whereas the low rates in MeCN suggtests deactivation of the catalytic species **4** by coordination of MeCN to the active metal center.[12] In THF, the cyclization of **5a** almost stopped within 1 h and some unidentified organic compounds were obtained as by-products. Comparison of the reaction rate with that using CuCl(bipy), **1**, and **2** is shown in entries 10–12, suggesting that catalytic activity of the cationic complex **4** is comparable to the conventional CuCl-bipyridine catalyst, and even higher than that using the mononuclear amidinate complexes **1** and **2**.

Table 1. Radical cyclization of **5a** (all reactions were carried out using 0.2 mmol of **5a** and 10 mol% of catalyst in 1.5 mL of solvent at 25 °C)

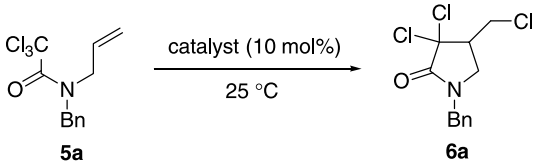

5a **6a**

Entry	Catalyst	Solvent	Time (h)	Yield (%)
1	**4** [Y=$B(C_6F_5)_4$]	CH_2Cl_2	0.5	94
2	**3a**	CH_2Cl_2	4	30
3	**3a**+$AgBF_4$	CH_2Cl_2	1	98
4	**3a**+$AgPF_6$	CH_2Cl_2	1	90
5	**3a**+$NaPF_6$	CH_2Cl_2	0.5	>99
6	**3a**+$NaBPh_4$	CH_2Cl_2	0.5	>99
7	**3a**+$NaBPh_4$	Benzene	0.5	38
8	**3a**+$NaBPh_4$	THF	0.5	37
9	**3a**+$NaBPh_4$	CH_3CN	0.5	<5
10	**1**	Toluene	4	85
11	**2**	Toluene	4	88
12	CuCl+Bipy	CH_2Cl_2	0.5	>99

A series of *N*-allyl α-trichloroacetamide derivatives **5a–d** was subjected to cyclization with 10 mol% of **3** and the anioic activator in dichloromethane at 25 °C. The reactions gave the desired product in quantitative yields except the case of *N*-phenyl derivative **5c** (Table 2, entries 1–5). Although the mononuclear ruthenium amidinates **1** and **2** were not efficient for the cyclization of *N*-tosyl derivateve **5b** (rt, 4 h; 31% for **1** and 0% for **2**, respectively), the cationic diruthenium amidinate **4** catalyzed the cyclization effectively to give the γ-lactam **6b** in quantitative yield (entry 2). The reactions of acetamides **5b** and **5d** proceeded smoothly to give the corresponding products in high yields even at low catalyst loadings (1–2.5 mol%) (entries 3 and 5). This catalyst system was also effective for the cyclization of α-monobromoacetamide **5e** and the γ-bromolactam **6e** was obtained in 94% yield (entry 6).

Table 2. Radical cyclization of *N*-allylpoliharoacetamides **5a–e** (all reactions were carried out using 0.2 mmol of **5**, 10 mol% of **3** and sadium salts in 1.5 mL of CH_2Cl_2 at 25 °C)

Entry	Substrate	Time (h)	Product	Yield (%)
1	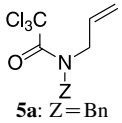 **5a**: Z=Bn	0.5	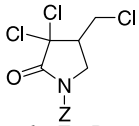 **6a**: Z=Bn	>99
2	**5b**: Z=Ts	0.5	**6b**: Z=Ts	>99
3[a]	**5b**: Z=Ts	3	**6b**: Z=Ts	92
4	**5c**: Z=Ph	1	**6c**: Z=Ph	52
5[b]	**5d**: Z=allyl	1	**6d**: Z=allyl	>99
6	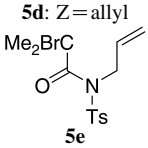 **5e**	4	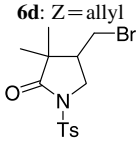 **6e**	94

[a] Catalyst (1 mol%) was used.
[b] Catalyst (2.5 mol%) was used.

The efficiency of **3**/$NaPF_6$ or $NaBPh_4$ as the catalyst eventually led to two important aspects in the γ-lactam synthesis by ATRC. First, the pyrrolidizine alkaloid precursor **6f**[13] was obtained in high yield as the sole product (1*R*,7a*S*) by the reaction of optically active **5f**[13a] with this catalyst system (Table 3, entry 1). It is noteworthy that the catalyst efficiency in this particular substrate is much higher than that with the copper catalysts; the reaction reportedly promoted by a stoichiometric amount of CuCl in MeCN at 160 °C,[13a] whereas the reaction with a catalytic amount of CuCl/bipyridine system took place at 80 °C (entry 4). In sharp contrast, the reaction with **3a** in the

Table 3. Cyclization of **5f** by copper or ruthenium catalysts

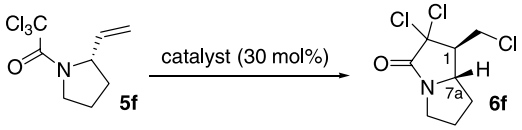

Entry	Catalyst	Solvent	Conditions	Yield (%)	Trans/cis[a]
1	**3a**+$NaPF_6$	CH_2Cl_2	rt, 3 h	90	0:100
2	**1**	Benzene	rt, 13 h	90	0:100
3	**2**	Benzene	rt, 3 h	85	0:100
4	CuCl/bipy	$ClCH_2CH_2Cl$	80 °C, 2 h	97	0:100

[a] Determined by ^1H NMR analysis.

presence of $NaPF_6$ proceeded at rt similar to those with **1** or **2** as shown in entries 2 and 3.[8c]

It is well known that radical cyclization of ω-olefinic haloamides at low temperatures has a problem of low yields of the product due to high rotational barrier (16–22 kcal/mol) of the C–N bond in the amide function.[14] As shown in Scheme 2, there are two possible rotamers, *anti*-**5f** and *syn*-**5f**, and *anti*-**5f** is the rotamer unfavorable for the cyclization. Preliminary DFT caluculations[15] suggest that there is no substantial energy difference between two rotamers (0.87 kcal/mol; B3LYP/6-311++G(2d,p)//B3LYP/6-31G(d) level); this rules out the assumption from simple molecular model consideration of **5f** that *anti*-**5f** may predominantly exist in solution because of substantial steric repulsion between the CCl_3 and the vinyl groups. Calculations of radical intermediates **A** indicates that the cyclization proceeds through a reaction pathway involving change of hybridization of the nitrogen atom from sp^2 (**A**) to sp^3 (**B** and **C**) prior to the carbon–carbon bond formation (Scheme 2). The resulting sp^3-hybridized cyclic radical species has four possible isomers, *cis*-**B**, *trans*-**B**, *cis*-**C**, and *trans*-**C**. Although *cis*-**B** is only the transition state capable of cyclization, the cis-orientation of the dichloroacetyl radical moiety to the vinyl group produces substantial steric repulsion between them, which is the most serious in *cis*-**B**. The reason of the slow copper-catalyzed

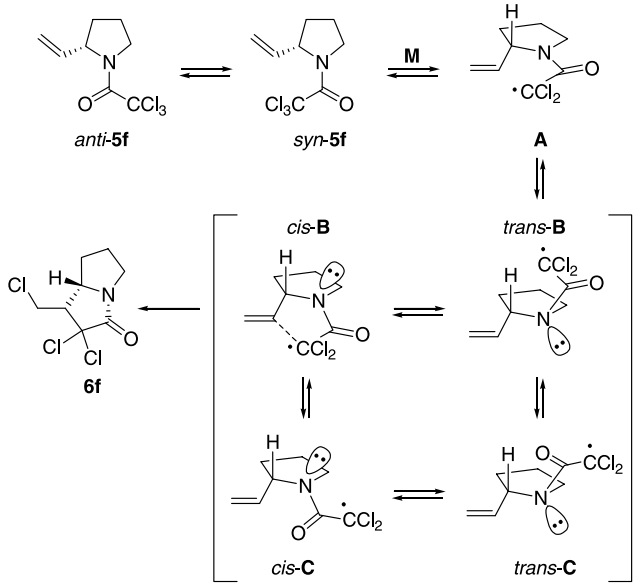

Scheme 2. The conformation of **5f** in the cyclization.

cyclization of **5f** can be attributed to the fact that *cis*-**B** is a thermodynamically less favorable transition state. A clue to understand the success of ruthenium amidinates for the low-temperature cyclization of **5f** is oxophilic nature of ruthenium amidinates, in particular that of catinic diruthenium amidinates, which could provide their coordination to the oxygen atom in the transition state **B**. As shown in the Scheme 3, the coordination makes *cis*-**B** to be a more favorable transition state than *cis*-**C**.

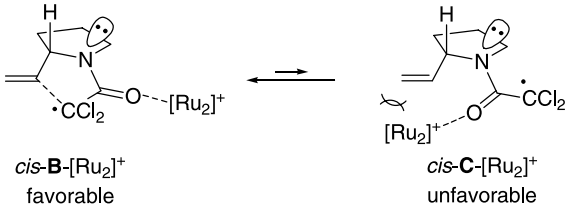

Scheme 3. The conformatin of $[Ru_2]^+$-coordinated *cis*-**B** and *cis*-**C**.

The second merit for the use of in situ generated **4** is high catalytic activity for the cyclization of an *N*-allyl-α,α-dichloroacetamide **5g** (Table 4). It is known that **5g** is a less reactive substrate than the trichlorinated homologue in the ATRC. In fact, with the conventional CuCl/bipy system, it is necessary to apply high reaction temperatures (>80 °C) or to load large amounts of the catalyst (~30 mol%) to obtain the product in good yields.[16] Although the neutral complex **3a** was not very effective for the cyclization of **5g** (12 h, 25% yield), the cationic diruthenium species prepared in situ from **3a** and $NaBPh_4$ (10 mol% each) gave the product **6g** in 88% yield, when the reaction was performed at 25 °C for 3 h (entry 1); this suggests that **3a**/$NaBPh_4$ is the most powerful catalyst for *N*-allyldichloroacetamides so far reported. The observed diastereoselectivity (trans/cis=7:1) is much different from that obtained by CuCl(bipy) at 83 °C (trans/cis=4:1, which was proved to be the thermal equiblium ratio in a separate experiment), indicating that the reaction with cationic diruthenium amidinate was controlled kinetically.[17,18]

2.3. Intermolecular atom-transfer radical addition

Intermolecular ATRA is generally slower than ATRC, and there are not many examples of the ATRA of α,α-dichlorocarbonyl compounds to olefins under mild conditions.[19] We first attempted the intermolecular addition reaction of α,α-dichloro-γ-lactam **6b** with 1 equimolar amount of olefins ([alkene]=0.133 M) at ambient temperature,

Table 4. Cyclization of **5g** by copper and ruthenium catalysts

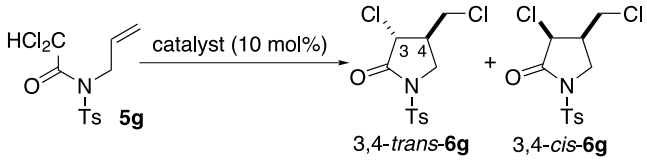

Entry	Catalyst	Solvent	Conditions	Yield (%)	Trans/cis[a]
1	**3a**+$NaBPh_4$	CH_2Cl_2	25 °C, 3 h	88	7.0:1
2	**3a**+$NaBPh_4$	$ClCH_2CH_2Cl$	45 °C, 1 h	39	6.6:1
3	CuCl/bipy	CH_2Cl_2	25 °C, 3 h	24	7.4:1
4	CuCl/bipy	$ClCH_2CH_2Cl$	83 °C, 1 h	95	4.0:1

[a] Determined by ^{1}H NMR analysis.

Table 5. Reaction of **6b** with various olefins (all reactions were carried out using 0.2 mmol of **6b**, 2.0 mmol of olefin and 0.02 mmol of catalyst in 1.5 mL of CH_2Cl_2)

Entry	Olefin	Catalyst	Conditions	Product	Yield (%)	Cis/trans[a]
1	TMS	**3a**+$NaBPh_4$	25 °C, 5 h	**7a**	24[b]	3.2:1
2		CuCl/bipy	25 °C, 12 h	**7a**	0[b]	—
3[c]		CuCl/bipy	83 °C, 1 h	**7a**	93[b]	5.7:1
4		**3a**+$NaBPh_4$	25 °C, 10 h	**7b**	57	5.7:1
5		CuCl/bipy	25 °C, 12 h	**7b**	<5	—
6[c]		CuCl/bipy	83 °C, 1 h	**7b**	>99	>99:1
7	MeO_2C	**3a**+$NaBPh_4$	25 °C, 5 h	**7c**	50[a]	—

[a] Determined by ^{1}H NMR analysis.
[b] Product was isolated after treatment with SiO_2.
[c] In dichloroethane.

however, the alkylated products were not detectable by ^{1}H NMR. In the presence of 10 equiv of alkenes ([alkene]= 1.33 M), this cationic diruthenium catalytic species is useful for activation of an α-chlorine atom of **6b** followed by intermolecular addition reaction to alkenes (Table 5). Although high reaction temperatures are required for the carbon–carbon bond forming reaction at the α-position of the 2-pyrroridinone **6b** catalyzed by the CuCl/bipy system,[17b] the reaction of **6b** (0.2 mmol) with 10 equiv of allyltrimethylsilane in the presence of in situ-generated cationic species (10 mol%) proceeded even at 25 °C to give the allylated product **7a** in 24% yield with 3.2:1 diastereomer ratio after treatment with SiO_2 for elimination of chlorotrimethylsilane (entries 1–3). Similarly, the reaction of **6b** with methylenecyclohexane proceeded at ambient temperature to afford the 1:1 adduct **7b** in 57% yield (entry 4). In these two cases, only the 1:1 adduct was formed without contamination of oligomers and polymers. The reason of low to moderate yields of the product is low conversion of the starting materials, which is caused by instability of the coordinatively unsaturated catalyst species. The diastereomer ratio of the adducts **7a** and **7b** were kinetically controlled (3.2:1 for **7a** and 5.7:1 for **7b**,

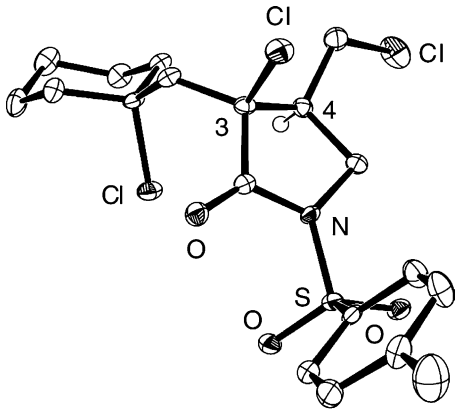

Figure 1. The ORTEP drawing of 3,4-*cis*-**7**. For clarify, only H atom at the C4 position is shown.

respectively), these are in contrast to the fact that the reactions catalyzed by the CuCl/bipy system at 83 °C afforded the thermodynamically controlled ratio (>88:12 for **7a** and >99:1 for **7b**, respectively)[17b] (entries 4 and 6). The relative stereochemistry of the major isomer of **7b** was determined to be 3,4-*cis* by X-ray diffraction (Fig. 1). Methyl methacrylate (MMA) also reacted with **6b** at rt; the conversion reached 90% after 5 h. The products identified were the adduct **7c** as four diastereomer mixtures (ca. 50% yield) and a product **6g** (ca. 5%) produced by reductive dechlorination. Although no poly(MMA) was formed under this conditions (1.33 M in CH_2Cl_2), some amounts of unidentified organic compounds, spectral data of which suggests to be telomers of MMA, were also detected (entry 7).

2.4. Atom-transfer radical polymerization

In the above sections, we have proved high catalytic activity of the coordinatively unsaturated diruthenium amidinate **4** having appropriate redox potentials for ATRC and ATRA for the production of organic products. Such high catalytic activity of **4** enables to lower the reaction temperature, which is advantageous for controlling the relative stereochemistry of newly formed stereocenters kinetically. Success of these studies prompted us to extend catalysis of the coordinatively unsaturated diruthenium amidinate to ATRP. It should be noted that there is the following important mechanistic points between ATRP and ATRA (or ATRC). First, both ATRP and ATRA/ATRC have the same initiation step, that is, reaction of a metal catalyst with an organic halide (R–X) to generate a radical species (R˙) and **M**–X. In the ATRA/ATRC, the initial radical species adds to a carbon–carbon double bond to form a new carbon radical (Scheme 4, **D**), which reacts with **M**-X to give the product. The striking difference of ATRP from ATRA/ATRC is that the intermediary radical species **D** successively reacted with many molecules of the vinyl monomer, which provides growth of the polymer chain (**E**). In many papers, a metal-capping species (R–X–**M**) is postulated as a dormant species, and reversible generation of active macromolecular radical species at the polymer end from the dormant species is followed by 'well-controlled' living-like chain growth in reacting with the monomer.[6] It is expected that use of coordinatively unsatrurated complex as the catalyst for ATRP accelerates both the initiation step and the reactivation of the dormant species; this should be advantageous to lower the reaction temperature and to take part in the facile activation of less reactive organic halide initiators. In contrast, a possible drawback deduced from our results of ATRA is instability of the coordinatively unsaturated species as a fragile catalyst, which may affect the polymerization behavior. A research on the same line was reported by Sawamoto and co-workers, in which a coordinatively unsaturated ruthenium complex, $Ru(Cp^*)Cl(PCy_3)$, catalyzes rapid but 'ill-controlled' polymerization of MMA to give poly(MMA) with quite broad (M_w/M_n=2.8–6.2) molecular weight distributions.[20]

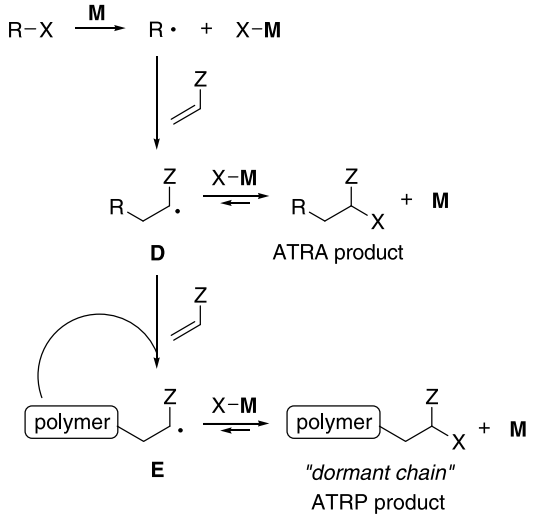

Scheme 4. Proposed mechanisms for ATRP.

A mixture of cationic diruthenium amidinate **4** [Y=PF_6] (19 μmol), MMA (2 mL, 19 mmol), ethyl α-bromoisobutylate **8** (38 μmol) was stirred in a sealed tube at 40 °C for 10 h (Table 6). The reaction using catalyst **4**, in situ-generated from **3a** and $NaPF_6$, produces poly(MMA) with M_n=37,000; M_w/M_n=1.8 in 35% yield as shown in entry 1. The relatively wide molecular weight distribution is dramatically improved when isolated complex **4** was used as the catalyst; poly(MMA) with M_w/M_n=1.3 was obtained in 32% yield (entry 2). When the reaction was carried out using toluene as the solvent, M_n of the formed polymer was apparently larger than that of the polymer obtained by the reaction without solvent (entries 2 vs 3). Although the conversions of MMA increased in both ethyl acetate and dichloroethane, the molecular weight distributions of formed polymer were broad (entries 4 and 5). We also examined the reaction with the catalyst/monomer ratio of 1:200, the polymerization of MMA ceased before reaching

Table 6. Polymerization of MMA with isolated complex **4** [Y=PF_6] (all reactions were carried out using 19 μmol of **4**, 38 μmol of ethyl α-bromoisobutylate **8**, 19 mmol of MMA in 2 mL of toluene at 40 °C for 10 h)

Entry	Solvent	Ratio (**4**/**8**/MMA)	Yield[a] (%)	M_n[b]	M_w/M_n[b]
1[c]	—	1:2:1000	35	37,000	1.8
2	—	1:2:1000	32	29,000	1.3
3	Toluene	1:2:1000	26	47,000	1.3
4	AcOEt	1:2:1000	45	40,000	1.8
5	$ClCH_2CH_2Cl$	1:2:1000	56	31,000	2.2
6	Toluene	1:2:200	20	7000	1.2
7[d]	Toluene	1:2:1000	35	29,000	1.3

[a] Isolated yield after precipitation.
[b] Determined by GPC analysis of the crude polymer.
[c] In situ-prepared catalyst was used.
[d] 25 °C for 20 h.

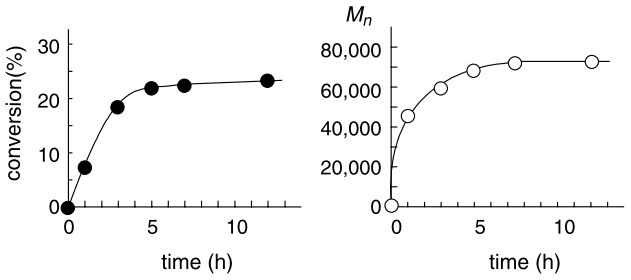

Figure 2. The plots of time versus conversion (left) and M_n (right) of the reaction of **4**/**8**/MMA=1:1:1000 in ethyl acetate at 40 °C.

completion (20% yield) and the polymer of M_n=7000 and M_w/M_n=1.2 was formed (entry 6). Although the conversions of MMA in the present polymerization in toluene were not so high (26–35%), the cationic complex **4** found to be effective for activation of an α-bromine atom of the dormant chain even at 25 °C and control the polymerization at the initial stage (entry 7). Despite the high catalytic activity for the polymerization of MMA, a disadvantage of **4** is its short life time as shown in the reaction profile (Fig. 2), in which the conversion of MMA and the M_n of formed polymer are both increasing at the initial stage, but the polymerization was terminated after 7 h.[21] It is apparent from the end-group analysis of the formed poly(MMA) using ^{13}C NMR that the polymerization proceeds with the atom transfer reaction to give poly(MMA) bearing terminal bromide (δ 58.9 ppm for the terminal α-carbon; $CH_2C(Me)(Br)CO_2Me$);[22] this is also supported from post-polymerization described below. The high activity of the cationic diruthenium amidinate **4** as the polymerization catalyst led to activation of a C–Br bond of macroinitiators, which is less reactive than that of commonly used organic initiators. The post-polymerization of MMA from poly(MMA) bearing a terminal bromide **9a** (M_n=7000; M_w/M_n=1.2), which was obtained by the reaction shown in Table 6, entry 5, as a macroinitiator proceeded even at 25 °C to afford the poly(MMA) of M_n=47,000 and M_w/M_n=1.3 (Table 7, entry 1). MMA can also be polymerized by the macroinitiator **9b**[23,24] derived from polybutylene oxides, [poly(THF)],[23b] bearing a 2-bromoisobutyl group at the polymer terminal (M_n=3800; M_w/M_n=1.2) at 25 °C to form the polymer of M_n=26,000 and M_w/M_n=1.2; the ^1H NMR spectrum of the obtained copolymer **10b** revealed that the product contains both poly(THF) and poly(MMA) segments (entry 2). In the conversion of this particular polymerization, the chain growth was terminated at ambient temperature (ca. 25 °C), after 30 and 40% of MMA was consumed. In sharp contrast, MMA was completely converted to the polymer in the reaction of **9b** with MMA at 40 °C (entry 3).[25,26] These results clearly showed that the coordinatevely unsaturated complex acts as effective catalyst for the ATRP using less reactive macromolecule initiators at low temperature.

3. Conclusion

It is well known that intramolecular radical addition (ATRC) is entropicaly more favorable than the intermolecular addition reaction (ATRA). Thus, the catalytic activity of the metal complexes in ATRC is dependent on how efficient the metal catalyst abstracts the halogen atom of organic halide initiators; in other words, the reaction is controlled by its initial step. In contrast, intermolecular radical addition to olefins (ATRA) is affected by concentration of olefins, and hence, the reactions are generally slower than ATRC. In ATRP, another important factor is involved in the reaction; efficient activation of the halogen atom at the polymer terminal by the metal catalyst, which may proceed through a dormant species shown in Scheme 4, is an essential key to well-controlled living-like polymerization. Since reactivation and chain growth of the polymer terminal take place many times during the polymerization, both efficiency and durability are required for the good ATRP catalyst. In our examinations for the coordinatively unsaturated diruthenium amidinate, $[(\eta^5\text{-}C_5Me_5)Ru(\mu_2\text{-}i\text{-}PrN{=}C(Me)N i\text{-}Pr)Ru(\eta^5\text{-}C_5Me_5)]^+$**4**, as the ATRC, ATRA, and ATRP catalyst, we found that **4** can effectively activate a C–X bond of organic or macromolecular halides.[27] In the cyclization and intermolecular addition reaction, the catalytic activity is often comparable to the conventional CuCl/bipy catalyst, and even higher in

Table 7. Radical polymerization of MMA using macroinitiator **9a** and **9b** (all reactions were carried out using 19 μmol of **4**, 19 μmol of **9**, 19 mmol of MMA in 2 mL of toluene)

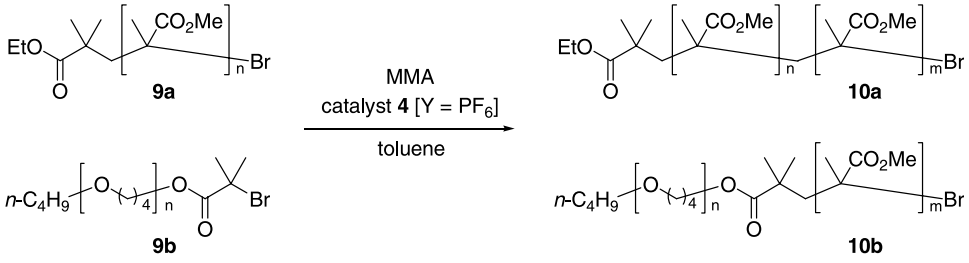

Entry	Initiator **9**		Conditions	Conversion (%)[a]	Yield (%)[b]	M_n[c]	M_w/M_n[c]
1	**9a**	M_n=7000, M_w/M_n=1.2	25 °C, 20 h	28	25	47,000	1.3
2	**9b**	M_n=3800, M_w/M_n=1.2	25 °C, 4 h	37	35	26,000	1.2
3	**9b**	M_n=2600, M_w/M_n=1.4	40 °C, 20 h	>95	90	71,000	1.6

[a] Determined by ^1H NMR analysis.
[b] Isolated yield after precipitation.
[c] Determined by GPC analysis of the crude polymer.

extreme cases. This clearly shows an advantage of coordinatively unsaturated complexes in catalyst efficiency for the halogen abstraction at the initial stage of the catalytic cycle, which especially contributes to rapid ATRC. This catalyst species is also active towards polymerization of methacrylate using macroinitiators at low temperature (rt to 40 °C), giving poly(MMA) and poly(THF)–poly(MMA) block copolymer with narrow molecular weight distributions, however, the polymerization is often accompanied by the catalyst deactivation leading to low conversion of the monomer. In other words, the present coordinatively unsaturated polymerisation catalyst has a strong point in the efficiency but not in the durability. Consequently, the results presented in this paper demonstrate that use of coordinatively unsaturated species is a reasonable strategy for the development of good catalysts for ATRC. For their application to ATRP, durability has somehow to be added to the catalyst to achieve high conversion of the monomer.

These findings provide important aspects in catalyst search for atom-transfer radical reactions.

4. Experimental

4.1. General methods

All reactions were carried out under a nitrogen or argon atmosphere. Solvents were distilled under an inert gas atmosphere from CaH_2 (dichloromethane and dichloroethane) or sodium/benzophenone (toluene) prior to use. Sodium tetraphenylborate was purchased from Wako Pure Chemical Ind, Ltd. Sodium hexafluorophosphate, ethyl α-bromoisobutylate **8** were purchased from Tokyo Chemical Industry Co., Ltd. ^{1}H and ^{13}C NMR spectra were measured on JEOL GSX-270 (270 MHz), Lambda 400 (400 MHz), Lambda 600 (600 MHz) spectrometers. Chemical shifts for ^{1}H NMR were described in parts per million downfield from tetramethylsilane as an internal standard ($\delta=0$) in $CDCl_3$, unless otherwise noted. Chemical shifts for ^{13}C NMR were expressed in parts per million in $CDCl_3$ as an internal standard ($\delta=77.1$), unless otherwise noted. IR spectra were measured on a JASCO FT/IR-550 spectrometer. Column chromatography was performed with silica gel (Merck, Art 7734). Elemental Analysis was performed by the Elemental Analysis Center, Faculty of Science, Kyushu University. Analytical thin-layer chromatography (TLC) was performed on glass plates and aluminum sheets precoated with silica gel (Merck, Kieselgel 60 F_{254}, layer thickness 0.25 and 0.2 mm, respectively). Visualization was accomplished by UV light (254 nm), anisaldehyde, and phosphomolybdic acid. GPC analyses of the polymers were performed with a JASCO DG-1580-83 degasser, PU-980 HPLC pump, UV-970 UV/vis detector, RI-930 RI detector, and CO-2065-plus column oven (at 40 °C) using a Shodex GPC-KF-804L connected with a GPC KF-805L in THF. Calibration was carried out on the basis of retention time of a standard sample of poly(methyl methacrylate) (Shodex Standard M-75) (7 samples (M_w/M_n=1.02–1.09), of which the M_n range is 1.84×10^3–1.99×10^6. Diruthenium amidinate complexes (**3** and **4d**),[9] *N*-Allyl-2,2,2-trichloroacetamides **5a–d**[3c] and poly(THF)[23] were prepared by our method. Other acetamides **5e**[13d] and **5f**[11a] were prepared by the literature method.

4.2. General procedure for the atom-transfer radical cyclization of *N*-allyl-α-halogenated acetamides catalyzed by in situ-generated cationic diruthenium amidinates

In a typical example, (η^5-C_5Me_5)Ru(μ^2-*i*-PrN=C(Me)N*i*-Pr)Ru(Cl)(η^5-C_5Me_5) (**3a**, 13.0 mg, 0.02 mmol), $NaBPh_4$ (6.9 mg, 0.02 mmol) and *N*-allyl-*N*-tosyl-2,2-dichloroacetamide (**5g**, 64.4 mg, 0.2 mmol) were measured into a flask, and the atmosphere was replaced by argon. Then freshly distilled, carefully degassed dichloromethane (1.5 mL) was added. After it was stirred for 3 h at 25 °C, the reaction mixture was filtered through a pad of Celite and Florisil, and then the filtrate was concentrated under reduced pressure. Purification by silica gel chromatography (1:1 hexane/ether) gave the cyclized product (**6g**) in 88% yield (56.7 mg): the cis/trans ratio was determined by ^{1}H NMR analysis.

4.2.1. 3,3-Dichloro-4-chloromethyl-1-benzyl-pyrrolidin-2-one (6a).[3c] ^{1}H NMR (600 MHz, $CDCl_3$): $\delta=3.03$–3.13 (m, 2H), 3.47 (m, 1H), 3.68 (dd, $J=11.2$, 9.5 Hz, 1H), 3.97 (dd, $J=11.2$, 3.7 Hz, 1H), 4.45 (d, $J=14.6$ Hz, 1H), 4.63 (d, $J=14.6$ Hz, 1H), 7.21–7.41 (m, 5H); ^{13}C NMR (150 MHz, $CDCl_3$): $\delta=41.1$, 47.4, 48.0, 51.7, 83.8, 128.3, 128.4, 129.2, 134.6, 166.1.

4.2.2. 3,3-Dichloro-4-chloromethyl-1-(*p*-toluenesulfonyl)-pyrrolidin-2-one (6b).[3c] ^{1}H NMR (600 MHz, $CDCl_3$): $\delta=2.46$ (s, 3H), 3.08 (dddd, $J=10.0$, 8.8, 7.1, 4.4 Hz, 1H), 3.56 (dd, $J=10.5$, 8.8 Hz, 1H), 3.66 (dd, $J=11.5$, 10.0 Hz, 1H), 3.93 (dd, $J=11.5$, 4.4 Hz, 1H), 4.24 (dd, $J=10.5$, 7.1 Hz, 1H), 7.37 (d, $J=8.3$ Hz, 2H), 7.93 (d, $J=8.3$ Hz, 2H); ^{13}C NMR (150 MHz, $CDCl_3$): $\delta=21.9$, 40.2, 47.5, 50.8, 82.7, 128.4, 130.1, 133.4, 146.5, 163.1.

4.2.3. 3,3-Dichloro-4-chloromethyl-1-phenyl-pyrrolidin-2-one (6c). White solid; mp 142 °C; IR (KBr): $\nu=1710$, 1594, 1496, 1417, 1306, 761, 750 cm^{-1}; ^{1}H NMR (600 MHz, $CDCl_3$): $\delta=3.26$ (dddd, $J=10.4$, 8.2, 7.1, 4.4 Hz, 1H), 3.74 (dd, $J=9.9$, 8.2 Hz, 1H), 3.85 (dd, $J=11.0$, 10.4 Hz, 1H), 4.09 (dd, $J=11.0$, 4.4 Hz, 1H), 4.10 (dd, $J=9.9$, 7.1 Hz, 1H), 7.26 (t, $J=7.1$ Hz, 1H), 7.43 (dd, $J=8.2$, 7.1 Hz, 2H), 7.64 (d, $J=8.2$ Hz, 2H); ^{13}C NMR (150 MHz, $CDCl_3$): $\delta=41.0$, 49.1, 51.1, 84.0, 120.3, 126.2, 129.2, 137.9, 164.4; elemental Anal. Calcd (%) for $C_{11}H_{10}Cl_3NO$: C, 47.51; H, 3.61; N, 5.04. Found: C, 47.43; H, 3.62; N, 5.03.

4.2.4. 3,3-Dichloro-4-chloromethyl-1-allyl-pyrrolidin-2-one (6d).[3a] ^{1}H NMR (600 MHz, $CDCl_3$): $\delta=3.10$ (dddd, $J=9.9$, 8.2, 7.7, 6.6 Hz, 1H), 3.22 (dd, $J=9.9$, 7.7 Hz, 1H), 3.57 (dd, $J=10.4$, 6.6 Hz, 1H), 3.73 (dd, $J=10.4$, 9.9 Hz, 1H), 3.95 (dd, $J=15.4$, 6.0 Hz, 1H), 3.98 (dd, $J=15.4$, 4.4 Hz, 1H), 3.99 (dd, $J=9.9$, 8.2 Hz, 1H), 5.26 (d, $J=17.0$ Hz, 1H), 5.29 (*d*, $J=10.4$ Hz, 1H), 5.73 (dddd, $J=17.0$, 10.4, 6.0, 4.4 Hz, 1H); ^{13}C NMR (150 MHz, $CDCl_3$): $\delta=41.0$, 46.4, 47.4, 51.7, 83.6, 119.7, 130.4, 165.7.

4.2.5. 3,3-Dimethyl-4-bromomethyl-1-(*p*-toluenesulfonyl)-pyrrolidin-2-on (6e).[12d] ^{1}H NMR (600 MHz,

$CDCl_3$): δ=0.89 (s, 3H), 1.16 (s, 3H), 2.44 (s, 3H), 2.45 (dddd, J=9.9, 8.8, 7.7, 4.4 Hz, 1H), 3.20 (t, J=9.9 Hz, 1H), 3.43 (dd, J=9.9, 4.4 Hz, 1H), 3.46 (dd, J=10.4, 8.8 Hz, 1H), 4.15 (dd, J=10.4, 7.7 Hz, 1H), 7.34 (d, J=8.2 Hz, 2H), 7.91 (d, J=8.2 Hz, 2H); ^{13}C NMR (150 MHz, $CDCl_3$): δ=17.8, 21.7, 23.4, 29.7, 45.0, 45.4, 48.8, 128.0, 129.7, 134.8, 145.3, 176.8.

4.2.6. (1*R*,7a*S*)-1-Chlorometyl-2,2-dichloro-hexahydropyrrolizin-3-one (6f).[11a] ^{1}H NMR (400 MHz, $CDCl_3$): δ=3.99 (dd, 1H), 3.86 (dd, 1H), 3.62 (m, 1H), 3.54 (m, 1H), 3.29 (m, 1H), 2.76 (m, 2H), 2.17 (m, 2H), 1.61 (m, 1H); ^{13}C NMR (100 MHz, $CDCl_3$): δ=26.7, 31.5, 40.6, 41.8, 61.3, 62.9, 87.0, 164.1.

4.2.7. 3-Chloro-4-chloromethyl-1-(*p*-toluenesulfonyl)-pyrrolidin-2-one (6g).[13a] *trans-Isomer*. ^{1}H NMR (600 MHz, $CDCl_3$): δ=2.46 (s, 3H), 2.82 (m, 1H), 3.68–3.78 (m, 3H), 4.11 (dd, J=10.2, 8.1 Hz, 1H), 4.34 (d, J=9.3 Hz, 1H), 7.34 (d, J=8.3 Hz, 2H), 7.94 (d, J=8.3 Hz, 2H); ^{13}C NMR (150 MHz, $CDCl_3$): δ=21.8, 42.3, 44.2, 47.0, 56.1, 128.3, 130.0, 134.3, 146.1, 166.7.

cis-Isomer. ^{1}H NMR (600 MHz, $CDCl_3$): δ=2.46 (s, 3H), 2.95 (ddddd, J=8.3, 7.6, 7.3, 6.8, 6.1 Hz, 1H), 3.53 (dd, J=11.5, 7.6 Hz, 1H), 3.66 (dd, J=10.3, 8.3 Hz, 1H), 3.71 (dd, J=11.5, 6.8 Hz, 1H), 4.13 (dd, J=10.3, 7.3 Hz, 1H), 4.44 (d, J=6.1 Hz, 1H), 7.37 (d, J=8.3 Hz, 2H), 7.92 (d, J=8.3 Hz, 2H); ^{13}C NMR (150 MHz, $CDCl_3$): δ=21.8, 40.4, 41.0, 47.9, 57.6, 128.2, 130.0, 134.0, 146.0, 166.8.

4.3. Reaction of α,α,γ-trichlorinated γ-lactam 6b and methylenecyclohexane

4.3.1. 3-Chloro-3-(1′-chlorocyclohexyl)methyl-4-chloromethyl-1-(*p*-toluenesulfonyl)pyrrolidin-2-one (7b).[14b] (η^5-C_5Me_5)Ru(μ^2-*i*-PrN=C(Me)N*i*-Pr)Ru(Cl)(η^5-C_5Me_5) (**3a**, 13.0 mg, 0.02 mmol), $NaBPh_4$ (6.9 mg, 0.02 mmol) and lactam (**6b**, 71.3 mg, 0.2 mmol) were measured into a flask, and the atmosphere was replaced by argon. Then freshly distilled, carefully degassed dichloromethane (1.5 mL) and methylenecyclohexane (240 μL, 2.0 mmol) were added. After it was stirred for 10 h at 25 °C, the reaction mixture was filtered through a pad of Celite and Florisil, and then the filtrate was concentrated under reduced pressure. Purification by silica gel chromatography (2:1 hexane/ether) gave the α-alkylated product (**7**) in 57% yield (51.2 mg). The cis/trans ratio was determined by ^{1}H NMR analysis.

cis-Isomer. Single crystals for the X-ray diffraction study were obtained from dichloromethane/hexane at rt. Colorless solid; mp 151–153 °C; ^{1}H NMR (400 MHz, $CDCl_3$): δ=1.06 (m, 1H), 1.38–1.81 (m, 8H), 1.91 (m, 1H), 2.44 (s, 3H), 2.47 (d, J=15.6 Hz, 1H), 2.75 (d, J=15.6 Hz, 1H), 3.47–3.54 (m, 2H), 3.63 (dd, J=11.0, 8.8 Hz, 1H), 4.01 (dd, J=11.2, 2.9 Hz, 1H), 4.34 (m, 1H), 7.35 (d, J=8.2 Hz, 2H), 7.90 (d, J=8.2 Hz, 2H); ^{13}C NMR (100 MHz, $CDCl_3$): δ=21.4, 21.7, 21.8, 24.7, 37.3, 42.0, 42.3, 42.4, 48.2, 49.5, 71.9, 72.9, 128.2, 129.8, 133.7, 145.9, 168.5.

trans-Isomer. ^{1}H NMR (400 MHz, $CDCl_3$): δ=1.02–2.02 (m, 10H), 2.44 (s, 3H), 2.50 (d, J=14.4 Hz, 1H), 2.90 (d, J=14.4 Hz, 1H), 3.40–3.69 (m, 3H), 3.71 (dd, J=11.2, 4.4 Hz, 1H), 4.25 (dd, J=10.0, 7.1 Hz, 1H), 7.35 (d, J=8.2 Hz, 2H), 7.90 (d, J=8.2 Hz, 2H); ^{13}C NMR (100 MHz, $CDCl_3$): δ=21.8, 22.7, 25.5, 29.5, 37.3, 41.5, 42.3, 44.7, 48.0, 49.5, 71.9, 72.9, 128.4, 129.6, 133.9, 145.8, 168.6.

4.3.2. 3-Allyl-3-chloro-4-chloromethyl-1-(*p*-toluenesulfonyl)-pyrrolidin-2-one 7a.[14b] *cis-Isomer*. ^{1}H NMR (600 MHz, $CDCl_3$): δ=2.42 (s, 3H), 2.75 (dd, J=14.1, 7.5 Hz, 1H), 2.80 (dd, J=14.1, 6.7 Hz, 1H), 2.81 (dddd, J=9.6, 9.2, 7.1, 5.3 Hz, 1H), 3.41 (dd, J=10.1, 9.6 Hz, 1H), 3.56 (dd, J=11.4, 9.2 Hz, 1H), 3.76 (dd, J=11.4, 5.3 Hz, 1H), 4.18 (dd, J=10.1, 7.1 Hz, 1H), 5.20 (d, J=10.3 Hz, 1H), 5.21 (d, J=17.0 Hz, 1H), 5.64 (dddd, J=17.0, 10.3, 7.5, 6.7 Hz, 1H), 7.33 (d, J=8.2 Hz, 2H), 7.88 (d, J=8.2 Hz, 2H); ^{13}C NMR (150 MHz, $CDCl_3$): δ=21.8, 40.9, 41.2, 42.9, 47.7, 71.1, 121.8, 128.1, 129.8, 130.3, 133.8, 145.9, 168.0.

trans-Isomer. ^{1}H NMR (600 MHz, $CDCl_3$): δ=2.45 (s, 3H), 2.48 (dd, J=15.8, 7.5 Hz, 1H), 2.77 (dd, J=15.8, 6.0 Hz, 1H), 2.87 (dddd, J=9.3, 6.2, 3.8, 3.1 Hz, 1H), 3.41 (dd, J=11.4, 9.3 Hz, 1H), 3.70 (dd, J=11.4, 3.8 Hz, 1H), 3.93 (dd, J=10.4, 3.1 Hz, 1H), 4.10 (dd, J=10.4, 6.2 Hz, 1H), 5.18 (d, J=10.4 Hz, 1H), 5.21 (d, J=17.4 Hz, 1H), 5.79 (dddd, J=17.4, 10.4, 7.5, 6.0 Hz, 1H), 7.35 (d, J=8.4 Hz, 2H), 7.94 (d, J=8.4 Hz, 2H); ^{13}C NMR (150 MHz, $CDCl_3$): δ=21.7, 37.8, 41.3, 46.5, 47.4, 70.1, 120.8, 128.2, 129.8, 130.0, 134.0, 145.8, 168.0.

4.3.3. Preparation of macroinitiator 9b. To a solution of $PhMe_2SiO$-[$(CH_2)_4O$]$_n$-C_4H_9 [M_n=2500, M_w/M_n=1.4] (300 mg, 0.12 mmol) in benzene (2 mL) was added ethyl α-bromoisobutylate (36 μL, 0.45 mmol). The mixture was stirred at ambient temperature for 20 h, then the reaction mixture was poured into methanol (25 mL) and concentrated under reduced pressure. The residue was dissolved in chloroform (0.5 mL) and was purified by precipitation by adding methanol (50 mL) at −30 °C gave the polymer **9b** in 70% yield (208 mg). ^{1}H NMR (270 MHz, $CDCl_3$): δ=0.89 (t, J=7.3 Hz, 3H; terminal CH_3), 1.40–1.80 (m; CH_2), 1.91 (s, 6H; CBrMe_2), 3.30–3.50 (m; OCH_2), 4.17 (t, J=6.3 Hz, 2H; OCH_2–^{n}Pr). The GPC analysis showed M_n=2600, M_W/M_n=1.4.

4.4. General procedure for the polymerization promoted by the isolated complex 4

In a typical example, a mixture of **4** [Y=PF_6] (10 mg, 19 μmol), MMA (2 mL, 19 mmol), **9b** [M_n=2600, M_W/M_n=1.4] (50 mg, 0.019 mmol), and toluene (2 mL) was placed in a glass tube. The mixture was degassed three times, and sealed in vacuo. After it was stirred at 40 °C for 20 h, the reaction mixture was dissolved in THF, passed through an alumina column, then concentrated under reduced pressure. The residue was dissolved in THF and was purified by precipitation by adding methanol (50 mL) gave the polymer **10b** in 90% yield (1.7 g). The GPC analysis showed M_n=71,000, M_W/M_n=1.6.

4.5. Electrochemical measurements

Cyclic voltammetric studies were carried out using a BAS

50B/W electrochemical analyzer in a globe box filled with purified nitrogen. The measurement was performed at rt using a ruthenium or copper complex (0.0015 mmol) in THF (5 mL) containing Bu_4NPF_6 (0.1 M) as a supporting electrolyte. A three-electrode cell was used, which was equipped with a platinum disk working electrode, a platinum wire counter electrode, and a silver reference electrode comprised of a silver wire in count with $AgNO_3$ (0.01 M) and Bu_4NPF_6 (0.2 M) in acetonitrile.

4.6. X-ray structure determination and details of refinement

X-ray-quality crystals of *cis*-**7b** were grown from a mixture of CH_2Cl_2 and hexane, and mounted on a loop. All measurements were made on a Rigaku Saturn CCD area detector with graphite monochromated Mo Kα radiation; $\lambda=0.71070$ Å. The crystal-to-detector distance was 45.01 mm. The data were collected at 123(1) K to a maximum 2θ value of 55.0°. The exposure rate was 12.0 s/° The data were corrected for Lorentz and polarization effects. The structure was solved by heavy-atom Patterson methods[29] and expanded using Fourier techniques.[30] The non-hydrogen atoms were refined anisotropically. Hydrogen atoms were refined using the riding model. The final cycle of full-matrix least-squares refinement on F^2 was based on 4675 observed reflections and 268 variable parameters. Neutral atom scattering factors were taken from Cromer and Waber.[31] All calculations were performed using the CrystalStructure[32,33] crystallographic software package. Final refinement details are collected in Table 8, and the numbering scheme employed is shown in Figure 1, which were drawn with ORTEP at 50% probability ellipsoid. Crystallographic data (excluding structure factors) for the structure has been deposited with the Cambridge Crystallographic Data Centre as supplementary publication no. CCDC-259053. Copies of the data can be obtained free of charge on application to CCDC, 12 Union Road, Cambridge CB21EZ, UK (fax: +44 1223 336 033; e-mail: deposit@ccdc.cam.ac.uk).

Table 8. Crystallographic data and structure refinement for 3,4-*cis*-**7b**

Formula	$C_{19}H_{24}Cl_3NO_3S$
FW	452.82
Crystal system	Triclinic
Space group	*P*-1 (#2)
Cell constants	
a (Å)	8.787(4)
b (Å)	10.892(5)
c (Å)	11.455(5)
α (°)	70.82(1)
β (°)	84.98(2)
γ (°)	89.56(2)
V (Å^3)	1031.3(8)
Z value	2
D_{calcd} (g/cm^3)	1.458
F (000)	472.00
μ (Mo Kα) (cm^{-1})	5.61
Radiation; λ (Å)	0.71070
Temperature (°C)	−150
Exposure rate (s/°)	12.0
$2\theta_{max}$ (°)	55.0
No. of total data collected	12,453
No. of unique data	4687 ($R_{int}=0.040$)
No. of obsd reflections	4675
No. of variables	268
Reflection/parameter ratio	17.44
Residuals	
*R*1 ($I>2\sigma$)	0.036
R (all reflections)	0.067
*wR*2 (all reflections)	0.066
GOF	1.000

Acknowledgements

This work was supported by a Grant-in-Aid for Scientific Research from the Ministry of Education, Culture, Sports, Science and Technology, Japan.

Supplementary data

Supplementary data associated with this article can be found, in the online version, at doi:10.1016/j.tet.2005.08.037. Tables of crystal structure parameters and details of data correction, bond angles and distances, and atomic positional and thermal parameters of 3,4-*cis*-**7**.

References and notes

1. (a) Giese, B. *Radicals in Organic Synthesis: Formation of Carbon–Carbon Bonds*; Pergamon: New York, 1986. (b) Curran, D. P. In Trost, B. M., Fleming, I., Eds.; Comprehensive Organic Synthesis; Pergamon: Oxford, 1991; Vol. 4, p 715. (c) *Radicals in Organic Synthesis*; Renaud, P., Sibi, M. P., Eds.; Wiley-VCH: Weinheim, 2001.
2. Asscher, M.; Vofsi, D. *J. Chem. Soc.* **1961**, 2261. **1963**, 1887, 3921.
3. (a) Nagashima, H.; Wakamatsu, H.; Ito, K.; Tomo, Y.; Tsuji, J. *Tetrahedron Lett.* **1983**, *23*, 2395. (b) Nagashima, H.; Wakamatsu, H.; Itoh, K. *J. Chem. Soc., Chem. Commun.* **1984**, 652. (c) Nagashima, H.; Ozaki, N.; Seki, K.; Ishii, M.; Itoh, K. *J. Org. Chem.* **1989**, *54*, 4497. (d) Nagashima, H.; Seki, K.; Ozaki, N.; Wakamatsu, H.; Itoh, K.; Tomo, Y.; Tsuji, J. *J. Org. Chem.* **1990**, *55*, 985. (e) Nagashima, H.; Ozaki, N.; Ishii, M.; Seki, K.; Washiyama, M.; Itoh, K. *J. Org. Chem.* **1993**, *58*, 464.
4. Reviews: (a) Iqbal, J.; Bhatia, B.; Nayyar, N. K. *Chem. Rev.* **1994**, *94*, 519. (b) Giese, B.; Kopping, B.; Gobel, T.; Dickhaut, J.; Thoma, G.; Kulicke, K. J.; Trach, F. *Org. React.* **1996**, *48*, 301. (c) Clark, A. J. *Chem. Soc. Rev.* **2002**, *31*, 1.
5. (a) Kato, M.; Kamigaito, M.; Sawamoto, M.; Higashimura, T. *Macromolecules* **1995**, *28*, 1721. (b) Wang, J. S.; Matyjaszewski, K. *J. Am. Chem. Soc.* **1995**, *117*, 5614. (c) Patten, T. E.; Xia, T.; Abernathy, K.; Matyjaszewski, K. *Science* **1996**, *272*, 866.
6. (a) *Controlled Radical Polymerization*; Matyjaszewski, K., Ed.; ACS Symposium Series 685; American Chemical Society: Washington, 1998. (b) Patten, T. E.; Matyjaszewski, K. *Adv. Mater.* **1998**, *10*, 901. (c) Sawamoto, M.; Kamigaito, M. In *Synthesis of Polymers*; Schlüter, A.-D., Ed.; Materials Science and Technology Series; Wiley-VCH: Weinheim, 1999. (d) Matyjaszewski, K.; Xia, J. *Chem. Rev.* **2001**, *101*, 2921. (e) Kamigaito, M.; Ando, T.; Sawamoto, M. *Chem. Rev.* **2001**, *101*, 3689.
7. (a) Minisci, F. *Acc. Chem. Res.* **1975**, *8*, 165. (b) Kochi, J. K.

Organometallic Mechanisms and Catalysis; Academic: New York, 1978. (c) Davis, R.; Groves, I. F. *J. Chem. Soc., Dalton Trans.* **1982**, 2281.

8. (a) Yamaguchi, Y.; Nagashima, H. *Organometallics* **2000**, *19*, 725. (b) Kondo, H.; Kageyama, A.; Yamaguchi, Y.; Haga, M.; Kirchner, K.; Nagashima, H. *Bull. Chem. Soc. Jpn.* **2001**, *74*, 1927. (c) Nagashima, H.; Gondo, M.; Masuda, S.; Kondo, H.; Yamaguchi, Y.; Matsubara, K. *Chem. Commun.* **2003**, 442. Also see: (d) Nagashima, H.; Kondo, H.; Hayashida, T.; Yamaguchi, Y.; Gondo, M.; Masuda, S.; Miyazaki, K.; Matsubara, K.; Kirchner, K. *Coord. Chem. Rev.* **2003**, *245*, 177.
9. (a) Kondo, H.; Yamaguchi, Y.; Nagashima, H. *J. Am. Chem. Soc.* **2001**, *123*, 500. (b) Kondo, H.; Matsubara, K.; Nagashima, H. *J. Am. Chem. Soc.* **2002**, *124*, 534.
10. Preliminary communication, see: Motoyama, Y.; Gondo, M.; Masuda, S.; Iwashita, Y.; Nagashima, H. *Chem. Lett.* **2004**, *33*, 442.
11. Matyjaszewski, K. *ACS Symp. Ser.* **1998**, *685*, 258.
12. Terasawa, J.; Kondo, H.; Matsumoto, T.; Kirchner, K.; Motoyama, Y.; Nagashima, H. *Organometallics* **2005**, *24*, 2713.
13. (a) Seijas, J. A.; Vazquez-Tato, M. P.; Castedo, L.; Estevez, R. J.; Onega, M.; Ruiz, M. *Tetrahedron* **1992**, *48*, 1637. (b) Ishibashi, H.; Uemura, N.; Nakatani, H.; Okazaki, M.; Sato, T.; Nakamura, N.; Ikeda, M. *J. Org. Chem.* **1993**, *58*, 2360.
14. (a) Stewart, W. S.; Siddall, T. H., III *Chem. Rev.* **1970**, *70*, 517. (b) Gansow, O. A.; Killough, J.; Burke, A. R. *J. Am. Chem. Soc.* **1971**, *93*, 4297. (c) Curran, D. P.; Tamine, J. *J. Org. Chem.* **1991**, *56*, 2746. (d) Iwamatsu, S.; Matsubara, K.; Nagashima, H. *J. Org. Chem.* **1999**, *64*, 9625. (e) Nagashima, H.; Isono, Y.; Iwamatsu, S. *J. Org. Chem.* **2001**, *66*, 315.
15. *Gaussian 98 package: Gaussian 98*, Revision A.11; Gaussian Inc.: Pittsburgh, PA,USA, 2001.
16. (a) Rachita, M. A.; Slough, G. A. *Tetrahedron Lett.* **1993**, *34*, 6821. (b) Clark, A. J.; Duncalf, D. J.; Filik, R. P.; Haddleton, D. M.; Thomas, G. H.; Wongtap, H. *Tetrahedron Lett.* **1999**, *40*, 3807. (c) Clark, A. J.; Filik, R. P.; Thomas, G. H. *Tetrahedron Lett.* **1999**, *40*, 4885. (d) Clark, A. J.; Filik, R. P.; Haddleton, D. M.; Radigue, A.; Sanders, C. J.; Thomas, G. H.; Smith, M. E. *J. Org. Chem.* **1999**, *64*, 8954.
17. It is known that equilibrium between the trans- and cis-isomers of this type of compounds easily took place in the presence of transition metal complexes over 80 °C, and the thermodynamically controlled ratio of *trans*-**6g** to *cis*-**6g** reached ca. 4:1: (a) Sloigh, G. A. *Tetrahedron Lett.* **1993**, *34*, 6825. (b) Iwamatsu, S.; Kondo, H.; Matsubara, K.; Nagashima, H. *Tetrahedron* **1999**, *55*, 1687.
18. DFT calculations (Ref. 15) (B3LYP/6-311++G(2d,p)//B3LYP/6-31G(d) level) of *cis*-**6g** and *trans*-**6g** were carried out to show that the *trans*-**6g** proved to be slightly stable (2.75 kJ/mol) than the cis-isomer.
19. Iron-based catalyst: (a) Forti, L.; Ghelfi, F.; Libertini, E.; Pagnoni, U. M.; Soragni, E. *Tetrahedron* **1997**, *53*, 17761. (b) Cu/bipyridine catalyst, see Ref. 17b.
20. Watanabe, Y.; Ando, T.; Kamigaito, M.; Sawamoto, M. *Macromolecules* **2001**, *34*, 4370.
21. In the reaction of MMA and initiator **8** catalyzed by **4** (**4**/**8**/MMA=1:1:1000), the M_n of formed poly(MMA) is linearly increased in increasing the conversion of MMA with narrow molecular weight distribution (M_w/M_n (1.2 in toluene) at the initial stage (<10% conversion), however, such relationship gradually deviates from the linearity because of the decomposition of the catalyst.
22. Ando, T.; Kamigaito, M.; Sawamoto, M. *Macromolecules* **2000**, *33*, 2819.
23. (a) Iura, T.; Matsubara, K.; Nagashima, H.; The Reports of Advanced Material Study; Kyushu University, 2000; Vol. 14, p 119. (b) Nagashima, H.; Suzuki, A.; Iura, T.; Ryu, K.; Matsubara, K. *Organometallics* **2000**, *19*, 3579.
24. Recent representative papers: (a) Narita, M.; Nomura, R.; Endo, T. *Macromolecules* **1998**, *31*, 2774. (b) Kajiwara, A.; Matyjaszewski, K. *Macromolecules* **1998**, *31*, 3489.
25. Matyjaszewski reported the polymerization of MMA with CuBr/dNbipy [dNbipy=4,4′-di(5-nonyl)-2,2′-bipyridine] using poly(THF)-derived bromopropionate as the initiator, in which the temperature over 90 °C (24 h, >97% conversion) was required for the reaction (Ref. 24b).
26. The reason why the conversion of MMA reached over 95% in the polymerization using poly(THF)-derived initiator **9b** is not clear at present. We assumed that the polyether moiety of both the initiator **9b** and the dormant chain might effectively stabilize the highly reactive diruthenium amidinate **4** with an oxophilic nature.
27. For the metal-catalyzed atom-transfer reactions, the redox mechanisms shown in Scheme 1 are often proposed, which involve a halogen atom transfer reaction from the formed M–X species to the carbon radical intermediates. Although possible involvement of free radical chain processes cannot be completely excluded in the ATRA, ATRC, and ATRP reactions presented in this paper, the following points strongly support the redox mechanism. First, the same coordinatively unsaturated complex catalyzes all of the ATRA, ATRC, and ATRP reactions; this suggests that these three reactions proceed through similar mechanisms. Second, free radical polymerization generally provides polymers with wide molecular weight distributions, and termination process is disproportionation (Ref. 28). In contrast, the ATRP presented in this paper achieves the production of polymers having a halogen atom end group with narrow M_w/M_ns; this strongly suggests interaction of the radical species at the polymer end with the metallic species leading to abstraction of the halogen atom from the M–X species by the polymer radical. As a consequence of the first and the second points, other two reactions, ATRA and ATRC, should also be promoted by the redox mechanism not involving the free radical chain process.
28. Kashiwagi, T.; Kitayama, T.; Masuda, E. *Macromolecules* **1986**, *19*, 2160.
29. Beurskens, P. T.; Admiraal, G.; Beurskens, G.; Bosman, W. P.; Garcia-Granda, S.; Gould, R. O.; Smits, J. M. M.; Smykalla, C. *PATTY: The DIRDIF program system*; Technical Report of the Crystallography Laboratory; University of Nijmegen: The Netherlands, 1992.
30. Beurskens, P. T.; Admiraal, G.; Beurskens, G.; Bosman, W. P.; de Gelder, R.; Israel, R.; Smits, J. M. M. *DIRDIF99: The DIRDIF-99 program system*; Technical Report of the Crystallography Laboratory; University of Nijmegen: The Netherlands, 1999.
31. Cromer, D. T.; Waber, J. T. In *International Tables for X-ray Crystallography*, *Vol. 4*; Kynoch: Birmingham, England, 1974; Table 2.2 A.
32. *CrystalStructure 3.6.0: Crystal Structure Analysis Package*, Rigaku and Rigaku/MSC (2000–2004); 9009 New Trails: Dr. The Woodlands TX 77381, USA.
33. Watkin, D. J.; Prout, C. K.; Carruthers, J. R.; Betteridge, P. W. *Crystals*; Chemical Crystallography Laboratory: Oxford, UK, 1996.

Available online at www.sciencedirect.com
SCIENCE DIRECT
Tetrahedron
ELSEVIER
Tetrahedron 61 (2005) 10227–10234

New pyrrolopyridazine derivatives as blue organic luminophors

K. M. K. Swamy,[a] Min Sun Park,[a] Su Jung Han,[b] Sook Kyung Kim,[a] Ju Hee Kim,[a] Chongmok Lee,[b] Hyunjin Bang,[a] Youngmee Kim,[b] Sung-Jin Kim[a,b] and Juyoung Yoon[a,b,*]

[a]*Division of Nano Sciences, Ewha Womans University, 11-1 Daehyon-Dong, Sodaemun-Ku, Seoul 120-750, Korea*
[b]*Department of Chemistry, Ewha Womans University, 11-1 Daehyon-Dong, Sodaemun-Ku, Seoul 120-750, Korea*

Received 14 May 2005; revised 10 August 2005; accepted 11 August 2005

Available online 2 September 2005

Abstract—New pyrrolopyridazine derivatives were synthesized as potential blue organic luminophors. Three different classes of pyrrolopyridazine derivatives were made, for example, aryl groups directly connected to the core PPY (pyrrolo[1,2-*b*]pyridazine-5,6,7-tricarboxylic acid trimethyl ester) moiety, aryl groups connected to the PPY via a vinylene linker and aryl groups connected to the PPY via an acetylene linker. Their optical and electrochemical properties were productively compared. One of the derivatives **2** showed a relative quantum yield as high as 0.9. Compound **8** in the vinyl bridged pyrrolopyridazine series has been characterized by its X-ray crystal structure analysis.

1. Introduction

Since the discovery of a thin-film organic electroluminescent device by the team at Kodak,[1a] organic light emitting diodes (OLED) have become the most promising new optoelectronic devices for practical industrial applications. Electroluminescent thin films of organic molecules have been extensively investigated because of their low operating voltage, tunable red-green-blue output colors, high brightness, mechanical flexibility and ease of fabrication.[1b] Although polymeric as well as small organic molecules are well established electroluminescent materials used in fabricating the thin film devices, smaller organic units were realized to be advantageous with facile emission color control and the easy fabrication of multilayer devices.[2] Investigations on synthesizing new blue luminous materials for applications in electroluminescent (EL) display have attracted great attention recently, but there are very few single component deep blue- and pure red-emitting dyes.[2]

Recently, Wudl et al. reported pyrrolopyridazine derivatives as a new class of blue organic luminophors. They demonstrated the possibility of tuning colors and energy levels by modifying the structures of these luminophors.[3] Herein, we report the synthesis of new pyrrolopyridazine derivatives, along with the optical properties of these new compounds. To study the relationship between optical properties and the effect of conjugation and substitution, we systematically designed and synthesized a series of luminophors containing a core pyrrolo[1,2-*b*]pyridazine-5,6,7-tricarboxylic acid trimethyl ester moiety. Three different classes of pyrrolopyridazine derivatives were synthesized, for example, aryl groups directly connected to the core PPY (pyrrolo[1,2-*b*]pyridazine-5,6,7-tricarboxylic acid trimethyl ester) moiety, aryl groups connected to the PPY via a vinylene linker and aryl groups connected to the PPY via an acetylene linker. Their comparative optical and electrochemical properties were investigated to study the effect of extended conjugation. Compound **8** in the vinyl bridged pyrrolopyridazine series has been characterized by its X-ray crystal structure analysis.

2. Results and discussion

2.1. Synthesis

For the synthesis of various pyrrolopyridazine derivatives, 3-iodopyridazine (**26**) was synthesized from 3,6-dichloropyridazine in four steps following the procedures reported elsewhere. The treatment of 3,6-dichloropyridazine with sodium iodide gave 3,6-diiodopyridazine, which was then reacted with hydrazine to give 6-iodo-3-pyridazinylhydrazine. This hydrazine was reacted with mercuric oxide to give 3-iodopyridazine.[4,5]

Keywords: Pyrrolopyridazine; Fluorescence; Luminophor; Blue luminophor; Sonogashira coupling; Blue shift; Red shift.
* Corresponding author. Tel.: +82 2 3277 2400; fax: +82 2 3277 2384; e-mail: jyoon@ewha.ac.kr

0040–4020/$ - see front matter © 2005 Elsevier Ltd. All rights reserved.
doi:10.1016/j.tet.2005.08.038

The 3-arylpyridazine derivatives (**14–16**) were synthesized as shown in Scheme 1 by modifying the literature procedures.[6] Synthesis of aryl pyridazines via Suzuki cross-coupling is a single step and more convenient than the reported method for the preparation of compound (**15**).[7] On the other hand, 3-(2-arylvinyl)pyridazine derivatives were also obtained in one step by the treatment of aromatic aldehydes with 3-methylpyridazine using the reported methodology (Scheme 2).[8a]

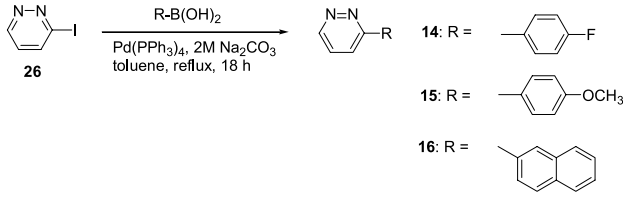

Scheme 1. Synthesis of 3-arylpyridazines (**14–16**) via Suzuki cross-coupling.

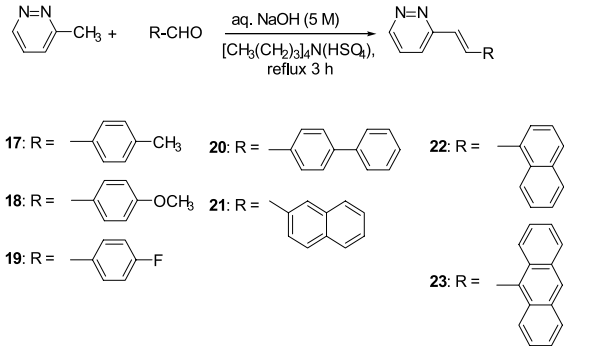

Scheme 2. Synthesis of 3-(2-aryl-vinyl)pyridazines (**17–23**).

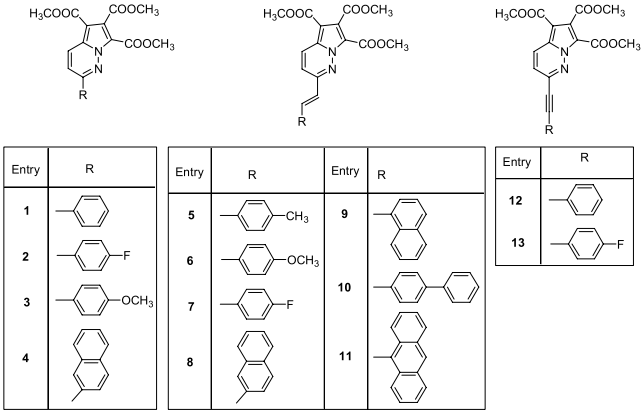

Figure 1. Luminophors synthesized (**1–13**).

The structural data of the compounds **18** and **19** were in a good agreement with the earlier reports.[8b,c] Sonogashira coupling[9] between 3-iodopyridazine and terminal alkynes in the presence of $(PPh_3)_2PdCl_2$ and CuI in basic condition yielded 3-arylethynylpyridazines (Scheme 3).

The luminescent pyrrolopyridazine derivatives (**1–13**) were prepared (Fig. 1) in one step via 1,3-dipolar cycloaddition reaction between 3-substituted pyridazines (aryl/vinylaryl/ethynylaryl) and dimethyl acetylenedicarboxylate (DMAD) in methanol at a low temperature as depicted in Scheme 4, by modifying the reported procedure.[3b]

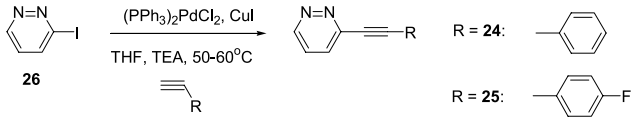

Scheme 3. 3-Arylethynylpyridazines (**24–25**) from Sonogashira reaction.

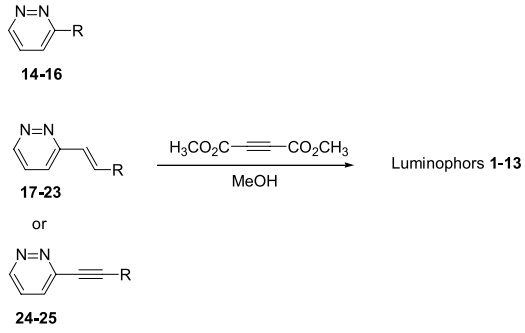

Scheme 4. Synthesis of luminophors (**1–13**).

2.2. X-ray crystal structure

A single crystal of compound **8** was grown from a CH_2Cl_2/MeOH solution and was characterized using X-ray

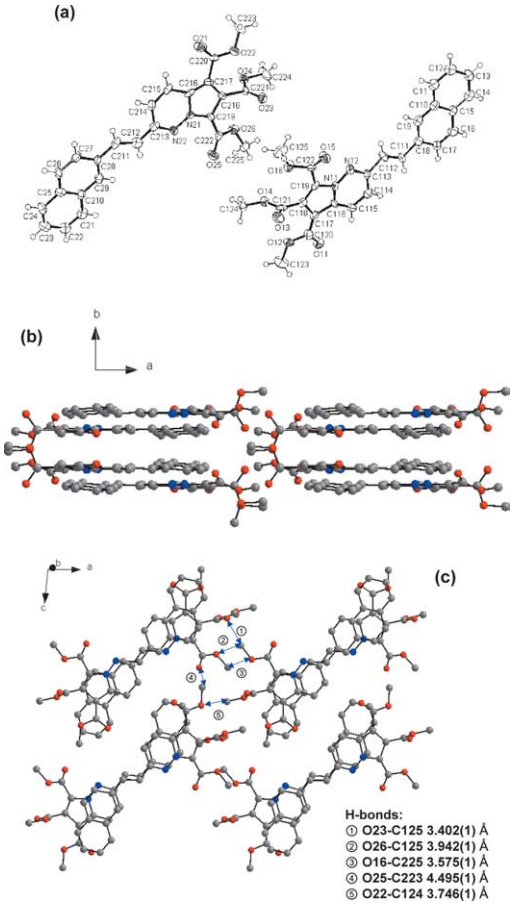

Figure 2. X-ray structure of **8** (in (b) and (c), blue: N and red: O).

crystallography. Figure 2 shows the π stacking of compound **8** in a head to tail mode. The molecules stack along the *b* axis and the average distance between the π planes was 3.66 Å (Fig. 2b). Hydrogen bonds between the oxygens and methyl group in the ester moieties were observed and the distances between these oxygens and carbons are in the range of 3.40–4.49 Å (Fig. 2c).

2.3. Optical properties

The absorption and fluorescence spectra of compounds **2**–**13** were recorded in DMSO, methanol, methylene chloride, and hexane solutions at room temperature. The relative quantum yields were determined using 9,10-diphenylanthracene in degassed hexane ($\Phi = 0.96$). The optical data for compound **1** was taken from the literature.[3]

As expected and illustrated in the cyclic voltametry data, significant red shifts were observed in UV as well as fluorescence for the compounds **6** and **7** being extended conjugation. Figure 3 exhibits that the second absorption bands of **7** (315 nm) and **6** (331 nm) are red-shifted compared with those of **2** (280 nm) and **3** (300 nm). These red shifts of compounds **6** and **7** were probably due to ground state stabilization arising from extended conjugation via vinylene linkage. The first absorption bands were assigned at around 350 nm for compound **1**, **2** and **3**. However, for compounds **5**, **6** and **7**, the absorption maximum around 320–340 nm was used as the excitation wavelength since the first absorption bands were overlapped with the second absorption bands. On the other hand, the compounds **12** and **13** bearing acetylene linkage displayed red shifts in their UV as well as fluorescence spectra (Figs 3 & 4) compared to those of **1** and **2**.

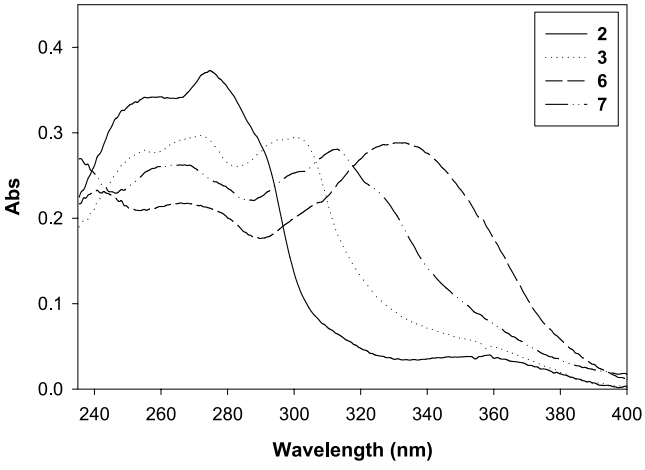

Figure 3. The UV absorption spectra of compounds **2**, **3**, **6** and **7** in dichloromethane.

Compound **2** displayed a relatively higher quantum yield values when compared to the compounds bearing extended conjugation moiety. As shown in Table 1, there was a dramatic difference in quantum yield between compounds **2** (90%) and **7** (27%). The compounds bearing aryl groups via a vinylene linkage (**5**–**11**) show relatively low fluorescent quantum yields. It is likely that the significant differences in these compounds resulted from the stronger electronic perturbation in the ground and excited states due to the extended conjugation provided by the vinylene linkage. On the other hand, the compounds **12** (44%) and **13** (52%) bearing acetylene linkage displayed better fluorescent quantum yield compared to those of compounds bearing vinylene linkage. The introduction of a fluorine atom on the aryl ring increased the fluorescent quantum yields in both cases (compound **2** vs **1** or **3**; compound **7** vs **5** or **6**; compound **13** vs **12**) (Table 1). Compounds with vinylene and acetylene spacers induced red shifts in their fluorescence λ_{max} by 5 and 18 nm, respectively. It is likely that extended conjugation enhances the intersystem crossing (ISC) rates thereby resulting in quenched emission for compounds **3**–**13**. The theory also gains significance in view that compounds **2**, **7** and **13** have relative higher quantum yield values when compared with the others in the corresponding series.

2.4. Electrochemical studies

Table 2 summarizes the cyclic voltametric data in CH_3CN containing 0.1 M tetrabutylammonium hexafluorophosphate with the scan rate of 0.1 V/s. The potential values of the first redox wave in the scan of both the positive and negative direction are included in Table 2 along with some multiple redox waves, which are known to be related to the HOMO and LUMO energy levels. Overall, as the interpretation of the electrochemical properties is similar to that reported by Wudl et al.[3a] their assignments can be applied to these compounds.

Compounds **1**–**3** show the oxidation potential at 1.89, 1.90, and 1.76 V, respectively, and the reduction potential at −1.59, −1.58, and −1.63 V, respectively, which indicates that the substituent group on the 2-phenyl group connected to PPY (pyrrolo[1,2-*b*]pyridazine-5,6,7-tricarboxylic acid trimethyl ester) affects the HOMO level slightly and the LUMO level trivially. Compounds **5**–**7** also showed a similar tendency. Compounds **1** and **4** exhibited almost the same oxidation and reduction potential, which implies that both the HOMO and LUMO level are not changed when the 2-phenyl or 2-naphthyl moiety are connected to PPY.

A relative large difference in the oxidation potential was found by a comparison of the (**2**, **7**), (**3**, **6**), and (**4**, **8**) couples, respectively. In compounds **2**, **3**, and **4**, the aromatic moieties were linked directly to position 2 of PPY while the same aromatic moieties were linked to position 2 of PPY via a vinylene linkage in compounds **7**, **6**, and **8**, respectively. Interestingly, compounds **7**, **6**, and **8** had lower oxidation potential than the corresponding compounds **2**, **3**, and **4** by 0.45, 0.37, and 0.24 V, respectively, while their reduction potentials remained similar within 0.08 V compared with their corresponding compounds. This indicates that such elongated conjugation at the position 2 in PPY mainly affects the HOMO as shown in compounds **1**–**3** and **5**–**7** (Table 2). It is likely that a vinylene linkage at position 2 affects the HOMO level but affects the LUMO level to a much lesser extent, however, no further effort to explain this phenomenon is made in this study. Figure 5 shows the cyclic voltammograms of compounds **6** and **3**, where an improvement in the reversibility in the reduction

Table 1. λ_{max} (nm) of absorption spectra, λ_{max} (nm) of fluorescence spectra, and relative efficiency (%) of compound **1–13**

Compd	Absorption (λ_{max}/nm)				Fluorescence [(λ_{max}/nm) (quantum efficiency (%))]			
	DMSO	MeOH	CH_2Cl_2	Hexane	DMSO	MeOH	CH_2Cl_2	Hexane
1	348[a]	346[a]	350[a]	351[a]	446 (81)[a]	443 (73)[a]	444 (68)[a]	442 (75)[a]
2	352	347	348	[b]	449 (90)	444 (85)	443 (79)	[b]
3	348	348	349	[b]	445 (51)	439 (43)	441 (41)	[b]
4	348	348	340	[b]	450 (39)	445 (22)	444 (31)	[b]
5	321	316	330	305	450 (9)	452 (8)	447 (7)	443 (27)
6	331	335	328	[b]	463 (5)	466 (8)	438 (9)	[b]
7	315	312	313	[b]	454 (27)	451 (25)	448 (23)	[b]
8	329	323	328	[b]	460 (9)	451 (12)	448 (8)	[b]
9	343	341	335	[b]	453 (8)	453 (11)	450 (12)	[b]
10	337	335	332	[b]	441 (6)	455 (10)	453 (8)	[b]
11	394	389	373	389	510 (5)	490 (8)	505 (13)	472 (28)
12	356	[b]	358	[b]	467 (44)	[b]	456 (41)	[b]
13	359	[b]	358	[b]	467 (52)	[b]	453 (50)	[b]

[a] Taken from Ref. 3a.
[b] Insoluble.

Table 2. Cyclic voltammetric data for **1–8**, **11**, and anthracene[a]

Compd	**1**	**2**	**3**	**4**	**5**	**6**	**7**	**8**	**11**	Anthracene
E_{ox}[b]	1.89/…[c]	1.90/…[c]	1.76/…[c]	1.90/…[c]	1.69/…[c]	1.39/…[c]	1.46/…[c]	1.66/…[c]	1.29/…[c]	1.28/…[c]
E_{red}[b]	−1.59/ −1.67	−1.58/ −1.66	−1.63/ −1.71	−1.57/ −1.64	−1.54/ −1.61	−1.55/ −1.63	−1.54/ −1.61	−1.48/…[d]	−1.45/…[d]	−1.92/ −1.99

[a] CVs were recorded at room temperature in CH_3CN/0.1 M $TBAPF_6$.
[b] E_{ox} and E_{red} are represented as E_{pa}/E_{pc} (V vs SCE), respectively.
[c] It is hard to measure the value because of lack of reversibility.
[d] It is hard to determine the exact value due to multiple redox waves.

0/−1 couple at $E=-1.59$ V of compound **6** compared with that of **3** are easily observed at a scan rate (ν) of 0.1 V/s (Fig. 5a and b). A 5-fold increase in the scan rate leads to an enhancement in the reversibility in the reduction process of compound **3** (Fig. 5c). Judging from the i_{pc}/i_{pa} ratio depending on ν, the half-life of the anion radical of compound **3** was approximately 1 s.[10] Such kinetic stabilization phenomena of the radical anion of compound **7** and **8** in the CVs depending on ν were also observed by comparing them with compounds **2** and **4**, respectively. The estimated half-life of the anion radical of compounds **2** and **4** was >1 s and a few seconds, respectively. The above redox potential measurement data were parallel with the optical measurement data, that is, the UV λ_{max} of compounds **7** and **6** is longer than that of compounds **2** and **3** by 35 and 31 nm, respectively.

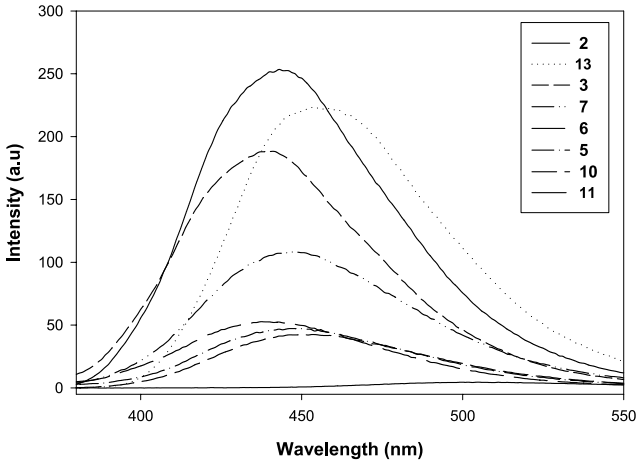

Figure 4. Fluorescence spectra of compounds **2**, **3**, **5**, **6**, **7**, **10**, **11** and **13** in dichloromethane.

Compound **11** had the lowest oxidation potential among compounds **5**, **8**, and **11**. The origin of this could be understood partially by observing the cyclic voltammograms of compound **11** and anthracene (An) in Figure 6. Anthracene itself shows an oxidation potential of $E=1.28$ V and a reduction potential of −1.95 V (Fig. 6b). The oxidation potential is retained in compound **11** (Fig. 6a). However, the reduction potential is in the similar range with the other species shown in Table 2. This suggests that the tuning of the HOMO level is possible via the covalent bonding of the substituent that has the lower oxidation potential. But it is also possible to lose some extent of the electrochemical reversibility as shown in Figure 6.

3. Conclusion

Twelve new luminescent pyrrolopyridazine pyrrolo[1,2-*b*] pyridazine-5,6,7-tricarboxylic acid trimethyl esters were synthesized from less expensive reagents and under mild reaction conditions. In this systematic investigation, three different classes of target molecules were synthesized, for example, aryl groups directly connected to the core PPY (pyrrolo[1,2-*b*]pyridazine-5,6,7-tricarboxylic acid trimethyl ester) moiety, aryl groups connected to the PPY via a vinylene linker and aryl groups connected to the PPY via an acetylene linker. Their optical and electrochemical properties were studied in detail and compared. One of these compounds was characterized by X-ray structure analysis. In particular, it was observed that, compounds bearing fluorine substituent were showing relatively higher quantum

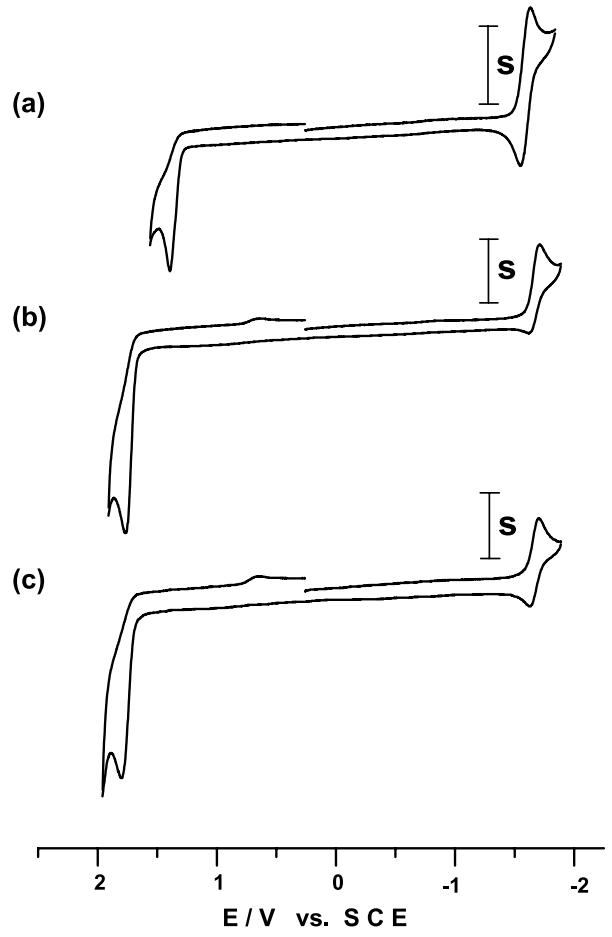

Figure 5. Cyclic voltammograms of 1 mM **6** (a) and **3** (b, c) at a glassy carbon disk electrode with negative scan direction; in CH_3CN containing 0.1 M $TBAPF_6$; $v=0.1$ V/s (a, b) or 0.5 V/s (c). The scale bar represents 20 (a, b) and 50 μA (c), respectively.

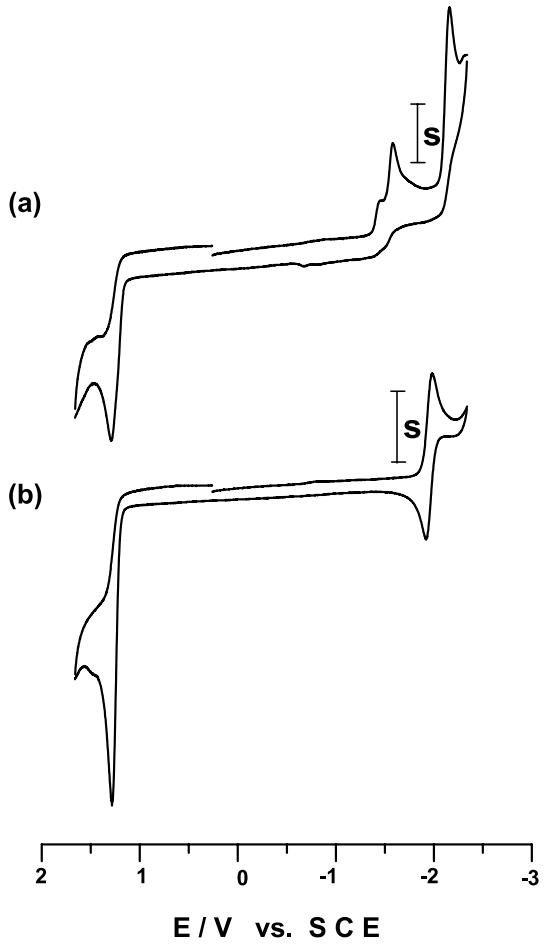

Figure 6. Cyclic voltammograms of 1 mM **11** (a) and anthracene (b) at a glassy carbon disk electrode with negative scan direction; in CH_3CN containing 0.1 M $TBAPF_6$; $v=0.1$ V/s. The scale bar represents 10 (a) and 20 μA (b), respectively.

yield values in comparison with the other substituents in that series. The possibility of tuning the colors and energy levels of these luminophors was studied by extending the π-system at the position 2 of the core PPY through a proper modification such as vinylene or acetylene linkage. We also demonstrated that pyrrolopyridazine systems bearing an aryl groups with a suitable electron donor/withdrawing groups can result in push–pull effects on the overall photochemical properties of the luminophors.

4. Experimental

4.1. General methods

Unless otherwise noted, materials were obtained from commercial suppliers and were used without further purification. Flash chromatography was carried out on silica gel 60 (230–400 mesh ASTM; Merck). Thin-layer chromatography (TLC) was carried out using Merck 60 F_{254} plates with a thickness of 0.25 mm. Preparative TLC was performed using Merck 60 F_{254} plates with a thickness of 1 mm.

Melting points were measured using a Büchi 530 melting point apparatus, and are uncorrected. ^{1}H NMR spectra were recorded using Bruker 250 MHz spectrometer with TMS as the internal standard. Fluorescence measurements were made on a RF-5301 PC Spectrofluorophotometer with excitation at 367 nm; both emission and excitation slit widths were 5 nm. Mass spectra were obtained using JMS-700 Mstation spectrometers.

3-Phenylpyridazine was purchased from Spec, Rijswijk, The Netherlands. Compound **1** was prepared following the published procedure.[3] Preparation of recently reported compound **15** involves four steps.[7] But in our case we could able to get the same in one step via Suzuki coupling. The vinyl derivatives such as **18** and **19** were confirmed with reported results.[8]

4.2. General procedure for the preparation of 2-arylpyrrolo[1,2-*b*]pyridazine-5,6,7-tricarboxylic acid trimethyl ester (1–4) and 2-(2-arylvinyl)pyrrolo[1,2-*b*]-pyridazine-5,6,7-tricarboxylic acid trimethyl ester (5–11)

Dimethyl acetylenedicarboxylate (DMAD) (1 mmol) was added dropwise to a stirring solution of 3-arylpyridazine/3-(2-arylvinyl)pyridazine (0.5 mmol) in anhydrous methanol (2 mL) at 0 °C. Stirring was continued at 0 °C for 1.5 h and then at ambient temperature 5 h. Solvents were

evaporated under reduced pressure and added 2 mL of methanol. Solid separated slowly on standing the solution at room temperature for 2–4 h. It was filtered, washed with small amount of methanol and dried in vacuo. The crude product was crystallized in dichloromethane/methanol. Yields were ranging from 20 to 30%.

4.2.1. 2-(4-Fluorophenyl)pyrrolo[1,2-*b*]pyridazine-5,6,7-tricarboxylic acid trimethyl ester (2). Mp 194–195 °C; ^{1}H NMR ($CDCl_3$) δ 8.66 (d, 1H, J=9.5 Hz), 8.12 (dd, 2H), 7.58 (d, 1H, J=9.5 Hz), 7.19 (m, 2H), 4.03 (s, 3H), 3.98 (s, 3H), 3.94 (s, 3H); ^{13}C NMR ($CDCl_3$) δ 166.4, 165.6, 162.8, 162.4, 158.7, 152.2, 131.0, 130.9, 130.6, 129.3, 129.1, 128.8, 128.5, 117.4, 116.5, 116.1, 102.8, 53.1, 52.2, 51.9; HRMS (FAB) m/z=387.0982 $(M+H)^+$, calcd for $C_{19}H_{16}FN_2O_6$=387.0992.

4.2.2. 2-(4-Methoxyphenyl)pyrrolo[1,2-*b*]pyridazine-5,6,7-tricarboxylic acid trimethyl ester (3). Mp 157–158 °C; ^{1}H NMR ($CDCl_3$) δ 8.57 (d, 1H, J=9.6 Hz), 8.02 (d, 2H, J=8.8 Hz), 7.55 (d, 1H, J=9.6 Hz), 7.01 (d, 2H, J=2.7 Hz), 4.02 (s, 3H), 3.97 (s, 3H), 3.92 (s, 3H), 3.88 (s, 3H); ^{13}C NMR ($CDCl_3$) δ 165.8, 162.8, 161.7, 158.8, 152.7, 130.6, 128.6, 128.1, 127.2, 117.3, 116.2, 114.6, 102.6, 55.4, 53.0, 52.1, 51.9; HRMS (FAB) m/z=399.1199 $(M+H)^+$, calcd for $C_{20}H_{19}N_2O_7$=399.1192. Anal. Calcd for $C_{20}H_{18}N_2O_7$: C, 60.30; H, 4.55; N, 7.03. Found: C, 60.03; H, 4.36; N, 7.26.

4.2.3. 2-Naphthalen-2-yl-pyrrolo[1,2-*b*]pyridazine-5,6,7-tricarboxylic acid trimethyl ester (4). Mp 180–182 °C; ^{1}H NMR ($CDCl_3$) δ 8.58 (d, 1H, J=9.5 Hz), 8.41 (s, 1H), 8.25 (dd, 1H, J_1=8.6 Hz and J_2=1.5 Hz), 7.94 (d, 2H, J=8.3 Hz), 7.86 (m, 1H), 7.70 (d, 1H, J=9.5 Hz), 7.53 (m, 2H), 4.04 (s, 3H), 3.98 (s, 3H), 3.92 (s, 3H); ^{13}C NMR ($CDCl_3$) δ 165.7, 162.8, 158.7, 152.8, 134.3, 133.1, 132.0, 130.7, 129.1, 128.8, 128.7, 128.4, 128.1, 127.8, 127.5, 127.2, 126.7, 123.9, 117.4, 116.5, 102.7, 53.0, 52.2, 51.9; HRMS (FAB) m/z=419.1243 $(M+H)^+$, calcd for $C_{23}H_{19}N_2O_6$=419.1243.

4.2.4. 2-(2-*p*-Tolylvinyl)pyrrolo[1,2-*b*]pyridazine-5,6,7-tricarboxylic acid trimethyl ester (5). Mp 240–241 °C; ^{1}H NMR ($CDCl_3$) δ 8.53 (d, 1H, J=9.6 Hz), 7.43–7.68 (m, 4H), 7.12–7.26 (m, 3H), 4.01 (s, 3H), 3.96 (s, 3H), 3.91 (s, 3H); ^{13}C NMR ($CDCl_3$) δ 165.7, 162.8, 158.8, 152.8, 139.7, 136.4, 132.8, 130.9, 129.7, 128.5, 127.6, 127.4, 123.5, 117.3, 116.0, 102.9, 53.0, 52.2, 51.9, 21.4; MS (FAB) m/z=409.3 $(M+H)^+$. Anal. Calcd for $C_{22}H_{20}N_2O_6$: C, 64.70; H, 4.94; N, 6.86. Found: C, 64.87; H, 4.97; N, 6.74.

4.2.5. 2-[2-(4-Methoxyphenyl)vinyl]pyrrolo[1,2-*b*]pyridazine-5,6,7-tricarboxylic acid trimethyl ester (6). Mp 216–217 °C; ^{1}H NMR ($CDCl_3$) δ 8.52 (d, 1H, J=9.6 Hz), 7.55 (d, 2H, J=8.8 Hz), 7.48 (d, 1H, J=9.6 Hz), 7.43 (d, 1H, J=2.7 Hz), 7.13 (d, 1H, J=16.5 Hz), 6.94 (d, 2H, J=8.8 Hz), 4.01 (s, 3H), 3.96 (s, 3H), 3.91 (s, 3H), 3.86 (s, 3H); ^{13}C NMR ($CDCl_3$) δ 165.8, 162.8, 160.7, 158.8, 152.9, 136.0, 130.9, 128.9, 128.4, 128.3, 127.5, 122.2, 117.2, 116.0, 114.4, 102.8, 55.4, 53.0, 52.2, 51.9; MS (FAB) m/z=425.3 $(M+H)^+$. Anal. Calcd for $C_{22}H_{20}N_2O_7$: C, 62.26; H, 4.75; N, 6.60. Found: C, 62.41; H, 4.79; N, 6.59.

4.2.6. 2-[2-(4-Fluorophenyl)vinyl]pyrrolo[1,2-*b*]pyridazine-5,6,7-tricarboxylic acid trimethyl ester (7). Mp 189–190 °C; ^{1}H NMR ($CDCl_3$) δ 8.58 (d, 1H, J=9.5 Hz), 7.61–7.02 (m, 8H), 4.01 (s, 3H), 3.95 (s, 3H), 3.87 (s, 3H); ^{13}C NMR ($CDCl_3$) δ 165.7, 165.4, 162.8, 159.70, 157.4, 152.4, 135.1, 131.8, 131.4, 130.9, 127.8, 124.3, 117.3, 116.2, 115.9, 114.8, 103.0, 53.0, 52.0, 51.8; MS (FAB) m/z=413.3 $(M+H)^+$. Anal. Calcd for $C_{21}H_{17}FN_2O_6$: C, 61.16; H, 4.16; N, 6.79. Found: C, 61.01; H, 4.26; N, 6.64.

4.2.7. 2-(2-Naphthalen-2-yl-vinyl)pyrrolo[1,2-*b*]pyridazine-5,6,7-tricarboxylic acid trimethyl ester (8). Mp 191–192 °C; ^{1}H NMR ($CDCl_3$) δ 8.53 (d, 1H, J=10.0 Hz), 7.95 (s, 1H), 7.85–7.77 (m, 4H), 7.68 (d, 1H, J=17.5 Hz), 7.52–7.43 (m, 3H), 7.38 (d, 1H, J=17.5 Hz), 4.02 (s, 3H), 3.97 (s, 3H), 3.91 (s, 3H); ^{13}C NMR ($CDCl_3$) δ 165.7, 162.7, 158.7, 152.5, 136.4, 133.8, 133.4, 133.0, 130.8, 128.7, 128.3, 127.8, 127.6, 126.8, 126.6, 124.6, 123.4, 117.3, 116.0, 102.9, 53.0, 52.2, 51.9; MS (FAB) m/z=445.3 $(M+H)^+$. Anal. Calcd for $C_{25}H_{20}N_2O_6$: C, 67.56; H, 4.54; N, 6.30. Found: C, 67.68; H, 4.46; N, 6.32.

4.2.8. 2-(2-Naphthalen-1-yl-vinyl)pyrrolo[1,2-*b*]pyridazine-5,6,7-tricarboxylic acid trimethyl ester (9). Mp 192–193 °C; ^{1}H NMR ($CDCl_3$) δ 8.57 (d, 1H, J=9.5 Hz), 8.35 (d, 1H, J=16.2 Hz), 8.22 (d, 1H, J=8.0 Hz), 7.85–7.89 (m, 3H), 7.52–7.59 (m, 4H), 7.32 (d, 1H, J=16.2 Hz), 4.03 (s, 3H), 3.97 (s, 3H), 3.93 (s, 3H); ^{13}C NMR ($CDCl_3$) δ 165.7, 162.8, 158.8, 152.6, 133.7, 133.3, 132.9, 131.3, 130.9, 129.7, 128.8, 128.7, 127.7, 127.1, 126.7, 126.1, 125.7, 124.6, 123.3, 117.4, 116.2, 102.9, 53.0, 52.2, 51.9; MS (FAB) m/z=445.3 $(M+H)^+$. Anal. Calcd for $C_{25}H_{20}N_2O_6$: C, 67.56; H, 4.54; N, 6.30. Found: C, 67.45; H, 4.54; N, 6.26.

4.2.9. 2-(2-Biphenyl-4-yl-vinyl)pyrrolo[1,2-*b*]pyridazine-5,6,7-tricarboxylic acid trimethyl ester (10). Mp 236–237 °C; ^{1}H NMR ($CDCl_3$) δ 8.56 (d, 1H, J=9.5 Hz), 7.59–7.71 (m, 6H), 7.52 (d, 1H, J=6.4 Hz), 7.34–7.49 (m, 4H), 7.26 (d, 1H), 4.01 (s, 3H), 3.97 (s, 3H), 3.92 (s, 3H); ^{13}C NMR ($CDCl_3$) δ 165.7, 162.8, 158.7, 152.6, 142.2, 140.3, 135.9, 134.5, 130.9, 128.9, 128.6, 127.9, 127.7, 127.6, 127.5, 127.0, 124.4, 117.3, 116.0, 102.9, 53.0, 52.2, 51.9; MS (FAB) m/z=471.3 $(M+H)^+$. Anal. Calcd for $C_{27}H_{22}N_2O_6$: C, 68.93; H, 4.71; N, 5.95. Found: C, 68.85; H, 4.78; N, 5.92.

4.2.10. 2-(2-Anthracen-9-yl-vinyl)pyrrolo[1,2-*b*]pyridazine-5,6,7-tricarboxylic acid trimethyl ester (11). Mp 209–210 °C; ^{1}H NMR ($CDCl_3$) δ 8.65 (d, 1H, J=9.5 Hz), 8.44 (d, 1H, J=16.7 Hz), 8.43 (s, 1H), 8.31 (m, 2H), 8.03 (m, 2H), 7.62 (d, 1H, J=9.6 Hz), 7.50 (m, 4H), 7.16 (d, 1H, J=16.7 Hz), 4.03 (s, 3H), 3.94 (s, 3H), 3.92 (s, 3H); ^{13}C NMR ($CDCl_3$) δ 178.7, 177.0, 173.8, 165.7, 162.8, 158.8, 152.1, 151.5, 133.4, 132.8, 131.4, 131.0, 130.4, 129.5, 128.9, 128.8, 128.0, 127.9, 126.5, 126.2, 125.7, 125.4, 125.3, 53.1, 52.2, 51.9; HRMS (FAB) m/z=495.1531 $(M+H)^+$, calcd for $C_{29}H_{23}N_2O_6$=495.1556.

4.3. General procedure for the preparation of 2-aryl-ethynyl-pyrrolo[1,2-*b*]pyridazine-5,6,7-tricarboxylic acid trimethyl ester (12–13)

Dimethyl acetylenedicarboxylate (DMAD) (1 mmol) was added dropwise to a stirring solution of 3-arylethynyl-pyridazine (0.5 mmol) in anhydrous methanol (6 mL) at 0 °C. Stirring was continued at 0 °C for 1.5 h and then at ambient temperature 24 h. Solvents were evaporated under vacuum and the residue, which contains tarry impurities was eluted on silica gel column using hexane + ethyl acetate 7:3. It was again crystallized in methanol with trace amount of dichloromethane. Yields were ranging from 15 to 20%.

4.3.1. 2-Phenylethynylpyrrolo[1,2-*b*]pyridazine-5,6,7-tricarboxylic acid trimethyl ester (12). Mp 188–189 °C; ^{1}H NMR ($CDCl_3$) δ 8.60 (d, 1H, J=9.4 Hz), 7.66–7.62 (m, 2H), 7.45–7.36 (m, 3H), 7.30 (d, 1H, J=10.00 Hz), 4.02 (s, 3H), 3.97 (s, 3H), 3.92 (s, 3H); ^{13}C NMR ($CDCl_3$) δ 165.4, 162.5, 158.5, 140.8, 132.3, 130.4, 129.9, 129.0, 128.5, 127.7, 121.2, 117.6, 103.2, 93.9, 84.9, 53.0, 52.4, 52.0; HRMS (FAB) m/z=393.1098 $(M+H)^+$, calcd for $C_{21}H_{17}N_2O_6$=393.1087. Anal. Calcd for $C_{21}H_{16}N_2O_6$: C, 64.28; H, 4.11; N, 7.14. Found: C, 64.26; H, 4.14; N, 7.40.

4.3.2. 2-(4-Fluorophenylethynyl)pyrrolo[1,2-*b*]pyridazine-5,6,7-tricarboxylic acid trimethyl ester (13). Mp 167–168 °C; ^{1}H NMR ($CDCl_3$) δ 8.61 (d, 1H, J=10 Hz), 7.67–7.59 (m, 2H), 7.29 (d, 1H, J=10 Hz), 7.14–7.08 (m, 2H), 4.02 (s, 3H), 3.97 (s, 3H), 3.92 (s, 3H); ^{13}C NMR ($CDCl_3$) δ 165.1, 162.5, 161.4, 158.5, 140.7, 134.4, 134.3, 130.4, 129.1, 127.8, 121.1, 117.6, 117.3, 117.2, 116.2, 115.8, 103.3, 92.8, 84.7, 53.1, 52.4, 52.0; HRMS (FAB) m/z=411.1007 $(M+H)^+$, calcd for $C_{21}H_{16}FN_2O_6$= 411.0992. Anal. Calcd for $C_{21}H_{15}FN_2O_6$: C, 61.47; H, 3.68; N, 6.83. Found: C, 61.62; H, 3.64; N, 7.00.

4.4. General procedure for the preparation 3-aryl-pyridazines via Suzuki cross-coupling (14–16)

These compounds were prepared according to a modified literature method.[6] A mixture of 3-iodopyridazine (2.42 mmol), arylboronic acid (3.64 mmol), $Pd(PPh_3)_4$ (0.075 mmol), toluene (20 mL) and Na_2CO_3 (2.6 mL, 2 M) was flushed with N_2 for 5 min under stirring. The reaction mixture was heated at 120 °C for 18–24 h under a N_2 atmosphere. After cooling to room temperature the solvents were evaporated to dryness under reduced pressure. EtOAc (80 mL) was added and the suspension was placed in an ultrasonic bath for 5 min. The mixture was filtered, washed the residue thoroughly with EtOAc (~40 mL) and the filtrate evaporated under reduced pressure to dryness. The residue was purified by flash column chromatography on silica gel using EtOAc.

4.4.1. 3-(4-Fluorophenyl)pyridazine (14). Mp 122–123 °C; ^{1}H NMR ($CDCl_3$) δ 9.15 (dd, 1H, J_1=4.9 Hz and J_2=1.6 Hz), 8.03–8.11 (m, 2H), 7.83 (dd, 1H, J_1=8.7 Hz and J_2=1.6 Hz), 7.54 (dd, 1H, J_1=8.6 Hz and J_2=4.8 Hz), 7.16–7.27 (m, 2H); ^{13}C NMR ($CDCl_3$) δ 166.4, 162.5, 158.7, 150.2, 132.8, 129.4, 129.2, 127.0, 123.8, 116.5, 116.2; HRMS (EI) m/z=174.0588 $(M)^+$, calcd for $C_{10}H_7FN_2$=174.0593.

4.4.2. 3-(4-Methoxyphenyl)pyridazine (15). Mp 107–108 °C; ^{1}H NMR ($CDCl_3$) δ 9.10 (dd, 1H, J_1=4.8 Hz and J_2=1.6 Hz), 8.03–8.08 (m, 2H), 7.80 (dd, 1H, J_1=8.7 Hz and J_2=1.6 Hz), 7.47 (dd, 1H, J_1=8.7 Hz and J_2=4.9 Hz), 7.02–7.08 (m, 2H), 3.89 (s, 3H); ^{13}C NMR ($CDCl_3$) δ 161.7, 159.4, 149.9, 129.16, 129.0, 128.8, 127.1, 123.6, 114.8, 114.3, 55.8; HRMS (EI) m/z=186.0789 $(M)^+$, calcd for $C_{11}H_{10}N_2O$=186.0793. Anal. Calcd for $C_{11}H_{10}N_2O$: C, 70.95; H, 5.41; N, 15.0. Found: C, 70.71; H, 5.49; N, 15.18.

4.4.3. 3-Naphthalen-2-yl-pyridazine (16). Mp 173–174 °C; ^{1}H NMR ($CDCl_3$) δ 9.20 (dd, 1H, J_1=4.8 Hz and J_2=1.6 Hz), 8.58 (d, 1H, J=102 Hz), 8.24 (dd, 1H, J_1= 8.6 Hz and J_2=1.8 Hz), 8.05–7.99 (m, 4H), 7.62–7.55 (m, 3H); ^{13}C NMR ($CDCl_3$) δ 159.4, 150.0, 134.1, 133.6, 133.4, 128.9, 128.8, 127.8, 127.2, 127.0, 126.8, 126.6, 124.2, 124.1; MS (FAB) m/z=206.2 $(M+H)^+$.

4.5. General procedure for the preparation of 3-(2-aryl-vinyl)pyridazine derivatives (17–23)

These compounds were prepared according to a modified literature method.[8a] Aromatic aldehyde (10 mmol) was slowly added over a period of 5 h to a mixture of the 3-methylpyridazine (10 mmol) and tetrabutylammonium hydrogen sulfate (1 mmol) in a hot aqueous solution (50 mL) of sodium hydroxide (5 M) under stirring. The reflux was maintained for 3 h. After cooling overnight the separated solid was filtered, washed with small amount of cold water and dried. The crude product was purified by eluting on silica gel column using ethyl acetate/hexane 1:1. Yields were ranging from 40 to 60%.

4.5.1. 3-(2-*p*-Tolyl-vinyl)pyridazine (17). Mp 121–122 °C; ^{1}H NMR ($CDCl_3$) δ 9.03 (dd, 1H, J_1=4.8 Hz and J_2= 1.6 Hz), 7.72–7.58 (m, 2H), 7.51 (s, 1H), 7.48 (s, 1H), 7.44 (dd, 1H, J_1=8.6 Hz, J_2=4.9 Hz), 7.31 (d, 1H, J=10.7 Hz), 7.19 (s, 1H), 7.14 (s, 1H), 2.38 (s, 3H); ^{13}C NMR ($CDCl_3$) δ 158.4, 149.5, 139.3, 135.1, 134.8, 133.2, 129.6, 129.2, 127.7, 127.3, 127.0, 126.3, 124.7, 123.9, 123.8, 21.4; MS (FAB) m/z=197.3 $(M+H)^+$.

4.5.2. 3-(2-Biphenyl-4-yl-vinyl)pyridazine (20). Mp 186–187 °C; ^{1}H NMR ($CDCl_3$) δ 9.05 (dd, 1H, J_1=4.8 Hz and J_2=1.5 Hz), 7.74 (d, 1H, J=16.5 Hz), 7.61–7.66 (m, 7H), 7.36–7.49 (m, 4H), 7.13 (d, 1H, J=16.5 Hz); ^{13}C NMR ($CDCl_3$) δ 158.3, 149.6, 141.8, 140.4, 134.9, 134.7, 128.9, 127.8, 127.6, 127.5, 127.3, 127.0, 126.4, 125.1, 123.9; MS (FAB) m/z=259.3 $(M+H)^+$.

4.5.3. 3-(2-Naphthalen-2-yl-vinyl)-pyridazine (21). Mp 166–167 °C; ^{1}H NMR ($CDCl_3$) δ 9.05 (dd, 1H, J_1=4.9 Hz and J_2=1.6 Hz), 7.95 (s, 1H), 7.79–7.88 (m, 5H), 7.66 (d, 1H, J=8.4 Hz), 7.42–7.51 (m, 4H); ^{13}C NMR ($CDCl_3$) δ 158.3, 149.7, 135.2, 133.7, 133.5, 133.4, 128.6, 128.5, 128.3, 127.8, 126.7, 126.6, 126.5, 125.5, 124.0, 123.4; MS (FAB) m/z=233.3 $(M+H)^+$. Anal. Calcd for $C_{16}H_{12}N_2$: C, 82.73; H, 5.21; N, 12.06. Found: C, 82.59; H, 5.25; N, 11.87.

4.5.4. 3-(2-Naphthalen-1-yl-vinyl)-pyridazine (22). Mp 82–83 °C; ^{1}H NMR ($CDCl_3$) δ 9.05 (dd, 1H, J_1=4.9 Hz and J_2=1.6 Hz), 8.54 (d, 1H, J=16.5 Hz), 8.29 (d, 1H, J= 7.6 Hz), 7.82–7.86 (m, 3H), 7.68 (dd, 1H, J_1=8.6 Hz and

J_2=1.6 Hz), 7.43–7.56 (m, 4H), 7.40 (d, 1H, J=16.5 Hz); ^{13}C NMR ($CDCl_3$) δ 158.2, 149.7, 133.7, 133.5, 132.2, 131.4, 129.4, 128.7, 127.7, 126.5, 126.4, 126.1, 125.6, 124.4, 124.3, 123.6; MS (FAB) m/z=233.3 $(M+H)^+$. Anal. Calcd for $C_{16}H_{12}N_2$: C, 82.73; H, 5.21; N, 12.06. Found: C, 82.56; H, 5.27; N, 11.99.

4.5.5. 3-(2-Anthracen-9-yl-vinyl)-pyridazine (23). Mp 172–173 °C; ^{1}H NMR ($CDCl_3$) δ 9.15 (dd, 1H, J_1=4.9 Hz and J_2=1.6 Hz), 8.66 (d, 1H, J=16.5 Hz), 8.45 (s, 1H), 8.36 (m, 2H), 8.03 (m, 2H), 7.72 (dd, 1H, J_1=8.6 Hz and J_2=1.6 Hz), 7.45–7.53 (m, 5H), 7.21 (d, 1H, J=16.5 Hz); ^{13}C NMR ($CDCl_3$) δ 157.8, 150.0, 133.6, 132.2, 131.4, 131.1, 129.6, 128.8, 127.5, 126.6, 125.9, 125.5, 125.3, 124.4; MS (FAB) m/z=283.3 $(M+H)^+$. Anal. Calcd for $C_{20}H_{14}N_2$: C, 85.08; H, 5.00; N, 9.92. Found: C, 84.88; H, 5.01; N, 9.73.

4.6. General procedure for the preparation of 3-(2-arylethynyl)pyridazines via Sonogashira coupling (24–25)

These compounds were prepared according to a modified literature method.[9] The suspension of iodopyridazine (2.91 mmol), $Pd(PPh_3)_2Cl_2$ (0.06 mmol) and copper(I) iodide (0.30 mmol), in dry THF (12 mL) and dry triethylamine (12 mL) was stirred at room temperature under argon atmosphere for 15 min. To this suspension the terminal alkyne (3.50 mmol), dissolved in dry THF (5 mL) was added. The reaction mixture was stirred for 5 h at 55–60 °C. The solvents were removed in vacuo, and the residue was dissolved in chloroform (50 mL) and filtered out the solids. The chloroform solution was washed with water (4×10 mL each), dried over Na_2SO_4 and evaporated the solvents in vacuo. The residue was purified on silica column using hexane+ethyl acetate 3:7 solvent mixture. Yields were ranging from 60 to 70%.

4.6.1. 3-Phenylethynylpyridazine (24). Mp 72–73 °C; ^{1}H NMR ($CDCl_3$) δ 9.14 (d, 1H, J=3.93 Hz), 7.71–7.61 (m, 3H), 7.42–7.38 (m, 4H); ^{13}C NMR ($CDCl_3$) δ 149.3, 148.4, 132.6, 132.2, 129.5, 129.6, 128.5, 125.7, 121.5, 93.9, 85.7; HRMS (EI) m/z=180.0692 $(M)^+$, calcd for $C_{12}H_8N_2$= 180.0687. Anal. Calcd for $C_{12}H_8N_2$: C, 79.98; H, 4.47; N, 15.55. Found: C, 79.88; H, 4.38; N, 15.60.

4.6.2. 3-(4-Fluorophenylethynyl)pyridazine (25). Mp 129–130 °C; ^{1}H NMR ($CDCl_3$) δ 9.18 (s, 1H), 7.66–7.52 (m, 4H), 7.19–7.06 (m, 2H); ^{13}C NMR ($CDCl_3$) δ 165.3, 161.3, 149.3, 134.3, 134.2, 129.5, 125.7, 117.6, 117.5, 116.1, 115.8, 92.8, 85.5; HRMS (EI) m/z=198.0611 $(M)^+$, calcd for $C_{12}H_7FN_2$=198.0593.

4.7. Cyclic voltammetry (CV) measurement

All the electrochemical measurements were carried out in acetonitrile solutions containing 1 mM electroactive compound and 0.1 M tetrabutylammonium hexafluorophosphate ($TBAPF_6$), respectively, at room temperature using a BAS 100B electrochemical analyzer. A glassy carbon disk (diameter 3 mm) and platinum wire were used as working and counter electrodes. The reference electrode used was $Ag|AgNO_3$ (0.1 M), and all the potential values were calibrated versus the ferrocene/ferrocenium ($Fc|Fc^+$) redox couple. The potential values shown in this text were then corrected to the saturated calomel electrode (SCE) on the basis of $Fc|Fc^+$ redox potential as 0.44 V versus SCE,[3a,10–12] unless otherwise specified. The potential scan rate was varied from 0.1 to 1 V/s to check the reversibility of redox waves. E_{pa} (anodic peak potential) and E_{pc} (cathodic peak potential) were shown for redox waves.

Acknowledgements

This work was supported by the Korea Research Foundation Grant funded by the Korean Government (MOEHRD) (KRF-R14-2003-014-01001-0) and by the SRC program of the Korea Science and Engineering Foundation (KOSEF) through the Center for Intelligent Nano-Bio Materials at Ewha Womans University (R11-2005-008-02001-0) K.M.K.S. is thankful to KOFST for Brain Pool Fellowship.

Supplementary data

Supplementary data associated with this article can be found, in the online version, at doi:10.1016/j.tet.2005.08.038

References and notes

1. (a) VanSlyke, S. A.; Tang, C. W. U.S. Patent 4,539,507, 1985. (b) Tang, C. W.; VanSlyke, S. A. *Appl. Phys. Lett.* **1987**, *51*, 913.
2. (a) Kido, J.; Okamoto, Y. *Chem. Rev.* **2002**, *102*, 2357. (b) Chen, C. H.; Shi, J. *Coord. Chem. Rev.* **1998**, *171*, 161.
3. (a) Mitsumori, T.; Bendikov, M.; Sedó, J.; Wudl, F. *Chem. Mater.* **2003**, *15*, 3759. (b) Cheng, Y.; Ma, B.; Wudl, F. *J. Mater. Chem.* **1999**, *9*, 2183.
4. Coad, P.; Coad, R. A.; Clough, S.; Hyepock, J.; Salisbury, R.; Wilkins, C. *J. Org. Chem.* **1963**, *28*, 218.
5. Haider, N.; Käferböck, J. *Heterocycles* **2000**, *53*, 2527.
6. Maes, B. U. W.; Lemière, G. L. F.; Dommisse, R.; Augustyns, K.; Haemers, A. *Tetrahedron* **2000**, *56*, 1777.
7. Lee, S. J.; Kang, S.; Lee, S. H.; Hwang, K. J.; Park, N. K.; Kim, Y. S. *Mater. Sci. Eng. C* **2004**, *24*, 349.
8. (a) Eynde, J. J. V.; Pascal, L.; Haverbeke, Y. V.; Dubois, P. *Synth. Commun.* **2001**, *31*, 3167. (b) Heinisch, G.; Mayrhofer, A. *Sci. Pharm.* **1982**, *50*, 120. (c) Guenter, A.; Gottfried, H. J. *Heterocycl. Chem.* **1984**, *21*, 435.
9. Storm, O.; Lüning, U. *Eur. J. Org. Chem.* **2003**, 3109.
10. (a) Nicholson, R. S.; Shain, I. *Anal. Chem.* **1964**, *36*, 706. (b) Kim, J. Y.; Lee, C.; Park, J. W. J. *J. Electroanal. Chem.* **2001**, *504*, 104.
11. Clerac, R.; Cotton, F. A.; Dunbar, K. R.; Lu, T.; Murillo, C. A.; Wang, X. *J. Am. Chem. Soc.* **2000**, *122*, 2272.
12. The potential values of compound **1** reported here are somewhat different from those in Ref. 1, but the potential values of anthracene are the same as those in Bard, A. J.; Faulkner, L. R. *Electrochemical Methods: Fundamentals and Applications*, 2nd ed.; Wiley: New York, 2001; p 81.

Available online at www.sciencedirect.com
SCIENCE DIRECT
Tetrahedron 61 (2005) 10235–10241
Tetrahedron

Novel method for synthesis of unsymmetrical bis(indolyl)alkanes catalyzed by ceric ammonium nitrate (CAN) under ultrasonic irradiation

Xiao-Fei Zeng, Shun-Jun Ji* and Shun-Yi Wang

Key Lab. of Organic Synthesis of Jiangsu Province, College of Chemistry and Chemical Engineering of Suzhou University, Suzhou, 215006 China

Received 9 May 2005; revised 8 August 2005; accepted 11 August 2005

Abstract—The reaction of indole with (1*H*-indol-3-yl)(alkyl) methanol was catalyzed efficiently by ceric ammonium nitrate under ultrasonic irradiation to afford the unsymmetrical bis(indolyl)alkane in good to excellent yields.

1. Introduction

Indole derivatives are known to possess various biological properties including antibacterial, cytotoxic, antioxidative and insecticidal activities, many indole derivatives are used as antibiotics in pharmaceuticals.[1] Among them, bisindolylalkanes (BIAs) are important class of bioactive metabolite.[2] With the continuing isolation of structurally more versatile BIAs,[3] the demand for efficient synthesis of BIAs become an increasing interest in organic synthesis.[4] In previous reports concering synthesis of BIAs, most of them involve the electrophilic substitution of indoles with various aldehydes or ketones in the presence of either protic[5] or Lewis acids.[6] Although the synthesis of symmetrical BIAs has been studied extensively throughout the last century, the synthesis of unsymmetrical BIAs is still highly sought-after in synthetic community.[7] To the best of our knowledge there were only two general synthetic approaches for the synthesis of unsymmetrical BIAs reported by Yannick Vallee[9,10] and Chakrabarty.[8] Yannick Vallee[9,10] firstly reported the synthesis of unsymmetrical BIAs, but the operation was complicated. Chakrabarty[8] reported that through the Michael reactions of 3-(2-nitrovinyl)indole with indoles, unsymmetrical BIAs also could be obtained, however, the method was limited to 2,2-bis(3-indolyl)-nitroethane derivatives. Furthermore, they were all suffered from long reaction time, low yields and complex handling.

In this report, as a continuous research of our previous work,[11] we wish to introduce a simple method for synthesis of unsymmetrical BIAs. Using this method, various BIAs can be obtained by changing different substrates (Scheme 1).

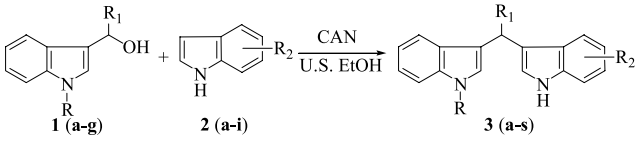

R= H, Ts
R_1= Ph, *n*-Nonanyl, *n*-Octanyl, *n*-Hexanyl, *n*-Butanyl
R_2= CH_3, H, BnO, Ts

Scheme 1.

In recent years, ceric ammonium nitrate (CAN) has received considerable attention as an inexpensive and easily available catalyst for various organic reactions such as oxidation, oxidative addition, nitration, photo-oxidation, deprotection, graft polymerization etc.[12] CAN as a catalyst to catalyze the reaction of indoles with carbonyl compounds to afford the symmetrical BIAs has been reported by Biswanath Das and co-workers.[13] However, the reaction must be performed using the toxic CH_3CN as solvent under the protection of N_2 atmosphere and was only limited to the synthesis of symmetrical BIAs.

Ultrasonic irradiation was demonstrated to be an efficient synthetic technique for activating various organic reactions

Keywords: Indoles; CAN; Ultrasound irradiation; Unsymmetrical bis(indolyl)methanes.
* Corresponding author. Tel.: +86 512 65880086; fax: +86 512 65880089; e-mail: shunjun@suda.edu.cn

0040–4020/$ - see front matter © 2005 Elsevier Ltd. All rights reserved.
doi:10.1016/j.tet.2005.08.040

proceeding via single electron transfer (SET) mechanism or radical route.[14] Many organic transformations can be accelerated by ultrasonic irradiation with fast reaction rate, short reaction time, high yields and sometimes good selectivity.[15]

In this report, we described an ultrasound-accelerated reaction of indoles with (1*H*-indol-3-yl) (alkyl)methanol[16] **1** using a catalytic amount of CAN, which provided an efficient route to the synthesis of unsymmetrical BIAs (Scheme 1).

2. Results and discussion

The reactions were first carried out using 1:1 molar ratio of (1*H*-indol-3-yl)(phenyl)methanol **1a** and **2b** along with a catalytic amount of CAN in different solvents under ultrasonic irradiation. The results were summarized in Table 1. It was observed that the reaction proceeded efficiently in the presence of CAN (10 mol%) and anhydrous alcohols (MeOH or EtOH, 2 mL) at room temperature, giving the unsymmetrical BIAs **3b** in excellent yields (92–96%) (Table 1, entries 1–2), (Scheme 2). Considering the lower toxicity of EtOH, thus we carried out this reaction in anhydrous EtOH. In addition, it has also been found that the same reaction did not progress well in *n*-PrOH and aqueous EtOH media under identical conditions, affording the product in 75 and 77% yields, respectively (Table 1, entries 3–4).

Table 1. The solvent effect of reaction of 5-methyl-indole with (1*H*-indol-3-yl)(phenyl)methanol **1a**[a]

Entry	Solvent	Time (h)	Yield (%)[b]
1	MeOH	3.5	96
2	EtOH	2.5	92
3	*n*-PrOH	4.5	75
4	90% EtOH	5	77

[a] All reactions were carried out using a catalytic amount of CAN (10 mol%) at room temperature.
[b] Isolated yields.

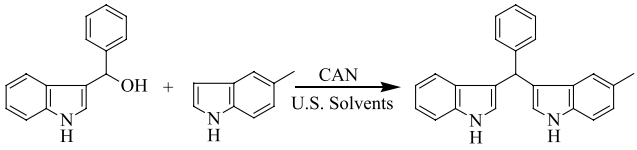

Scheme 2.

The reaction of (1*H*-indol-3-yl)(phenyl)methanol **1a** with **2b** was then carried out using different Lewis acids under ultrasonic irradiation at room temperature. As shown in Table 2, it was found that the other two ceric salts $Ce(NO_3)_3$ and $Ce_2(C_2O_4)_3$ (Table 2, entries 2–3) did not improve the reaction under identical reaction conditions in comparison to CAN. Furthermore, it was found that the reaction could also be carried out using Lewis acid $Bi(NO_3)_3$ (Table 2, entry 4), but the yield was relatively low (71%). Therefore, CAN was found to be superior in terms of conversion and reaction time (Scheme 3).

Table 2. Lewis acid mediated reaction of 5-methyl-indole with (1*H*-indol-3-yl)(phenyl)methanol **1a**[a]

Entry	Lewis acid	Time (h)	Yield (%)[b]
1	CAN	2.5	92
2	$Ce(NO_3)_3$	4.5	89
3	$Ce_2(C_2O_4)_3$	6.5	40
4	$Bi(NO_3)_3$	2.5	71

[a] All reactions were carried out using 10 mol% catalyst under sonic irradiation.
[b] Isolated yields.

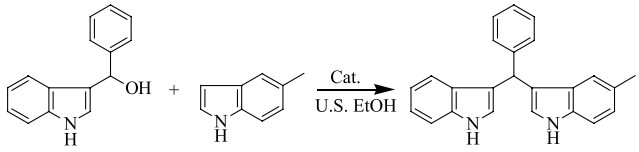

Scheme 3.

Prompted by this success, we extended the reaction of (1*H*-indol-3-yl)(alkyl)methanol **1a** with a wide range of other substituted indole compounds under similar conditions at room temperature, furnishing the unsymmetrical BIAs in good to excellent yields (Table 3). Our findings reflected the wide applicability and usefulness of this method. In all cases, the reactions proceeded efficiently to give the corresponding unsymmetrical BIAs in moderate to excellent yields (75–96%). Even aliphatic substrates such as 1-(1*H*-indol-3-yl)decan-1-ol **1b**, (1*H*-indol-3-yl)methanol **1d**, 1-(1*H*-indol-3-yl)pentan-1-ol **1e**, 1-(1*H*-indol-3-yl)heptan-1-ol **1f** and 1-(1*H*-indol-3-yl)nonan-1-ol **1g**could also react with substituted indoles to afford the desired products **3g**, **3m**–**3s** in good yields (80–96%, Table 3, entries 7 and 14–20). The reactions were clean and the products were obtained in moderate to excellent yields without the formation of any by-products. However, the reaction of 5-nitroindole **2i** and phenyl(1-tosyl-1*H*-indol-3-yl)methanol **1c** did not occur under above conditions (Table 3, entry 13), (Scheme 4).

3. Conclusions

In summary, we have developed a simple, novel and efficient synthetic protocol for the synthesis of unsymmetrical BIAs using a catalytic amount of CAN under ultrasonic irradiation at room temperature. It is superior to the existing synthetic routes to the synthesis of unsymmetrical BIAs for a number of reasons, viz. (i) it is fast and efficient, employs a cheap, non-toxic CAN as the catalyst and involves a simple work-up; (ii) using this method, we can obtain various BIAs simply by changing different substrates.

Table 3. Reaction of indoles with (1*H*-indol-3-yl)(phenyl)methanol **1a–d**[a]

Entry	1	2	Product (3)	Time (h)	Yield (%)[b]
1	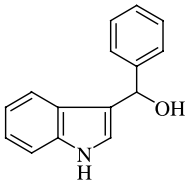 **1a**	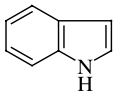 **2a**	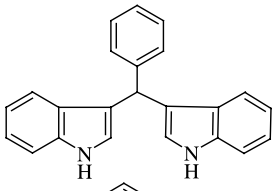 **3a**	2	93
2	**1a**	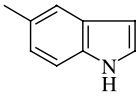 **2b**	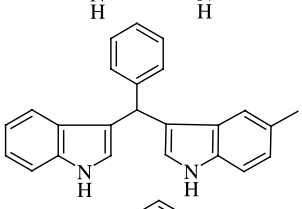 **3b**	2.5	92
3	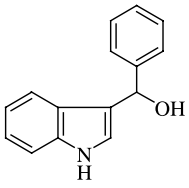 **1a**	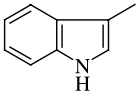 **2c**	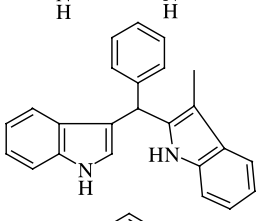 **3c**	2.5	89
4	**1a**	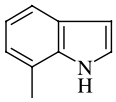 **2d**	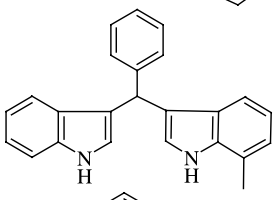 **3d**	2.5	95
5	**1a**	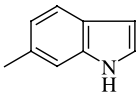 **2e**	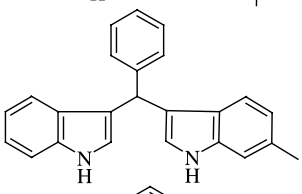 **3e**	2.5	96
6	**1a**	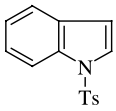 **2f**	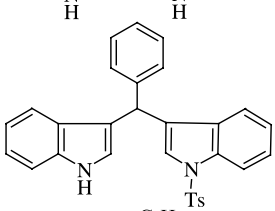 **3f**	2	89
7	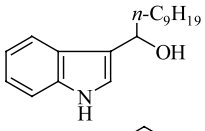 **1b**	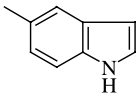 **2b**	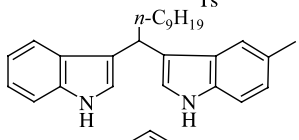 **3g**	2.5	90
8	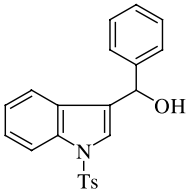 **1c**	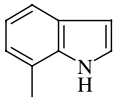 **2d**	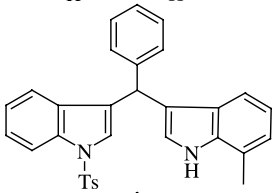 **3h**	3.5	75
9	**1c**	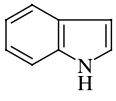 **2a**	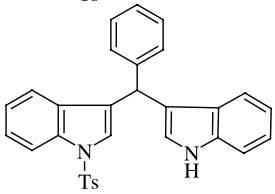 **3f**	2.5	92

Table 3 (*continued*)

Entry	1	2	Product (3)	Time (h)	Yield (%)[b]
10	**1c**	**2b**	**3i**	3.5	78
11	**1c**	**2g**	**3j**	2.5	77
12	**1c**	**2h**	**3k**	3	85
13	**1c**	**2i**	**3l**	5	nr[c]
14	**1d**	**2h**	**3m**	2.5	86
15	**1d**	**2c**	**3n**	2.5	80
16	**1e**	**2b**	**3o**	2.5	96
17	**1e**	**2d**	**3p**	2.5	84
18	**1f**	**2b**	**3q**	2.5	82
19	**1g**	**2b**	**3r**	2.5	80
20	**1g**	**2d**	**3s**	2.5	86

[a] All reactions were carried out in anhydrous ethanol at room temperature under ultrasound irridiation, employing 10 mol% CAN.
[b] Isolated yields. All products are fully characterized by IR, ^{1}HNMR, HRMS and mp etc.
[c] No reaction.

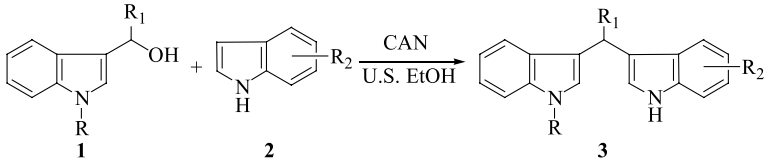

Scheme 4.

4. Experimental

4.1. General

Melting points were recorded on an Electrothermal digital melting point apparatus and uncorrected. ^{1}H NMR (400 MHz) spectra were recorded on a Varian Mercury MHz spectrometer in $CDCl_3$. IR Spectra were obtained on a Nicolet FT-IR500 spectrophotometer using KBr pellets. High resolution mass spectra were obtained using GCT-TOF instrument. Ultrasonic irradiation was performed in a KQ-250E ultrasonic cleaner with a frequency of 40 KHz and a normal power of 250 W. The reaction flask was located in the water bath of the ultrasonic cleaner.

4.2. Typical experimental procedure

A mixture of (1*H*-indol-3-yl)(phenyl)methanol **1a** (0.112 g, 0.5 mmol), 5-methylindole **2b** (0.066 g, 0.5 mmol), CAN (0.028 g, 0.05 mmol) and anhydrous EtOH (2 mL) was irradiated under ultrasound in an open vessel at room temperature until the disappearance of the starting material (2.5 h, checked by TLC). After standing for 2 h, the reaction mixture was poured into water and the precipitated solid was collected, washed with warm water (about 80 °C, 2× 10 mL). The crude mixture was purified by flash column chromatography (EtOAc/petroleum ether 1:4) to afford the pure product.

4.2.1. 1*H*, 1′*H*-3, 3′-Phenylmethanediyl-bis-indole, 3a. Brown powder; mp 142–144 °C; IR (KBr): ν 3395, 2863 cm^{-1}; ^{1}H NMR (400 MHz, $CDCl_3$): δ 5.90 (s, 1H), 6.66 (s, 2H), 7.02 (t, J=5.6 Hz, 2H), 7.18 (t, J=7.2 Hz, 2H), 7.23 (d, J=7.2 Hz, 1H), 7.29 (t, J=8.2 Hz, 3H), 7.36 (d, J=8.0 Hz, 3H), 7.40 (d, J=8.4 Hz, 2H), 7.89 (s, 2H), HRMS [found: *m*/*z*, 322.1445 (M^+); calcd for $C_{23}H_{18}N_2$: M, 322.1470].

4.2.2. 3-((5-Methyl-1*H*-indol-3-yl)(phenyl)methyl)-1*H*-indole, 3b. Brown solid; mp 87–89 °C; IR (KBr): ν 3409, 2960, 2842 cm^{-1}; ^{1}H NMR (400 MHz, $CDCl_3$): δ 2.49 (s, 3H), 5.89 (s, 1H), 6.66 (s, 2H), 6.92–7.03 (m, 3H), 7.16–7.30 (m, 5H), 7.35–7.41 (m, 4H), 7.83 (s, 1H), 7.90 (s, 1H), HRMS [found: *m*/*z*, 336.1614 (M^+); calcd for $C_{24}H_{20}N_2$: M, 336.1626].

4.2.3. 3-((3-Methyl-1*H*-indol-2-yl)(phenyl)methyl)-1*H*-indole, 3c. Black powder; mp 101–103 °C; IR (KBr): ν 3407, 2960, 2853 cm^{-1}; ^{1}H NMR (400 MHz, $CDCl_3$): δ 2.27 (s, 3H), 5.95 (s, 1H), 6.70 (s, 1H), 7.00 (t, J=5.6 Hz, 1H), 7.11 (t, J=2.8 Hz, 2H), 7.17–7.25 (m, 3H), 7.27–7.38 (m, 6H), 7.36 (d, J=8.0 Hz, 2H), 7.58 (d, J=4.8 Hz, 1H), 7.67 (s, 1H), 8.05 (s, 1H), HRMS [found: *m*/*z*, 336.1610 (M^+); calcd for $C_{24}H_{20}N_2$: M, 336.1626].

4.2.4. 3-((7-Methyl-1*H*-indol-3-yl)(phenyl)methyl)-1*H*-indole, 3d. Brown powder; mp 145–147 °C; IR (KBr): ν 3406, 3385, 2925, 2848 cm^{-1}; ^{1}H NMR (400 MHz, $CDCl_3$): δ 2.36 (s, 3H), 5.87 (s, 1H), 6.61 (s, 1H), 6.66 (s, 1H), 7.00 (s, 1H), 7.01 (s, 1H), 7.06–7.35 (m, 6H), 7.37–7.40 (m, 4H), 7.82 (s, 1H), 7.90 (s, 1H), HRMS [found: *m*/*z*, 336.1613 (M^+); calcd for $C_{24}H_{20}N_2$: M, 336.1626].

4.2.5. 3-((6-Methyl-1*H*-indol-3-yl)(phenyl)methyl)-1*H*-indole, 3e. Pink powder; mp 91–93 °C; IR (KBr): ν 3409, 2918, 2956 cm^{-1}; ^{1}H NMR (400 MHz, $CDCl_3$): δ 2.44 (s, 3H), 5.87 (s, 1H), 6.58 (s, 1H), 6.66 (s, 1H), 6.61 (s, 1H), 6.99 (s, 1H), 7.00–7.40 (m, 10H), 7.77 (s, 1H), 7.89 (s, 1H), HRMS [found: *m*/*z*, 336.1609 (M^+); calcd for $C_{24}H_{20}N_2$: M, 336.1626].

4.2.6. 3-((1*H*-Indol-3-yl)(phenyl)methyl)-1-tosyl-1*H*-indole, 3f. Yellow solid; mp 196–198 °C; IR (KBr): ν 3430 cm^{-1}; ^{1}H NMR (400 MHz, $CDCl_3$): δ 2.38 (s, 3H), 5.73 (s, 1H), 6.57 (d, J=7.2 Hz, 1H), 7.00–7.12 (m, 3H), 7.20–7.30 (m, 16H), 7.39 (d, J=7.6 Hz, 1H), 7.62 (d, J=8.0 Hz, 1H), 7.98 (d, J=7.6 Hz, 2H), HRMS [found: *m*/*z*, 476.1547 (M^+); calcd for $C_{30}H_{24}N_2O_2S$: M, 476.1558].

4.2.7. 3-(1-(2-Methyl-1*H*-indol-3-yl)decyl)-1*H*-indole, 3g. Brown solid; mp: 105–107 °C; IR (KBr): ν 3418, 2925, 2853 cm^{-1}; ^{1}H NMR (400 MHz, $CDCl_3$): δ 0.88 (t, J=4.6 Hz, 3H), 1.24–1.42 (m, 14H), 2.18–2.23 (m, 2H), 2.43 (s, 3H), 4.55 (t, J=6.8 Hz, 1H), 6.90 (s, 2H), 6.95–7.06 (m, 3H), 7.14 (t, J=7.2 Hz, 1H), 7.19 (s, 1H), 7.28 (d, J=8.0 Hz, 1H), 7.47 (d, J=7.6 Hz, 1H), 7.60 (d, J=8.0 Hz, 1H), 7.71 (s, 1H), 7.76 (s, 1H), HRMS [found: *m*/*z*, 386.2731 (M^+); calcd for $C_{26}H_{32}N_2$: M, 386.2722].

4.2.8. 3-((7-Methyl-1*H*-indol-3-yl)(phenyl)methyl)-1-tosyl-1*H*-indole, 3h. Yellow solid; mp 103–105 °C; IR (KBr): ν 3418, 2960, 2919 cm^{-1}; ^{1}H NMR (400 MHz, $CDCl_3$): δ 2.38 (s, 3H), 2.51 (s, 3H), 5.72 (s, 1H), 6.57 (s, 1H), 6.93–7.12 (m, 5H), 7.19–7.30 (m, 8H), 7.62 (d, J=7.6 Hz, 2H), 7.92 (s, 1H), 7.98 (d, J=7.2 Hz, 1H), HRMS [found: *m*/*z*, 490.1698 (M^+); calcd for $C_{31}H_{26}N_2O_2S$: M, 490.1715].

4.2.9. 3-((5-Methyl-1*H*-indol-3-yl)(phenyl)methyl)-1-tosyl-1*H*-indole, 3i. Pink powder; mp 245–247 °C; IR (KBr): ν 3430, 2919, 2858 cm^{-1}; ^{1}H NMR (400 MHz, $CDCl_3$): δ 2.37 (s, 6H), 5.71 (s, 1H), 6.52 (s, 1H), 7.04 (s, 2H), 7.11 (d, J=6.8 Hz, 2H), 7.20 (d, J=8.4 Hz, 2H), 7.24–7.29 (m, 8H), 7.64 (d, J=8.0 Hz, 2H), 7.98 (d, J=8.4 Hz, 1H), HRMS [found: *m*/*z*, 490.1673 (M^+); calcd for $C_{31}H_{26}N_2O_2S$: M, 490.1715].

4.2.10. 5-(Benzyloxy)-3-(phenyl(1-tosyl-1*H*-indol-3-yl)methyl)-1*H*-indole, 3j. Yellow solid; mp 93–95 °C; IR (KBr): ν 1647, 1617 cm^{-1}; ^{1}H NMR (400 MHz, $CDCl_3$): δ

2.19 (s, 3H), 4.90 (s, 2H), 5.67 (s, 1H), 6.54 (d, $J=1.6$ Hz, 1H), 6.84 (d, $J=2.4$ Hz, 1H), 6.96–6.99 (m, 1H), 7.06–7.15 (m, 4H), 7.23–7.41 (m, 8H), 7.62 (d, $J=8.0$ Hz, 2H), 7.90 (s, 1H), 7.97 (d, $J=8.8$ Hz, 1H), HRMS [found: *m/z*, 582.1912 (M^+); calcd for $C_{37}H_{30}N_2O_3S$: M, 582.1977].

4.2.11. 3-((2-Methyl-1*H*-indol-3-yl)(phenyl)methyl)-1-tosyl-1*H*-indole, 3k. Pink powder; mp 235–237 °C; IR (KBr): ν 3433, 2929, 2860 cm^{-1}; ^1H NMR (400 MHz, $CDCl_3$): δ 2.33 (s, 3H), 2.45 (s, 3H), 5.73 (s, 1H), 6.55 (s, 1H), 7.01 (s, 2H), 7.11 (d, $J=7.2$ Hz, 2H), 7.20 (d, $J=8.4$ Hz, 2H), 7.22–7.27 (m, 8H), 7.64 (d, $J=8.4$ Hz, 2H), 7.95 (d, $J=8.0$ Hz, 1H), HRMS [found: *m/z*, 490.1644 (M^+); calcd for $C_{31}H_{26}N_2O_2S$: M, 490.1715].

4.2.12. 3-((2-Methyl-1*H*-indol-3-yl)methyl)-1*H*-indole, 3m. Red powder; mp 131–134 °C; IR (KBr): ν 3396, 3388, 2960 cm^{-1}; ^1H NMR (400 MHz, $CDCl_3$): δ 4.25 (s, 2H), 2.40 (s, 3H), 7.04 (s, 1H), 7.08–7.12 (m, 3H), 7.15–7.18 (m, 1H), 7.21–7.27 (m, 1H), 7.40 (d, $J=8.0$ Hz, 1H), 7.50–7.56 (m, 2H), 7.68 (s, 1H), 8.06 (s, 1H), HRMS [found: *m/z*, 260.1311 (M^+); calcd for $C_{31}H_{26}N_2O_2S$: M, 260.1313].

4.2.13. 3-((3-Methyl-1*H*-indol-3-yl)methyl)-1*H*-indole, 3n. Red powder; mp 136–138 °C; IR (KBr): ν 3399, 3389, 2958 cm^{-1}; ^1H NMR (400 MHz, $CDCl_3$): δ 4.28 (s, 2H), 2.34 (s, 3H), 7.07 (s, 1H), 7.09–7.15 (m, 3H), 7.18–7.19 (m, 1H), 7.21–7.25 (m, 1H), 7.41 (d, $J=8.4$ Hz, 1H), 7.50–7.56 (m, 2H), 7.80 (s, 1H), 8.02 (s, 1H), HRMS [found: *m/z*, 260.1304 (M^+); calcd for $C_{31}H_{26}N_2O_2S$: M, 260.1313].

4.2.14. 3-(1-(1*H*-Indol-3-yl)pentyl)-5-methyl-1H-indole, 3o. Red powder; mp 67–69 °C; IR (KBr): ν 3412, 3408, 2958 cm^{-1}; ^1H NMR (400 MHz, $CDCl_3$): δ 0.97 (t, $J=8.4$ Hz, 3H), 1.29–1.33 (m, 4H), 1.39–1.41 (m, 2H), 2.47 (s, 3H), 4.44 (t, $J=7.2$ Hz, 1H), 6.92–6.98 (m, 3H), 7.03 (t, $J=7.6$ Hz, 1H), 7.14 (t, $J=7.4$ Hz, 1H), 7.21 (d, $J=8.0$ Hz, 1H), 7.32 (d, $J=8.0$ Hz, 1H), 7.38 (s, 1H), 7.54–7.62 (m, 1H), 7.80 (s, 1H), 7.89 (s, 1H), HRMS [found: *m/z*, 316.1946 (M^+); calcd for $C_{22}H_{24}N_2$: M, 316.1939].

4.2.15. 3-(1-(1*H*-Indol-3-yl)pentyl)-7-methyl-1H-indole, 3p. Red powder; mp 81–83 °C; IR (KBr): ν 3410, 3400, 2950 cm^{-1}; ^1H NMR (400 MHz, $CDCl_3$): δ 0.98 (t, $J=8.0$ Hz, 3H), 1.27–1.33 (m, 4H), 1.39–1.42 (m, 2H), 2.45 (s, 3H), 4.44 (t, $J=7.2$ Hz, 1H), 6.93–6.97 (m, 3H), 7.05 (t, $J=7.2$ Hz, 1H), 7.16 (d, $J=7.6$ Hz, 1H), 7.20 (d, $J=8.0$ Hz, 1H), 7.31 (d, $J=8.4$ Hz, 1H), 7.39 (s, 1H), 7.56–7.60 (m, 1H), 7.81 (s, 1H), 7.88 (s, 1H), HRMS [found: *m/z*, 316.1925 (M^+); calcd for $C_{22}H_{24}N_2$: M, 316.1939].

4.2.16. 3-(1-(5-Methyl-1*H*-indol-3-yl)heptyl)-1*H*-indole, 3q. Red powder; mp 89–91 °C; IR (KBr): ν 3417, 3410, 2955 cm^{-1}; ^1H NMR (400 MHz, $CDCl_3$): δ 1.01 (t, $J=8.0$ Hz, 3H), 1.45–1.60 (m, 10H), 2.43 (s, 3H), 4.46 (t, $J=7.2$ Hz, 1H), 6.95–7.05 (m, 5H), 7.14 (t, $J=7.6$ Hz, 1H), 7.32 (d, $J=8.0$ Hz, 1H), 7.45–7.47 (m, 1H), 7.59 (d, $J=7.6$ Hz, 1H), 7.82 (s, 1H), 7.88 (s, 1H), HRMS [found: *m/z*, 344.2270 (M^+); calcd for $C_{24}H_{28}N_2$: M, 344.2252].

4.2.17. 3-(1-(5-Methyl-1*H*-indol-3-yl)nonyl)-1*H*-indole, 3r. Brown powder; mp 78–81 °C; IR (KBr): ν 3400, 3195, 2951 cm^{-1}; ^1H NMR (400 MHz, $CDCl_3$): δ 0.87 (t, $J=8.4$ Hz, 3H), 1.25–1.39 (m, 12H), 2.19–2.22 (m, 2H), 2.46 (s, 3H), 4.46 (t, $J=7.2$ Hz, 1H), 6.95–7.05 (m, 5H), 7.14 (t, $J=7.6$ Hz, 1H), 7.32 (d, $J=8.0$ Hz, 1H), 7.45–7.47 (m, 1H), 7.59 (d, $J=7.6$ Hz, 1H), 7.82 (s, 1H), 7.88 (s, 1H), HRMS [found: *m/z*, 372.2581 (M^+); calcd for $C_{26}H_{32}N_2$: M, 372.2565].

4.2.18. 3-(1-(7-Methyl-1*H*-indol-3-yl)nonyl)-1*H*-indole, 3s. Red powder; mp 95–97 °C; IR (KBr): ν 3397, 3389, 2959 cm^{-1}; ^1H NMR (400 MHz, $CDCl_3$): δ 0.85 (t, $J=8.0$ Hz, 3H), 1.23–1.39 (m, 14H), 2.46 (s, 3H), 4.46 (t, $J=7.2$ Hz, 1H), 6.95–7.04 (m, 5H), 7.14 (t, $J=8.0$ Hz, 2H), 7.32 (d, $J=8.0$ Hz, 1H), 7.60 (d, $J=8.0$ Hz, 1H), 7.84 (s, 1H), 7.91 (s, 1H), HRMS [found: *m/z*, 372.2581 (M^+); calcd for $C_{26}H_{32}N_2$: M, 372.2565].

Acknowledgements

The work was partially supported by a research grant from the Innovation Project for Graduate student of Jiangsu Province, the Key Laboratory of Organic Synthesis of Jiangsu Province (No. JSK008) and the National Science Foundation of Jiangsu Province (No. BK2004038). This work was also supported by the National Natural Science Foundation of China (No. 20172039 and 20472062).

References and notes

1. (a) Sundberg, R. J. *The Chemistry of Indoles*; Academic: New York, 1970. (b) Lounasmaa, M.; Tolvanen, A. *Nat. Prod. Rep.* **2000**, *17*, 175–183. (c) Hibino, S.; Chozi, T. *Nat. Prod. Rep.* **2001**, *18*, 66–71.
2. (a) Porter, J. K.; Bacon, C. W.; Robbins, J. D.; Himmelsbach, D. S.; Higman, H. C. *J. Agric. Food Chem.* **1977**, *25*, 88–93. (b) Osawa, T.; Namiki, M. *Tetrahedron Lett.* **1983**, *24*, 4719–4921. (c) Fahy, E. M.; Potts, B. C.; Faulkner, D. J.; Smith, K. *J. Nat. Prod.* **1991**, *54*, 564–569. (d) Bell, R.; Carmell, S.; Sar, N. *J. Nat. Prod.* **1994**, *57*, 1587–1590. (e) Bifulco, G.; Bruno, I.; Riccio, R.; Lavayre, J.; Bourdy, G. *J. Nat. Prod.* **1995**, *58*, 1254–1260.
3. (a) Garbe, T. R.; Kobayashi, M.; Shimizu, N.; Takesue, N.; Ozawa, M.; Yukawa, H. *J. Nat. Prod.* **2000**, *63*, 596–598. (b) Veluri, R.; Oka, I.; Wagner-Dobler, I.; Laatsch, H. *J. Nat. Prod.* **2003**, *66*, 1520–1523.
4. (a) Yadav, J. S.; Reddy, B. V. S.; Murthy, Ch. V. S.; Kumar, G. M.; Madan, Ch. R. *Synthesis* **2001**, 783–789. (b) Chakrabarty, M.; Ghosh, N.; Basak, R.; Harigaya, Y. *Tetrahedron Lett.* **2002**, *43*, 4075–4078. (c) Nagarajan, R.; Perumal, P. T. *Tetrahedron* **2002**, *58*, 1229–1233. (d) Bandgar, B. P.; Shaikh, K. A. *Tetrahedron Lett.* **2003**, *44*, 1959–1961. (e) Mahadevan, A.; Sard, H.; Gonzalez, M.; McKew, J. C. *Tetrahedron Lett.* **2003**, *44*, 4589–4591. (f) Reddy, A. V.; Ravinder, K.; Reddy, V. L. N.; Goud, T. V.; Ravikanth, V.; Venkateswarlu, Y. *Synth. Commun.* **2003**, *33*, 3687–3696. (g) Nagarajan, R.; Perumal, P. T. *Chem. Lett.* **2004**, *33*, 288. (h) Li, J.; Zhou, M.; Li, B. G.; Zhang, G. L. *Synth. Commun.* **2004**, *34*, 275–283.
5. (a) Roomi, M.; MacDonald, S. *Can. J. Chem.* **1970**, *48*,

139–142. (b) Gregorovich, B.; Liang, K.; Clugston, D.; MacDonald, S. *Can. J. Chem.* **1968**, *46*, 3291–3294.
6. (a) Woland, W.; Venkiteswaren, M.; Richards, C. *J. Org. Chem.* **1961**, *26*, 4241–4248. (b) Banerji, J.; Chatterjee, A.; Manna, S.; Pascard, C.; Prange, T.; Shoolery, J. *Heterocycles* **1981**, *15*, 325–333. (c) Chatterjee, A.; Manna, S.; Banerji, J.; Pascard, C.; Prange, T.; Shoolery, J. *J. Chem. Soc., Perkin Trans. 1* **1980**, 553–559. (d) Babu, G.; Sridhar, N.; Perumal, P. T. *Synth. Commun.* **2000**, *30*, 1609–1616.
7. Chakrabarty, M.; Ramkrishna, B.; Yoshihiro, H. *Heterocycles* **2001**, *55*(12), 2431–2447.
8. Chakrabarty, M.; Basak, R.; Ghosh, N. *Tetrahedron Lett.* **2001**, *42*, 3913–3915.
9. Denis, J.-N.; Mauger, H.; Vallee, Y. *Tetrahedron Lett.* **1997**, *38*, 8515–8518.
10. Chalaye-Mauger, H.; Denis, J.-N.; Averbuch-Pouchot, M.-T.; Vallee, Y. *Tetrahedron* **2000**, *56*, 791–804.
11. (a) Ji, S.-J.; Wang, S.-Y.; Zhang, Y.; Loh, T.-P. *Tetrahedron* **2004**, *60*, 2051–2055. (b) Ji, S.-J.; Zhou, M.-F.; Gu, D.-G.; Wang, S.-Y.; Loh, T.-P. *Synlett* **2003**, *13*, 2077–2079. (c) Ji, S.-J.; Zhou, M.-F.; Gu, D.-G.; Jiang, Z.-Q.; Loh, T.-P. *Eur. J. Org. Chem.* **2004**, 1584–1587. (d) Gu, D.-G.; Ji, S.-J.; Jiang, Z.-Q.; Zhou, M.-F.; Loh, T.-P. *Synlett* **2005**, *6*, 959–963. (e) Ji, S.-J.; Wang, S.-Y. *Synlett* **2003**, *13*, 2074–2076. (f) Wang, S.-Y.; Ji, S.-J.; Loh, T.-P. *Synlett* **2003**, *13*, 2377–2379. (g) Ji, S.-J.; Wang, S.-Y. *Ultrason. Sonochem.* **2005**, 339–344.
12. For review on CAN mediated reactions see: (a) Hwu, J. R.; King, K. Y. *Curr. Sci.* **2001**, *81*, 1043–1053. (b) Molander, G. A. *Chem. Rev.* **1992**, *92*, 29–89. (c) Ho, T. L. *Organic Synthesis by Oxidation with Metal Compounds*; Plenum: New York, 1986; and references cited therein. (d) Imamoto, T. *Lanthanide Reagents in Organic Synthesis*; Academic: London, 1994; p 119. (e) Nair, V.; Mathew, J.; Prabhakaran, J. *Chem. Soc. Rev.* **1997**, 127–144. For examples, see: (f) Nair, V.; Panicker, S. B.; Nair, L. G.; George, T. G.; Augustine, A. *Synlett* **2003**, 156–160. (g) Baciocchi, E.; Ruzziconi, R. *Synth. Commun.* **1988**, *18*, 1841–1851. (h) Baciocchi, E.; Ruzziconi, R. *J. Org. Chem.* **1986**, *51*, 1645–1651. (i) Baciocchi, E.; Ruzziconi, R. *Gazz. Chim. Ital.* **1986**, *116*, 671–678.
13. Ramesh, C. N.; Ravindranath, B. D. *J. Chem. Res. (S)* **2003**, 72–74.
14. (a) Einhorn, C.; Einhorn, J.; Luche, J. L. *Synthesis* **1989**, 787–793. (b) Singh, V.; Sapehiyia, V.; Kad, G. L. *Synthesis* **2003**, 198–205.
15. For review, see: (a) Luche, J. L. *Synthetic Organic Sonochemistry*; Plenum: New York, 1998. (b) Mason, T. *J. Chem. Soc. Rev.* **1997**, *26*, 443–451. For examples, see: (a) Palacios, M. L. D.; Comdom, R. F. P. *Synth. Commun.* **2003**, *33*, 1777–1789. (d) Li, J.-T.; Yang, W.-Z.; Wang, S.-X.; Li, S.-H.; Li, T.-S. *Ultrason. Sonochem.* **2002**, *9*, 237–241. (e) Wang, S.-X.; Li, J.-T.; Yang, W.-Z.; Li, T.-S. *Ultrason. Sonochem.* **2002**, *9*, 159–165. (f) Li, J.-T.; Li, T.-S.; Li, L.-J.; Cheng, X. *Ultrason. Sonochem.* **1999**, *6*, 199–206. (g) Qin, Z.; Chen, F.; Xie, Y. *Prog. Chem.* **1998**, *10*, 65–71. (h) Li, J.-T.; Yang, W.-Z.; Chen, G.-F.; Li, T.-S. *Synth. Commun.* **2003**, *33*, 2619–2629. (i) Jayasree, J.; Rao, J. M. *Synth. Commun.* **1996**, *26*, 3717–3726. (j) Bettadaiah, B. K.; Gurudutt, K. N.; Srinivas, P. *Synth. Commun.* **2003**, *33*, 2293–2304. (k) Yang, J.-H.; Li, J.-T.; Zhao, J.-L.; Li, T.-S. *Synth. Commun.* **2004**, *34*, 993–1002. (l) Chandrasekhar, S.; Narsihmulu, Ch.; Jagadeshwar, V. *Synlett* **2002**, *5*, 771–773. (m) Ando, T.; Cork, D. G.; Kimura, T. *Chem. Lett.* **1986**, *173*, 665–667. (n) Fuentes, A.; Sinisterra, J. V. *Tetrahedron Lett.* **1986**, *27*, 2967–2970. (o) Yadav, J. S.; Subba Reddy, B. V.; Srinivas, C.; Srihari, P. *Synlett* **2001**, *6*, 854–856. (p) Ji, S.-J.; Shen, Z.-L.; Gu, D.-G.; Wang, S.-Y. *J. Organomet. Chem.* **2004**, *689*, 1843–1848. (q) Li, J.-T.; Lin, Z.-P.; Qi, N.; Li, T.-S. *Synth. Commun.* **2004**, *34*, 4339–4346. (r) Comdom, R. F. P.; Palacios, M. L. D. *Synth. Commun.* **2003**, *33*, 921–930. (s) Winum, J. Y.; Kamal, M.; Leydet, A. *Tetrahedron Lett.* **1996**, *37*, 1781–1784. (t) Ji, S.-J.; Shen, Z.-L.; Wang, S.-Y. *Chin. Chem. Lett.* **2003**, *14*, 663–666. (u) Fernando, C.; Wanda, P. A.; Demetrius, V.; Cristiano, R. M.; Silva Lopes, E. C.; Rodrigo, C. R.; Silveira, G. P. C.; Pavam, C. H. *Tetrahedron* **2002**, *58*, 7437–7447. (v) Yadav, J. S.; Reddy, B. V. S.; Reddy, K. S. *Tetrahedron* **2003**, *59*, 5333–5336. (w) Zhang, J.; Duan, W.; Cai, J. *Tetrahedron* **2004**, *60*, 1665–1669. (x) Xu, Q.-Y.; Chao, B.; Wang, Y.-M.; Donald, C. D. *Tetrahedron* **1997**, *53*, 12131–12146.
16. Gordon, W.; Gribble Richard, A.; Silva Mark, S. G. *Synth. Commun.* **1999**, *29*, 729–747.

Available online at www.sciencedirect.com
SCIENCE DIRECT
Tetrahedron 61 (2005) 10242–10253
Tetrahedron

[2]Pseudorotaxanes based on the cryptand/monopyridinium recognition motif

Feihe Huang,[a,†] Arnold L. Rheingold,[b] Carla Slebodnick,[a] Amanda Ohs,[b] Karen A. Switek[a,‡] and Harry W. Gibson[a,*]

[a]*Department of Chemistry, Virginia Polytechnic Institute and State University, Blacksburg, VA 24061, USA*
[b]*Department of Chemistry and Biochemistry, University of California, San Diego, La Jolla, CA 92093-0358, USA*

Received 13 June 2005; revised 9 August 2005; accepted 10 August 2005

Available online 9 September 2005

Abstract—The first cryptand/monopyridinium [2]pseudorotaxanes were prepared from five bis(*m*-phenylene)-32-crown-10- and one bis(*m*-phenylene)-26-crown-8-based cryptand hosts and three monopyridinium guests. These pseudorotaxanes were studied by proton NMR spectroscopy, mass spectrometry, and X-ray crystallography. Association constants ranged from 141 M^{-1} to 1.86×10^4 M^{-1} in 1:1 acetone: chloroform at 22 °C.

1. Introduction

Threaded structures, such as pseudorotaxanes, rotaxanes, catenanes, polypseudorotaxanes, polyrotaxanes, and polycatenanes, have been widely studied due to not only their topological importance but also their potential applications.[1] Up to now, the main host–guest recognition motifs used for fabrication of these threaded structures are bis(*p*-phenylene)-34-crown-10/paraquat,[2] crown ether/secondary ammonium salts,[3] benzylic tetraamide macrocycle/amides or phenolates,[4] cyclic bisparaquat/electron-rich aromatics,[5] cyclodextrins/hydrophobic compounds,[6] calixarene/paraquat,[7] cryptand/paraquat,[8] dibenzo-24-crown-8/1,2-bispyridiniumethane salts,[9] and cucurbituril/paraquat or secondary ammonium salts.[10] These recognition motifs are mainly based on hydrogen bonding, π–π stacking, charge transfer, and hydrophilic–hydrophobic interactions. Metal–ligand coordinations have also been widely used in the preparation of threaded structures.[11]

The first cryptand was reported in 1968.[12a] The original objective for preparing cryptands was to bind metal ions and small organic molecules strongly by encapsulation.[12] Recently, progress has been made in synthesis of cryptands and supramolecular cryptands[13] that can complex large organic guests, such as paraquat derivatives and bis(secondary ammonium) salts. We reported very strong complexations between a cryptand and paraquat derivatives in 1999.[8d] Later, we reported cooperative complexation between a cryptand and a bisparaquat derivative,[8e] two pseudorotaxane-like cryptand/paraquat [3]complexes,[8f] and the formation of dimers of cryptand/paraquat inclusion complexes driven by dipole–dipole and face-to-face π-stacking interactions.[8g] Specifically, a bis(*m*-phenylene)-32-crown-10-based diester cryptand with a pyridyl nitrogen atom located at a site occupied by either water or a PF_6 anion in analogous crown ether based complexes exhibited a very high association constant $K_a=5.0\times10^6$ M^{-1} with paraquat in acetone, 9000 times greater than the crown ether system.[8h] We also found that the formation of supramolecular cryptands by chelation of difunctional macrocycles can improve the complexations with paraquat derivatives,[14a] a bis(secondary ammonium) salt,[14b] and a bisparaquat derivative.[14c] These cryptands and supramolecular cryptands have proven to be much better hosts for organic guests than corresponding simple crown ethers.[8,14] Cryptands have also been used in the binding of inorganic anions,[15] anionic colorimetric dyes,[15] acetic acid,[16] and ion-pairs.[17]

Simple monopyridinium salts have been widely studied in chemistry not only due to their easy availability, but also

Keywords: Host–guest systems; Self-assembly; Pseudorotaxane; Cryptand; Pyridinium.
* Corresponding author. Tel.: +1 540 231 8242; fax: +1 540 231 8517; e-mail: hwgibson@vt.edu
† Present address: Department of Chemistry, University of Utah, 315 South 1400 East, Salt Lake City, UT 84112-0850, USA.
‡ Summer Undergraduate Research participant, 1999, supported by the National Science Foundation through DMR 922487 REU. Present address: Department of Chemistry, University of Minnesota, Minneapolis, MN 55455-0431, USA.

0040–4020/$ - see front matter © 2005 Elsevier Ltd. All rights reserved.
doi:10.1016/j.tet.2005.08.036

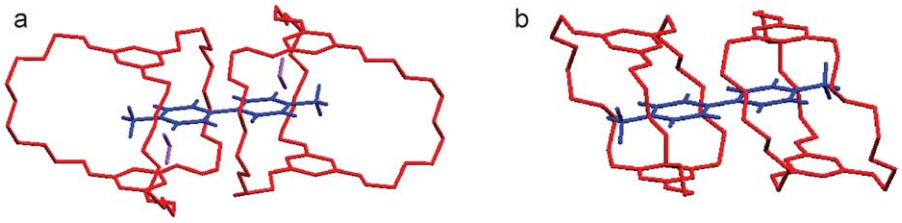

Figure 1. X-ray structures of **1a**·**2**·**1a**·$2H_2O$ (a) and **1b**·**2**·**1b** (b).[8f]

because of their potential applications.[18] For the most recent examples, they have been used in the synthesis of novel monomeric and homodimeric cyanine dyes for nucleic acid detection,[18e] preparation of cationic lipids in gene delivery,[18f] fabrication of novel stilbazolium analogues as second-order nonlinear optical materials,[18g] and manufacture of amperometric sensors.[18h] However, monopyridinium salts have been rarely used in preparation of threaded structures. A few examples are the Beer systems based on ion-pair recognition by ditopic hosts.[19]

Here we report the first cryptand/monopyridinium [2] pseudorotaxanes, which are based on a new cryptand/monopyridinium recognition motif. The formation of these pseudorotaxanes is mainly driven by hydrogen bonding and face-to-face π-stacking interactions.

2. Results and discussion

2.1. Design of cryptand/monopyridinium [2] pseudorotaxanes

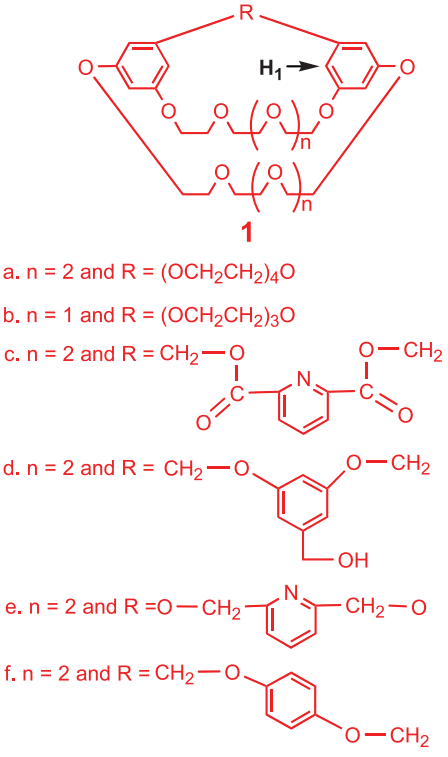

The design of these cryptand/monopyridinium [2]pseudorotaxanes was inspired by the formation of two 2:1 pseudorotaxane-like cryptand/paraquat [3]complexes (Fig. 1).[8f] On the basis of these structures in which each paraquat unit is shared by two cryptand moieties, we theorized that these cryptands[8d,f,h] should be able to complex monopyridinium derivatives. The folded complexes of monopyridinium salts and crown ethers reported by Lämsä et al.[20] also piqued our interest. Therefore, monopyridinium derivatives **3** were prepared and their complexation with cryptands **1** was studied.

2.2. Syntheses of cryptand hosts and monopyridinium guests

The preparation of bis(*m*-phenylene)-32-crown-10- and bis(*m*-phenylene)-26-crown-8-based cryptand hosts **1** followed previously reported procedures.[8d,f,h] Monopyridinium salts **3a** and **3b** were made by the reaction of ethyl isonicotinate with an excess of the alkyl bromide or iodide followed by ion exchange with ammonium hexafluorophosphate. Monopyridinium salt **3c** was synthesized according to a reported method.[21] All these monopyridinium salts were purified by recrystallization in deionized water and dried under vacuum at 100 °C.

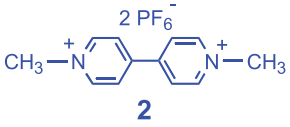

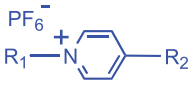

a. $R_1 = C_6H_5CH_2$, $R_2 = COOC_2H_5$;
b. $R_1 = CH_3$, $R_2 = COOC_2H_5$;
c. $R_1 = CH_3$, $R_2 = CH_3$

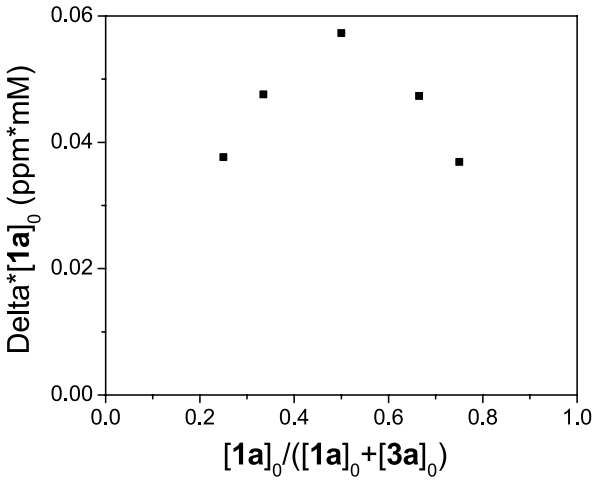

Figure 2. Job plot showing the 1:1 stoichiometry of the complex between **1a** and **3a** in acetone-d_6. $[\mathbf{1a}]_0+[\mathbf{3a}]_0=2.00$ mM. $[\mathbf{1a}]_0$ and $[\mathbf{3a}]_0$ are initial concentrations of **1a** and **3a**. Delta = chemical shift change for H_1 of **1a**.

2.3. Complexation of cryptand hosts 1 with monopyridinium salts 3

The yellow color of solutions of these cryptands with monopyridinium derivatives is not as intense as that of solutions of these cryptands with paraquat derivatives.[8d,f–h] A Job plot[22] (Fig. 2) based on proton NMR data demonstrated that the complex between **1a** and **3a** was of 1:1 stoichiometry in acetone solution. In the same way, it was found that other complexes between **1** and **3** also had 1:1 stoichiometry in solution (see Supplementary data).

Three solutions containing **1a**, **3a**, and equimolar **1a** and **3a** were characterized by proton NMR in 1:1 acetone:chloroform (Fig. 3). These NMR spectra indicated that exchange was fast for this complexation system. After complexation, significant upfield shifts were observed for the pyridinium protons (H_6 and H_7) of guest **3a**, the aromatic protons (H_1), and α-ethyleneoxy protons (H_2) of host **1a**. Furthermore, benzylic protons (H_8) of **3a** and β-ethyleneoxy protons (H_4) of **1a** move upfield, while phenyl and ester methylene

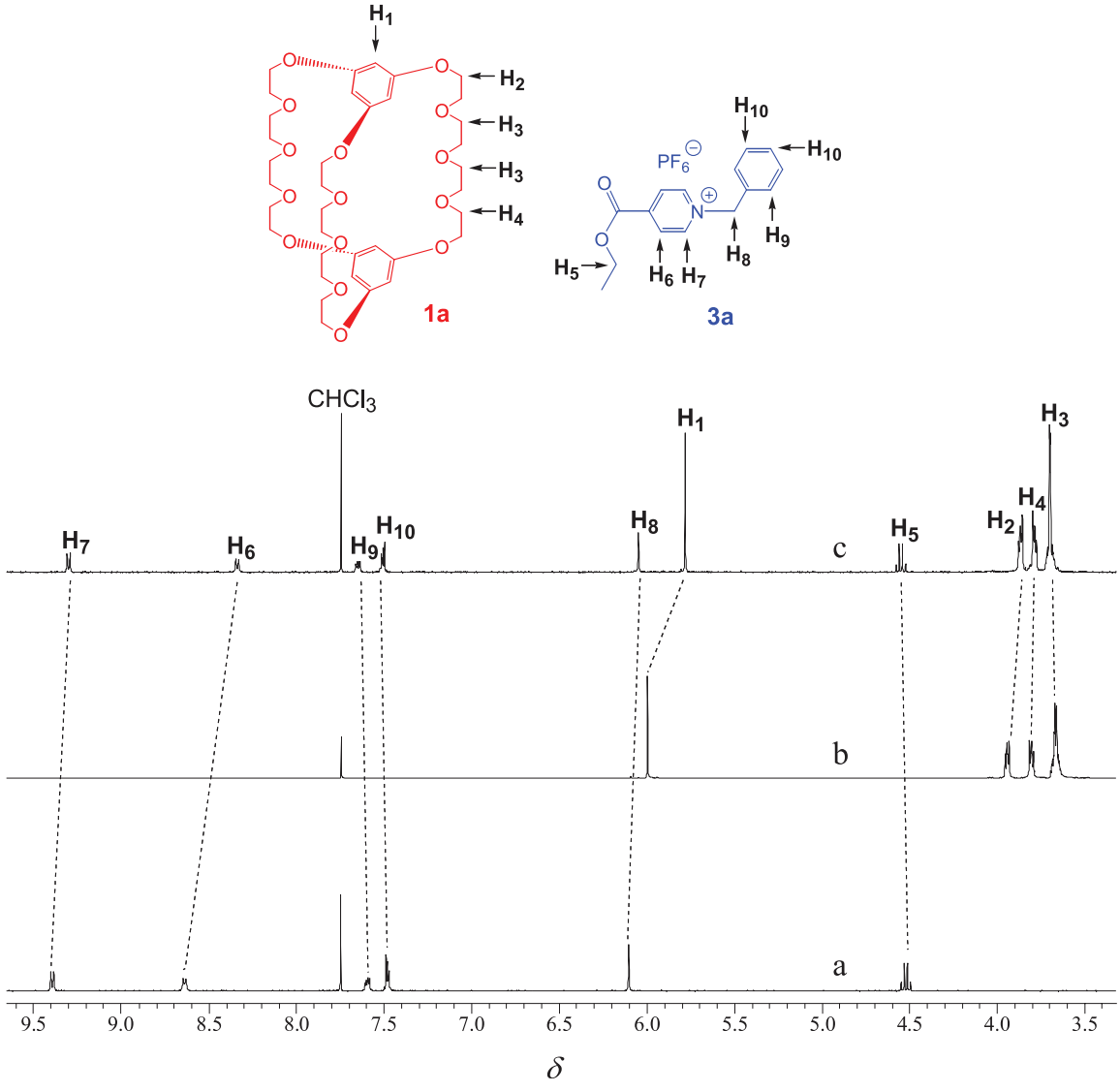

Figure 3. Partial proton NMR spectra (400 MHz, 1:1 $CDCl_3$:CD_3COCD_3, 22 °C) of monopyridinium salt **3a** (a, bottom), cryptand **1a** (b, middle), and 3.00 mM initial concentrations of both **1a** and **3a** (c, top).

protons (H_9, H_{10}, and H_5) of **3a** and ethyleneoxy protons H_3 of **1a** move downfield.

The association constants $\{(K_a=[\mathbf{1}\cdot\mathbf{3}]/[\mathbf{1}])[\mathbf{3}]_0-[\mathbf{1}\cdot\mathbf{3}]\}$ for these cryptand/monopyridinium complexes were determined using the chemical shifts of protons H_1 of the cryptands (Tables 1 and 2). The K_a values of the three complexes of **1a** are similar, but they are higher in 1:1 acetone:chloroform than in acetone (Table 1) because of the decreased polarity of the former.

Table 1. Association constants (K_a)[a] for **1a**/monopyridinium complexes

Solvent	**1a**·**3a**	**1a**·**3b**	**1a**·**3c**
Acetone	182±20	173±40	193±31
1:1 acetone: chloroform	588±60	426±59	536±48

[a] $K_a=[\mathbf{1}\cdot\mathbf{3}]/[\mathbf{1}]([\mathbf{3}]_0-[\mathbf{1}\cdot\mathbf{3}])$ M^{-1} at 22 °C. Cited values and error bars are means and standard deviations from determinations at 4 or 5 different concentrations.

The K_a value of the complex **1a**·**3a** of the larger 32-crown-10-based cryptand is about four times that of the complex **1b**·**3a** of the smaller 26-crown-8-based cryptand (Table 2). In the ethyleneoxy bridges of the cryptands, the aliphatic oxygen atoms are more basic than the phenolic oxygen atoms because of *p*-π conjugation in the latter; since there are more aliphatic oxygen atoms in **1a** (9) than in **1b** (6) it is understandable that K_a is larger for **1a**·**3a** than **1b**·**3a**, as also observed in the case of **1a**·**2** and **1b**·**2**.[8f]

For complexation of monopyridinium salt **3a**, **1c** is by far the best host (Table 2). The small increase in association constant from **1d**·**3a** to **1e**·**3a** is the result of the introduction of an additional binding site, the pyridyl nitrogen atom, on the third 7-atom bridge of **1e**. The notable 30-fold increase in association constant from **1a**·**3a** to **1c**·**3a** is due to the introduction of a better binding site, the pyridyl nitrogen atom, and more optimal cavity size resulting from the 9-atom third arm, just as we have seen in complexations between these cryptands and paraquat derivatives.[8d,f,h] These interactions were confirmed by the X-ray analyses described below.

2.4. Electrospray ionization mass spectrometric characterization of cryptand/monopyridinium [2]pseudorotaxanes

Some of these cryptand/monopyridinium complexes were characterized by electrospray ionization mass spectrometry and their 1:1 stoichiometries were confirmed (Table 3; also see Supplementary data). The mass spectrum for **1a**·**3a** is given in Figure 4 as an example. No peaks related to other stoichiometries were found.

2.5. Solid state structures of [2]pseudorotaxanes 1a·3a and 1c·3a

X-ray analyses were done on yellow crystals of **1a**·**3a** and colorless crystals of **1c**·**3a** grown by vapor diffusion of pentane into equimolar acetone solutions of the corresponding cryptand and monopyridinium salt. These crystal structures (Figs. 5 and 6) demonstrate that these complexes are [2]pseudorotaxanes. For both **1a**·**3a** and **1c**·**3a**, the main stabilization interactions are hydrogen bonding and face-to-face π-stacking interactions in the solid state. Two methylene hydrogens on the ethyl ester group and an α-pyridinium hydrogen of **3a** are involved in hydrogen bonding (**D**, **E**, **F** of Fig. 5; **I**, **J**, and **K** of Fig. 6) with oxygen atoms on ethyleneoxy chains of the cryptand hosts with similar lengths and angles. The β-pyridinium hydrogens of **3a** are not involved in interactions with the cryptand hosts. The pyridinium ring of **3a** nicely lies at the midpoint between the two phenylene rings of the cryptand hosts, presumably in order to maximize face-to-face π-stacking. However, there are some differences. First,

Table 2. Association constants (K_a)[a] for cryptand/**3a** complexes

	1a·**3a**	**1b**·**3a**	**1c**·**3a**	**1d**·**3a**	**1e**·**3a**	**1f**·**3a**
K_a (M^{-1})	588±60	141±21	18.6(±2.0)×10^3	332±33	423±42	1.31(±0.12)×10^3
Relative K_a	4.2±1.0	1.0	1.3(±0.4)×10^2	2.4±0.6	3.0±0.8	9.3±2.3
$-\Delta G_{295\,K}$ (kcal/mol)	3.74±0.05	2.90±0.09	5.76±0.06	3.40±0.06	3.54±0.06	4.21±0.05

[a] $K_a=[\mathbf{1}\cdot\mathbf{3}]/[\mathbf{1}]([\mathbf{3}]_0-[\mathbf{1}\cdot\mathbf{3}])$, measured in 1:1 acetone/chloroform at 22 °C. Cited values and error bars are means and standard deviations from determinations at 4 or 5 different concentrations.

Table 3. Observed mass/charge ratios for 1:1 cryptand/monopyridinium complexes in CH_3CN:$CHCl_3$ 4:1 by electrospray ionization mass spectrometry

Complex	$[\mathbf{1}\cdot\mathbf{3}+Na]^+$	$[\mathbf{1}\cdot\mathbf{3}+Li-HOCH_2CH_2OH]^+$	$[\mathbf{1}\cdot\mathbf{3}-PF_6]^+$
1a·**3a**[a]	1136.4 (10%)	1058.8 (10%)	968.6 (100%)
1a·**3b**[b]	1060.5 (6%)	982.6 (7%)	892.6 (100%)
1a·**3c**	1002.6 (1%)	924.8 (8%)	834.6 (100%)
1c·**3a**[c]	1137.4 (5%)		969.3 (64%)
1d·**3a**[d]			942.5 (43%)
1e·**3a**[d,e]			913.4 (28%)

[a] Also found for **1a**·**3a**: *m*/*z* 892.7 $[\mathbf{1}\cdot\mathbf{3}-PF_6-C_6H_5+H]^+$ (6%).
[b] Also found for **1a**·**3b**: *m*/*z* 864.6 $[\mathbf{1}\cdot\mathbf{3}-PF_6-C_2H_4]^+$ (14%).
[c] Four more peaks were found for **1c**·**3a**: *m*/*z* 1123.3 $[\mathbf{1}\cdot\mathbf{3}+Na-CH_3+H]^+$ (4%), 955.3 $[\mathbf{1}\cdot\mathbf{3}-PF_6-CH_3+H]^+$ (100%), 912.3 $[\mathbf{1}\cdot\mathbf{3}-HPF_6-C_6H_6+Na-H]^+$ (24%), and 898.3 $[\mathbf{1}\cdot\mathbf{3}-PF_6-C_6H_6+Li]^+$ (29%).
[d] The base peak was at *m*/*z* 242.2, corresponding to $[\mathbf{3}-PF_6]^+$.
[e] Also found for **1e**·**3a**: *m*/*z* 1059.4 $[\mathbf{1}\cdot\mathbf{3}+H]^+$ (1%).

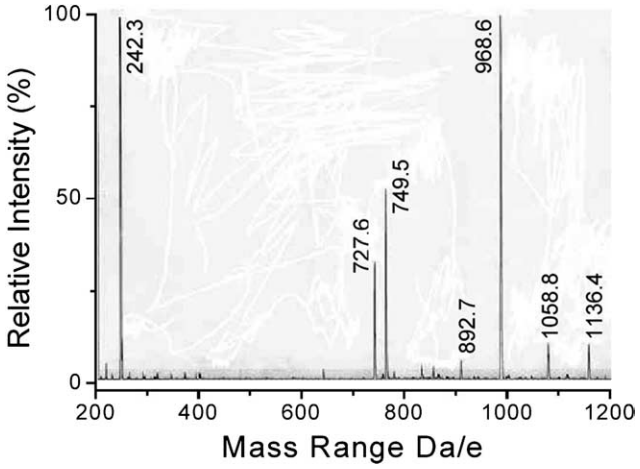

Figure 4. Electrospray mass spectrum of a solution of **1a** and **3a** in a mixture of acetonitrile and chloroform (4:1). Assignments of main peaks: *m*/*z* 1136.4 [**1a**·**3a**+Na]$^+$, 1058.8 [**1a**·**3a**+Li−$HOCH_2CH_2OH$]$^+$, 968.6 [**1a**·**3a**−PF_6]$^+$, 892.7 [**1a**·**3a**−PF_6−C_6H_5+H]$^+$, 749.5 [**1a**+Na]$^+$, 727.6 [**1a**+H]$^+$, and 242.3 [**3a**−PF_6]$^+$.

one α-pyridinium hydrogen of **3a** is connected to cryptand **1a** indirectly by a water bridge (**A**, **B**, and **C** of Fig. 5), while this α-pyridinium hydrogen of **3a** is connected to **1c** directly by a hydrogen bond (**H** of Fig. 6) to the pyridyl nitrogen atom on the host, whose third bridge is shorter (9 atoms) than that of **1a** (13 atoms). Second, one benzylic hydrogen of **3a** is involved in hydrogen bonding between the host and guest in **1a**·**3a** (**G** of Fig. 5), while neither of them are involved in hydrogen bonding to the host in **1c**·**3a** (Fig. 6).

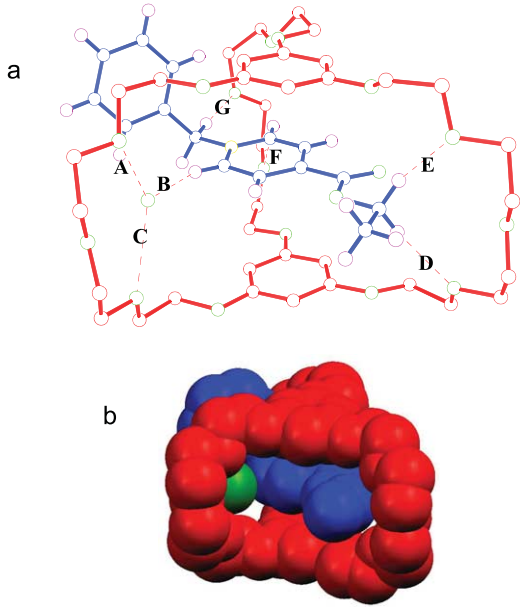

Figure 5. Ball-stick (a) and space-filling (b) views of one unique host–guest complex (the other is similar) in the X-ray structure of **1a**·**3a**. Compound **1a** is red, **3a** is blue, and the water molecule is green. The PF_6 counterion, other solvent molecules, and the hydrogens on **1a** were omitted for clarity. In the ball-stick view, oxygens are green, nitrogen is yellow, and hydrogens are magenta. In the space-filling view, all hydrogens were omitted. Hydrogen-bond parameters: C(O)···O distances (Å), H···O distances (Å), C(O)–H···O angles (degrees) **A**, 2.89, not available, not available; **B**, 3.13, 2.30, 146; **C**, 2.87, not available, not available; **D**, 3.26, 2.33, 157; **E**, 3.33, 2.51, 140, **F**, 3.18, 2.60, 120; **G**, 3.34, 2.35, 175. Face-to-face π-stacking parameters: centroid–centroid distances (Å) 3.83, 3.83; ring plane/ring plane inclinations (degrees): 3.8, 1.4.

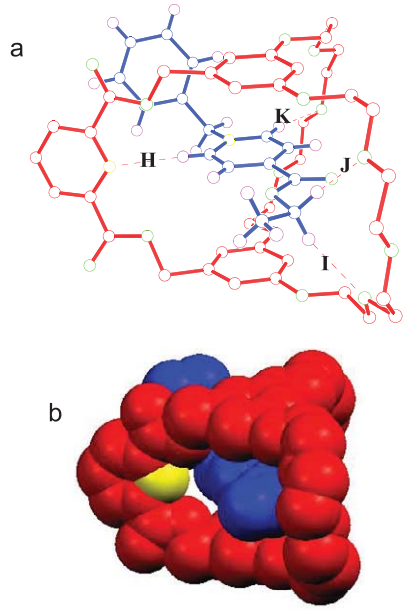

Figure 6. Ball-stick (a) and space-filling (b) views of the X-ray structure of **1c**·**3a**. Compound **1c** is red and **3a** is blue. The PF_6 counterion, solvent molecules, and the hydrogens on **1c** were omitted for clarity. Oxygens are green, nitrogens are yellow, and hydrogens are magenta. In the ball-stick view, oxygens are green, nitrogen is yellow, and hydrogens are magenta. In the space-filling view, all hydrogens were omitted. Hydrogen-bond parameters: C···O(N) distances (Å), H···O(N) distances (Å), C–H···O(N) angles (degrees) **H**, 3.61, 2.78, 149; **I**, 3.41, 2.49, 157; **J**, 3.28, 2.37, 154; **K**, 3.57, 2.65, 168. Face-to-face π-stacking parameters: centroid–centroid distances (Å) 3.91, 3.91; ring plane/ring plane inclinations (degrees): 6.1, 3.5.

Third, the centroid–centroid distance between the phenylene rings of the cryptand host in **1a**·**3a** is 6.88 Å, while this distance is 6.98 Å in **1c**·**3a**. This is presumably due in part to the shorter (9 atoms in **1c** versus 13 atoms in **1a**) and more rigid third arm of **1c**, which pushes the phenylene rings apart. This difference is consistent with the fact that charge transfer interactions between the host and guest in **1a**·**3a** are stronger than those in **1c**·**3a**; the crystals **1a**·**3a** of are yellow, while the crystals of **1c**·**3a** are colorless. Nonetheless, the additional pyridyl binding site in the host confers a ∼50% increase in the stability (Δ*G*) of **1c**·**3a** versus **1a**·**3a** (Table 2). It is interesting to note that the pyridyl nitrogen's location in **1c**·**3a** (Fig. 6) is almost the same as the bridging water's oxygen atom in **1a**·**3a** (Fig. 5); this feature was the basis of our original design of this cryptand.[8h]

The ^{1}H NMR chemical shift changes of host **1a** upon complexation are consistent with an 'averaged' structure in solution similar to that of **1a**·**3a** in the solid state (Fig. 5). Protons H_1, H_2 and H_4 are in shielding regions of the pyridinium or terminal phenylene ring of the guest **3a**, while H_3 resides in the deshielding environment of both the pyridinium and terminal phenylene rings of the guest **3a**. The downfield shift of the ethyl ester methylene (H_5) and phenylene protons (H_9 and H_{10}) of the guest **3a** is consistent with their positions in the deshielding region of the aromatic moieties of the cryptand host **1a**. The upfield shift of the pyridinium (H_6 and H_7) and benzylic protons (H_8) of the guest **3a** is consistent with their positions in the shielding region of the aromatic moieties of the cryptand host **1a**.

2.6. Solid state structures of cryptand 1b and [2]pseudorotaxane 1b·3a

Colorless crystals of cryptand **1b** were grown by slow evaporation of an acetone solution of **1b**, while yellow crystals of [2]pseudorotaxane **1b·3a** were grown by vapor diffusion of pentane into an equimolar acetone solution of cryptand **1b** and monopyridinium salt **3a**. The X-ray crystal structures of **1b** and **1b·3a** are shown in Figure 7. The two phenylene rings of **1b** are not parallel to each other, but exhibit a twist angle of 20° (Fig. 7a). The centroid–centroid distance between them is 4.78 Å. Comparison of the crystal structures of **1b** and **1b·3a** (Fig. 7a and b) shows that the cryptand host **1b** stretches so that the twist angle and centroid–centroid distance between two phenylene rings of **1b** are changed to 6.2° and 6.37 Å, respectively, due to the threading of the monopyridinium guest **3a** through its cavity. Similar to the crystal structures of the above two bis(*m*-phenylene)-32-crown-10-based cryptand/monopyridnium [2]pseudorotaxanes **1a·3a** (Fig. 5) and **1c·3a** (Fig. 6), the bis(*m*-phenylene)-26-crown-8- based cryptand/monopyridnium complex **1b·3a** is also a [2]pseudorotaxane, it is also stabilized by hydrogen bonding and face-to-face π-stacking interactions in the solid state, the two β-pyridinium hydrogens of **3a** are not involved in interactions with the cryptand host, and the pyridinium ring of **3a** nicely lies at the mid-point between the two phenylene rings of **1b**. However, at least two differences are observed. First, both α-pyridinium hydrogen atoms of **3a** are connected to the cryptand host by single hydrogen bonds in **1a·3a** and **1c·3a**, while one α-pyridinium hydrogen of **3a** is connected to cryptand **1b** by two hydrogen bonds (**L** and **M** of Fig. 7) and the other α-pyridinium hydrogen atom is connected to **1b** by one hydrogen bond (**O** of Fig. 7). Second, both methylene hydrogen atoms on the ethyl ester group of **3a** are connected to the cryptand host by hydrogen bonds in **1a·3a** and **1c·3a**, while only one methylene hydrogen atom on the ethyl ester group of **3a** is connected to cryptand **1b** by a hydrogen bond (**N** of Fig. 7).

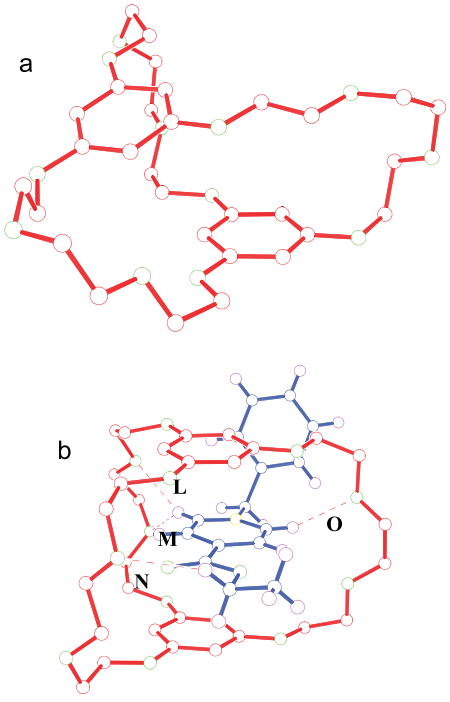

Figure 7. Ball-stick view of the X-ray structures of cryptand **1b** (a) and [2]pseudorotaxane **1b·3a** (b). Compound **1b** is red and **3a** is blue. The PF_6 counterion, solvent molecules, and the hydrogens on **1b** were omitted for clarity. Oxygens are green, nitrogens are yellow, and hydrogens are magenta. Hydrogen-bond parameters: C···O distances (Å), H···O distances (Å), C–H···O angles (degrees) **L**, 3.32, 2.48, 148; **M**, 3.15, 2.36, 141; **N**, 3.48, 2.58, 151; **O**, 3.26, 2.59, 128. Face-to-face π-stacking parameters: centroid–centroid distances (Å) 3.51, 3.51; ring plane/ring plane inclinations (degrees): 0.8, 5.7.

In total the binding of guest **3a** by cryptand **1b** is ~20% weaker (ΔG) than by cryptand **1a** (Table 2); this ultimately is due to the shorter arms of **1b** (10 atoms) versus **1a** (13 atoms) and the resultant changes in geometry of the host.

2.7. Solid state structures of [2]pseudorotaxane 1d·3a

It is interesting that two different types of yellow crystals of **1d·3a** were obtained by vapor diffusion of pentane into acetone solutions of the components. Therefore, two different X-ray structures (Fig. 8a and b), in which complex **1d·3a** has different co-conformations, were obtained. This is possibly due to the flexibility of the ethyl ester group at 4-position of the pyridinium ring of guest **3a**. For both

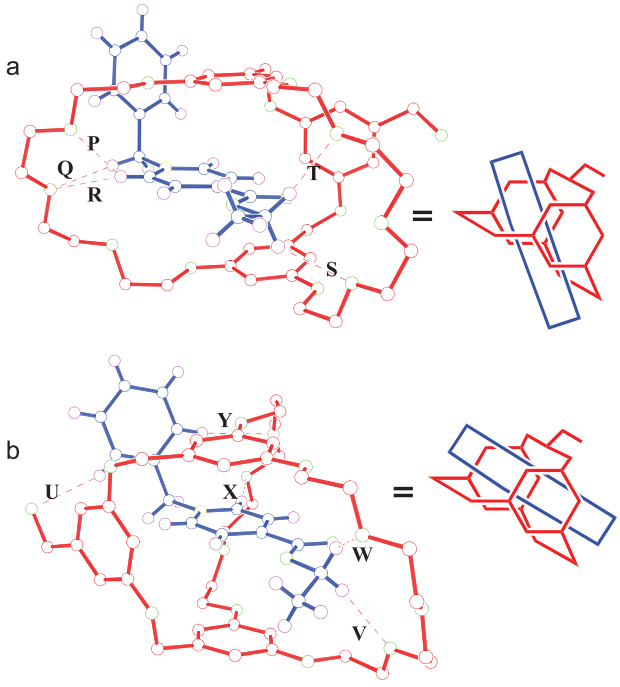

Figure 8. Ball-stick view of the X-ray structures of dimorphic forms of **1d·3a**. Compound **1d** is red and **3a** is blue. The PF_6 counterion, solvent molecules, and the hydrogens on **1d** were omitted for clarity. Oxygens are green, nitrogens are yellow, and hydrogens are magenta. (a) Hydrogen-bond parameters: C···O(N) distances (Å), H···O(N) distances (Å), C–H···O(N) angles (degrees) **P**, 3.17, 2.44, 134; **Q**, 3.56, 2.64, 156; **R**, 3.38, 2.51, 153; **S**, 3.49, 2.66, 141; **T**, 3.34, 2.42, 153. Face-to-face π-stacking parameters: centroid–centroid distances (Å) 3.68, 4.29; ring plane/ring plane inclinations (degrees): 5.9, 12.2; (b) hydrogen-bond parameters: C···O(N) distances (Å), H···O(N) distances (Å), C–H···O(N) angles (degrees) **U**, 3.49, 2.63, 153; **V**, 3.24, 2.34, 153; **W**, 3.27, 2.57, 128; **X**, 3.22, 2.29, 172; **Y**, 3.40, 2.53, 155. Face-to-face π-stacking parameters: centroid–centroid distances (Å) 4.20, 3.98; ring plane/ring plane inclinations (degrees): 5.8, 3.2. Edge-to-face π-stacking parameters: hydrogen–centroid distance (Å) 2.51, carbon–centroid distance (Å) 3.38, carbon–hydrogen–centroid angle (degrees): 155.

crystal structures, complex **1d·3a** is a pseudorotaxane, the main stabilization interactions are hydrogen bonding and face-to-face π-stacking interactions in the solid state, and there are hydrogen bonds that involve methylene hydrogens on the ethyl ester group of **3a** (**S**, **T**, **V**, and **W** of Fig. 8). There are at least two noteworthy points in comparison with the above three pseudorotaxane crystal structures. First, one benzylic hydrogen of **3a** is involved in hydrogen bonding between the host and guest in **1a·3a** (**G** of Fig. 5) and one of the two crystal structures of **1d·3a** (**Q** of Fig. 8a), while neither of them are involved in hydrogen bonding to the host in **1b·3a** (Fig. 7), **1c·3a** (Fig. 6), and the other crystal structure of **1d·3a** (Fig. 8b). Second, the pyridinium ring of **3a** nicely lies at the mid-point between the two phenylene rings of the cryptand host in **1a·3a** (Fig. 5), **1b·3a** (Fig. 7) and **1c·3a** (Fig. 6), while the distances between the pyridinium ring of **3a** and the two phenylene rings of the cryptand host are not equal to each other in the two crystal structures of **1d·3a** (Fig. 8a and b). A possible reason for this is that hydrogen bonding is more important than face-to-face π-stacking interactions for this complex, so the three aromatic rings are placed in this way to maximize hydrogen bonding.

There are at least five major differences in the two crystal structures of **1d·3a**. First, the most important difference is that the monopyridinium guest **3a** is threaded through the cavity of the 32-crown-10 part of the cryptand host in one crystal structure (Fig. 8a), while the 32-crown-10 part forms a taco complex conformation with the monopyridinium guest in the other (Fig. 8b). Second, none of the hydrogens on the terminal phenylene ring of **3a** are involved in hydrogen bonding between the cryptand host and the monopyridinium guest in one crystal structure of **1d·3a** (Fig. 8a) [nor in the above pseudorotaxane crystal structures (Figs. 5–7)], while there are two hydrogen bonds involving two different hydrogens on the terminal phenylene ring of **3a** in the other crystal structure of **1d·3a** (**U** and **Y** of Fig. 8b). Third, one benzylic hydrogen of **3a** is involved in hydrogen bonding with the host in one form of **1d·3a** (**Q** of Fig. 8a), while neither of them is involved in hydrogen bonding in the other (Fig. 8b). Fourth, there are two hydrogen bonds between the host and guest based on one α-pyridinium hydrogen of **3a** in one crystal structure of **1d·3a** (**P** and **R** of Fig. 8a), while there is only one of this type of hydrogen bond in the other (**X** of Fig. 8b). Fifth, there is an edge-to-face π-stacking interaction between the pyridinium ring of **3a** and the phenylene ring of the third bridge of **1d** in one crystal structure (Fig. 8b), but not in the other (Fig. 8a) [nor in the above pseudorotaxane crystal structures (Figs. 5–7)]. Edge-to-face π-stacking interactions were observed before in our studies of crown ether/bis(secondary ammonium) complexes.[3b,c]

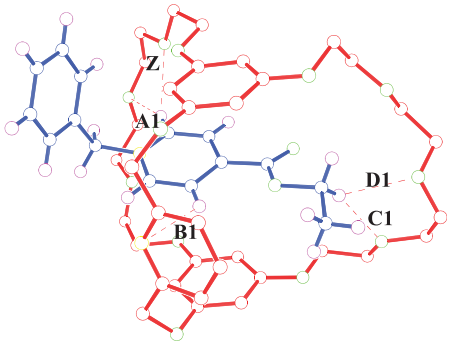

Figure 9. Ball-stick view of [2]pseudorotaxane **1e·3a**. Compound **1e** is red and **3a** is blue. The PF_6 counterion, solvent molecules, and the hydrogens on **1e** were omitted for clarity. Oxygens are green, nitrogens are yellow, and hydrogens are magenta. Hydrogen-bond parameters: C···O distances (Å), H···O distances (Å), C–H···O angles (degrees) **Z**, 3.11, 2.45, 127; **A1**, 3.25, 2.35, 159; **B1**, 3.36, 2.73, 125; **C1**, 3.27, 2.36, 153; **D1**, 2.99, 2.50, 111. Face-to-face π-stacking parameters: centroid–centroid distances (Å) 4.05, 4.18; ring plane/ring plane inclinations (degrees): 10.6, 10.3.

2.8. Solid state structure of [2]pseudorotaxane 1e·3a

Pale yellow crystals of [2]pseudorotaxane **1e·3a** were grown by vapor diffusion of pentane into an acetone solution of monopyridinium salt **3a** and excess cryptand **1e**. The X-ray crystal structure of **1e·3a** is shown in Figure 9. Similar to the crystal structures of the above four cryptand/monopyridnium [2]pseudorotaxanes (Figs. 5–8), bis(*m*-phenylene)-32-crown-10-based cryptand/monopyridnium complex **1e·3a** is also a [2]pseudorotaxane and it is also stabilized by hydrogen bonding and face-to-face π-stacking interactions in the solid state. However, there are three points that are worth mentioning. First, what is unique here is that one β-pyridinium hydrogen of **3a** is involved in hydrogen bonding (**B1** of Fig. 9) to the pyridyl nitrogen atom of cryptand **1e**, while β-pyridinium hydrogens of **3a** are not involved in hydrogen bonding with the cryptand host in the crystal structures of the above mentioned cryptand/monopyridnium [2]pseudorotaxanes (Figs. 5–8). Second, one methylene hydrogen atom on the ethyl ester group of **3a** is involved in two hydrogen bonds (**C1** and **D1** in Fig. 9) and the other is not involved in any hydrogen bonding to the cryptand host in **1e·3a**, while both methylene hydrogen atoms on the ethyl ester group of **3a** are connected to the cryptand host by one hydrogen bond in the above mentioned bis(*m*-phenylene)-32-crown-10-based cryptand/monopyridnium [2]pseudorotaxanes (Figs. 5, 6, and 8). Third, both α-pyridinium hydrogens of **3a** are hydrogen bonded to the cryptand host directly or indirectly in the crystal structures of cryptand/monopyridnium [2]pseudorotaxanes

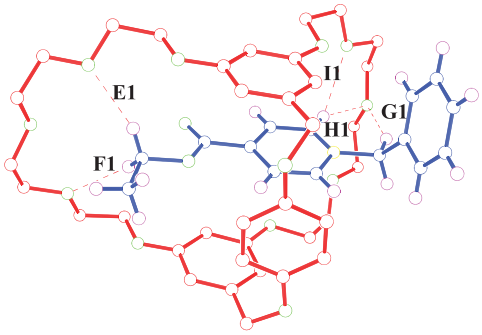

Figure 10. Ball-stick view of [2]pseudorotaxane **1f·3a**. Compound **1f** is red and **3a** is blue. The PF_6 counterion, solvent molecules, and the hydrogens on **1f** were omitted for clarity. Oxygens are green, nitrogens are yellow, and hydrogens are magenta. Hydrogen-bond parameters: C···O distances (Å), H···O distances (Å), C–H···O angles (degrees) **E1**, 3.36, 2.41, 162; **F1**, 3.29, 2.42, 146; **G1**, 3.54, 2.63, 152; **H1**, 3.26, 2.36, 158; **I1**, 3.15, 2.52, 123. Face-to-face π-stacking parameters: centroid–centroid distances (Å) 3.91, 4.39; ring plane/ring plane inclinations (degrees): 2.8, 2.3. Edge-to-face π-stacking parameters: hydrogen–centroid distance (Å) 2.75, carbon–centroid distance (Å) 3.53, carbon–hydrogen–centroid angle (degrees): 140.

1a·3a (**A**, **B**, **C**, and **F** in Fig. 5), **1c·3a** (**H** and **K** in Fig. 6), and **1b·3a** (**L**, **M**, and **O** in Fig. 7), while only one α-pyridinium hydrogen of **3a** is involved in hydrogen bonding to the cryptand host in **1d·3a** (**P** and **R** in Fig. 8a and **X** in Fig. 8b) and **1e·3a** (**Z** and **A1** in Fig. 9).

Cryptands **1d** and **1e** have the same ring sizes. The slightly higher binding ability of **1e** can be attributed to the presence of the pyridyl nitrogen binding site. Because of its reduced ring size, **1e** is a very much poorer (by >2 kcal/mol in ΔG, Table 2) host for **3a** than the larger cryptand **1c** in spite of the greater basicity of its pyridyl nitrogen atom.[23]

2.9. Solid state structure of [2]pseudorotaxane 1f·3a

Pale yellow crystals of [2]pseudorotaxane **1f·3a** were grown by vapor diffusion of pentane into an acetone solution of monopyridinium salt **3a** and excess cryptand **1f**. The X-ray crystal structure of **1f·3a** is shown in Figure 10. Similar to the crystal structures of the above five cryptand/monopyridnium complexes (Figs. 5–9), complex **1f·3a** is also a [2]pseudorotaxane and it is also stabilized by hydrogen bonding and face-to-face π-stacking interactions in the solid state. The crystal structure (Fig. 10) of **1f·3a** is the same as one crystal structure (Fig. 8a) of **1d·3a** in terms of which hydrogen atoms are involved in hydrogen bonds to the cryptand host. That is to say, for both of them, one benzylic hydrogen is involved in a hydrogen bond (**Q** in Fig. 8a and **G1** in Fig. 10), one α-pyridinium hydrogen is involved in two hydrogen bonds (**P** and **R** in Fig. 8a and **H1** and **I1** in Fig. 10), and both methylene hydrogen atoms on the ethyl ester group are involved in hydrogen bonding (**S** and **T** in Fig. 8a and **E1** and **F1** in Fig. 10) between the cryptand host and monopyridinium guest. Similar to the second crystal structure of **1d·3a** (Fig. 8b), **1f·3a** is also stabilized by an edge-to-face π-stacking interaction between the pyridinium ring of **3a** and the phenylene ring on the third bridge of the cryptand host (Fig. 10).

1f is a better host for **3a** than *meta* homolog **1d** (Table 2, ~20% change in ΔG); this can be attributed to the nicely positioned aromatic ring of **1f**, which allows more efficient edge-to-face interactions with the guest.

3. Conclusions

In summary, we demonstrated that threaded structures (pseudorotaxanes) can be efficiently prepared based on a new cryptand/monopyridinium recognition motif. Though monopyridinium salts do not complex these cryptands as strongly as paraquat derivatives, they have better solubility in organic solvents than paraquat derivatives. Moreover, once interlocked structures (rotaxanes or catenanes) based on monopyridinium salts are made, they have the potential to be reduced in order to prepare neutral interlocked structures.[24] Also the starting materials to make monopyridinium salts are much cheaper than those for preparing paraquat derivatives. Recently we have demonstrated that the simple crown ether bis(*m*-phenylene)-32-crown-10 also complexes monopyridinium salts, yielding X-ray structures similar to those reported here, albeit with lower association constants ($<100\ M^{-1}$ in 1:1 acetone/chloroform at 22 °C).[25] Currently we are focusing on using this new recognition motif to construct novel supramolecular systems and have recently used closely related tris(monopyridinium) guests with cryptand **1a** in preparation of novel C_3 symmetric [2]pseudorotaxanes.[26]

4. Experimental

4.1. General procedures

All solvents were HPLC or GC grade. Low-resolution electrospray ionization mass spectroscopy was carried out on a TSQ Finnigan LC/MS/MS instrument. Elemental analyses were carried out by Atlantic Microlabs, Norcross, GA. X-ray diffraction data of cryptand **1b** and pseudorotaxanes **1a·3a**, **1b·3a**, **1e·3a**, and **1f·3a** were collected on an Oxford Diffraction XCalibur2™ diffractometer equipped with the Enhance X-ray Source™ (Mo K_α radiation; $\lambda=0.71073$ Å) and a Sapphire 2™ CCD detector by the phi and omega scan method. For every data collection, the chosen crystal was mounted on a nylon CryoLoop™ (Hampton Research) with Krytox® Oil (DuPont). X-ray diffraction experiments of pseudorotaxanes **1c·3a** and **1d·3a** were carried out on a Bruker SMART CCD diffractometer equipped with Mo K_α radiation ($\lambda=0.71073$ Å) and a graphite monochromator by the phi and omega scan method. The data collection routine, unit cell refinement, and data processing were carried out with the program CrysAlis.[27] Melting points were taken in capillary tubes and are uncorrected.

4.1.1. 4-Carbethoxy-1-benzylpyridinium hexafluorophosphate (3a). To a 50 mL three-necked round bottom flask equipped with a magnetic stirrer and a condenser were added 3.42 g (20.0 mmol) of benzyl bromide and 10 mL of acetonitrile. To this solution was added a solution of ethyl isonicotinate (1.51 g, 10.0 mmol) in 10 mL of acetone and the mixture was stirred at reflux for 48 h. The reaction mixture was cooled to room temperature and the precipitate was filtered. The solid was boiled in $CHCl_3$ and filtered. This solid was dissolved in a minimum volume of deionized water. To this solution was added NH_4PF_6 until no further precipitation was observed. The precipitate was filtered and recrystallized from deionized water three times to afford **3a** as white crystals, 3.21 g (83%), mp 173.9–174.6 °C. ^{1}H NMR (400 MHz, acetone-d_6, 22 °C): $\delta=1.45$ (t, $J=7.2$ Hz, 3H), 4.54 (q, $J=7.2$ Hz, 2H), 6.23 (s, 2H), 7.52–7.56 (m, 3H), 7.66–7.70 (m, 2H), 8.73 (d, $J=6.8$ Hz, 2H), 9.51 (d, $J=6.8$ Hz, 2H); elemental Anal. Calcd for $C_{15}H_{16}O_2N_1P_1F_6$: C, 46.50; H, 4.17; N, 3.62. Found: C, 46.70, 46.53; H, 4.03, 3.99; N, 3.66, 3.74.

4.1.2. 4-Carbethoxy-1-methylpyridinium hexafluorophosphate (3b). Compound **3b**, prepared in a similar way as **3a**, was obtained as white crystals (81%), mp 127.8–128.5 °C. ^{1}H NMR (400 MHz, acetone-d_6, 22 °C): $\delta=1.46$ (t, $J=7.2$ Hz, 3H), 4.55 (q, $J=7.2$ Hz, 2H), 4.78 (s, 3H), 8.70 (d, $J=6.8$ Hz, 2H), 9.37 (d, $J=6.8$ Hz, 2H); elemental Anal. Calcd for $C_9H_{12}O_2N_1P_1F_6$: C, 34.72; H, 3.89; N, 4.50. Found: C, 34.77, 34.75; H, 3.84, 3.73; N, 4.55, 4.47.

4.2. Complexation studies by proton NMR

All solutions were prepared as follows. Precisely weighed amounts of dried hosts and guests were added into separate screw cap vials. The solvent was added with to-deliver volumetric pipets. Then specific volumes of each fresh solution were mixed to yield the desired concentrations. For example, in order to make three solutions, 0.500 mM **1a**/1.00 mM **3a**, 0.500 mM **1a**/2.00 mM **3a**, and 0.500 mM **1a**/5.00 mM **3a**, a 1.00 mM solution of **1a** was made first by adding 5.00 mL of acetone-d_6 with a 5.00 mL to-deliver pipette into a screw cap vial containing 3.63 mg (0.00500 mmol) of **1a**. Then 0.300 mL of this solution was added with a 0.300 mL to-deliver pipet to each of three vials that contained 0.300 mL of 2.00 mM, 0.300 mL of 4.00 mM, and 0.300 mL of 10.0 mM of **3a** separately. ^{1}H NMR data were collected on a temperature controlled Varian Unity (or an Inova) 400 MHz spectrometer. Acetone-d_6 and 1:1 acetone-d_6:chloroform-d were chosen as the NMR solvents because all compounds used here have relatively good solubilities in them.

4.3. Determination of association constants ($K_{\mathbf{a},\mathbf{1}\cdot\mathbf{3}}$) for [2]pseudorotaxanes 1·3

^{1}H NMR characterizations were done on solutions with constant $[\mathbf{1}]_0$ and varied $[\mathbf{3}]_0$. Based on these NMR data, $\Delta_{0,\mathbf{1}}$, the difference in δ values for H_1 of **1** in the uncomplexed and fully complexed species, was determined by the extrapolation of a plot of $\Delta=\delta-\delta_u$ versus $1/[\mathbf{3}]_0$ in the high initial concentration range of **3**. The resultant $\Delta_{0,\mathbf{1}}$ values for **1a**·**3a**, **1a**·**3b**, **1a**·**3c**, **1b**·**3a**, **1c**·**3a**, **1d**·**3a**, **1e**·**3a**, and **1f**·**3a** were 0.429 (acetone) and 0.450 ppm (1:1 acetone/chloroform), 0.206 (acetone) and 0.277 ppm (1:1 acetone/chloroform), 0.185 (acetone) and 0.242 ppm (1:1 acetone/chloroform), 0.117 ppm (1:1 acetone/chloroform), 0.144 ppm (1:1 acetone/chloroform), 0.134 ppm (1:1 acetone/chloroform), 0.283 ppm (1:1 acetone/chloroform), and 0.503 ppm (1:1 acetone/chloroform), respectively. Then $K_{a,\mathbf{1}\cdot\mathbf{3}}$ values at different $[\mathbf{1}]_0$ and $[\mathbf{3}]_0$ were calculated from $K_{a,\mathbf{1}\cdot\mathbf{3}}=(\Delta_{\mathbf{1}}/\Delta_{0,\mathbf{1}})/\{1-(\Delta_{\mathbf{1}}/\Delta_{0,\mathbf{1}})\}\{[\mathbf{3}]_0-(\Delta_{\mathbf{1}}/\Delta_{0,\mathbf{1}})[\mathbf{1}]_0\}$. The values and errors of $K_{a,\mathbf{1}\cdot\mathbf{3}}$ in Tables 1 and 2 are mean values and standard derivations of $K_{a,\mathbf{1}\cdot\mathbf{3}}$ values at four or five points with different $[\mathbf{1}]_0$ and $[\mathbf{3}]_0$ in the range $\Delta_{\mathbf{1}}/\Delta_{0,\mathbf{1}}=0.2$–0.8.

4.4. X-ray analysis of 1a·3a (Fig. 5)

The structure was solved by direct methods using SIR-92[28] and refined using SHELXTL NT.[29] The asymmetric unit of the structural model comprises two crystallographically independent host/guest complexes plus an additional half a guest salt and 5.38 water molecules. After locating the main residues and the waters within and around the periphery of the residues, additional residual electron density that was presumably evaporated/disordered solvent could not be modeled successfully. Consequently, the SQUEEZE[30] subroutine of the program package PLATON[31] was used to identify potential solvent/void regions and subtract any electron density contribution in this region from the structure factors. A total of 639.4 Å^3 void space was identified (9.7% of total cell volume), but electron density totaling only 3 e$^-$ was subtracted. Presumably the strong non-bonding interactions between the host and guest allowed the solvent to evaporate without the sample losing crystallinity. The final refinement model involved anisotropic displacement parameters for non-hydrogen atoms, except the disordered atoms in the host molecules. A riding model was used for all hydrogen atoms. No hydrogen positions were located or calculated for the water molecules. Data were collected on an Oxford Diffraction Sapphire 2 CCD diffractometer by the omega scan method in a range $1.4°\leq\theta\leq19.8°$. Crystal data: block, yellow, $0.34\times0.22\times0.12$ mm^3, $C_{54.75}H_{79.373}F_{7.50}N_{1.25}O_{20.19}P_{1.25}$, FW=1259.33, triclinic, space group P-1, $a=10.8768(10)$, $b=23.3640(18)$, $c=27.605(3)$ Å, $\alpha=103.533(7)$, $\beta=100.307(8)°$, $\gamma=97.849(7)$, $V=6592.6(10)$ Å^3, $Z=4$, $D_c=1.269$ g cm^{-3}, $T=100$ K, $\mu=1.37$ cm^{-1}, 32,144 measured reflections, 23,206 independent reflections [R(int)=0.0540], 1646 parameters, 164 restraints, $F(000)=2658$, $R_1=0.2109$, $wR_2=0.2957$ (all data), $R_1=0.0981$, $wR_2=0.2387$ [$I>2\sigma(I)$], maximum residual density 0.696 e Å^{-3}, and goodness-of-fit (F^2)=0.966. Crystallographic data (excluding structure factors) for the structures in this paper have been deposited with the Cambridge Crystallographic Data Centre as supplementary publication numbers CCDC 274457–274464. Copies of the data can be obtained, free of charge, on application to CCDC, 12 Union Road, Cambridge CB2 1EZ, UK [fax: +44 (0)1223 336033 or e-mail: deposit@ccdc.cam.ac.uk].

4.5. X-ray analysis of 1b (Fig. 7a)

The structure was solved by the direct methods using SIR-92[28] and refined by full-matrix least squares using Crystals.[32] Non-hydrogen atoms were treated anisotropically and hydrogen atoms were placed in calculated positions. Crystal data: prism, colorless, $0.32\times0.15\times0.10$ mm^3, $C_{30}H_{44}O_{13}$, FW=612.67, triclinic, space group P-1, $a=11.1123(11)$, $b=12.0045(15)$, $c=13.1472(18)$ Å, $\alpha=68.838(12)$, $\beta=75.51(1)$, $\gamma=67.07(1)°$, $V=1494.0(3)$ Å^3, $Z=2$, $D_c=1.362$ g cm^{-3}, $T=100$ K, $\mu=1.06$ cm^{-1}, 16,286 measured reflections, 9297 independent reflections [R(int)=0.02], 389 parameters, $F(000)=656$, $R_1=0.0578$, $wR_2=0.0543$ (all data), $R_1=0.0497$, $wR_2=0.0533$ [$I>1\sigma(I)$], maximum residual density 0.40 e Å^{-3}, and goodness-of-fit (F^2)=1.1248.

4.6. X-ray analysis of 1b·3a (Fig. 7b)

The structure was solved by direct methods and refined using SHELXTL NT.[29] The asymmetric unit of the structure comprises one crystallographically independent host–guest complex. The final refinement model involved anisotropic displacement parameters for non-hydrogen atoms and a riding model for all hydrogen atoms. Crystal data: plate, yellow, $0.058\times0.148\times0.244$ mm^3, $C_{45}H_{58}F_6NO_{14}P$, FW=981.89, monoclinic, space group $P2_1/n$, $a=10.1411(15)$, $b=21.048(4)$, $c=21.152(3)$ Å, $\beta=93.236(12)°$, $V=4507.7(12)$ Å^3, $Z=4$, $D_c=1.447$ g cm^{-3}, $T=100$ K, $\mu=1.55$ cm^{-1}, 22,096 measured reflections, 7972 independent reflections [R(int)=0.0709], 605 parameters, $F(000)=2064$, $R_1=0.1326$, $wR_2=0.0966$ (all data), $R_1=0.0613$, $wR_2=0.0777$ [$I>2\sigma(I)$], maximum residual density 0.316 e Å^{-3}, and goodness-of-fit (F^2)=0.986.

4.7. X-ray analysis of 1c·3a (Fig. 6)

SADABS[33] absorption corrections were applied. The structure was solved by direct methods and refined by full-matrix least squares procedure on F^2 using SHELXTL.[29] Non-hydrogen atoms were refined with anisotropic displacement coefficients, and hydrogen atoms were treated as idealized contributions. Crystal data: blade, colorless, $0.10\times0.10\times0.03$ mm^3, $C_{52}H_{61}F_6N_2O_{19}P$, FW=1163.00, monoclinic, space group $P2_1/n$, $a=14.742(3)$, $b=20.650(3)$, $c=19.244(3)$ Å, $\beta=104.346(3)°$, $V=5675.5(17)$ Å^3, $Z=4$, $D_c=1.361$ g cm^{-3}, $T=208(2)$ K, $\mu=1.42$ cm^{-1}, 29,441 measured reflections, 7401 independent reflections [R(int)=0.0685], 721 parameters, 0 restraints, $F(000)=2432$, $R_1=0.1534$, $wR_2=0.3107$ (all data), $R_1=0.1076$, $wR_2=0.2779$ [$I>2\sigma(I)$], maximum residual density 1.531 e Å^{-3}, and goodness-of-fit (F^2)=1.068.

4.8. X-ray analysis of 1d·3a (Fig. 8a)

The structure was solved by direct methods and refined by full-matrix least squares procedure on F^2 using the SHELXTL.[29] Non-hydrogen atoms were refined with anisotropic displacement coefficients, and hydrogen atoms were treated as idealized contributions. Crystal data: plate, pale yellow, $0.30\times0.30\times0.20$ mm^3, $C_{57.50}H_{76}F_6NO_{16}P$, FW=1182.16, triclinic, space group P-1, $a=11.0155(9)$, $b=13.3102(11)$, $c=21.2726(18)$ Å, $\alpha=89.0340(10)$, $\beta=81.7310(10)$, $\gamma=68.0420(10)°$, $V=2860.3(4)$ Å^3, $Z=2$, $D_c=1.373$ g cm^{-3}, $T=100$ K, $\mu=1.38$ cm^{-1}, 22,605 measured reflections, 11,128 independent reflections [R(int)=0.0223], 712 parameters, $F(000)=1250$, $R_1=0.0674$, $wR_2=0.1520$ (all data), $R_1=0.0533$, $wR_2=0.1436$ [$I>2\sigma(I)$], maximum residual density 1.592 e Å^{-3}, and goodness-of-fit (F^2)=1.090.

4.9. X-ray analysis of 1d·3a (Fig. 8b)

SADABS[33] absorption corrections were applied. The structure was solved by direct methods and refined by full-matrix least squares procedure on F^2 using SHELXTL.[29] Non-hydrogen atoms were refined with anisotropic displacement coefficients, and hydrogen atoms were treated as idealized contributions. Crystal data: plate, pale yellow, $0.30\times0.25\times0.20$ mm^3, $C_{55}H_{70}F_6NO_{16}P$, FW=1146.09, monoclinic, space group $P2_1/c$, $a=10.661(4)$, $b=29.733(10)$, $c=17.235(6)$ Å, $\beta=97.731(6)°$, $V=5413(3)$ Å^3, $Z=4$, $D_c=1.406$ g cm^{-3}, $T=100$ K, $\mu=1.43$ cm^{-1}, 11,150 measured reflections, 7411 independent reflections [R(int)=0.0370], 716 parameters, $F(000)=2416$, $R_1=0.0715$, $wR_2=0.1025$ (all data), $R_1=0.0438$, $wR_2=0.0919$ [$I>2\sigma(I)$], maximum residual density 0.353 e Å^{-3}, and goodness-of-fit (F^2)=0.983.

4.10. X-ray analysis of 1e·3a (Fig. 9)

The structure was solved by direct methods and refined using SHELXTL NT.[29] The asymmetric unit of the structure comprises one crystallographically independent host–guest complex. The final refinement model involved anisotropic displacement parameters for non-hydrogen atoms and a riding model for all hydrogen atoms. Crystal data: block, pale yellow, $0.275\times0.327\times0.356$ mm^3, $C_{50}H_{61}F_6N_2O_{14}P$, FW=1058.98, monoclinic, space group $P2_1/c$, $a=23.9952(17)$, $b=13.4583(10)$, $c=16.0394(12)$ Å, $\beta=105.273(6)°$, $V=4996.7(6)$ Å^3, $Z=4$, $D_c=1.408$ g cm^{-3}, $T=100$ K, $\mu=1.46$ cm^{-1}, 54,370 measured reflections, 14,618 independent reflections [R(int)=0.0288], 659 parameters, $F(000)=2224$, $R_1=0.0647$, $wR_2=0.1196$ (all data), $R_1=0.0549$, $wR_2=0.1146$ [$I>2\sigma(I)$], maximum residual density 0.307 e Å^{-3}, and goodness-of-fit (F^2)=1.195.

4.11. X-ray analysis of 1f·3a (Fig. 10)

The structure was solved by direct methods and refined using SHELXTL NT.[29] The asymmetric unit of the structure comprises one crystallographically independent host–guest complex. The final refinement model involved anisotropic displacement parameters for non-hydrogen atoms and a riding model for all hydrogen atoms. Crystal data: needle, pale yellow, $0.14\times0.17\times0.56$ mm^3, $C_{54}H_{68}F_6NO_{15}P$, FW=1116.06, monoclinic, space group $P2_1/c$, $a=11.377(2)$, $b=18.145(3)$, $c=27.106(5)$ Å, $\beta=99.856(17)°$, $V=5513.2(18)$ Å^3, $Z=4$, $D_c=1.345$ g cm^{-3}, $T=100$ K, $\mu=1.37$ cm^{-1}, 30,997 measured reflections, 12,702 independent reflections [R(int)=0.0330], 697 parameters, $F(000)=2352$, $R_1=0.1069$, $wR_2=0.1907$ (all data), $R_1=0.0647$, $wR_2=0.1647$ [$I>2\sigma(I)$], maximum residual density 0.583 e Å^{-3}, and goodness-of-fit (F^2)=1.112.

Acknowledgements

This research was supported by the National Science Foundation (DMR0097126) and the American Chemical Society Petroleum Research Fund (40223-AC7). We also thank NSF (Grant CHE-0131128) for funding of the purchase of the Oxford Diffraction Xcalibur2 single crystal diffractometer.

Supplementary data

Supplementary data associated with this article can be found, in the online version, at doi:10.1016/j.tet.2005.08.036. Job plots showing the 1:1 stoichiometry of the other complexes between **1** and **3** in 1:1 acetone/chloroform and electrospray ionization mass spectra of some cryptand/monopyridinium pseudorotaxanes.

References and notes

1. Gibson, H. W. In *Large Ring Molecules*; Semlyen, J. A., Ed.; Wiley: New York, 1996; pp 191–262. Philp, D.; Stoddart, J. F. *Angew. Chem., Int. Ed.* **1996**, *35*, 1155–1196. Raymo, F. M.; Stoddart, J. F. *Chem. Rev.* **1999**, *99*, 1643–1664. *Catenanes, Rotaxanes, and Knots*; Sauvage, J.-P., Dietrich-Buchecker, C. O., Eds.; Wiley-VCH: Weinheim, 1999. Mahan, E.; Gibson, H. W. In *Cyclic Polymers*; Semlyen, A. J., Ed. 2nd ed.;

Kluwer: Dordrecht, 2000; pp 415–560. Hubin, T. J.; Busch, D. H. *Coord. Chem. Rev.* **2000**, *200–202*, 5–52. Panova, I. G.; Topchieva, I. N. *Russ. Chem. Rev.* **2001**, *70*, 23–44.

2. Allwood, B. L.; Spencer, N.; Shahriari-Zavareh, H.; Stoddart, J. F.; Williams, D. J. *J. Chem. Soc., Chem. Commun.* **1987**, 1064–1066. Ashton, P. R.; Philp, D.; Reddington, M. V.; Slawin, A. M. Z.; Spencer, N.; Stoddart, J. F.; Williams, D. J. *J. Chem. Soc., Chem. Commun.* **1991**, 1680–1683. Huang, F.; Jones, J. W.; Slebodnick, C.; Gibson, H. W. *J. Am. Chem. Soc.* **2003**, *125*, 14458–14464.
3. (a) Fyfe, M. C. T.; Stoddart, J. F. *Adv. Supramol. Chem.* **1999**, *5*, 1–53. (b) Bryant, W. S.; Guzei, I.; Rheingold, A. L.; Gibson, H. W. *Org. Lett.* **1999**, *1*, 47–50. (c) Huang, F.; Zakharov, L. N.; Rheingold, A. L.; Jones, J. W.; Gibson, H. W. *Chem. Commun.* **2003**, 2122–2123. (d) Jones, J. W.; Gibson, H. W. *J. Am. Chem. Soc.* **2003**, *125*, 7001–7004. (e) Hung, W.-C.; Liao, K.-S.; Liu, Y.-H.; Peng, S.-M.; Chiu, S.-H. *Org. Lett.* **2004**, *6*, 4183–4186. (f) Lowe, J. N.; Fulton, D. A.; Chiu, S.-H.; Elizarov, A. M.; Cantrill, S. J.; Rowan, S. J.; Stoddart, J. F. *J. Org. Chem.* **2004**, *69*, 4390–4402.
4. Vögtle, F.; Hunten, A.; Vogel, E.; Buschbeck, S.; Safarowsky, O.; Recker, J.; Parham, A.-H.; Knott, M.; Müller, W. M.; Muller, U.; Okamoto, Y.; Kubota, T.; Lindner, W.; Francotte, E.; Grimme, S. *Angew. Chem., Int. Ed.* **2001**, *40*, 2468–2471. Hunter, C. A.; Low, C. M. R.; Packer, M. J.; Spey, S. E.; Vinter, J. G.; Vysotsky, M. O.; Zonta, C. *Angew. Chem., Int. Ed.* **2001**, *40*, 2678–2682. Leigh, D. A.; Wong, J. K. Y.; Dehez, F.; Zerbetto, F. *Nature* **2003**, *424*, 174–179. Schalley, C. A.; Reckien, W.; Peyerimhoff, S.; Baytekin, B.; Vögtle, F. *Chem. Eur. J.* **2004**, *10*, 4777–4789. Leigh, D. A.; Venturini, A.; Wilson, A. J.; Wong, J. K. Y.; Zerbetto, F. *Chem. Eur. J.* **2004**, *10*, 4960–4969. Hernández, J. V.; Kay, E. R.; Leigh, D. A. *Science* **2004**, *306*, 1532–1537.
5. Odell, B.; Reddington, M. V.; Slawin, A. M. Z.; Spencer, N.; Stoddart, J. F.; Williams, D. J. *Angew. Chem., Int. Ed. Engl.* **1988**, *27*, 1547–1550. Liu, Y.; Flood, A. H.; Stoddart, J. F. *J. Am. Chem. Soc.* **2004**, *126*, 9150–9151. Deng, W.-Q.; Muller, R. P.; Goddard, W. A., III *J. Am. Chem. Soc.* **2004**, *126*, 13562–13563.
6. Ogino, H. *J. Am. Chem. Soc.* **1981**, *103*, 1303–1304. Yamanari, K.; Shimura, Y. *Chem. Lett.* **1982**, *12*, 1959–1962. Gonzalez, B.; Cuadrado, I.; Alonso, B.; Casado, C. M.; Moran, M.; Kaifer, A. E. *Organometallics* **2002**, *21*, 3544–3551. Pang, Y.; Ritter, H.; Tabatabai, M. *Macromolecules* **2003**, *36*, 7090–7093. Okada, M.; Harada, A. *Org. Lett.* **2004**, *6*, 361–364.
7. Arduini, A.; Ferdani, R.; Pochini, A.; Secchi, A.; Ugozzoli, F. *Angew. Chem., Int. Ed.* **2000**, *39*, 3453–3456. Arduini, A.; Calzavacca, F.; Pochini, A.; Secchi, A. *Chem. Eur. J.* **2003**, *9*, 793–799.
8. (a) Rowan, A. E.; Aarts, P. P. M.; Koutstaal, K. W. M. *Chem. Commun.* **1998**, 611–612. (b) Gunter, M. J.; Jeynes, T. P.; Johnston, M. R.; Turner, P.; Chen, Z. *J. Chem. Soc., Perkin Trans. 1* **1998**, 1945–1957. (c) Elemans, J. A. A. W.; Claase, M. B.; Aarts, P. P. M.; Rowan, A. E.; Schenning, A. P. H. J.; Nolte, R. J. M. *J. Org. Chem.* **1999**, *64*, 7009–7016. (d) Bryant, W. S.; Jones, J. W.; Mason, P. E.; Guzei, I. A.; Rheingold, A. L.; Nagvekar, D. S.; Gibson, H. W. *Org. Lett.* **1999**, *1*, 1001–1004. (e) Huang, F.; Fronczek, F. R.; Gibson, H. W. *J. Am. Chem. Soc.* **2003**, *125*, 9272–9273. (f) Huang, F.; Gibson, H. W.; Bryant, W. S.; Nagvekar, D. S.; Fronczek, F. R. *J. Am. Chem. Soc.* **2003**, *125*, 9367–9371. (g) Huang, F.; Zhou, L.; Jones, J. W.; Gibson, H. W.; Ashraf-Khorassani, M. *Chem. Commun.* **2004**, 2670–2671. (h) Huang, F.; Switek, K. A.; Zakharov, L. N.; Fronczek, F. R.; Slebodnick, C.; Lam, M.; Golen, J. A.; Bryant, W. S.; Mason, P.; Rheingold, A. L.; Ashraf-Khorassani, M.; Gibson, H. W. *J. Org. Chem.* **2005**, *70*, 3231–3241.
9. Loeb, S. J.; Wisner, J. A. *Angew. Chem., Int. Ed.* **1998**, *37*, 2838–2840. Hubbard, A. L.; Davidson, G. J. E.; Patel, R. H.; Wisner, J. A.; Loeb, S. J. *Chem. Commun.* **2004**, 138–139.
10. Kim, H.-J.; Jeon, W. S.; Ko, Y. H.; Kim, K. *Proc. Natl. Acad. Sci. U.S.A.* **2002**, *99*, 5007–5011. Choi, S. W.; Lee, J. W.; Ko, Y. H.; Kim, K. *Macromolecules* **2002**, *35*, 3526–3531. Tuncel, D.; Steinke, J. H. G. *Chem. Commun.* **2002**, 496–497. Tuncel, D.; Steinke, J. H. G. *Macromolecules* **2004**, *37*, 288–302. Sindelar, V.; Moon, K.; Kaifer, A. E. *Org. Lett.* **2004**, *6*, 2665–2668.
11. Dietrich-Buchecker, C.; Colasson, B.; Fujita, M.; Hori, A.; Geum, N.; Sakamoto, S.; Yamaguchi, K.; Sauvage, J.-P. *J. Am. Chem. Soc.* **2003**, *125*, 5717–5725. Flamigni, L.; Talarico, A. M.; Chambron, J.-C.; Heitz, V.; Linke, M.; Fujita, N.; Sauvage, J.-P. *Chem. Eur. J.* **2004**, *10*, 2689–2699. Kwan, P. H.; MacLachlan, M. J.; Swager, T. M. *J. Am. Chem. Soc.* **2004**, *126*, 8638–8639. Perret-Aebi, L.-E.; von Zelewsky, A.; Dietrich-Buchecker, C.; Sauvage, J.-P. *Angew. Chem., Int. Ed.* **2004**, *43*, 4482–4485.
12. (a) Simmons, H. E.; Park, C. H. *J. Am. Chem. Soc.* **1968**, *2429-2431*, 2431–2432. (b) Reviews: Dietrich, B. In Lehn, J.-M., Atwood, J. L., Davies, J. E. D., McNicol, D. D., Vogtle, F., Eds.; Comprehensive Supramolecular Chemistry; Pergamon: Oxford, 1996; Vol. 1, pp 153–211. Lucht, B. L.; Collum, D. B. *Acc. Chem. Res.* **1999**, *32*, 1035–1042. Reed, C. A.; Bolskar, R. D. *Chem. Rev.* **2000**, *100*, 1075–1120. Kaes, C.; Katz, A.; Hosseini, M. W. *Chem. Rev.* **2000**, *100*, 3553–3590.
13. Supramolecular cryptands have been referred to as 'pseudo-cryptands'. For the first such reference see: Nabeshima, T.; Inaba, T.; Sagae, T.; Furukawa, N. *Tetrahedron Lett.* **1990**, *31*, 3919–3922. For examples of recent references see: (a) Romain, H.; Florence, D.; Alain, M. *Chemistry* **2002**, *8*, 2438–2445. (b) Nabeshima, T.; Yoshihira, Y.; Saiki, T.; Akine, S.; Horn, E. *J. Am. Chem. Soc.* **2003**, *125*, 28–29. For a review see: Nabeshima, T.; Akine, S.; Saiki, T. *Rev. Heteroat. Chem.* **2000**, *22*, 219–239.
14. (a) Jones, J. W.; Zakharov, L. N.; Rheingold, A. L.; Gibson, H. W. *J. Am. Chem. Soc.* **2002**, *124*, 13378–13379. (b) Huang, F.; Zakharov, L. N.; Rheingold, A. L.; Jones, J. W.; Gibson, H. W. *Chem. Commun.* **2003**, 2122–2123. (c) Huang, F.; Guzei, I. A.; Jones, J. W.; Gibson, H. W. *Chem. Commun.* **2005**, 1693–1695.
15. Niikura, K.; Bisson, A. P.; Anslyn, E. V. *J. Chem. Soc., Perkin Trans. 2* **1999**, 1111–1114.
16. Hashizume, M.; Tobey, S.; Lynch, V. M.; Anslyn, E. V. *Supramol. Chem.* **2002**, *14*, 511–517.
17. Mahoney, J. M.; Beatty, A. M.; Smith, B. D. *J. Am. Chem. Soc.* **2001**, *123*, 5847–5848. Mahoney, J. M.; Stucker, K. A.; Jiang, H.; Carmichael, I.; Brinkmann, N. R.; Beatty, A. M.; Noll, B. C.; Smith, B. D. *J. Am. Chem. Soc.* **2005**, *127*, 2922–2928.
18. Recent publications: (a) Yamada, D. S.; Misono, T.; Tsuzuki, S. *J. Am. Chem. Soc.* **2004**, *126*, 9682–9872. (b) Rashkin, M. J.; Hughes, R. M.; Calloway, N. T.; Waters, M. L. *J. Am. Chem. Soc.* **2004**, *126*, 13320–13325. (c) Zhao, D.; Fei, Z.; Geldbach, T. J.; Scopelliti, R.; Dyson, P. J. *J. Am. Chem. Soc.* **2004**, *126*, 15876–15882. (d) Pittelkow, M.; Christensen, J. B.; Meijer, E. W. *J. Polym. Sci., Polym. Chem.* **2004**, *42*, 3792–3799. (e) Vasilev, A.; Deligeorgiev, T.; Gadjev, N.;

Drexhage, K.-H. *Dyes Pigm.* **2005**, *66*, 135–142. (f) Ilies, M. A.; Johnson, B. H.; Makori, F.; Miller, A.; Seitz, W. A.; Thompson, E. B.; Balaban, A. T. *Arch. Biochem. Biophys.* **2005**, *435*, 217–226. (g) Tsuji, K.; Nishimura, N.; Duan, X.-M.; Okada, S.; Oikawa, H.; Matsuda, H.; Nakanishi, H. *Bull. Chem. Soc. Jpn.* **2005**, *78*, 180–186. (h) Colilla, M.; Darder, M.; Aranda, P.; Ruiz-Hitzky, E. *Chem. Mater.* **2005**, *17*, 708–715.

19. Curiel, D.; Beer, P. D.; Paul, R. L.; Cowley, A.; Sambrook, M. R.; Szemes, F. *Chem. Commun.* **2004**, 1162–1163. Sambrook, M. R.; Beer, P. D.; Wisner, J. A.; Paul, R. L.; Cowley, A. R. *J. Am. Chem. Soc.* **2004**, *126*, 15364–15365.
20. Lämsä, M.; Huuskonen, J.; Rissanen, K.; Pursiainen, J. *Chem. Eur. J.* **1998**, *4*, 84–92.
21. Che, C. M.; Kwong, H. L.; Poon, C. K.; Yam, V. W. W. *J. Chem. Soc., Dalton Trans.: Inorg. Chem.* **1990**, 3215–3219.
22. Job, P. *Ann. Chim.* **1928**, *9*, 113–203.
23. Huang, F.; Switek, K. A.; Gibson, H. W. *Chem. Commun.* **2005**, 3655–3657.
24. Quaternized monopyridinium nuclei can be easily reduced by sodium borohydride to the neutral tetrahydro derivatives. See: *Pyridine and its Derivatives*; Shaw, E. N., Klingsberg, E., Eds.; Interscience: New York, 1960; pp 47–55; Part 2. Paquette, L. A. *Modern Heterocyclic Chemistry*; W. A. Benjamin: New York, 1968; pp 240–241.
25. Huang, F.; Slebodnick, C.; Ratliff, A. E.; Gibson, H. W. *Tetrahedron Lett.* **2005**, *46*, 6019–6022.
26. Huang, F.; Fronczek, F.; Ashraf-Khorassani, M.; Gibson, H. W. *Tetrahedron Lett.* **2005**, *46*, 6765–6769.
27. *CrysAlis*, v1.170; Oxford Diffraction: Wroclaw, Poland, 2002.
28. Burla, M. C.; Camalli, M.; Cascarano, G.; Giacovazzo, C.; Polidori, G.; Spagna, R.; Viterbo, D. *J. Appl. Crystallogr.* **1989**, *22*, 389–393.
29. Sheldrick, G. M. *SHELXTL NT*, version 6.12; Bruker Analytical X-ray Systems Inc.: Madison, Wisconsin WI, USA, 2001.
30. Van der Sluis, P.; Spek, A. L. *Acta Crystollgr., Sect. A: Found. Crystallogr.* **1990**, *46*, 194–201.
31. Spek, A. L. *J. Appl. Crystallogr.* **2003**, *36*, 7–13.
32. Watkin, D. J.; Prout, C. K.; Carruthers, J. R.; Betteridge, P. W.; Cooper, R. I. *Crystals*; Chemical Crystallography Laboratory: University of Oxford, Oxford, 2000.
33. Sheldrick, G. M. *SADABS*, version 2.01, Bruker/Siemens Area Detector Absorption Correction Program; Bruker AXS: Madison, Wisconsin WI, USA, 1998.

Available online at www.sciencedirect.com
SCIENCE DIRECT
Tetrahedron
ELSEVIER
Tetrahedron 61 (2005) 10254–10261

Resolution of non-protein amino acids via the microbial protease-catalyzed enantioselective hydrolysis of their *N*-unprotected esters

Toshifumi Miyazawa,* Kiwamu Imagawa, Hiroe Minowa, Toyoko Miyamoto and Takashi Yamada

Department of Chemistry, Faculty of Science and Engineering, Konan University, Higashinada-ku, Kobe 658-8501, Japan

Received 11 July 2005; revised 8 August 2005; accepted 8 August 2005

Available online 26 August 2005

Abstract—In the *Aspergillus oryzae* protease-catalyzed ester hydrolysis, substitution of *N*-unprotected amino acid esters for the corresponding *N*-protected amino acid esters resulted in a large enhancement of the hydrolysis rate, while the enantioselectivity was deteriorated strikingly when the substrates employed were the conventional methyl esters. This difficulty was overcome by employing esters bearing a longer alkyl chain such as the isobutyl ester. Utilizing this ester, amino acids carrying an aromatic side chain were resolved with excellent enantioselectivities ($E=50$ to >200). With amino acids bearing an aliphatic side chain also, good results in terms of the hydrolysis rate and enantioselectivity were obtained by employing such an ester as the isobutyl ester. Moreover, the enantioselectivity proved to be enhanced further by conducting the reaction at low temperature. This procedure was applicable to the case where the enantioselectivity was not high enough even by the use of the isobutyl ester.

1. Introduction

Microbial proteases from a variety of sources are commercially available. They have been employed mainly for food processing and as detergent ingredients. Although they possess some properties favorable as synthetic catalysts—they are inexpensive, stable and easy to handle, and they require no added cofactors, they have rarely been exploited for organic syntheses, except subtilisins, the most important members of which are subtilisin Carlsberg (from *Bacillus licheniformis*) and subtilisin BPN′ (from *Bacillus amyloliquefaciens*). Not only racemic amino acid esters but also other racemic carboxylic acid esters have been resolved with subtilisins.[1] Furthermore, the former subtilisin has been utilized for the transesterification between *N*-protected amino acid esters and alcohols[2] and for the regioselective acylation of polyhydroxy compounds such as carbohydrates,[3] because of its unique robustness in organic solvents. The latter subtilisin, including its variants, has frequently been applied to peptide synthesis.[4] We also have been making a search for the effective use of microbial proteases in organic syntheses. We exploited previously *Aspergillus oryzae* protease (Amano protease A) and *Bacillus subtilis* protease (Amano protease N) for the resolution of non-protein amino acids via the enantioselective hydrolysis of their *N*-protected esters.[5] Recently, we have also reported the utilization of *Aspergillus melleus* protease (Amano protease P) and *A. oryzae* protease as catalysts for peptide bond formation via the kinetically controlled approach[6] and of *B. subtilis* protease via the thermodynamically controlled approach.[7] On these lines, we have preliminarily reported on the resolution of non-protein amino acids via the enantioselective hydrolysis of their *N*-unprotected esters employing *A. oryzae* protease.[8,9] During the course of the investigation, we have found that the enantioselectivity of the hydrolysis can be significantly improved by choosing an appropriate ester grouping and by lowering the reaction temperature. In this paper, we describe further relevant details.

Besides some 20 amino acids universally distributed as protein constituents in living organisms, there are hundreds of other amino acids of non-protein origin.[10] Homochiral non-protein amino acids, including those synthetic compounds which have not been found in nature, are useful building blocks for the synthesis of analogs of biologically active peptides such as toxins, antibiotics, hormones, and enzyme inhibitors[11] and versatile chiral starting materials or

Keywords: Resolution; Non-protein amino acids; *Aspergillus oryzae* protease; Enantioselective hydrolysis; Isobutyl ester; Low temperature.
* Corresponding author. Tel.: +81 784314341; fax: +81 784352539; e-mail: miyazawa@base2.ipc.konan-u.ac.jp

0040–4020/$ - see front matter © 2005 Elsevier Ltd. All rights reserved.
doi:10.1016/j.tet.2005.08.033

chiral auxiliaries for other synthetic purposes.[12] For the supply of non-protein amino acids in quantity, the chemical synthesis of racemic forms followed by their optical resolution is still the preferable way, though a number of methods have been developed for the asymmetric syntheses of amino acids.[13] For the resolution of racemic amino acids, enzymatic methods have often been employed besides chemical methods based on the formation of diastereomeric salts or derivatives.[14,15] Hydrolytic enzymes have often been used for the purpose. Acylase I (aminoacylase; *N*-acylamino acid amidohydrolase) is the most frequently used enzyme in the chemoenzymatic preparation of the L (≡*S*) forms of amino acids from the racemic *N*-acyl derivatives. An extensive study has been conducted of the substrate specificity of porcine kidney acylase and the mold enzyme from *A. oryzae*, especially for the resolution of unnatural and rarely occurring amino acids.[16] However, the most commonly used enzymes such as porcine renal acylase I are not always applicable to the resolution of non-protein amino acids. Accordingly, it is worthwhile to develop novel enzymatic resolution methods for them. Ester hydrolysis has been utilized for the enzyme-based resolution procedures for amino acids.[17] The mammalian protease α-chymotrypsin is one of the most popular enzymes which have been employed for such a purpose. We also have exploited some microbial lipases and porcine pancreatic lipase for the resolution of non-protein amino acids through the enantioselective hydrolysis of their *N*-protected esters.[18] The success of the lipase-mediated methods prompted us to examine microbial proteases for the same purpose.

2. Results and discussion

As stated above, we investigated previously the resolution of non-protein amino acids via the enantioselective hydrolysis of the methyl esters of their *N*-benzyloxycarbonyl (*Z*) derivatives using two microbial proteases from *B. subtilis* (Amano protease N) and *A. oryzae* (Amano protease A), the former protease generally yielding better results than the latter one.[5a] When *B. subtilis* protease was employed, amino acids bearing an aliphatic side chain as well as those with an aromatic side chain were resolved with good to excellent enantioselectivities in phosphate buffer containing 20% (v/v) DMF. In some cases, however, the hydrolysis rates were rather slow, which makes the method less practical. Since the *N*-*Z*-amino acid methyl esters used as substrates generally had low solubilities in water, the addition of such a polar solvent as DMF was inevitable, which should be responsible for the often observed slow hydrolysis. Consequently, we intended to examine amino acid esters bearing a free α-amino group as substrates for the microbial protease-catalyzed hydrolysis which have better solubilities than the corresponding *N*-protected derivatives in the expectation of an enhancement of the hydrolysis rate.

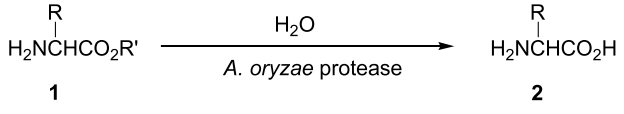

Scheme 1. *A. oryzae* protease-catalyzed hydrolysis of amino acid esters (**1**). See Tables 1 and 2 for R and R′.

Initially, the methyl esters of several phenylalanines bearing a halogen atom on the benzene ring (**1**, R = X-PhCH$_2$) were subjected to hydrolysis with *A. oryzae* protease[19] at the initial pH of 7 and at 30 °C (Scheme 1). After the desired degree of conversion (ca. 40%), the liberated amino acid (**2**) was isolated and its enantiomeric excess (ee) was determined by HPLC analysis on a chiral ligand-exchange column.[20] The results are compiled in Table 1. As anticipated, the hydrolysis of the methyl esters of these *N*-unprotected, halogenated phenylalanines proceeded much more smoothly than that of the corresponding *N*-protected methyl esters. Thus, ca. 40% conversion was reached after dozens of minutes instead of dozens of hours for the *N*-protected derivatives. However, the enantioselectivities deteriorated strikingly compared with those observed with the corresponding *N*-protected derivatives,[21] as judged from the values of enantiomeric ratio (*E*).[22]

Accordingly, the influence of ester groupings was examined next using 4-fluorophenylalanine (**1**, R = 4-F-PhCH$_2$) as a model amino acid in the expectation of a possible enhancement of enantioselectivity even at the cost of some reduction in the hydrolysis rate (entries 1–5, Table 1). In the resolution of carboxylic acids via the enzyme-catalyzed ester hydrolysis, the methyl or ethyl ester is ordinarily a preferable one, because esters carrying a longer alkyl chain are usually hydrolyzed at reduced rates. Activated esters such as the 2-chloroethyl or 2,2,2-trifluoroethyl ester are sometimes employed in order to enhance the rate of ester hydrolysis. On the other hand, the influence of the alcohol moiety of esters on the enantioselectivity of hydrolysis is not fully understood: relevant data have scarcely been accumulated in the literature.[23] As can be seen from the table, the use of the isopropyl ester resulted in a large retardation of hydrolysis with a slight improvement of enantioselectivity (entry 2). In the case of the benzyl ester, the hydrolysis proceeded very smoothly with a distinct enlargement in the *E* value (entry 5). It was gratifying to find that the use of the *n*-butyl (entry 3) or the isobutyl ester (entry 4) resulted in no retardation of the hydrolysis and yet a marked enhancement of enantioselectivity. Especially with the *n*-butyl ester, the hydrolysis proceeded in an almost enantiospecific manner, the *E* value being evaluated to be >200.[24] Of these two esters, the isobutyl ester was chosen in order to avoid the handling of the stinking *n*-butyl alcohol in the preparation of *n*-butyl esters and after their hydrolysis. Thus, the resolution of other halogenated phenylalanines was examined by employing their isobutyl esters as substrates. A marked enhancement of enantioselectivity was achieved by replacing the methyl ester with the isobutyl ester (entries 7, 9, and 11). The reaction was changed from almost non-enantiospecific to specific with 4-chlorophenylalanine. Excellent enantioselectivities were attained also in all the other cases employing the isobutyl esters as substrates (entries 12–l4). The marked enhancement of enantioselectivity by switching the methyl ester to the isobutyl ester observed here imply that the role of the ester moiety becomes relatively important in the substrate recognition by the protease when an acylamino group is replaced by a free amino group.

Furthermore, the influence of ester groupings was also explored with *N*-unprotected amino acids bearing an

Table 1. *A. oryzae* protease-catalyzed hydrolysis of aromatic amino acid esters (**1**)[a]

Entry	R	R′	Conversion (%)	Time (min)	ee_P (%)[b]	*E*
1	4-F-$PhCH_2$	Me	48	79	47	4.2
2	4-F-$PhCH_2$	*i*-Pr[c]	35	230	67	7.1
3	4-F-$PhCH_2$	*n*-Bu[c]	34	24	99	>200
4	4-F-$PhCH_2$	*i*-Bu[c]	47	25	97	170
5	4-F-$PhCH_2$	Bzl[c]	39	5	91	37
6	3-F-$PhCH_2$	Me	23	30	84	15
7	3-F-$PhCH_2$	*i*-Bu	33	30	98	150
8	2-F-$PhCH_2$	Me	24	45	7.5	1.2
9	2-F-$PhCH_2$	*i*-Bu	44	55	92	50
10	4-Cl-$PhCH_2$	Me	43	59	46	3.7
11	4-Cl-$PhCH_2$	*i*-Bu	46	30	98	>200
12	2-Cl-$PhCH_2$	*i*-Bu	38	20	99	>200
13	4-Br-$PhCH_2$	*i*-Bu	52	25	91	120
14	$PhCH_2$	*i*-Bu	31	24	>99	>200

[a] Reactions were conducted as described in the Section 4 using 0.2 mmol of DL-**1** in the form of the hydrochloride (or hydrobromide).
[b] Enantiomeric excess of the liberated amino acid.
[c] Hydrobromide.

aliphatic side chain. The results obtained when a series of esters of norvaline (2-aminopentanoic acid; **1**, R=*n*-Pr) were subjected to hydrolysis with *A. oryzae* protease (Table 2). The pH of the reaction mixture was maintained at 7 by automatic titration with 0.1 M NaOH during the hydrolysis. DMSO (20%, v/v) was added to the phosphate buffer to increase the solubility of the alkyl esters larger than the *n*-butyl ester (entries 9–12). In the case of the *n*-pentyl ester, it was ascertained that the addition of DMSO had no harmful effects on the enzymatic hydrolysis: the reaction was little retarded and the enantioselectivity was not affected at all (entries 8 and 9). When normal alkyl esters are compared, the enantioselectivity was increased almost progressively with the length of the ester alkyl chain from methyl to *n*-heptyl (entries 1–6, and 8–11). The longer *n*-octyl ester (entry 12) yielded an *E* value as low as that obtained with the methyl ester, and in addition, the reaction was extremely slow. Of all the esters examined, the isobutyl ester gave an enantioselectivity of the highest rank even in the shortest reaction time. Therefore, this ester was chosen for further studies, making it easier to compare the results with those with the aromatic amino acids mentioned above. Thus, rather high enantioselectivities were attained in the hydrolysis of the isobutyl esters of other aliphatic amino acids (entries 16, 19, 21, and 22). However, they were lower than those observed with the aromatic amino acid derivatives. As stated below, we found that conducting the hydrolysis at low temperature was quite effective in improving further the enantioselectivity.

In all the cases mentioned above, the preferential hydrolysis of the L-enantiomers was confirmed by comparison with

Table 2. *A. oryzae* protease-catalyzed hydrolysis of aliphatic amino acid esters (**1**)[a]

Entry	R	R′	Conversion (%)	Time (min)	ee_P (%)[b]	*E*
1	*n*-Pr	Me	40	170	58	5.5
2	*n*-Pr	Et	40	280	72	10
3	*n*-Pr	*n*-Pr	40	250	75	12
4	*n*-Pr	*i*-Pr	40	510	82	18
5	*n*-Pr	*n*-Bu	40	150	88	30
6	*n*-Pr	*i*-Bu	40	77	92	45
7[c]	*n*-Pr	*i*-Bu	40	400	97	130
8	*n*-Pr	*n*-Pentyl	40	180	91	40
9[d]	*n*-Pr	*n*-Pentyl	40	190	91	40
10[d]	*n*-Pr	*n*-Hexyl	42	120	92	50
11[d]	*n*-Pr	*n*-Heptyl	40	96	94	63
12[d]	*n*-Pr	*n*-Octyl	14	23 h	70	5.9
13	*n*-Bu	Me	40	160	53	4.6
14	*n*-Bu	Et	39	200	67	7.8
15	*n*-Bu	*n*-Pr	39	170	86	24
16	*n*-Bu	*i*-Bu	40	140	95	76
17[c]	*n*-Bu	*i*-Bu	41	19.7 h	98	>200
18	Et	Me	40	390	38	5.5
19	Et	*i*-Bu	40	190	78	14
20[c]	Et	*i*-Bu	40	22.3 h	95	78
21	*i*-Bu	*i*-Bu	40	320	94	66
22	*n*-Pentyl	*i*-Bu[e]	33	280	89	27
23	*i*-Pentyl	*i*-Bu[e]	33	14.5 h	77	11

[a] Reactions were conducted as described in the Section 4 using 0.4 mmol of DL-**1** in the form of the hydrochloride (or tosylate) in 0.1 M phosphate buffer (pH 7.0) without DMSO at 30 °C, unless otherwise noted.
[b] Enantiomeric excess of the liberated amino acid.
[c] Reactions were conducted at 5 °C.
[d] Reactions were conducted in 0.1 M phosphate buffer (pH 7.0) containing 20% (v/v) DMSO.
[e] Tosylate.

authentic samples prepared form the optically active amino acids, if available, on HPLC or suggested from the regularity of elution order of the enantiomers on HPLC.[20] This stereochemical preference is the same as that observed in the hydrolysis of racemic *N*-*Z*-amino acid 2-chloroethyl or 2,2,2-trifluoroethyl esters mediated by lipases[18] or proteases.[5,25]

We examined next the possibility of improving the enantioselectivity by lowering temperature in the *A. oryzae* protease-catalyzed hydrolysis of the isobutyl esters of 2-aminobutanoic acid (**1**, R=Et) and norvaline.[26] It is widely believed that in enzymatic reactions, as in the conventional chemical reactions, lower temperatures lead to higher enantioselectivity; this has been supported by a number of experimental results.[27,28] A rational understanding of such a temperature effect on enantioselectivity has been proposed.[29] When $-RT\ln E$ is plotted against absolute temperature (T), a straight line should be obtained ($-RT\ln E=\Delta\Delta H^{\ddagger}-T\Delta\Delta S^{\ddagger}$).[30] If the racemic temperature (T_r), at which no enantiomeric discrimination occurs, is high above the ordinary temperature, the enantioselectivity will increase with decreasing temperature. As shown in Figure 1, when $-RT\ln E$ obtained from the E value at each temperature was plotted against T, straight lines were obtained for the hydrolysis of the isobutyl esters of both the amino acids. The temperature range examined here was 5–45 °C. The existence of a linear relationship between $-RT\ln E$ and T indicates that the temperature effect on the enantioselectivity of the enzymatic hydrolyses is governed by the above-mentioned equation and the enzyme retains its active conformation within the temperature range examined. In both the cases, T_r's were high (80 °C for 2-aminobutatnoic acid; 93 °C for norvaline); thus, when the reaction temperature was lowered from 30 to 5 °C, the hydrolysis time became much longer, but a largely enhanced enantioselectivity was obtained in each case (entries 20 and 7, respectively, in Table 2). This is also the case with the isobutyl ester of norleucine (2-aminohexanoic acid; **1**, R=*n*-Bu): the reaction was almost enantiospecific at 5 °C (entry 17).

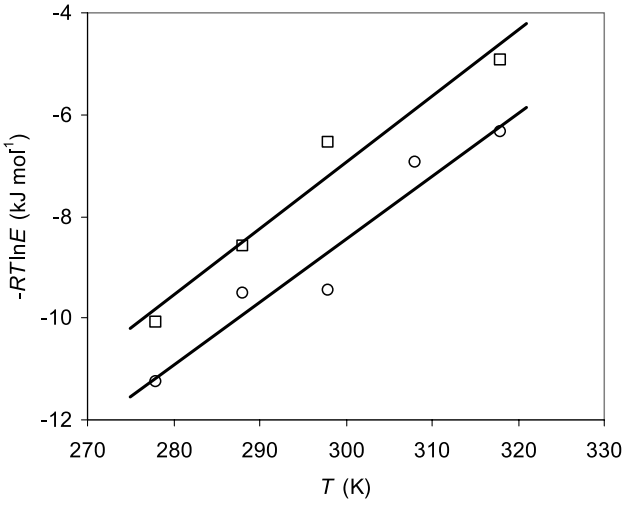

Figure 1. Influence of temperature (T) on the difference in the activation free energy ($\Delta\Delta G^{\ddagger}=-RT\ln E$) between the enantiomers for the *A. oryzae* protease-catalyzed hydrolysis of isobutyl esters of 2-aminobutanoic acid (square) and norvaline (circle).

3. Conclusion

In this work, we have shown that in the hydrolysis of amino acid esters with a free α-amino group catalyzed by *A. oryzae* protease, the enantioselectivity can be enhanced greatly by employing esters with a longer alkyl chain such as the isobutyl ester. The enhancement of enantioselectivity by modifying the alcohol moiety of the substrate ester seems to be rather general, and this possibility should be considered when the enantioselectivity is inadequate with the methyl or ethyl ester conventionally used in the ester hydrolysis mediated by hydrolytic enzymes. Furthermore, we have shown that the enantioselectivity of the hydrolysis reaction catalyzed by the microbial protease can be enhanced significantly by conducting the reaction at low temperature. In cases in which T_r exists above the ordinary temperature (this must be often the case), there must be such a possibility. The relevant results accumulated recently support this idea. In the reactions conducted in water with organic cosolvents or in organic solvents, it is usually easy to lower the reaction temperature even below 0 °C, which may lead to a significant enhancement of enantioselectivity. As the majority of enzymes used for biotransformations are not thermally stable, reactions at higher temperatures are largely restricted, while lowering temperature seems to have less operational limits.

4. Experimental

4.1. General

^{1}H NMR spectra were obtained at 300 MHz on a Varian Unity 300 spectrometer using DMSO-d_6 as a solvent with TMS as an internal standard unless otherwise noted. Mp were determined on a Yamato MP-21 apparatus and are uncorrected. Optical rotations were measured using a JASCO DIP-4 digital polarimeter. All organic solvents were distilled following standard protocols and dried over molecular sieves prior to use. Petroleum ether refers to the fraction with distillation range 30–70 °C. Protease from *A. oryzae* (protease A) was supplied by Amano Pharmaceutical Co. (Japan) and had a specific activity of 10 U/mg solid (pH 7.0) (one Amano unit is defined as the enzyme quantity which hydrolyzes casein to produce color equivalent to 400 mg of L-Tyr per 60 min at 37 °C, according to the supplier).

4.2. Preparation of amino acid esters

The physical and ^{1}H NMR data of the amino acid esters prepared are compiled in Table 3. Elemental analysis data of all the new compounds are available as Supplementary material.

4.2.1. As hydrochlorides (or tosylates). The method for preparing amino acid methyl esters[35] was modified as illustrated below for the preparation of DL-2-aminobutanoic acid isobutyl ester hydrochloride. Thionyl chloride (16 ml)

Table 3. Physical and ^{1}H NMR data of DL-amino acid esters

DL-amino acid ester (**1**) hydrochloride			
R	R′	Mp (°C)[a]	^{1}H NMR δ_H (DMSO-d_6)
4-F-PhCH$_2$	Me	169–170 [C]	3.03–3.17 (2H, m), 3.67 (3H, s), 4.26 (1H, t, J=6.6 Hz), 7.11–7.28 (4H, m), 8.47 (3H, s)
4-F-PhCH$_2$	*i*-Pr[b]	198–199 [C]	1.22 (3H, d, J=6.3 Hz), 1.23 (3H, d, J=6.3 Hz), 3.02–3.17 (2H, m), 3.87 (1H, t, J=6.3 Hz), 4.97 (1H, septet, J=6.3 Hz), 7.13–7.30 (4H, m), 8.59 (3H, s)
4-F-PhCH$_2$	*n*-Bu[b]	116–117 [C]	0.89 (3H, t, J=7.2 Hz), 1.20–1.50 (2H, m), 1.51–1.66 (2H, m), 3.03–3.17 (2H, m), 4.08–4.20 (2H, m), 4.26 (1H, t, J=6.6 Hz), 7.10–7.30 (4H, m), 8.57 (3H, s)
4-F-PhCH$_2$	*i*-Bu[b]	127–129 [C]	0.76 (3H, d, J=6.6 Hz), 0.77 (3H, d, J=6.6 Hz), 1.60–1.81 (1H, m), 3.06–3.27 (2H, d of ABq, J=14.0, 8.0, 5.7 Hz), 3.75–3.86 (2H, m), 4.33 (1H, dd, J=8.0, 5.7 Hz), 7.09–7.31 (4H, m), 8.70 (3H, s)
4-F-PhCH$_2$	Bzl[b]	199–201 [C]	3.03–3.18 (2H, m), 4.27 (1H, t, J=6.6 Hz), 5.23 (1H, s), 7.11–7.28 (4H, m), 7.33–7.45 (5H, m), 8.67 (3H, s)
3-F-PhCH$_2$	Me	160–162 [C]	3.09–3.21 (2H, m), 3.67 (3H, s), 4.31 (1H, t, J=6.6 Hz), 7.05–7.37 (4H, m), 8.58 (3H, s)
3-F-PhCH$_2$	*i*-Bu	137–138.5 [D]	0.76 (3H, d, J=6.9 Hz), 0.77 (3H, d, J=6.9 Hz), 1.66–1.83 (1H, m), 3.05–3.25 (2H, d of ABq, J=14.0, 7.8, 5.7 Hz), 3.78–3.87 (2H, m), 4.33 (1H, dd, J=7.8, 5.7 Hz), 7.06–7.40 (4H, m), 8.70 (3H, s)
2-F-PhCH$_2$	Me	159–160 [D]	3.08–3.24 (2H, m), 3.62 (3H, s), 4.16 (1H, dd, J=6.0, 5.7 Hz), 7.13–7.37 (4H, m), 8.65 (3H, s)
2-F-PhCH$_2$	*i*-Bu	139–142 [D]	0.71 (3H, d, J=6.6 Hz), 0.73 (3H, d, J=6.6 Hz), 1.60–1.76 (1H, m), 3.06–3.26 (2H, d of ABq, J=14.0, 8.7, 5.7 Hz), 3.70–3.86 (2H, d of ABq, J=10.5, 6.6 Hz), 4.33 (1H, dd, J=8.7, 5.7 Hz), 7.14–7.37 (4H, m), 8.74 (3H, s)
4-Cl-PhCH$_2$	Me	183–184 [C], lit.[31] 177–178	3.05–3.18 (2H, m), 3.67 (3H, s), 4.27 (1H, t, J=6.6 Hz), 7.22–7.40 (4H, m), 8.47 (3H, s)
4-Cl-PhCH$_2$	*i*-Bu	149–151 [D]	0.76 (3H, d, J=6.6 Hz), 0.77 (3H, d, J=6.6 Hz), 1.65–1.82 (1H, m), 3.02–3.23 (2H, m), 3.77–3.87 (2H, m), 4.24–4.30 (1H, m), 7.25–7.40 (4H, m), 8.70 (3H, s)
2-Cl-PhCH$_2$	*i*-Bu	128–131 [D]	0.76 (3H, d, J=6.6 Hz), 0.77 (3H, d, J=6.6 Hz), 1.66–1.82 (1H, m), 3.00–3.23 (2H, m), 3.76–3.87 (2H, m), 4.25–4.30 (1H, m), 7.21–7.41 (4H, m), 8.69 (3H, s)
4-Br-PhCH$_2$	*i*-Bu	162–164 [C]	0.78 (3H, d, J=6.6 Hz), 0.79 (3H, d, J=6.6 Hz), 1.67–1.85 (1H, m), 3.00–3.20 (2H, d of ABq, J=14.1, 7.8, 6.0 Hz), 3.77–3.88 (2H, m), 4.25–4.29 (1H, m), 7.18–7.52 (4H, m), 8.54 (3H, s)
PhCH$_2$	*i*-Bu	129–131 [B]	0.74 (3H, d, J=6.6 Hz), 0.75 (3H, d, J=6.6 Hz), 1.64–1.82 (1H, m), 3.00–3.24 (2H, d of ABq, J=13.8, 8.1, 5.7 Hz), 3.75–3.86 (2H, d of ABq, J=10.1, 6.1 Hz), 4.26 (1H, dd, J=8.1, 5.7 Hz), 7.22–7.35 (5H, m), 8.63 (3H, s)
n-Pr	Me	116–117 [C], lit.[32] 116–117	0.85 (3H, t, J=7.4 Hz), 1.21–1.45 (2H, m), 1.74 (2H, q-like, J= ca. 7.4 Hz), 3.72 (3H, s), 3.95 (1H, t, J=6.3 Hz), 8.62 (3H, s)
n-Pr	Et	66–68 [D], lit.[33] ca. 65[c]	0.87 (3H, t, J=7.2 Hz), 1.22 (3H, t, J=7.2 Hz), 1.20–1.50 (2H, m), 1.76 (2H, q-like, J= ca. 7.5 Hz), 3.92 (1H, t, J=6.3 Hz), 4.11–4.26 (2H, m), 8.62 (3H, s)
n-Pr	*n*-Pr	68–71 [E][d]	0.87 (3H, t, J=7.2 Hz), 0.90 (3H, t, J=7.2 Hz), 1.20–1.51 (2H, m), 1.62 (2H, sextet, J=7.0 Hz), 1.70–1.82 (2H, m), 3.96 (1H, t, J=6.3 Hz), 4.04–4.17 (2H, m), 8.58 (3H, s)
n-Pr	*i*-Pr	96–97 [F]	0.87 (3H, t, J=7.2 Hz), 1.22 (3H, d, J=6.3 Hz), 1.23 (3H, d, J=6.3 Hz), 1.20–1.50 (2H, m), 1.69–1.81 (2H, m), 3.87 (1H, t, J=6.3 Hz), 4.98 (1H, septet, J=6.3 Hz), 8.60 (3H, s)
n-Pr	*n*-Bu	76–77 [D]	0.87 (3H, t, J=7.2 Hz), 0.89 (3H, t, J=7.2 Hz), 1.20–1.50 (4H, m), 1.51–1.65 (2H, m), 1.70–1.81 (2H, m), 3.96 (1H, t, J=6.3 Hz), 4.08–4.21 (2H, m), 8.55 (3H, s)
n-Pr	*i*-Bu	84–86 [A]	0.86 (3H, t, J=7.2 Hz), 0.89 (6H, d, J=6.6 Hz), 1.22–1.48 (2H, m), 1.76 (2H, q-like, J= ca. 7.5 Hz), 1.83–1.96 (1H, m), 3.87–3.98 (3H, m), 8.60 (3H, s)
n-Pr	*n*-Pentyl	78–79 [C]	0.86 (3H, t, J=7.2 Hz), 0.87 (3H, t, J=7.2 Hz), 1.19–1.50 (6H, m), 1.55–1.64 (2H, m), 1.69–1.81 (2H, m), 3.96 (1H, t, J=6.3 Hz), 4.07–4.21 (2H, m), 8.54 (3H, s)
n-Pr	*n*-Hexyl	78–79 [C]	0.86 (3H, t, J=7.2 Hz), 0.87 (3H, t, J=7.2 Hz), 1.19–1.50 (8H, m), 1.55–1.64 (2H, m), 1.70–1.81 (2H, m), 3.96 (1H, t, J=6.3 Hz), 4.07–4.21 (2H, m), 8.55 (3H, s)
n-Pr	*n*-Heptyl	69–72 [B]	0.84 (3H, t, J=7.2 Hz), 0.86 (3H, t, J=7.2 Hz), 1.18–1.48 (10H, m), 1.53–1.63 (2H, m), 1.68–1.79 (2H, m), 3.96 (1H, t, J=6.3 Hz), 4.06–4.20 (2H, m), 8.51 (3H, s)
n-Pr	*n*-Octyl	73–74 [G]	0.85 (3H, t, J=7.2 Hz), 0.87 (6H, d, J=6.6 Hz), 1.19–1.50 (12H, m), 1.55–1.64 (2H, m), 1.70–1.81 (2H, m), 3.96 (1H, t, J=6.3 Hz), 4.06–4.21 (2H, m), 8.54 (3H, s)
n-Bu	Me	117–119 [C], lit.[32] 122–123	0.85 (3H, t, J=6.9 Hz), 1.17–1.42 (4H, m), 1.71–1.83 (2H, m), 3.73 (3H, s), 3.96 (1H, t, J=6.3 Hz), 8.54 (3H, s)
n-Bu	Et	81–82 [D]	0.86 (3H, t, J=6.9 Hz), 1.22 (3H, t, J=7.2 Hz), 1.17–1.43 (4H, m), 1.72–1.84 (2H, m), 3.93 (1H, t, J=6.3 Hz), 4.11–4.27 (2H, m), 8.55 (3H, s)
n-Bu	*n*-Pr	82–84 [E]	0.86 (3H, t, J=6.9 Hz), 0.90 (3H, t, J=7.2 Hz), 1.17–1.42 (4H, m), 1.63 (2H, sextet, J=7.0 Hz), 1.72–1.83 (2H, m), 3.93 (1H, t, J=6.3 Hz), 4.04–4.18 (2H, m), 8.54 (3H, s)
n-Bu	*i*-Bu	56–57 [B]	0.84 (3H, t, J=7.2 Hz), 0.89 (6H, d, J=6.6 Hz), 1.17–1.43 (4H, m), 1.78 (2H, q-like, J= ca. 7.3 Hz), 1.82–1.96 (1H, m), 3.87–3.99 (3H, m), 8.55 (3H, s)
Et	Me	146–148 [C], lit.[34] 139	0.89 (3H, t, J=7.5 Hz), 1.82 (2H, d of q, J=7.5, 6.0 Hz), 3.72 (3H, s), 3.94 (1H, t, J=6.0 Hz), 8.65 (3H, s)

Table 3 (*continued*)

DL-amino acid ester (**1**) hydrochloride			
R	R′	Mp (°C)[a]	^{1}H NMR δ_H (DMSO-d_6)
Et	*i*-Bu	72–73 [A]	0.90 (6H, d, J=6.3 Hz), 0.92 (3H, t, J=7.5 Hz), 1.80–1.97 (3H, m), 3.88–4.00 (3H, m), 8.60 (3H, s)
i-Bu	*i*-Bu	106–108 [B]	0.87–0.90 (12H, m), 1.63 (2H, t, J=7.0 Hz),1.67–1.79 (1H, m), 1.81–1.97 (1H, m), 3.88–3.971 (3H, m), 8.55 (3H, s)
n-Pentyl	*i*-Bu	oil[e]	0.85 (3H, t, J=6.9 Hz), 0.90 (6H, d, J=6.9 Hz), 1.18–1.46 (6H, m), 1.73–1.83 (2H, m), 1.83–1.97 (1H, m), 3.87–3.99 (3H, m), 8.63 (3H, s)
i-Pentyl	*i*-Bu	116–118 [B][f]	0.84 (3H, d, J=6.6 Hz), 0.85 (3H, d, J=6.6 Hz), 0.91 (6H, d, J=6.6 Hz), 1.06–1.37 (2H, m), 1.44–1.58 (1H, m), 1.72–1.99 (3H, m), 3.88–4.01 (3H, m), 8.54 (3H, s)

[a] Recrystallization solvent: A, EtOAc–ether; B, ether–petroleum ether; C, MeOH–ether; D, EtOH–ether; E, 1-propanol–ether; F, 2-propanol–ether; G, 1-octanol.
[b] Hydrobromide.
[c] Tosylate, mp 123–124 °C (D).
[d] Tosylate, mp 85–86 °C (C).
[e] Tosylate, mp 103–104 °C (D).
[f] Tosylate, mp 132–134 °C (D).

was added dropwise below 0 °C under stirring to isobutyl alcohol (2-methyl-1-propanol; 98 ml) which had been precooled to −10 °C. After 15 min the DL-amino acid (4.46 g) was added and the reaction mixture was stirred at 50 °C for 60 h. The mixture was evaporated under reduced pressure, and the residue was recrystallized from ethyl acetate–petroleum ether to yield white needles; 7.25 g (86%); mp 66–68 °C. Other DL-amino acid ester hydrochlorides were prepared in essentially the same manner and purified by recrystallization from an appropriate solvent (shown in the table). In some cases, the hydrochlorides obtained were converted to the tosylates which became crystalline more easily.

4.2.2. As hydrobromides. The preparation of DL-4-fluorophenylalanine isobutyl ester hydrobromide is described as a typical example. *N*-*Z*-DL-4-fluorophenylalanine[36] (252 mg) was reacted with isobutyl alcohol (70 μl) in the presence of 1-ethyl-3-(3-dimethylaminopropyl)-carbodiimide hydrochloride (170 mg) and 4-dimethylaminopyridine (50 mg) in anhydrous dichloromethane (3 ml) according to Dhaon et al.[37] The crude isobutyl ester (218 mg) thus obtained was treated with 25% HBr in acetic acid (3 ml) to yield the debenzyloxycarbonylated product, which was recrystallized from MeOH–ether; yield, 224 mg (96% from the *N*-*Z*-amino acid); mp 127–129 °C. Other DL-amino acid ester hydrobromides were prepared in essentially the same manner and purified by recrystallization from MeOH–ether.

4.3. *A. oryzae* protease-catalyzed hydrolysis of aromatic amino acid esters

An amino acid ester hydrochloride (or hydrobromide) (0.2 mmol) was dissolved in 2.5 ml of 0.1 M phosphate buffer (pH 7.0). The pH was adjusted to 7.0 with 0.5 M NaOH. On the other hand, a protease preparation (20 mg) was added to 1 ml of the same buffer, mixed up and centrifuged (12,000 rpm, 20 min), and 0.5 ml of the supernatant was added to the above substrate solution. The resulting mixture was shaken (180 strokes per minute) at 30 °C. The reaction was monitored by HPLC on a Nucleosil 5C_8 column (4.6 mm I.D.×150 mm; Chemco Scientific Co., Japan). The liquid chromatograph employed was a Shimadzu LC-10AS instrument equipped with a Rheodyne 7725i sample injector, an SPD-10A variable wavelength UV monitor and a Chromatopac C-R6A data processor under the following conditions: mobile phase, 10–30% (v/v) solution of CH_3CN in water containing trifluoroacetic acid (0.1%); flow rate, 1.0 ml min^{-1}; column temperature, 30 °C; detection, UV at 254 nm. After the desired degree of conversion (ca. 40%), the reaction mixture was adjusted to pH 9 with 0.5 M NaOH and extracted several times with ethyl acetate to remove the unreacted ester. The aqueous layer was adjusted to pH 7 with 1 M HCl and evaporated to dryness under reduced pressure. The residue was dissolved in a small amount of distilled water and analyzed by chiral HPLC (vide infra) to obtain the ee value of the liberated amino acid. The results are shown in Table 1.

4.4. *A. oryzae* protease-catalyzed hydrolysis of aliphatic amino acid esters

An amino acid ester hydrochloride (or tosylate) (0.4 mmol) was dissolved in 2.5 ml of 0.1 M phosphate buffer (pH 7.0) with/without DMSO (0.6 ml). The pH was adjusted to 7.0 with 0.5 M NaOH. The protease solution (0.5 ml) prepared as above from a protease preparation (20 mg) was added to the above substrate solution. The resulting mixture was stirred at a constant temperature in the range of 5–45 °C. The pH was maintained at 7.0 by automatic titration with 0.1 M NaOH using an AUT-1 automatic pH titrator equipped with an ABT-1 automatic burette (TOA Electronics, Japan). The progress of the reaction was followed by the consumption of the alkali. After the desired degree of conversion (ca. 40%), the reaction mixture was treated as above to separate the liberated amino acid, which was analyzed by chiral HPLC to obtain its ee value. The results are shown in Table 2.

4.5. Chiral HPLC analysis

The optical purities of the resulting amino acids were determined by chiral HPLC on a Sumichiral OA-5000 column (4.6 mm I.D.×150 mm; Sumika Chemical Analysis Service, Japan).[20] HPLC analysis was performed on the same liquid chromatograph as stated above under the following conditions: mobile phase, 0.5–5 mM copper(II) sulfate in water–2-propanol (85/15–99/1, v/v); flow rate, 1 ml min^{-1}; column temperature, 30 °C; detection, UV at 254 nm.

Acknowledgements

The authors are grateful to Amano Pharmaceutical Co. for the generous gift of the protease used in this study. This work was financially supported in part by a Grant-in-Aid for Scientific Research from the Ministry of Education, Science, Sports and Culture of Japan. M. Kawagishi is acknowledged for some preliminary experiments.

Supplementary data

Supplementary data associated with this article can be found, in the online version, at doi:10.1016/j.tet.2005.08.033

References and notes

1. Gais, H. J.; Theil, F. Enzyme Catlaysis in Organic Synthesis. In Drauz, K., Waldmann, H., Eds.; Wiley-VCH: Weinheim, 2002; pp 407–412.
2. Santos, A. M.; Vidal, M.; Pacheco, Y.; Frontera, J.; Báez, C.; Omellas, O.; Barletta, G.; Griebenow, K. *Biotechnol. Bioeng.* **2001**, *74*, 295–308.
3. Altreuter, D. H.; Dordick, J. S.; Clark, D. S. *J. Am. Chem. Soc.* **2002**, *124*, 1871–1876.
4. Kullmann, W. *Enzymatic Peptide Synthesis*; CRC: Boca Raton, Florida, 1987; pp 47–48.
5. (a) Miyazawa, T.; Iwanaga, H.; Yamada, T.; Kuwata, S. *Chirality* **1992**, *427*, 431. (b) Miyazawa, T. In *Fluorine-Containing Amino Acids: Synthesis and Properties*; Kukhar', v. p., Soloshonok, V. A., Eds.; Wiley: Chichester, 1995.
6. Miyazawa, T.; Hiramatsu, M.; Murashima, T.; Yamada, T. *Biocatal. Biotransform.* **2003**, *21*, 93–100.
7. Miyazawa, T.; Masaki, S.; Tanaka, K.; Yamada, T. *Lett. Pept. Sci.* **2003**, *10*, 83–87.
8. Miyazawa, T.; Minowa, H.; Miyamoto, T.; Imagawa, K.; Yanagihara, R.; Yamada, T. *Tetrahedron: Asymmetry* **1997**, *8*, 367–370.
9. *A. oryzae* protease has been employed for the enantioselective hydrolysis of carboxylic acid esters, especially sterically demanding α,α-disubstituted carboxylic esters: (a) Fülling, G.; Sih, C. J. *J. Am. Chem. Soc.* **1987**, *109*, 2845–2846. (b) Feichter, C.; Faber, K.; Griengl, H. *J. Chem. Soc., Perkin Trans. 1* **1991**, 653–654. (c) Yang, S.; Hayden, W.; Faber, K.; Griengl, H. *Synthesis* **1992**, 365–366. (d) Berger, B.; de Raadt, A.; Griengl, H.; Hayden, W.; Hechtberger, P.; Klempier, N.; Faber, K. *Pure Appl. Chem.* **1992**, *64*, 1085–1088.
10. Hunt, S. The Non-protein Amino Acids. In *Chemistry and Biochemistry of the Amino Acids*; Barrett, G. C., Ed.; Chapman and Hall: London, 1985; pp 55–138.
11. Roberts, D. C.; Vellaccio, F. In *Unusual Amino Acids in Peptide Synthesis*; Gross, E., Meienhofer, J., Eds.; The Peptides; Academic: New York, 1983; Vol. 5, pp 341–449.
12. Coppola, G. M.; Schuster, H. F. In *Asymmetric Synthesis: Construction of Chiral Molecules Using Amino Acids*; Wiley: New York, 1987.
13. Duthaler, R. O. *Tetrahedron* **1994**, *50*, 1539–1650.
14. Barrett, G. C. Resolution of amino acids. In *Chemistry and Biochemistry of the Amino Acids*; Barrett, G. C., Ed.; Chapman and Hal: London, 1985; pp 338–353.
15. Williams, R. M. *Synthesis of Optically Active α-Amino Acids*; Pergamon: Oxford, 1989.
16. Chenault, H. K.; Dahmer, J.; Whitesides, G. M. *J. Am. Chem. Soc.* **1989**, *111*, 6354–6364.
17. Miyazawa, T. *Amino Acids* **1999**, *16*, 191–213.
18. Miyazawa, T.; Iwanaga, H.; Ueji, S.; Yamada, T. *Biocatal. Biotransform.* **2000**, *17*, 445–458.
19. Contrary to the hydrolysis of the methyl esters of *N*-protected amino acids,[5a] *A. oryzae* protease generally gave better results than *B. subtilis* protease towards the esters of *N*-unprotected amino acids examined in the present work. Therefore, the former protease was employed in the following studies.
20. On a Sumichiral OA-5000 column: Miyazawa, T.; Minowa, H.; Imagawa, K.; Yamada, T. *Chromatographia* **2004**, *60*, 45–50.
21. In the case of 3-fluorophenylalanine (**1**, R=3-F-$PhCH_2$) alone, an acceptable enantioselectivity was obtained ($E=15$).
22. Chen, C.-S.; Fujimoto, Y.; Girdukas, G.; Sih, C. J. *J. Am. Chem. Soc.* **1982**, *104*, 7294–7299.
23. An example of a marked improvement of the enantioselectivity can be seen in the lipase-catalyzed hydrolysis of 8-acetoxy-10-bromoundec-9-enoic acid esters by using the *n*-butyl ester instead of the methyl ester as the substrate: Bhalerao, U. T.; Dasaradhi, L.; Neelakantan, P.; Fadnavis, N. W. *J. Chem. Soc., Chem. Commun.* **1991**, 1197–1198.
24. Faber, K. *Biotransformations in Organic Chemistry*, 4 ed.; Springer: Berlin, 2000; p 42.
25. Miyazawa, T.; Iwanaga, H.; Yamada, T.; Kuwata, S. *Biotechnol. Lett.* **1994**, *16*, 373–378.
26. Preliminary communication: Miyazawa, T.; Imagawa, K.; Yanagihara, R.; Yamada, T. *Biotechnol. Tech.* **1997**, *11*, 931–933.
27. For a review on the low temperature effect on lipase-catalyzed reactions, see: Sakai, T. *Tetrahedron: Asymmetry* **2004**, *15*, 2749–2756.
28. Pham, V. T.; Phillips, R. S. *J. Am. Chem. Soc.* **1990**, *112*, 3629–3632.
29. (a) Phillips, R. S. *Enzyme Microb. Technol.* **1992**, *14*, 417–419. (b) Phillips, R. S. *TIBTECH* **1996**, *14*, 13–l6.
30. The *E* value is defined as the ratio of the specificity constants, k_{cat}/K_m, between the enantiomers:[22] $E=(k_{cat}/K_m)S/(k_{cat}/K_m)R$. Thus, $-RT\ln E$ corresponds to the difference in the activation free energy $\Delta\Delta(G^{\ddagger})$ between the enantiomers: $-RT\ln E=\Delta\Delta G^{\ddagger}$. The temperature dependence of $\Delta\Delta G^{\ddagger}$ can be given by the equation $\Delta\Delta G^{\ddagger}=\Delta\Delta H^{\ddagger}-T\Delta\Delta S^{\ddagger}$.
31. Łankiewicz, L.; Kasprzykowski, F.; Grzonka, Z.; Kettmann, U.; Hermann, P. *Bioorg. Chem.* **1989**, *17*, 275–280.

32. Smith, E. L.; Polglase, W. J. *J. Biol. Chem.* **1949**, *180*, 1209–1223.
33. Curtius, T. *J. prakt. Chem.* **1930**, *125*, 211–302.
34. Curtius, T.; Müller, E. *Ber.* **1904**, *37*, 1261–1279.
35. Brenner, M.; Huber, W. *Helv. Chim. Acta* **1953**, *36*, 1109–1115.
36. Miyazawa, T.; Nakajo, S.; Nishikawa, M.; Hamahara, K.; Imagawa, K.; Ensatsu, E.; Yanagihara, R.; Yamada, T. *J. Chem. Soc., Perkin Trans. 1* **2001**, 82–86.
37. Dhaon, M. K.; Olsen, R. K.; Ramasamy, K. *J. Org. Chem.* **1982**, *47*, 1962–1965.

Available online at www.sciencedirect.com
SCIENCE DIRECT
Tetrahedron
Tetrahedron 61 (2005) 10262–10276

Direct alkenylation of arylamines at the *ortho*-position with magnesium alkylidene carbenoids and some theoretical studies of the reactions

Tsuyoshi Satoh,[a,*] Yumi Ogino[a] and Kaori Ando[b,*]

[a]*Department of Chemistry, Faculty of Science, Tokyo University of Science; Kagurazaka, Shinjuku-ku, Tokyo 162-8601, Japan*
[b]*College of Education, University of the Ryukyus, Nishihara-cho, Okinawa 903-0213, Japan*

Received 22 July 2005; accepted 5 August 2005

Available online 12 September 2005

Abstract—1-Chlorovinyl *p*-tolyl sulfoxides were synthesized from ketones and chloromethyl *p*-tolyl sulfoxide in high yields. Treatment of the sulfoxides with isopropylmagnesium chloride at −78 °C in toluene gave magnesium alkylidene carbenoids (α-chloro alkenylmagnesium chlorides), which were treated with *N*-lithio arylamines to afford *ortho*-alkenylated arylamines in moderate yields. The reaction, in some cases, proceeded in a highly stereospecific manner at the carbon bearing the chlorine and the sulfinyl group. The structures of the α-chloro alkenylmagnesium chlorides and the reactivity of the *N*-lithio *meta*-substituted anilines were studied at the B3LYP and MP2 levels of theory with the 6-31(+)G* basis set. This reaction offers a quite novel and direct alkenylation of arylamines at the *ortho*-position of the aromatic ring.

1. Introduction

Arylamines, including anilines, are undoubtedly one of the most important and fundamental compounds in organic chemistry. Arylamines have been widely used as the material for medicine, dyes, and other chemical products. In view of this importance of arylamines, innumerable studies are still being actively carried out concerning their chemistry and synthesis.[1]

The alkylation of the aromatic ring of arylamines is quite important chemistry for the synthesis of derivatives of arylamines. However, direct alkylation of arylamines having a free amino group is not a so easily accessible process. For example, under normal Friedel–Crafts alkylation conditions, the reaction is inhibited by complex formation of the amino group with the acid catalyst. An even more difficult process is the direct alkenylation of the arylamines. To the best of our knowledge, only two reports concerning the direct alkenylation of arylamines on the aromatic ring have been published so far by Sartori et al.[2] and Yamaguchi et al.[3] Sartori's group synthesized 1,1-diarylethylenes directly from substituted anilines and phenylacetylene in the presence of montmorillonite KSF.[2] Yamaguchi's group synthesized *ortho*-vinylated anilines directly from anilines with ethyne in the presence of $SnCl_4$–Bu_3N.[3]

We recently reported a new method for the generation of magnesium alkylidene carbenoids **3** from 1-chlorovinyl *p*-tolyl sulfoxides **2**, which were synthesized from ketones **1** and chloromethyl *p*-tolyl sulfoxide in three steps in high yields,[4] with a Grignard reagent[5] via a sulfoxide–magnesium exchange reaction.[6] From the generated magnesium alkylidene carbenoids **3**, a new method for the synthesis of *tetra*-substituted olefins[7] and allenes[8] was realized.

In continuation of our interest in the development of new synthetic methods by utilizing the generated magnesium alkylidene carbenoids **3** in organic synthesis, we investigated the reaction of **3** with *N*-lithio amines and found that the reaction with *N*-lithio arylamines gave *ortho*-alkenylated arylamines **4** in moderate to good yields (Scheme 1).[9] In this paper we describe in detail the direct alkenylation of arylamines at the *ortho*-position with magnesium alkylidene carbenoids and theoretical studies of the reaction.

Keywords: Sulfoxide–magnesium exchange reaction; Magnesium alkylidene carbenoid; Alkenylation; *ortho*-Alkenylated arylamine; Theoretical study.
* Corresponding authors. Tel.: +81 3 5228 8272; fax: +81 3 3235 2214; e-mail: tsatoh@ch.kagu.tus.ac.jp

0040–4020/$ - see front matter © 2005 Elsevier Ltd. All rights reserved.
doi:10.1016/j.tet.2005.08.035

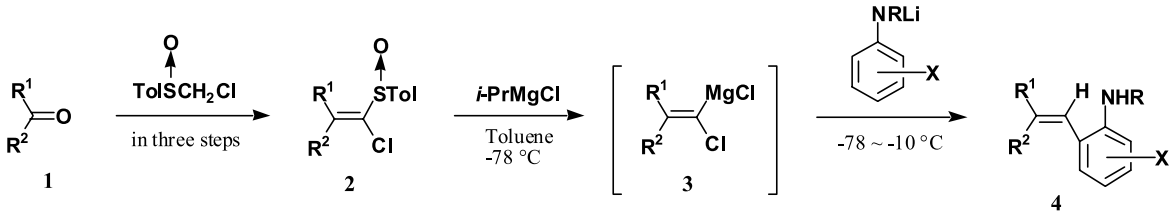

Scheme 1.

2. Results and discussion

2.1. Direct *ortho*-alkenylation of arylamines including aniline with the magnesium alkylidene carbenoid 6

1-Chlorovinyl *p*-tolyl sulfoxide **5**, which was synthesized from 1,4-cyclohexanedione mono ethylene ketal and chloromethyl *p*-tolyl sulfoxide in high yield,[4,7] in dry THF was treated with *t*-BuMgCl (0.12 equiv) at −78 °C to remove a trace of moisture in the reaction mixture. After 10 min, *i*-PrMgCl (2.8 equiv) was added to the reaction mixture. The sulfoxide–magnesium exchange reaction took place instantaneously to give the magnesium alkylidene carbenoid **6**.[8b] First, reaction of **6** with *N*-lithio piperidine and *N*-lithio *n*-hexylamine was investigated, however, only a rather complex mixture was obtained with these *N*-lithio alkylamines.

Next, the reaction was investigated with *N*-litho arylamines. *N*-litho aniline (3 equiv), which was generated from aniline and *n*-BuLi in THF at −78 °C, was added to the solution of the magnesium alkylidene carbenoid **6**, generated as above, through a cannula at −78 °C and the temperature of the reaction mixture was gradually allowed to warm to −10 °C. We obtained a colorless crystalline product in 25% yield. The product showed $C_{15}H_{19}NO_2$ as the molecular formula and N–H absorption on its IR spectrum. At this stage two products, alkenyl aniline **7a** and enamine **8**, were expected to be produced. ^{1}H NMR showed two NH protons and only four aromatic protons (δ 6.69 (1H, d), 6.73 (1H, t), 6.98 (1H, d), 7.06 (1H, t)). From the coupling pattern of these aromatic protons and the ^{13}C NMR, the structure of the product was unambiguously determined to be the *ortho*-alkenylated aniline **7a** (Scheme 2).

We were somewhat surprised and pleased by this result because no report has been published on the reaction of anilines with alkylidene carbenes (or carbenoids).[10] In addition, this reaction was recognized to be a quite novel and direct alkenylation of arylamines on the aromatic ring.

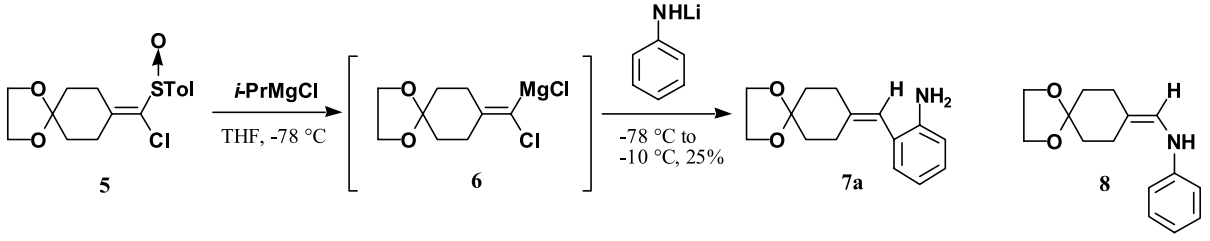

Scheme 2.

Table 1. Conditions for the *ortho*-alkenylation of aniline

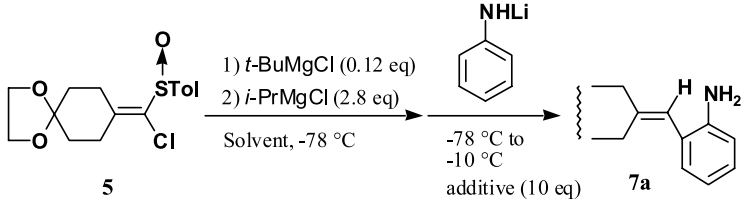

Entry	Solvent	Additive	Yield of **7a** %
1	THF	No	25
2	CPME[a]	No	9
3	Toluene	No	49
4	Toluene	DMPU[b]	14
5	Toluene	HMPA	14
6	Toluene	12-Crown-6	16
7	Toluene	TMEDA	25
8	Toluene	DME	37
9	Toluene	CPME[a]	40

[a] Cyclopentyl methyl ether.
[b] 1,3-Dimethyl-3,4,5,6-tetrahydro-2(1*H*)pyrimidinone.

Table 2. Synthesis of *ortho*-alkenylated arylamines **7** by the reaction of magnesium alkylidene carbenoid **6** with *N*-lithio arylamines

Entry	Arylamine[a]	*ortho*-Alkenylated arylamine **7**	(Yield, %)
1	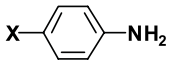	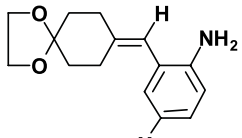 **7b** X=OCH_3 **7c** X=Cl	(44) (28)
2			
3	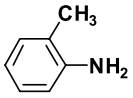	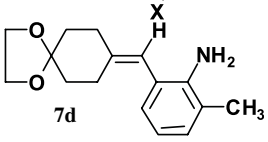 **7d**	(32)
4	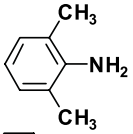	—[b]	
5	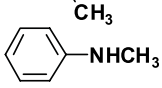	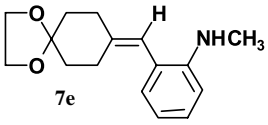 **7e**	(38)
6	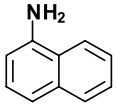	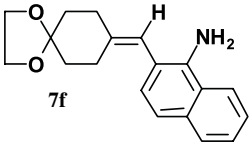 **7f**	(66)
7	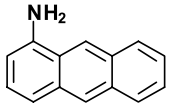	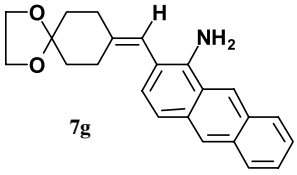 **7g**	(60)

[a] Three equivalents of *N*-lithio arylamines were reacted with **6**.
[b] No *para*-alkenylated product was obtained.

First of all, we investigated the best conditions for this *ortho*-alkenylation and the results are summarized in Table 1.

The use of cyclopentyl methyl ether (CPME) as a solvent gave a miserable yield (entry 2). As shown in entry 3, toluene was found to be a good solvent for the reaction and 49% yield of **7a** was obtained. Encouraged by this result, several reaction conditions were investigated in toluene in the presence of an additive. However, the additives investigated were found to be ineffective (entries 4–9). We decided to use toluene as the solvent without any additive throughout this study.

Next, we investigated the generality of this reaction of the magnesium alkylidene carbenoid **6** with other *N*-lithio arylamines under the conditions described above and the results are summarized in Table 2. The reaction with the aniline having an electron-donating group (OCH_3) at the 4-position gave a similar yield of **7b** (entry 1), however, the aniline having an electron-withdrawing group (Cl) gave **7c** in markedly diminished yield (entry 2). The reaction with *ortho*-toluidine gave the *ortho*-alkenylated aniline **7d** (entry 3). Interestingly, 2,6-dimethylaniline gave no *para*-alkenylated aniline. This result indicated that this reaction only gives *ortho*-alkenylated products.

N-Methylaniline gave an *ortho*-alkenylated product **7e** in 38% yield (entry 5). Interestingly, the reaction with 1-aminonaphthalene and 1-aminoanthracene gave much better yields of the *ortho*-alkenylated aryl amines **7f** and **7g**, respectively, (entries 6 and 7).

The reaction of the magnesium alkylidene carbenoid **6** with *meta*-substituted anilines is quite interesting because the regioisomers are expected to be obtained. We investigated the reaction with four *meta*-substituted anilines and the results are summarized in Table 3.

The reaction with *meta*-anisidine gave two products and the main product was found to have the alkenyl group at a more hindered position **7h** (entry 1). In the previous communication, we reported that the reason for this regioselectivity may be the chelation of the magnesium alkylidene carbenoid **6** between the amino group and the methoxy group.[9] However, all other *meta*-substituted anilines, even *meta*-methylaniline, which has no ability for the chelation, gave more hindered alkenylated compounds as main products (entries 2–4), although the yields were not satisfactory. The theoretical study for this regioselectivity is discussed later (vide infra).

2.2. Study for the reaction mechanism

At this stage, we investigated the mechanism of this reaction

Table 3. Synthesis of *ortho*-alkenylated arylamines **7** by the reaction of magnesium alkylidene carbenoid **6** with *meta*-substituted *N*-lithio anilines

Entry	*meta*-Substituted anilin[a]	*ortho*-Alkenylated arylamine **7**	(Yield, %)
1	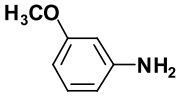	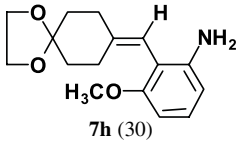 **7h** (30)	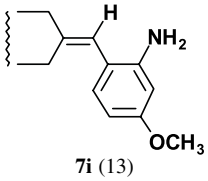 **7i** (13)
2	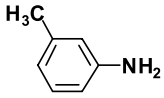	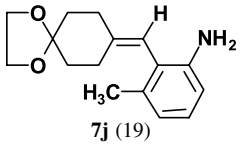 **7j** (19)	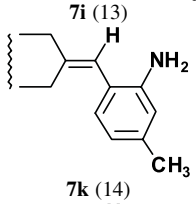 **7k** (14)
3	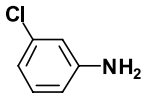	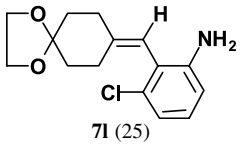 **7l** (25)	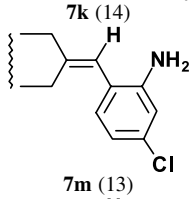 **7m** (13)
4	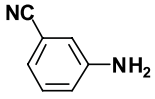	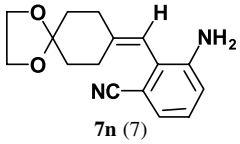 **7n** (7)	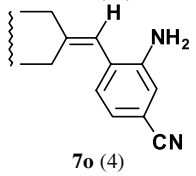 **7o** (4)

[a] Three equivalents of *meta*-substituted *N*-lithio aniline was reacted with **6**.

by using aniline-2,3,4,5,6-d_5 (Scheme 3). The reaction of the magnesium alkylidene carbenoid **6** with *N*-lithio aniline-2,3,4,5,6-d_5 **A** was carried out in toluene and *ortho*-alkenylated aniline **9** was obtained. The deuterium incorporation of **9** at the olefinic carbon was measured by ^{1}H NMR and the deuterium incorporation was found to be 25%. From this result, we propose the mechanism of this reaction as follows (Scheme 3).

The *N*-lithio arylamine **A** is present in the resonance form,

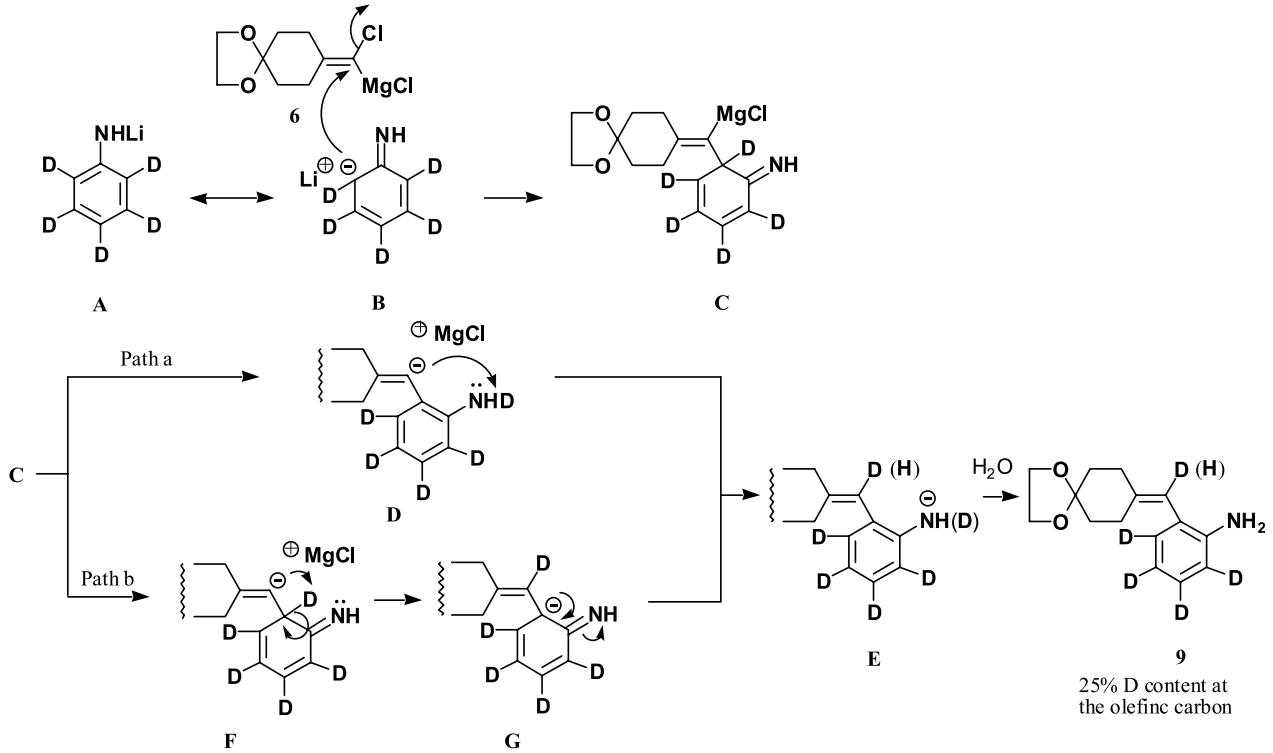

Scheme 3.

Table 4. Synthesis of *ortho*-alkenylated arylamines by the reaction of magnesium alkylidene carbenoid derived from **10** with *N*-lithio arylamines

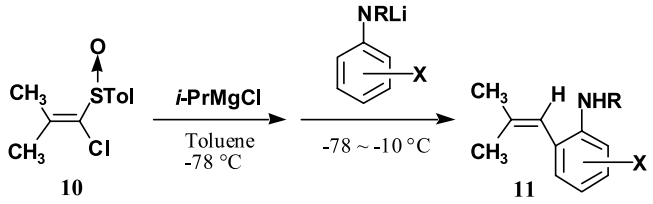

Entry	Arylamine[a]	*ortho*-Alkenylated arylamine		(Yield, %)
1	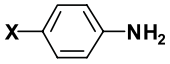	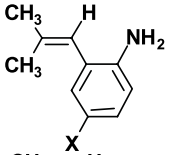	**11a** X=H	(43)
2			**11b** X=OCH_3	(43)
3	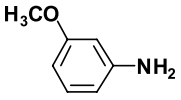	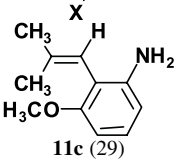 **11c** (29)	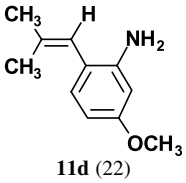 **11d** (22)	
4	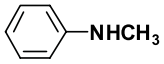	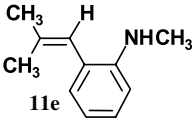 **11e**		(46)
5	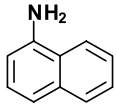	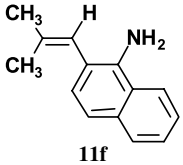 **11f**		(81)
6	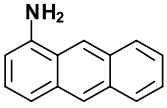	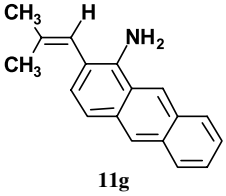 **11g**		(79)

[a] Three equivalents of *N*-lithio arylamine was reacted with the carbenoid derived from **10**.

lithium α-imino carbanion **B**. The reaction of **B** with the magnesium alkylidene carbenoid **6** takes place with inversion of the configuration at the carbenoid carbon to give the intermediate **C**. The inversion of the configuration in the reaction of lithium alkylidene carbenoids with alkyllithium has been reported by Walborsky et al.[11] Oku et al.[12] and Narasaka et al.[13] We will discuss later the structure of the carbenoid and the reaction by B3LYP and MP2 calculations (vide infra).

Two pathways (path a and b) were postulated for the mechanism from the intermediate **C** to the product **9**. Thus, the intermediate **C** is first aromatized (intermolecular transfer of the deuterium from the carbon to the nitrogen was presumed to be take place) to give the alkenylmagnesium **D**. Then the alkenyl anion picks up the proton or deuterium on the nitrogen to give **E**, which was treated with water to afford **9** (path a). Less than 50% deuterium incorporation on the olefinic carbon was anticipated in path a. The other mechanism (path b) is as follows: the alkenyl anion first picks up the deuterium on the carbon next to the imine **F** to give an anion having deuterium on the olefinic carbon **G**. The intermediate **G** is aromatized to give **E**. Close to 100% deuterium incorporation was expected in path b. As described above, because the obtained *ortho*-alkenylated aniline **9** had 25% of deuterium on the olefinic carbon, this reaction was proved to proceed via path a.

2.3. Synthesis of the aryl amines having 2-methyl-1-propene at the *ortho*-position

To investigate the generality of this reaction, we further studied this reaction using 1-chlorovinyl *p*-tolyl sulfoxide **10** derived from acetone and the results are summarized in Table 4. Entries 1 and 2 show that quite similar yields were obtained with aniline and *p*-anisidine. The reaction with *m*-anisidine gave two products and the main product was again found to be the more sterically hindered **11c** (entry 3). *N*-methylaniline gave better yield compared with the result in Table 2, entry 5. Again, much better yields were obtained from the reaction of the magnesium alkylidene carbenoid with 1-aminonaphthalene and 1-aminoanthracene (entries 5 and 6).

Table 5. The reaction of the magnesium alkylidene carbenoids derived from *E*- and *Z*-1-chlorovinyl *p*-tolyl sulfoxides with *N*-lithio aniline, *N*-lithio 1-aminonaphthalene and *N*-lithio 1-aminoanthracene

Entry	Arylamine[a]		Product	*E*/*Z*[b]	(Yield, %)
1	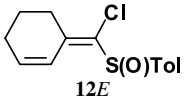 **12***E*	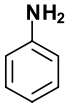	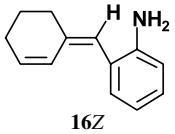 **16***Z*	6:94	(53)
2	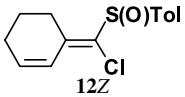 **12***Z*	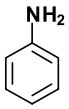	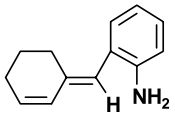 **16***E*	94:6	(46)
3	**12***E*	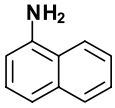	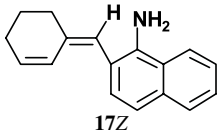 **17***Z*	3:97	(65)
4	**12***Z*	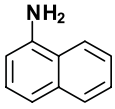	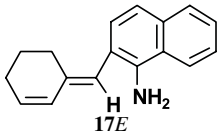 **17***E*	95:5	(71)
5	**12***E*	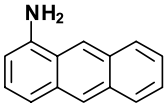	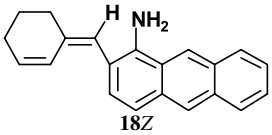 **18***Z*	22:78	(69)
6	**12***Z*	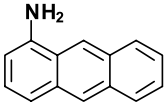	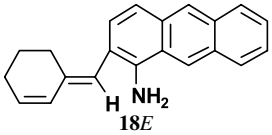 **18***E*	84:16	(66)
7	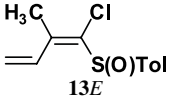 **13***E*	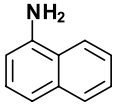	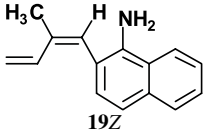 **19***Z*	4:96	(68)
8	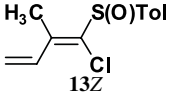 **13***Z*	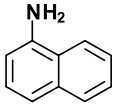	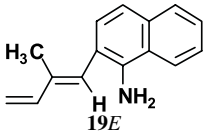 **19***E*	94:6	(62)
9	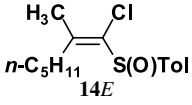 **14***E*	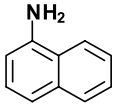	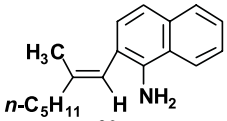 **20***E*	44:56	(54)
10	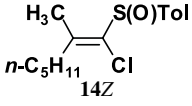 **14***Z*	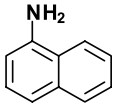	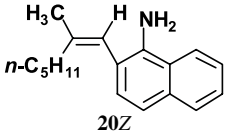 **20***Z*	34:66	(55)
11	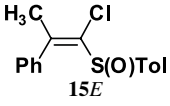 **15***E*	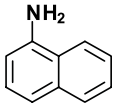	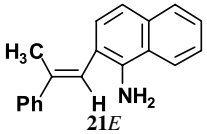 **21***E*	6:94	(61)
12	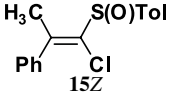 **15***Z*	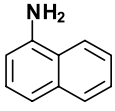	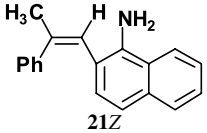 **21***Z*	25:75	(45)

[a] Three equivalents of *N*-lithio aniline, *N*-lithio 1-aminonaphthalene and *N*-lithio 1-aminoanthracene were reacted with the magnesium alkylidene carbenoids.
[b] The ratio of *E*/*Z* was determined from their ^{1}H NMR.

Table 6. Quenching of the magnesium alkylidene carbenoid derived from **12** and **15** with water

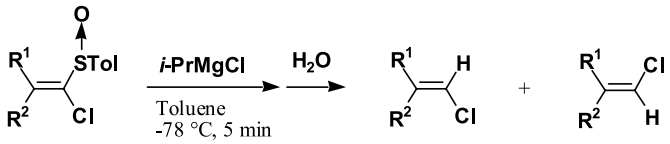

12 and **15**

Entry	1-Chlorovinyl *p*-tolyl sulfoxide	Alkenylchloride
1	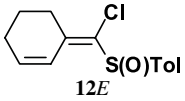 **12***E*	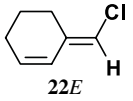 **22***E*
2	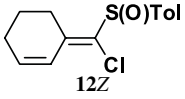 **12***Z*	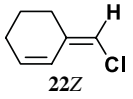 **22***Z*
3	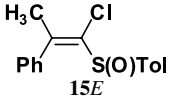 **15***E*	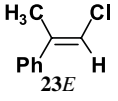 **23***E*
4	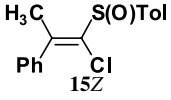 **15***Z*	**23***E* + 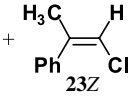 **23***Z* **23***E*:**23***Z*=35:65

2.4. Stereochemistry of the reaction

Next, we investigated the stereochemistry of these reactions. First of all, stereoisomers of the 1-chlorovinyl *p*-tolyl sufoxides (**12**–**15**) were synthesized from unsymmetrical ketones (2-cyclohexenone, methyl vinyl ketone, 2-heptanone, and acetophenone) and the reaction was carried out with aniline, 1-aminonaphthalene and 1-aminoanthracene. The results are summarized in Table 5. Quite interestingly, the reaction of the magnesium alkylidene carbenoids derived from **12***E* and **12***Z* with aniline and 1-aminonaphthalene gave *Z-ortho*-alkenylated arylamines **16***Z* and **17***Z*, and *E-ortho*-alkenylated arylamines **16***E* and **17***E*, respectively, with high stereospecificity (entries 1–4). The reaction of **12***E* and **12***Z* with 1-aminoanthracene gave also the *ortho*-alkenylated 1-aminoanthracenes, **18***Z* and **18***E*, stereospecifically although the stereospecificity was somewhat lower (entries 5 and 6). The 1-chlorovinyl *p*-tolyl sulfoxide derived from methyl vinyl ketone **13** showed again quite high stereospecificity with 1-aminonaphthalene to give **19***Z* and **19***E* (entries 7 and 8).

Further, this reaction was carried out with the 1-chlorovinyl *p*-tolyl sulfoxides derived from unsymmetrical dialkyl ketone (2-heptanone) **14** and alkyl aryl ketone (acetophenone) **15** with 1-aminonaphthalene. Quite interestingly, both vinyl sulfoxides **14***E* and **14***Z* gave mainly *Z*-isomer **20***Z* (entries 9 and 10), namely, the reactions with **14** show stereoselectivity. The reaction with **15***E* and **15***Z* showed also stereoselectivity. In this case, **15***E* exclusively gave **21***Z*

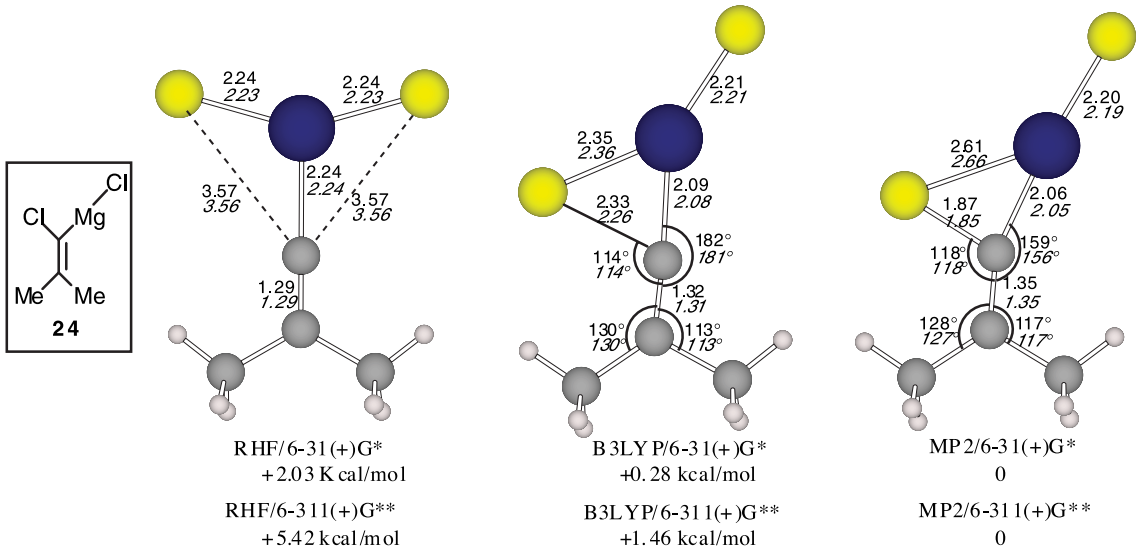

Figure 1. Geometries of 1-chloro-2-methylpropenylmagnesium chloride **24** optimized at the RHF, B3LYP, and MP2 levels of theory with the 6-31(+)G* and 6-311(+)G** basis sets. The energies of these geometries were calculated at the CCSD(T) method with the corresponding basis set.

in high stereoselectivity (entry 11). The reaction with **15***Z* gave **21***Z*, however, the selectivity was lower than the reaction with **15***E* (entry 12).

The stereospecificity and the stereoselectivity mentioned above are explained as follows. If the configuration of the magnesium alkylidene carbenoids generated from 1-chlorovinyl *p*-tolyl sulfoxides derived from α,β-unsaturated ketones is stable enough in the reaction conditions, the *N*-lithio arylamine attacks backside to the chlorine atom to give the product stereospecifically. On the other hand, if the configuration of the magnesium alkylidene carbenoids generated from the 1-chlorovinyl *p*-tolyl sulfoxide derived from dialkyl ketone or alkyl aryl ketone is not stable under the reaction conditions, both isomers of the magnesium alkylidene carbenoids are present in equilibrium before the alkenylation and from the more stable isomer the main product is produced.

In order to obtain the information on the stability of the magnesium alkylidene carbenoids, we treated **12** and **15** with *i*-PrMgCl at −78 °C for 5 min and the generated magnesium alkylidene carbenoids were quenched with water. The results are summarized in Table 6. As anticipated, the reaction of **12***E* and **12***Z* gave **22***E* and **22***Z*, respectively, without any presence of the isomer (entries 1 and 2). These results imply that the configuration of the generated magnesium alkylidene carbenoids is stable for at least 5 min. The reaction of **15***E* gave **23***E* exclusively, however, **15***Z* gave a mixture of **23***E* and **23***Z*. These results imply that the magnesium alkylidene carbenoid generated from **15***E* and **15***Z* is unstable.[7] These results are consistent with the stereospecificity and the stereoselectivity shown in Table 5. We studied the stability for the geometry of the magnesium alkylidene carbenoids by calculation and will discuss this later (vide infra).

2.5. Theoretical studies for the α-chloro alkenylmagnesium chlorides and the reactivity of the *N*-lithio *meta*-substituted anilines

To better understand these substitution reactions of the magnesium alkylidene carbenoids (α-chloro alkenylmagnesium chlorides), we studied them computationally. All calculations were performed using the Gaussian 98 program.[14] The frequency calculations on the optimized structures gave only harmonic frequencies and confirmed that they are minima. The structures of the α-chloro alkenylmagnesium chlorides were first studied using the RHF, B3LYP, and MP2 levels of theory with the 6-31(+)G*[15] basis set. The obtained geometries of 1-chloro-2-methylpropenyl-magnesium chloride **24** are shown in Figure 1.

The magnesium atom interacts with the vinyl chloride strongly at the RHF level and the structure is a complex of the alkenyl carbene with $MgCl_2$ rather than the α-chloro alkenylmagnesium chloride. This structure is not compatible with our experimental results. On the other hand, both the B3LYP and MP2 geometries are the α-halo alkenylmagnesium chloride where the C–Cl bond is bridged by the magnesium atom. The ^{13}C NMR study[16,17] of the α-bromo alkyllithium compounds showed considerable weakening of the C–Br bonds and the theoretical studies reported a bridging geometry for H_2CLiCl,[18] CH_2=FLi,[19] and RR′C=CLiX (X=Cl, Br).[13]

In order to know, which α-chloro alkenylmagnesium chloride structure is more reliable, the energies were computed using a higher level of the correlation method, CCSD(T)/6-31(+)G*, on these geometries. The relative energies are +2.03, 0.28, and 0 kcal/mol, respectively. Although the Cl–Mg distance of the MP2 geometry is longer than that of the B3LYP by 0.26 Å, those CCSD(T) energies are not much different. The MP2 geometry was reoptimized with constraining the Cl–Mg distance to 2.45, 2.50, and 2.55 Å at the MP2/6-31(+)G* level and the relative CCSD(T) energies were −0.09, −0.13 and −0.08 kcal/mol, respectively. Therefore, the real structure seems to be between the B3LYP structure and the MP2 structure and is closer to the latter. To see the basis set effects, the structures were also calculated using 6-311(+)G**. Since the geometries are almost the same as the 6-31(+)G* basis for all the RHF, B3LYP, and MP2 levels of theory, the 6-31(+)G* basis set is as good as the 6-311(+)G** basis set for the structure of α-chloro alkenylmagnesium chloride.

Stereospecific formation of the alkenyl aniline was observed when the conjugated α-chloro alkenylmagnesium chlorides were used. Therefore, the structures of the conjugated α-chloro alkenylmagnesium chlorides were further studied. The optimized structures for *E*- and *Z*-1-chloro-2-methyl-1, 3-butadienylmagnesium chloride **25** are shown in Figure 2. There are three characteristic differences between **24** (see Fig. 1) and **25**. The distances between the Mg and the vinyl-Cl is much longer, the C–Cl bond is shorter, and the C=C–

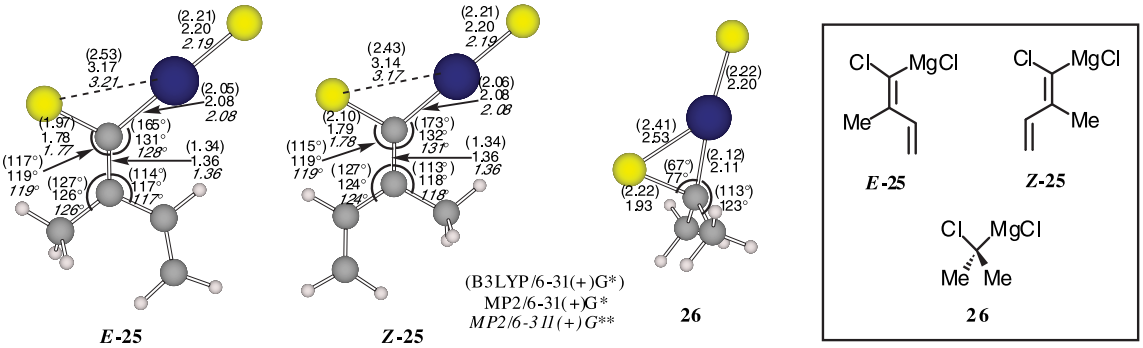

Figure 2. Geometries of *E*-**25**, *Z*-**25**, and **26** optimized at the B3LYP/6-31(+)G*, and MP2/6-31(+)G*, and MP2/6-311(+)G**.

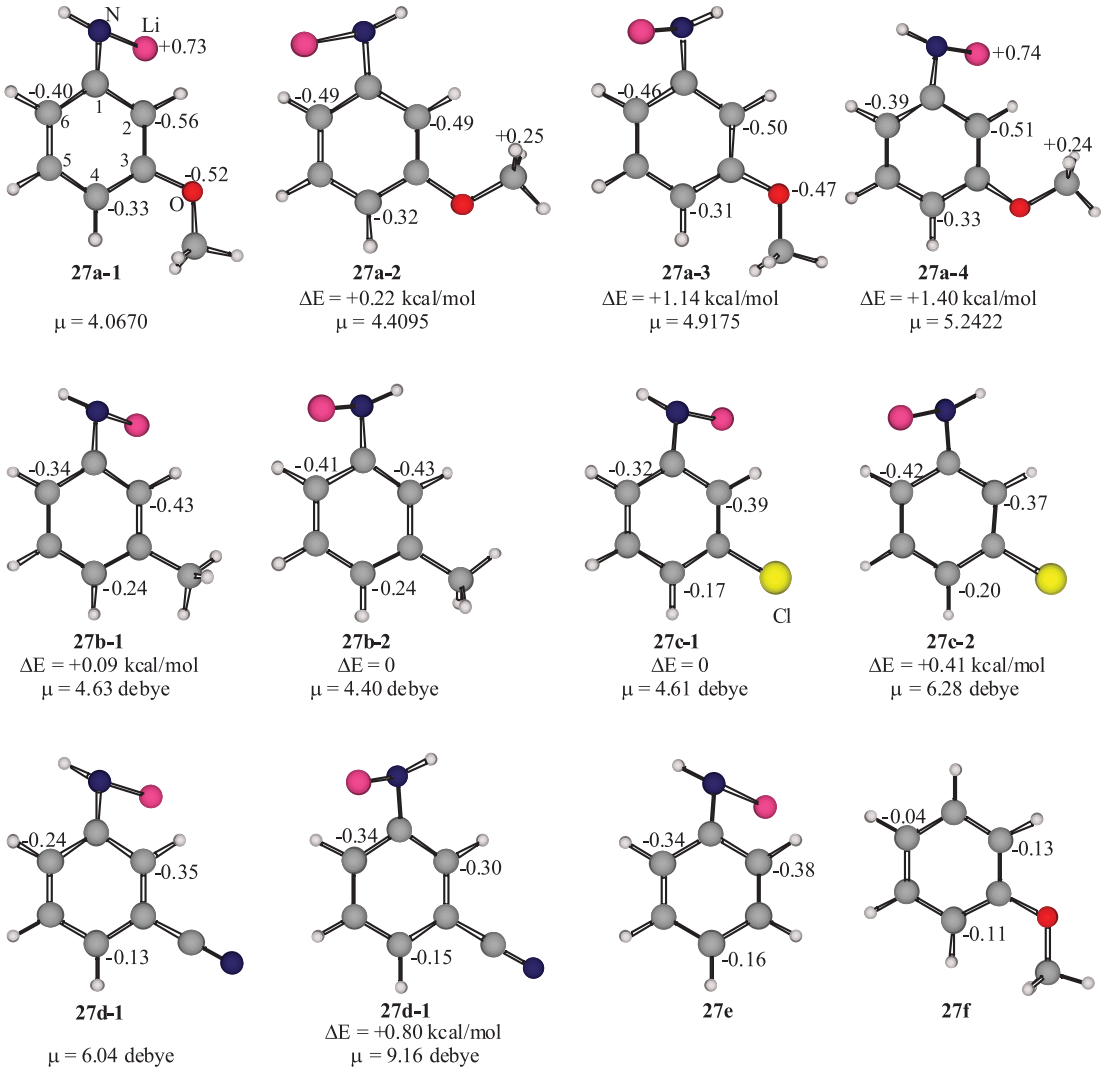

Figure 3. Optimized structures of *N*-lithio *meta*-substituted anilines **27** at the MP2/6-31(+)G* level of theory. Atomic charges with hydrogens summed into heavy atoms were calculated using the CHelpG scheme of Breneman (MP2/6-31(+)G* density=MP2 pop=CHelpG).

Mg angle is smaller in **25** at both the B3LYP and MP2 levels of theory. Thus, the conjugated systems are geometrically stabilized. The charges computed by natural population analysis (MP2/6-31(+)G* density=MP2 pop=NPA) show a more negative charge on the vinyl-Cl in **24** and the alkyl-Cl in 2-chloro-2-propanylmagnesium chloride **26** than on the vinyl-Cl in **25** (the values are as follows: *E*-**25**, −0.06; *Z*-**25**, −0.07; **24**, −0.18; **26**, −0.22).[20] In these cases, the Mg–Cl distances correspond to the amount of the negative charge on the vinyl-Cl. That is, the shorter the Mg–Cl distances, the more negative charge on the Cl. Only a small amount of the negative charge is placed on the vinyl-Cl due to the charge delocalization in the conjugated systems **25**. Thus, the interaction between the Mg and the Cl is weaker in **25** than those in **24** and **26**. This weaker interaction increases the geometrical stabilization, and, therefore, stereospecific reaction can be expected.

For the reaction with *meta*-substituted anilines, the more hindered alkenylated compounds were obtained as main products. To see the reactivity of these *N*-lithio *meta*-substituted anilines **27**, the electrostatic potential-derived charges using the CHelpG scheme of Breneman (MP2/6-31(+)G* density=MP2 pop=CHelpG) were calculated with the structures optimized at the MP2/6-31(+)G* level. The results are shown in Figure 3.

Four conformers **27a-1**–**27a-4** were obtained for *N*-lithio *meta*-anisidine. The more negative atom charge (−0.56) was found on the carbon-2 in the most stable conformer **27a-1**. The same value (−0.49) was obtained on both the carbon-2 and the carbon-6 in **27a-2**, which is 0.22 kcal/mol less stable than **27a-1**. In the other two conformers (**27a-3** and **27a-4**), the more negative charge was also found on the carbon-2. Thus, the obtained product selectivity corresponds well to the negative charges on both the carbon-2 and the carbon-6, and the conformer stability.

There are two conformers for *N*-lithio *meta*-methylaniline (**27b-1** and **27b-2**). Although the more negative charge was found on the carbon-2 in both conformers, the difference is small in the more stable **27b-2**. Therefore, the less selective formation of **7j** was found (see Table 3, entry 2). There are also two conformers for both *N*-lithio *meta*-chloroaniline and *N*-lithio *meta*-cyanoaniline (**27c** and **27d**). The more negative charges were found on the carbon-2 in the more

stable conformers **27c**-**1** and **27d**-**1**. Compared to **27a**, the less negative charges found in **27c** and **27d** are thought to be a reason for the lower product yields. In these cases, all the more stable conformers have smaller dipole moment. Since the reaction was performed in toluene with low polarity ($\varepsilon=2.379$), the conformers with lower dipole moment are stabilized. In fact, the energy differences are in proportion to the differences of the dipole moment in **27b–d**.

For **27a**, not only the dipole moment, but also the MeO conformation is important for the conformer stability. The electrostatic interaction of the lithium with the carbon-2 and the oxygen stabilizes **27a**-**1**. On the other hand, this stabilization was reduced in **27a**-**4** due to the electrostatic interaction between the negative carbon-2 and the positive methyl group. The electrostatic repulsion between the carbon-2 and the oxygen destabilizes **27a**-**3** compared with **27a**-**2**. Furthermore, the dipole moment increases in the order of **27a**-**1**, **27a**-**2**, **27a**-**3**, and **27a**-**4**. Thus, the energy differences of these conformers can be explained on the basis of the dipole moment and the electrostatic interaction. The electrostatic potential-derived charges were also calculated for *N*-lithio aniline **27e** and anisole **27f**. The strongly electron-donating lithioamino group increases the negative charge on both the ortho positions with the lithium side more. Thus, the CHelpG results explain the experimental reactivity and the selectivity very well.

3. Experimental

3.1. General

All melting points are uncorrected. ^{1}H NMR spectra were measured in a $CDCl_3$ solution with JEOL JNM-LA 500 spectrometer. Electron-impact mass spectra (MS) were obtained at 70 eV by direct insertion. Silica gel 60 (Merck) containing 0.5% fluorescence reagent 254 and a quartz column were used for column chromatography and the products having UV absorption were detected by UV irradiation. In experiments requiring a dry solvent, toluene was distilled from CaH_2 and THF was distilled from diphenylketyl.

5,[7] **10**,[21] **12***E*,[4] **12***Z*,[4] **15***E*,[7] and **15***Z*[7] are known compounds.

3.1.1. 2-(1,4-Dioxaspiro[4.5]dec-8-ylidenemethyl)phenylamine (7a). To a solution of **5** (98.1 mg; 0.3 mmol) in 6 mL of dry toluene in a flame-dried flask at −78 °C under argon atmosphere was added *t*-BuMgCl (0.036 mmol) dropwise with stirring. After 10 min, *i*-PrMgCl (0.84 mmol) was added dropwise to the reaction mixture at −78 °C to give the magnesium alkylidene carbenoid **6**. *n*-BuLi (0.93 mmol) was added to a solution of aniline (0.082 mL; 0.90 mmol) in 4 mL of dry toluene in an another flame-dried flask at −78 °C under argon atmosphere to give the lithium anilide. This solution was added to a solution of the carbenoid **6** through a cannula. Temperature of the reaction mixture was gradually allowed to warm to −10 °C. The reaction was quenched by satd aq NH_4Cl and the whole was extracted with $CHCl_3$. The organic layer was washed once with water and dried over $MgSO_4$. After removal of the solvent, the product was purified by silica gel column chromatography to give **7a** (35.9 mg; 49%) as colorless needles; mp 118–119 °C (AcOEt/hexane); IR (KBr) 3464 (NH), 3371 (NH), 2946, 2894, 1631, 1491, 1454, 1116, 1079, 1029, 904, 754 cm^{-1}; ^{1}H NMR δ 1.67 (2H, t, J=6.4 Hz), 1.80 (2H, t, J=6.4 Hz), 2.35 (2H, t, J=6.6 Hz), 2.46 (2H, dt, J=6.4 Hz), 3.67 (2H, br s), 3.98 (4H, s), 6.09 (1H, s), 6.69 (1H, d, J=8.0 Hz), 6.73 (1H, t, J=7.5 Hz), 6.98 (1H, d, J=7.4 Hz), 7.06 (1H, t, J=7.0 Hz). ^{13}C NMR δ 26.3, 33.6, 35.5, 36.3, 64.4 (2C), 108.7, 115.0, 118.0, 119.2, 123.6, 127.7, 130.1, 142.4, 144.3. MS *m*/*z* (%) 245 (M^+, 100), 200 (30), 183 (19), 159 (27), 144 (44), 130 (39), 107 (70), 106 (45). Anal. Calcd for $C_{15}H_{19}NO_2$: C, 73.44; H, 7.81; N 5.71. Found: C, 72.99; H, 7.75; N, 5.48.

3.1.2. 2-(1,4-Dioxaspiro[4.5]dec-8-ylidenemethyl)-4-methoxyphenylamine (7b). Colorless oil; IR (neat) 3445 (NH), 3362 (NH), 2948, 1604, 1498, 1274, 1239, 1120, 1082, 1035 cm^{-1}; ^{1}H NMR δ 1.67 (2H, t, J=6.4 Hz), 1.80 (2H, t, J=6.6 Hz), 2.37 (2H, t, J=6.1 Hz), 2.45 (2H, t, J=6.1 Hz), 3.43 (2H, br s), 3.74 (3H, s), 3.98 (4H, m), 6.09 (1H, s), 6.58 (1H, d, J=2.8 Hz), 6.65 (1H, s), 6.67 (1H, d, J=2.8 Hz). MS *m*/*z* (%) 275 (M^+, 100), 230 (22), 212 (8), 189 (15), 174 (22), 160 (16), 137 (55), 122 (15), 117 (8). Calcd for $C_{16}H_{21}NO_3$: *M*, 275.1520. Found: *m*/*z* 275.1523.

3.1.3. 4-Chloro-2-(1,4-dioxaspiro[4.5]dec-8-ylidenemethyl)phenylamine (7c). Colorless oil; IR (neat) 3469 (NH), 3369 (NH), 2951, 2884, 1615, 1488, 1275, 1248, 1120, 1082, 1033 cm^{-1}; ^{1}H NMR δ 1.67 (2H, t, J=6.6 Hz), 1.79 (2H, t, J=6.6 Hz), 2.33 (2H, t, J=6.6 Hz), 2.45 (2H, t, J=6.6 Hz), 3.66 (2H, br s), 3.98 (4H, s), 6.01 (1H, s), 6.61 (1H, d, J=8.5 Hz), 6.94 (1H, d, J=2.4 Hz), 7.00 (1H, dd, J=8.4, 2.5 Hz). MS *m*/*z* (%) 279 (M^+, 98), 234 (28), 218 (14), 193 (20), 178 (22), 164 (36), 158 (28), 141 (100), 130 (12), 121 (18), 95 (20), 86 (12), 77 (10), 55 (12), 42 (12). Calcd for $C_{15}H_{18}ClNO_2$: *M*, 279.1025. Found: *m*/*z* 279.1025.

3.1.4. 2-(1,4-Dioxaspiro[4.5]dec-8-ylidenemethyl)-6-methylphenylamine (7d). Colorless crystals; mp 105–106 °C (AcOEt/hexane); IR (KBr) 3454 (NH), 3369 (NH), 2954, 2879, 2853, 1625, 1588, 1477, 1464, 1119, 1083, 1031, 919, 751 cm^{-1}; ^{1}H NMR δ 1.66 (2H, t, J=6.6 Hz), 1.80 (2H, t, J=6.4 Hz), 2.18 (3H, s), 2.35 (2H, t, J=6.4 Hz), 2.46 (2H, t, J=6.4 Hz), 3.65 (2H, br s), 3.98 (4H, m), 6.11 (1H, s), 6.67 (1H, t, J=7.3 Hz), 6.87 (1H, d, J=7.3 Hz), 6.97 (1H, d, J=7.3 Hz). MS *m*/*z* (%) 259 (M^+, 100), 214 (28), 196 (12), 186 (6), 173 (33), 158 (46), 144 (36), 130 (10), 121 (62), 99 (6). Calcd for $C_{16}H_{21}NO_2$: *M*, 259.1570. Found: *m*/*z* 259.1570. Anal. Calcd for $C_{16}H_{21}NO_2$: C, 74.10; H, 8.16; N 5.40. Found: C, 73.97; H, 8.12; N, 5.37.

3.1.5. [2-(1,4-Dioxaspiro[4.5]dec-8-ylidenemethyl)phenyl]methylamine (7e). Colorless crystals; mp 70–71 °C (hexane); IR (KBr) 3424 (NH), 2947, 2884, 2813, 1601, 1578, 1507, 1166, 1120, 1082, 1034, 909, 749 cm^{-1}; ^{1}H NMR δ 1.65 (2H, t, J=6.6 Hz), 1.80 (2H, t, J=6.6 Hz), 2.33 (2H, t, J=6.6 Hz), 2.45 (2H, t, J=6.6 Hz), 2.86 (3H, s), 3.79 (1H, br s), 3.98 (4H, m), 6.03 (1H, s), 6.62 (1H, d, J=8.3 Hz), 6.68 (1H, dt, J=7.4, 0.9 Hz), 6.96 (1H, d, J=

7.4 Hz), 7.18 (1H, dt, J=8.3, 1.2 Hz). MS m/z (%) 259 (M^+, 100), 214 (24), 173 (24), 158 (50), 144 (28), 130 (18), 120 (42), 99 (11), 91 (11), 77 (6). Calcd for $C_{16}H_{21}NO_2$: M, 259.1571. Found: m/z 259.1574. Anal. Calcd for $C_{16}H_{21}NO_2$: C, 74.10; H, 8.16; N, 5.40. Found: C, 73.67; H, 7.89; N, 5.40.

3.1.6. 2-(1,4-Dioxaspiro[4.5]dec-8-ylidenemethyl) naphthalen-1-ylamine (7f). Colorless needles; mp 123–124 °C (AcOEt/hexane); IR (KBr) 3472 (NH), 3383 (NH), 2948, 2883, 1615, 1566, 1432, 1403, 1120, 1080, 1033, 758, 735 cm^{-1}; ^1H NMR δ 1.67 (1H, t, J=6.4 Hz), 1.84 (1H, t, J=6.4 Hz), 2.35 (2H, t, J=6.6 Hz), 2.52 (2H, t, J=6.5 Hz), 3.96–4.00 (4H, m), 4.21 (2H, br s), 6.28 (1H, s), 7.15 (1H, d, J=8.6 Hz), 7.27 (1H, d, J=8.3 Hz), 7.41–7.44 (2H, m), 7.76–7.77 (1H, m), 7.81–7.82 (1H, m). MS m/z (%) 295 (M^+, 100), 250 (20), 234 (6), 232 (8), 208 (10), 194 (20), 180 (35), 156 (82). Calcd for $C_{19}H_{21}NO_2$: M, 295.1570. Found: m/z 295.1562. Anal. Calcd for $C_{19}H_{21}NO_2$: C, 77.26; H, 7.17; N, 4.74. Found: C, 77.15; H, 7.16; N, 4.75.

3.1.7. 2-(1,4-Dioxaspiro[4.5]dec-8-ylidenemethyl) anthracen-1-ylamine (7g). Colorless amorphous; IR (KBr) 3469 (NH), 3390 (NH), 2944, 2879, 1610, 1428, 1383, 1119, 1087, 1035, 909, 870, 737 cm^{-1}; ^1H NMR δ 1.70 (2H, t, J=6.6 Hz), 1.86 (2H, t, J=6.4 Hz), 2.39 (2H, t, J=6.1 Hz), 2.54 (2H, t, J=6.1 Hz), 3.97–4.01 (4H, m), 4.36 (2H, br s), 6.32 (1H, s), 7.16 (1H, d, J=8.6 Hz), 7.41–7.46 (3H, m), 7.95–7.97 (1H, m), 7.98–8.0 (1H, m), 8.34 (1H, s), 8.38 (1H, s). MS m/z (%) 345 (M^+, 100), 300 (15), 243 (15), 206 (60), 193 (6). Calcd for $C_{23}H_{23}NO_2$: M, 345.1717. Found: m/z 345.1707.

3.1.8. 2-(1,4-Dioxaspiro[4.5]dec-8-ylidenemethyl)-3-methoxyphenylamine (7h). Colorless oil; IR (neat) 3469 (NH), 3371 (NH), 2949, 2886, 2838, 1615, 1471, 1258, 1210, 1122, 1081, 1034 cm^{-1}; ^1H NMR δ 1.67 (2H, t, J=6.4 Hz), 1.81 (2H, t, J=6.4 Hz), 2.15 (2H, t, J=6.4 Hz), 2.49 (2H, t, J=6.4 Hz), 3.69 (2H, br s), 3.76 (3H, s), 3.97 (4H, m), 5.88 (1H, s), 6.31 (1H, d, J=8.2 Hz), 6.36 (1H, d, J=8.3 Hz), 7.02 (1H, t, J=8.2 Hz). MS m/z (%) 275 (M^+, 100), 230 (26), 213 (16), 189 (34), 174 (40), 160 (24), 136 (63), 130 (10), 117 (8), 106 (15). Calcd for $C_{16}H_{21}NO_3$: M, 275.1520. Found: m/z 275.1520.

3.1.9. 2-(1,4-Dioxaspiro[4.5]dec-8-ylidenemethyl)-5-methoxyphenylamine (7i). Colorless crystals; mp 87–88 °C (AcOEt/hexane); IR (KBr) 3466 (NH), 3363 (NH), 2953, 2901, 1599, 1622, 1578, 1506, 1209, 1081, 1030, 903 cm^{-1}; ^1H NMR δ 1.66 (2H, t, J=6.4 Hz), 1.79 (2H, t, J=6.6 Hz), 2.35 (2H, t, J=6.6 Hz), 2.44 (2H, t, J=6.6 Hz), 3.69 (2H, br s), 3.76 (3H, s), 3.97–3.99 (4H, m), 6.03 (1H, s), 6.26 (1H, d, J=2.7 Hz), 6.31 (1H, dd, J=8.2, 2.7 Hz), 6.88 (1H, d, J=8.2 Hz). MS m/z (%) 275 (M^+, 100), 230 (26), 214 (20), 189 (30), 174 (22), 160 (23), 136 (75), 130 (6), 117 (8). Calcd for $C_{16}H_{21}NO_3$: M, 275.1521. Found: m/z 275.1525. Anal. Calcd for $C_{16}H_{21}NO_3$: C, 69.79; H, 7.69; N, 5.09. Found: C, 69.74; H, 7.54; N, 5.13.

3.1.10. 2-(1,4-Dioxaspiro[4.5]dec-8-ylidenemethyl)-3-methylphenylamine (7j) and 2-(1,4-dioxaspiro[4.5]dec-8-ylidenemethyl)-5-methylphenylamine (7k). The reaction gave an inseparable mixture of **7j** and **7k**. Colorless oil; IR (neat) 3468 (NH), 3370 (NH), 2948, 2884, 1610, 1466, 1120, 1083, 757 cm^{-1}; ^1H NMR (vinylic proton and aromatic protons of **7j**) δ 5.95 (s), 6.55 (d, J=7.9 Hz), 6.60 (d, J=7.3 Hz), 6.96 (t, J=7.8 Hz); ^1H NMR (vinylic proton and aromatic protons of **7k**) δ 6.06 (s), 6.52 (s), 6.55 (d, J=7.9 Hz), 6.86 (d, J=7.7 Hz). MS m/z (%) 259 (M^+, 100), 214 (38), 173 (30), 158 (54), 144 (48), 120 (80). Calcd for $C_{16}H_{21}NO_2$: M, 259.1572. Found: m/z 259.1577.

3.1.11. 3-Chloro-2-(1,4-dioxaspiro[4.5]dec-8-ylidenemethyl)phenylamine (7l). Colorless oil; IR (neat) 3474 (NH), 3368 (NH), 2952, 2884, 1615, 1471, 1447, 1120, 1083, 1034, 908 cm^{-1}; ^1H NMR δ 1.65–1.70 (2H, m), 1.78–1.84 (2H, m), 2.12–2.16 (2H, m), 2.48–2.52 (2H, m), 3.79 (2H, br s), 3.95–4.00 (4H, m), 5.92 (1H, s), 6.58 (1H, d, J=8.0 Hz), 6.77 (1H, d, J=8.0 Hz), 6.97 (1H, t, J=8.0 Hz). MS m/z (%) 279 (M^+, 100), 234 (26), 218 (18), 193 (28), 178 (32), 164 (42), 158 (23), 141 (73). Calcd for $C_{15}H_{18}ClNO_2$: M, 279.1024. Found: m/z 279.1018.

3.1.12. 5-Chloro-2-(1,4-dioxaspiro[4.5]dec-8-ylidenemethyl)phenylamine (7m). Colorless oil; IR (neat) 3469 (NH), 3371 (NH), 2948, 2883, 1608, 1466, 1120, 1083, 1034, 908, 758 cm^{-1}; ^1H NMR δ 1.65 (2H, t, J=6.6 Hz), 1.79 (2H, t, J=6.6 Hz), 2.31 (2H, t, J=6.6 Hz), 2.44 (2H, t, J=6.6 Hz), 3.73 (2H, br s), 3.98 (4H, m), 6.00 (1H, s), 6.67 (1H, s), 6.68 (1H, d, J=8.3 Hz), 6.87 (1H, d, J=8.3 Hz). MS m/z (%) 279 (M^+, 100), 250 (8), 234 (26), 220 (8), 217 (20), 193 (26), 178 (29), 164 (38), 158 (20), 141 (65). Calcd for $C_{15}H_{18}ClNO_2$: M, 279.1024. Found: m/z 279.1022.

3.1.13. 3-Amino-2-(1,4-dioxaspiro[4.5]dec-8-ylidenemethyl)benzonitrile (7n). Colorless oil; IR (neat) 3472 (NH), 3369 (NH), 2953, 2885, 2272 (CN), 1621, 1463, 1121, 1084, 1033, 909 cm^{-1}; ^1H NMR δ 1.68–1.84 (4H, m), 2.21 (2H, m), 2.58 (2H, m), 3.88 (2H, br s), 3.95–3.99 (4H, m), 6.06 (1H, s), 6.86 (1H, dd, J=7.8, 0.9 Hz), 7.04 (1H, dd, J=7.8, 0.9 Hz), 7.12 (1H, t, J=7.8 Hz). MS m/z (%) 270 (M^+, 100), 241 (22), 225 (40), 209 (28), 197 (38), 169 (32), 155 (40), 131 (23), 99 (34). Calcd for $C_{16}H_{18}N_2O_2$: M, 270.1367. Found: m/z 270.1362.

3.1.14. 3-Amino-4-(1,4-dioxaspiro[4.5]dec-8-ylidenemethyl)benzonitrile (7o). Colorless oil; IR (neat) 3475 (NH), 3370 (NH), 2953, 2923, 2874, 2229 (CN), 1627, 1424, 1117, 1083, 1032, 909 cm^{-1}; ^1H NMR δ 1.67 (2H, t, J=6.6 Hz), 1.81 (2H, t, J=6.6 Hz), 2.31 (2H, t, J=6.4 Hz), 2.47 (2H, t, J=6.4 Hz), 3.87 (2H, br s), 3.97–4.00 (4H, m), 6.03 (1H, s), 6.92 (1H, d, J=1.2 Hz), 6.99 (1H, dd, J=7.6, 1.2 Hz), 7.03 (1H, d, J=7.6 Hz). MS m/z (%) 270 (M^+, 100), 257 (10), 241 (15), 225 (28), 208 (30), 197 (19), 183 (23), 169 (52), 155 (57), 132 (99), 99 (40), 86 (44). Calcd for $C_{16}H_{18}N_2O_2$: M, 270.1367. Found: m/z 270.1370.

3.1.15. 2-(2-Methylpropenyl)phenylamine (11a). Colorless oil; IR (neat) 3466 (NH), 3376 (NH), 3022, 2968, 2930, 2855, 1615, 1491, 1454, 1299, 750 cm^{-1}; ^1H NMR δ 1.71 (3H, s), 1.91 (3H, s), 3.66 (2H, br s), 6.06 (1H, s), 6.69 (1H, d, J=7.6 Hz), 6.73 (1H, t, J=7.6 Hz), 7.00 (1H, d, J=7.6 Hz), 7.05 (1H, t, J=7.6 Hz). MS m/z (%) 147 (M^+, 100), 117 (30), 106 (30), 91 (11), 77 (13), 65 (11). Calcd for $C_{10}H_{13}N$: M, 147.1047. Found: m/z 147.1049.

3.1.16. 4-Methoxy-2-(2-methylpropenyl)phenylamine (11b). Colorless oil; IR (neat) 3440 (NH), 3363 (NH), 2929, 2852, 1603, 1497 cm^{-1}; ^1H NMR δ 1.73 (3H, d, J= 1.2 Hz), 1.91 (3H, d, J=1.2 Hz), 3.43 (2H, br s), 3.74 (3H, s), 6.06 (1H, br s), 6.61 (1H, m), 6.65 (2H, m). MS m/z (%) 177 (M^+, 100), 162 (85), 147 (18), 134 (8), 117 (12), 91 (8). Calcd for $C_{11}H_{15}NO$: M, 177.1152. Found: m/z 117.1154.

3.1.17. 3-Methoxy-2-(2-methylpropenyl)phenylamine (11c). Colorless oil; IR (neat) 3462 (NH), 3376 (NH), 2930, 2852, 1618, 1506, 1294, 1205, 1168, 1030 cm^{-1}; ^1H NMR δ 1.59 (3H, s), 1.94 (3H, d, J=1.3 Hz), 3.71 (2H, br s), 3.78 (3H, s), 5.91 (1H, br s), 6.32 (1H, d, J=8.0 Hz), 6.37 (1H, d, J=8.0 Hz), 7.02 (1H, t, J=8.0 Hz). MS m/z (%) 177 (M^+, 80), 162 (100), 147 (30), 131 (12), 117 (8), 106 (16), 91 (10), 77 (18), 65 (6). Calcd for $C_{11}H_{15}NO$: M, 177.1153. Found: m/z 117.1153.

3.1.18. 5-Methoxy-2-(2-methylpropenyl)phenylamine (11d). Colorless oil; IR (neat) 3473 (NH), 3377 (NH), 2932, 2836, 1612, 1468, 1257, 1129, 1092, 1055, 770 cm^{-1}; ^1H NMR δ 1.70 (3H, s), 1.89 (3H, s), 3.70 (2H, br s), 3.76 (3H, s), 5.99 (1H, s), 6.26 (1H, d, J=2.8 Hz), 6.31 (1H, dd, J=8.3, 2.8 Hz), 6.90 (1H, d, J=8.3 Hz). MS m/z (%) 178 (12), 177 (M^+, 100), 162 (66), 136 (48), 131 (10), 117 (10), 91 (8). Calcd for $C_{11}H_{15}NO$: M, 177.1152. Found: m/z 177.1150.

3.1.19. *N*-Methyl-*N*-[2-(2-methylpropenyl)phenyl]amine (11e). Colorless oil; IR (neat) 3429 (NH), 2911, 2814, 1602, 1578, 1506, 1459, 748 cm^{-1}; ^1H NMR δ 1.69 (3H, d, J= 0.9 Hz), 1.91 (3H, d, J=1.3 Hz), 2.85 (3H, s), 3.76 (1H, br s), 6.00 (1H, br s), 6.61 (1H, d, J=7.3 Hz), 6.68 (1H, t, J= 7.3 Hz), 6.98 (1H, d, J=7.3 Hz), 7.16 (1H, t, J=7.3 Hz). MS m/z (%) 161 (M^+, 100), 146 (84), 131 (36), 118 (58), 115 (12), 91 (16), 77 (12), 65 (6). Calcd for $C_{11}H_{15}N$: M, 161.1204. Found: m/z 161.1206.

3.1.20. 2-(2-Methylpropenyl)naphthalen-1-ylamine (11f). Colorless oil; IR (neat) 3469 (NH), 3383 (NH), 3054, 2929, 1610, 1565, 1507, 1430, 1400 cm^{-1}; ^1H NMR δ 1.72 (3H, s), 1.97 (3H, d, J=1.2 Hz), 4.20 (2H, br s), 6.25 (1H, s), 7.17 (1H, d, J=8.3 Hz), 7.27 (1H, d, J=8.3 Hz), 7.41–7.44 (2H, m), 7.77 (1H, dd, J=6.6, 2.5 Hz), 7.81–7.83 (1H, m). MS m/z (%) 197 (M^+, 100) 182 (85), 167 (30), 156 (22), 90 (6), 28 (24). Calcd for $C_{14}H_{15}N$: M, 197.1204. Found: m/z 197.1211.

3.1.21. 2-(2-Methylpropenyl)anthracen-1-ylamine (11g). Colorless crystals; mp 98–100 °C (hexane); IR (KBr) 3469 (NH), 3383 (NH), 3050, 2960, 2926, 1617, 1527, 1402, 1387, 891, 873, 735 cm^{-1}; ^1H NMR δ 1.75 (3H, s), 2.00 (3H, d, J=1.2 Hz), 4.34 (2H, br s), 6.30 (1H, s), 7.19 (1H, d, J=8.5 Hz), 7.41–7.46 (3H, m), 7.95–7.97 (1H, m), 7.99 (1H, m), 8.34 (1H, s), 8.39 (1H, s). MS m/z (%) 247 (M^+, 100), 232 (26), 217 (20), 202 (6), 115 (8), 28 (24). Calcd for $C_{18}H_{17}N$: M, 247.1360. Found: m/z 247.1370. Anal. Calcd for $C_{18}H_{17}N$: C, 87.41; H, 6.93; N, 5.66. Found: C, 87.69; H, 6.87; N, 5.57.

3.1.22. (*E*)-1-Chloro-2-methyl-1-(*p*-tolylsulfinyl)-1,3-butadiene (13*E*) and (*Z*)-1-chloro-2-methyl-1-(*p*-tolylsulfinyl)-1,3-butadiene (13*Z*). A solution of chloromethyl *p*-tolyl sulfoxide (1.0 g; 5.3 mmol) in dry THF (5 mL) was added dropwise to a solution of LDA (7.95 mmol) in 20 mL of THF at −78 °C. The solution was stirred at −78 °C for 10 min, then methyl vinyl ketone (0.648 mL: 7.95 mmol) was added. The reaction mixture was stirred for 10 min and the reaction was quenched by satd aq NH_4Cl. The whole was extracted with $CHCl_3$. The organic layer was washed once with water and dried over $MgSO_4$. The solvent was evaporated to leave the adducts as colorless crystals. The adducts were dissolved in a mixture of acetic anhydride (11.2 mL) and pyridine (21.4 mL). 4-Dimethylaminopyridine (108 mg; 0.88 mmol) was added to the solution and the reaction mixture was stirred at room temperature for 15 h. The acetic anhydride and pyridine were evaporated under vacuum and the residue was purified by silica gel column chromatography to give the acetate (1.21 g; 76%) as a colorless oil (a mixture of two diastereomers); IR (neat) 2995, 2945, 1739 (CO), 1370, 1239 (COC), 1092, 1065 (SO) cm^{-1}.

A solution of the acetate (205 mg; 0.68 mmol) in dry THF (4 mL) was added dropwise to a solution of *N*-lithio 2-piperidone [1.7 mmol; prepared from *n*-BuLi (1.7 mmol) and 2-piperidone (169 mg; 1.7 mmol) in THF (4 mL) at 0 °C] in THF at 25 °C. The mixture was stirred at 25 °C for 30 min. The reaction was quenched by satd aq NH_4Cl and the whole was extracted with $CHCl_3$ and the organic layer was washed three times with water. The organic layer was dried over $MgSO_4$. The solvent was evaporated to leave colorless crystals, which were purified by silica gel column chromatography to give **13***E* (79 mg; 48%) and **13***Z* (79 mg; 48%).

Compound **13***E*: Colorless needles; mp 103–104 °C (AcOEt/hexane); IR (KBr) 3095, 3053, 3024, 2918, 1555, 1494, 1417, 1086, 1059 (SO), 922, 899, 807 cm^{-1}; ^1H NMR δ 2.13 (3H, s), 2.41 (3H, s), 5.50 (1H, d, J=11.0 Hz), 5.63 (1H, d, J=16.8 Hz), 7.30 (2H, d, J=7.9 Hz), 7.47 (1H, dd, J=16.8, 11.0 Hz), 7.48 (2H, d, J=7.9 Hz). MS m/z (%) 240 (M^+, 15), 223 (12), 205 (10), 188 (16), 175 (18), 157 (25), 139 (46), 124 (46), 117 (52), 105 (25), 89 (72), 77 (20), 65 (100). Calcd for $C_{12}H_{13}ClOS$: M, 240.0374. Found: m/z 240.0369. Anal. Calcd for $C_{12}H_{13}ClOS$: C, 59.87; H, 5.44; Cl, 14.73; S, 13.32. Found: C, 59.89; H, 5.29; Cl, 14.73; S, 13.09.

Compound **13***Z*: Colorless crystals; mp 77–78 °C (AcOEt/hexane); IR (KBr) 3050, 3002, 2957, 1564, 1492, 1447, 1418, 1087, 1060 (SO), 939, 891, 810 cm^{-1}; ^1H NMR δ 2.40 (3H, s), 2.41 (3H, s), 5.56 (1H, d, J=11.0 Hz), 5.69 (1H, d, J=17.4 Hz), 6.93 (1H, dd, J=17.4, 11.0 Hz), 7.31 (2H, d, J=8.3 Hz), 7.49 (2H, d, J=8.3 Hz). MS m/z (%) 240 (M^+, 20), 223 (22), 192 (15), 187 (15), 177 (22), 157 (65), 139 (45), 123 (55), 105 (30), 91 (40), 77 (20), 65 (100). Calcd for $C_{12}H_{13}ClOS$: M, 240.0374. Found: m/z 240.0371. Anal. Calcd for $C_{12}H_{13}ClOS$: C, 59.87; H, 5.44; Cl, 14.73; S, 13.32. Found: C, 59.92; H, 5.21; Cl, 14.62; S, 13.08.

3.1.23. (*E*)-1-Chloro-2-methyl-1-(*p*-tolylsulfinyl)-1-heptene (14*E*) and (*Z*)-1-chloro-2-methyl-1-(*p*-tolylsulfinyl)-1-heptene (14*Z*). These compounds were synthesized from chloromethyl *p*-tolyl sulfoxide and 2-heptanone in a similar way as described above. The acetates were isolated by silica

gel column chromatography to give more polar acetate-P (55%) as a colorless oil and less polar acetate-L (39%) as colorless crystals.

Acetate-P; IR (neat) 2956, 2870, 1732 (CO), 1494, 1461, 1369, 1243 (COC), 1154, 1093, 1066 (SO), 1018, 820, 516 cm^{-1}; ^1H NMR δ 0.89 (3H, t, J=7.0 Hz), 1.20–1.43 (6H, m), 1.71 (3H, s), 1.87–1.93 (1H, m), 2.14 (3H, s), 2.17–2.20 (1H, m), 2.42 (3H, s), 5.25 (1H, s), 7.33 (2H, d, J=8.3 Hz), 7.47 (2H, d, J=8.3 Hz). MS m/z (%) 344 (M^+, 2), 205 (32), 140 (87), 139 (36), 109 (26), 91 (16), 65 (6), 43 (100). Calcd for $C_{17}H_{25}ClO_3S$: M, 344.1213. Found: m/z 344.1216.

Acetate-L: Colorless crystals; mp 64–65 °C (AcOEt/hexane); IR (KBr) 2950, 2931, 1726 (CO), 1242 (COC), 1087, 1463 (SO), 515 cm^{-1}; ^1H NMR δ 0.92 (3H, t, J=7.0 Hz), 1.33–1.48 (6H, m), 1.61 (3H, s), 1.99–2.06 (1H, m), 2.09 (3H, s), 2.35–2.40 (1H, m), 2.42 (3H, s), 5.38 (1H, s), 7.33 (2H, d, J=8.0 Hz), 7.47 (2H, d, J=8.0 Hz). MS m/z (%) 344 (M^+, 2), 205 (32), 140 (50), 139 (33), 109 (25), 91 (15), 65 (6), 43 (100). Calcd for $C_{17}H_{25}ClO_3S$: M, 344.1231. Found: m/z 344.1233. Anal. Calcd for $C_{17}H_{25}ClO_3S$: C, 59.20; H, 7.31; Cl, 10.28; S, 9.3. Found: C, 59.18; H, 7.36; Cl, 10.15; S, 9.23.

Treatment of the acetate-L and acetate-P with *N*-lithio 2-piperidone in THF at 25 °C gave **14***Z* (93%) and **14***E* (96%), respectively.

Compound **14***E*: Colorless oil; IR (neat) 2957, 2929, 2860, 1493, 1456, 1088, 1061 (SO), 808 cm^{-1}; ^1H NMR δ 0.87 (3H, t, J=7.0 Hz), 1.26–1.31 (4H, m), 1.45–1.50 (2H, m), 2.31 (3H, s), 2.33 (2H, t, J=8.0 Hz), 2.41 (3H, s), 7.30 (2H, d, J=7.9 Hz), 7.46 (2H, d, J=7.9 Hz). MS m/z (%) 284 (M^+, 26), 267 (100), 211 (24), 175 (32), 140 (36), 139 (26), 123 (21), 91 (36), 89 (17), 65 (17). Calcd for $C_{15}H_{21}ClO_3S$: M, 284.1002. Found: m/z 284.0994.

Compound **14***Z*: Colorless oil; IR (neat) 2957, 2929, 2861, 1493, 1456, 1088, 1062 (SO), 808 cm^{-1}; ^1H NMR δ 0.94 (3H, t, J=6.6 Hz), 1.38–1.41 (4H, m), 1.50–1.59 (2H, m), 2.00 (3H, s), 2.41 (3H, s), 2.73 (2H, t, J=7.9 Hz), 7.31 (2H, d, J=7.9 Hz), 7.49 (2H, d, J=8.2 Hz). MS m/z (%) 284 (M^+, 85), 267 (100), 211 (75), 175 (56), 140 (90), 139 (63), 123 (56), 91 (72), 89 (68), 55 (42), 41 (42). Calcd for $C_{15}H_{21}ClOS$: M, 284.1001. Found: m/z 284.0993.

3.1.24. (*Z*)-2-(Cyclohex-2-enylidenemethyl)phenylamine (16*Z*). Colorless oil; IR (neat) 3467 (NH), 3376 (NH), 3030, 2932, 2829, 1615, 1489, 1453, 747 cm^{-1}; ^1H NMR δ 1.81 (2H, quintet, J=6.2 Hz), 2.18–2.20 (2H, m), 2.48 (2H, t, J=6.0 Hz), 3.69 (2H, br s), 5.87–5.91 (1H, m), 6.01 (1H, s), 6.35 (1H, d, J=10.8 Hz), 6.69 (1H, d, J=7.6 Hz), 6.73 (1H, t, J=7.3 Hz), 7.04–7.07 (2H, m). MS m/z (%) 185 (M^+, 100), 170 (15), 157 (64), 143 (14), 130 (34), 115 (10), 106 (52), 91 (13), 77 (14). Calcd for $C_{13}H_{15}N$: M, 185.1204. Found: m/z 185.1210.

3.1.25. (*E*)-2-(Cyclohex-2-enylidenemethyl)phenylamine (16*E*). Colorless oil; IR (neat) 3461 (NH), 3375 (NH), 3021, 2931, 2862, 2829, 1615, 1489, 1454 cm^{-1}; ^1H NMR δ 1.68 (2H, quintet, J=6.2 Hz), 2.16–2.19 (2H, m), 2.47 (2H, dt, J=6.3, 1.5 Hz), 3.69 (2H, br s), 5.88–5.91 (1H, m), 6.10 (1H, s), 6.25 (1H, d, J=10.0 Hz), 6.69 (1H, d, J=8.0 Hz), 6.74 (1H, t, J=7.5 Hz), 7.04–7.07 (2H, m). MS m/z (%) 185 (M^+, 100), 170 (13), 157 (63), 143 (13), 130 (33), 115 (10), 106 (52), 91 (12), 77 (12). Calcd for $C_{13}H_{15}N$: M, 185.1204. Found: m/z 185.1212.

3.1.26. (*Z*)-2-(Cyclohex-2-enylidenemethyl)naphthalen-1-ylamine (17*Z*). Colorless crystals; mp 71–73 °C (hexane); IR (KBr) 3478 (NH), 3392 (NH), 2928, 2856, 2822, 1614, 1403, 790, 736 cm^{-1}; ^1H NMR δ 1.84 (2H, quintet, J=6.2 Hz), 2.20–2.21 (2H, m), 2.53 (2H, t, J=6.3 Hz), 4.16 (2H, br s), 5.88–5.91 (1H, m), 6.18 (1H, s), 6.32 (1H, dd, J=10.0, 0.9 Hz), 7.23 (1H, d, J=8.3 Hz), 7.26 (1H, d, J=8.3 Hz), 7.40–7.43 (2H, m), 7.74–7.76 (1H, m), 7.78–7.80 (1H, m). MS m/z (%) 235 (M^+, 100), 220 (10), 207 (42), 193 (8), 180 (30), 167 (6), 156 (18), 143 (6). Calcd for $C_{17}H_{17}N$: M, 235.1359. Found: m/z 235.1353.

3.1.27. (*E*)-2-(Cyclohex-2-enylidenemethyl)naphthalen-1-ylamine (17*E*). Colorless oil; IR (neat) 3472 (NH), 3385 (NH), 3054, 3021, 2930, 2862, 2829, 1615, 1403, 806, 758, 737 cm^{-1}; ^1H NMR δ 1.68 (2H, quintet, J=6.2 Hz), 2.17–2.20 (2H, m), 2.46 (2H, t, J=6.2 Hz), 4.18 (2H, br s), 5.90–5.93 (1H, m), 6.29 (1H, s), 6.31 (1H, d, J=10.1 Hz), 7.22 (1H, d, J=8.6 Hz), 7.26 (1H, d, J=8.6 Hz), 7.39–7.43 (2H, m), 7.74–7.76 (1H, m), 7.79–7.80 (1H, m). MS m/z (%) 235 (M^+, 100), 220 (10), 207 (44), 193 (8), 180 (30), 167 (8), 156 (18), 143 (6). Calcd for $C_{17}H_{17}N$: M, 235.1360. Found: m/z 235.1366.

3.1.28. (*Z*)-2-(Cyclohex-2-enylidenemethyl)athracen-1-ylamine (18*Z*). Colorless amorphous; IR (KBr) 3456 (NH), 3382 (NH), 2929, 2858, 1618, 875, 738 cm^{-1}; ^1H NMR δ 1.85 (2H, quintet, J=6.2 Hz), 2.21–2.23 (2H, m), 2.55 (2H, t, J=5.9 Hz), 4.34 (2H, br s), 5.91–5.94 (1H, m), 6.22 (1H, s), 6.37 (1H, dd, J=10.0, 0.9 Hz), 7.24 (1H, dd, J=8.7, 1.9 Hz), 7.40–7.43 (3H, m), 7.93–7.97 (2H, m), 8.31 (1H, s), 8.34 (1H, s). MS m/z (%) 285 (M^+, 100), 257 (16), 230 (16), 206 (10), 193 (6). Calcd for $C_{21}H_{19}N$: M, 285.1516. Found: m/z 285.1509.

3.1.29. (*E*)-2-(Cyclohex-2-enylidenemethyl)athracen-1-ylamine (18*E*). Colorless crystals; mp 114–115 °C (hexane); IR (KBr) 3462 (NH), 3389 (NH), 2928, 2827, 1613, 869, 737 cm^{-1}; ^1H NMR δ 1.71 (2H, quintet, J=6.1 Hz), 2.19–2.21 (2H, m), 2.49 (2H, t, J=6.0 Hz), 4.35 (2H, br s), 5.91–5.95 (1H, m), 6.33–6.34 (2H, m), 7.24 (1H, d, J=8.5 Hz), 7.41–7.43 (3H, m), 7.93–7.97 (2H, m), 8.31 (1H, m), 8.35 (1H, s). MS m/z (%) 285 (M^+, 100), 256 (18), 230 (18), 206 (10). Calcd for $C_{21}H_{19}N$: M, 285.1517. Found: m/z 285.1521. Anal. Calcd for $C_{21}H_{19}N$: C, 88.38; H, 6.71; N, 4.91. Found: C, 87.79; H, 6.44; N, 4.86.

3.1.30. (*Z*)-2-(2-Methylbuta-1,3-dienyl)naphthalen-1-ylamine (19*Z*). Colorless crystals; mp 51–52 °C (hexane); IR (KBr) 3476 (NH), 3391 (NH), 3055, 2979, 2930, 1618, 1404, 900, 810, 762, 738 cm^{-1}; ^1H NMR δ 2.07 (3H, s), 4.21 (2H, br s), 5.14 (1H, d, J=10.7 Hz), 5.36 (1H, d, J=17.4), 6.47 (1H, s), 6.65 (1H, dd, J=17.4, 10.7 Hz), 7.19 (1H, d, J=8.3 Hz), 7.26 (1H, d, J=8.3 Hz), 7.41–7.45 (2H, m), 7.75–7.77 (1H, m), 7.79–7.81 (1H, m). MS m/z (%) 209 (M^+, 100), 194 (84), 178 (20), 165 (12), 152 (8), 139 (6), 96

(12). Calcd for $C_{15}H_{15}N$: *M*, 209.1204. Found: *m/z* 209.1207. Anal. Calcd for $C_{15}H_{15}N$: C, 86.08; H, 7.22; N, 6.69. Found: C, 85.85; H, 7.24; N, 6.69.

3.1.31. (*E*)-2-(2-Methylbuta-1,3-dienyl)naphthalen-1-ylamine (19*E*). Colorless oil; IR (neat) 3474 (NH), 3388 (NH), 3055, 2918, 1615, 1403, 902, 797, 760, 737 cm^{-1}; ^1H NMR δ 1.89 (3H, s), 4.22 (2H, br s), 5.16 (1H, d, J=10.7 Hz), 5.33 (1H, d, J=17.4 Hz), 6.55 (1H, s), 6.66 (1H, dd, J=17.4, 10.7 Hz), 7.21 (1H, d, J=8.2 Hz), 7.28 (1H, d, J=8.2 Hz), 7.42–7.46 (2H, m), 7.77–7.78 (1H, m), 7.81–7.83 (1H, m). MS *m/z* (%) 209 (M^+, 100), 194 (88), 178 (20), 165 (14), 152 (10), 139 (6), 115 (6), 96 (14). Calcd for $C_{15}H_{15}N$: *M*, 209.1203. Found: *m/z* 209.1203.

3.1.32. (*Z*)-2-(2-Methylhept-1-enyl)naphthalen-1-ylamine (20*Z*). Colorless oil; IR (neat) 3467 (NH), 3386 (NH), 2927, 2857, 1611, 1400, 1380 cm^{-1}; ^1H NMR δ 0.81 (3H, t, J=6.9 Hz), 1.13–1.23 (4H, m), 1.42 (2H, quintet, J=7.6 Hz), 1.94 (3H, s), 2.07 (2H, t, J=7.8 Hz), 4.17 (2H, br s), 6.23 (1H, s), 7.14 (1H, d, J=8.3 Hz), 7.26 (1H, d, J=9.2 Hz), 7.40–7.45 (2H, m), 7.76 (1H, m), 7.81 (1H, d, J=7.3 Hz). MS *m/z* (%) 253 (M^+, 100), 196 (50), 182 (54), 167 (12), 156 (23), 143 (23). Calcd for $C_{18}H_{23}N$: *M*, 253.1828. Found: *m/z* 253.1822.

3.1.33. (*E*)-2-(2-Methylhept-1-enyl)naphthalen-1-ylamine (20*E*). Colorless oil; IR (neat) 3472 (NH), 3384 (NH), 2928, 2856, 1615, 1403, 800, 760, 734 cm^{-1}; ^1H NMR δ 0.94 (3H, t, J=6.4 Hz), 1.38 (4H, m), 1.57 (2H, t, J=6.7 Hz), 1.69 (3H, s), 2.24 (2H, t, J=7.5 Hz), 4.18 (2H, br s), 6.25 (1H, s), 7.17 (1H, d, J=8.3 Hz), 7.27 (1H, d, J=8.3 Hz), 7.40–7.45 (2H, m), 7.76 (1H, d, J=8.0 Hz), 7.81 (1H, d, J=7.7 Hz). MS *m/z* (%) 253 (M^+, 100), 238 (6), 196 (53), 182 (61), 167 (13), 156 (25), 143 (23). Calcd for $C_{18}H_{23}N$: *M*, 253.1829. Found: *m/z* 253.1837.

3.1.34. (*Z*)-2-(2-Phenylpropenyl)naphthalen-1-ylamine (21*Z*). Colorless crystals; mp 110–112 °C (AcOEt/hexane); IR (KBr) 3487 (NH), 3391 (NH), 2965, 2926, 2869, 1614, 1406, 804, 760, 748, 696 cm^{-1}; ^1H NMR δ 2.32 (3H, s), 4.24 (2H, br s), 6.55 (1H, s), 6.86 (1H, d, J=8.6 Hz), 7.02 (1H, d, J=8.6 Hz), 7.13–7.20 (5H, m), 7.36–7.42 (2H, m), 7.65–7.67 (1H, m), 7.76 (1H, d, J=8.0 Hz). MS *m/z* (%) 259 (M^+, 92), 244 (100), 215 (8), 182 (11), 167 (10), 156 (18), 121 (12). Calcd for $C_{19}H_{17}N$: *M*, 259.1359. Found: *m/z* 259.1355. Anal. Calcd for $C_{19}H_{17}N$: C, 87.99; H, 6.61; N, 5.40. Found: C, 87.82; H, 6.58; N, 5.48.

3.1.35. (*E*)-2-(2-Phenylpropenyl)naphthalen-1-ylamine (21*E*). Colorless amorphous; IR (KBr) 3484 (NH), 3399 (NH), 3049, 2919, 2851, 1608, 1404, 761, 740, 697 cm^{-1}; ^1H NMR δ 2.16 (3H, s), 4.27 (2H, br s), 6.90 (1H, s), 7.28 (1H, d, J=8.3 Hz), 7.32–7.34 (2H, m), 7.40 (2H, t, J=7.6 Hz), 7.44–7.48 (2H, m), 7.61 (2H, d, J=8.0 Hz), 7.79–7.81 (1H, m), 7.84–7.86 (1H, m). MS *m/z* (%) 259 (M^+, 92), 244 (100), 215 (8), 182 (11), 167 (8), 156 (17), 122 (8), 121 (9). Calcd for $C_{19}H_{17}N$: *M*, 259.1360. Found: *m/z* 259.1364.

3.1.36. (*E*)-3-Cholromethylenecyclohexene (22*E*). To a solution of **12** (80 mg; 0.3 mmol) in 6 mL of dry toluene in a flame-dried flask at −78 °C under argon atmosphere was added *t*-BuMgCl (0.036 mmol) dropwise with stirring. After 10 min, *i*-PrMgCl (0.84 mmol) was added dropwise to the reaction mixture at −78 °C to give the magnesium alkylidene carbenoid. After 5 min, the reaction was quenched by satd aq NH_4Cl and the whole was extract with $CHCl_3$. The organic layer was washed once with water and dried over $MgSO_4$. After removal of the solvent, the product was purified by silica gel column chromatography to give 19.7 mg (51%) of **22*E*** as a colorless oil; IR (neat) 2941, 2867, 2834, 1694, 835, 795, 755 cm^{-1}; ^1H NMR δ 1.71 (2H, quintet, J=6.3 Hz), 2.11–2.15 (2H, m), 2.46 (2H, dt, J=6.3, 2.1 Hz), 5.83–5.87 (1H, m), 5.91 (1H, s), 6.06 (1H, dt, J=10.1, 2.0 Hz). MS *m/z* (%) 128 (M^+, 40), 113 (6), 93 (100), 79 (82), 77 (66). Calcd for C_7H_9Cl: *M*, 128.0393. Found: *m/z* 128.0390.

3.1.37. (*Z*)-3-Cholromethylenecyclohexene (22*Z*). Colorless oil; IR (neat) 2940, 2866, 2832, 818, 758, 731 cm^{-1}; ^1H NMR δ 1.70–1.75 (2H, m), 2.16–2.20 (2H, m), 2.30–2.33 (2H, m), 5.72 (1H, s), 6.01–6.05 (1H, m), 6.55–6.58 (1H, m). MS *m/z* (%) 128 (M^+, 32) 113 (9), 93 (67), 83 (100), 79 (47), 77 (46). Calcd for C_7H_9Cl: *M*, 128.0393. Found: *m/z* 128.0391.

3.1.38. (*E*)-(2-Chloro-1-methylvinyl)benzene (23*E*). Colorless oil; IR (neat) 3080, 3059, 2923, 1494, 1443, 801, 749, 695 cm^{-1}; ^1H NMR δ 2.20 (3H, d, J=1.2 Hz), 6.32 (1H, q, J=1.4 Hz), 7.27–7.31 (1H, m), 7.32–7.34 (4H, m). MS *m/z* (%) 152 (M^+, 100), 115 (56), 103 (33), 91 (47), 78 (42). Calcd for C_9H_9Cl: *M*, 152.0393. Found: *m/z* 152.0397.

3.1.39. (*Z*)-(2-Chloro-1-methylvinyl)benzene (23*Z*). Colorless oil; IR (neat) 3059, 2970, 2916, 1494, 1442, 835, 762, 697 cm^{-1}; ^1H NMR δ 2.09 (3H, d, J=1.5 Hz), 6.11 (1H, q, J=1.5 Hz), 7.28–7.32 (1H, m), 7.37–7.38 (4H, m). MS *m/z* (%) 152 (M^+, 100) 115 (56), 103 (33), 91 (18), 78 (43). Calcd for C_9H_9Cl: *M*, 152.0393. Found: *m/z* 152.0390.

Acknowledgements

This work was supported by a grant from the Ministry of Education, Culture, Sports, Science and Technology of Japan to promote multi-disciplinary research project, which is gratefully acknowledged.

References and notes

1. Barton, D. H. R.; Ollis, W. D. In Sutherland, I. O., Ed.; Comprehensive Organic Chemistry; Pergamon: Oxford, 1979; Vol. 2, pp 131–184.
2. Arienti, A.; Bigi, F.; Maggi, R.; Marzi, E.; Moggi, P.; Rastelli, M.; Sartori, G.; Tarantola, F. *Tetrahedron* **1997**, *53*, 3795–3804.
3. (a) Yamaguchi, M.; Arisawa, M.; Hirama, M. *Chem. Commun.* **1998**, 1399–1400. (b) Yamaguchi, M.; Arisawa, M. *Farumashia* **1999**, *35*, 145–149.
4. Satoh, T.; Kawashima, T.; Takahashi, S.; Sakai, K. *Tetrahedron* **2003**, *59*, 9599–9607.

5. Satoh, T.; Takano, K.; Someya, H.; Matsuda, K. *Tetrahedron Lett.* **1995**, *36*, 7097–7100.
6. (a) Satoh, T. *J. Synth. Org. Chem. Jpn.* **1996**, *54*, 481–489. (b) Satoh, T. *J. Synth. Org. Chem. Jpn.* **2003**, *61*, 98–110. (c) Satoh, T. *Chem. Rec.* **2004**, *3*, 329–341.
7. Satoh, T.; Takano, K.; Ota, H.; Someya, H.; Matsuda, K.; Koyama, M. *Tetrahedron* **1998**, *54*, 5557–5574.
8. (a) Satoh, T.; Sakamoto, T.; Watanabe, M. *Tetrahedron Lett.* **2002**, *43*, 2043–2046. (b) Satoh, T.; Sakamoto, T.; Watanabe, M.; Takano, K. *Chem. Pharm. Bull.* **2003**, *51*, 966–970.
9. Preliminary results of this study was reported as a communication: Satoh, T.; Ogino, Y.; Nakamura, M. *Tetrahedron Lett.* **2004**, *45*, 5785–5789.
10. (a) Stang, P. J. *Chem. Rev.* **1978**, *78*, 383–405. (b) Oku, A.; Harada, T. *J. Synth. Org. Chem. Jpn.* **1986**, *44*, 736–755. (c) Oku, A. *J. Synth. Org. Chem. Jpn.* **1990**, *48*, 710–723. (d) Kirmse, W. *Angew. Chem., Int. Ed.* **1997**, *36*, 1164–1170.
11. (a) Duraisamy, M.; Walborsky, H. M. *J. Am. Chem. Soc.* **1984**, *106*, 5035–5037. (b) Walborsky, H. M.; Duraisamy, M. *Tetrahedron Lett.* **1985**, *26*, 2743–2746. (c) Rachon, J.; Goedken, V.; Walborsky, H. M. *J. Am. Chem. Soc.* **1986**, *108*, 7435–7436. (d) Topolski, M.; Duraisamy, M.; Rachon, J.; Gawronski, J.; Gawronska, K.; Goedken, V.; Walborsky, H. M. *J. Org. Chem.* **1993**, *58*, 546–555.
12. (a) Harada, T.; Nozaki, Y.; Yamaura, Y.; Oku, A. *J. Am. Chem. Soc.* **1985**, *107*, 2189–2190. (b) Oku, A.; Harada, T.; Hattori, K.; Nozaki, Y.; Yamaura, Y. *J. Org. Chem.* **1988**, *53*, 3089–3098.
13. Yanagisawa, H.; Miura, K.; Kitamura, M.; Narasaka, K.; Ando, K. *Bull. Chem. Soc. Jpn.* **2003**, *76*, 2009–2026.
14. Frisch, M. J.; Trucks, G. W.; Schlegel, H. B.; Scuseria, G. E.; Robb, M. A.; Cheeseman, J. R.; Zakrzewski, V. G.; Montgomery, J. A., Jr.; Stratmann, R. E.; Burant, J. C.; Dapprich, S.; Millam, J. M.; Daniels, A. D.; Kudin, K. N.; Strain, M. C.; Farkas, O.; Tomasi, J.; Barone, V.; Cossi, M.; Cammi, R.; Mennucci, B.; Pomelli, C.; Adamo, C.; Clifford, S.; Ochterski, J.; G. Petersson, A.; Ayala, P. Y.; Cui, Q.; Morokuma, K.; Malick, D. K.; Rabuck, A. D.; Raghavachari, K.; Foresman, J. B.; Cioslowski, J.; Ortiz, J. V.; Baboul, A. G.; Stefanov, B. B.; Liu, G.; Liashenko, A.; Piskorz, P.; Komaromi, I.; Gomperts, R.; Martin, R. L.; Fox, D. J.; Keith, T.; Al-Laham, M. A.; Peng. C. Y.; Nanayakkara, A.; Challacombe, M.; Gill, P. M. W.; Johnson, B.; Chen, W.; Wong, M. W.; Andres, J. L.; Gonzalez, C.; Head-Gordon, M.; Replogle, E. S.; Pople, J. A. *Gaussian 98*, Revision A.9; Gaussian Inc., Pittsburgh PA, 1998.
15. For both Mg and Li, the 6-31G* basis set was used.
16. Seebach, D.; Siegel, H.; Müllen, K.; Hiltbrunner, K. *Angew. Chem., Int. Ed. Engl.* **1979**, *18*, 784–785.
17. (a) Seebach, D.; Siegel, H.; Gabriel, J.; Hässig, R. *Helv. Chim. Acta* **1980**, *63*, 2046–2053. (b) Seebach, D.; Hässig, R.; Gabriel, J. *Helv. Chim. Acta* **1983**, *66*, 308–337.
18. Schleyer, P. v. R.; Clark, T.; Kos, A. J.; Spitznagel, G. W.; Rohde, C.; Arad, D.; Houk, K. N.; Rondan, N. G. *J. Am. Chem. Soc.* **1984**, *106*, 6467–6475.
19. (a) Pelter, A.; Kvicala, J.; Parry, D. E. *J. Chem. Soc., Perkin Trans. 1* **1995**, 2681–2682. (b) Wang, B.; Deng, C. *Chem. Phys. Lett.* **1988**, *147*, 99–104.
20. The electrostatic potential-derived charges using the CHelpG scheme of Breneman: *E*-**25**, −0.118; *Z*-**25**, −0.138; **24**, −0.141; **26**, −0.28. The Mulliken charges: *E*-**25**, +0.13; *Z*-**25**, +0.14; **24**, −0.11; **26**, −0.19.
21. Satoh, T.; Ota, H. *Tetrahedron* **2000**, *56*, 5113–5122.

Available online at www.sciencedirect.com
SCIENCE DIRECT
Tetrahedron
Tetrahedron 61 (2005) 10277–10284

A general strategy for the synthesis of azapeptidomimetic lactams

Robert L. Broadrup, Bei Wang and William P. Malachowski*

Department of Chemistry, Bryn Mawr College, Bryn Mawr, PA 19010-2899, USA

Received 22 July 2005; accepted 5 August 2005

Available online 24 August 2005

Abstract—A selection of azapeptidomimetics containing constraining lactam rings have been prepared by Mitsunobu cyclization of serine/homologated serine-azaalanine derivatives. These include sterically-congested β-lactams, as well as γ-butyrolactam and δ-valerolactam analogs. A novel azaamino acid acylation method was developed to prepare the sterically demanding α-benzyl-serine-azaalanine precursor. In all cases, the Mitsunobu conditions were highly efficient in forming the desired azapeptidomimetic lactams. The reported process represents a general strategy for the synthesis of peptidomimetic structures with a constraining lactam ring.

1. Introduction

Peptidomimetic structures are the frequent focus of synthetic efforts because they mimic or enhance biologically relevant properties of proteins, but avoid the normal metabolic liabilities.[1] Lactam rings have been a common peptidomimetic target since the seminal work of Freidinger.[1f,2] γ-Butyro-, δ-valero- and ε-caprolactam containing peptidomimetics have been synthesized[2] with a variety of techniques to generate conformationally constrained peptidomimetics. Subsequent research has demonstrated a variety of peptidomimetic lactam applications, many with important biological activity.[3] Recently, even the smaller β-lactam peptidomimetic structures have been synthesized and shown to mimic the β-turn secondary structure and biological activity of melanostatin.[4] Peptidomimetic β-lactams have also shown activity as protease inhibitors.[5]

Similarly, azapeptides or related derivatives have been used as peptide surrogates. They usually create structurally analogous, but metabolically stable peptide mimics, which retain the biological activity of their peptide analogs.[6] Recent reports have demonstrated their unique conformational effects[7] and potent enzyme inhibition.[8]

With the goal of extending our previously described synthetic process[9] to a greater array of peptidomimetic lactam structures, we focused on demonstrating that the method would apply to γ-butyrolactams, δ-valerolactams and more complex β-lactams. Described herein are successful strategies to accomplish this goal. The results demonstrate the utility of the intramolecular Mitsunobu reaction of acyl hydrazides for the synthesis of peptidomimetic structures containing a variety of lactam rings embedded in the peptide backbone.

2. Results and discussion

2.1. Azapeptidomimetic quaternary β-lactams

Recent research from Palomo and co-workers[4] has shown the utility of α-alkyl-α-amino-β-lactam peptidomimetics, which contain a quaternary carbon at C-3 of the β-lactam. Use of an α-alkyl-serine derivative with our previously reported method[9] would permit the efficient synthesis of structurally related azapeptidomimetic lactams. We chose to demonstrate this process with α-benzyl-serine, as the aromatic side chain would facilitate chromatographic methods.

A retrosynthetic analysis of β-lactam **1** (Scheme 1) begins with the cyclization of acyl hydrazide **2** under Mitsunobu

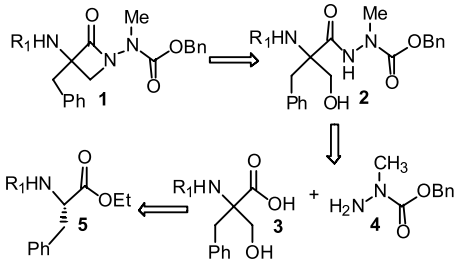

Scheme 1. Retrosynthetic analysis for azapeptidomimetic quaternary lactams.

Keywords: Peptidomimetic; Lactams; Azapeptide; Mitsunobu reaction.
* Corresponding author. Tel.: +1 610 526 5016; fax: +1 610 526 5086; e-mail: wmalacho@brynmawr.edu

0040–4020/$ - see front matter © 2005 Elsevier Ltd. All rights reserved.
doi:10.1016/j.tet.2005.08.029

conditions. The acyl hydrazide could be obtained by coupling α-benzyl-serine derivative **3** and azaalanine derivative **4**. Compound **3** could be prepared by hydroxymethylation of *N*-protected phenylalanine ethyl ester **5**. The benzyl ester of azaalanine **4** could arise from the reaction between methyl hydrazine and benzyl chloroformate.

The α-benzyl-serine derivative **3** was synthesized via modification of a reported α-hydroxymethylation protocol (Scheme 2).[10] *N*-Benzylidene-phenylalanine ethyl ester **7** was prepared by the reaction of phenylalanine ethyl ester **6** with benzaldehyde. Hydroxymethylation of **7** occurred by deprotonation with lithium diisopropylamide (LDA) and reaction of the resulting enolate with sublimed formaldehyde. The hydrolytically labile imine group made purification difficult, so the crude product was immediately hydrolyzed to the α-benzyl serine ethyl ester **9** with 1 N HCl. The hydrophilic nature of **9** also made purification difficult, so the most effective procedure was to immediately protect the amine of **9** as a *tert*-butoxycarbonyl (Boc) carbamate. Isolation and purification of **10** was more easily accomplished and the three step process afforded **10** in 53% yield. Finally, hydrolysis of the ethyl ester with lithium hydroxide in ethanol and water gave *N*-Boc-α-benzyl-serine **3**.

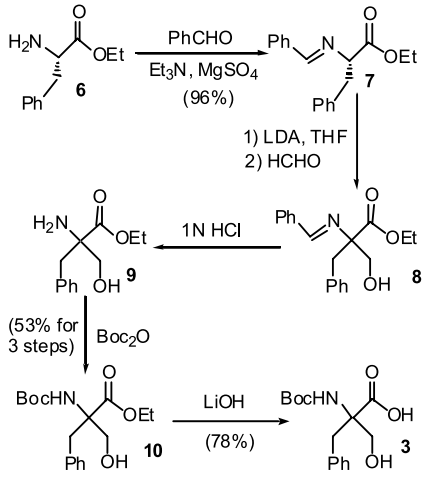

Scheme 2. Synthesis of α-benzyl-serine derivative **3**.

The benzyl ester of azaalanine **4** (Scheme 1) was synthesized from methyl hydrazine and benzyl chloroformate as previously described.[9] In our earlier report, 2-ethoxy-1-ethoxycarbonyl-1,2-dihydroquinoline (EEDQ) was determined to be the most efficient coupling agent for joining azaalanine and serine derivatives. However, attempts to couple the weakly nucleophilic azaalanine with the more hindered serine derivative **3** proved unsucccessful. After screening a variety of coupling agents, the best, albeit modest, yield was obtained by employing *O*-(benzotriazol-1-yl)-1,1,3,3-tetramethyluronium hexafluorophosphate (HATU), which afforded the desired hydrazide **2** in 38% yield (Scheme 3).

Unsatisfied with a modest coupling yield, we explored an alternative approach, which activated the acid group to nucleophilic acyl substitution via a β-lactone. Over the last decade, β-lactone derivatives have been elegantly exploited

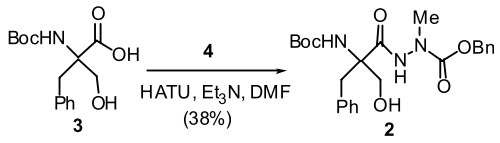

Scheme 3. Coupling of **3** and **4**.

as versatile intermediates.[11] The work of Vederas[12] has permitted the efficient synthesis of β-lactones from serine, however, the vast majority of recent reports with serine β-lactones have focused on reactions at the β-carbon.[12,13] Although there are a few reports that describe reactions at the carbonyl,[14] to the best of our knowledge, there are no reports that describe β-lactones as useful acylating agents for the synthesis of hindered peptides.[15]

Nevertheless, we converted **3** into the corresponding β-lactone **11** (Scheme 4) using triphenylphosphine (Ph_3P) and diethyl azodicarboxylate (DEAD) in 72% yield.[12] Although no reaction occurred when the β-lactone was combined with **4**, pre-activation of **4** by reaction with trimethyl aluminum afforded a dimethylaluminum–hydrazide complex, which efficiently reacted at the acyl group of β-lactone **11** to afford a 68% yield of the desired azapeptide **2**.

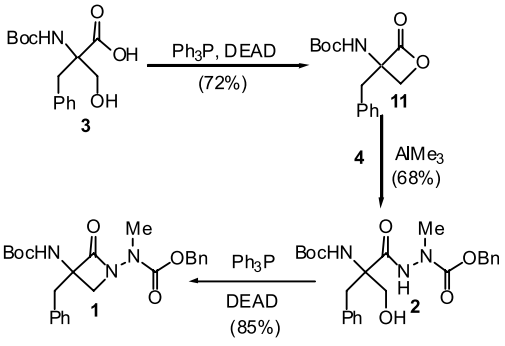

Scheme 4. Synthesis of azadipeptide β-lactam **1**.

With an improved procedure for the synthesis of the serine-azaalanine derivative, **2** was then subjected to Mitsunobu conditions (Ph_3P, DEAD) to afford the desired C-3 benzyl β-lactam azapeptidomimetic **1** in high yield. Elaboration of the azapeptide on the amino and carboxy terminal ends mirrored procedures already described[9] with the exception that the more active coupling agent HATU was used to couple at the hindered amino group to make **12** (Scheme 5). The tetrapeptidomimetic **13** was synthesized in an overall yield of 11% from **6** with the longest linear sequence being 12 steps. This process could be made stereoselective if asymmetric methods of α-alkyl-serine synthesis were applied.[16]

2.2. Azapeptidomimetic γ-butyrolactams and δ-valerolactams

A unified strategy for the synthesis of larger lactams was envisioned in the retrosynthetic plan shown in Scheme 6. Briefly, homologues of serine **16** would be coupled with azaamino acids **4** and the product **15** subjected to Mitsunobu conditions to afford the azapeptidomimetic lactams **14**. The

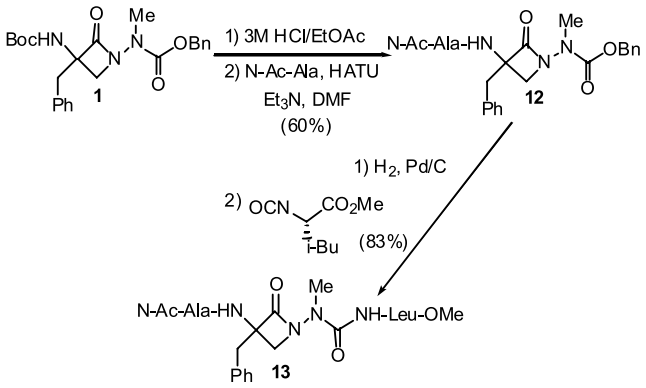

Scheme 5. Elaboration of **1** to a tetrapeptidomimetic β-lactam.

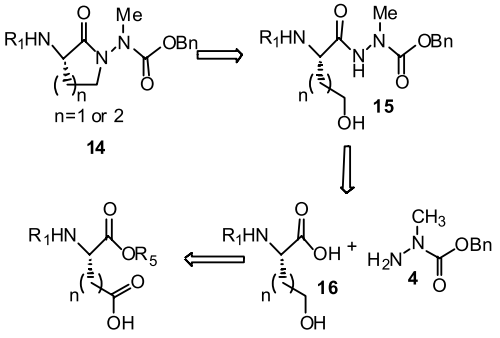

Scheme 6. Retrosynthetic plan for azapeptidomimetic γ-butyrolactams and δ-valerolactams.

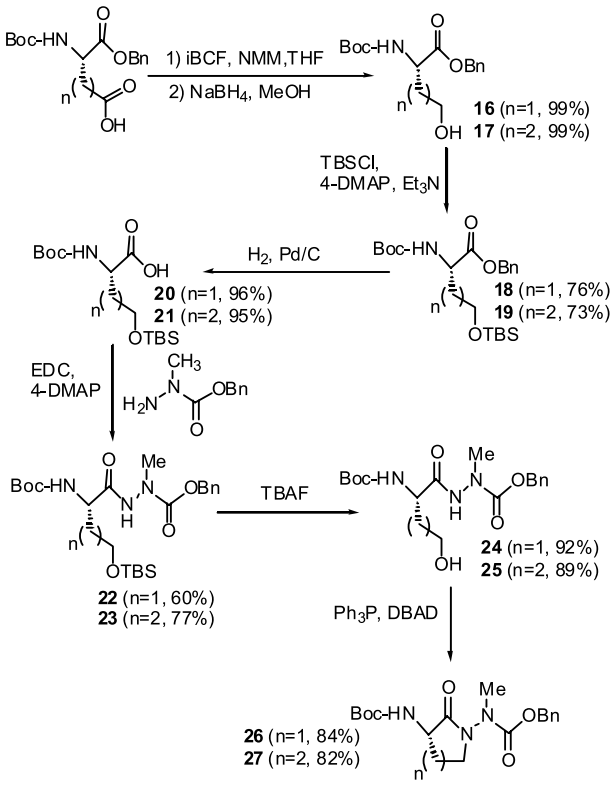

Scheme 7. Synthesis of azapeptidomimetic γ-butyrolactams and δ-valerolactams.

plan called for selective reduction of the side chain carboxylic acid in aspartic and glutamic acid to afford the homologated serine derivatives **16**.

Synthesis of the homologated serine derivatives began with reduction of the commercially available α-benzyl *N*-*tert*-butoxycarbonyl-aspartic acid (Boc-Asp-OBn) and α-benzyl *N*-(*tert*)-butoxycarbonyl-glutamic acid (Boc-Glu-OBn). A modified mixed anhydride/$NaBH_4$ reduction procedure[17] provided alcohols **16** and **17** (Scheme 7) in 99% yield along with some minor contaminant. Protection of the alcohol in **16** and **17** was necessary to avoid side reactions such as competing lactonization. Selective deprotection under hydrogenation conditions ($Pd/C/H_2$) afforded the free acids **20** and **21** in 96 and 95% yield, respectively.

Coupling of the homologated serine derivatives **20** and **21** with benzyl azaalanine **4** was best accomplished with *N*-(3-dimethylaminopropyl)-*N*′-ethylcarbodiimide (EDC) to afford the azadipeptidomimetic structures **22** and **23** in 60 and 77% yield, respectively. EEDQ coupling was unsatisfactory because the quinoline side product was difficult to separate from **22** and **23**. Tetrabutylammonium fluoride (TBAF) mediated deprotection of **22** and **23** provided the alcohol substrates (**24** and **25**) for the lactamization process.

A slight modification to the Mitsunobu conditions used for β-lactam synthesis was required to provide optimized yields of the larger lactam rings. One important side reaction that occurred in the γ-butyrolactam synthesis was a competing intermolecular substitution reaction by the reduced azo dicarboxylate side product.[18] To reduce the intermolecular reaction, azadipeptide concentration was reduced and the temperature was lowered to 0 °C. In addition, the phosphine was combined with the azodicarboxylate and activated prior to introduction of the azadipeptidomimetics **24** and **25**. The modified Mitsunobu conditions afforded the γ-butyrolactam **26** and the δ-valerolactam **27** in 84 and 82%, respectively. Extension of the γ-butyrolactam and δ-valerolactam in the manner shown for **1** in Scheme 5 was successfully accomplished with the methods previously described.[9] Preliminary experiments to form seven or eight member ring azapeptidomimetic lactams have not met with success.

3. Conclusion

Mitsunobu conditions have been successfully applied to the synthesis of three more azapeptidomimetic lactams. The synthesis of a sterically demanding β-lactam azadipeptidomimetic, a γ-butyrolactam and a δ-valerolactam illustrate the versatility of the reported method for the synthesis of peptidomimetic structures with a constraining lactam ring. The reactions described here and in the previous publication[9] demonstrate the ability to create peptidomimetic lactam scaffolds with variations at every peptide residue. Previously reported methods[2,4] have not demonstrated similar versatility.

4. Experimental

4.1. General

Unless otherwise stated, all air- or moisture-sensitive reactions were performed with magnetic stirring in flame-dried glassware under an argon atmosphere using dry, distilled solvents. Tetrahydrofuran (THF) and dichloromethane (CH_2Cl_2) were dried over microwave-activated 4 Å molecular sieves (beads, 8–12 mesh). Triethylamine (Et_3N) was distilled from calcium hydride. All other commercially obtained reagents were used as received. All reactions were monitored by thin-layer chromatography (TLC) using precoated 250 micron softlayer silica gel GF uniplates (Analtech). TLC plates were visualized with UV light (254 nm), ninhydrin, potassium permanganate, or ammonium molybdate sprays. Flash chromatography was performed with the indicated solvent system using 60 Å (230–400 mesh, particle size 0.040–0.063 mm) normal phase silica gel. 'Concentrated' refers to the removal of solvent with a rotary evaporator at normal water aspirator pressure followed by further evacuation with a two-stage mechanical pump unless otherwise indicated. Yields refer to chromatographically and spectroscopically pure compounds, except as otherwise indicated. All new compounds were determined to be >95% pure by NMR, HPLC, GC or elemental analysis as indicated (see Supplementary materials). All melting points were determined with an open capillary. ^1H and ^{13}C NMR spectra were recorded at 300 and 75 MHz, respectively. Chemical shifts were reported in δ values relative to tetramethylsilane in ^1H NMR standard and the solvent peak in ^{13}C NMR. Peak splitting patterns in the NMR are reported as follows: s, singlet; d, doublet; t, triplet; q, quartet; m, multiplet; br, broad. GC analyses were performed with an EI-MS detector fitted with a 30 m×0.25 mm column filled with crosslinked 5% PH ME siloxane (0.25 μm film thickness); gas pressure: 7.63 psi He. The method for analysis of all samples involved heating from 70 to 250 °C (10 °C/min), then from 250 to 260 °C (2 °C/min) and finally holding at 260 °C for 2 min. HPLC analyses were performed with an RID and UV detector at 254 nm fitted with a 5 μ silica gel column (250×4.6 mm); eluted with 90:10 *n*-hexane/IPA at 1 mL/min. Elemental analyses were conducted by QTI, Whitehouse, NJ.

4.1.1. *N*-Benzylidene-L-phenylalanine ethyl ester (7). To a solution of phenylalanine ethyl ester hydrochloride salt 1 (2.88 g, 12.5 mmol) in CH_2Cl_2 (40 mL), triethylamine (5.5 mL) and benzaldehyde (1.32 mL, 13 mmol), anhydrous magnesium sulfate (7 g) was added at room temperature. The mixture was stirred overnight. The resulting mixture was filtered and the filtrate was concentrated to white solid. The product was partitioned between ether (50 mL) and water (100 mL), and the aqueous layer extracted with ether (2×50 mL). The combined ether layers were dried over anhydrous $MgSO_4$, filtered and concentrated to give benzylidene phenylalanine ethyl ester **7** (3.35 g, 96%) as colorless oil, which was used without further purification. The product matched the spectroscopic data for the same compound already reported in the literature.[10]

4.1.2. *N*-Boc-α-benzyl-serine ethyl ester (10). To a cold (−78 °C) solution of diisopropylamine (6.53 mL, 49.8 mmol) in THF (15 mL), butyllithium (1.6 M in hexane, 31.1 mL, 49.8 mmol) was added dropwise and the mixture was stirred at −78 °C for 30 min. To the LDA in THF was then added dropwise a solution of **7** (13.1 g, 46.6 mmol) in THF (50 mL). The mixture was stirred at −78 °C for 30 min and then warmed to 0 °C. Formaldehyde gas [prepared from paraformaldehyde (7.0 g) by heating at 180 °C] was introduced by a stream of nitrogen during a 30 min period. The reaction mixture was then warmed to room temperature and stirred for an hour. The reaction was partitioned between ice-cold ammonium chloride solution (100 mL) and ether (100 mL) and separated. The aqueous layer was extracted with ether and the combined organic layers were dried over anhydrous $MgSO_4$, and concentrated under reduced pressure to give an orange oil **8** (12.6 g crude).

The residue from the hydroxymethylation reaction was treated with 1 N hydrochloric acid solution (70 mL) and stirred for 30 min. The aqueous layer was separated from the orange organic layer and washed with CH_2Cl_2 (10 mL). The aqueous layer was saturated with sodium hydrogen carbonate to pH ~ 8. CH_2Cl_2 (100 mL) was added to the solution, followed by *tert*-butyl dicarbonate (9.20 g, 42.2 mmol). The mixture was stirred for 4 h and separated. The organic layer was washed with saturated NaCl solution, dried over anhydrous $MgSO_4$, and concentrated. The residue was purified by silica gel column chromatography (eluted with hexane/EtOAc 3:1) to give **10** (8.0 g, three steps 53%) as a colorless oil. ^1H NMR ($CDCl_3$) δ 7.22 (m, 3H), 7.08 (m, 2H), 5.39 (s, 1H), 4.18 (m, 3H), 3.86 (d, J=11.2 Hz, 1H), 3.42 (s, br, 1H), 3.37 (d, J=13.6 Hz, 1H), 3.10 (d, J=12.6 Hz, 1H), 1.46 (s, 9H), 1.20 (t, J=6.9 Hz, 3H). ^{13}C NMR ($CDCl_3$) δ 171.2, 154.4, 134.6, 129.3, 129.2, 127.6, 126.3, 79.3, 65.3, 64.8, 61.2, 36.9, 27.6, 13.3. IR (CH_2Cl_2) 3600–2500, 1706, 1498, 1162 cm^{-1}. HRMS calcd for $C_{17}H_{25}NO_5+Na^+$ 346.1630, found 346.1628.

4.1.3. *N*-Boc-α-benzyl-serine (3). To a cold (0 °C) solution of ester **10** (2.43 g, 7.5 mmol) in ethanol (30 mL), lithium hydroxide monohydrate (0.6 g, 14.3 mmol) in water (20 mL) was added. The mixture was then warmed to room temperature and stirred for 4 h. After concentration, the residue was partitioned between water and ether. The water layer was washed with ether twice, then acidified with 1 M HCl and extracted with CH_2Cl_2. The organic layer was washed with saturated NaCl solution, dried over anhydrous $MgSO_4$ and concentrated to give **3** (1.73 g, 78% yield) as a yellow oil. ^1H NMR ($CDCl_3$) δ 7.44 (m, br, 2H), 7.16 (m, 3H), 7.05 (m, 2H), 5.35 (s, 1H), 4.12 (d, J=11.4 Hz, 1H), 3.87 (d, J=11.1 Hz, 1H), 3.26 (d, J=13.6 Hz, 1H), 3.04 (d, J=13.6 Hz, 1H), 1.38 (s, 9H). ^{13}C NMR ($CDCl_3$) δ 174.3, 155.0, 134.4, 129.4, 127.9, 126.6, 79.9, 64.8, 36.6, 27.7. IR ($CDCl_3$) 3415, 2982, 1706, 1498 cm^{-1}. HRMS calcd for $C_{15}H_{21}NO_5+Na^+$ 318.1317, found 318.1327.

4.1.4. *N*-Boc-α-amino-α-benzyl-β-lactone (11). To a cold (−78 °C) solution of triphenylphosphine (2.86 g, 10.9 mmol) in THF (70 mL), diethyl azodicarboxylate (DEAD) (1.72 mL, 10.9 mmol) was added dropwise over 5 min. The solution was stirred at −78 °C for 10 min. A solution of **3** (3.07 g, 10.4 mmol) in THF (15 mL), which

was then added dropwise to the mixture over 30 min. After complete addition, the mixture was stirred at −78 °C for 20 min. The mixture was then slowly warmed to room temperature overnight. The reaction solution was concentrated. The residue was purified by silica gel column chromatography (eluted with hexane/EtOAc 3:1–1:1) to give **11** (2.06 g, 72%) as white crystals, which could be recrystallized from EtOAc/hexane, mp=139–140 °C. R_f=0.43 (3:1 hexane/EtOAc). ^{1}H NMR ($CDCl_3$) δ 7.40–7.23 (m, 5H), 4.99 (s, 1H), 4.66 (s, 1H), 4.31 (d, J=5.0 Hz, 1H), 3.26 (d, J=14.2 Hz, 1H), 3.26 (d, J=14.2 Hz, 1H), 1.44 (s, 4H). ^{13}C NMR ($CDCl_3$) δ 171.3, 154.4, 133.5, 130.1, 129.5, 129.4, 128.3, 81.7, 70.5, 70.2, 39.5, 28.2. IR ($CDCl_3$) 3435, 1838, 1717 cm^{-1}. Anal. Calcd for $C_{15}H_{19}NO_4$: C, 64.97; H, 6.91; N, 5.05. Found C, 64.82; H, 7.11; N, 5.07.

4.1.5. Benzyl *N*-(*tert*-butoxycarbonyl)-α-benzyl-serine-azaalanine (2). To a solution of hydrazine **4**[9] (2.10 g, 11.7 mmol) in CH_2Cl_2 (4 mL), trimethyl aluminum (2.0 M in toluene, 5.83 mL, 11.7 mmol) was added dropwise and stirred at room temperature for 1 h. β-Lactone **11** (1.10 g, 4.66 mmol) in CH_2Cl_2 (4 mL) was added to the mixture and stirred overnight. The mixture was quenched with pH 7 phosphate buffer and extracted with CH_2Cl_2. The organic extracts were combined, dried over anhydrous $MgSO_4$ and concentrated. The residue was purified by silica gel column chromatography (eluted with hexane/EtOAc 1:1–2:1) to give **9** (1.4 g, 68%) as colorless crystal. ^{1}H NMR ($CDCl_3$) δ 8.9 (m, br, 1H), 7.20 (m, 10H), 5.59 (s, 1H), 5.13 (q, J=12.0 Hz, 2H), 4.61 (s, br, 1H), 3.78 (s, br, 1H), 3.41 (s, br, 2H), 3.22 (s, 4H), 1.40 (s, 9H). ^{13}C NMR ($CDCl_3$) δ 173, 157.7, 155.5, 136.0, 130.9, 128.6, 80.5, 68.7, 66.7, 63.7, 38.4, 36.3, 28.6. IR ($CDCl_3$) 3407, 2981, 1715, 1694 cm^{-1}.

4.1.6. 1-[(*N*-Methyl,*N*-benzyloxycarbonyl)-amino]-3-benzyl-3-[(*tert*-butoxycarbonyl)-amino]-2-azetidinone (1). Triphenylphosphine (1.25 g, 4.78 mmol) was added to a solution of **2** (2.08 g, 4.55 mmol) in THF (40 mL) and stirred for 3 min. Diethyl azodicarboxylate (DEAD) (0.753 mL, 4.78 mmol) was added in three portions over 15 min. The mixture was stirred overnight and concentrated. The residue was purified by silica gel column chromatography (eluted with hexane/EtOAc 3:1) to give **1** (1.7 g, 85%) as white crystals, mp=115–116 °C. ^{1}H NMR ($CDCl_3$) δ 7.22 (m, 10H), 5.12 (s, 2H), 4.99 (s, 1H), 3.83 (s, 2H), 3.61 (s, 1H), 3.15 (s, 2H), 2.95 (s, 3H), 1.43 (s, 9H). ^{13}C NMR ($CDCl_3$) δ 166.5, 154.8, 154.2, 135.5, 134.7, 130.0, 128.5, 128.3, 127.9, 127.2, 80.4, 68.3, 65.5, 54.4, 39.1, 35.5, 28.2. IR ($CDCl_3$) cm^{-1}: 3431, 2981, 1784, 1716. Anal. Calcd for $C_{24}H_{29}N_3O_5$: C, 65.59; H, 6.65; N, 9.56. Found C, 65.38; H, 6.74; N, 9.42.

4.1.7. 1-[(*N*-Methyl,*N*-benzyloxycarbonyl)-amino]-3-benzyl-3-[(*N*-acetyl-L-alanine)amino]-2-azetidinone (12). To a cold (0 °C) solution of 3 N HCl/EtOAc (15 mL), β-lactam **1** (1.46 g, 3.32 mmol) was added and the reaction was stirred, while slowly warming to room temperature. After 1.5 h, the reaction was stopped and concentrated in vacuo. Reconcentration from $CHCl_3$ gave 1.6 g crude **12** as the hydrochloride salt. ^{1}H NMR (CD_3OD) δ 9.40 (br s, 2H), 7.26 (m, 10H), 4.93 (q, J=12, 16.8, 12.0 Hz, 2H), 4.17 (s, 1H), 3.67 (s, 1H), 3.48 (br s, 2H), 2.92 (s, 3H). Crude **12** (1.6 g), *N*-acetyl-L-alanine (0.48 g, 3.65 mmol) and HATU (1.26 g, 3.32 mmol) were dissolved in DMF (15 mL). The mixture was cooled to 0 °C and treated with Et_3N (0.925 mL, 6.64 mmol). Stirring was continued in the ice bath for 1 h and then the reaction was warmed to room temperature and stirred overnight. The reaction was diluted with H_2O (30 mL), extracted with ethyl acetate (4×10 mL), The combined organic layers were washed with 1 N HCl (2×10 mL), 5% $NaHCO_3$ (2×10 mL), brine (10 mL), anhydrous $MgSO_4$ and concentrated. The residue was purified by silica gel column chromatography (eluted with 5% MeOH/CH_2Cl_2) to give **12** (0.9 g, 60%) as an oil. The oil was crystallized in cold EtOAc to a white solid, mp=174–178 °C. ^{1}H NMR ($CDCl_3$) δ 7.25 (m, 10H), 6.90 (d, rotamer, 1H), 6.15 (d, rotamer, 1H), 5.10 (q, J=19.2, 12.0 Hz, 2H), 4.42 (q, J=15, 7.2 Hz, 1H), 3.86 (br s, 1H), 3.61 (br s, 1H), 3.12 (br s, 2H), 3.01 (s, rotamer, 2H), 2.88 (s, rotamer, 1H), 1.94 (s, 3H), 1.27 (d, J=7.2 Hz, 3H). ^{13}C NMR ($CDCl_3$) δ 172.7, 170.7, 155.4, 136.0, 134.7, 129.0, 127.9, 68.8, 65.9, 54.2, 49.0, 39.2, 35.7, 23.4, 18.2. IR ($CDCl_3$) 3428, 3052, 2988, 1788, 1721, 1687, 1421, 1264 cm^{-1}. HRMS calcd for $C_{24}H_{28}N_4O_5$+Na^+475.1957, found 475.1971.

4.1.8. 1-[(*N*-Methyl)-amino]-3-benzyl-3-[(*N*-acetyl-L-alanine)amino]-2-azetidinone. β-Lactam **12** (0.45 g, 0.99 mmol) was dissolved in methanol (10 mL) at room temperature under nitrogen, and Pd/C (4.5 mg) was added to the solution. The reaction atmosphere was purged with H_2, stirring for 30 min. The reaction material was filtered through Celite and concentrated to a white solid (0.30 g, 95%), which was used immediately without further purification. ^{1}H NMR (CD_3OD) δ 7.26 (m, 5H), 4.31 (m, 1H), 3.60 (dd, J=4.8, 2.4 Hz, 1H), 3.50 (dd, J=13.2, 5.1 Hz, 1H), 3.13 (d, J=7.2 Hz, 2H), 2.16 (d, J=18.6 Hz, 3H), 1.95 (s, 3H), 1.30 (dd, J=9.9, 7.2 Hz, 3H). ^{13}C NMR ($CDCl_3$) δ 175.5, 173.6, 169.3, 136.2, 132.1, 130.0, 128.8, 66.5, 53.8, 52.9, 36.0, 23.0, 18.5. IR ($CDCl_3$) 3295, 3294, 1752, 1654, 1542 cm^{-1}.

4.1.9. 1-[[*N*-Methyl,*N*-carbonyl-L-(methylleucyl)]-amino]-3-benzyl-3-[(*N*-acetyl-L-alanine)amino]-2-azetidinone (13). 1-[(*N*-Methyl)-amino]-3-benzyl-3-[(*N*-acetyl-L-alanine)amino]-2-azetidinone (0.30 g, 0.94 mmol) was dissolved in a mixture of dry CH_2Cl_2 (8 mL) and DMF (5 mL), and cooled to 0 °C under N_2. Leucine isocyanate, methyl ester[19] (0.34 g, 2 mmol) was added as a CH_2Cl_2 solution (4 mL). *N*,*N*-diisopropylethylamine (0.44 mL, 2.5 mmol) was added 2 min later. The solution was stirred and allowed to slowly warm to room temperature. After 20 h, the reaction was quenched with 10% citric acid (15 mL) and extracted with EtOAc (2×15 mL). The organic layer was washed with 10% citric acid (1×10 mL), H_2O (1×10 mL), brine (1×10 mL), dried over anhydrous $MgSO_4$ and concentrated to give crude white wet crystals (0.48 g). The residue was purified by silica gel column chromatography (5% MeOH/CH_2Cl_2) to give **13** (0.40 g, 87%) as an oil. The oil was crystallized in EtOAc/hexanes, mp=155–158 °C. ^{1}H NMR ($CDCl_3$) as rotamers δ 7.84 (s, 0.5H), 7.74 (s, 0.5H), 7.32 (m, 5H), 4.57 (dt, J=7.2, 2.7 Hz, 1H), 4.40 (m, 0.5H), 4.29 (m, 0.5H), 3.91 (d, J=5.1 Hz, 0.5H), 3.80 (d, J=5.1 Hz, 0.5H), 3.66 (s, 3H), 3.55 (dd, J=7.5, 5.1 Hz, 1H), 3.24 (t, J=13.8 Hz, 1H), 3.04 (dd, J=13.5, 7.8 Hz, 1H), 2.38 (d, J=12.9 Hz, 3H), 2.00 (d,

J=5.7 Hz, 3H), 1.75 (m, 1H), 1.60 (m, 2H), 1.35 (t, J= 6.9 Hz, 3H), 0.87 (m, 6H). ^{13}C NMR ($CDCl_3$) as rotamers δ 175.0, 174.3, 173.1, 172.8, 171.5, 170.8, 167.5, 167.0, 157.3, 133.0, 130.9, 129.0, 128.2, 66.0, 52.8, 52.5, 52.3, 52.2, 50.9, 50.8, 49.0, 48.8, 40.7, 40.2, 38.5, 38.4, 36.8, 25.1, 24.8, 23.4, 23.3, 21.7, 21.6, 18.0, 17.3. IR (neat) 3293, 2958, 1787, 1753, 1654, 1551 cm^{-1}. HRMS calcd for $C_{24}H_{35}N_5O_6+Na^+$512.2486, found 512.2490.

4.1.10. (2*S*)-2-*tert*-Butoxycarbonylamino-4-hydroxybutyric acid benzyl ester (16). Boc-Asp-OBn (3.00 g, 9.28 mmol) was dissolved in dry THF (46 mL) and cooled to −15 °C. 4-Methylmorpholine (1.02 mL, 9.28 mmol) was added, followed by dropwise addition of isobutyl chloroformate (1.20 mL, 9.28 mmol) to give a white suspension, which was stirred for 10 min. Sodium borohydride (1.05 g, 27.8 mmol) was added, followed by dropwise addition of anhydrous MeOH (93 mL) through a pressure-equalized dropping funnel, which lead to gaseous evolution. The reaction was stirred an additional 10 min after the MeOH addition, and 1 M aqueous HCl (18.6 mL) was added dropwise. The reaction was concentrated and the remaining crude mixture was extracted with EtOAc (3×65 mL), and the combined organic layers were washed with 1 M HCl (1×37 mL), H_2O (2×45 mL), 5% $NaHCO_3$ (1×46 mL), H_2O (3×45 mL), and dried over Na_2SO_4. The crude product was concentrated and purified by flash chromatography (3:7–1:1 EtOAc/Hexanes). Compound **16** was isolated as a clear, colorless viscous oil in 99.4% yield (2.85 g) with some minor contamination clearly visible in ^{1}H and ^{13}C NMR. The product matched the spectroscopic data for the same compound already reported in the literature.[20]

4.1.11. (2*S*)-2-*tert*-Butoxycarbonylamino-5-hydroxypentanoic acid benzyl ester (17). Reaction procedure identical to **16** except Boc-Glu-OBn was used. Column chromatography provided a clear, colorless viscous oil in 98.6% yield with some minor contamination clearly visible in ^{1}H and ^{13}C NMR. The product matched the spectroscopic data for the same compound already reported in the literature.[20,21]

4.1.12. (2*S*)-2-*tert*-Butoxycarbonylamino-4-(*tert*-butyldimethyl-silanyloxy)-butyric acid benzyl ester (18). To a solution of **16** (2.77 g, 8.94 mmol) in 25 mL dry CH_2Cl_2, was added Et_3N (1.49 mL, 10.7 mmol), 4-DMAP (54.6 mg, 0.45 mmol), and TBDMS-Cl (1.48 g, 9.83 mmol) to give a clear, colorless solution, which was stirred overnight. The colorless suspension was then washed with H_2O (1×4 mL), saturated aqueous NH_4Cl (1×4 mL), and dried over Na_2SO_4. The organic layer was concentrated and purified by flash chromatography (1:4 EtOAc/Hexanes) to afford a clear, colorless oil in 76% yield. ^{1}H NMR ($CDCl_3$) δ 7.35 (s, 5H), 5.73 (br s, 1H), 5.18 (q, J=15.6, 12.4 Hz, 2H), 4.43 (br s, 1H), 3.75–3.60 (m, 2H), 2.15–1.85 (m, 2H), 1.43 (s, 9H), 0.90 (s, 9H), 0.04 (s, 6H). ^{13}C NMR ($CDCl_3$) δ 172.57, 155, 135.88, 128.71, 128.44, 128.38, 79.64, 67.00, 60.36, 52.76, 33.96, 28.51, 26.04, 18.32, −5.43, −5.47. IR (CH_2Cl_2) 3409, 2957, 2931, 2858, 1720 cm^{-1}. GC: room temperature 17.49 min. HRMS calcd for $C_{22}H_{37}NO_5Si+Na^+$446.2339, found 446.2345.

4.1.13. (2*S*)-2-*tert*-Butoxycarbonylamino-5-(*tert*-butyldimethyl-silanyloxy)-pentanoic acid benzyl ester (19). Reaction procedure identical to **18** except **17** was used as the starting material. Column chromatography provided a clear, colorless oil in 72.7% yield. ^{1}H NMR ($CDCl_3$) δ 7.35 (s, 5H), 5.30–5.10 (m, 3H), 4.35 (br s, 1H), 3.70–3.50 (m, 2H), 2.00–1.50 (m, 4H), 1.44 (s, 9), 0.89 (s, 9H), 0.04 (s, 6H). ^{13}C NMR ($CDCl_3$) δ 172.90, 155, 135.74, 128.76, 128.52, 128.40, 80, 67.10, 62.48, 53.59, 29.30, 28.63, 28.53, 26.13, 18.49, −5.16. IR (CH_2Cl_2) 3361, 2956, 2930, 2887, 2858, 1718 cm^{-1}. GC: room temperature 18.32 min. HRMS calcd for $C_{23}H_{39}NO_5Si+Na^+$460.2495, found 460.2494.

4.1.14. 2-*tert*-Butoxycarbonylamino-4-(*tert*-butyldimethyl-silanyloxy)-butyric acid (20). To a solution of **18** (2.82 g, 6.65 mmol) in MeOH (12 mL) was added 0.28 g 10% Pd/C to give a black suspension, which was evacuated and flushed with hydrogen three times before being stirred under hydrogen for 5 h. The black suspension was evacuated and flushed with argon, filtered through a pad of Celite and concentrated to give a clear, colorless viscous oil in 95.9% yield (2.13 g), which was used without further purification. ^{1}H NMR ($CDCl_3$) δ 8.47 (br s, 1H), 5.85 (br s, 1H), 4.33 (br s, 1H), 2.20–1.90 (m, 2H), 1.44 (s, 9H), 0.91 (s, 9H), 0.07 (s, 6H). ^{13}C NMR ($CDCl_3$) δ 175.73, 155.88, 81.04, 66.16, 50.63, 45.65, 31.04, 28.72, 28.66, 26.19, 26.04, 8.86. IR (CH_2Cl_2) 3409, 2931, 1686 cm^{-1}.

4.1.15. (2*S*)-2-*tert*-Butoxycarbonylamino-5-(*tert*-butyldimethyl-silanyloxy)-pentanoic acid (21). Reaction procedure identical to **20** except **19** was used and a clear, colorless viscous oil was obtained in 95.1% yield, which was used without further purification. ^{1}H NMR ($CDCl_3$) δ 10.10 (br s, 1H), 5.31 (br s, 1H), 4.29 (br s, 1H), 3.66 (t, J= 5.9 Hz, 2H), 2.00–1.55 (m, 4H), 1.45 (s, 9H), 0.90 (s, 9H), 0.06 (s, 6H). ^{13}C NMR ($CDCl_3$) δ 156.29, 80.56, 67, 63.07, 53.64, 28.63, 26.03, 25.87, 18.75, 18.37, 17.98, −3.21, −4.95, −4.99. IR (CH_2Cl_2) 3345, 2931, 2859, 1715 cm^{-1}. HRMS calcd for $C_{16}H_{33}NO_5Si+Na^+$370.2026, found 370.2038.

4.1.16. (2*S*)-*N*′-[2-*tert*-Butoxycarbonylamino-4-(*tert*-butyl-dimethyl-silanyloxy)-butyryl]-*N*-methyl-hydrazinecarboxylic acid benzyl ester (22). To a solution of **20** (2.13 g, 6.39 mmol) in 17.0 mL dry CH_2Cl_2 at −15 °C were added **4**[9] (1.10 g, 6.09 mmol) in 6.50 mL, dry CH_2Cl_2, EDC (1.40 g, 7.30 mmol), and 4-DMAP (0.82 g, 6.69 mmol) to give a light buff suspension, which was allowed to warm to room temperature overnight. The clear, light buff solution was washed with H_2O (1×4 mL), brine (1×4 mL), and dried over Na_2SO_4. The organic layer was concentrated and purified by flash chromatography (1:4–1:1 EtOAc/Hexanes) to afford a clear, colorless viscous oil in 60.0% yield (1.81 g). ^{1}H NMR ($CDCl_3$) δ 8.58 (br s, 1H), 7.32 (s, 5H), 5.87 (br s, 1H), 5.25–5.00 (m, 2H), 4.24 (br s, 1H), 4.00–3.50 (br m, 2H), 3.19 (s, 3H), 1.92 (br s, 2H), 1.42 (s, 9H), 0.90 (s, 9H), 0.05 (s, 6H). ^{13}C NMR ($CDCl_3$) δ 171, 156.15, 136, 128.66, 128.36, 128.21, 80, 68.23, 61.06, 52, 37, 34, 28.48, 26.02, 18.24, −5.38, −5.46. IR (CH_2Cl_2) 3314, 2956, 2930, 1694 cm^{-1}. GC: room temperature 15.77 min. HRMS calcd for $C_{24}H_{41}N_3O_6Si+Na^+$518.2662, found 518.2679.

4.1.17. (2*S*)-*N*′-[2-*tert*-Butoxycarbonylamino-5-(*tert*-butyl-dimethyl-silanyloxy)-pentanoyl]-*N*-methyl-hydrazinecarboxylic acid benzyl ester (23). Reaction procedure identical to **22** except **21** was used. Purification by flash chromatography provided a clear, colorless viscous oil in 76.9% yield. ^{1}H NMR ($CDCl_3$) δ 8.53 (br s, 1H), 7.26 (s, 5H), 4.95–5.40 (m, 3H), 4.13 (br s, 1H), 3.56 (br s, 2H), 3.18 (s, 3H), 1.50–2.00 (m, 4H), 1.42 (s, 9H), 0.89 (s, 9H), 0.06 (s, 6H). ^{13}C NMR ($CDCl_3$) δ 171, 156.34, 156.17, 136.35, 128.87, 128.59, 128.51, 80.60, 68.48, 63.43, 52.86, 29.49, 28.70, 28.37, 26.37, 18.75, 1.42, −4.93, −5.02. IR (CH_2Cl_2) 3293, 2955, 2930, 2858, 1680 cm^{-1}. GC: room temperature 16.67 min. HRMS calcd for $C_{25}H_{43}N_3O_6Si+Na^+$532.2819, found 532.2837.

4.1.18. (2*S*)-*N*′-(2-*tert*-Butoxycarbonylamino-4-hydroxy-butyryl)-*N*-methyl-hydrazinecarboxylic acid benzyl ester (24). To a solution of **22** (1.00 g, 2.02 mmol) in dry THF (8.1 mL) at −15 °C was added TBAF as a 1.0 M solution in THF (2.06 mL, 2.06 mmol). The reaction was stirred for 1 h at −15 °C and 30 min at room temperature. The clear, light brown solution was recooled to 0 °C, and 2 mL aqueous saturated NH_4Cl were added. This mixture was diluted to about 50 mL with EtOAc, washed with brine (1×2 mL), and dried over Na_2SO_4. The organic layer was concentrated to a clear, light brown oil, which was purified by flash chromatography 70% EtOAc/Hexanes to 100% EtOAc to afford a white foam in 91.5% yield (0.704 g). ^{1}H NMR ($CDCl_3$) δ 9.45 (br s, 1H), 7.32 (br s, 5H), 5.66 (br s, 1H), 5.12 (br s, 2H), 4.40 (br s, 1H), 3.8–3.6 (m, 2H), 3.18 (s, 3H), 1.85 (m, 2H), 1.42 (s, 9H). ^{13}C NMR ($CDCl_3$) δ 171.96, 171.81, 171.355, 156.92, 156.22, 136.23, 128.91, 128.74, 128.68, 128.45, 125.92, 80.99, 68.58, 58.46, 50.14, 49.80, 38.386, 37.77, 36.59, 30.72, 28.64. IR (CH_2Cl_2) 3299, 2978, 1688 cm^{-1}. HPLC: room temperature 10.86 min. HRMS calcd for $C_{18}H_{27}N_3O_6+Na^+$404.1798, found 404.1812.

4.1.19. (2*S*)-*N*′-(2-*tert*-Butoxycarbonylamino-5-hydroxy-pentanoyl)-*N*-methyl-hydrazinecarboxylic acid benzyl ester (25). Reaction procedure identical to **24** except **23** was used and a white foam was obtained in 89.0% yield. Spectral data suggest contamination with hydrate or TBDMS deprotection byproduct. ^{1}H NMR ($CDCl_3$) δ 9.19, (br s, 1H), 7.32 (br s, 5H), 5.75–5.35 (m, 1H), 5.21 (br s, 2H), 4.45–4.15 (br m, 1H), 3.80–3.30 (m, 3H), 2.00–1.10 (m, 13H). ^{13}C NMR ($CDCl_3$) δ 172, 156, 136, 128.91, 128.68, 81, 68.61, 62.69, 52, 37, 30, 28.70, 27.93. IR (CH_2Cl_2) 3424, 2978, 1686 cm^{-1}. HPLC: room temperature 13.47 min. GC: room temperature 14.60 min. HRMS calcd for $C_{19}H_{29}N_3O_6+Na^+$418.1954, found 418.1964.

4.1.20. (2*S*)-(3-*tert*-Butoxycarbonylamino-2-oxo-pyrrolidin-1-yl)-methyl-carbamic acid benzyl ester (26). Triphenylphosphine (0.30 g, 1.15 mmol), DBAD (0.26 g, 1.15 mmol), and anhydrous THF (40 mL) were stirred at room temperature for 10 min and cooled to 0 °C. The contents of this flask were then cannulated into a solution of **24** (0.400 g, 1.05 mmol) in anhydrous THF (52 mL) at 0 °C, and the solution was stirred overnight at 0 °C. The clear, colorless solution was then concentrated and purified by flash chromatography 3:7–1:1 EtOAc/Hexanes to provide a colorless glass in 84% yield (0.32 g). ^{1}H NMR as rotamers ($CDCl_3$) δ 7.45–7.25 (m, 5H), 5.3–4.9 (m, 3H), 4.65–4.00 (m, 1.3H), 3.70–3.30 (m, 1.7H), 3.25–3.10 (m, 3H), 2.80–2.50 (br m, 1H), 2.15–1.80 (m, 1H), 1.45 (s, 9H). ^{13}C NMR ($CDCl_3$) as rotamers δ 171.07, 155.99, 155.31, 137.06, 136.83, 136.11, 129.01, 128.95, 128.83, 128.74, 128.53, 128.37, 128.31, 128.24, 80.57, 70.39, 68.69, 68.07, 67.83, 66.16, 50.85, 50.55, 44.46, 43.99, 43.51, 36.63, 35.84, 35.18, 31.04, 28.96, 28.71, 27.67, 27.36. IR (CH_2Cl_2) 3348, 2978, 1710 cm^{-1}. GC: room temperature 18.73 min. EI-MS *m/z* (rel int.): 363.10 (0.06, $M^{+\cdot}$), 307 (6, M^+-56), 172 (11, M^+-191), 91 (100, $^+CH_2Ph$). HRMS calcd for $C_{18}H_{25}N_3O_5+Na^+$386.1692, found 386.1681.

4.1.21. (2*S*)-(3-*tert*-Butoxycarbonylamino-2-oxo-piperidin-1-yl)-methyl-carbamic acid benzyl ester (27). Reaction procedure identical to **26** except **25** was used and a clear, colorless viscous oil was obtained in 82% yield (0.16 g). ^{1}H NMR ($CDCl_3$) as rotamers δ 7.40–7.20 (m, 5H), 5.45–5.00 (m, 3H), 4.30–3.90 (m, 1H), 3.75–3.35 (m, 2H), 3.20–3.00 (m, 3H), 2.50–2.30 (m, 1H), 2.10–1.55 (m, 3H), 1.45 (m, 9H). ^{13}C NMR ($CDCl_3$) as rotamers δ 169, 168, 156, 156.5, 128.73, 128.48, 128.19, 128.14, 127.75, 80, 68.25, 52, 50.5, 50, 39, 38, 36.17, 35.43, 34, 28.52, 27, 21.16, 21, 20. IR (CH_2Cl_2) 3416, 2976, 1715, 1678 cm^{-1}. GC: room temperature 19.21 min. EI-MS *m/z* (rel. int.): 377 (0.04, $M^{+\cdot}$), 321 (16, M^+-56), 186 (8, M^+-191), 120 (14, M^+-257), 91 (100, $^+CH_2Ph$). HRMS calcd for $C_{19}H_{27}N_3O_5+Na^+$400.1848, found 400.1843.

Acknowledgements

We gratefully acknowledge financial support from the National Science Foundation and Bryn Mawr College.

Supplementary data

Supplementary data associated with this article can be found, in the online version, at doi:10.1016/j.tet.2005.08.029. Copies of ^{1}H/^{13}C NMR spectra for compounds **1**–**3**, **7**, **10**–**13**, **18**–**27** and the precursor to **13**. A copy of the ^{1}H NMR of the precursor to **12**. A copy of HPLC data for compound **24**. Copies of GC data for compounds **18**, **19**, **22**, **23**, and **25**–**27**. Copies of IR and MS data for compounds **26** and **27**.

References and notes

1. A recent selection of peptidomimetics reviews: (a) Martin-Martinez, M.; Patino-Molina, R.; Garciα-Lopez, M. T.; Gonzalez-Muniz, R. *Mini-Rev. Med. Chem.* **2004**, *4*, 669–680. (b) Holder, J. R.; Haskell-Luevano, C. *Med. Res. Rev.* **2004**, *24*, 325–356. (c) Andronati, S. A.; Karaseva, T. L.; Krysko, A. A. *Curr. Med. Chem.* **2004**, *11*, 1183–1211. (d) Schiller, P. W.; Weltrowska, G.; Schmidt, R.; Nguyen, T. M.-D.; Berezowska, I.; Lemieux, C.; Ngoc, N. N.; Carpenter, K. A.; Wilkes, B. C. *Drug Discovery Strategies and Methods* **2004**, 147–173. (e) Belvisi, L.; Colombo, L.; Manzoni, L.;

Potenza, D.; Scolastico, C. *Synlett* **2004**, *9*, 1449–1471. (f) Freidinger, R. M. *J. Med. Chem.* **2003**, *46*, 5553–5566. (g) Nakanishi, H.; Kahn, M.; Ibsen, H. Design of peptidomimetics. In *Practice of Medical Chemistry* 2nd ed.; 2003; pp 477–500. (h) Derian, C. K.; Maryanoff, B. E.; Andrade-Gordon, P.; Zhang, H.-C. *Drug Dev. Res.* **2003**, *59*, 355–366. (i) Luthman, K.; Hacksell, U. Peptides and peptidomimetics. In *Textbook of Drug Design and Discovery* 3rd ed.; 2002; pp 459–485.

2. (a) Freidinger, R. M.; Veber, D. F.; Perlow, D. S.; Brooks, J. R.; Saperstein, R. *Science* **1980**, *210*, 656–658. (b) Freidinger, R. M.; Perlow, D. S.; Veber, D. F. *J. Org. Chem.* **1982**, *47*, 104–109. (c) Bell, I. M.; Beshore, D. C.; Gallicchio, S. N.; Williams, T. M. *Tetrahedron Lett.* **2000**, 1141–1145.
3. (a) Cascieri, M. A.; Chicchi, G. G.; Freidinger, R. M.; Colton, C. D.; Perlow, D. S.; Williams, B.; Curtis, N. R.; McKnight, A. T.; Maguire, J. J.; Veber, D. F.; Liang, T. *Mol. Pharmacol.* **1986**, *29*, 34–38. (b) Freidinger, R. M.; Perlow, D. S.; Randall, W. C.; Saperstein, R.; Arison, B. H.; Veber, D. F. *Int. J. Pept. Protein Res.* **1984**, *23*, 142–150. (c) Thorsett, E. D.; Harris, E. E.; Aster, S. D.; Peterson, E. R.; Taub, D.; Patchett, A. A. *Biochem. Biophys. Res. Commun.* **1983**, *111*, 166–171. (d) Thorsett, E. D.; Harris, E. E.; Aster, S. D.; Peterson, E. R.; Tristram, E. W.; Snyder, J. P.; Springer, J. P.; Patchett, A. A. In *Peptides, Structure and Function*, Proceedings of the Eighth American Peptide Symposium; Pierce Chemical Company: Rockford, IL, 1983; pp 555–558. (e) Aubé, J. In *Advances in Amino Acid Mimetics and Peptidomimetics*, *Vol. 1*; JAI: Greenwich, CT, 1997; pp 193–232. (f) Halab, L.; Gosselin, F.; Lubell, W. D. *Biopolymers (Pept. Sci.)* **2000**, *55*, 101–122. (g) Simpson, J. C.; Ho, C.; Shands, E. F. B.; Gershengorn, M. C.; Marshall, G. R.; Moeller, K. D. *Bioorg. Med. Chem.* **2002**, *10*, 291–302. (h) Hoffmann, T.; Waibel, R.; Gmeiner, P. *J. Org. Chem.* **2003**, *68*, 62–69.
4. (a) Palomo, C.; Aizpurua, J. M.; Benito, A.; Miranda, J. I.; Fratila, R. M.; Matute, C.; Domercq, M.; Gago, F.; Martin-Santamaria, S.; Linden, A. *J. Am. Chem. Soc.* **2003**, *125*, 16243–16260. (b) Palomo, C.; Aizpurua, J. M.; Benito, A.; Galarza, R.; Khamrai, U. K.; Vazquez, J.; de Pascual-Teresa, J.; Nieto, P. M.; Linden, A. *Angew. Chem., Int. Ed.* **1999**, *38*, 3056–3058.
5. (a) Achilles, K.; Schneider, M.; Schirmeister, T.; Otto, H.-H. *Pharmazie* **2000**, *55*, 798. (b) Achilles, K.; Schirmeister, T.; Otto, H.-H. *Arch. Pharm.* **2000**, *333*, 243.
6. (a) Zega, A. *Curr. Med. Chem.* **2005**, *12*, 589–597. (b) Gante, J. *Synthesis* **1989**, 405–413.
7. (a) Che, Ye.; Marshall, G. R. *J. Org. Chem.* **2004**, *69*, 9030–9042. (b) Melendez, R. E.; Lubell, W. D. *J. Am. Chem. Soc.* **2004**, *126*, 6759–6764.
8. (a) Bailey, M. D.; Halmos, T.; Goudreau, N.; Lescop, E.; Llinas-Brunet, M. *J. Med. Chem.* **2004**, *47*, 3788–3799. (b) Ekici, O. D.; Goetz, M. G.; James, K. E.; Li, Z. Z.; Rukamp, B. J.; Asgian, J. L.; Caffrey, C. R.; Hansell, E.; Dvorak, J.; McKerrow, J. H.; Potempa, J.; Travis, J.; Mikolajczyk, J.; Salvesen, G. S.; Powers, J. C. *J. Med. Chem.* **2004**, *47*, 1889–1892. (c) James, K. E.; Asgian, J. L.; Li, Z. Z.; Ekici, O. D.; Rubin, J. R.; Mikolajczyk, J.; Salvesen, G. S.; Powers, J. C. *J. Med. Chem.* **2004**, *47*, 1553–1574. (d) Bouget, K.; Aubin, S.; Delcros, J.-G.; Arlot-Bonnemains, Y.; Baudy--Floc'h, M. *Bioorg. Med. Chem.* **2003**, *11*, 4881–4889.
9. Malachowski, W. P.; Tie, C.; Wang, K.; Broadrup, R. L. *J. Org. Chem.* **2002**, *67*, 8962.
10. Calcagni, A.; Rossi, D.; Lucente, G. *Synthesis* **1981**, 445–447.
11. For reviews of β-lactone synthesis and reactions see: (a) Yang, H. W.; Romo, D. *Tetrahedron* **1999**, *55*, 6403–6434. (b) Pommier, A.; Pons, J.-M. *Synthesis* **1993**, 441–459.
12. (a) Arnold, L. D.; Kalantar, T. H.; Vederas, J. C. *J. Am. Chem. Soc.* **1985**, *107*, 7105–7109. (b) Ramer, S. E.; Moore, R. N.; Vederas, J. C. *Can. J. Chem.* **1986**, *64*, 706. (c) Pansare, S. V.; Huyer, G.; Arnold, L. D.; Vederas, J. C. *Org. Synth.* **1991**, *70*, 1.
13. (a) Arnold, L. D.; Drover, J. C. G.; Vederas, J. C. *J. Am. Chem. Soc.* **1987**, *109*, 4649–4659. (b) Arnold, L. D.; May, R. G.; Vederas, J. C. *J. Am. Chem. Soc.* **1988**, *110*, 2237–2241. (c) Pansare, S. V.; Vederas, J. C. *J. Org. Chem.* **1989**, *54*, 2311–2316. (d) Shao, H.; Wang, S. H. H.; Lee, C. W.; Osapay, G.; Goodman, M. *J. Org. Chem.* **1995**, *60*, 2956–2957. (e) Smith, N. D.; Goodman, M. *Org. Lett.* **2003**, *5*, 1035–1037. (f) Smith, N. D.; Wohlrab, A. M.; Goodman, M. *Org. Lett.* **2005**, *7*, 255–258.
14. (a) Sheehan, J. C.; Hasspacher, K.; Yeh, Y. L. *J. Am. Chem. Soc.* **1959**, *81*, 6086. (b) Shanzer, A.; Libman, J. *J. Chem. Soc., Chem. Commun.* **1983**, 846–847.
15. For an example of an aluminum-mediated hydroxamate ring-opening of a β-lactone see: Nelson, S. G.; Cheung, W. S.; Kassick, A. J.; Hifiker, M. A. *J. Am. Chem. Soc.* **2002**, *124*, 13654–13655.
16. For a selection of asymmetric α-alkyl-serine syntheses see: (a) Groth, U.; Chiang, Y.-C.; Schollkopt, U. *Liebigs Ann. Chem.* **1982**, 1756–1757. (b) Sano, S.; Miwa, T.; Liu, X.-K.; Ishii, T.; Takehisa, T.; Shiro, M.; Nagao, Y. *Tetrahedron: Asymmetry* **1998**, *9*, 3615–3618. (c) Seebach, D.; Aebi, J. D.; Gander-Coquoz, M.; Naef, R. *Helv. Chim. Acta* **1987**, *70*, 1194–1216. (d) Moon, S. H.; Ohfune, Y. *J. Am. Chem. Soc.* **1994**, *116*, 7405–7406.
17. Sibrian-Vazquez, M.; Spivak, D. A. *Synlett* **2002**, *7*, 1105.
18. *O*-alkylation has been seen with the related Mitsunobu reaction of acyl hydroxamates in e-caprolactam synthesis, see for example: (a) Maurer, P. J.; Miller, M. J. *J. Am. Chem. Soc.* **1983**, *105*, 240–245. (b) Maurer, P. J.; Miller, M. J. *J. Org. Chem.* **1981**, *46*, 2835–2836. Nevertheless, we did not see any *O*-alkylation products based on a close analysis of NMR and IR (see supplementary materials).
19. (a) Nowick, J. S.; Powell, N. A.; Nguyen, T. M.; Noronha, G. *J. Org. Chem.* **1992**, *57*, 7364. (b) Tsai, J. H.; Takaoka, L. R.; Powell, N. A.; Nowick, J. S. *Org. Synth.* **2000**, *78*, 220.
20. Jackson, R. F. W.; Moore, R. J.; Dexter, C. S.; Elliott, J.; Mowbray, C. E. *J. Org. Chem.* **1998**, *63*, 7875.
21. Yokokawa, F.; Inaizumi, A.; Shioiri, T. *Tetrahedron* **2005**, *61*, 1459–1480.

Available online at www.sciencedirect.com
SCIENCE DIRECT
Tetrahedron
ELSEVIER
Tetrahedron 61 (2005) 10285–10290

Biomimic transformation of resveratrol

Yoshiaki Takaya, Kenji Terashima, Junko Ito, Yue-Hua He, Maki Tateoka, Naho Yamaguchi and Masatake Niwa*

Faculty of Pharmacy, Meijo University, Tempaku, Nagoya, 468-8503, Japan

Received 20 July 2005; revised 4 August 2005; accepted 5 August 2005

Available online 24 August 2005

Abstract—Resveratrol was treated with several kinds of peroxidases and inorganic reagents so as to prepare ε-viniferin. Among several inorganic reagents, which were investigated in this study, thallium(III) nitrate in methanol gave (±)-ε-viniferin in the yield of 68%. On the other hand, peroxidases did not lead to ε-viniferin, but some stilbenedimers such as pallidol, resveratrol *trans*-dehydrodimer, and leachianol F were obtained.

1. Introduction

There are many oligostilbenes isolated from Vitaceaeous plants, and they are generated from a stilbene, resveratrol (**1**). Some of them are the enantiomers of oligostilbenes from plants of other families, such as Dipterocarpaceae, Leguminosae, Cyperaceae, and Gnetaceae.[1] For instance, (+)-ε-viniferin (**2a**), a resveratrol dimer, and (+)-hopeaphenol (**3a**), a resveratrol tetramer, are obtained from Vitaceaeous plants, but their enantiomers (**2b** and **3b**, respectively), are from plants of other families. It is estimated that the stereochemistry of the oligostilbenes from Vitaceaeous plants are initially regulated when two molecules of resveratrol (**1**) oxidatively couple to form (+)-ε-viniferin (**2a**), and based on the stereochemistry of **2a**, further biotransformations are estimated to occur (Fig. 1).

In our previous papers, we reported the transformation from (+)-ε-viniferin (**2a**) to (−)-vitisin B (**4**), (+)-vitisin C (**5**), (+)-hopeaphenol (**3a**), and (−)-isohopeaphenol (**6**) by using horseradish peroxidase,[2,3] and from (+)-ε-viniferin (**2a**) to (+)-ampelopsin A (**7**), (+)-ampelopsin B (**8**), (−)-ampelopsin D (**9**), and (+)-ampelopsin F (**10**) under acidic conditions.[3,4] But we have never obtained ε-viniferin (**2**) by the transformation of resveratrol (**1**). Resveratrol (**1**) is supposed to dimerize oxidatively by peroxidase or phenoloxidase in plant cells to afford ε-viniferin (**2**). Langcake and Pryce reported the treatment of resveratrol (**1**) with horseradish peroxidase.[5] According to their result, ε-viniferin (**2**) was not obtained by the reaction but resveratrol-*trans*-dehydrodimer (**11**) was. Sako et al. also investigated the nonenzymatical oxidative coupling of resveratrol with several inorganic oxidative reagents, but

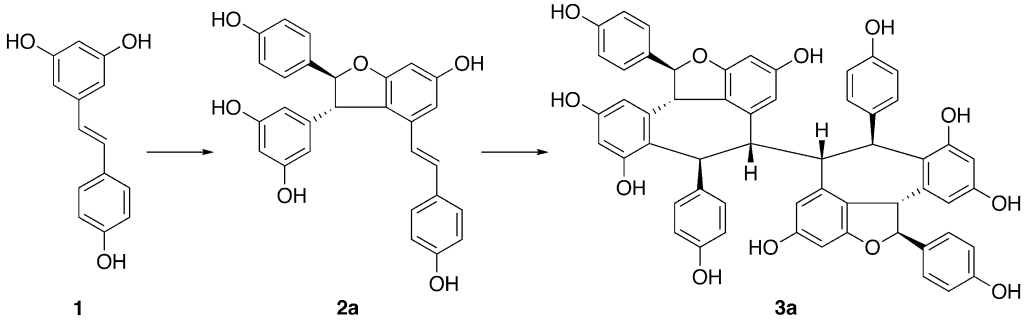

Figure 1. Plausible biogenesis of oligostilbenes.

Keywords: Resveratrol; Peroxidase; ε-Viniferin; Thallium(III) nitrate.
* Corresponding author. Tel.: +81 52 832 1781; fax: +81 52 834 8090; e-mail: masa@ccmfs.meijo-u.ac.jp

0040–4020/$ - see front matter © 2005 Elsevier Ltd. All rights reserved.
doi:10.1016/j.tet.2005.08.023

they reported that the formation of ε-viniferin (**2**) was not observed.[6]

In this study, to substantiate the hypothesis to form (+)-ε-viniferin from resveratrol (**1**) in Vitaceaeous plants, we investigated the participation of peroxidase and inorganic oxidizing reagents in oligomerization of resveratrol (**1**). As the result, the treatment of thallium(III) nitrate led to ε-viniferin (**2**) in good yield, and potassium hexacyanoferrate, and iron(III) chloride also gave **2**, whereas no commercially available peroxidases, which were tested in this study, provided ε-viniferin (**2**).

2. Results and discussion

2.1. Synthesis of resveratrol (1)

In this study, synthetic resveratrol (**1**) under the procedure shown in Scheme 1 was used for the transformation with oxidizing reagents. The starting material, methyl 3,5-dihydroxybenzoate (**13**), was *tert*-butyldimethylsilylated followed by reduction of the methoxy carbonyl group with lithium aluminum hydride to afford 3,5-bis(*tert*-butyldimethylsilyloxy)benzyl alcohol (**14**). Compound **14** was converted to the benzyl chloride (**15**), and **15** was transformed into phosphonate (**16**). Resveratrol (**1**) was obtained by the reaction of **16** and 4-*tert*-butyldimetylsilyloxybenzaldehyde (**18**),[7] which was prepared from 4-hydroxybenzaldehyde (**17**), followed by deprotection. No *cis*-isomer of **1** was found in this preparation.

2.2. Treatment of resveratrol (1) with oxidizing reagents

Resveratrol (**1**) was treated with several inorganic oxidizing reagents in certain solvents as shown in Table 1. These reagents are usually used for phenol oxidation.[8] Among them, thallium(III) nitrate (TTN) in methanol at −50 °C transformed resveratrol (**1**) to (±)-ε-viniferin (**2**), consuming 30% of the starting material, within 5 min along with 56% of recovered resveratrol (**1**). But when this reaction was carried out at over 0 °C, the reaction gave just a complex mixture. The product obtained by the reaction at −50 °C was analyzed by HPLC equipped with CD detector using a chiral column. As the result, the product was revealed to be a mixture of (+)- and (−)-ε-viniferins (**2a** and **2b**) as shown in Figure 2. Potassium hexacyanoferrate(III) is also a good reagent to form ε-viniferin (**2**), and

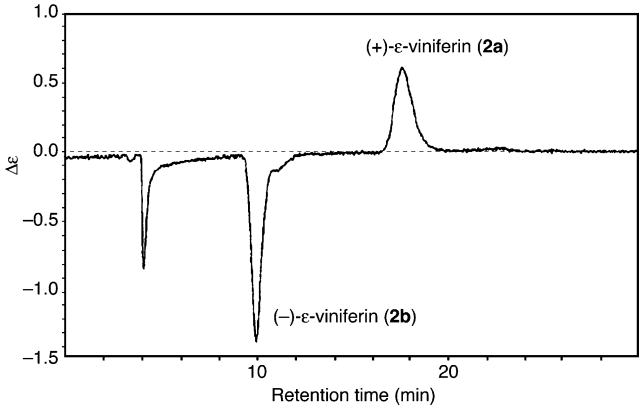

Figure 2. Analysis of the reaction mixture of TTN treatment.

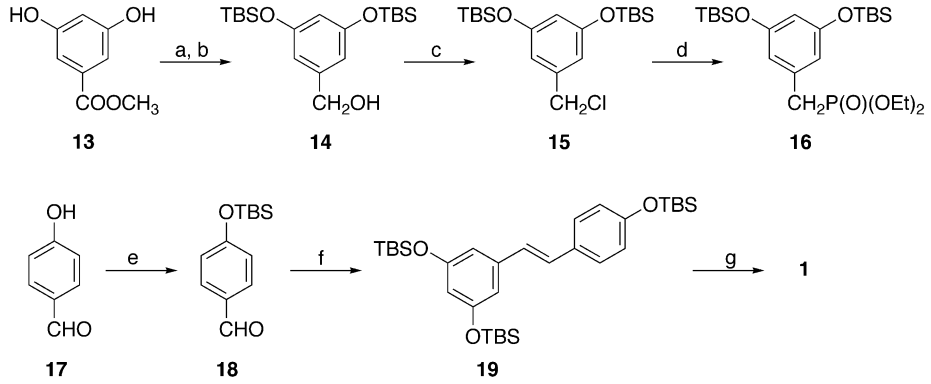

Scheme 1. Synthesis of resveratrol (**1**). Reaction conditions: (a) TBSCl, imidazole, DMF, rt; (b) $LiAlH_4$, THF, 0 °C; (c) *p*-TsCl, Et_3N, DMAP, CH_2Cl_2, rt; (d) $P(OEt)_3$, NaI; (e) TBSCl, imidazole, DMF, rt; (f) **16** NaH, THF, −55 °C; (g) concd HCl, EtOH, rt.

Table 1. Treatment of resveratrol (**1**) with oxidizing reagents

Reagents	Solvent	Temperature (°C)	Time	**2** (%)	**11** (%)	**12** (%)
$Tl(NO_3)_3$	MeOH	−50	5 min	30.1	—	—
$Tl(NO_3)_3$	MeOH	−30	5 min	3.9	—	—
$K_3[Fe(CN)_6]$	MeOH	25	10 min	21.9	22.5	15.7
$Ce(SO_4)_2$	MeOH	−50	26 h	3.7	8.4	—
$FeCl_3$	Acetone	25	20 h	0.9	97.0	1.5
MnO_2	CH_2Cl_2	25	24 h	—	91.0	9.0

The percentage in this table means the 'degree of transformation (%DT)'. See Section 3.

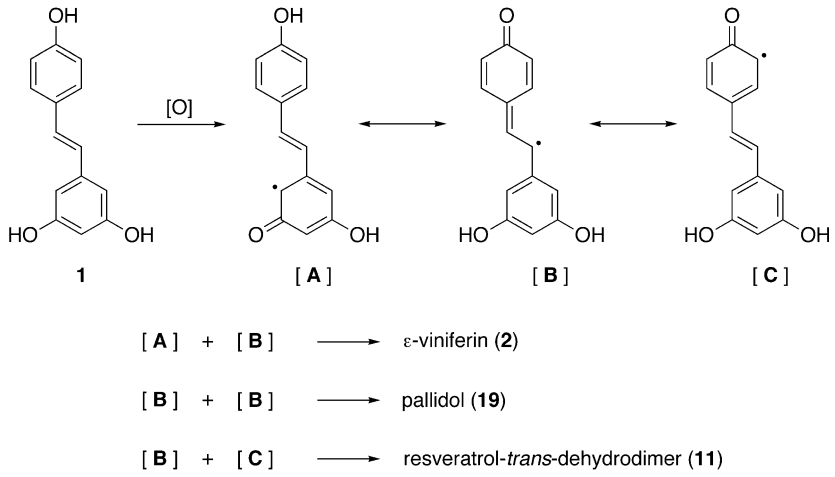

Scheme 2. Hypothesis for the dimerization of resveratrol (**1**).

cerium(IV) sulfate, and iron(III) chloride afforded ε-viniferin (**2**), though the yields were low. On the other hand, iron(III) chloride, and manganese(IV) oxide mainly gave (±)-resveratrol-*trans*-dehydrodimer (**11**). The mechanism for the dimerization of resveratrol (**1**) is suggested as shown in Scheme 2. When the reaction occurs in a short period, as in the case using TTN, the intermediate [**A**] would generate predominantly and then it reacts with intermediate [**B**] to afford ε-viniferin (**2**). Resveratrol-*trans*-dehydrodimer (**11**) is supposed to form by the reaction of intermediate [**B**] and [**C**]. On the basis of our result obtained when we used iron(III) chloride, and mangan(IV) oxide, and the result reported,[6] during the long reaction time and at comparatively higher temperature when **11** was mainly provided, sterically less hindered intermediate [**C**] would be easily involved in the reaction. But an appropriate account for the distinction of the reactivity cannot be made only with this evidence (Table 1).

2.3. Treatment of resveratrol (1) with peroxidases

ε-Viniferin (**2**) is supposed to generate from resveratrol (**1**) via oxidative coupling with peroxidase or phenoloxidase via the proposed intermediates shown in Scheme 2. In order to investigate the participation of peroxidase in the formation of ε-viniferin (**2**), resveratrol (**1**) was treated with several commercially available peroxidases in two kinds of solvents. In this study, we used peroxidases from soybean, fungus (*Arthromyces ramosus*), and horseradish. The reactions were carried out at 27 °C, because when we tried it at 37 °C, the reaction gave only a complex mixture. As the result, ε-viniferin (**2**) was not obtained by using any of the peroxidases tested, though several resveratrol dimers were obtained (Table 2). In all cases, (±)-resveratrol-*trans*-dehydrodimer (**11**)[5] and (±)-pallidol (**12**)[9,10] were major products and compounds **20** and **21** (Fig. 3), all of which were estimated to form via two molecules of intermediate

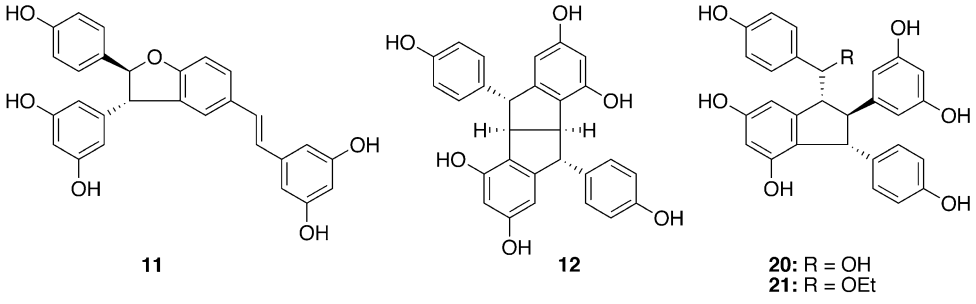

Figure 3. Products obtained by the treatment of resveratrol (**1**) with oxidizing reagents and peroxidases.

Table 2. Diversity of the products obtained by the treatment of resveratrol (**1**) with peroxidases

Origins of peroxidases	Solvent	**11** (%)	**12** (%)	**20** (%)	**21** (%)
Glycine max	aq Acetone	21.4	7.2	1.8	—
Arthromyces ramosus	aq Acetone	18.4	7.4	4.6	—
Horseradish	aq Acetone	12.6	10.2	—	—
Glycine max	aq EtOH	12.1	9.5	5.2	8.6
Arthromyces ramosus	aq EtOH	13.1	5.0	4.6	8.2

The percentage in this table means the 'degree of transformation (%DT)'. See Section 3.

[**B**] in Scheme 2, were obtained as minor products. Accordingly, some specific oxidizing enzymes would be involved to form ε-viniferin (**2**) in the plants. The reaction time in each case was short enough (0.5–1.5 h) to form ε-viniferin (**2**), if the reaction proceeded like that with inorganic oxidizing reagents. Furthermore, the pattern of the reaction was the same as those, which were observed when (+)-ε-viniferin (**2a**) was treated horseradish peroxidase to form (−)-vitisin B, (+)-vitisin C, (+)-hopeaphenol, and (−)-isohopeaphenol.[2,3] So, judging from the evidence, no intermediate [**A**] seemed to be generated in those enzymatic reactions, and the reaction proceeded via the less hindered intermediates [**B**] and [**C**]. Because resveratrol-*trans*-dehydrodimer (**11**) was resulted from intermediate [**B**] and [**C**], and other products, a mixture of (±)-leachianols F and G (**20**),[11] and a mixture of (±)-quadrangularin B and C (**21**),[9] were formed via two molecules of intermediate [**B**].

3. Experimental

3.1. General

UV and IR spectra were recorded on JASCO Ubest V-560 (cell length 10 mm) and FT-IR-410 spectrophotometers, respectively. Optical rotations were measured with a JASCO P-1020 polarimeter (cell length 100 mm). ^{1}H and ^{13}C NMR spectra were recorded on JEOL ALPHA-600 (^{1}H: 600 MHz and ^{13}C: 150 MHz), JEOL ECP-500 (^{1}H: 500 MHz and ^{13}C: 125 MHz), and JEOL ALPHA-400 (^{1}H: 400 MHz and ^{13}C: 100 MHz) spectrometers. Chemical shifts for ^{1}H and ^{13}C NMR are given in parts per million (δ) relative to solvent signal (chloroform-*d*: δ_H 7.26 and δ_C 77.0, methanol-d_4: δ_H 3.30 and δ_C 49.0, acetone-d_6: δ_H 2.04 and δ_C 24.9) as internal standards, respectively. LR and HR FAB-MS were obtained with JEOL JMS HX-110 using *m*-nitrobenzyl alcohol as matrix. Analytical TLC was performed on silica gel 60 F_{254} (Merck). Column chromatography was carried out on silica gel BW-820MH (Fuji Silysia Chemicals, Co. Ltd). ODS (Develosil ODS UG-5, ϕ20×250 mm, Nomura Chemical, Seto, Japan), C-8 (Develosil C8-5, ϕ20×250 mm, Nomura Chemical, Seto, Japan), and C-8 (YMC-Pack C8, ϕ20×250 mm, YMC, Kyoto, Japan) columns were used for preparative HPLC, and C-8 (Develosil C8-5, ϕ4.6×250 mm, Nomura Chemical, Seto, Japan) column were used for analytical HPLC. Peroxidases from soybean (*Glycine max*), *A. ramosus* were purchased from Sigma and peroxidase from horseradish were from Wako Pure Chemicals, Osaka, Japan.

3.2. Synthesis of resveratrol (1)

3.2.1. 3,5-Bis(*tert*-butyldimetylsilyloxy)benzyl alcohol (14). To a solution of methyl 3,5-dihydroxybenzoate (**13**, 50.0 g) in DMF (300 mL), imidazole (21.6 g) and *tert*-butyldimethylsilyl chloride (TBSCl) (48.8 g) was added and stirred at rt for 21 h. The reaction solution was extracted with ethyl acetate, and the ethyl acetate layer was washed with water and brine, dried over anhydrous magnesium sulfate. The solvent was removed in vacuo, and the crude product was purified by silica-gel column chromatography using hexane/ethyl acetate 97:3 as an eluent to afford methyl 3,5-bis(*tert*-butyldimetylsilyloxy)benzoate (**23**) (115 g, 97.5%). Compound **23** (109 g) was dissolved to THF (350 mL), and lithium aluminum hydride (5.6 g) was added at 0 °C. After 20 h, the reaction mixture was extracted with ethyl acetate, and the ethyl acetate layer was washed with water and brine, dried over anhydrous magnesium sulfate, and evaporated. The residue was purified by silica-gel column chromatography using hexane/ethyl acetate 95:5 as an eluent to give alcohol **14** (89.9 g, 88.7%).

3,5-Bis(tert-butyldimetylsilyloxy)benzoate (**23**). ^{1}H NMR (600 MHz, $CDCl_3$) δ 7.10 (2H, d, J=2.2 Hz), 6.50 (1H, t, J=2.2 Hz), 3.86 (3H, s), 0.96 (18H, s), 0.18 (12H, s); EI-MS *m*/*z* 396 (M^+).

3,5-Bis(tert-butyldimetylsilyloxy)benzyl alcohol (**14**). ^{1}H NMR (400 MHz, $CDCl_3$) δ 6.44 (2H, d, J=2.2 Hz), 6.23 (1H, t, J=2.2 Hz), 4.54 (2H, s), 0.95 (18H, s), 0.17 (12H, s); EI-MS *m*/*z* 368 (M^+).

3.2.2. 3,5-Bis(*tert*-butyldimetylsilyloxy)benzyl chloride (15). *p*-Toluenesulfonyl chloride (44.4 g) was added to the CH_2Cl_2 solution (400 mL) of alcohol (**14**, 71.4 g), triethylamine (32.5 mL), and 4-dimethylaminopyridine (DMAP) (11.9 g) at 0 °C. The reaction solution was stirred at rt for 12 h, and extracted with chloroform. The organic layer was washed with water and brine, dried over anhydrous magnesium sulfate and evaporated. The crude product was purified by silica-gel chromatography using hexane/ethyl acetate 95:5 as an eluent to give chloride **15** (45.7 g, 61.0%).

3,5-Bis(tert-butyldimetylsilyloxy)benzyl chloride (**15**). ^{1}H NMR (600 MHz, $CDCl_3$) δ 6.45 (2H, d, J=1.8 Hz), 6.26 (1H, t, J=1.8 Hz), 4.43 (2H, s), 0.96 (18H, s), 0.18 (12H, s); EI-MS *m*/*z* 386, 388 (M^+).

3.2.3. Diethyl [3,5-bis(*tert*-butyldimetylsilyloxy)phenyl] methylphosphonate (16). To a mixture of chloride (**15**, 31.5 g) and triethyl phosphite (23.7 mL), NaI (1.3 g) was added, and stirred at 135 °C for 3 h. Triethyl phosphite (23.7 mL) and NaI (1.3 g) was added again and stirred another 3 h. The reaction solution was extracted with ethyl acetate. The organic layer was washed with water and brine, dried over anhydrous magnesium sulfate, and evaporated. The crude product was purified by silica-gel chromatography using hexane/ethyl acetate 7:3 as an eluent to afford phosphonate (**16**) (34.2 g, 86.1%).

Diethyl [3,5-bis(tert-butyldimetylsilyloxy)phenyl]methylphosphonate (**16**). ^{1}H NMR (600 MHz, $CDCl_3$) δ 6.43 (2H, d, J=2.2 Hz), 6.26 (1H, t, J=2.2 Hz), 4.00 (4H, m), 3.03 (2H, d, J=21.6 Hz), 1.25 (6H, t, J=7.0 Hz), 0.94 (18H, s), 0.19 (12H, s); EI-MS *m*/*z* 488 (M^+).

3.2.4. 4-(*tert*-Butyldimetylsilyloxy)benzaldehyde (18). To a solution of methyl 3,5-dihydroxybenzoate (**17**, 16.8 g) in DMF (100 mL), imidazole (11.3 g) and TBSCl (25.0 g) was added and stirred at rt for 21 h. The reaction solution was extracted with ethyl acetate, and the ethyl acetate layer was washed with water and brine, dried over anhydrous magnesium sulfate. The solvent was removed in vacuo, and the crude product was purified by silica-gel column chromatography using hexane/ethyl acetate 95:5 as an eluent to afford compound **18** (18.9 g, 58.1%).

4-(tert-Butyldimetylsilyloxy)benzaldehyde (**18**). ^{1}H NMR (600 MHz, $CDCl_3$) δ 9.89 (1H, s), 7.79 (2H, d, J=8.8 Hz), 6.95 (2H, d, J=8.8 Hz), 0.99 (9H, s), 0.25 (6H, s); EI-MS m/z 236 (M^+).

3.2.5. 3,5,4′-Tris(*tert*-butyldimetylsilyloxy)stilbene (19). A solution of phosphonate (**16**, 23.4 g) in THF (40 mL) was added dropwise to a suspension of NaH (2.45 g) in THF (20 mL) at −55 °C for 1 h, and the reaction mixture was stirred at 0 °C for 1 h. The mixture was cooled to −55 °C again, and a solution of compound **18** (12.5 g) in THF (20 mL) was added dropwise for 1 h. The reaction temperature was raised to 0 °C for 3 h, and was kept at 0 °C for 20 h. The solution was stirred at rt for 6 h, neutralized with 2 M HCl, and extracted with ethyl acetate. The ethyl acetate layer was washed with water and brine, dried over anhydrous magnesium sulfate, and evaporated. The crude product was purified by silica-gel column chromatography using chloroform/methanol 97:3 as an eluent to give compound **19** (13.9 g, 50.8%).

3,5,4′-Tris(tert-butyldimetylsilyloxy)stilbene (**19**). ^{1}H NMR (600 MHz, $CDCl_3$) δ 7.37 (2H, d, J=8.7 Hz), 6.95 (1H, d, J=16.5 Hz), 6.84 (1H, d, J=16.5 Hz), 6.82 (2H, d, J=8.7 Hz), 6.59 (2H, d, J=2.2 Hz), 6.24 (2H, d, J=2.2 Hz), 0.96 (27H, s), 0.19 (18H, s); EI-MS m/z 570 (M^+).

3.2.6. Resveratrol (1). To a solution of compound **19** (5.7 g) in ethanol (12 mL), a mixture of concd HCl (20 mL) and ethanol (100 mL) was added, and stirred at rt for 26 h. The reaction solution was evaporated and extracted with ethyl acetate. The ethyl acetate layer was washed with water and brine, dried over anhydrous magnesium sulfate, and evaporated. The crude product was purified by silica-gel chromatography using chloroform/methanol 95:5 as an eluent to give resveratrol (**1**) (1.8 g, 79.0%).

3.3. Evaluation of the reactivity

In this study, 'Degree of transformation' was defined as follows. This term means the amount of resveratrol (**1**), which was consumed to form stilbenedimers, and the values (%DT) are used throughout the following investigations.

Degree of transformation (%DT)=(mole of product×2)/(mole of resveratrol (**1**))×100.

3.4. Treatment of resveratrol (1) with oxidizing reagents

3.4.1. Treatment with thallium(III) nitrate. To a solution of resveratrol (5 mg) in methanol (1.5 mL), $Tl(NO_3)_3$ (10.7 mg) was added at −50 °C. The solution was stirred at −50 °C for 30 min under N_2 atmosphere. Water (1 mL) was added to the solution and the reaction mixture was extracted with ethyl acetate. The organic layer was washed with water and brine, died over anhydrous magnesium sulfate, evaporated. The crude product was purified by preparative HPLC equipped with ODS column using a mixed solvent of methanol/water 6:4 as an eluent to give ε-viniferin (**2**, 1.5 mg, 30.1%DT), along with the recovered resveratrol (**1**, 2.8 mg, 56%).

The resulted ε-viniferin (**2**) was submitted to HPLC analysis by using a chiral column (Chiralpak AD, ϕ4.6×150 mm, Daicel Chemical Industries, Osaka) by using hexane/isopropyl alcohol/trifluoroacetic acid 80:20:0.5 as a mobile phase at flow rate of 1 mL/min.

3.4.2. Treatment with potassium hexacyanoferrate(III). To a solution of resveratrol (**1**, 7.7 mg) in methanol (1 mL), a mixed solution of K_2CO_3 (4.1 mg) and $K_3[Fe(CN)_6]$ (9.8 mg) in 0.5 mL of water was added at rt. After 10 min, the reaction mixture was analyzed by HPLC with C-8 column using a mixed solvent of methanol/water 6:4 as an eluent at 0.5 mL/min, and the amount of a product was quantified on the basis of the area of the peak. ε-Viniferin (**2**, Rt=10.0 min, 21.9%DT), resveratrol-*trans*-dehydrodimer (**11**, Rt=14.9 min, 22.5%DT), and pallidol (**12**, Rt=6.7 min, 15.7%DT) was detected along with recovered resveratrol (**1**, Rt=9.1 min, 39.9%).

3.4.3. Treatment with cerium(IV) sulfate. To a solution of resveratrol (**1**, 1.0 mg) in methanol (1 mL), $CeSO_4$ (1.4 mg) was added at −50 °. After 26 h, the reaction mixture extracted with ethyl acetate and water. The organic layer was washed with water, brine, and dried over anhydrous magnesium sulfate, and evaporated. The residue was analyzed by HPLC with C-8 column using a mixed solvent of methanol/water 6:4 as an eluent at 0.5 mL/min, and the amount of a product was quantified on the basis of the area of the peak. ε-Viniferin (**2**, 3.7%DT), and resveratrol-*trans*-dehydrodimer (**11**, 8.4%DT) was detected along with recovered resveratrol (**1**, 53%).

3.4.4. Treatment with iron(III) chloride. To a solution of resveratrol (**1**, 6.1 mg) in acetone (1 mL), $FeCl_3$ (4.4 mg) was added at rt. After 20 h, the reaction mixture was analyzed by HPLC with C-8 column using a mixed solvent of methanol/water 6:4 as an eluent at 0.5 mL/min, and the amount of a product was quantified on the basis of the area of the peak. ε-Viniferin (**2**, 0.9%DT), resveratrol-*trans*-dehydrodimer (**11**, 97%DT), and pallidol (**12**, 1.5%DT) was detected.

3.5. Treatment of resveratrol (1) with peroxidases

3.5.1. General procedure of treatment with peroxidases in aqueous acetone. A mixture of resveratrol (ca. 10 mg), acetone (1 mL), water (1 mL), 0.5 M phosphate buffer (pH 6.0) (0.4 mL) and enzyme solution (0.1 mL in 0.5 M phosphate buffer (pH 6.0)) was stirred at 27 °C for 5 min. Then 30% H_2O_2 (3 μL) was added to this reaction solution. After 30 min, the reaction solution was extracted with ethyl acetate. The organic layer was washed with water, and brine, dried over anhydrous magnesium sulfate, and evaporated. The residue was fractionated by preparative HPLC with C-8 column (YMC) using a mixed solvent of methanol/water 1:1.

3.5.1.1. Peroxidase from soybean (*Glycine max*). For this reaction, resveratrol (10.8 mg) and peroxidase from soybean (*G. max*) as a solution (4 mg/mL) were used. Crude product of 6.3 mg was obtained, and by the preparative HPLC of the product, resveratrol-*trans*-dehydrodimer (**11**, 2.3 mg, 21.4%), pallidol (**12**, 0.8 mg, 7.2%), and a mixture of leachianol F and G (**20**, 0.2 mg, 1.8%) were obtained.

3.5.1.2. Peroxidase from *Arthromyces ramosus*. For this reaction, resveratrol (10.4 mg) and peroxidase from *A. ramosus* as a solution (4 mg/mL) were used. Crude product of 8.5 mg was obtained, and by the preparative HPLC of the product, resveratrol-*trans*-dehydrodimer (**11**, 1.9 mg, 18.4%), pallidol (**12**, 0.8 mg, 7.4%), and a mixture of leachianol F and G (**20**, 0.5 mg, 4.6%) were obtained.

3.5.1.3. Peroxidase from horseradish. For this reaction, resveratrol (10.4 mg) and peroxidase from horseradish as a solution (10 mg/mL) were used. Crude product of 7.9 mg was obtained, and by the preparative HPLC of the product, resveratrol-*trans*-dehydrodimer (**11**, 1.3 mg, 12.6%), and pallidol (**12**, 1.1 mg, 10.2%) were obtained.

3.5.2. General procedure of treatment with peroxidases in aqueous ethanol. A mixture of resveratrol (50 mg), ethanol (5 mL), water (5 mL), 0.5 M phosphate buffer (pH 6.0) (2 mL) and enzyme solution (0.5 mL in 0.5 M phosphate buffer (pH 6.0)) was stirred at 27 °C for 5 min. Then 30% H_2O_2 (15 μL) was added to this reaction solution. After 30 min, wet 1 g of Amberlite XAD-2 (Organo, Tokyo) was added to the solution and eluted with water, 50% aqueous methanol, methanol, and acetone. The acetone elute was evaporated and fractionated by preparative HPLC with C-8 column (Develosil) using a mixed solvent of methanol/water 1:1.

3.5.2.1. Peroxidase from soybean (*Glycine max*). Peroxidase from soybean (*G. max*) was used as a solution (40 μg/mL). By the preparative HPLC, resveratrol-*trans*-dehydrodimer (**11**, 6.0 mg, 12.1%), pallidol (**12**, 4.9 mg, 9.5%), a mixture of leachianol F and G (**20**, 2.7 mg, 5.2%), and a mixture of quadrangularin B and C (**21**, 4.7 mg, 8.6%) were obtained.

3.5.2.2. Peroxidase from *Arthromyces ramosus*. Peroxidase from *A. ramosus* was used as a solution (4 mg/mL). By the preparative HPLC, resveratrol-*trans*-dehydrodimer (**11**, 6.5 mg, 13.1%), pallidol (**12**, 2.6 mg, 5.0%), a mixture of leachianol F and G (**20**, 2.4 mg, 4.6%), and a mixture of quadrangularin B and C (**21**, 4.5 mg, 8.2%) were obtained.

Acknowledgements

This research was financially supported by a Grant-in-Aid for High-Tech Research Center Project and for The Advancement of Graduate School from the Ministry of Education, Culture, Sports, Science and Technology of Japan, which are gratefully acknowledged.

References and notes

1. Takaya, Y.; Niwa, M. *Trends Heterocycl. Chem.* **2001**, *7*, 41–54.
2. Ito, J.; Niwa, M. *Tetrahedron* **1996**, *52*, 9991–9998.
3. Takaya, Y.; Yan, K.-X.; Terashima, K.; He, Y.-H.; Niwa, M. *Tetrahedron* **2002**, *58*, 9265–9271.
4. Takaya, Y.; Yan, K.-X.; Terashima, K.; Ito, J.; Niwa, M. *Tetrahedron* **2002**, *58*, 7259–7265.
5. Langcake, P.; Pryce, R. J. *J. Chem. Soc., Chem. Commun.* **1977**, 208–210.
6. Sako, M.; Hosokawa, H.; Ito, T.; Iinuma, M. *J. Org. Chem.* **2004**, *69*, 2598–2600.
7. Nikaido, M.; Aslanian, R.; Scavo, F.; Helquist, P.; Aakermark, B.; Baeckvall, J. E. *J. Org. Chem.* **1984**, *49*, 4738–4740.
8. Yamamura, S. *The Chemistry of Phenol*; Wiley: West Sussex, England, 2003; pp 1153–1346.
9. Waffo-Teguo, P.; Lee, D.; Cuendet, M.; Mérillon, J.-M.; Pezzuto, J. M.; Kinghorn, A. D. *J. Nat. Prod.* **2001**, *64*, 136–138.
10. Adesanya, S. A.; Nia, R.; Martin, M.-T.; Boukamcha, N.; Montagnac, A.; Païs, M. *J. Nat. Prod.* **1999**, *62*, 1694–1695.
11. Ohyama, M.; Tanaka, T.; Iinuma, M. *Phytochemistry* **1995**, *38*, 733–740.

Available online at www.sciencedirect.com
SCIENCE DIRECT
Tetrahedron
ELSEVIER
Tetrahedron 61 (2005) 10291–10302

1,9-Bis(*N*,*N*-dimethylaminomethyl)dipyrromethanes in the synthesis of porphyrins bearing one or two *meso* substituents

Dazhong Fan, Masahiko Taniguchi, Zhen Yao, Savithri Dhanalekshmi and Jonathan S. Lindsey*

Department of Chemistry, North Carolina State University, Raleigh, NC, 27695-8204, USA

Received 18 April 2005; revised 4 August 2005; accepted 5 August 2005

Available online 1 September 2005

Abstract—A synthesis of 5,15-disubstituted zinc-porphyrins has been developed that employs condensation of a 1,9-bis(*N*,*N*-dimethylaminomethyl)dipyrromethane + a dipyrromethane in refluxing ethanol containing zinc acetate followed by oxidation with DDQ. The *N*,*N*-dimethylaminomethylation of the dipyrromethane was achieved via Eschenmoser's reagent (*N*,*N*-dimethylmethyleneammonium iodide) in CH_2Cl_2 at room temperature. The synthesis is compatible with diverse substituents (e.g., alkyl, aryl, ester, acetal) and enables rapid synthesis of *trans*-AB-, A_2-, and A-porphyrins. The synthesis of >40 zinc porphyrins has been surveyed; 13 zinc porphyrins were isolated in yields of 5–20% without detectable scrambling.

1. Introduction

Porphyrins bearing only one or two substituents present a compact architecture suitable for a wide variety of applications or further synthetic elaboration. For substituents at the *meso*-positions, the methodology established for preparing porphyrins bearing four distinct *meso*-substituents would appear applicable. The route to such ABCD-porphyrins entails condensation of a dipyrromethane + dipyrromethane-1,9-dicarbinol, where the four substituents are introduced via the *meso*-positions of both dipyrromethane species and the carbinol units at the 1- and 9-positions.[1] The corresponding synthesis of A-porphyrins, *trans*-AB-porphyrins, and also *trans*-A_2-porphyrins[2] would employ *meso*-substituted dipyrromethanes with no substituents at the carbinol sites. To our surprise, condensations with dipyrromethanes bearing primary carbinol groups proceeded poorly, giving a mixture of porphyrins and overall low yields.[3] No better alternatives (other than statistical condensations) to A-porphyrins or *trans*-AB-porphyrins have been developed. This limitation prompted us to investigate C1 synthons having greater reactivity than primary carbinol groups for the rational synthesis of porphyrins bearing one or two *meso*-substituents.

A wide variety of C1 synthons have been employed in porphyrin chemistry, either as functional groups (aldehyde,[4] hydroxymethyl[3]) attached to a pyrrolic species or as added reagents (formic acid,[5] trimethyl orthoformate,[6] formaldehyde,[2] and imines[7]). A key consideration in the use of dipyrromethanes is the possibility of acidolysis followed by undesired recombination of dipyrromethane-derived fragments, affording undesired porphyrin species (i.e., scrambling). The possibility of scrambling constrains the nature of the reactive groups employed as C1 synthons (e.g., aldehyde or hydroxymethyl) and reaction conditions that can be employed.

The aminomethyl group is an attractive candidate for the C1 synthon leading to porphyrinic macrocycles because of ease of introduction, the possibility that reaction can be carried out without added acid catalysts, and biomimetic analogy. Indeed, an aminomethylpyrrole (porphobilinogen, **A**)[8] is the biosynthetic precursor of all naturally occurring porphyrinic macrocycles (Chart 1). Aminomethylpyrroles have been prepared by the condensation of pyrrole derivatives with aldehydes and amines.[9] The advent of *N*,*N*-dimethylmethyleneammonium iodide (Eschenmoser's reagent),[10] designed for reactions with corrins, also facilitated the synthesis of aminomethylpyrrolic compounds. To construct porphyrinic macrocycles from aminomethylpyrroles, three different approaches have been investigated: (1) self-condensation of an aminomethylpyrrole (e.g., **B** or **C**);[11,12] (2) condensation of a bis(aminomethyl)pyrrole (e.g., **D** or **E**) with a pyrrole derivative;[11,13,14] and (3) 3 + 1 condensation of a bis(aminomethyl)pyrrole **D** with a tripyrrane.[14,15] These approaches are attractive in their simplicity but have the potential limitation of forming a mixture of porphyrin

Keywords: Dipyrromethane; Aminomethylation; Porphyrin; Zinc.
* Corresponding author. Tel.: +1 9195156406; fax: +1 9195132830; e-mail: jlindsey@ncsu.edu

0040–4020/$ - see front matter © 2005 Elsevier Ltd. All rights reserved.
doi:10.1016/j.tet.2005.08.028

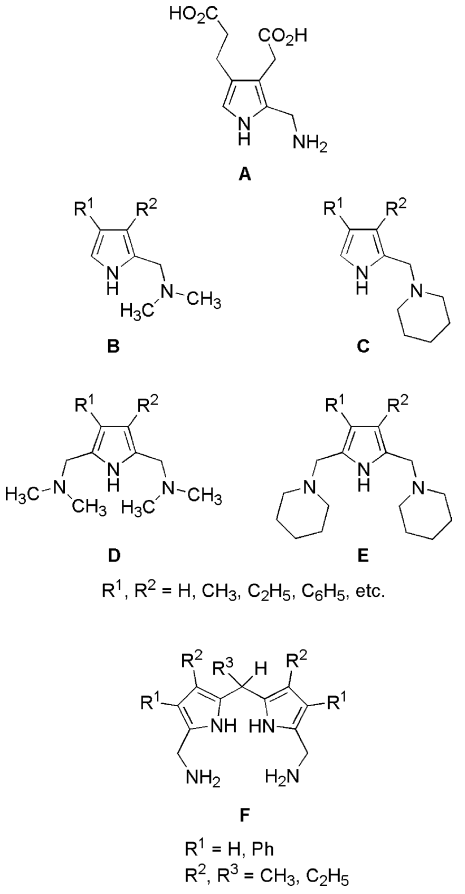

Chart 1.

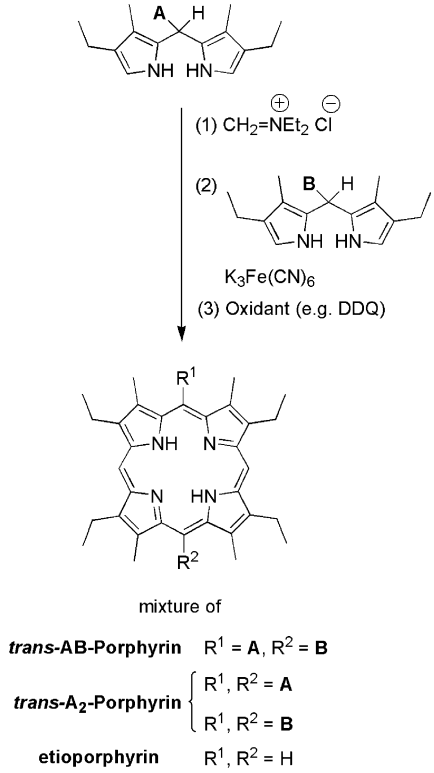

Scheme 1.

regioisomers depending on the β-substitution pattern of the pyrrolic substrates.

Although aminomethyl-dipyrromethanes can be attractive precursors for porphyrinic macrocycles, aminomethyl-dipyrromethane derivatives (**F**) have been mainly used for the synthesis of expanded porphyrins, such as porphocyanine.[16] To our knowledge, the only previous example of aminomethyl-dipyrromethane derivatives in porphyrin chemistry is Hombrecher's synthesis of *meso*-substituted etioporphyrins:[17] treatment of a dipyrromethane with a Mannich reagent ($CH_2{=}NEt_2Cl$) gave the 1,9-bis(*N*,*N*-diethylaminomethyl)dipyrromethane (not isolated), which upon condensation with a dipyrromethane in situ afforded a mixture including a *trans*-AB-porphyrin, A-porphyrins, and etioporphyrin (Scheme 1).

In this paper, we report the synthesis of *trans*-AB-, *trans*-A_2-, and A-porphyrins via a [2+2] condensation of a bis(aminomethyl)dipyrromethane+a dipyrromethane. The dipyrromethanes lack β-substituents. *N*,*N*-Dimethylaminomethylation of a dipyrromethane is achieved with Eschenmoser's reagent. The survey of the scope of reaction encompassed 14 dipyrromethanes and led to examination of the synthesis of >40 zinc porphyrins.

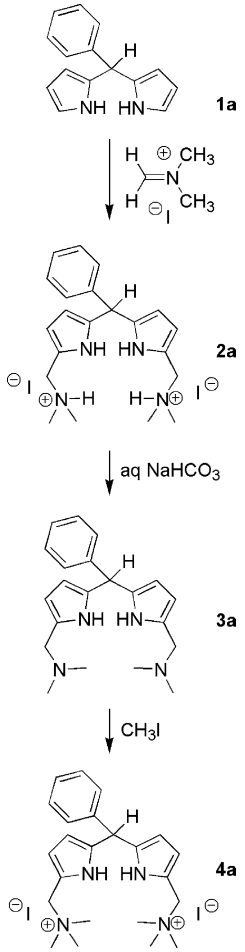

Scheme 2.

2. Results and discussion

2.1. Synthesis of aminomethyl derivatives of 5-phenyldipyrromethane

A series of aminomethyl derivatives of 5-phenyldipyrromethane was prepared as shown in Scheme 2. Treatment of 5-phenyldipyrromethane (**1a**)[18] with Eschenmoser's reagent[10] at room temperature smoothly gave the dipyrromethane-bis(ammonium iodide) **2a**, which was easily isolated by precipitation upon addition of ethyl ether. Alternatively, treatment of the reaction mixture containing **2a** with aqueous $NaHCO_3$ quantitatively gave the corresponding free amine, 1,9-bis(*N*,*N*-dimethylaminomethyl)-dipyrromethane (**3a**). The reaction of **3a** with methyl iodide gave the quaternized ammonium salt **4a**.

2.2. Optimization of the reaction conditions for porphyrin formation

Porphyrin formation via a [2+2] condensation was first examined by the reaction of free base bis(aminomethyl) dipyrromethane **3a**+dipyrromethane **1b**[19] under various conditions. In each case, the yield of porphyrin was determined by absorption spectroscopy and the occurrence of scrambling was assessed by laser-desorption mass spectrometry (LD-MS).[20,21] Initially, several reagents (oxidant, acid, and metal template) were examined for the reaction in CH_2Cl_2/EtOH 3:1. The major findings are as follows:

Table 1. Effect of reagents in porphyrin formation via **3a**+**1b**[a]

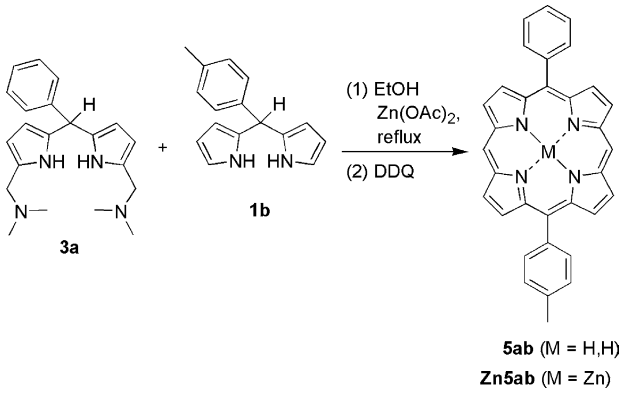

Entry	Reagent 1	Reagent 2	Product	Yield (%)[b]
1	—	—	—	0
2	—	DDQ[c]	**5ab**	7
3	$K_3Fe(CN)_6$	—	**5ab**	5
4	$K_3Fe(CN)_6$	DDQ[c]	**5ab**	7
5	Acid[d]	DDQ[c]	—	0
6	$Zn(OAc)_2$	—	**Zn5ab**	2
7	$Zn(OAc)_2$	DDQ[c]	**Zn5ab**	13

[a] Reaction conditions: 10 mM reactants in CH_2Cl_2/EtOH 3:1 under reflux exposed to air for 18 h in the presence or absence of reagents [$K_3Fe(CN)_6$ (0.1, 1, or 10 equiv) or $Zn(OAc)_2$ (10 equiv)].

[b] The yields of porphyrin were calculated upon absorption spectroscopy of small aliquots from the reaction mixture.

[c] Following the general reaction condition, the reaction mixture was treated with 3/4 equiv of DDQ per pyrrole unit (30 mM).

[d] Trifluoroacetic acid (TFA), trichloroacetic acid (TCA), acetic acid, or propionic acid.

(*1*) *Oxidant*. The condensation of **3a**+**1b** in CH_2Cl_2/EtOH 3:1 under reflux for 16 h (without any oxidant other than air) gave no porphyrin (Table 1, entry 1). However, further treatment of the reaction mixture with DDQ afforded free base porphyrin **5ab** in 7% yield (entry 2). Smith employed $K_3Fe(CN)_6$ as an oxidant for porphyrin formation from a bis(aminomethyl)pyrrole.[14] Inclusion of $K_3Fe(CN)_6$ in the condensation of **3a**+**1b** afforded porphyrin **5ab** in 5% yield (entry 3). The yield increased to 7% upon further oxidation with DDQ (entry 4). No added catalyst is required for formation of the putative porphyrinogen, however, oxidation cannot be achieved with air or $K_3Fe(CN)_6$ but requires use of DDQ.

(*2*) *Acid*. Trifluoroacetic acid, trichloroacetic acid, acetic acid, or propionic acid was examined as an acid catalyst (entry 5). At room temperature, no porphyrin formation was observed.

(*3*) *Metal template*. The condensation of **3a**+**1b** in the presence of $Zn(OAc)_2$ in CH_2Cl_2/EtOH 3:1 under reflux gave zinc porphyrin **Zn5ab** in 2% yield (entry 6). Oxidation of the reaction mixture with DDQ afforded **Zn5ab** in up to 13% yield without scrambling (entry 7). No free base porphyrin was detected. This method provides a simple procedure for the formation of a *trans*-AB-porphyrin.

The required reagents for the porphyrin-forming reaction from a bis(aminomethyl)dipyrromethane are $Zn(OAc)_2$ and DDQ. Further modification of the reaction conditions was investigated by changing the following factors:

(*4*) *Solvent*. EtOH gave the best result out of six solvents that were examined (THF, MeOH, toluene, CH_2Cl_2, $CHCl_3$, EtOH). In alcohol solvents, the reaction proceeded rapidly and was complete in 1 h. A longer reaction time was required with halogenated solvents.

(*5*) *Amount of* $Zn(OAc)_2$. The highest yield of porphyrin was obtained when 10 mol equiv of $Zn(OAc)_2$ was used. The yield decreased to one third with a stoichiometric amount of $Zn(OAc)_2$.

(*6*) *Concentration*. The effects of reactant concentration were examined over the range from 1 to 316 mM. The highest yield (~12% spectroscopic yield) was obtained at 10 mM (Fig. 1A).

(*7*) *Reaction time*. The yield of porphyrin as a function of time upon condensation of **3a** and **1b** (to form porphyrin **Zn5ab**) is shown in Figure 1B. The condensation was essentially complete within ~2 h.

From these studies, the best conditions for porphyrin formation are as follows: **3a** (10 mM), **1b** (10 mM), and $Zn(OAc)_2$ (10 equiv) in EtOH under reflux for ~2 h, followed by treatment with DDQ (3/4 equiv per pyrrolic unit) at room temperature for 15 min. Application of this method afforded *trans*-AB-porphyrin **Zn5ab** in 16% yield without detectable scrambling.

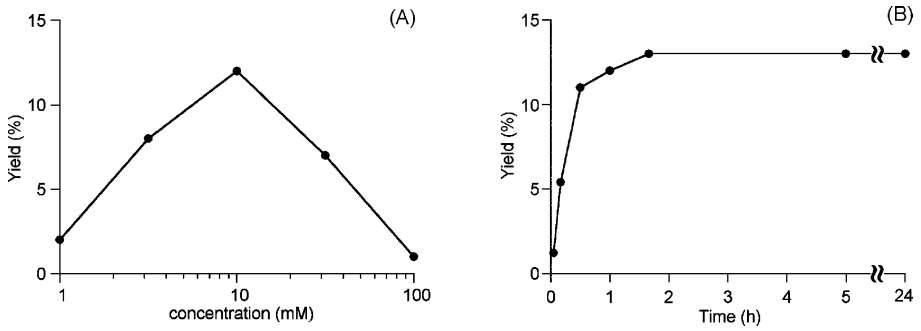

Figure 1. (A) Effect of concentration of dipyrromethane species in porphyrin formation (**3a**+**1b**). Reaction conditions were as follows: [$Zn(OAc)_2$ (10 equiv) in EtOH at reflux in air for 5 h, data points are at 1, 3.16, 10, 31.6, 100, and 316 mM], then treated with 3/4 equiv of DDQ per pyrrole unit. The yields of porphyrin were determined using absorption spectroscopy by removing small aliquots from the reaction mixture; (B) the yield of porphyrin as a function of time upon reaction of bis(*N*,*N*-dimethylaminomethyl)dipyrromethane **3a**+dipyrromethane **1b** with $Zn(OAc)_2$ under reflux in EtOH (the concentration of each reactant is 10 mM) exposed to air.

2.3. Reactivity of free base amine (3a) versus ammonium salts (2a and 4a) of dipyrromethanes

The reactivity of free base amine (**3a**) versus amine salt (**2a** or **4a**) was examined under the optimized conditions described above and also in the absence of $Zn(OAc)_2$ and/or DDQ (Table 2). The highest yields were obtained for all three substrates (**2a**, **3a**, **4a**) upon use of both $Zn(OAc)_2$ and DDQ. This result was somewhat surprising, because we anticipated that the quaternized ammonium salt might react in the absence of $Zn(OAc)_2$. With either $Zn(OAc)_2$ or DDQ present, the bis(ammonium) salts of the dipyrromethane (**2a**, **4a**) exhibited reactivity comparable to each other and greater than that of the free base amine **3a**. However, the highest yield overall was observed with the free base amine derivative **3a**. All subsequent porphyrin-forming reactions were performed with free base 1,9-bis(*N*,*N*-dimethylaminomethyl)dipyrromethane analogues of **3a**.

2.4. Synthesis of *trans*-AB-, *trans*-A_2-, and A-porphyrins. Probing aryl/alkyl/H substituents

A series of known dipyrromethanes (**1a**–**n**)[1,18,19,22–31] was prepared by application of a new solventless synthesis that entails treatment of an aldehyde dissolved in 100 equiv of pyrrole with a mild Lewis acid ($InCl_3$) at room temperature.[32] Each dipyrromethane (**1a**–**n**) was reacted with Eschenmoser's reagent at room temperature followed by workup with aqueous $NaHCO_3$ (aqueous K_2CO_3 was used for the synthesis of **3i**), affording the corresponding free base 1,9-bis(*N*,*N*-dimethylaminomethyl)dipyrromethane (**3a**–**n**) in 43–91% yield (Table 3).

Table 2. Effect of reagents and amine [free amine (**3a**) versus amine salt (**2a** or **4a**)] in porphyrin formation[a]

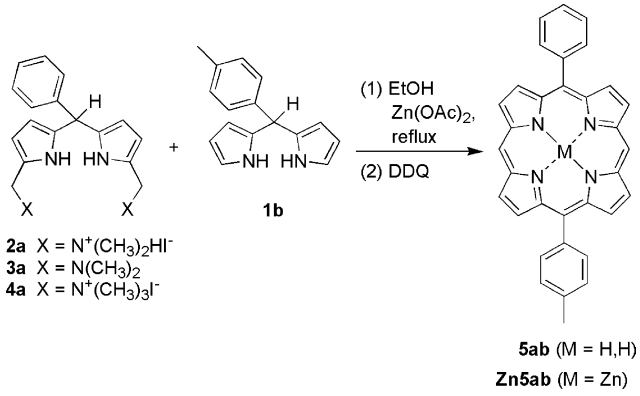

Substrate	Yield (%)[b]			
Step (1):	—	—	$Zn(OAc)_2$	$Zn(OAc)_2$
Step (2):	—	DDQ	—	DDQ
2a	1 (**5ab**)	6 (**5ab**)	4 (**Zn5ab**)[c]	10 (**Zn5ab**)
3a	0	0	0	13 (**Zn5ab**)
4a	<1 (**5ab**)	6 (**5ab**)	2 (**Zn5ab**)	8 (**Zn5ab**)

[a] Reaction conditions: 10 mM reactants and 10 equiv of $Zn(OAc)_2$ in EtOH under reflux exposed to air for 18 h, then treated with 3/4 equiv of DDQ per pyrrole unit (30 mM).
[b] The yields of porphyrin were calculated using absorption spectroscopy by removing small aliquots from the reaction mixture.
[c] LD-MS showed the presence of free base porphyrin **5ab**.

Table 3. Synthesis of 5-substituted-1,9-bis(*N*,*N*-dimethylaminomethyl)dipyrromethanes **3a–n**[a]

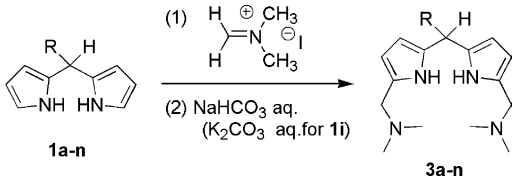

R		Yield (%)[b]	R		Yield (%)[b]
a		68	**h**		83
b	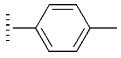	91	**i**		63
c	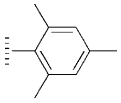	64	**j**	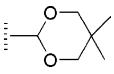	75
d	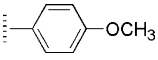	85	**k**		43
e	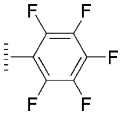	87	**l**	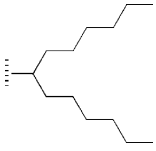	81
f		68	**m**		66
g	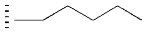	87	**n**	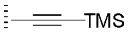	86

[a] Reaction conditions: 100 mM dipyrromethane **1a–n** and 2 equiv of Eschenmoser's reagent in CH_2Cl_2 at room temperature for 1 h, then washed with saturated aqueous $NaHCO_3$ (K_2CO_3 for **1i**).
[b] Isolated yield.

The scope of porphyrin formation was examined using the 1,9-bis(*N*,*N*-dimethylaminomethyl)dipyrromethanes (Scheme 3, Table 4). Emphasis was placed on (1) variation of the substituents; (2) assessment of any scrambling processes; and (3) yields of porphyrin. Altogether, the preparation of **28** *trans*-AB-porphyrins was examined. The yields of porphyrin were determined spectroscopically and ranged from <1 to 19% depending on the substituents and combination of the dipyrromethane precursors. Note that a given porphyrin can be made in two ways by switching the combination of the 1,9-bis(*N*,*N*-dimethylaminomethyl)-dipyrromethane (**3**) and dipyrromethane (**1**). For example, **1e**+**3d** afforded the zinc porphyrin **Zn5de** in <1% yield while **1d**+**3e** gave **Zn5de** in 15% yield. In all cases where the better of the two possible combinations was employed, the yields ranged from 12 to 19%. In those cases where the porphyrin was isolated (**Zn5ab** and **Zn5ac**), the isolated yields compared well with the spectroscopic yield. Scrambling was observed only in the reaction of 5-(pentafluorophenyl)dipyrromethane (**1e**)+1,9-bis(*N*,*N*-dimethylaminomethyl)-5-pentyldipyrromethane (**3g**) (8% yield, level 2 scrambling). The scrambling problem could be overcome by reversal of the substituents; thus, reaction of **1g**+**3e** afforded the same target porphyrin in 15% yield with no detectable scrambling. In general, the reaction of 5-(pentafluorophenyl)dipyrromethane (**1e**) proceeded in low yield and/or scrambling whereas the same *meso*-substituent could be well accommodated upon use of 1,9-bis(*N*,*N*-dimethylaminomethyl)-5-(pentafluorophenyl)-dipyrromethane (**3e**). Taken together, the results upon condensation of a dipyrromethane+1,9-bis(*N*,*N*-dimethyl-aminomethyl)dipyrromethane are superior to those of the reaction of a 1,9-bis(hydroxymethyl)-5-substituted-dipyrro-methane+a 5-substituted-dipyrromethane, which resulted in extensive scrambling.[3]

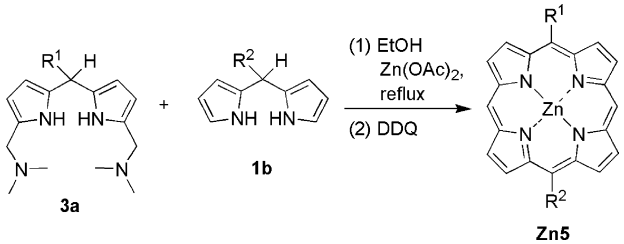

Scheme 3.

The results illustrate the effects of substituents (alkyl or aryl) on the yields of the *trans*-AB-porphyrins and the relative reactivity of those groups when present on the dipyrromethane (**1**) versus 1,9-bis(dimethylaminomethyl)-dipyrromethane (**3**). The yields of porphyrin are insensitive to the presence of an alkyl versus aryl group on either dipyrromethane or 1,9-bis(dimethylaminomethyl)dipyrro-methane reactants. However, in the synthesis of porphyrins bearing only one *meso*-substituent (A-porphyrin), the combination of unsubstituted dipyrromethane and 5-sub-stituted 1,9-bis(dimethylaminomethyl)dipyrromethane affords higher yields than the reverse combination.

Table 4. Formation of *trans*-AB- and A-porphyrins **Zn5** via **3a–g,i**+**1a–g,i**[a]

		3a 	**3b** 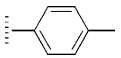	**3c** 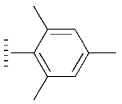	**3d** 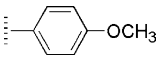	**3e** 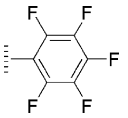	**3f** Methyl	**3g** *n*-Pentyl	**3i** H
1a		—	13	11	11	18	7	15	5
1b	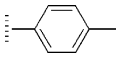	14 (16)[b]	—	11	9	13	6	16	5
1c	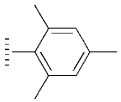	18 (15)[b]	18	—	10	18	12	16	6
1d	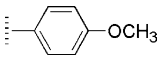	12	13	12	—	15	6	14	5
1e	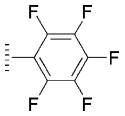	<1	6[c]	<1	<1	—	4	8[c]	2
1f	Methyl	13	13	16	12	12	—	16	4
1g	*n*-Pentyl	18	16	16	15	15	11	—	8
1i	H	13	19	14	11	8	9	16	—

[a] The yields of porphyrin were determined by absorption spectroscopy of small aliquots from the reaction mixture. All reactions gave level 0 scrambling (detected by LD-MS analysis) unless noted otherwise. Reaction conditions: 10 mM reactants and 10 equiv of $Zn(OAc)_2$ in EtOH under reflux exposed to air for 3 h, then treated with 3/4 equiv of DDQ per pyrrole unit (30 mM). The combination that gives the better yield of porphyrin is underlined.

[b] Isolated yield.

[c] Level 2 scrambling.

Table 5. Synthesis of *trans*-AB-, A_2-, and A-porphyrins **Zn5** with diverse substituents[a]

Bis(aminomethyl)dipyrromethane		Dipyrromethane		Porphyrin	Yield (%)[b]
trans-AB-porphyrin					
3j	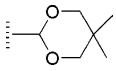	**1b**	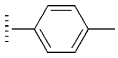	**Zn5bj**	10
3k		**1b**	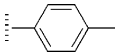	**Zn5bk**	14
3l	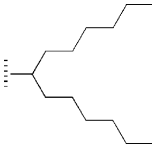	**1b**	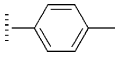	**Zn5bl**	15
3m		**1b**	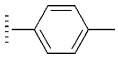	**Zn5bm**	5
3g	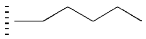	**1h**		**Zn5gh**	17
3a		**1n**	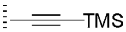	**Zn5an**	6
3j	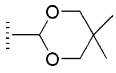	**1n**	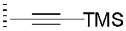	**Zn5jn**	1
A-porphyrin					
3j	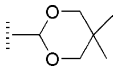	**1i**		**Zn5ij**	12
3k		**1i**		**Zn5ik**	17
3l	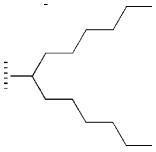	**1i**		**Zn5il**	20
3m		**1i**		**Zn5im**	5
trans-A_2-porphyrin					
3l	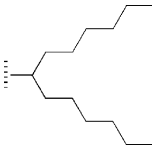	**1l**	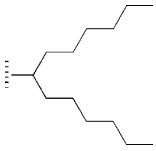	**Zn5ll**	15

[a] All reactions give level 0 scrambling (assessed by LD-MS analysis). Reaction conditions: 10 mM reactants and 10 equiv of $Zn(OAc)_2$ in refluxing EtOH exposed to air for 2 h, then treated with 3/4 equiv of DDQ per pyrrole unit (30 mM).
[b] Isolated yields.

2.5. Synthesis of *trans*-AB-, *trans*-A_2-, and A-porphyrins. Scope with diverse substituents

We examined the synthesis of a series of *trans*-AB-, *trans*-A_2-, and A-porphyrins bearing diverse substituents (Table 5). Each porphyrin was purified by short passage over a pad of silica. 5-(*p*-Tolyl)dipyrromethane (**1b**) was reacted with a series of 1,9-bis(dimethylaminomethyl)-dipyrromethanes bearing diverse substituents **3j–m**, including acetal,[27] allyl,[28] swallowtail,[29] and carboethoxy[30] groups. In each case, no scrambling was observed and the isolated yields of the *trans*-AB-porphyrins ranged from 5 to 15%. In the same manner, a *trans*-AB-porphyrin (**Zn5gh**) bearing two alkyl groups was prepared in 17% yield. When a 5-TMS-ethynyldipyrromethane (**1n**) was employed, the yield of porphyrin was low (**Zn5an** and **Zn5jn**). Very little change was obtained upon use of the TMS-ethynyl unit in the bis(*N*,*N*-dimethylaminomethyl)dipyrromethane species.

A similar series of reactions was performed with unsubstituted dipyrromethane (**1i**) and 5-substituted 1,9-bis(*N*,*N*-dimethylaminomethyl)dipyrromethanes **3j–m**. The corresponding A-porphyrins (**Zn5ij**, **Zn5ik**, **Zn5il**, and **Zn5im**) were obtained in yields of 5–20%. *trans*-AB-porphyrins bearing a single swallowtail substituent (**Zn5bl** and **Zn5il**) were obtained smoothly. A *trans*-A_2-porphyrin (**Zn5ll**) was obtained by using a dipyrromethane and a bis(*N*,*N*-dimethylaminomethyl)dipyrromethane each bearing swallowtail substituents at the 5-position. The success of these approaches is in contrast to the failure encountered upon attempted reaction of a dipyrromethane-1-carbinol bearing a swallowtail substituent at the 1-position.[29]

In general, the substituents that can be introduced with this method are quite diverse and open up a number of applications. The acetal group (**Zn5bj**, **Zn5ij**) can be converted to an aldehyde,[27] the allyl group (**Zn5bk**, **Zn5ik**) can be used for surface attachment,[28] the swallowtail group (**Zn5bl**, **Zn5il**, **Zn5ll**) can suppress aggregation and thereby increase the solubility of the porphyrin,[29] and the ester (**Zn5bm**, **Zn5im**) provides a motif for apical coordination in self-assembly processes.

3. Outlook

The synthesis of porphyrins bearing one or two *meso*-substituents (A-porphyrin, *trans*-AB-porphyrin) requires use of a C1 synthon that provides greater reactivity than that of a primary carbinol group. The *N*,*N*-dimethylaminomethyl group serves as an effective C1 synthon owing to the ease of introduction, reactivity in the absence of an added Brønsted acid, and reaction under mild conditions without detectable acidolysis. The method described herein affords rather modest yields of zinc porphyrins. The low yields are offset by the absence of scrambling, the broad scope, and the ease of implementation.

4. Experimental

4.1. General

All ^{1}H NMR (400 MHz) and ^{13}C NMR (100 MHz) spectra were obtained in $CDCl_3$ unless noted otherwise. Porphyrins were analyzed by laser desorption mass spectrometry without a matrix (LD-MS).[21] Fast atom bombardment mass spectrometry (FAB-MS) data are reported for the molecule ion or protonated molecule ion. Column chromatography was performed with flash silica. Each new compound (except salt **4a**) was >95% pure as determined by ^{1}H NMR spectroscopy. For each zinc porphyrin, only the principal absorption maxima are reported.

4.2. Noncommercial compounds

The dipyrromethanes **1a**,[18] **1b**,[19] **1c**,[22] **1d**,[23] **1e**,[24] **1f**,[25] **1g**,[19] **1h**,[1] **1i**,[26] **1j**,[27] **1k**,[28] **1l**,[29] **1m**,[30] **1n**[31] were prepared using a new method that entails reaction of an aldehyde in 100 equiv of pyrrole containing a Lewis acid (e.g., $InCl_3$).[32]

4.3. Spectroscopic yield determinations

Yields of porphyrin-forming reactions were determined by removal of aliquots from the reaction mixture, treatment with DDQ, followed by absorption spectroscopy of the oxidized product. For example, an ethanol solution of **3a** (1.00 mL, 20.0 mM stock solution, 20.0 μmol of **3a**) and an ethanol solution of **1b** (1.00 mL, 20.0 mM stock solution, 20.0 μmol of **1b**) were combined and treated with $Zn(OAc)_2$ (36.6 mg, 200 μmol), affording [**3a**]=[**1a**]=10 mM. The reaction mixture was refluxed for a designated period. A sample of DDQ (13.6 mg, 60.0 μmol) was added and the mixture was stirred for 10 min at room temperature, then triethylamine (13 μL, 100 μmol) was added. An aliquot (25 μL) of the reaction mixture was removed and diluted with THF (500 μL, 21 times dilution), then 50 μL of this diluted reaction mixture was added to a 1-cm pathlength cuvette containing 3.00 mL of THF (61 times dilution) and the absorption spectrum was recorded (total dilution 1281 times). The yield of the porphyrin was determined by the intensity of the Soret band (412 nm, ε=500,000 M^{-1} cm^{-1}) measured from the apex to the base of the red edge of the band. In this manner, a Soret band absorption of 1.00 corresponded to a porphyrin yield of 26%.

4.4. Standard procedures

4.4.1. Aminomethylation of a dipyrromethane, exemplified for 1,9-bis(*N*,*N*-dimethylaminomethyl)-5-phenyldipyrromethane (3a). A solution of **1a** (667 mg, 3.00 mmol) in CH_2Cl_2 (30 mL) at room temperature was treated with *N*,*N*-dimethylmethyleneammonium iodide (Eschenmoser's reagent; employed as a fine powder; 1.17 g, 6.30 mmol). After 1 h, CH_2Cl_2 (100 mL) and aqueous $NaHCO_3$ (100 mL) were added to the reaction mixture. The organic phase was dried (Na_2SO_4) and then concentrated to dryness. Addition of hexanes/CH_2Cl_2 afforded a precipitate, which upon filtration was obtained as a pale yellow solid (600 mg, 59%): mp 76–78 °C; ^{1}H NMR δ 2.17 (s, 12H), 3.33 (s, 4H), 5.37 (s, 1H), 5.72–5.74 (m, 2H), 5.89–5.91 (m, 2H), 7.19–7.31 (m, 5H), 8.07–8.18 (br, 2H); ^{13}C NMR δ 44.3, 45.0, 56.7, 106.8, 107.3, 126.7, 128.36, 128.48, 128.9, 132.5, 142.4. Anal. Calcd for $C_{21}H_{28}N_4$: C, 74.96; H, 8.39; N, 16.65. Found: C, 74.76; H, 8.63; N, 16.27.

4.4.2. Porphyrin formation from 1,9-bis(*N*,*N*-dimethylaminomethyl)dipyrromethanes, exemplified for Zn(II)-5-mesityl-15-phenylporphyrin (Zn5ac) via 3a+1c. A solution of **3a** (168 mg, 0.500 mmol) and 5-mesityldipyrromethane (**1c**, 132 mg, 0.500 mmol) in ethanol (50 mL) at room temperature was treated with $Zn(OAc)_2$ (917 mg, 5.00 mmol). The mixture was heated to reflux. After 2 h, the reaction mixture was allowed to cool to room temperature. A sample of DDQ (340 mg, 1.50 mmol) was added and the mixture was stirred for 15 min. Triethylamine (355 μL, 2.50 mmol) was added and the reaction mixture was concentrated to dryness. Column chromatography [silica, hexanes/CH_2Cl_2 1:1] afforded a purple solid (42.4 mg, 15%); ^{1}H NMR δ 1.85 (s, 6H), 2.68 (s, 3H), 7.34 (s, 2H), 7.80–7.82 (m, 3H), 8.25–8.28 (m, 2H), 9.00 (d, J=4.4 Hz, 2H), 9.14 (d, J=4.4 Hz, 2H), 9.41 (d, J=4.4 Hz, 2H), 9.45 (d, J=4.4 Hz, 2H), 10.30 (s, 2H); ^{13}C NMR δ 21.7, 22.0, 106.1, 118.7, 120.2, 126.9, 127.7, 128.0, 131.6, 131.9, 132.5, 132.7, 134.8, 137.8, 139.0, 139.6, 142.9, 149.65, 149.74, 150.17, 150.31. Anal. Calcd for $C_{35}H_{26}N_4Zn$: C, 74.01; H, 4.61; N, 9.86. Found: C, 74.27; H, 4.72; N, 9.53; LD-MS obsd 565.9, calcd 566.14 ($C_{35}H_{26}N_4Zn$); λ_{abs} 412, 544 nm.

4.5. Synthesis of 1,9-dialkylated dipyrromethanes

4.5.1. Hydroiodide salt of 1,9-bis(*N*,*N*-dimethylaminomethyl)-5-phenyldipyrromethane (2a). A solution of **1a** (222 mg, 1.00 mmol) in CH_2Cl_2 (10 mL) at room temperature was treated with *N*,*N*-dimethylmethyleneammonium iodide (fine powder form; 389 mg, 2.10 mmol). After 1 h, the mixture was diluted with ethyl ether (30 mL), causing formation of a precipitate. A pale yellow solid (542 mg,

91%) was collected by filtration: mp 138–140 °C; ^{1}H NMR δ 2.97 (d, J=5.2 Hz, 12H), 4.54 (d, J=5.2 Hz, 4H), 5.45 (s, 1H), 5.79–5.81 (m, 2H), 6.19–6.21 (m, 2H), 7.20–7.29 (m, 5H), 8.90–9.10 (br, 2H), 10.40 (s, 2H); ^{13}C NMR δ 43.03, 43.08, 44.6, 55.2, 108.9, 113.6, 118.2, 126.7, 128.43, 128.54, 135.0, 143.0; FAB-MS obsd 465.18, calcd 465.16 [$(M-I)^+$] ($M=C_{21}H_{30}IN_4$).

4.5.2. Hydroiodide salt of 1,9-bis(*N*,*N*-trimethylaminomethyl)-5-phenyldipyrromethane (4a). A solution of **3a** (336 mg, 1.00 mmol) in dry CH_2Cl_2 (10 mL) was treated with CH_3I (3.00 mmol) at room temperature in 1 h. The reaction mixture was filtered, washed with a small amount of cold THF, and concentrated to dryness, affording a pale yellow solid (400 mg, 65%, >80% pure): mp 186–188 °C; ^{1}H NMR (DMSO-d_6) δ 3.37 (s, 18H), 4.80 (s, 4H), 5.90 (s, 1H), 6.18 (s, 2H), 6.69 (s, 2H), 7.60–7.76 (m, 5H), 11.50–11.68 (br, 2H); ^{13}C NMR (DMSO-d_6) δ 43.2, 51.4, 54.37, 54.41, 61.8, 107.9, 113.6, 118.1, 126.7, 128.1, 128.4, 135.8, 1425.4; FAB-MS obsd 493.21, calcd 493.18 [$(M-I)^+$] ($M=C_{23}H_{34}IN_4$).

4.5.3. 1,9-Bis(*N*,*N*-dimethylaminomethyl)-5-(*p*-tolyl) dipyrromethane (3b). Following the standard procedure, reaction of 1.00 mmol of **1b** afforded a pale yellow solid (320 mg, 91%): mp 62–64 °C; ^{1}H NMR δ 2.17 (s, 12H), 2.32 (s, 3H), 3.29–3.38 (m, 4H), 5.34 (s, 1H), 5.74–5.75 (m, 2H), 5.90–5.91 (m, 2H), 7.09 (s, 4H), 8.27–8.35 (br, 2H); ^{13}C NMR δ 21.3, 44.1, 45.2, 56.9, 106.8, 107.6, 128.4, 128.9, 129.4, 133.1, 136.5, 139.6; FAB-MS obsd 350.2483, calcd 350.2470 ($C_{22}H_{30}N_4$).

4.5.4. 1,9-Bis(*N*,*N*-dimethylaminomethyl)-5-mesityldipyrromethane (3c). Following the standard procedure, reaction of 1.00 mmol of **1c** afforded a pale yellow solid (240 mg, 64%): mp 43–45 °C; ^{1}H NMR δ 2.09 (s, 6H), 2.18 (s, 12H), 2.27 (s, 3H), 3.34 (s, 4H), 5.77–5.79 (m, 2H), 5.82 (s, 1H), 5.92–5.93 (m, 2H), 6.83 (s, 2H), 8.18–8.34 (br, 2H); ^{13}C NMR δ 20.91, 21.03, 38.9, 45.1, 56.8, 106.4, 108.0, 127.9, 130.4, 131.7, 135.1, 136.4, 137.7; FAB-MS obsd 378.2785, calcd 378.2783 ($C_{24}H_{34}N_4$).

4.5.5. 1,9-Bis(*N*,*N*-dimethylaminomethyl)-5-(4-methoxyphenyl)dipyrromethane (3d). Following the standard procedure, reaction of 1.00 mmol of **1d** afforded a pale yellow solid (310 mg, 85%): mp 65–66 °C; ^{1}H NMR δ 2.15 (s, 12H), 3.28–3.36 (m, 4H), 3.77 (s, 3H), 5.30 (s, 1H), 5.71–5.73 (m, 2H), 5.90–5.91 (m, 2H), 6.80–6.82 (m, 2H), 7.09–7.11 (m, 2H), 8.30–8.45 (br, 2H); ^{13}C NMR δ 43.6, 45.2, 55.5, 56.9, 106.9, 107.6, 114.0, 128.9, 129.6, 133.3, 134.8, 158.5; FAB-MS obsd 366.2411, calcd 366.2420 ($C_{22}H_{30}N_4O$).

4.5.6. 1,9-Bis(*N*,*N*-dimethylaminomethyl)-5-(pentafluorophenyl)dipyrromethane (3e). Following the standard procedure, reaction of 1.00 mmol of **1e** afforded a yellow solid (370 mg, 87%): mp 38–40 °C; ^{1}H NMR δ 2.19 (s, 12H), 3.30–3.41 (m, 4H), 5.82 (s, 1H), 5.87–5.88 (m, 2H), 5.94–5.95 (m, 2H), 8.50–8.60 (br, 2H); ^{13}C NMR δ 33.5, 45.2, 56.8, 107.3, 107.9, 116.2–116.5 (m), 128.3, 129.8, 136.5–136.8 (m), 139.0–139.3 (m, two peaks were overlapped), 141.5–141.8 (m), 143.8–144.0 (m), 146.3–146.4 (m); FAB-MS obsd 426.1825, calcd 426.1843 ($C_{21}H_{23}F_5N_4$).

4.5.7. 1,9-Bis(*N*,*N*-dimethylaminomethyl)-5-methyldipyrromethane (3f). Following the standard procedure, reaction of 1.00 mmol of **1f** afforded a pale yellow solid (140 mg, 51%): mp 113–115 °C; ^{1}H NMR δ 1.57 (d, J=8.0 Hz, 3H), 2.16 (s, 12H), 3.32 (s, 4H), 4.07–4.12 (m, 1H), 5.87–5.91 (m, 4H), 8.12–8.24 (br, 2H); ^{13}C NMR δ 20.6, 32.1, 45.1, 56.8, 104.2, 107.4, 128.4, 135.2; FAB-MS obsd 274.31, calcd 274.22 ($C_{16}H_{26}N_4$).

4.5.8. 1,9-Bis(*N*,*N*-dimethylaminomethyl)-5-*n*-pentyldipyrromethane (3g). Following the standard procedure, reaction of 1.00 mmol of **1g** afforded a brown oil (290 mg, 87%); ^{1}H NMR δ 0.85 (t, J=6.4 Hz, 3H), 1.27 (s, 6H), 1.92–1.94 (m, 2H), 2.37 (s, 12H), 3.59–3.67 (m, 4H), 3.92–3.95 (m, 1H), 5.89–5.90 (m, 2H), 5.97–5.98 (m, 2H), 9.10–9.24 (br, 2H); ^{13}C NMR δ 14.3, 22.8, 27.5, 31.9, 34.8, 38.2, 45.2, 56.9, 105.0, 107.4, 128.5, 134.1; FAB-MS obsd 330.2774, calcd 330.2783 ($C_{20}H_{34}N_4$).

4.5.9. 1,9-Bis(*N*,*N*-dimethylaminomethyl)-5-*n*-hexyldipyrromethane (3h). Following the standard procedure, reaction of 1.00 mmol of **1h** afforded a yellow solid (278 mg, 80%): mp 88–90 °C; ^{1}H NMR δ 0.85 (t, J=6.4 Hz, 3H), 1.24–1.29 (m, 8H), 1.89–1.91 (m, 2H), 2.16 (s, 12H), 3.29–3.37 (m, 4H), 3.88 (t, J=7.6 Hz, 1H), 5.87–5.90 (m, 4H), 8.10–8.20 (br, 2H); ^{13}C NMR δ 14.3, 22.8, 27.8, 29.4, 31.9, 34.7, 38.1, 45.2, 56.9, 105.0, 107.4, 128.4, 134.1; FAB-MS obsd 344.2859, calcd 344.2940 ($C_{21}H_{36}N_4$).

4.5.10. 1,9-Bis(*N*,*N*-dimethylaminomethyl)dipyrromethane (3i). Following the standard procedure with slight modification (K_2CO_3 was used instead of $NaHCO_3$), reaction of 1.00 mmol of **1i** afforded a pale yellow solid (152 mg, 63%): mp 74–76 °C; ^{1}H NMR δ 2.17 (s, 12H), 3.33 (s, 4H), 3.84 (s, 2H), 5.82–5.83 (m, 2H), 5.88–5.90 (m, 2H), 8.55–8.70 (br, 2H); ^{13}C NMR δ 27.0, 45.2, 56.9, 105.9, 107.8, 128.6, 129.7; FAB-MS obsd 261.2091, calcd 261.2079 ($C_{15}H_{24}N_4$).

4.5.11. 1,9-Bis(*N*,*N*-dimethylaminomethyl)-5-(5,5-dimethyl-1,3-dioxan-2-yl)dipyrromethane (3j). Following the standard procedure, reaction of 1.00 mmol of **1j** afforded a colorless solid (280 mg, 75%): mp 92–94 °C; ^{1}H NMR δ 0.72 (s, 3H), 1.12 (s, 3H), 2.18 (s, 12H), 3.32 (d, J=13.2 Hz, 2H), 3.41 (d, J=13.2 Hz, 2H), 3.48 (d, J=13.2 Hz, 2H), 3.72 (d, J=13.2 Hz, 2H), 4.30 (d, J=4.0 Hz, 1H), 4.80 (d, J=4.0 Hz, 1H); 5.79–5.81 (m, 2H), 5.88–5.89 (m, 2H), 8.80–8.90 (br, 2H); ^{13}C NMR δ 22.0, 23.2, 30.5, 42.6, 45.2, 57.0, 103.7, 107.0, 107.2, 128.8, 129.5; FAB-MS obsd 374.2680, calcd 374.2682 ($C_{21}H_{34}N_4O_2$).

4.5.12. 5-Allyl-1,9-bis(*N*,*N*-dimethylaminomethyl)dipyrromethane (3k). Following the standard procedure, reaction of 1.00 mmol of **1k** afforded a brown oil (130 mg, 43%); ^{1}H NMR δ 2.14 (s, 12H), 2.68–2.72 (m, 2H), 3.32–3.33 (m, 4H), 4.00–4.03 (m, 1H), 4.98–5.08 (m, 2H), 5.76–5.83 (m, 1H), 5.89–5.90 (m, 4H), 8.20–8.40 (br, 2H); ^{13}C NMR δ 38.2, 39.3, 45.2, 56.9, 105.2, 107.5, 116.7, 128.6, 133.4, 136.8; FAB-MS obsd 300.2308, calcd 300.2314 ($C_{18}H_{28}N_4$).

4.5.13. 1,9-Bis(*N*,*N*-dimethylaminomethyl)-5-(tridec-7-yl)dipyrromethane (3l). Following the standard procedure, reaction of 1.00 mmol of **1l** afforded a brown oil (180 mg, 81%); ^{1}H NMR δ 0.86 (t, J=7.2 Hz, 6H), 1.13–1.35 (m, 20H), 1.81–1.91 (m, 1H), 2.16 (s, 12H), 3.30 (d, J=13.2 Hz, 2H), 3.39 (d, J=13.2 Hz, 2H), 3.97 (d, J=6.4 Hz, 2H), 5.85–5.86 (m, 2H), 5.89–5.90 (m, 2H), 8.15–8.33 (br, 2H); ^{13}C NMR δ 14.3, 22.9, 27.2, 29.9, 31.6, 32.1, 41.8, 42.1, 45.1, 56.9, 105.9, 107.5, 127.9, 132.9; FAB-MS obsd 442.4033, calcd 442.4035 ($C_{28}H_{50}N_4$).

4.5.14. 1,9-Bis(*N*,*N*-dimethylaminomethyl)-5-(ethoxycarbonyl)dipyrromethane (3m). Following the standard procedure, reaction of 1.00 mmol of **1m** afforded a brown oil (230 mg, 69%); ^{1}H NMR δ 1.27 (t, J=7.2 Hz, 3H), 2.17 (s, 12H), 3.28 (d, J=12.0 Hz, 2H), 3.45 (d, J=12.0 Hz, 2H), 4.20 (q, J=7.2 Hz, 2H), 4.99 (s, 1H), 5.89–5.93 (m, 4H), 8.80–9.00 (br, 2H); ^{13}C NMR δ 14.3, 44.6, 45.1, 56.7, 61.8, 106.9, 107.8, 127.2, 129.4, 171.6; FAB-MS obsd 333.2291, calcd 332.2212 ($C_{18}H_{28}N_4O_2$).

4.5.15. 1,9-Bis(*N*,*N*-dimethylaminomethyl)-5-[2-(trimethylsilyl)ethynyl]dipyrromethane (3n). Following the standard procedure, reaction of 1.00 mmol of **1n** afforded a brown solid (290 mg, 81%): mp 73–76 °C; ^{1}H NMR δ 0.19 (s, 9H), 2.18 (s, 12H), 3.35 (d, J=3.2 Hz, 4H), 5.15 (s, 1H), 5.90–5.91 (m, 2H), 5.96–5.97 (m, 2H), 8.30–8.40 (br, 2H); ^{13}C NMR δ 0.2, 31.6, 45.2, 56.8, 87.7, 104.1, 106.0, 107.6, 129.1, 129.4.

4.6. Synthesis of Zn(II)porphyrins

4.6.1. Zn(II)-5-(4-methylphenyl)-15-phenylporphyrin (Zn5ab) via 3a+1b. Following the standard procedure, reaction of 0.500 mmol of **3a** and **1b** afforded a purple solid (43 mg, 16%); ^{1}H NMR (THF-d_8) δ 2.75 (s, 2H), 7.58–7.62 (m, 2H), 7.77–7.83 (m, 2H), 8.13–8.18 (m, 2H), 8.26–8.29 (m, 2H), 9.11–9.15 (m, 2H), 9.15–9.19 (m, 2H), 9.41–9.47 (m, 2H), 10.31 (s, 2H); ^{13}C NMR (THF-d_8) δ 21.7, 106.6, 120.3, 120.6, 127.4, 128.1, 128.2, 132.2, 132.3, 132.7, 132.9, 135.7, 135.8, 137.8, 141.6, 144.6, 150.61, 150.64, 151.0, 151.2; LD-MS obsd 538.5; FAB-MS obsd 538.1150, calcd 538.1136 ($C_{33}H_{22}N_4Zn$); λ_{abs} 413, 539 nm.

4.6.2. Zn(II)-5-(5,5-dimethyl-1,3-dioxan-2-yl)-15-(4-methylphenyl)porphyrin (Zn5bj) via 3j+1b. Following the standard procedure, reaction of 1.00 mmol of **3j** and **1b** afforded a purple solid (58.0 mg, 10%); ^{1}H NMR (THF-d_8) δ 1.17 (s, 3H), 2.00 (s, 3H), 2.74 (s, 3H), 4.30–4.39 (m, 4H), 7.60 (d, J=8.0 Hz, 2H), 8.07 (s, 1H), 8.14 (d, J=8.0 Hz, 2H), 9.18 (d, J=4.0 Hz, 2H), 9.43 (d, J=4.0 Hz, 2H), 9.56 (d, J=4.0 Hz, 2H), 10.18 (d, J=4.0 Hz, 2H), 10.34 (s, 2H); ^{13}C NMR (THF-d_8) δ 21.7, 23.0, 31.7, 80.8, 106.4, 108.0, 113.2, 121.5, 128.1, 131.8, 132.0, 132.5, 132.9, 135.6, 137.8, 141.6, 150.36, 150.48, 150.51, 151.3; LD-MS obsd 575.9; FAB-MS obsd 576.1519, calcd 576.1504 ($C_{33}H_{28}N_4O_2Zn$); λ_{abs} 409, 541 nm.

4.6.3. Zn(II)-5-allyl-15-(4-methylphenyl)porphyrin (Zn5bk) via 3k+1b. Following the standard procedure, reaction of 1.00 mmol of **3k** and **1b** afforded a purple solid (70.0 mg, 14%); ^{1}H NMR (THF-d_8) δ 2.75 (s, 3H), 5.15–5.20 (m, 2H), 5.73–5.75 (m, 2H), 6.81–6.88 (m, 1H), 7.61 (d, J=8.0 Hz, 2H), 8.15 (d, J=8.0 Hz, 2H), 9.13 (d, J=4.0 Hz, 2H), 9.36–9.37 (m, 4H), 9.59 (d, J=4.0 Hz, 2H), 10.13 (s, 2H); ^{13}C NMR (THF-d_8) δ 21.8, 40.0, 106.12, 106.18, 115.5, 116.6, 120.1, 128.1, 130.4, 132.2, 132.72, 132.81, 135.7, 137.7, 141.7, 143.7, 150.26, 150.44, 151.26, 151.42; LD-MS obsd 501.9; FAB-MS obsd 502.1118, calcd 502.1136 ($C_{30}H_{22}N_4Zn$); λ_{abs} 412, 545 nm.

4.6.4. Zn(II)-5-(4-methylphenyl)-15-(tridec-7-yl)porphyrin (Zn5bl) via 3l+1b. Following the standard procedure, reaction of 1.00 mmol of **3l** and **1b** afforded a purple solid (100 mg, 15%); ^{1}H NMR δ 0.69–0.72 (m, 6H), 1.06–1.11 (m, 12H), 1.33–1.42 (m, 2H), 1.58–1.66 (m, 2H), 2.75 (s, 3H), 2.80–2.89 (m, 2H), 3.00–3.10 (m, 2H), 5.38–5.42 (m, 1H), 7.60 (d, J=7.6 Hz, 2H), 8.13 (d, J=7.6 Hz, 2H), 9.12–9.14 (m, 2H), 9.39–9.40 (m, 2H), 9.50–9.53 (m, 2H), 9.90 (d, J=4.8 Hz, 1H), 9.99 (d, J=4.8 Hz, 1H), 10.26 (s, 2H); ^{13}C NMR δ 14.2, 21.8, 22.7, 29.9, 31.9, 43.0, 47.4, 105.7, 106.0, 119.7, 125.0, 127.6, 130.3, 131.3, 131.69, 131.72, 132.1, 132.5, 132.74, 134.77, 137.3, 139.9, 147.7, 149.1, 149.4, 149.72, 149.74, 150.53, 150.58, 152.0; LD-MS obsd 644.7; FAB-MS obsd 644.2899, calcd 644.2857 ($C_{40}H_{44}N_4Zn$); λ_{abs} 412, 545 nm.

4.6.5. Zn(II)-5-ethoxycarbonyl-15-(4-methylphenyl)porphyrin (Zn5bm) via 3m+1b. Following the standard procedure, reaction of 1.00 mmol of **3m** and **1b** afforded a purple solid (25.0 mg, 5%); ^{1}H NMR (THF-d_8) δ 1.82 (t, J=7.2 Hz, 3H), 2.73 (s, 3H), 5.08 (q, J=7.2 Hz, 2H), 7.61 (d, J=8.0 Hz, 2H), 8.11 (d, J=7.6 Hz, 2H), 9.04 (d, J=4.4 Hz, 2H), 9.38 (d, J=4.4 Hz, 2H), 9.49 (d, J=4.4 Hz, 2H), 9.66 (d, J=4.8 Hz, 2H), 10.30 (s, 2H); ^{13}C NMR (THF-d_8) δ 14.4, 20.8, 62.2, 106.71, 106.83, 107.3, 127.2, 131.11, 131.15, 132.40, 132.53, 134.7, 137.1, 140.4, 149.2, 149.70, 149.77, 150.1, 172.2; LD-MS obsd 535.6; FAB-MS obsd 534.1059, calcd 534.1034 ($C_{30}H_{22}N_4O_2Zn$); λ_{abs} 410, 541 nm.

4.6.6. Zn(II)-5-hexyl-15-*n*-pentylporphyrin (Zn5gh) from 3g+1h. Following the standard procedure, reaction of 0.600 mmol of **3g** and **1h** afforded a purple solid (80.0 mg, 17%); ^{1}H NMR δ 0.94–1.03 (m, 6H), 1.40–1.46 (m, 2H), 1.51–1.61 (m, 4H), 1.83–1.88 (m, 4H), 2.54–2.59 (m, 4H), 4.94–4.98 (m, 4H), 9.34 (d, J=4.4 Hz, 4H), 9.58 (d, J=4.4 Hz, 4H), 10.00 (s, 2H); ^{13}C NMR (THF-d_8) δ 13.7, 13.8, 22.9, 23.0, 30.4, 32.3, 32.9, 35.28, 35.34, 39.1, 39.4, 104.5, 118.81, 118.82, 128.8, 131.6, 148.9, 150.3; LD-MS obsd 526.6; FAB-MS obsd 526.2088, calcd 526.2075 ($C_{31}H_{34}N_4Zn$); λ_{abs} 411, 546 nm.

4.6.7. Zn(II)-5-phenyl-15-[2-(trimethylsilyl)ethynyl]porphyrin (Zn5an) from 3a+1n. Following the standard procedure, reaction of 1.00 mmol of **3a** and **1n** afforded a purple solid (30.1 mg, 6%); ^{1}H NMR (THF-d_8) δ 0.69 (s, 9H), 7.79–7.81 (m, 3H), 8.22–8.24 (m, 2H), 8.79 (d, J=4.4 Hz, 2H), 9.34 (d, J=4.4 Hz, 2H), 9.45 (d, J=4.4 Hz, 2H), 9.85 (d, J=4.4 Hz, 2H), 10.22 (s, 2H); ^{13}C NMR (THF-d_8) δ 0.8, 98.5, 100.2, 106.0, 107.7, 122.5, 127.5, 128.4, 131.9, 132.3, 133.13, 133.24, 135.6, 135.8, 144.3, 150.5, 150.8, 151.0, 153.6; LD-MS obsd 545.5; FAB-MS obsd 544.1061, calcd 544.1062 ($C_{31}H_{24}N_4SiZn$); λ_{abs} 424, 556, 595 nm.

4.6.8. Zn(II)-5-(5,5-dimethyl-1,3-dioxan-2-yl)-15-[2-(trimethylsilyl)ethynyl]porphyrin (Zn5jn) from 3j+1n. Following the standard procedure, reaction of 1.00 mmol of **3j** and **1n** afforded a purple solid (5.70 mg, 1%); ^{1}H NMR δ 7.98 (s, 2H), 9.30 (d, J=4.8 Hz, 2H), 9.40 (d, J=4.8 Hz, 2H), 9.75 (d, J=4.0 Hz, 2H), 10.08 (d, J=4.0 Hz, 2H), 10.11 (s, 2H); LD-MS obsd 583.406; FAB-MS obsd 582.1473, calcd 582.1429 ($C_{31}H_{30}N_4O_2SiZn$); λ_{abs} 417, 551, 587 nm.

4.6.9. Zn(II)-5-(5,5-dimethyl-1,3-dioxan-2-yl)porphyrin (Zn5ij) from 3j+1i. Following the standard procedure, reaction of 1.00 mmol of **3j** and **1i** afforded a purple solid (56.0 mg, 12%); ^{1}H NMR δ 1.17 (s, 3H), 2.01 (s, 3H), 4.30–4.40 (m, 4H), 8.09 (s, 1H), 9.41 (s, 4H), 9.53 (d, J=4.0 Hz, 2H), 10.15 (s, 1H), 10.19 (d, J=4.0 Hz, 2H), 10.25 (s, 2H); ^{13}C NMR (THF-d_8) δ 21.6, 30.3, 79.4, 104.4, 104.6, 106.6, 108.8, 112.1, 129.6, 130.5, 130.9, 131.1, 131.4, 132.3, 133.7, 148.52, 148.59, 148.87, 148.90, 149.1, 149.5, 150.3, 152.6; LD-MS obsd 485.6; FAB-MS obsd 486.1057, calcd 486.1034 ($C_{26}H_{22}N_4O_2Zn$); λ_{abs} 403, 535 nm.

4.6.10. Zn(II)-5-allylporphyrin (Zn5ik) from 3k+1i. Following the standard procedure, reaction of 1.00 mmol of **3k** and **1i** afforded a purple solid (71.2 mg, 17%); ^{1}H NMR δ 5.17–5.22 (m, 2H), 5.94–5.96 (m, 2H), 6.89–6.96 (m, 1H), 9.46–9.47 (m, 6H), 9.72–9.73 (m, 2H), 10.17 (s, 1H), 10.19 (s, 2H); ^{13}C NMR (THF-d_8) δ 41.0, 105.51, 105.54, 106.42, 106.46, 116.4, 117.9, 131.2, 133.56, 133.63, 133.65, 144.6, 151.1, 151.4, 151.91, 152.03; LD-MS obsd 412.1; FAB-MS obsd 412.0632, calcd 412.0666 ($C_{23}H_{16}N_4Zn$); λ_{abs} 406, 538 nm.

4.6.11. Zn(II)-5-(tridec-7-yl)porphyrin (Zn5il) from 3l+1i. Following the standard procedure, reaction of 1.00 mmol of **3l** and **1i** afforded a purple solid (123 mg, 22%); ^{1}H NMR δ 0.67–0.70 (m, 6H), 1.02–1.17 (m, 12H), 1.33–1.43 (m, 2H), 1.60–1.64 (m, 2H), 2.81–2.89 (m, 2H), 3.01–3.07 (m, 2H), 5.40–5.44 (m, 1H), 9.42–9.46 (m, 4H), 9.51 (d, J=4.0 Hz, 1H), 9.54 (d, J=4.0 Hz, 1H), 9.92 (d, J=5.2 Hz, 1H), 10.01 (d, J=5.2 Hz, 1H), 10.13 (s, 1H), 10.25 (s, 2H); ^{13}C NMR δ 14.2, 22.8, 29.9, 31.9, 43.1, 47.5, 103.8, 105.0, 105.2, 125.5, 130.2, 131.2, 131.63, 131.77, 131.83, 131.98, 132.01, 147.4, 148.7, 148.9, 149.2, 149.55, 149.60, 151.5; LD-MS obsd 555.8; FAB-MS obsd 554.2439, calcd 554.2388 ($C_{33}H_{38}N_4Zn$); λ_{abs} 406, 538 nm.

4.6.12. Zn(II)-5-ethoxycarbonylporphyrin (Zn5im) from 3m+1i. Following the standard procedure, reaction of 1.00 mmol of **3m** and **1i** afforded a purple solid (22.0 mg, 5%); ^{1}H NMR (THF-d_8) δ 1.82 (t, J=7.2 Hz, 3H), 5.09 (q, J=7.2 Hz, 2H), 9.51–9.55 (m, 6H), 9.68 (d, J=4.4 Hz, 2H), 10.35 (s, 2H), 10.37 (s, 1H); ^{13}C NMR (THF-d_8) δ 14.4, 62.2, 105.7, 106.4, 108.8, 131.1, 131.7, 132.33, 132.46, 148.7, 149.50, 149.75, 150.12, 171.8; LD-MS obsd 443.9; FAB-MS obsd 444.0566, calcd 444.0565 ($C_{23}H_{16}N_4O_2Zn$); λ_{abs} 403, 535 nm.

4.6.13. Zn(II)-5,15-bis(tridec-7-yl)porphyrin (Zn5ll) from 3l+1l. Following the standard procedure, reaction of 0.800 mmol of **3l** and **1l** afforded a purple solid (81.0 mg, 14%); ^{1}H NMR δ 0.68–0.71 (m, 12H), 1.01–1.14 (m, 24H), 1.31–1.39 (m, 4H), 1.54–1.62 (m, 4H), 2.76–2.85 (m, 4H), 2.97–3.07 (m, 4H), 5.32–5.37 (m, 2H), 9.46–9.50 (m, 4H), 9.84–9.86 (m, 2H), 9.92–9.94 (m, 2H), 10.21 (s, 2H); ^{13}C NMR δ 14.2, 22.7, 29.8, 31.9, 42.8, 47.2, 104.93, 105.21, 105.49, 124.0, 130.02, 130.25, 130.95, 131.17, 131.50, 131.82, 147.12, 147.37, 149.18, 149.45, 149.72, 149.76, 152.04, 152.10; LD-MS obsd 736.0; FAB-MS obsd 736.4412, calcd 736.4422 ($C_{46}H_{64}N_4Zn$); λ_{abs} 412, 548 nm.

Acknowledgements

This research was supported by a grant from the NIH (GM36238). Mass spectra were obtained at the Mass Spectrometry Laboratory for Biotechnology. Partial funding for the facility was obtained from the North Carolina Biotechnology Center and the National Science Foundation.

References and notes

1. Rao, P. D.; Dhanalekshmi, S.; Littler, B. J.; Lindsey, J. S. *J. Org. Chem.* **2000**, *65*, 7323–7344.
2. Brückner, C.; Posakony, J. J.; Johnson, C. K.; Boyle, R. W.; James, B. R.; Dolphin, D. *J. Porphyrins Phthalocyanines* **1998**, *2*, 455–465.
3. Geier, G. R., III; Callinan, J. B.; Rao, P. D.; Lindsey, J. S. *J. Porphyrins Phthalocyanines* **2001**, *5*, 810–823.
4. (a) Markovac, A.; MacDonald, S. F. *Can. J. Chem.* **1965**, *43*, 3364–3371. (b) Clarke, O. J.; Boyle, R. W. *Tetrahedron Lett.* **1998**, *39*, 7167–7168.
5. Arsenault, G. P.; Bullock, E.; MacDonald, S. F. *J. Am. Chem. Soc.* **1960**, *82*, 4384–4389.
6. Baldwin, J. E.; Crossley, M. J.; Klose, T.; O'Rear, E. A., III; Peters, M. K. *Tetrahedron* **1982**, *38*, 27–39.
7. Tabushi, I.; Sakai, K.-i.; Yamamura, K. *Tetrahedron Lett.* **1978**, *19*, 1821–1824.
8. (a) Westall, R. G. *Nature* **1952**, *170*, 614–616. (b) Cookson, G. H.; Rimington, C. *Nature* **1953**, *171*, 875–876. (c) Shemin, D.; Russell, C. S. *J. Am. Chem. Soc.* **1953**, *75*, 4873–4874. (d) Cookson, G. H.; Rimington, C. *Biochem. J.* **1954**, *57*, 476–484.
9. (a) Bachman, G. B.; Heisey, L. V. *J. Am. Chem. Soc.* **1946**, *68*, 2496–2499. (b) Herz, W.; Dittmer, K.; Cristol, S. J. *J. Am. Chem. Soc.* **1947**, *69*, 1698–1700.
10. Schreiber, J.; Maag, H.; Hashimoto, N.; Eschenmoser, A. *Angew. Chem., Int. Ed.* **1971**, *10*, 330–331.
11. Eisner, U.; Linstead, R. P. *J. Chem. Soc.* **1955**, 3742–3749.
12. (a) Eisner, U.; Linstead, R. P.; Parkes, E. A.; Stephen, E. *J. Chem. Soc.* **1956**, 1655–1661. (b) Eisner, U. *J. Chem. Soc.* **1957**, 854–858. (c) Eisner, U.; Lichtarowicz, A.; Linstead, R. P. *J. Chem. Soc.* **1957**, 733–739. (d) Bullock, E.; Johnson, A. W.; Markham, E.; Shaw, K. B. *J. Chem. Soc.* **1958**, 1430–1440. (e) Friedman, M. *J. Org. Chem.* **1965**, *30*, 859–863. (f) Egorova, G. D.; Solev'ev, K. N.; Shul'ga, A. M. *Russ. J. Gen. Chem.* **1967**, *37*, 333–336. (g) Whitlock, H. W.; Hanauer, R. *J. Org. Chem.* **1968**, *33*, 2169–2171. (h) Kinoshita, H.; Tanaka, S.; Nishimori, N.; Dejima, H.; Inomata, K. *Bull. Chem. Soc. Jpn.* **1992**, *65*, 2660–2667. (i) Tabushi, I.; Sakai, K.-i.; Yamamura, K. *Tetrahedron Lett.* **1978**, *19*, 1821–1824.

13. Nguyen, L. T.; Senge, M. O.; Smith, K. M. *Tetrahedron Lett.* **1994**, *35*, 7581–7584.
14. Nguyen, L. T.; Senge, M. O.; Smith, K. M. *J. Org. Chem.* **1996**, *61*, 998–1003.
15. Siri, O.; Smith, K. M. *Tetrahedron Lett.* **2003**, *44*, 6103–6105.
16. (a) Dolphin, D.; Rettig, S. J.; Tang, H.; Wijesekera, T.; Xie, L. Y. *J. Am. Chem. Soc.* **1993**, *115*, 9301–9302. (b) Boyle, R. W.; Xie, L. Y.; Dolphin, D. *Tetrahedron Lett.* **1994**, *35*, 5377–5380. (c) Xie, L. Y.; Boyle, R. W.; Dolphin, D. *J. Am. Chem. Soc.* **1996**, *118*, 4853–4859.
17. (a) Hombrecher, H. K.; Horter, G. *Liebigs Ann. Chem.* **1991**, 219–227. (b) Hombrecher, H. K.; Horter, G.; Arp, C. *Tetrahedron* **1992**, *48*, 9451–9460. (c) Schell, C.; Hombrecher, H. K. *Bioorg. Med. Chem.* **1999**, *7*, 1857–1865. (d) Schell, C.; Hombrecher, H. K. *Chem. Eur. J.* **1999**, *5*, 587–598.
18. Mizutani, T.; Ema, T.; Tomita, T.; Kuroda, Y.; Ogoshi, H. *J. Am. Chem. Soc.* **1994**, *116*, 4240–4250.
19. Hammel, D.; Erk, P.; Schuler, B.; Heinze, J.; Müllen, K. *Adv. Mater.* **1992**, *4*, 737–739.
20. Littler, B. J.; Ciringh, Y.; Lindsey, J. S. *J. Org. Chem.* **1999**, *64*, 2864–2872.
21. Srinivasan, N.; Haney, C. A.; Lindsey, J. S.; Zhang, W.; Chait, B. T. *J. Porphyrins Phthalocyanines* **1999**, *3*, 283–291.
22. Lee, C.-H.; Lindsey, J. S. *Tetrahedron* **1994**, *50*, 11427–11440.
23. Lee, C.-H.; Kim, J.-Y. *Bull. Korean Chem. Soc.* **1996**, *17*, 215–217.
24. Boyle, R. W.; Karunaratne, V.; Jasat, A.; Mar, E. K.; Dolphin, D. *Synlett* **1994**, 939–940.
25. Oddo, B.; Cambieri, F. *Gazz. Chim. Ital.* **1940**, *70*, 559–564.
26. Wang, Q. M.; Bruce, D. W. *Synlett* **1995**, 1267–1268.
27. Balakumar, A.; Muthukumaran, K.; Lindsey, J. S. *J. Org. Chem.* **2004**, *69*, 5112–5115.
28. Liu, Z.; Yasseri, A. A.; Loewe, R. S.; Lysenko, A. B.; Malinovskii, V. L.; Zhao, Q.; Surthi, S.; Li, Q.; Misra, V.; Lindsey, J. S.; Bocian, D. F. *J. Org. Chem.* **2004**, *69*, 5568–5577.
29. Thamyongkit, P.; Speckbacher, M.; Diers, J. R.; Kee, H. L.; Kirmaier, C.; Holten, D.; Bocian, D. F.; Lindsey, J. S. *J. Org. Chem.* **2004**, *69*, 3700–3710.
30. Trova, M. P.; Gauuan, P. J. F.; Pechulis, A. D.; Bubb, S. M.; Bocckino, S. B.; Crapo, J. D.; Day, B. J. *Bioorg. Med. Chem.* **2003**, *11*, 2695–2707.
31. Wilson, G. S.; Anderson, H. L. *Synlett* **1996**, 1039–1040.
32. Laha, J. K.; Dhanalekshmi, S.; Taniguchi, M.; Ambroise, A.; Lindsey, J. S. *Org. Process Res. Dev.* **2003**, *7*, 799–812.

Available online at www.sciencedirect.com
SCIENCE DIRECT
Tetrahedron
ELSEVIER
Tetrahedron 61 (2005) 10303–10308

Synthesis of 4-halophosphaisocoumarins via halocyclization of 2-(1-alkynyl)phenylphosphonates

Ai-Yun Peng[a,b] and Yi-Xiang Ding[b,*]

[a]*School of Chemistry & Chemical Engineering, Sun Yat-sen University, 135 Xingangxi Lu, Guangzhou 510275, China*
[b]*Shanghai Institute of Organic Chemistry, Chinese Academy of Sciences, 354 Fenglin Lu, Shanghai 200032, China*

Received 21 June 2005; revised 1 August 2005; accepted 2 August 2005

Abstract—A series of 4-halophosphaisocoumarins were prepared with high regioselectivity in good to excellent yields under mild conditions by the reaction of 2-(1-alkynyl)phenylphosphonic acid diesters with I_2 in $CHCl_3$ or ICl in CH_2Cl_2, or by the reaction of 2-(1-alkynyl)phenylphosphonic acid monoesters with NBS or NCS in DMF. Whether the alkynylphosphonates could cyclize or not was affected by the substituents, reaction solvents and electrophiles. A rationale for this reaction is discussed.

1. Introduction

4-Chloroisocoumarins **1** are effective irreversible inhibitors of serine proteases[1] and potent inhibitors of amyloid peptide production.[2] Since there is a remarkable similarity in bioactivities between the carbon species and their phosphorus counterparts,[3] one would anticipate that phosphorus 4-chloroisocoumarin analogs **2–4** might have potential bioactivities similar to those of the 4-chloroisocoumarins reported herein (Fig. 1).

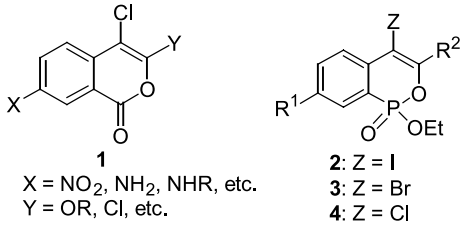

Figure 1. 4-Chloroisocoumarins and 4-haolophosphaisocoumarins.

In a recent communication, we described the synthesis of 4-iodophosphaisocoumarins **2** via iodocyclization of 2-(1-alkynyl)phenylphosphonic acid diesters with I_2 or ICl.[4] However, the bromo- and chlorophosphaisocoumarins **3** and **4** remain unknown compounds as yet. On the other hand, during the course of preparing **2**, we found that this iodocyclization reaction showed very high 6-*endo*-dig[5] regioselectivity and the yields of **2** were dependent on the substituents of the substrates and the strength of the electrophiles. We think it is necessary to further study the cyclization of phosphonates to C–C triple bond with other electrophiles and synthesize more type of phosphaisocoumarins for future bioassays. Herein, we wish to present a detailed study on the halocyclization of 2-(1-alkynyl)-phenylphosphonates with I_2, ICl, NBS and NCS, respectively, and discuss the plausible mechanisms in this paper.

2. Results and discussion

We first examined the reaction of 2-(phenylethynyl) phenylphosphonate **5a** with 2.0 equiv of iodine in several different organic solvents at room temperature. It was obvious that the reaction was highly dependent on the type of solvent used (Table 1, entries 1–5). In CH_3CN and DMF, the diiodide **6a** was the major product (entries 1, 2); in benzene, a ketone byproduct **7a** was isolated (entry 3) (Fig. 2). Fortunately, when the reaction was run in $CHCl_3$ or CH_2Cl_2, the desired product **2a** was produced in good yield (entries 4, 5).

To explore the scope of this reaction, other 2-(1-alkynyl) phenylphosphonic acid diesters **5** with a variety of substituents were allowed to react with I_2 in $CHCl_3$ or with ICl in CH_2Cl_2 and the results are summarized in Table 1. I_2 was efficient in most cases and a series of 4-iodophosphaisocoumarins were obtained in good to excellent yields. However, **5c** with an H group on the

Keywords: Synthesis; Phosphonates; Alkynes; 4-Halophosphaisocoumarins; Halocyclization.
* Corresponding author. Tel.: +86 21 54925334; fax: +86 21 64166128; e-mail: dingyx@mail.sioc.ac.cn

0040–4020/$ - see front matter © 2005 Elsevier Ltd. All rights reserved.
doi:10.1016/j.tet.2005.08.032

Table 1. Synthesis of phosphaisocoumarins via iodocyclization of **5**[a]

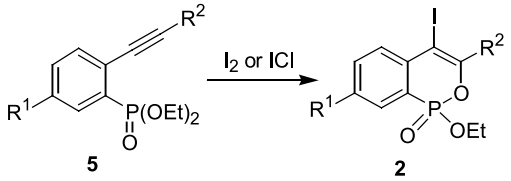

5 **2**

Entry	R^1	R^2	Solvent	Product(s)	Yield (%)[b]
1	H	C_6H_5	CH_3CN	**6a**	85
2	H	C_6H_5	DMF	**6a**	65
3	H	C_6H_5	PhH	**2a**+**7a**	35+15
4	H	C_6H_5	CH_2Cl_2	**2a**	80
5	H	C_6H_5	$CHCl_3$	**2a**	83
6	H	*n*-C_4H_9	$CHCl_3$	**2b**	70
7	H	H	$CHCl_3$	**2c**+**6c**	4+65
8[b]	H	H	CH_2Cl_2	**2c**	35
9	Cl	4-EtC_6H_4	$CHCl_3$	**2d**+**7d**	64+30
10[c]	Cl	4-EtC_6H_4	$CHCl_3$	**2d**	78
11	Cl	C_6H_5	$CHCl_3$	**2e**+**7e**	67+25
12[c]	Cl	C_6H_5	$CHCl_3$	**2e**	80
13	Cl	*n*-C_4H_9	$CHCl_3$	**2f**	64
14	Cl	Cyclopropyl	$CHCl_3$	**2g**	76
15	Cl	CH_2OCH_3	$CHCl_3$	**2h**	46
16	Cl	$SiMe_3$	$CHCl_3$	**2i**	0
17[b]	Cl	$SiMe_3$	CH_2Cl_2	**2i**	82
18	CH_3O	C_6H_5	$CHCl_3$	**2j**	93

[a] All reactions were conducted at room temperature with 2.0 equiv of I_2 in solvent for 12 h and the solvent was used as received unless otherwise specified.
[b] The reaction was carried out at room temperature with 1.2 equiv of ICl in CH_2Cl_2 under N_2 for 10 h.
[c] In this reaction, the solvent $CHCl_3$ was distilled from calcium hydride.

acetylenic moiety (R^2=H) gave the diiodide as the major product (entry 7). A bulky $SiMe_3$ group (entry 16) totally halted the reaction and the starting material **5i** was completely recovered under these conditions. Use of the strong electrophile ICl instead of I_2 afforded the desired products **2c** and **2i** in moderate yields for **5c** and **5i** (entries 8 and 17). It is also worth mentioning that for the reactions of **5d** and **5e** (entries 9 and 11), the corresponding α-ketone byproducts **7d** and **7e** resulting from water attacking onto the iodonium intermediates were also isolated (entries 9 and 11);[4] the α-ketone byproducts could be reduced substantially when the above reactions were carried out in anhydrous $CHCl_3$ (entries 10 and 12) (Fig. 2).

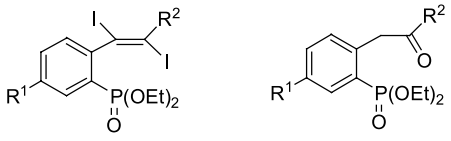

6 **7**

Figure 2. The structures of **6** and **7**.

We next studied the bromocyclization reaction of **5a**. Under the similar conditions used for the iodocyclization of **5a**, the reaction of **5a** with 2.0 equiv of NBS in $CHCl_3$ at room temperature for 48 h did not lead to any cyclization products but rather to an unidentified product (Scheme 1). This result was not surprising. Iodocyclization of unsaturated compounds is one of the most important procedures to construct various heterocycles containing N, O, S atoms.[6] However, there are far fewer reports about bromocyclization reactions[7] and especially chlorocyclization reactions,[7a,b] probably because of the stability of the corresponding halonium intermediates decreasing in the order of I>Br>Cl.[8] It has been reported that iodocyclization of alkenylphosphonic acid diesters could proceed smoothly, while under the similar conditions, bromocyclization of the same substrates only led to dibromides.[9] Although Shibuya and co-workers at last synthesized phostones by bromocyclization of alkenylphosphonic acid monoesters, they did not extend it to the chlorocyclization reactions.[10] The weak nucleophilicity of phosphonyl group and the lower reactivity of alkynes towards electrophilic reagents than that of alkenes might add more challenge to our proposed halocyclization reactions.

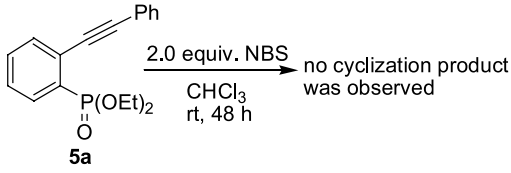

5a

Scheme 1. The reaction of **5a** with NBS in $CHCl_3$.

We then investigated the reaction of 2-(phenylethynyl) phenylphosphonic acid monoester **8a** with NBS. When using $CHCl_3$ as the solvent, the reaction of **8a** with 2.0 equiv of NBS at room temperature for 24 h afforded only a trace amount of the cyclization product **3a**. However, we were pleased to see that when using DMF as the solvent, the reaction of **8a** with NBS gave **3a** as the single product in 74% isolated yield (Table 2, entry 1). We thought that the solvents had a large effect on the reaction largely because the solvent DMF could act as a Lewis base to enhance the nucleophilicity of the phosphonyl oxygen.[11]

To explore the scope of this bromocyclization reaction, a series of 2-(1-alkynyl)phenylphosphonic monoesters **8** were

Table 2. Synthesis of phosphaisocoumarins via bromo- and chlorocyclization of **8**[a]

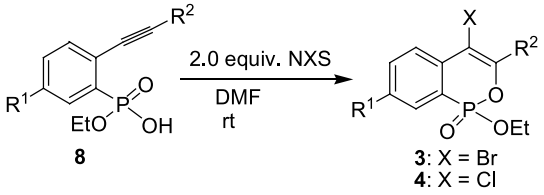

Entry	R^1	R^2	NXS	Product	Yield (%)[b]
1	H	C_6H_5	NBS	**3a**	74
2	Cl	C_6H_5	NBS	**3b**	84
3	Cl	4-EtC_6H_4	NBS	**3c**	85
4	Cl	Cyclopropyl	NBS	**3d**	73
5	Cl	*n*-C_4H_9	NBS	**3e**	85
6	Cl	CH_2OCH_3	NBS	**3f**	Trace
7	CH_3O	C_6H_5	NBS	**3g**	51
8	H	C_6H_5	NCS	**4a**	73
9	Cl	C_6H_5	NCS	**4b**	66
10	Cl	4-EtC_6H_4	NCS	**4c**	69
11	Cl	Cyclopropyl	NCS	**4d**	73
12	Cl	*n*-C_4H_9	NCS	**4e**	Trace
13	Cl	CH_2OCH_3	NCS	**4f**	Trace
14	CH_3O	C_6H_5	NCS	**4g**	Trace

[a] All reactions were conducted at room temperature with 2.0 equiv of NBS or NCS in DMF for 24 h.
[b] Isolated yield.

allowed to react with NBS or NCS in DMF at room temperature and the results are summarized in Table 2. Apparently, the substituents and electrophiles have large effects on the reaction. The substrates **8a–d** with aryl and cyclopropyl groups on the acetylenic moiety could react with both NBS and NCS to give the desired products in good to excellent yields (entries 1–4, 8–11). The substrate **8f** with an electron-withdrawing methoxymethyl group did not participate in either bromo- or chlorocyclization reaction (entries 6 and 13). The reaction of **8e** having a *n*-butyl group on the acetylenic moiety with NBS produced the desired product **3e** in 85% yield (entry 5), but most of the starting material **8e** was recovered even after extended exposure to NCS under the same conditions (entry 12). Moreover, the reaction of **8g** bearing an electron-donating methoxy group on the benzene with NBS gave the product **3g** only in 51% yield (entry 7), and the chlorocyclization of **8g** did not proceed at all under our conditions (entry 14). It is also worth mentioning that no 5-*exo*-dig[5] cyclization products were detected in each case. The bromo- and chlorocyclization products are assigned as **3** and **4** based on comparison of their IR, ^{1}H NMR, ^{31}P NMR spectrum with those of **2**.[4]

We rationalized our results by plausible mechanisms shown in Scheme 2. Electrophilic addition of I_2, ICl, NBS or NCS to the C–C triple bond might form the corresponding intermediates **A**, **B** or **C**; their stabilities and the nucleophilicity of the phosphonyl oxygen play crucial roles in determining whether the alkynylphosphonates will cyclize or not. Intramolecular nucleophilic attack by the phosphonyl oxygen onto the position 2 of **A** or **C** would give the desired products **2**, **3** or **4**. Alternatively, the phosphonyl oxygen might also attack onto the position 1 of **A** or **B** to give the five-membered-ring products. However, all the examined substrates showed high regioselectivity for six-membered-ring products, indicating that the 5-*exo*-dig process was very disadvantageous for 2-(1-alkynyl)phenylphosphonates. The above regioselectivity might be caused by the following factors: (1) the longer bond lengths of C–P and P–O would make the phosphonyl oxygen much closer to the farther position of the triple bonds; (2) the tetrahedral phosphonates might further increase the ring strain and lower the stabililty of the corresponding five-membered-ring products. Thus, the substrates (e.g., **8e** and **8g**), bearing groups that can better stabilize the benzylic cations **B** other than intermediates **C**, did not proceed the chlorocyclization reactions smoothly (Table 2, entries 12, 14). By way of contrast, the substituents have fewer effects on the iodo- and bromocyclization than on the chlorocyclization, probably because iodonium ions compete more effectively with open carbocations than bromonium ions, chloronium ions compete less effectively,[8] and it is difficult for open carbocations **B** to form the desired cyclization products.

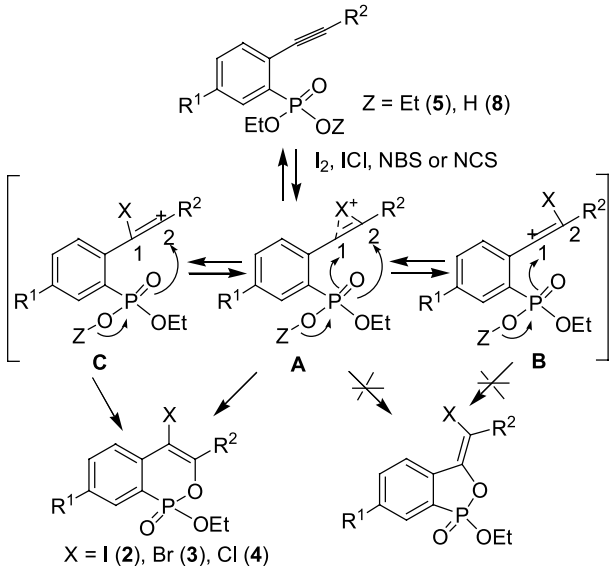

Scheme 2. Plausible mechanisms of the halocyclization of 2-(1-alkynyl) phenylphosphonates.

3. Conclusions

In conclusion, a series of 4-iodophosphaisocoumarins were prepared with high regioselectivity in good yields via iodocyclization of 2-(1-alkynyl)phenylphosphonic acid diesters with I_2 in $CHCl_3$ or ICl in CH_2Cl_2, and 4-bromo- and 4-chlorophosphaisocoumarins were synthesized by the reaction of 2-(1-alkynyl)phenylphosphonic acid monoesters with NBS and NCS in DMF. These halocyclization reactions have been much affected by the substituents of the substrates, reaction solvents and electrophiles, which could be rationalized by the proposed mechanisms in this paper.

4. Experimental

4.1. General

NMR spectra were all recorded on a Varian Mercury 300 spectrometer using $CDCl_3$ as the solvent. The ^1H NMR spectra used $CDCl_3$ (with TMS) as the internal reference at 7.27 ppm. ^{31}P NMR spectra used the 85% H_3PO_4 as the external reference. MS spectra were determined using a HP5989A mass spectrometer. IR spectra were measured on a Y-Zoom Cursor instrument. Starting materials **5** and **8** were prepared as described previously.[11]

4.2. General procedure for the halocyclization of 5 by I_2

A mixture of **5** (0.50 mmol) and I_2 (1.00 mmol) was dissolved in $CHCl_3$ (5.0 mL). After stirring at room temperature for 12 h, the reaction mixture was then diluted with EtOAc and washed with 5% aqueous $Na_2S_2O_3$. The organic phase was washed with brine, dried (Na_2SO_4), and evaporated in vacuo. The residue was chromatographed on silica gel using hexane/EtOAc as eluent to give the corresponding product **2**.

4.3. General procedure for the halocyclization of 5 by ICl

To the substrate **5** (0.10 mmol) was added ICl (0.12 mmol) in CH_2Cl_2 (1.2 mL), and the resulting mixture was stirred in the dark under nitrogen at room temperature for 10 h. The reaction mixture was then diluted with EtOAc and washed with 5% aqueous $Na_2S_2O_3$. The organic phase was washed with brine, dried (Na_2SO_4), and evaporated in vacuo. The residue was chromatographed on silica gel using hexane/EtOAc as eluent to give the product **2**.

For the characterization data of compounds **2** in Table 1, see the Supporting information of Ref. 4.

4.4. Characterization data for compounds 6a, 6c, 7d, and 7e listed in Table 1

4.4.1. Diethyl 2-((*E*)1,2-diiodo-2-phenylvinyl)phenylphosphonate (6a). Red oil. ^1H NMR (300 MHz, $CDCl_3$): δ 8.20–8.23 (m, 2H), 7.50–7.88 (m, 7H), 3.97–4.11 (m, 4H), 1.28 (t, $J=6.9$ Hz, 6H); MS (EI), *m/z* (%): 441 [$(M-I)^+$, 5], 412 (2), 385 (2), 241 (82), 213 (28), 185 (100), 167 (22), 105 (19), 77 (25); IR (film, cm^{-1}): ν 3062, 2924, 1596, 1450, 1209, 1146, 1099, 1019, 934.

4.4.2. Diethyl 2-((*E*)1,2-diiodovinyl)phenylphosphonate (6c). Red oil. ^1H NMR (300 MHz, $CDCl_3$): δ 7.83–7.93 (m, 1H), 7.33–7.53 (m, 2H), 7.11–7.23 (m, 2H), 4.00–4.19 (m, 4H), 1.25–1.34 (m, 6H); MS (EI), *m/z* (%): 365 [$(M-I)^+$, 86], 336 (30), 309 (100), 291 (10), 182 (46), 165 (23), 153 (43), 136 (26), 118 (21); IR (film, cm^{-1}): ν 3058, 2980, 1592, 1466, 1391, 1243, 1140, 1081, 1049, 1024, 970.

4.4.3. {5-Chloro-2-[2-(4-ethyl-phenyl)-2-oxo-ethyl]-phenyl}-phosphonic acid diethyl ester (7d). Pale yellow oil. ^1H NMR (300 MHz, $CDCl_3$): δ 7.90–7.98 (m, 3H), 7.19–7.50 (m, 4H), 4.66 (s, 2H), 3.96–4.11 (m, 4H), 2.72 (q, $J=7.5$ Hz, 2H), 1.20–1.27 (m, 9H); MS (EI), *m/z* (%): 394 (M^+, 1), 291 (2), 254 (6), 178 (6), 150 (49), 133 (100), 105 (92), 77 (39); IR (film, cm^{-1}): ν 2969, 1686, 1606, 1478, 1384, 1250, 1221, 1182, 1106, 1019, 971. Anal. Calcd for $C_{20}H_{24}ClO_4P$: C, 60.82; H, 6.14. Found: C, 61.03; H, 6.18.

4.4.4. [5-Chloro-2-(2-oxo-2-phenyl-ethyl)-phenyl]-phosphonic acid diethyl ester (7e). Pale yellow oil. ^1H NMR (300 MHz, $CDCl_3$): δ 7.51–8.06 (m, 7H), 7.24–7.29 (m, 1H), 4.73 (s, 2H), 4.03–4.17 (m, 4H), 1.25 (dt, $J_1=7.2$ Hz, $J_2=2.4$ Hz, 6H); MS (EI), *m/z* (%): 366 (M^+, 6), 261 (1), 228 (2), 187 (4), 165 (2), 105 (100), 77 (28); IR (film, cm^{-1}): ν 2982, 1691, 1598, 1478, 1384, 1330, 1250, 1217, 1150, 1019, 969; HRMS (EI): calcd for $C_{18}H_{20}ClO_4P$ (M^+): 366.07877. Found: 366.07821.

4.5. General procedures for the preparation of 3 and 4

A mixture of **8** (0.50 mmol), NBS (1.00 mmol) or NCS (1.00 mmol) was dissolved in DMF (5.0 mL). After stirring at room temperature for 24 h, the reaction mixture was then diluted with EtOAc and washed with 5% aqueous $Na_2S_2O_3$. The organic phase was washed with brine, dried (Na_2SO_4), and evaporated in vacuo. The residue was chromatographed on silica gel using hexane–EtOAc (5/1–2/1) as eluent to give the corresponding product **3** or **4**. The isolated yield and the physical data for **3** and **4** are as follows:

4.5.1. 1-Ethoxy-3-phenyl-4-bromobenzo[*c*][1,2]oxaphosphinine 1-oxide (3a). White solid, mp 109–110 °C. Yield: 74%. ^1H NMR (300 MHz, $CDCl_3$): δ 7.92–8.01 (m, 2H), 7.71–7.88 (m, 3H), 7.45–7.56 (m, 4H), 4.25–4.31 (m, 2H), 1.36 (t, $J=6.9$ Hz, 3H); ^{31}P NMR (121 MHz, $CDCl_3$): δ 9.94; MS (EI), *m/z* (%): 364 (M^+, 97), 336 (100), 279 (9), 257 (12), 239 (38), 229 (1), 165 (19), 105 (54), 77 (43); IR (KBr, cm^{-1}): ν 2992, 1608, 1446, 1268, 1234, 1070, 1019, 970. Anal. Calcd for $C_{16}H_{14}BrO_3P$: C, 52.62; H, 3.87. Found: C, 52.55; H, 3.88.

4.5.2. 7-Chloro-1-ethoxy-3-phenyl-4-bromobenzo[*c*][1,2]oxaphosphinine 1-oxide (3b). White solid, mp 109–110 °C. Yield: 84%. ^1H NMR (300 MHz, $CDCl_3$): δ 7.83–7.96 (m, 2H), 7.65–7.74 (m, 3H), 7.46–7.48 (m, 3H), 4.26–4.36 (m, 2H), 1.38 (t, $J=6.9$ Hz, 3H); ^{31}P NMR (121 MHz, $CDCl_3$): δ 14.24; MS (EI), *m/z* (%): 400 (97), 398 (M^+, 75), 372 (100), 273 (16), 263 (10), 199 (10), 163 (14), 105 (28), 77 (25); IR (KBr, cm^{-1}): ν 2999, 1594, 1467, 1385, 1285, 1246, 1160, 1069, 1009, 973. Anal. Calcd for $C_{16}H_{13}BrClO_3P$: C, 48.09; H, 3.29. Found: C, 48.11; H, 3.18.

4.5.3. 7-Chloro-1-ethoxy-3-(4-ethylphenyl)-4-bromobenzo[*c*][1,2]oxaphosphinine 1-oxide (3c). White solid, mp 121–122 °C. Yield: 85%. ^{1}H NMR (300 MHz, $CDCl_3$): δ 7.82–7.94 (m, 2H), 7.64–7.67 (m, 3H), 7.28–7.30 (m, 2H), 4.25–4.35 (m, 2H), 2.72 (q, J=7.8 Hz, 2H), 1.37 (t, J=6.9 Hz, 3H), 1.29 (t, J=7.8 Hz, 3H); ^{31}P NMR (121 MHz, $CDCl_3$): δ 8.34; MS (EI), *m*/*z* (%): 426 (M^+, 78), 428 (100), 400 (69), 385 (55), 319 (12), 291 (9), 255 (11), 189 (23), 105 (14), 77 (18); IR (KBr, cm^{-1}): ν 2965, 1592, 1461, 1281, 1268, 1158, 1065, 1028, 1018, 974. Anal. Calcd for $C_{18}H_{17}BrClO_3P$: C, 50.55; H, 4.01. Found: C, 50.45; H, 3.93.

4.5.4. 7-Chloro-4-bromo-3-cyclopropyl-1-ethoxybenzo[*c*][1,2]oxaphosphinine 1-oxide (3d). White solid, mp 82–83 °C. Yield: 73%. ^{1}H NMR (300 MHz, $CDCl_3$): δ 7.72–7.79 (m, 2H), 7.57–7.61 (m, 1H), 4.15–4.26 (m, 2H), 2.40–2.50 (m, 1H), 1.36 (t, J=6.9 Hz, 3H), 1.16–1.24 (m, 1H), 0.95–1.04 (m, 3H); ^{31}P NMR (121 MHz, $CDCl_3$): δ 9.05; MS (EI), *m*/*z* (%): 362 (M^+, 30), 364 (39), 336 (38), 255 (100), 237 (24), 220 (13), 209 (23), 175 (13), 139 (10), 99 (6), 75 (4); IR (KBr, cm^{-1}): ν 2988, 1600, 1465, 1392, 1284, 1266, 1161, 1062, 1018, 970. Anal. Calcd for $C_{13}H_{13}BrClO_3P$: C, 42.95; H, 3.60. Found: C, 43.01; H, 3.59.

4.5.5. 3-Butyl-4-bromo-7-chloro-1-ethoxy-benzo[*c*][1,2]oxaphosphinine 1-oxide (3e). Pale yellow oil. Yield: 85%. ^{1}H NMR (300 MHz, $CDCl_3$): δ 7.72–7.81 (m, 2H), 7.57–7.61 (m, 1H), 4.22–4.27 (m, 2H), 2.69–2.78 (m, 2H), 1.62–1.70 (m, 2H), 1.23–1.46 (m, 5H), 0.95 (t, J=7.2 Hz, 3H); ^{31}P NMR (121 MHz, $CDCl_3$): δ 12.39; MS (EI), *m*/*z* (%): 380 [$(M+2)^+$, 100], 378 (M^+, 77), 352 (26), 323 (52), 271 (90), 229 (64), 101 (6), 75 (7); IR (film, cm^{-1}): ν 2959, 1609, 1466, 1389, 1287, 1273, 1081, 1033, 971. Anal. Calcd for $C_{14}H_{17}BrClO_3P$: C, 44.30; H, 4.51. Found: C, 44.64; H, 4.47.

4.5.6. 7-Methoxy-1-ethoxy-3-phenyl-4-bromobenzo[*c*][1,2]oxaphosphinine 1-oxide (3g). White solid, mp 125–126 °C. Yield: 51%. ^{1}H NMR (300 MHz, $CDCl_3$): δ 7.88–7.94 (m, 1H), 7.70–7.74 (m, 2H), 7.35–7.47 (m, 4H), 7.21–7.25 (m, 1H), 4.22–4.32 (m, 2H), 3.92 (s, 3H), 1.37 (t, J=7.2 Hz, 3H); ^{31}P NMR (121 MHz, $CDCl_3$): δ 10.37; MS (EI), *m*/*z* (%): 394 (M^+, 100), 396 (96), 366 (94), 351 (50), 269 (4), 259 (16), 195 (4), 105 (31), 77 (34); IR (KBr, cm^{-1}): ν 2985, 1598, 1486, 1280, 1261, 1154, 1030, 1020, 948. Anal. Calcd for $C_{17}H_{16}BrO_4P$: C, 51.67; H, 4.08. Found: C, 51.90; H, 4.37.

4.5.7. 1-Ethoxy-3-phenyl-4-chlorobenzo[*c*][1,2]oxaphosphinine 1-oxide (4a). White solid, mp 100–101 °C. Yield: 73%. ^{1}H NMR (300 MHz, $CDCl_3$): δ 7.76–7.91 (m, 5H), 7.46–7.60 (m, 4H), 4.21–4.33 (m, 2H), 1.35 (t, J=7.2 Hz, 3H); ^{31}P NMR (121 MHz, $CDCl_3$): δ 14.28; MS (EI), *m*/*z* (%): 320 (M^+, 80), 292 (100), 235 (15), 199 (9), 165 (17), 105 (49), 77 (51); IR (KBr, cm^{-1}): ν 2995, 1609, 1446, 1388, 1268, 1235, 1159, 1020, 967. Anal. Calcd for $C_{16}H_{14}ClO_3P$: C, 59.92; H, 4.40. Found: C, 59.70; H, 4.25.

4.5.8. 7-Chloro-1-ethoxy-3-phenyl-4-chlorobenzo[*c*][1,2]oxaphosphinine 1-oxide (4b). White solid, mp 138–139 °C. Yield: 66%. ^{1}H NMR (300 MHz, $CDCl_3$): δ 7.67–7.92 (m, 5H), 7.46–7.49 (m, 3H), 4.25–4.35 (m, 2H), 1.37 (t, J=6.9 Hz, 3H); ^{31}P NMR (121 MHz, $CDCl_3$): δ 12.19; MS (EI), *m*/*z* (%): 354 (M^+, 70), 326 (100), 269 (8), 233 (4), 199 (8), 163 (13), 105 (39), 77 (36); IR (KBr, cm^{-1}): ν 2979, 1601, 1467, 1387, 1285, 1268, 1161, 1011, 969. Anal. Calcd for $C_{16}H_{13}Cl_2O_3P$: C, 54.11; H, 3.69. Found: C, 54.12; H 3.49.

4.5.9. 7-Chloro-1-ethoxy-3-(4-ethylphenyl)-4-chlorobenzo[*c*][1,2]oxaphosphinine 1-oxide (4c). White solid, mp 105–107 °C. Yield: 69%. ^{1}H NMR (300 MHz, $CDCl_3$): δ 7.84–7.92 (m, 2H), 7.66–7.75 (m, 3H), 7.29–7.32 (m, 2H), 4.25–4.35 (m, 2H), 2.73 (q, J=7.8 Hz, 2H), 1.36 (t, J=6.9 Hz, 3H), 1.29 (t, J=7.5 Hz, 3H); ^{31}P NMR (121 MHz, $CDCl_3$): δ 8.30; MS (EI), *m*/*z* (%): 382 (M^+, 100), 354 (85), 339 (82), 319 (19), 290 (11), 255 (15), 189 (14), 105 (12), 77 (18); IR (KBr, cm^{-1}): ν 2966, 1599, 1468, 1290, 1269, 1161, 1075, 1011, 972. Anal. Calcd for $C_{18}H_{17}Cl_2O_3P$: C, 56.42; H, 4.47. Found: C, 56.36; H, 4.54.

4.5.10. 4,7-Dichloro-3-cyclopropyl-1-ethoxy-benzo[*c*][1,2]oxaphosphinine 1-oxide (4d). White solid, mp 62–63 °C. Yield: 73%. ^{1}H NMR (300 MHz, $CDCl_3$): δ 7.59–7.81 (m, 3H), 4.15–4.26 (m, 2H), 2.33–2.43 (m, 1H), 1.35 (t, J=6.9 Hz, 3H), 1.16–1.24 (m, 1H), 0.94–1.04 (m, 3H); ^{31}P NMR (121 MHz, $CDCl_3$): δ 9.05; MS (EI), *m*/*z* (%): 318 (M^+, 72), 320 (47), 290 (100), 255 (94), 237 (27), 220 (15), 209 (37), 175 (21), 139 (15), 99 (9), 75 (10); IR (KBr, cm^{-1}): ν 2955, 1612, 1467, 1380, 1266, 1220, 1156, 1070, 1025, 988. Anal. Calcd for $C_{13}H_{13}Cl_2O_3P$: C, 48.93; H, 4.11. Found: C, 48.83; H 4.58.

References and notes

1. Powers, J. C.; Asgian, J. L.; Ekici, Ö.D.; James, K. E. *Chem. Rev.* **2002**, *102*, 4639–4750 and references therein.
2. Bihel, F.; Quelever, G.; Lelouard, H.; Petit, A.; Alves da Costa, C.; Pourquie, O.; Checler, F.; Thellend, A.; Pierre, P.; Kraus, J.-L. *Bioorg. Med. Chem.* **2003**, *11*, 3141–3152.
3. (a) Dillon, K. B.; Mathey, F.; Nixon FRS, J. F. *Phosphorus: The Carbon Copy*; Wiley: Chichester, 1998. (b) Quin, L. D. *A Guide to Organophosphorus Chemistry*; Wiley: New York, 2000; Chapter 11.
4. Peng, A.-Y.; Ding, Y.-X. *Org. Lett.* **2004**, *6*, 1119–1121.
5. Baldwin, J. E. *J. Chem. Soc., Chem. Commun.* **1976**, 734–736.
6. For the leading references, see: (a) review: Frederickson, M.; Grigg, R. *Org. Prep. Proced. Int.* **1997**, *29*, 33–62. (b) Flynn, B. L.; Verdier-Pinard, P.; Hamel, E. *Org. Lett.* **2001**, *3*, 651–654. (c) Knight, D. W.; Redfern, A. L.; Gilmore, J. *J. Chem. Soc., Perkin Trans. 1* **2002**, 622–628. (d) Rossi, R.; Carpita, A.; Bellina, F.; Stabile, P.; Mannina, L. *Tetrahedron* **2003**, *59*, 2067–2081. (e) Yao, T.; Larock, R. C. *J. Org. Chem.* **2003**, *68*, 5936–5942. (f) Barluenga, J.; Trincado, M.; Rubio, E.; González, M. J. *Angew. Chem., Int. Ed.* **2003**, *42*, 2406–2409. (g) Kang, S. H.; Lee, S. B.; Park, C. M. *J. Am. Chem. Soc.* **2003**, *125*, 15748–15749. (h) Yue, D.; Larock, R. C. *Org. Lett.* **2004**, *6*, 1037–1040.
7. (a) Krafft, G. A.; Katzenellenbogen, J. A. *J. Am. Chem. Soc.* **1981**, *103*, 5459–5466. (b) Nagarajan, A.; Balasubramanian, T. R. *Indian J. Chem., Sect. B* **1988**, *27*, 380. (c) Steinmann,

J. G.; Phillips, J. H.; Sanders, W. J.; Kiessling, L. L. *Org. Lett.* **2001**, *3*, 3557–3559.
8. Smith, M. B.; March, J. *Advanced Organic Chemistry*, 5th ed.; Wiley: New York, 2001; Chapter 15.
9. Zhao, Y.-F.; Yan, S.-J.; Zhai, C. *J. Org. Chem.* **1985**, *50*, 2136–2140.
10. Yokomatsu, T.; Shioya, Y.; Iwasawa, H.; Shibuya, S. *Heterocycles* **1997**, *46*, 463–472.
11. Peng, A.-Y.; Ding, Y.-X. *J. Am. Chem. Soc.* **2003**, *125*, 15006–15007.

Available online at www.sciencedirect.com
SCIENCE DIRECT
Tetrahedron
Tetrahedron 61 (2005) 10309–10320

Cation and anion fluorescent and electrochemical sensors derived from 4,4′-substituted biphenyl

Ana M. Costero,[a,*] M. José Bañuls,[a] M. José Aurell,[a] Luis E. Ochando[b] and Antonio Doménech[c]

[a]*Departamento de Química Orgánica, Universitat de València, Dr. Moliner 50, 46100-Burjassot, Valencia, Spain*
[b]*Departamento de Geología, Universitat de València, Valencia, Dr. Moliner 50, 46100-Burjassot, Valencia, Spain*
[c]*Departamento de Química Analítica, Universitat de València, Valencia, Dr. Moliner 50, 46100-Burjassot, Valencia, Spain*

Received 10 June 2005; revised 2 August 2005; accepted 2 August 2005

Abstract—Five new fluorescent macrocyclic ligands derived from biphenyl are described. These new compounds can be used in cation and anion recognition and sensing. Their fluorescent and electrochemical properties are studied and the influence of the biphenyl conformation on these properties is considered. The X-ray single crystal structure of one of the described ligands has been determined.

1. Introduction

Supramolecular chemistry has evolved to a coherent and lively body of concepts and has been progressive growing incorporating novel areas of investigation. Among all these areas one of the most attractive fields of research is that of programmed systems in which the recognition process is further coupled to a specific action. Among several examples of programmed supramolecular systems we will focus our research on the field of chemosensing where the recognition process is coupled to the specific action of signalling. One of the best approximations towards the development of chemosensors consists in coupling of two subunits each one displaying differentiable functions: the binding site and the signalling subunit. In the former resides the role of coordination to a certain species, whereas the task of the later consists in signalling the coordination event via changes in a physical property. In the approach of 'binding site-signalling subunit' these two subunits are covalently linked. To use fluorescent signalling subunits gives rise to fluorescent chemosensors whereas to use of electroactive systems allow the design of electrochemical chemosensors.[1] Most of the chemosensors prepared following this approach work inducing modifications in the electronic properties of the signalling unit but there are less examples of chemosensors based on conformational changes induced in the complexation process.[2] Among these later systems ligands derived from biphenyl systems have been widely used with different goals. Thus, some authors have reported their use as anion and cation fluorescent sensors due to the influence of the dihedral angle between both aromatic rings in their fluorescent behaviour.[3] On the other hand the introduction of different substituents on the biphenyl system gives rise to strong modifications not only in its fluorescent but also its electrochemical properties. Recently our research group has prepared different macrocyclic ligands directly bound to the 2,2′ positions of 4,4′-disubstituted biphenyls to be used as cationic or anionic sensors using their fluorescent or electrochemical properties.[4] These studies demonstrated that both the size of the cavity and the flexibility were two important factors not only for complexation but also for sensing. For this reason we now report the synthesis, complexation and electrochemical studies of several new compounds containing different functional groups and also different sizes in the binding cavity.

2. Results and discussion

The compounds studied in this research are reflected in Chart 1. The synthesis of ligands **1**, **2** and **3** is now described whereas the synthesis of compounds **4**, **5** and **6** has been previously published.[5] Preparation of **1** was accomplished by the method outlined in Scheme 1.

Ligand **1** was prepared from **6** by reduction with borane–tetrahydrofurane. Under these conditions the amide groups were reduced providing **1** as a yellow solid (Scheme 1).

Keywords: Chemosensors; Electrochemistry; Fluorescence; Biphenyl; Cations; Anions.
* Corresponding author. Tel.: +34 963544410; fax: +34 963543152; e-mail: ana.costero@uv.es

0040–4020/$ - see front matter © 2005 Elsevier Ltd. All rights reserved.
doi:10.1016/j.tet.2005.08.010

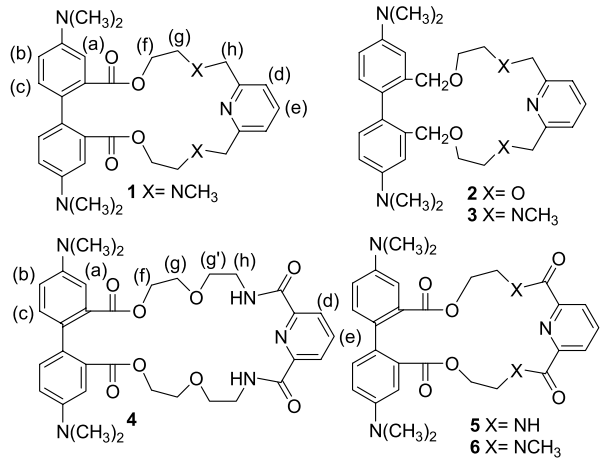

Chart 1.

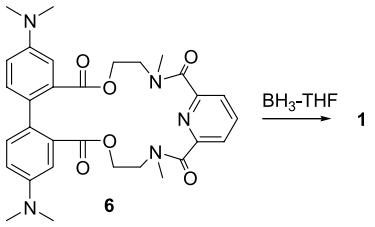

Scheme 1.

Preparation of ligands **2** and **3** was carried out as shown in Scheme 2 by reaction between 2,2′-bis(chloromethyl)-4,4′-bis(dimethylamino)biphenyl, whose synthesis was previously described,[6] and the corresponding chains. For the obtention of these chains different pathways were used. Thus, 2,6-pyridindicarbaldehyde, **7**, was prepared from 2,6-pyridindimethanol employing selenium oxyde following the procedure described in the literature.[7] The dialdehyde was then treated with *N*-methyl ethanolamine and sodium borohydride to give 2,6-bis[*N*-methyl-*N*-(2-hydroxyethyl)aminomethyl]pyridine (**8**) (Scheme 3).

In the case of compound **2**, 2,6-pyridinedimethanol was reacted with methyl bromoacetate and then, the formed diester was reduced with lithium borohydride providing 2,6-bis[(2-hydroxy)ethoxymethyl]pyridine (**9**).[8]

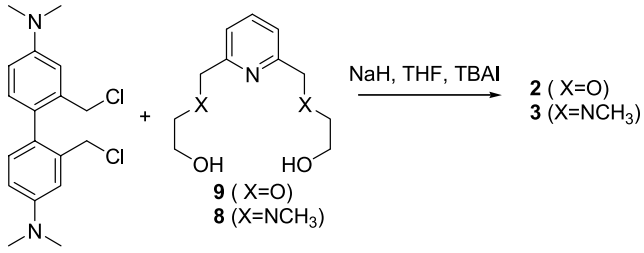

Scheme 2.

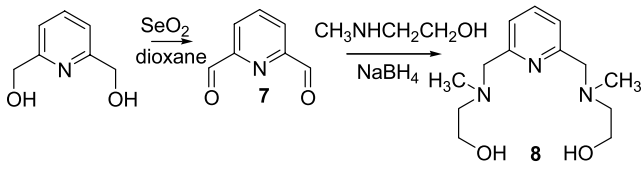

Scheme 3.

2.1. X-ray

X-ray single-crystal studies were performed on compound **1** (Fig. 1). Suitable crystals were obtained by slow evaporation of a solution of **1** in methanol–hexane. As can be seen in the structure, ligand **1** presented a diminution of the rigidity in the structure in comparison with other related compounds.[4b,5] This fact leads to an increase of the size inside the cavity.

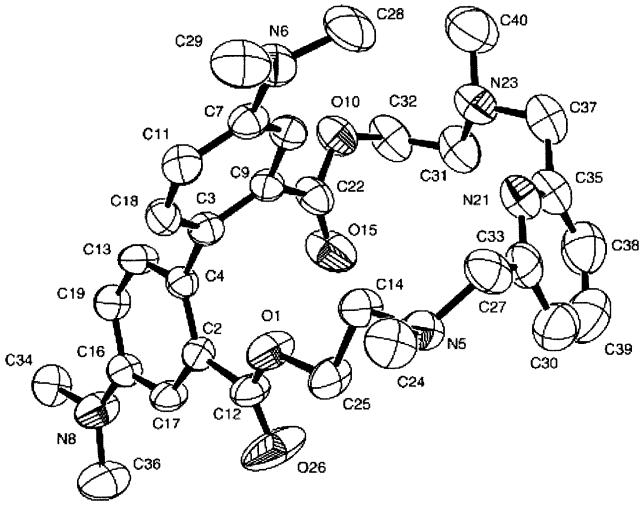

Figure 1. Molecular structure with crystallographic numbering scheme for compound **1**. For clarity, only an average position of O(26) has been drawn. This atom is disordered over two sites with occupancies at 50%.

The ester groups were almost coplanar to the biphenyl rings (O(26A)–C(12)–C(2)–C(17)=3.0°, O(26B)–C(12)–C(2)–C(17)=22.0° O(15)–C(22)–C(9)–C(20)=135.3°). The biphenyl unit shows a dihedral angle almost perpendicular (Angle between the average planes of each phenyl ring=88.6°). This fact seems to be related with the substitution in the pyridine ring, thus, ligands containing amide groups instead of amine groups present dihedral angles smaller than 90°.

On the other hand, methyl groups of amines lie in the same side of the mean plane defined of the cavity (C(24)–N(5)–C(27)–C(33)=174.4°, C(40)–N(23)–C(37)–C(35)=167.5°). This fact is in agreement with the situation of maximum packing required for the consecution of the single crystal. Stereoscopic view of crystal packing of the structure is shown in Figure 2.

3. Complexation experiments

3.1. Cation complexation

The ability of ligands **1**–**4** in cation complexation was firstly studied with Cd^{2+} and Zn^{2+} as their nitrate salts by using ^{1}H NMR techniques. The four compounds were able to form the corresponding complexes but the observed results depended on the ligand used. Thus, the ^{1}H NMR spectrum of the complex formed between ligand **1** and $Cd(NO_3)_2$ and $Zn(NO_3)_2$ in $CDCl_3$ suggested that complexation was

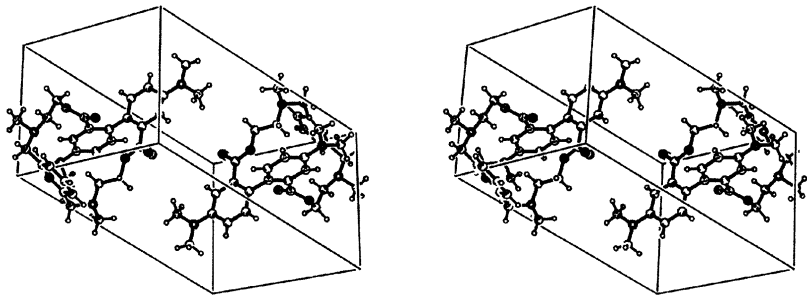

Figure 2. Stereoscopic view of crystal packing of the structure of compound **1**.

Table 1. ^{1}H NMR shifts for the hydrogen in ligand **1** and its complexes with $Cd(NO_3)_2$ and $Zn(NO_3)_2$ in $CDCl_3$

	H_a	H_b	H_c	H_d	H_e	H_f	H_g	H_h	H_i	H_j
1	7.15	6.75	6.94	7.51	7.12	3.92	2.53, 2.27	3.69, 3.51	2.32	2.91
1·$Cd(NO_3)_2$	7.06	7.05	6.86	7.80	7.17	3.35	3.90, 2.53	4.83, 4.22	2.10	3.02
1·$Zn(NO_3)_2$	7.20	7.01	6.82	7.62	7.23	3.69	3.03, 2.73	4.15, 3.88	2.44	2.97

carried out with the nitrogen atoms. This proposal agreed with the shift observed in the NMR signals of H_h ($\Delta\delta=0.46$, 0.37 ppm and 1.14, 0.71 for Zn^{2+} and Cd^{2+}, respectively), H_g ($\Delta\delta=0.50$, 0.46 ppm and 1.37, 0.26 for Zn^{2+} and Cd^{2+}, respectively) and even H_d ($\Delta\delta=0.11$ ppm and 0.29 for Zn^{2+} and Cd^{2+}, respectively) corresponding to the pyridine moiety (Table 1).

When similar studies were carried out with ligands **2** and **3** all the signals in the NMR spectra of the complex were very broad in CD_3CN as well as in $CDCl_3$. Probably the higher flexibility of these ligands made the interchange process faster than with ligand **1** but not faster enough in the NMR time scale to observe sharp signals. Variable temperature experiments were carried out from −40 to 55 °C but no improvement was observed with both solvents.

By contrast, the alkaline cations Li^+ and Na^+ as their picrate salts gave rise to better resolved signals in their corresponding ^{1}H NMR spectra in $(CD_3)_2CO$ (Fig. 3). With both ligands clear modifications were observed in the benzylic hydrogen atoms of the biphenyl moiety what agreed with the stronger interaction between the hard alkaline cations with the ether groups than with the amine nitrogen atoms. By using this technique the 1:1 stoichiometry and the complexation constants for these salts were determined. The results showed in Table 2 demonstrated that the changes in the heteroatoms have not too much influence in the complexation constant. What is more, these values are close to that obtained with the related compound containing five ether groups that showed a value of log $K=$ 2.0 for the complexation constant with sodium picrate in the same solvent.[9]

Finally, the ability of ligand **4** for complexing Cd^{2+} and Zn^{2+} salts was also studied using RMN techniques and the modifications observed in the shifts of the signals are showed in Table 3. It is clear that the presence of ester and amide groups makes the ligand more rigid and precludes an efficient binding of the cations.

Due to the fluorescent properties of the tetramethylbenzidine moiety, studies of complexation using this technique were carried out with ligands **1**–**4** (Fig. 4). These experiments have allowed to determining not only the complexation constants but also the 1:1 stoichiometry of the

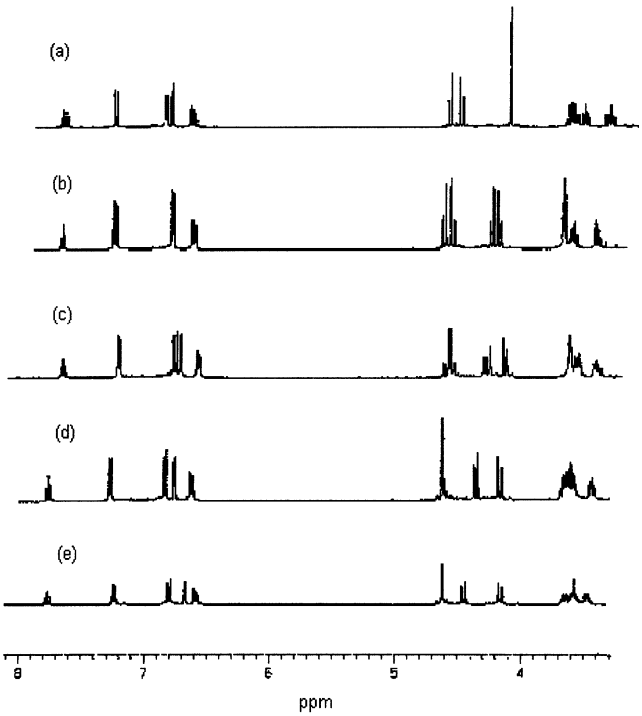

Figure 3. ^{1}H NMR spectra in $(CD_3)_2CO$ of (a) free ligand **2**; (b) ligand **2**+ 0.1 equiv LiPic; (c) ligand **2**+0.3 equiv LiPic; (d) ligand **2**+0.5 equiv LiPic; (e) ligand **2**+1.0 equiv LiPic.

Table 2. Log K for ligands **2** and **3** with alkaline cations in $(CD_3)_2CO$ by using NMR techniques

Ligand	Li Pic	Na Pic
2	1.9 (0.1)	2.1(0.1)
3	2.4 (0.1)	2.6 (0.1)

Table 3. ^{1}H NMR shifts for the hydrogen in ligand **4** and its complexes with $Cd(NO_3)_2$ and $Zn(NO_3)_2$ in $CDCl_3$

	NH	H_a	H_b	H_c	H_d	H_e	H_f	$H_{g,g',h}$	CH_3
4	8.50	7.16	6.92	7.07	8.29	8.15	4.25–3.80	3.68–3.40	2.90
4·$Zn(NO_3)_2$	8.62	7.17	6.94	7.05	8.31	8.19	4.28–4.13	3.70–3.42	2.93
4·$Cd(NO_3)_2$	8.59	7.16	6.93	7.04	8.29	8.16	4.30–4.14	3.72–3.41	2.93

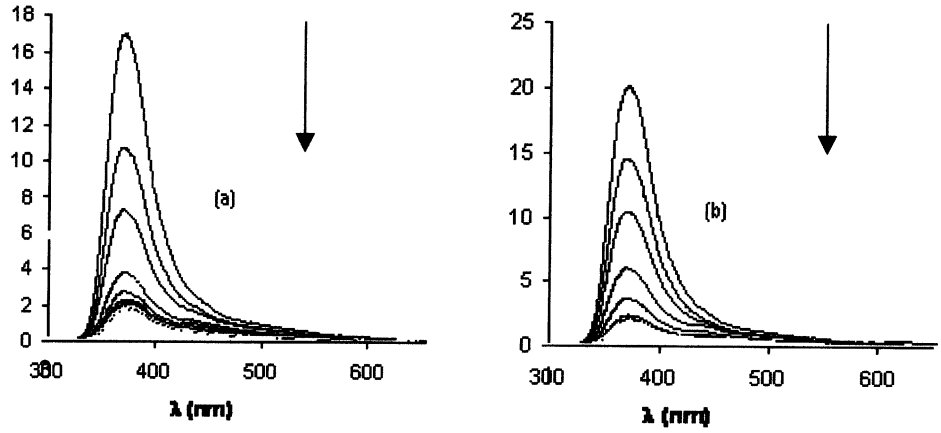

Figure 4. Fluorescence spectra of **3** after addition of (a) Zn^{2+} and (b) Cd^{2+} at 20 °C, $\lambda_{exc}=300$ nm. Initial concentration of ligand was 10^{-5} M in CH_3CN and the salt was added until high excess.

formed complex (Fig. 5). All these experiments were carried out in CH_3CN with Zn^{2+} and Cd^{2+} as their triflate salts.

The four studied ligands gave rise to a quenching of the fluorescence in the presence of different transition metal cations. A similar quenching of the fluorescence has also been observed in complexation experiments with other ligands containing tetramethylbenzidine subunits.[4a,10] In the studied ligands, the coordination of cations inside the coronand cavity modifies the dihedral angle between both byphenyl aromatic rings and this variation gives rise to the modification in the fluorescent properties.

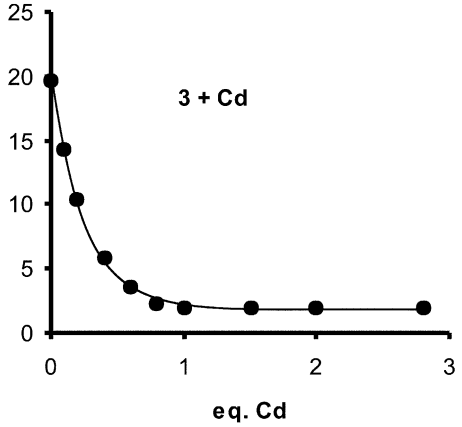

Figure 5. Stoichiometry determination for ligand **3** with Cd^{2+} in acetonitrile using fluorescence meassurements.

The values reflected in Table 4 demonstrated the influence of the coronand amine groups on the complexation ability. Thus, ligand **1** and **3** make stronger complex with both cations than ligand **2**. On the other hand, the similar results obtained with ligands **1** and **3** demonstrated that the substitution of an ester group for an ether group has a small influence on complexation. Even though, the experimental conditions were different the results

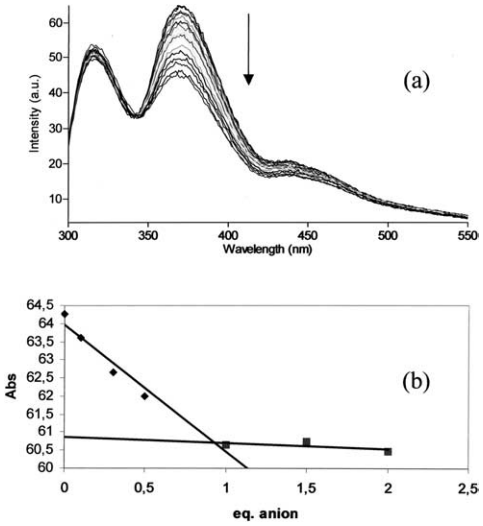

Figure 6. (a) Fluorescence spectra of **3**+HEPES after addition of increasing of $TBAHSO_4$ at 20 °C, $\lambda_{exc}=275$ nm. Initial concentration of ligand was 10^{-5} M in CH_3CN; (b) stoichiometry determination.

Table 4. Log *K* values for the complexation of Cd^{2+} and Zn^{2+} as triflate salts with ligands **1**–**4** in CH_3CN using fluorescence techniques

Ligand	**1**	**2**	**3**	**4**	**5**	**6**
Cd^{2+}	5.0 (0.2)	3.6 (0.1)	6.2 (0.2)	2.8 (0.1)	1.6[a]	1.9[a]
Zn^{2+}	5.1 (0.2)	—	5.8 (0.2)	2.9 (0.1)	1.5[a]	2.2[a]

[a] These values are determined for nitrate salts and by using ^{1}H NMR techniques.[5]

Table 5. Log *K* values for the complexation of F^-, AcO^- and HSO_4^- as tetrabutylammonium salts with ligands **1** and **3** in CH_3CN using fluorescence techniques

Ligand	F^-	AcO^-	HSO_4^-
1	4.9 (0.1)	5.0 (0.1)	4.7 (0.1)
3	5.7 (0.3)	5.3 (0.4)	5.0 (0.4)

previously published for ligand **5** and **6** demonstrated the strong influence of the amide group reduction in the complexing ability.

3.2. Anion complexation

Anion complexation was studied with ligands **1** and **3** due to the presence of amino groups susceptible to be protonated and became anion receptors. The studied anions were F^-, Br^-, I^-, AcO^- and HSO_4^- as their tetrabutylammonium salts after protonation of the corresponding ligands by using HEPES 0.01 M, pH 6, in dioxane/water 70:30. Fluorescence studies showed that 1:1 complexes were produced with F^-, AcO^- and HSO_4^- (Fig. 6). The complexation constants were determined by using Specfit[11] and are shown in Table 5.

Br^- and I^- showed a continuous quenching of the fluorescence that can not be related to the complexation event but to the heavy atom effect. On the other hand, the obtained results showed that each ligand complexed the three anions, F^-, AcO^- and HSO_4^- with similar constants values. However, ligand **3** showed higher constants than ligand **1** probably due to its higher flexibility. The presence of the ester groups in ligand **1** made it less suitable for adopting the appropriate geometry for anion complexation.

4. Electrochemical studies

The electrochemical response of compounds **1–4** in MeCN solution has been studied, as well as the electrochemistry of such macrocyclic receptors in the presence of an excess of different metal ions, namely, Li^+, Na^+, K^+, Mg^{2+}, Ca^{2+}, Ba^{2+}, Ni^{2+} and Zn^{2+}. The electrochemical response at glassy carbon and platinum electrodes is dominated by two successive one-electron transfer processes involving the oxidation of the diaminobiphenyl moiety above +1.0 V versus AgCl/Ag.

4.1. Electrochemistry of free ligand 1–4

As shown in Figure 7, corresponding to a 10^{-3} mM solution of **4** in 0.10 M Bu_4NPF_6/MeCN, the CV response of that receptor consists of three overlapped anodic peaks at +0.82 (Ia), +0.95 (IIa), and +1.10 V (IIIa) coupled with their cathodic counterparts at +0.76 (Ic), +0.87 (IIc), and +1.06 V (IIIc). A similar response was obtained for all receptors (peak potentials in Table 6).

Figure 7. CVs of a 10^{-3} mM **4** solution in 0.10 M Bu_4NPF_6/MeCN. Potential scan rate 100 mV/s.

The response of such bis(dimethylamino)biphenyl-containing receptors is consistent with that reported for the oxidation of aromatic compounds.[12] Thus, the parent neutral ligand, L, is reversibly oxidized to the corresponding radical cation $L^{\cdot+}$ and a dication, L^{2+}, in two successive one-electron transfer steps. On a first examination, these can correspond to the Ia/Ic and IIa/IIc couples. The presence of an additional couple IIIa/IIIc can be rationalized taking into account that the overall oxidation process is accompanied by a significant stereochemical modification: there is a transition from the dihedral neutral molecule, to the planar dication. Accordingly, one can assume that the first electron-transfer step yields a non-planar cation radical ($L^{\cdot+}$) that undergoes to some extent a relatively slow pre-organization process:[13]

$$L = L^{\cdot+} + e^- \quad (1)$$

$$L^{\cdot+}(\text{dihedral}) = (L^{\cdot+})^*(\text{planar}) \quad (2)$$

followed by the second electron transfer of both radical

Table 6. Peak potential data in mV versus AgCl/Ag for ligands **1–4** in MeCN solution (0.10 M Bu_4NPF_6). From CVs at 100 mV/s at platinum electrode

	Anodic peaks (Ep (mV))			Cathodic peaks (Ep (mV))		
Ligand	Ia	IIa	IIIa	Ic	IIc	IIIc
1	+0.76	+0.86	+1.00	+0.68	+0.79	+0.92
2	+0.74	+0.92	+1.09	+0.72	+0.84	—
3	+0.74	+0.88	+1.04	+0.69	+0.88	+1.0
4	+0.82	+0.95	+1.10	+0.76	+0.87	+1.06

cations:

$$(L^{\cdot+})^*(\text{planar}) = (L^{2+})^*(\text{planar}) + e^- \quad (3)$$

$$L^{\cdot+}(\text{dihedral}) = (L^{2+})^*(\text{planar}) + e^- \quad (4)$$

attributable, respectively, to the IIa/IIc and IIIa/IIIc couples (Fig. 8).

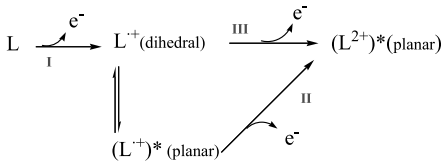

Figure 8.

In both cases, however, the dication comproportionates with the parent ligand within the second reduction process,

$$L^{2+} + L = 2L^{\cdot+} \quad (5)$$

to yield the cation radical which can be further oxidized to L^{2+}. Accordingly, the second voltammetric wave (II or III) is enhanced with respect to the first (I) as described in literature for different two-step redox processes.[14] Depending on the extent of the comproportionation reaction (5), IIa/IIc and IIIa/IIIc couples are more or less enhanced with respect to the Ia/Ic couple, thus the voltammetric profile consists on two separate peaks or two overlapping peaks.

4.2. Electrochemistry of L–M^{n+} complexes

The electrochemical response of L plus M^{n+} solutions is quite similar to that previously described. As shown in Figure 9, in the presence of an excess (four times) of metal salts, the voltammetric pattern is similar to that of the parent ligands. However, some peak potential shifts and changes in the voltammetric profile with respect the voltammetry of the non-coordinated ligands were recorded. The voltammetry of *L* plus M^{n+} systems can be interpreted in terms of the formation of ion-pair complexes that experience ligand-centred electrochemical processes:

$$\left[\frac{L}{M^+A^-}\right] = \left[\frac{L^{\cdot+}}{M^+A^-}\right] + e^- \quad (6)$$

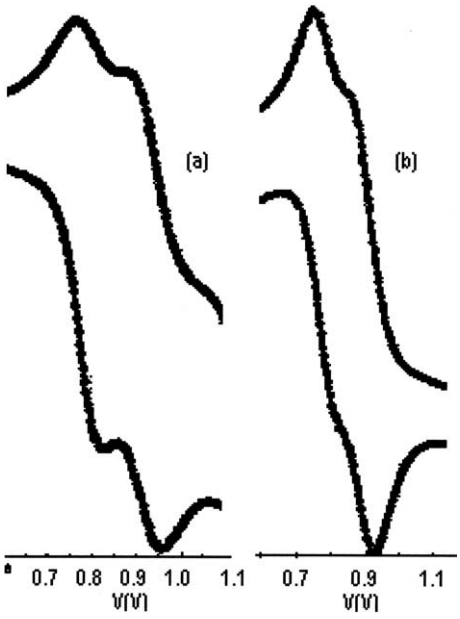

Figure 9. CVs of (a) a 2.0 mM **4** solution in 0.10 M Bu_4NPF_6/MeCN; (b) **4**+four times excess of Zn^{2+}. Potential scan rate 100 mV/s.

$$\left[\frac{L^{\cdot+}}{M^+A^-}\right](\text{dihedral}) = \left[\frac{L^{\cdot+}}{M^+A^-}\right]^*(\text{planar}) \quad (7)$$

$$\left[\frac{L^{\cdot+}}{M^+A^-}\right]^*(\text{planar}) = \left[\frac{L^{2+}}{M^+A^-}\right]^*(\text{planar}) + e^- \quad (8)$$

$$\left[\frac{L^{\cdot+}}{M^+A^-}\right](\text{dihedral}) = \left[\frac{L^{2+}}{M^+A^-}\right]^*(\text{planar}) + e^- \quad (9)$$

Peak potential values are summarized in Table 7.

Accordingly, complexation may influence the potential and relative height of the voltammetric peaks: (i) by modulating the thermochemical stability of the complex species; (ii) by modifying the kinetic of the comproportionation and preorganization reactions. To rationalize these effects, electrostatic, electronic, stereochemical and solvation factors should be considered.[15] First of all, it should be noted that, assuming reversibility, the formal potentials of the different couples are related with the equilibrium constants of the complexes formed with the oxidized and reduced forms. In view of the reversibility of the electrochemical processes I, II and III, formal electrode potentials $E^{0\prime}$, for such processes can be calculated from the

Table 7. Peak potential data in mV versus AgCl/Ag for ligands **1–4** in MeCN solution (0.10 M Bu_4NPF_6)

	Anodic peaks			Cathodic peaks		
Ligand	Ia	IIa	IIIa	Ic	IIc	IIIc
2	+0.74	+0.92	+1.09	+0.72	+0.84	—
2+Li^+	+0.82	+0.98	+1.32	+0.77	+0.94	+1.18
2+Zn^{2+}		+0.85	+0.99		+0.75	+0.91
3	+0.74	+0.88	+1.04	+0.69	+0.88	+1.0
3+Li^+		+0.83	+0.98		+0.76	+0.90
3+Zn^{2+}		+0.81	—		+0.72	—
4	+0.82	+0.95	+1.10	+0.76	+0.87	+1.06
4+Li^+		+0.94	+1.1		+0.89	+1.04
4+Zn^{2+}	+0.83	+0.93	—	+0.73	+0.88	—

From CVs at 100 mV/s at platinum electrode.

Table 8. Log K_{com} and log $K_{com'}$ for ligands **1**–**4** free and in the presence of cations

Ligand	**1**	**2**	Li^+-**2**	Zn^{2+}-**2**	**3**	Li^+-**3**	Zn^{2+}-**3**	**4**	Li^+-**4**	Zn^{2+}-**4**
Log K_{com}	−1.78	−2.54	−3.13	—	−2.79	—	—	−2.03	—	−2.15
Log $K_{com'}$	−4.07	—	−7.71	−2.54	−5.17	−2.45	—	−4.19	−2.63	—

half sum of the cathodic and anodic peak potentials ($E^{0\prime}=(E_{pc}+E_{pa})/2$). Thus, the shift in the formal potentials recorded upon complexation satisfies (V at 298 K):

$$E^{0'}(I) = 0.059 \log\left(\frac{K(\mathrm{L})}{K(\mathrm{L}^{\cdot+})}\right) \tag{10}$$

$$E^{0\prime}(\mathrm{II}) = 0.059 \log\left(\frac{K(\mathrm{L}^{\cdot+})}{K(\mathrm{L}^{2+})^*}\right) \tag{11}$$

$$E^{0\prime}(\mathrm{III}) = 0.059 \log\left(\frac{K(\mathrm{L}^{\cdot+})}{K(\mathrm{L}^{2+})^*}\right) \tag{12}$$

where $K(L)$, $K(L^{\cdot+})$, $K(L^{\cdot+})^*$, and $K(L^{2+})^*$ are the equilibrium constants for the complexation of a given metal ion, M^{n+}, with the neutral ligand, the radical cation (non-planar and planar), and the dication, respectively.

Electrochemical data allow for a direct determination of the equilibrium constant for the comproportionation reaction described by Eq. 5 and its analogues for metal complexes:

$$\log K_{com} = \left(\frac{(E^{0\prime}(I)-E^{0\prime}(II)}{0.059}\right) \tag{13}$$

$$\log K_{com\prime} = \left(\frac{E^{0\prime}(I)-E^{0\prime}(III)}{0.059}\right) \tag{14}$$

The estimated values are summarized in Table 8.

The differences between ligand and ligand+metal ion voltammograms result from the superposition of thermodynamic factors and kinetic ones and can be summarized in the following way:

(a) In some cases (Li^+-**2**) the peaks Ia/Ic are displaced towards more positive potentials. This effect can be in principle associated to an electrostatic cause: upon complexation, the system acquires a certain additional positive charge, thus decreasing its oxidation ability.
(b) In some cases (Li^+-**4**) the peaks IIa/IIc are negatively displaced even merging with the Ia/Ic couple that remains essentially unchanged. This effect, consisting in a relative destabilization of the $L^{\cdot+}$ complexes towards disproportionation, cannot be explained by electrostatic considerations. Probably it should be attributed to stereochemical factors: in these cases metal coordination favours the acquirement of a nearly coplanar geometry, thus favouring oxidation.
(c) In some cases (Li^+-**3**) (Fig. 10), the couple IIIa/IIIc is enhanced at the expense of the couple IIa/IIc. This effect, observed for small cations, can be associated to the adoption of a different coordination environment that makes difficult the adoption of a coplanar geometry. Then, Eq. 7 is fast, and the second electron transfer represented by Eq. 8 predominates over that represented by Eq. 9. In other cases, however, the couple IIIa/IIIc disappears. This is attributable to a fast acquirement of the planar geometry after the initial one-electron transfer step.
(d) In some cases, the voltammograms (Li^+-**4**) show a decrease in reversibility, as denoted by the appearance of a significant decrease of cathodic peaks, as can be seen on comparing Figure 11a and b. Reversibility of a couple can be interpreted in terms of the ability of the ligand or ligand+metal ion systems to promote

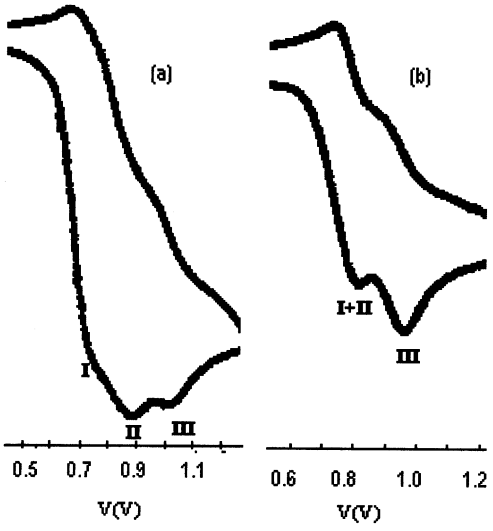

Figure 10. CVs of (a) a 2.0 mM **3** solution in 0.10 M Bu_4NPF_6/MeCN; (b) **3**+four times excess of Li^+. Potential scan rate 100 mV/s.

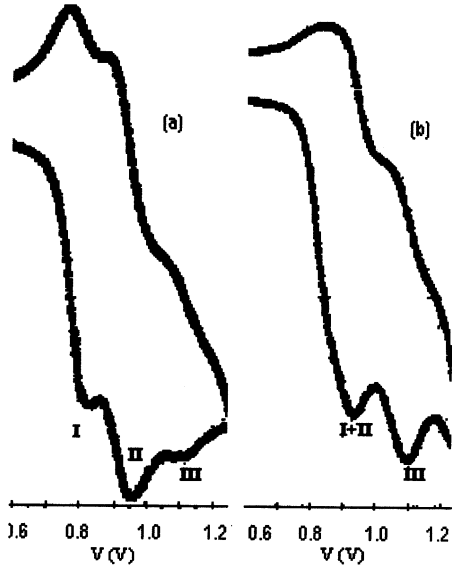

Figure 11. CVs of (a) a 2.0 mM **4** solution in 0.10 M Bu_4NPF_6/MeCN; (b) **4**+four times excess of Li^+. Potential scan rate 100 mV/s.

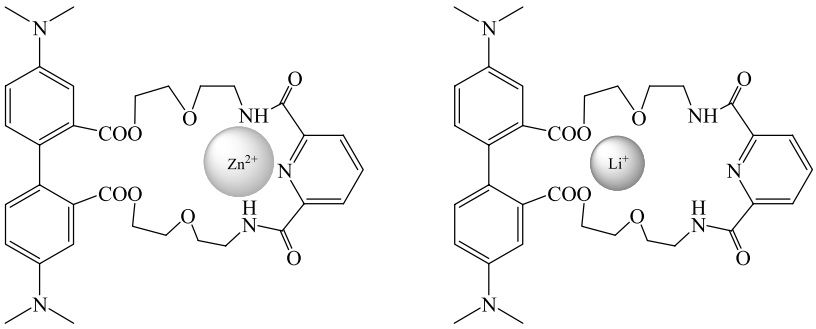

Figure 12.

structural rearrangements compatible with the structural requisites for stabilizing both oxidation states.[16] Since in non-reversible cases the peak potential values are similar to those in reversible systems, the loss of reversibility can be associated to the lowering of the rate of preorganization of the ligand. This result from ligand topology and ligand flexibility.

The most remarkable facts for compounds **3** and **4** were, that in the case of complexation with alkaline and alkaline-earth cations, peaks I and II overlapped, and peak III suffered an increase in its intensity. These features suggest that in such cases the dihedral/planar interconversion of the radical cation is fast. By contrast, with zinc cation and ligand **4**, peak III disappeared totally and it was not observed overlapping of peaks II and I. These facts were explained based on the different character of lithium and zinc. Thus, the hard character of lithium placed it close to the biphenyl moiety, making difficult the oxidation through the planar radical cation. In the case of zinc, because of its soft character, it is located close to the pyridine zone, so the oxidation through the planar geometry is possible (Fig. 12). On the other hand, **2** with transition metals showed that the preferred way for the oxidation was through the non-planar radical cation. This behaviour can be related to the presence of only one nitrogen atom in this compound that could allow the complex to adopt a different geometry. Finally, the addition of transition metal cations improved significantly the reversibility of the cyclic voltammetry.

5. Conclusions

The results obtained in complexation experiments carried out with ligands **1**–**4** allows to establish the influence of the different functional group in the cavity on the binding efficiency. Thus, substitution of amide groups by the corresponding amine functions (compounds **1** and **6**) has stronger influence in complexation than the change of ester by ether groups (compounds **1** and **3**). On the other hand, the rigidity of compound **4** (two ester and two amide groups) makes it few suitable for complexing transition metal cations, even though the size of the cavity is larger than in the other described compounds. It is also remarkable the small influence that the substitution of N by O atoms has in the complexation of alkali metal cations (compounds **2** and **3**).

In relation to anion recognition, it could be concluded that anion geometry has not influence in the fluorescent response what suggest the interaction with the anion is mostly related to acid–base reactions.

On the other hand, electrochemical studies can be summarized in two points: firstly, the existence of two different pathways in the two-electron oxidation. One of these routes goes through a dihedral radical-cation being the intermediate in the second pathway a planar system. Secondly, the obtained results in the presence of metal cations suggest that transition metal cations place themselves close to the nitrogen atoms. By contrast, the alkaline cations are preferably co-ordinated with the oxygen atoms present in the ligand.

6. Experimental

6.1. General methods

All commercially available reagents were used without further purification. Water sensitive reactions were performed under argon. Column chromatography was carried out on SDS activated neutral aluminium oxide (0.05–0.2 mm; activity degree 1). IR spectra were recorded on a Perkin-Elmer 1750 FT-IR and a Bruker Equinox 55 FT-IR. NMR spectra were recorded with Bruker Avance 300/500 and Varian Unity-300/400 spectrometers. Chemical shifts are reported in parts per million downfield from TMS. Spectra were referenced to residual undeuterated solvent. High-resolution mass spectra were taken with a Fisons VG-AUTOSPEC and those using the eletrospray ionizing technique were recorded on an HPLC-MS with ion trap Bruker 3000-Esquire Plus. UV spectra were run at 20 °C (thermostated) on a Shimadzu UV-2102 PC. Fluorescence spectra were carried out in a Varian Cary Eclipse Fluorimeter.

6.1.1. Synthesis of *N*,*N*′-dimethyl-2,2′-TMB-2,16-dicarboxy-6,9,12-triaza-8,10-pyridine-19-crown-2 (1). In a two-neck round bottom flask, under argon, **6** (0.670 g, 1.2 mmol) was dissolved in dry THF (10 ml) and stirred at room temperature. BH_3–THF 1 M (24 ml) was added dropwise over this solution. The mixture was stirred at room temperature for 24 h. Then, the reaction was quenched by adding aqueous HCl 1 M. The reaction was stirred for 2 h and neutralizing with NaOH pellets until pH 7. THF was

removed under vacuum and the aqueous layer was continuously extracted with hot chloroform for 24 h. Organic layer was dried with anhydrous sodium sulphate and filtered off. The solvent was evaporated under vacuum to give, after column chromatography purification (neutral alumina, AcOEt), compound **1** as a yellow solid (0.174 g, 32%). Mp: 168–169 °C. IR (KBr): 3140 (Ar–H), 2841 (CH_3, CH_2), 1721 (C=O), 1607 (C=C), 1256 (C–O), 862 cm^{-1}. NMR ^1H ($CDCl_3$) δ (ppm): 7.51 (1H, t, $J=7.7$ Hz, Py-H), 7.17 (2H, d, $J=2.6$ Hz, Ar–H), 7.14 (2H, d, $J=7.7$ Hz, Py-H), 6.96 (2H, d, $J=8.5$ Hz, Ar–H), 6.77 (2H, dd, $J_1=2.8$ Hz, $J_2=8.7$ Hz, Ar–H), 4.05–3.91 (4H, m, CH_2–OOC), 3.72 (2H, d, $J=13.2$ Hz, CH_2-py), 3.54 (2H, d, $J=13.3$ Hz, CH_2-py), 2.91 (6H, s, $(CH_3)_2N$), 2.58 (2H, m, CH_2–N), 2.32 (3H, s, CH_3–N), 2.29 (2H, m, CH_2–N). NMR ^{13}C ($CDCl_3$) δ (ppm): 166.9, 156.1, 148.0, 135.8, 130.5, 130.0, 129.4, 121.5, 114.2, 112.5, 61.9, 60.8, 52.6, 42.4, 39.6. HRMS (E.I.): M^+ calcd for $C_{31}H_{39}N_5O_4$ 545.2274, found 545.2276.

6.1.2. Synthesis of 2,2′-TMB-9-aza-8,10-pyridine-19-crown-4 (2). In a two-neck round bottom flask, under argon, a stirred solution of 2,6-bis((2-hydroxy)ethoxymethyl) pyridine (**9**) (0.227 g, 1 mmol) and NaH 60% mineral oil (0.120 g, 3 mmol) in THF (50 ml) was refluxed for 2 h. 2,2′-bis(chloromethyl)-4,4′-bis(dimethylamine) biphenyl (0.335 g, 1 mmol) and sodium iodide (5 mg) in THF (50 ml) was added dropwise over this solution. The mixture was heated for 48 h and quenched with water. THF was removed under vacuum, the aqueous layer was extracted with ethyl acetate (3×25 ml) and organic layers were washed with brine, dried with anhydrous sodium sulphate and evaporate under reduce pressure. Column chromatography (neutral alumina, AcOEt) gave ligand **2** as pale brown oil (0.097 g, 20%). IR (KBr): 2858, 1607 (C=C), 1494, 1453, 1348 and 1084 cm^{-1}. NMR ^1H ($CDCl_3$) δ (ppm): 7.60 (1H, t, $J=7.8$ Hz, Py-H), 7.24 (2H, d, $J=7.8$ Hz, Py-H), 6.92 (2H, d, $J=8.4$ Hz, Ar–H), 6.87 (2H, d, $J=2.7$ Hz, Ar–H), 6.65 (2H, dd, $J_1=2.7$ Hz, $J_2=8.4$ Hz, Ar-H), 4.54 (2H, d, $J=12.3$ Hz, CH_2–OAr), 4.44 (2H, d, $J=12.3$ Hz, CH_2–O), 4.07 (4H, s, CH_2–O), 3.60–3.55 (4H, m, CH_2–O), 3.52–3.42 (4H, m, CH_2–O), 3.31–3.24 (4H, m, CH_2–O), 2.91 (12H, s, $(CH_3)_2$–N). NMR ^{13}C ($CDCl_3$) δ (ppm): 158.0, 150.1, 137.9, 137.5, 134.6, 131.2, 122.3, 112.4, 111.6, 74.3, 71.5, 69.9, 69.6, 41.2. HRMS (E.I.): M^+ calcd for $C_{29}H_{37}N_3O_4$ 491.2784, found 491.2834.

6.1.3. Synthesis of *N*,*N*′-dimethyl-2,2′-TMB-6,9,12-triaza-8,10-pyridine-19-crown-2 (3). Following the same procedure employed in the synthesis of **2**, 2,6-bis(*N*-methyl, *N*-2-hydroxyethyl)methylamine pyridine (**8**) (0.253 g, 1 mmol) and 2,2′-bis(chloromethyl)-4,4′-bis(dimethylamine)biphenyl (0.335 g, 1 mmol) gave ligand **3** after column chromatography (neutral alumina, AcOEt/MeOH, 98:2) as a brown sirup (0.171 g, 33%). IR (KBr): 3376, 2850, 1607 (C=C), 1494, 1453, 1348, 1089 and 806 (C–N) cm^{-1}. NMR ^1H ($CDCl_3$) δ (ppm): 7.67 (1H, t, $J=7.7$ Hz, Py-H), 7.27 (2H, d, $J=7.7$ Hz, Ar–H), 6.87 (2H, d, $J=7.7$ Hz, Py-H), 6.84 (2H, d, $J=3.0$ Hz, Ar–H), 6.70 (2H, dd, $J_1=3.0$ Hz, $J_2=7.7$ Hz, Ar–H), 4.27 (2H, d, $J=11.8$ Hz, CH_2–OAr), 4.12 (2H, d, $J=11.8$ Hz, CH_2–OAr), 3.73 (4H, s, CH_2–N), 3.49–3.33 (4H, m, CH_2–O), 2.97 (12H, s, $(CH_3)_2$–N), 2.62 (4H, t, $J=6.2$ Hz, CH_2–N), 2.00 (6H, s, CH_3–N). NMR ^{13}C ($CDCl_3$) δ (ppm): 157.0, 149.5, 137.2, 136.2, 130.3, 127.4, 122.0, 111.8, 110.7, 70.2, 67.3, 62.4, 54.3, 43.0, 39.5. HRMS (E.I.): M^+ calcd for $C_{31}H_{43}N_5O_2$ 517.3417, found 517.3415.

6.1.4. Synthesis of 2,6-bis[*N*-methyl-*N*-(2-hydroxyethyl) aminomethyl] pyridine (8). 2,6-Bis(hydroxymethyl)pyridine (1.4 g, 10 mmol) and SeO_2 (1.105 g, 10 mmol) were refluxed for 4 h in dry 1,4-dioxane (25 ml), then filtered in hot and the solvent evaporated under vacuum. 2,6-Pyridinedicarbaldehyde was used in the following step without further purification. 2,6-Pyridinedicarbaldehyde (0.638 g, 4.7 mmol) and *N*-methyl ethanolamine (0.75 ml, 9.4 mmol) were refluxed in anhydrous ethanol (25 ml) during 4 h. Then, the mixture was cooled at room temperature, sodium borohydride was added (3.556 g, 94 mmol) and the reaction was stirred overnight. Finally, the reaction was quenched by refluxing with water during 5 h. Solvent was removed by distillation under reduced pressure and the aqueous layer was continuously extracted in hot chloroform for 24 h. The organic layer was dried with sodium sulphate and the solvent removed providing compound gave product **8** as a pale yellow oil (0.975 g, 82%). IR (KBr): 3362 (OH), 2949, 1594 (C=C), 1455, 1036 (C–O), 873, 787 cm^{-1}. NMR ^1H ($CDCl_3$) δ (ppm): 7.58 (1H, t, $J=7.6$ Hz, Py-H), 7.06 (2H, d, $J=7.6$ Hz, Py-H), 4.32 (2H, br s, OH), 3.65 (4H, s, CH_2–Ar), 3.60 (4H, t, $J=5.2$ Hz, CH_2–O), 2.59 (4H, t, $J=5.2$ Hz, CH_2–N), 2.24 (6H, s, CH_3–N).NMR ^{13}C ($CDCl_3$) δ (ppm): 158.7, 137.6, 122.0, 63.1, 59.8, 59.2, 43.1. HRMS (E.I.): M^+ calcd for $C_{13}H_{23}N_3O_2$ 253.1790, found 253.1783.

6.1.5. Synthesis of 2,6-bis[(2-hydroxy)ethoxymethyl] pyridine (9). Synthesis of dimethyl 2,6-bis-pyridinedimethoxyethanoate. The reaction was carried out under argon atmosphere. A suspension of 2,6-pyridinedimethanol (3 g, 21.5 mmol) and sodium hydride 60% mineral oil (2.3 g, 57.2 mmol) in dry THF (100 ml) was stirred at room temperature for 20 min. Then, methyl bromoacetate (6.2 ml, 64.5 mmol) in dry THF (40 ml) was added dropwise and the mixture heated (60 °C) for 10 h. The reaction was stopped by adding water; THF was evaporated under vacuum and the aqueous layer was extracted with ethyl acetate (3× 25 ml), washed with brine and dried over anhydrous sodium sulphate. Evaporation of the solvent and column chromatography (silica, CH_2Cl_2/$(CH_3)_2CO$ 95:5) provided the desired compound as a yellow oil (5.492 g, 90%). NMR ^1H ($CDCl_3$) δ (ppm): 7.34 (1H, t, $J=7.5$ Hz, Py-H), 7.00 (2H, d, $J=7.5$ Hz, Py-H), 4.29 (4H, s, CH_2–Ar), 3.81 (4H, s, CH_2–O), 3.30 (6H, s, CH_3–O). NMR ^{13}C (CD_3OD) δ (ppm): 167.3, 154.5, 140.1, 120.4, 74.2, 66.8, 52.3.

Dimethyl 2,6-bis-pyridinedimethoxyethanoate (1.935 g, 6.83 mmol) in anhydrous ethanol (60 ml) was cooled at 0 °C and vigorously stirred. Lithium borohydride (0.458 g, 21 mmol) was carefully added in portions. The mixture remained stirred at room temperature for 15 h, then quenched with water and the ethanol was evaporated under reduced pressure. The aqueous layer was continuously extracted with hot chloroform for 24 h; the organic layer was dried over anhydrous sodium sulphate and concentrated to give **9** as pale yellow oil (1.240 g, 80%).

NMR ^{1}H ($CDCl_3$) δ (ppm): 7.63 (1H, t, $J=8.0$ Hz, Py-H), 7.19 (2H, d, $J=8.0$ Hz, Py-H), 5.00 (2H, br s, OH), 4.67 (4H, s, CH_2–Ar), 3.77 (4H, br m, CH_2–O), 3.73 (4H, br m, CH_2–O). NMR ^{13}C (CD_3OD) δ (ppm): 158.2, 138.0, 120.9, 73.8, 73.3, 62.0.

6.2. X-ray structure analysis of ligand 1

Intensity measurements were made on an Enraf-Nonius CAD4 diffractometer using a colourless prismatic single crystal of dimensions $0.41\times0.20\times0.18$ mm. Graphite-monochromated Mo K_α radiation ($\lambda=0.71073$ Å) and ω-scan technique was used. Data collection was carried out at room temperature. Three reference reflections were measured every 2 h as an intensity and orientation check and no significant fluctuation was noticed during the collection of the data. Lorentz-polarization correction was made. The crystal structure was solved by direct methods using the SHELX system[16] and refined by full-matrix least-squares techniques[17] on F^2. The non-hydrogen atoms were refined anisotropically. All the hydrogen atoms were found by Fourier synthesis in the refinement process. Molecular graphics of the structure (Fig. 1) was made with ORTEP[18]. Stereoscopic view of crystal packing of the structure (Fig. 2) was performed with PLATON/PLUTON graphics system.[19] Part of the publication material was made with WinGX publication routines.[20]

Information concerning crystallographic data collection is summarized in Table 9. Atomic coordinates and equivalent isotropic displacement parameters are shown in Table 10. Additional crystallographic data (bond lengths and angles, anisotropic displacement parameters, hydrogen coordinatesand torsion angles, excluding structure factors) for this structure have been deposited with the Cambridge Crystallographic Datra Centre as supplementary publication number CCDC 273729. Copies of the data can be obtained, free of charge, on application to CCDC, 12 Union Road, Cambridge CB2 1EZ, UK.

Table 9. Crystal data and structure refinement for **1**

Empirical formula	$C_{31}\ H_{39}\ N_5\ O_4$	
Formula weight	545.67	
Temperature	293(2) K	
Wavelength	0.71073 Å	
Crystal system	Triclinic	
Space group	*P*-1	
Unit cell dimensions	$a=9.4339(2)$ Å	$\alpha=68.081(3)^\circ$
	$b=11.3474(2)$ Å	$\beta=71.502(3)^\circ$
	c=15.6222(2) Å	$\gamma=86.250(3)^\circ$
Volume	1468.64(4) $Å^3$	
Z	2	
Density (calculated)	1.234 Mg/m^3	
Absorption coefficient	0.083 mm^{-1}	
F(000)	584	
Crystal size	$0.41\times0.20\times0.18$ mm^3	
Theta range for data collection	2.29–26.24°	
Index ranges	$0\le h\le11$, $-14\le k\le14$, $-18\le l\le19$	
Reflections collected	6300	
Independent reflections	5923 [R(int)=0.0418]	
Completeness to theta=26.24°	99.9%	
Refinement method	Full-matrix least-squares on F^2	
Data/restraints/parameters	5923/0/526	
Goodness-of-fit on F^2	0.908	
Final *R* indices [$I>2$sigma(I)]	$R1=0.0518$, $wR2=0.1246$	
R indices (all data)	$R1=0.2605$, $wR2=0.1775$	
Largest diff. peak and hole	0.198 and -0.246 e $Å^{-3}$	

6.3. NMR titrations with cations. General procedure

In a NMR tube, the NMR ^{1}H spectrum of a well known concentration of free ligand was recorded. Then, an aliquot of a known solution of the metallic salt was added (0.1 equiv aprox), the mixture was stirred for 30 s, the solvent was evaporated to raise the initial volume (using argon flow) and the spectrum was again recorded. This procedure was repeated several times until the concentration of the salt was larger than the ligand and no variation of the signals was observed. The plot of the variation of the chemical shifts versus the ratio between the salt and the ligand gave the titration curve and so the stoichiometry of the complex. The constant value was calculated making use of the program Clinp 2.0.[21]

Table 10. Atomic coordinates ($\times10^4$) and equivalent isotropic displacement parameters ($Å^2\times10^3$) for **1**

	X	*y*	*z*	*U*(eq)
O(1)	6341(2)	2898(2)	3329(2)	65(1)
C(3)	4015(4)	1870(3)	3194(2)	41(1)
O(10)	4849(3)	2364(2)	703(2)	60(1)
N(8)	1259(3)	6329(3)	3689(3)	70(1)
N(5)	9835(3)	1328(3)	2860(2)	48(1)
C(4)	3415(3)	3108(3)	3250(2)	38(1)
C(2)	4189(4)	4041(3)	3342(2)	41(1)
C(7)	5107(4)	−528(3)	3193(3)	45(1)
N(6)	5687(3)	−1681(3)	3176(2)	57(1)
C(14)	8280(4)	1616(4)	2931(4)	52(1)
C(12)	5787(4)	4002(4)	3288(3)	50(1)
C(9)	4714(3)	1682(3)	2324(2)	40(1)
C(17)	3463(4)	5108(3)	3479(3)	48(1)
C(13)	1949(4)	3332(3)	3260(3)	50(1)
C(18)	3836(4)	816(3)	4042(3)	46(1)
O(15)	5502(4)	3803(2)	1196(2)	85(1)
C(16)	1980(4)	5282(3)	3531(2)	46(1)
N(21)	9915(3)	1452(3)	609(2)	61(1)
C(19)	1258(5)	4385(3)	3390(3)	52(1)
C(11)	4365(4)	−350(3)	4050(3)	47(1)
N(23)	7588(4)	1831(3)	−457(2)	66(1)
O(26A)	6430(30)	4750(20)	3390(20)	108(9)
O(26B)	6600(30)	4930(20)	3080(20)	97(6)
C(20)	5226(4)	498(3)	2329(3)	46(1)
C(27)	10,555(5)	855(4)	2083(3)	61(1)
C(25)	7927(4)	2762(4)	3196(4)	59(1)
C(22)	5049(4)	2744(4)	1369(3)	55(1)
C(32)	5424(6)	3206(5)	−311(3)	68(1)
C(24)	9938(6)	419(5)	3787(3)	63(1)
C(28)	6618(7)	−1751(5)	2266(4)	78(1)
C(34)	−300(5)	6454(5)	3808(4)	68(1)
C(29)	5852(7)	−2613(4)	4067(4)	71(1)
C(30)	11,342(5)	2996(5)	736(4)	79(1)
C(31)	7089(6)	3126(4)	−695(3)	72(1)
C(33)	10,611(4)	1821(4)	1093(3)	59(1)
C(35)	9980(5)	2281(4)	−289(3)	66(1)
C(36)	1988(7)	7164(6)	3946(6)	92(2)
C(37)	9209(5)	1813(6)	−814(4)	77(1)
C(40)	6898(7)	1108(7)	−843(5)	97(2)
C(39)	11,412(6)	3809(6)	−182(5)	94(2)
C(38)	10,719(6)	3444(5)	−701(4)	87(2)

U(eq) is defined as one third of the trace of the orthogonalized U^{ij} tensor.

6.4. Fluorescence titrations with cations. General procedure

The spectrum of free ligand (3.0 ml, 10^{-5} M) in acetonitrile was recorded. Then, an aliquot of a solution 10^{-3} M in the metallic salt and 10^{-5} M in the ligand was added (0.1 equiv), the mixture was stirred for 30 s and the spectrum was recorded. This procedure was repeated several times until the concentration of the salt was larger than the ligand and no variation of the signals was observed. The plot of the variation of the absorbance/emission versus the ratio between the salt and the complex gave the titration curve and so the stoichiometry of the complex. The constant value was calculated making use of the program Clinp 2.0.[21]

6.5. Fluorescence titrations with anions. General procedure

The spectrum of free ligand (3.0 ml, 10^{-5} M) in dioxane/water 70:30, HEPES 0.01 M, pH 6, was recorded. Then, an aliquot of a solution 10^{-3} M in the metallic salt and 10^{-5} M in the ligand was added (0.1 equiv), the mixture was stirred for 30 s and the spectrum was recorded. This procedure was repeated several times until the concentration of the salt was larger than the ligand and no variation of the signals was observed. The plot of the variation of the absorbance/emission versus the ratio between the salt and the complex gave the titration curve and so the stoichiometry of the complex. The constant value was calculated making use of the program Specfit.[11]

6.6. Electrochemical experiments

Electrochemical measurements were performed at 298 K in a conventional three-electrode cell under argon atmosphere. Nominal ca. 2.0 mM concentrations of the ligand were used in dry MeCN using tetrabuthylammonium hexafluorophosphate (0.10 M) as a supporting electrolyte. A four times excess of metallic salts was used in each case (triflate salts for the transition metal cations and perchlorate for alkaline cations). Experiments were performed using a BAS CV 50 W equipment using a BAS MF2012 glassy carbon electrode (GCE) (geometrical area 0.071 cm^2), and a BAS MF2014 platinum electrode (geometrical area 0.018 cm^2) as a working electrode. A platinum wire auxiliary electrode and a AgCl (3 M NaCl)/Ag reference electrode separated from the test solution by a salt bridge only containing supporting electrolyte completed the electrode arrangement. The potential of such reference electrode was −35 mV versus the saturated calomel reference electrode (SCE).

Acknowledgements

The present research has been financed by DGCYT (PPQ2002-00986) and Generallitat Valenciana Grupos 03/206. We acknowledge the Universitat de Valencia (S.C.I.E.) for most of the equipment employed. One of us (M.J.B.) acknowledges the Generalitat Valenciana for a PhD grant.

Supplementary data

Supplementary data associated with this article can be found, in the online version, at doi:10.1016/j.tet.2005.08.010

References and notes

1. (a) Fabbrizzi, L.; Poggi, A. *Chem. Soc. Rev.* **1995**, *24*, 197–202. (b) De Silva, A. P.; Gunaratne, H. Q. N.; Gunnlaugsonn, T.; Huxley, A. J. M.; McCoy, C. P.; Radamacher, J. T.; Rice, T. E. *Chem. Rev.* **1997**, *97*, 1515–1566. (c) Full issue of *Coord. Chem. Rev.* **2000**, 205 (d) Rurack, K.; Resch-Genger, U. *Chem. Soc. Rev.* **2002**, *31*, 116–127. (e) Martínez-Máñez, R.; Sancenón, F. *Chem. Rev.* **2003**, *103*, 4419–4504.
2. Weinig, H-G. ; Krauss, R.; Seydack, M.; Bendig, J.; Koert, U. *Chem. Eur. J.* **2001**, *7*, 2075–2088.
3. (a) McFarland, S. A.; Finney, N. S. *J. Am. Chem. Soc.* **2001**, *123*, 1260–1261. (b) Lee, D. H.; Im, J. H.; Lee, J-H. ; Hong, J-I. *Tetrahedron Lett.* **2002**, *43*, 9637–9640. (c) Cody, J.; Fahrni, C. J. *Tetrahedron* **2004**, *60*, 11099–11107.
4. (a) Costero, A. M.; Gil, S.; Sanchis, J.; Peransí, S.; Sanz, V.; Williams, J. A. G. *Tetrahedron* **2004**, *60*, 6327–6334. (b) Costero, A. M.; Aurell, M. J.; Bañuls, M. J.; Ward, M. D.; Argent, S. *Tetrahedron* **2004**, *60*, 9471–9478.
5. Costero, A. M.; Aurell, M. J.; Bañuls, M. J.; Ochando, L. E.; Tamarit, F. J.; Domenech, A. *J. Inclus. Phen. And Macrocyclic Chem.* **2003**, *45*, 241–249.
6. Costero, A. M.; Andreu, C.; Monrabal, E.; Martínez-Máñez, R.; Soto, J.; Padrilla-Tosta, M. J.; Pardo, T.; Ochando, E. L.; Amigó, J. M. *J. Chem. Soc., Dalton Trans.* **2000**, 361–367.
7. Alcock, N. W.; Kingston, R. G.; Moore, P.; Pierpoint, C. *J. Chem. Soc., Dalton Trans.* **1984**, 1937–1943.
8. Neugebauer, F. A.; Funk, B.; Staab, H. A. *Tetrahedron Lett.* **1994**, *35*, 4755–4758.
9. Costero, A. M.; Andreu, C.; Pitarch, M.; Andreu, R. *Tetrahedron* **1996**, *52*, 3683–3692.
10. Costero, A. M.; Sanchis, J.; Gil, S.; Sanz, V.; Ramírez de Arellano, M. C.; Williams, J. A. G.. *Supramol. Chem.* **2004**, *16*, 435–446.
11. SPECFIT/32™ GLOBAL ANALYSIS SYSTEM v.3.0, Spectrum Associates (Marlborough, MA, USA). www.bio-logic.info/rapid-kinetics/specfit.html.
12. Perrin, C. L. *Organic Polarography*; Interscience: New York, 1969; p 280.
13. Doménech, A.; Costero, A. M.; Bañuls, M. J., Aurell, M. J. *Electrochim Acta* **2005**, *50*, 4063–4075.
14. Yoon, K. B.; Huh, T. J.; Kochi, J. K. *J. Phys. Chem.* **1995**, *99*, 7042–7043.
15. (a) Golub, G.; Cohen, H.; Paoletti, P.; Bencini, A.; Messori, L.; Bertini, I.; Meyerstein, D. *J. Am. Chem. Soc.* **1995**, *117*, 8353–8361. (b) Barefield, E. K.; Freeman, G. M.; Van Derveer, D. G. *Inorg. Chem.* **1986**, *25*, 552–558. (c) Lay, P. A. *J. Phys. Chem.* **1986**, *90*, 878–885. (d) Richardson, D. E. *Inorg. Chem.* **1990**, *29*, 3213–3217. (e) Izatt, R. M.; Bradshaw, J. S.; Nielsen, S. A.; Lamb, J. D.; Christensen, J. J. *Chem. Rev.* **1985**, *85*, 271–339.

16. Sanaullah, K. K.; Glass, R. S.; Wilson, G. S. *J. Am. Chem. Soc.* **1993**, *115*, 592–600.
17. Sheldrick, G. M. *SHELX97*: Programs for Crystal Structure Analysis (Release 97-2). University of Göttingen, Germany, 1997.
18. Farrugia, L. J. ORTEP-3 for Windows. *J. Appl. Crystallogr.* **1997**, *30*, 565.
19. PLATON/PLUTON (a) Spek, A. L. *Acta Crystallogr., Sect. A* **1990**, *46*, C34. (b) Spek, A. L. *PLATON*: A Multipurpose Crystallographic Tool, Utrecht University, Utrecht, The Netherlands, 1998.
20. Farrugia, L. J. *J. Appl. Crystallogr.* **1999**, *32*, 837–838.
21. Available from Kholin Y. V., Konyaev D. S., Merny S. A. in www.bestnet.kharkov.ua/kholin/clinp.html.

Available online at www.sciencedirect.com
SCIENCE DIRECT
Tetrahedron
Tetrahedron 61 (2005) 10321–10330

Synthesis of cyclopropyl silyl ethers and their facile ring opening by photoinduced electron transfer as key step in radical/radical cationic cascade reactions

Prashant A. Waske and Jochen Mattay*

Organische Chemie I, Fakultät für Chemie, Universität Bielefeld, Postfach 100131, 33501 Bielefeld, Germany

Received 6 April 2005; revised 29 June 2005; accepted 1 August 2005

Available online 26 August 2005

Abstract—Various ring-fused cyclopropyl silyl ethers with an benzylic, olefinic or acetylenic side chain have been synthesized. Upon oxidative photoinduced electron transfer (PET) the cyclopropane ring opens and forms a reactive β-keto radical, which undergoes intramolecular cyclization. In some cases we observed only formation of ring opened non-cyclized products. With olefinic side chain 5-*exo-trig* mode of cyclization rather than 6-*endo-trig* mode of cyclization takes place whereas in case of acetylenic side chain we observed 6-*endo* cyclization.

1. Introduction

Since almost three decades radical cascade reactions (also called domino reactions) have often been used for synthesizing polycyclic compounds.[1–5] Still the tin hydride method introduced by Giese et al. is one of the mostly applied method to perform radical chain processes despite some disadvantages. In order to circumvent toxic tin reagents and to facilitate the working-up procedures, for example, electron transfer activation has been introduced to generate radical or radical ions.[5b,6] In these reactions metal salts are generally used as oxidizing and reducing agents, respectively. Another way to generate radical ions is possible by the photoinduced electron transfer (PET).[7] This procedure has several advantages: metal reagents and other toxic compounds are avoided, the working-up procedures are often very easy, and in general, photochemistry certainly provides powerful methods for a new and sustainable chemistry.[8]

Upon oxidative photoinduced electron transfer (PET) the cyclopropane ring opens and forms a reactive β-keto radical, which undergoes intramolecular cyclization. The oxidative ring-opening reactions of cyclopropanone acetals with carbonyl compounds via PET have been already studied by Akira Oku and co-workers.[8d–g] Recently, we have reported on radical/radical ionic cascade reactions initiated by photoinduced electron transfer (PET).[9–11] All these reactions have in common that the redox properties of molecules are changed upon excitation, that is, both the electron donating as well as electron accepting behavior of the excited species are drastically enhanced. This leads either to oxidative PET or to reductive PET processes. For details of PET and for special synthetic procedures such as sensitization and co-sensitization processes see, for example, Refs. 9–11.

Here, we will report on some further examples of PET initiated radical/radical cationic cascade reactions of bicyclic cyclopropyl silyl ethers functionalized by unsaturated side chains leading to polycyclic compounds. We were especially interested in checking the suitability of alkyne and arene groups in comparison of simple alkenes (Scheme 1).

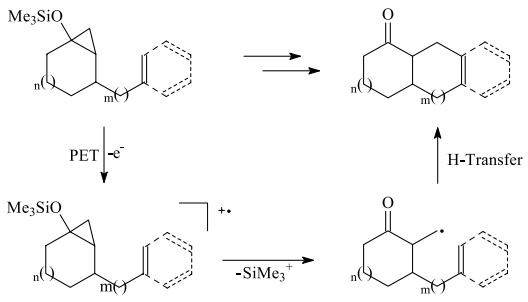

Scheme 1.

Keywords: Siloxy cyclopropanes; Domino reactions; Electron transfer; Polycycles; Radical ions; Radical reactions.
* Corresponding author. Tel.: +49 521 1062072; fax: +49 521 1066417; e-mail: mattay@uni-bielefeld.de

0040–4020/$ - see front matter © 2005 Elsevier Ltd. All rights reserved.
doi:10.1016/j.tet.2005.08.034

2. Results and discussion

2.1. Preparation of cyclopropyl silyl ethers

The silyl enol ethers were prepared by the copper catalyzed conjugate addition of various Grignard Reagent (GR) to the enones followed by trapping of the enolates with trimethylsilyl chloride (Scheme 2). The addition of propargyl magnesium bromide catalyzed by CuI to 2-cyclohexenone did not afford the expected product, however, use of the procedure developed by Lee[12] afforded the propargylated silyl enol ether in good yield. In general the corresponding bromides were used for the preparation of GR. In case of benzyl bromide we observed only the formation of 1,2-diphenyl ethane. This problem was circumvented by using benzyl chloride. The 1:1 mixture of diethyl ether/THF proved to be the best solvent for the preparation of GR and conjugate addition reactions. The selective cyclopropanation of respective silyl enol ethers in presence of alkenes or alkyne were successfully carried out using diethylzinc, methylene iodide and methylene chloride as the solvent of choice. Unfortunately, these conditions were not successful for related cyclopropanation of *tert*-butyl dimethyl silyl enol ethers, but we found that the corresponding trimethyl silyl enol ether **11** could be cyclopropanated in 75% yield.

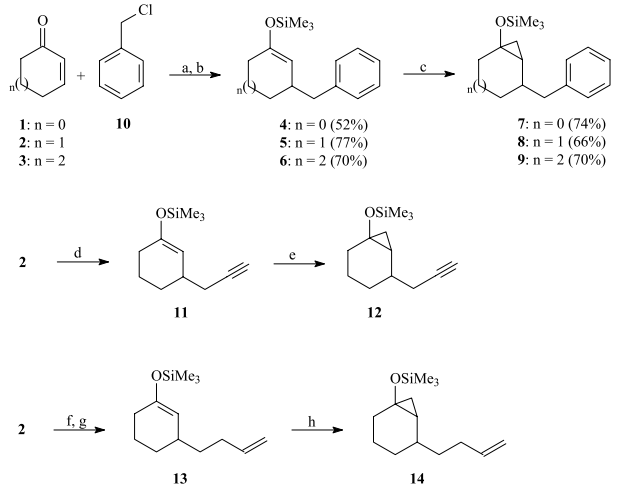

Scheme 2. (a) Mg metal, dry THF/diethyl ether 0 °C; (b) CuI, TMS-Cl, −78 °C, Et_3N, rt; (c) Et_2Zn, CH_2I_2, CH_2Cl_2, rt, 12 h; (d) in metal, propargyl bromide, dry THF, rt, 1 h, Me_2S, TMSOTf, 3 h, (65%); (e) Et_2Zn, CH_2I_2, CH_2Cl_2, 2 days, (75%); (f) Mg metal, 4-bromobut-1-ene, dry THF/diethyl ether, 0 °C; (g) CuI, TMS-Cl, −78 °C, 3 h, Et_3N, rt, (54%); (h) Et_2Zn, CH_2I_2, CH_2Cl_2, 2 h, (84%).

In case of 2-phenyl-1-bromo ethane, we did not observe any formation of GR. To overcome this problem we converted the less reactive bromide to the iodide by refluxing it with NaI in acetone (Scheme 3). The primary alkyllithium was readily prepared at −78 °C (dry ice–acetone bath) under an atmosphere of dry, deoxygenated argon by addition of 2.2 mol equiv of commercial *tert*-butyllithium (*t*-BuLi) in pentane to an approximately 0.1 M solution of **16** in dry *n*-pentane–diethyl ether (3/2 by volume).[13] The CuI catalyzed conjugate addition of this organolithium compound to 2-cyclohexenone in presence of TMS-Cl afforded silyl enol ether **17**.

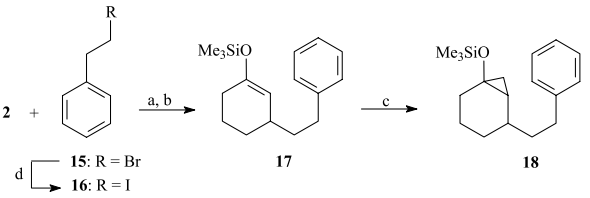

Scheme 3. (a) *t*-BuLi, THF, −78 °C to rt; (b) CuI, TMS-Cl, −78 °C, Et_3N, rt, (62%); (c) Et_2Zn, CH_2I_2, CH_2Cl_2, 12 h, (36%); (d) NaI, acetone, reflux 2 h, (72%).

The 3-substituted enones were prepared from the reaction of vinylogous ester **19** with GR prepared from corresponding bromides or chlorides (Scheme 4). The enone **20** is a very important intermediate in pharmaceutical industry, besides of several filed patents and to the best of our knowledge no one has reported its actual synthesis. We prepared enone **20** by the reaction of 3-ethoxy-2-cycloheptenone **19**[9] and benzyl magnesium chloride in 91% yield. Treatment of enone **20** with lithiumdiisopropylamine (LDA) in presence of TMS-Cl afforded its silyl enol ether **21**, which was cyclopropanated to **22** in 81% yield, using Et_2Zn, CH_2I_2 in CH_2Cl_2.

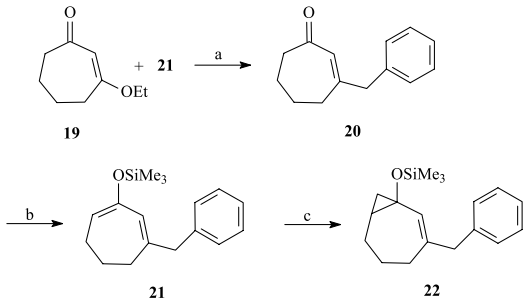

Scheme 4. (a) Mg metal, dry THF/diethyl ether, 0 °C, 3 h, (91%); (b) LDA, TMS-Cl, dry THF, −78 °C to rt, 2 h, (90%); (c) Et_2Zn, CH_2I_2, CH_2Cl_2, 12 h, (81%).

The cyclohexenone **23** was synthesized by treatment of 3-ethoxy-2-cyclohexenone and GR prepared from 4-bromo-2-methyl-1-butene and subsequent acid hydrolysis (Scheme 5).[14] Treatment of **23** with methyl lithium under

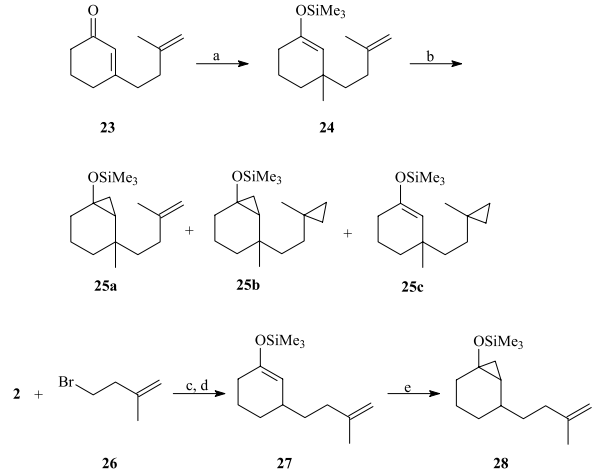

Scheme 5. (a) CuI, MeLi, 0 °C, 10 min, −78 °C, TMS-Cl, 3 h, Et_3N, rt, (75%); (b) Et_2Zn, CH_2I_2, CH_2Cl_2; (c) Mg metal, THF/diethyl ether, 0 °C; (d) CuI, TMS-Cl, −78 °C, Et_3N, rt, (83%); (e) Et_2Zn, CH_2I_2, CH_2Cl_2, 12 h, (65%).

our previously developed conditions gave enol ether **24** in 75% yield. The cyclopropanation of **24** with Et_2Zn, CH_2I_2 in various solvents resulted in the mixture of products **25a–c** in poor yields.

However, the enol ether **27** was prepared in good yield by copper catalyzed conjugate addition of GR as shown in Scheme 5. The silyl enol ether **27** could be cyclopropanated in 65% yield by using our standard conditions.

2.2. Photoinduced electron transfer (PET) cyclizations

The deoxygenated solutions of respective cyclopropyl silyl ethers in dry acetonitrile containing the PET sensitizer dicyanoanthracene (DCA) were irradiated in a Rayonet photochemical reactor using 420 nm lamps. All the reactions were monitored by GC or GC–MS.

The irradiation of **8** and **9** in dry acetonitrile resulted in the formation of tricyclic products **29** and **30** with high stereoselectivity (Scheme 6). The formation of these products can be explained as follows—for details of the mechanism see Ref. 9 (cf. Scheme 2): the sensitizer DCA gets electronically excited at 420 nm and thus is enabled to oxidize the substrate to its radical cation. Exocyclic cyclopropane ring opening leads to the formation of a β-keto radical, which further cyclizes to the tricyclic products. The last step is the elimination of a hydrogen atom to retain the aromatic ring. Surprisingly we observed only formation of cis isomers. The structure and stereochemistry were assigned using modern NMR techniques such as ^{1}H COSY, HMBC, HMQC and NOESY. The cyclopropane **7** under PET condition leads to the formation of non-cyclized ring enlarged products (scheme 7). In this case cyclopropyl ring opening takes place via endocyclic cleavage, indicating the formation of the thermodynamically favored more stable secondary radical. Obviously the formation of a new strained polycyclic product is energically disfavored.

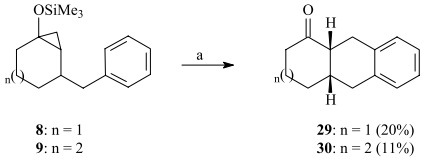

8: n = 1
9: n = 2

29: n = 1 (20%)
30: n = 2 (11%)

Scheme 6. (a) DCA, acetonitrile, irradiated for 12 h at 420 nm.

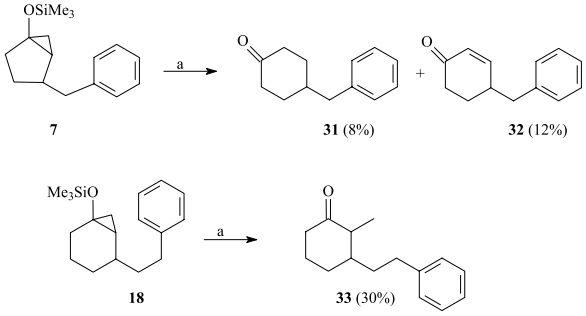

7 **31** (8%) **32** (12%)

18 **33** (30%)

Scheme 7. (a) DCA, acetonitrile, irradiated for 12 h at 420 nm.

Irradiation of **18** leads to the exocyclic ring opened noncyclized product **33** as well. In this case intra-molecular cyclization was not observed due to the large distance between exocyclic radical and phenyl ring. To explain the two contrasting ring opening results from very similar structures, we propose that both processes involve the endocyclic ring opening (cleavage of bond 'b', see Scheme 8) as first step[9] followed by a reversible ring-closure process. If $n=1$ or 2 and $m=1$ or 2 (as in case of **8**, **9** and **18**), reclosure could became more facile leading to a cyclohexylmethyl radical, which attack the phenyl ring depending on the chain lengths of its tether. If $n=0$ (as in case of **7**) the formation of ring enlarged product is favored leading to **31** and the α-β unsaturated ketone **32**, respectively. The structure of cyclopropane radical cations and their reactivity has been already discussed by Roth and co-workers.[15] Further, mechanistic investigations are underway using flash laser photolysis and quantum chemical calculations and will be published separately.[9b,9c]

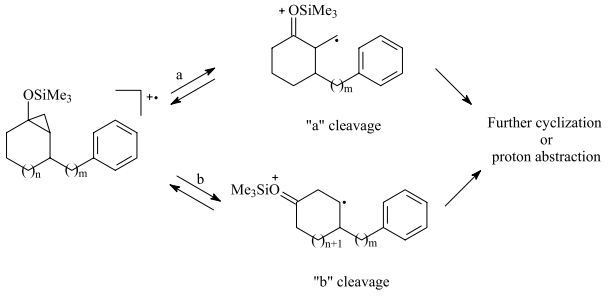

Scheme 8. cleavage of exocyclic (a) and endocyclic (b) C–C bond.

In accordance with this rationalization treatment of **14** and **28** under PET conditions leads to the cleavage of bond 'b', the formed cyclic radical undergoes 5-*exo-trig* cyclization affording products **34** and **35** due to the higher reactivity of alkenes rather than arenes in radical additions (Scheme 9). In these cases the final step is saturation of the radical, which takes places either by direct abstraction of hydrogen from solvent molecule or by reduction to the corresponding anion by the sensitizer radical anion followed up by protonation (e.g., by traces of water in the highly hygroscopic acetonitrile).[9] The stereochemistry at ring junction is cis, and was confirmed by NOESY analysis.

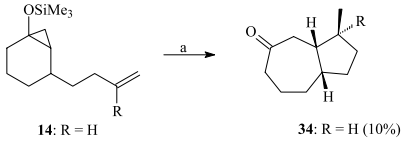

14: R = H
28: R = Me

34: R = H (10%)
35: R = Me (14%)

Scheme 9. (a) DCA, acetonitrile, irradiated for 12 h at 420 nm.

In case of **22** we observed formation of the bicyclic product **36** as only one isomer (31%) in which both substituents are cis to each other (Scheme 10). This is not surprising for products, which contain a bicyclooctenone substructure because of the high ring strain of the corresponding trans products. In addition, we observed some traces of product **37**, which indicates that the second cyclization step is energetically disfavored. The propargyl substituted

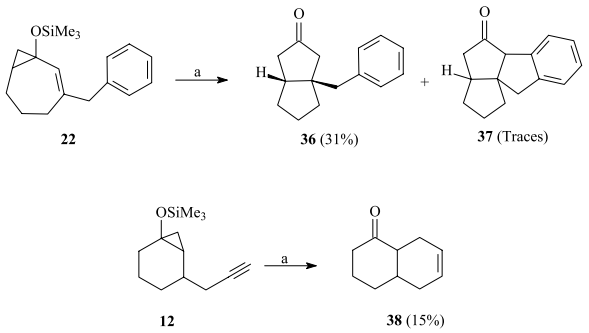

Scheme 10. (a) DCA, acetonitrile, irradiated for 12 h at 420 nm.

compound **12** was irradiated under PET conditions afforded the bicyclic product **38** via 6-*endo* cyclization. If the cyclopropane ring would have opened in a endocyclic way, the formed secondary radical must cyclize in a 5-*endo* mode, which is known to be disfavored according to the Baldwin–Beckwith rules.[16,17]

3. Conclusion

Various new ring-fused cyclopropyl silyl ethers with an benzylic, olefinic or acetylenic side chain have been synthesized in good yields. We have also been able to demonstrate that the PET induced ring opening of cyclopropyl silyl ethers is quite suitable for the production of polycylic compounds with high stereoselectivity. PET oxidative initiated reactions of these cyclopropyl silyl ethers lead to β-carbonyl radical cationic species and β-keto-radicals, respectively, which can be used for the construction of polycyclic compounds.[9] The termination step is supposed to be either a hydrogen radical transfer from the solvent (acetonitrile) or a stepwise electron transfer/protonation by traces of water in the solvent.

4. Experimental

4.1. General

^{1}H and ^{13}C NMR were recorded using Bruker DRX 500 or Bruker Avance 600 spectrometer. Spectra were recorded in $CDCl_3$; chemical shifts were calibrated to the residual $CHCl_3$ (δH = 7.24 ppm, δC = 77.00 ppm). IR spectra were recorded on a Perkin-Elmer 841 spectrometer. HRMS were recorded on AutospecX (Vacuum Generators, Manchester). GC/MS were recorded on a Shimadzu GC 17A/QP 5050A equipped with a 5MS capillary column (Hewlett Packard). GC analysis were carried out using Shimadzu GC-2010, equipped with HP-5MS (Hewlett Packard) capillary column (column length 25.0 m, inner diameter 0.20 mm). Analytical thin-layer chromatography was performed on a aluminum sheets coated with 0.20 mm silica gel with fluorescent indicator UV_{254} (Macherey-Nagel GmbH). Column chromatography was performed on silica gel MN60 (70–230 mesh; Macherey-Nagel GmbH). Photochemical reactions were performed using an RPR-100 Rayonet photochemical chamber reactor (Southern New England Ultraviolet Company) with RPR 4190 Å lamps that show an emission maximum at 419 ± 15 nm at half bandwidth. All reactions were carried out under an atmosphere of argon. All solvents were distilled prior to use; dry solvents were prepared using standard procedures, dry acetonitrile was stored over activated molecular sieves (size 4 Å). DCA was prepared using literature known method and recrystallized from toluene. All commercially available compounds were used as received unless stated otherwise.

4.2. General procedure A

Synthesis of silyl enol ethers. To a stirred suspension of magnesium metal (Mg), catalytic amount of iodine crystals and dry THF–diethyl ether (1/1 by volume) were added corresponding bromide or chloride (1.2 equiv) in such that the solution was slightly boiling, after addition the solution was heated under reflux for 1 h. This GR was added to the previously cooled suspension of CuI (1 equiv) in THF. The reaction temperature was maintained 0 °C for 10 min and then cooled to −78 °C by using dry ice–acetone bath. The solution of corresponding enones and TMS-Cl in dry THF were added dropwise and stirred for 3 h. Triethyl amine was added and reaction mixture was brought to room temperature (rt), reaction was monitored by GC–MS. Solvents were removed under high vacuum; *n*-pentane was added and the mixture was quickly filtered. The solvent was evaporated under reduced pressure and the crude product was used immediately for the next reaction.

4.3. General procedure B

Synthesis of silyl enol ether by LDA. The solution of diisopropyl amine in dry THF was placed in a oven dried apparatus under argon atmosphere and cooled to 0 °C. *n*-BuLi (1.6 M in hexane) were added dropwise, the stirring was continued for next 25 min and the reaction mixture was cooled to −78 °C using dry ice–acetone bath, followed by addition of respective enones in dry THF. The solution was stirred for 1 h and neat TMS-Cl was added. The solution was brought to rt and stirred for an additional hour at this temperature (monitored by GC–MS). After removal of solvent under reduced pressure, the residue was diluted with *n*-pentane. The precipitate of lithium chloride was removed by filtration; the solvent was removed under vacuum. The product was used immediately for next reaction.

4.4. General procedure C

Cyclopropanation of silyl enol ethers. The respective silyl enol ether was placed in dry apparatus under argon atmosphere, dry dichloromethane was added. The solution was cooled to 0 °C using ice bath, diethyl zinc (1.0 M in hexane) was added. After stirring for 10 min, the solution of diiodomethane in dry THF was added dropwise, the reaction mixture was warmed to rt and stirred for 2–24 h. The conversion was monitored by Gas Chromatography (GC), after complete consumption of starting material; the solution was carefully hydrolyzed by saturated aqueous solution of ammonium chloride until complete dissolution of zinc salt. The aqueous phase was separated and extracted two times with diethyl ether; collective organic layers were washed with water and dried over sodium sulphate. The

solvent was evaporated and the residue was purified with kugelrohr distillation.

4.5. General procedure D

PET oxidative reaction. The solution of cyclopropyl silyl ether and PET sensitizer DCA in dry acetonitrile was placed into a dry Pyrex tubes (diameter 12 mm, length 20 cm, capacity 12 mL). Flushed with argon for 25 min and irradiated for 12–24 h using 420 nm lamps. After complete consumption of starting material (monitored by GC and GC–MS), solvent removed under vacuum and the residue was purified by silica gel column chromatography (EtOAc/Cyclohexane).

4.5.1. Synthesis of 3-benzyl-1-trimethylsilyloxylcyclopent-1-ene (4).[20] Following general procedure A; cyclopentenone **1** (820 mg, 10 mmol) was treated with GR prepared from benzyl chloride (2.9 mL, 25 mmol) and Mg metal (610 mg, 25 mmol) in presence of CuI (1.90 g, 10 mmol) and TMS-Cl (1.5 mL, 12 mmol), gave silyl enol ether **4** (1.254 g, 70%). GC–MS (EI, 70 eV): *m/z* (%)=246 (M^+, 1), 155 (100), 139 (4), 115 (1), 91 (6) 75 (10).

4.5.2. Synthesis of 3-benzyl-1-trimethylsilyloxylcyclohex-1-ene (5). Following General procedure A; cyclohexenone **2** (1.705 g, 17.77 mmol) was treated with GR prepared from benzyl chloride (5.1 mL, 44.7 mmol) and Mg metal (911 mg, 37.3 mmol) in presence of CuI (3.376 g, 17.7 mmol) and TMS-Cl (2.2 mL, 17.7 mmol), gave **5** (3.755 g, 77%). GC–MS (EI, 70 eV): *m/z* (%)=260 (M^+, 1), 245 (6), 169 (100), 153 (4), 139 (1), 128 (2), 115 (4), 91 (31), 75 (32), 65 (14).

4.5.3. Synthesis of 3-benzyl-1-trimethylsilyloxylcyclohept-1-ene (6). Following General procedure A; cycloheptenone **3** (550 mg, 5 mmol) was treated with GR prepared form benzyl chloride (1.4 mL, 12.5 mmol) and Mg metal (305 mg, 12.5 mmol) in presence of CuI (950 mg, 5 mmol) and TMS-Cl (0.8 mL, 6 mmol), gave **6** (150 mg, 70%). GC–MS (EI, 70 eV): *m/z* (%)=274 (M^+, 1), 184 (100), 167 (2), 141 (1), 115 (1), 103 (1), 91 (9), 73 (56).

4.5.4. Synthesis of 2-propargyl-1-trimethylsililoxylcyclohex-1-ene (11).[12] To a stirred solution of **2** (145 mg, 1.5 mmol) in dry THF (3 mL) were added successfully dimethyl sulfide (0.1 mL, 1.95 mmol) and TMSOTf (366 mg, 1.65 mmol) at −78 °C under a argon atmosphere. After 10 min, organoindium reagent generated in situ from indium metal (344 mg, 1.65 mmol) and propargyl bromide (0.55 mL, 4.7 mmol) in THF at rt was added and mixture was stirred at −78 °C for 30 min. The reaction mixture was quenched with saturated aqueous solution of $NaHCO_3$. The aqueous layer was extracted with ether (3×25 mL) and combined organic layers were washed with water, brine and dried with sodium sulphate, filtered and concentrated under reduced pressure, gave **11** (204 mg, 65%). GC–MS (EI, 70 eV): *m/z* (%)=208 (M^+, 1), 168 (41), 150 (2), 110 (1), 96 (1), 78 (3), 72 (100), 61 (3), 44 (22).

4.5.5. Synthesis of 3-(but-3-enyl)-1-trimethylsilyloxylcyclohex-1-ene (13).[19] Following general procedure A; compound **2** (960 mg, 10 mmol) was treated with GR prepared from 1-bromo-3-butene (2.970 g, 22 mmol) and Mg metal (536 mg, 22 mmol) in presence of CuI (1.90 g, 10 mmol) and TMS-Cl (2.8 mL, 22 mmol), gave silyl enol ether **13** (1.20 g, 54%). GC–MS (EI, 70 eV): *m/z* (%)=223 (M^+, 2), 170 (26), 152 (12), 136 (2), 114 (4), 100 (19).

4.5.6. Synthesis of 3-(2-phenylethyl)-1-trimethylsilyloxylcyclohex-1-ene (17). Solution of 2-phenyl-1-iodo ethane **16** (1.919 g, 8.27 mmol) was placed in a dry apparatus equipped with argon balloon, magnetic needle and septum 15 mL dry *n*-pentane–diethyl ether (3/2 by volume) was added. The solution was cooled to −78 °C by using dry ice-acetone bath, the stirrer was started and solution of *t*-BuLi (1.160 g, 18.2 mmol) in *n*-pentane was then added dropwise via argon flushed syringe. Stirring was then continued at −78 °C for additional 5 min, the cooling bath was then removed and mixture was allowed to warm and stand at rt for 1 h to consume the unreacted *t*-BuLi. The mixture was then added dropwise to a solution of CuI (826 mg, 4.35 mmol) in dry diethyl ether at 0 °C, stirring was continued for 10 min and then solution was cooled to −78 °C. The solution of cyclohexenone **2** (391 mg, 4.35 mmol) and TMS-Cl (0.8 mL, 6.525 mmol) were added via syringe. Reaction was monitored by GC and workedup as reported in general procedure A, gave silyl enol ether **17** (692 mg, 62%). GC–MS (EI, 70 eV): *m/z* (%)=274 (M^+, 1), 183 (100), 156 (2), 144 (5), 129 (6), 117 (2), 105 (3), 91 (13), 85 (2), 73 (59).

4.5.7. Synthesis of 6-benzyl-1-trimethylsilyloxyl-1,6-cycloheptadiene (21). Following general procedure B; enone **20** (70 mg, 0.35 mmol) was treated with LDA prepared from diisopropyl amine and (42 mg, 0.42 mmol) and *n*-Butyllithium (0.3 mL, 0.38 mmol) in presence of TMS-Cl (0.06 mL, 0.52 mmol). Gave enol ether **21** (85 mg, 90%). GC–MS (EI, 70 eV): *m/z* (%)=272 (M^+, 52), 257 (17), 181 (9), 165 (13), 153 (9), 141 (3), 128 (3), 115 (4), 91 (35), 73 (100).

4.5.8. Synthesis of 3-methyl-3-(3-methylbut-3-enyl)-1-trimethylsilyloxylcyclohex-1-ene (24). CuI (695 mg, 3.698 mmol) was taken in a dry 25 mL round bottom flask; 10 mL of dry diethyl ether was added and solution was cooled to 0 °C using ice bath and MeLi (168 mg, 7.681 mol) was added. The stirring was continued for additional 10 min and then solution was cooled to −78 °C using dry ice acetone bath. The solution of **2** (500 mg, 3.048 mmol) and TMS-Cl (0.6 mL, 6.096 mmol) in 5 mL dry diethyl ether was added via syringe. The reaction was monitored by GC and reaction mixture was worked up using general procedure A, gave silyl enol ether **24** (570 mg, 75%). GC–MS (EI, 70 eV): *m/z* (%)=252 (M^+, 1), 237 (4), 183 (100), 170 (6), 162 (2), 118 (2), 105 (3), 91 (5), 73 (80).

4.5.9. Synthesis of 3-(3-methylbut-3-enyl)-1-trimethylsilyloxylcyclohex-1-ene (27). Following general procedure A; compound **2** was treated with GR prepared form 4-bromo-2-methyl-1-butene (5.02 g, 33.7 mmol) and Mg metal (720 mg, 30 mmol) in presence of CuI (2.850 g, 15 mmol) and TMS-Cl (2.3 mL, 18 mmol), gave enol ether **27** (2.80 g, 83%). GC–MS (EI, 70 eV): *m/z* (%)=238 (M^+, 1), 182 (52), 170 (8), 147 (8), 105 (4), 73 (100), 52 (2).

4.5.10. Synthesis of 4-benzyl-1-trimethylsilyloxylbicyclo[3.1.0]hexane (7).[20] Following general procedure C; to a stirred solution of silyl enol ether **4** (2.429 g, 9.87 mmol) in 10 mL dichloromethane, was added diethyl zinc (30.2 mL, 23.6 mmol). Solution was cooled to 0 °C using ice bath and neat CH_2I_2 (3.277 g, 12.2 mmol) was added dropwise over a period of 15 min, reaction mixture was brought to rt and stirred for 12 h. Reaction was monitored by GC and usual workup gave **7** (1.90 g, 74%) as colorless oil. GC–MS (EI, 70 eV): *m/z* (%)=260 (M^+, 2), 245 (4), 231 (6), 169 (98), 142 (10), 127 (11), 103 (91), 79 (17), 73 (100).

4.5.11. Synthesis of 4-benzyl-1-trimethylsilyloxylbicyclo[4.1.0]hepane (8). Following general procedure C; to a stirred solution of silyl enol ether **5** (1.49 g, 5.38 mmol) in 5 mL dichloromethane, was added diethyl zinc (14.4 mL, 11.3 mmol). Solution was cooled to 0 °C using ice bath and neat CH_2I_2 (2.821 g, 10.56 mmol) was added dropwise over a period of 15 min, reaction mixture was brought to rt and stirred for 12 h and usual workup gave **8** (980 mg, 66%) as colorless oil. IR (neat): υ=2928, 2862, 1704, 1453 cm^{-1}. ^1H NMR (500 MHz, $CDCl_3$): δ=0.15 (s, 9H), 0.30 (dd, 1H, J=5.6, 5.6 Hz), 0.83–0.89 (m, 1H), 0.90–0.99 (m, 3H), 1.55–1.64 (m, 1H), 1.65–1.75 (m, 2H), 1.84 (ddd, 1H, J=5.0, 13.8, 5.6 Hz), 2.18 (dd, 1H, J=3.7, 13.2 Hz), 2.70 (dd, 1H, J=7.8, 8.0 Hz), 2.81 (dd, 1H, J=7.5, 7.5 Hz), 7.19 (dd, 3H, J=7.5, 7.5 Hz), 7.27 (dd, 2H, J=8.1, 6.9 Hz) ppm. ^{13}C NMR (125 MHz, $CDCl_3$): δ=1.40 (CH_3), 19.00 (CH_2), 21.00 (CH_2), 24.29 (CH), 26.88 (CH_2), 31.98 (CH_2), 39.64 (CH), 44.35 (CH_2), 57.41 (C), 125.72 (CH), 128.14 (C), 128.96 (CH), 140.00 (CH) ppm. GC–MS (EI, 70 eV): *m/z* (%)=274 (M^+, 1), 259 (3), 246 (5), 245 (2), 231 (9), 185 (10), 184 (60), 183 (100), 169 (11), 156 (15), 155 (26), 142 (13), 130 (17), 129 (9), 93 (13), 91 (25).

4.5.12. Synthesis of 4-benzyl-1-trimethylsilyloxylbicyclo[5.1.0]octane (9). Following general procedure C; to a stirred solution of silyl enol ether **6** (1.37 g, 5 mmol) in 5 mL dichloromethane, was added diethyl zinc (14.4 mL, 11.3 mmol). Solution was cooled to 0 °C using ice bath and neat CH_2I_2 (1.53 g, 5.629 mmol) was added dropwise over a period of 15 min, reaction mixture was brought to rt and stirred for 12 h, usual workup gave **9** (1.0 g, 70%) as a colorless oil. IR (neat): υ=2932, 2368, 2344, 1702, 1456 cm^{-1}. ^1H NMR (500 MHz, $CDCl_3$): δ=0.05 (s, 9H), 0.25 (m, 1H), 0.50–0.70 (m, 1H), 0.94 (dd, 2H, J=4.3, 2.5 Hz), 1.03 (dd, 2H, J=10.6, 10.6 Hz), 1.49–1.60 (m, 2H), 1.63–1.77 (m, 1H), 1.88 (d, 1H, J=13.8 Hz), 2.10–2.25 (dm, 2H, J=14.4 Hz), 2.40 (dd, 1H, J=8.1, 8.1 Hz), 2.56 (dd, 1H, J=6.9, 6.9 Hz), 7.15 (ddd, 3H, J=1.2, 4.3, 6.2 Hz), 7.25 (dd, 2H, J=7.5, 8.7 Hz) ppm. ^{13}C NMR (125 MHz, $CDCl_3$): δ=1.20 (CH_3), 24.97 (CH), 28.09 (CH_2), 31.78 (CH_2), 38.34 (CH), 38.86 (CH_2), 43.12 (CH_2), 44.48 (CH_2), 69.65 (C), 125.64 (CH), 128.14 (CH), 129.32 (CH), 141.32 (C) ppm. GC–MS (EI, 70 eV): *m/z* (%)=288 (M^+, 3), 273 (3), 259 (6), 231 (5), 197 (71), 184 (12), 170 (39), 157 (26), 144 (29), 130 (11), 114 (5), 91 (23), 73 (100). HRMS: Calcd for $C_{18}H_{28}OSi$ (M^+) 288.190944, found 288.190933.

4.5.13. Synthesis of 4-(prop-2-ynyl)-1-trimethylsilyloxylbicyclo[4.1.0]heptane (12). Following general procedure C; to a stirred solution of silyl enol ether **11** (150 mg, 0.433 mmol) in 2 mL dichloromethane, was added diethyl zinc (2.2 mL, 1.03 mmol). Solution was cooled to 0 °C using ice bath and neat CH_2I_2 (211 mg, 0.793 mmol) was added dropwise over a period of 15 min, reaction mixture was brought to rt and stirred for 2 days, usual workup gave **12** (120 mg, 75%) as colorless oil. IR (neat): υ=2929, 2866, 1715, 1686 cm^{-1}. ^1H NMR (500 MHz, $CDCl_3$): δ=0.13 (s, 3H), 0.18 (s, 6H), 0.82–0.93 (m, 1H), 1.15–1.35 (m, 2H), 1.68–1.78 (m, 3H), 1.90–1.99 (m, 3H), 2.12 (tt, 2H), 2.20–2.30 (m, 2H) ppm. ^{13}C NMR (125 MHz, $CDCl_3$): δ=0.90 (Si–(CH_3)$_3$), 22.08 (CH_2), 22.58 (CH_2), 25.00 (CH_2), 35.18 (CH_2), 33.41 (CH), 33.99 (CH), 38.04 (CH), 69.21 (C), 84.10 (C) ppm. GC–MS (EI, 70 eV): *m/z* (%)=222 (M^+, 1), 206 (7), 154 (2), 131 (3), 116 (2), 93 (5), 77 (2), 72 (100).

4.5.14. Synthesis of 5-(but-3-enyl)-1-trimethylsilyloxylbicyclo[4.1.0]heptane (14).[19] Following general procedure C; to a stirred solution of silyl enol ether **13** (223 mg, 1 mmol) in 2 mL dichloromethane, was added diethyl zinc (2.9 mL, 2.32 mmol). Solution was cooled to 0 °C using ice bath and neat CH_2I_2 (264 mg, 0.9 mmol) was added dropwise over a period of 15 min, reaction mixture was brought to rt and stirred for 2 days, usual workup gave **14** (200 mg, 84%) as a colorless oil. GC–MS (EI, 70 eV): *m/z* (%)=238 (M^+, 2), 194 (8), 183 (9), 166 (3), 155 (3), 142 (3), 132 (2), 126 (4), 114 (3), 104 (2), 90 (5), 74 (30), 72 (100), 67 (6), 59 (5), 44 (14).

4.5.15. Synthesis of 4-(2-phenylethyl)-1-trimethylsilyloxylcyclohex-1-ene (18). Following general procedure C; to a stirred solution of silyl enol ether **17** (652 mg, 2.525 mmol) in 2.5 mL dichloromethane, was added diethyl zinc (7.6 mL, 6.04 mmol). Solution was cooled to 0 °C using ice bath and neat CH_2I_2 (1.362 g, 5.10 mmol) was added dropwise over a period of 15 min, reaction mixture was brought to rt and stirred for 2 days, usual workup gave **18** (545 mg, 36%) as a colorless oil. IR (neat): υ=2920, 28,235, 1704, 1453 cm^{-1}. ^1H NMR (500 MHz, $CDCl_3$): δ=0.14 (s, 9H), 0.85–0.86 (m, 1H), 1.10–1.40 (m, 2H), 1.50–1.65 (m, 6H), 1.80–1.90 (m, 1H), 1.96–2.10 (m, 2H), 2.40–2.55 (m, 1H), 2.60–2.70 (m, 1H), 7.16 (dd, 2H, J=6.2, 7.0 Hz), 7.27 (dd, 2H, J=7.0, 8.0 Hz) ppm. ^{13}C NMR (125 MHz, $CDCl_3$): δ=20.48 (CH_2), 27.14 (CH_2), 29.13 (CH_2), 30.48 (CH_2), 33.55 (CH_2), 34.55 (CH), 34.97 (CH_2), 51.00 (C), 125.57 (CH), 125.63 (C), 128.27 (CH), 128.32 (CH) ppm. GC–MS (EI, 70 eV): *m/z* (%)=288 (M^+, 6), 184 (17), 183 (100), 144 (4), 127 (3), 91 (14), 75 (18).

4.5.16. Synthesis of 3-benzyl-1-trimethylsilyloxylbicyclo[5.1.0]oct-2-ene (22). Following general procedure C; to a stirred solution of silyl enol ether **21** (118 mg, 0.433 mmol) in 2 mL dichloromethane, was added diethyl zinc (1.3 mL, 1.03 mmol). Solution was cooled to 0 °C using ice bath and neat CH_2I_2 (117 mg, 0.438 mmol) was added dropwise over a period of 15 min, reaction mixture was brought to rt and stirred for 12 h, usual workup gave **22** (100 mg, 81%) as a colorless oil. IR (neat): υ=2929, 2863, 1706, 1662, 1455, 1376 cm^{-1}. ^1H NMR (500 MHz, $CDCl_3$): δ=0.19 (dd, 1H, J=1.8, 5.0 Hz), 0.70–0.77 (m, 1H), 0.78–0.83 (m, 1H), 0.85–0.97 (m, 2H), 1.50–1.68 (m, 1H), 1.74–1.86 (m, 2H), 2.18–2.28 (m, 1H), 3.15 (d, 2H,

J=3.8 Hz), 5.55 (s, 1H), 7.03 (dd, 2H, J=2.0, 7.0 Hz), 7.13 (dd, 2H, J=5.0, 7.0 Hz), 7.18 (dd, 1H, J=7.5, 6.9 Hz) ppm. ^{13}C NMR (125 MHz, $CDCl_3$): δ=1.32 (CH_3), 21.24 (CH_2), 22.55 (CH_2), 25.42 (CH), 28.33 (CH_2), 31.07 (CH_2), 45.76 (CH_2), 57.60 (C), 126.04 (CH), 127.37 (CH), 128.19 (CH), 128.98 (C), 129.11 (CH), 139.59 (C) ppm. GC–MS (EI, 70 eV): m/z (%)=286 (M^+, 20), 271 (14), 257 (15), 244 (8), 196 (20), 195 (100), 179 (7), 167 (12), 91 (35), 73 (83). HRMS: Calcd for $C_{18}H_{26}OSi$ (M^+) 286.175294, found 286.175284.

4.5.17. Synthesis of 4-(3-methylbut-3-enyl)-1-trimethylsilyloxylbicyclo[4.1.0]heptane (28). Following general procedure C; to a stirred solution of silyl enol ether **27** (133 mg, 0.561 mmol) in 2 mL dichloromethane, was added diethyl zinc (0.6 mL, 0.49 mmol). Solution was cooled to 0 °C using ice bath and neat CH_2I_2 (135 mg, 0.505 mmol) was added dropwise over a period of 15 min, reaction mixture was brought to rt and stirred for 12 h, usual workup gave **28** (91 mg, 65%) as a colorless oil. IR (neat): υ=2917, 2873, 1558 cm^{-1}. ^{1}H NMR (500 MHz, $CDCl_3$): δ=0.12 (s, 9H), 0.30 (t, 1H, J=3.5 Hz), 0.80–0.98 (m, 3H), 1.30 (td, 2H, J=7.3, 7.0 Hz), 1.41–1.68 (m, 4H), 1.70 (ddd, 4H, J=6.2, 5.4, 4.2 Hz), 2.00 (ddd, 3H, J=6.8, 7.2, 7.7 Hz), 4.68 (s, 2H) ppm. ^{13}C NMR (125 MHz, $CDCl_3$): δ=1.43 (CH_3), 18.95 (CH_2), 21.20 (CH_2), 22.50 (CH_2), 24.80 (CH), 31.20 (CH_2), 35.60 (CH_2), 36.30 (CH_2), 37.80 (CH), 57.23 (C), 109.00 (CH_2), 146.00 (C) ppm. GC–MS (EI, 70 eV): m/z (%)=252 (M^+, 2), 195 (17), 183 (14), 196 (4), 162 (4), 155 (2), 143 (5), 107 (26), 93 (7), 79 (7), 75 (26), 73 (100), 55 (10). HRMS: Calcd for $C_{15}H_{28}OSi$ (M^+) 252.19094, found 252.18994.

4.6. General procedure E

Synthesis of 3-substituted enones by reaction of vinylogous ester with GR: The GR was prepared analogously to the general procedure A, under argon atmosphere, the vinylogous ester in dry THF was added dropwise to the solution of GR at 0 °C, after addition reaction mixture was brought to rt and stirred for additional hour, water was added and reaction mixture was acidified with dilute HCl, solution was stirred for next 1 h, ether phase was separated and aqueous phase was extracted with ether, collective ether phases were washed with $NaHCO_3$ (aqueous, Saturated), water, brine and dried over sodium sulphate, concentrated under reduced pressure and residue was purified by silica gel column chromatography (EtOAc/cyclohexane).

4.6.1. Synthesis of 3-benzyl-2-cycloheptene-1-one (20). Follwing general procedure E; under argon atmosphere 3-ethoxy-2-cycloheptene-1-one **19** (500 mg, 3.246 mmol) was treated with GR prepared from benzyl chloride (449 mg, 3.57 mmol) and Mg metal (85 mg, 3.5 mmol) in THF–ether (1/1 by volume). The crude product was purified using silica gel column chromatography (25% EtOAc in cyclohexane) afforded enone **20** (590 mg, 91%). IR (neat): υ=2939, 2865, 1658, 1492, 1454, 1265 cm^{-1}. ^{1}H NMR (500 MHz, $CDCl_3$): δ=1.64–1.70 (m, 2H), 1.71–1.78 (m, 2H), 2.34 (t, 2H, J=6.2 Hz), 2.56 (t, 2H, J=6.4 Hz), 3.46 (s, 2H), 5.94 (s, 1H), 7.15 (d, 2H, J=7.0 Hz), 7.28 (ddd, 1H, J=4.0, 7.0, 8.0 Hz), 7.29 (dd, 2H, J=2.0, 8.0 Hz) ppm. ^{13}C NMR (125 MHz, $CDCl_3$): δ=21.28 (CH_2), 25.17 (CH_2), 32.31 (CH_2), 42.25 (CH_2), 47.09 (CH_2), 126.77 (CH), 128.58 (CH), 129.09 (CH), 130.61 (CH), 137.58 (C), 160.09 (C), 204.07 (C=O) ppm. GC–MS (EI, 70 eV): m/z (%)=158 (M^+, 7), 129 (13), 115 (11), 109 (100), 92 (1), 91 (21), 81 (46), 79 (22), 81 (46), 79 (22), 67 (14), 65 (36).

4.6.2. *cis*-3,4,4a,9,9a,10-Hexahydro-1(2*H*)-antracenone (29).[22] Following general procedure D; the solution of cyclopropane **8** (200 mg, 0.72 mmol) and DCA (55 mg, 0.24 mmol) in 120 mL dry acetonitrile was filled into Pyrex irradiation tubes, flushed with argon for 20 min and irradiated for 12 h using 420 nm lamps. The residue was purified by silica gel column chromatography (9% EtOAc in cyclohexane) to afford **29** (29 mg, 20%). IR (KBr): υ=2377, 2320, 1718, 1689, 1519 cm^{-1}. NMR (^{1}H, ^{13}C, ^{13}C-DEPT); ^{1}H NMR (500 MHz, $CDCl_3$): δ=1.54 (dddd, 1H, J=3.7, 3.7, 3.7, 3.1 Hz), 1.74 (tttt, 1H, J=4.0, 3.7, 4.0, 4.0 Hz), 1.82–1.93 (m, 1H), 2.04 (dq, 1H, J=1.2, 1.2 Hz), 2.11 (qq, 1H, J=2.8, 2.9 Hz), 2.40 (dddd, 2H, J=5.6, 6.9, 6.2, 6.2 Hz), 2.46–2.53 (1H, m), 2.69 (dd, 1H, J=11.9, 11.9 Hz), 2.92 (d, 1H, J=10.0 Hz), 2.96 (t, 2H, J=2.8 Hz), 7.04 (dd, 1H, J=2.5, 6.2 Hz), 7.10 (ddd, 2H, J=7.2, 5.4, 1.8 Hz), 7.16 (dd, 1H, J=2.5, 3.1 Hz) ppm. ^{13}C NMR (125 MHz, $CDCl_3$): δ=26.05 (CH_2), 28.63 (CH_2), 32.69 (CH_2), 37.79 (CH_2), 40.74 (CH_2), 41.91 (CH_2), 50.82 (CH), 125.72 (CH), 125.91 (CH), 128.42 (CH), 129.30 (CH), 135.04 (CH), 135.04 (C), 135.36 (C), 211.80 (C=O) ppm. NMR (^{1}H COSY, HMBC, HMQC and NOESY):

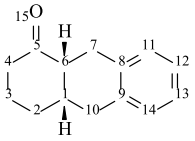

HMBC correlations of C-6 (50.82) to H-6 (δ 2.40), C-4 (41.91) to H-4 (2.50), C-1 (40.74) to H-1 (1.82–1.93), C-10 (37.79) to H-7 and H-10 (2.69 and 2.96), C-2 (32.69), to H-2 (1.54 and 2.04), C-7 (28.63) H-7 (2.96), C-3 (26.05), H-3 (1.54; 1.74; 2.04; 2.11). NOESY correlation of H-6 and H-1 leads to the assignment of cis ring fusion. GC–MS (EI, 70 eV): m/z (%)=200 (M^+, 100), 185 (27), 167 (24), 154 (47), 142 (21), 129 (59), 115 (17), 91 (13), 77 (18).

4.6.3. (5a*R*,10a*S*)-5,5a,7,8,9,10,10a,11-Octahydro-6*H*-cyclohepta[*b*]naphthalene-6-one (30). Following general procedure D; the solution of cyclopropane **9** (200 mg, 0.69 mmol) and DCA (30 mg, 0.131 mmol) in 120 mL dry acetonitrile was filled into Pyrex irradiation tubes, flushed with argon for 20 min and irradiated for 12 h using 420 nm lamps. The residue was purified by silica gel column chromatography (9% EtOAc in cyclohexane) to afford **30** (23 mg, 16%). IR (KBr): υ=2925, 2857, 1690, 1454 cm^{-1}. NMR (^{1}H, ^{13}C, ^{13}C-DEPT, ^{1}H COSY, HMBC, HMQC and NOESY); ^{1}H NMR (500 MHz, $CDCl_3$): δ=1.37 (ddd, 2H, J=12.5, 10.0, 9.8 Hz), 1.46–1.70 (m, 3H), 1.71–1.80 (m, 2H), 1.81–2.10 (m, 1H), 2.41 (ddt, 2H, J=6.3, 6.3, 2.0 Hz), 2.51–2.60 (2H, m), 2.65 (dt, 2H, J=11.0, 8.0 Hz), 2.84 (ddd, 2H, J=16.0, 16.2, 11.5 Hz), 7.09 (ddd, 3H, J=8.0, 3.0, 4.0 Hz), 7.26 (dd, 1H, J=6.9, 3.7 Hz) ppm. ^{13}C NMR (125 MHz, $CDCl_3$): δ=25.79 (CH_2), 32.74 (CH_2), 35.79 (CH_2), 35.52 (CH), 37.75 (CH_2), 41.19 (CH_2), 44.22 (CH_2),

54.92 (CH), 125.92 (CH), 128.25 (CH), 128.47 (CH), 128.58 (CH), 135.16 (C), 136.31 (C), 215.64 (C=O) ppm.

NMR (^{1}H COSY, HMBC, HMQC and NOESY):

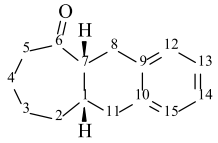

HSQC correlation of C-7 (54.92) to H-7 (2.51–2.60), C-5 (41.19) to H-5 (2.54), C-2 (41.19) to H-2 (2.50–2.65), C-11 (35.75) to (1.81–2.10 and 2.40–2.70 and 2.84), C-8 (32.74) to H-8 (2.84), C-3 (25.79) to H-3 (1.54 and 2.10). NOESY correlation between H-1 and H-7 lead to the assignment of cis ring fusion. GC–MS (EI, 70 eV): *m/z* (%)=214 (M^+, 90), 210 (6), 199 (20), 181 (26), 172 (11), 167 (3), 157 (15), 155 (17), 142 (28), 129 (100), 115 (35), 91 (15), 80 (10), 77 (16). HRMS: Calcd for $C_{15}H_{18}O$ (M^+) 214.1359, found 214.1347.

4.6.4. Benzylcyclohexanone (31)[23a] and 4-benzyl-2-cyclohexen-1-one (32).[23b] Following general procedure D; the solution of cyclopropane **7** (100 mg, 0.384 mmol) and DCA (25 mg, 0.109 mmol) in 60 mL dry acetonitrile was filled into Pyrex irradiation tubes, flushed with argon for 20 min and irradiated for 12 h using 420 nm lamps. The residue was purified by silica gel column chromatography (9% EtOAc in cyclohexane) to afford products **31** (6 mg, 8%) and **32** (9 mg, 12%). *Ketone* (**31**): IR (KBr): υ=1718, 1654 cm^{-1}. NMR (^{1}H, ^{13}C, ^{13}C-DEPT); ^{1}H NMR (500 MHz, $CDCl_3$): δ=1.20–1.37 (m, 1H), 1.42 (dq, 2H, *J*=4.3, 3.7 Hz), 1.99 (td, 3H, *J*=3.1, 4.3 Hz), 2.20–2.40 (m, 4H), 2.60 (d, 2H, *J*=6.9 Hz), 7.15 (d, 2H, *J*=6.9 Hz), 7.20 (t, 1H, *J*=7.2 Hz), 7.28 (t, 2H, *J*=7.2 Hz) ppm. ^{13}C NMR (150 MHz, $CDCl_3$): δ=26.91 (CH_2), 38.14 (CH), 40.76 (CH_2), 42.19 (CH_2), 126.11 (CH), 128.35 (CH), 129.01 (CH), 140.36 (C), 211.20 (C=O) ppm. NMR (^{1}H COSY, HMBC, HMQC):

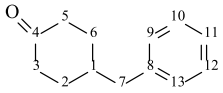

HMBC correlation of C-8 (140.36) to H-7 (2.60), C-7 (42.19) to H-1 (1.99), C-1 (38.14) to H-6 and H-2 (1.42) and H-5; H-2 (2.20–2.40) and H-7 (2.60), C-4 (211.20), to H-5; H-3; (2.20–2.40) and H-7 (2.60); H-6. COSEY correlation of H-2 to H-1; H-13; H-9 and H-1 to H-6; H-7 and H-2. GC–MS (EI, 70 eV): *m/z* (%)=188 (M^+, 1), 187 (7), 186 (50), 168 (60), 129 (8), 127 (2), 115 (4), 91 (100), 77 (6), 74 (1.2), 65 (54), 63 (13). *Enone* (**32**): IR (KBr): υ=1716, 1673 cm^{-1}. NMR (^{1}H, ^{13}C, ^{13}C-DEPT); ^{1}H NMR (500 MHz, $CDCl_3$): δ=1.66 (tdd, 1H, *J*=4.7, 4.3, 5.0 Hz), 1.99 (dtd, 1H, *J*=4.3, 5.0, 4.7 Hz), 2.27 (dtd, 1H, *J*=5.0, 4.5, 5.0 Hz), 2.42 (tt, 1H, *J*=4.8, 4.8 Hz), 2.65 (dd, 2H, *J*=8.5, 5.4 Hz), 2.72 (ddd, 1H, *J*=10.3, 5.3, 1.5 Hz), 5.92 (dd, 1H, *J*=1.8, 10.2 Hz), 6.77 (dt, 1H, *J*=2.0, 10.0 Hz), 7.13 (d, 2H, *J*=6.9 Hz), 7.18 (dd, 1H, *J*=1.8, 7.4 Hz), 7.26 (dd, 2H, *J*=1.8, 7.3 Hz) ppm. ^{13}C NMR (125 MHz, $CDCl_3$): δ=28.62 (CH_2), 36.79 (CH_2), 37.95 (CH), 40.90 (CH_2), 128.60 (CH), 128.56 (CH), 129.05 (CH), 129.31 (CH), 138.80 (C), 153.80 (CH), 199.70 (C=O) ppm. NMR (^{1}H COSY, HMBC, HMQC):

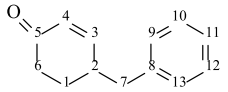

HMBC correlation of C-8 (138.80), to H-7 (2.65), H-9; H-13 (7.13), C-2 to (37.95) H-1a (1.66); H-1b (1.99), H-6a and H-6b (2.42); H-7 (2.65); H-3 (5.92) and H-4 (6.77), C-5 (199.70) to H-1; H-6; H-4. GC–MS (EI, 70 eV): *m/z* (%)=187 (M^+, 4), 186 (33), 168 (4), 158 (1), 129 (5), 127 (2), 115 (3), 91 (100), 79 (2), 77 (4), 65 (37), 51 (11).

4.6.5. 1-Methyl-3-(2-phenylethyl)-cyclohexanone (33). Following general procedure D; the solution of cyclopropane **18** (100 mg, 0.347 mmol) and DCA (45 mg, 0.19 mmol) in 50 mL dry acetonitrile was filled into Pyrex irradiation tubes, flushed with argon for 20 min and irradiated for 12 h using 420 nm lamps. The residue was purified by silica gel column chromatography (9% EtOAc in cyclohexane) to afford **33** (23 mg, 30%). IR: (KBr): υ=3391, 2961, 2932, 2866, 1710, 1452, 1070, 1452, 1070, 1070 cm^{-1}. ^{1}H NMR (500 MHz, $CDCl_3$): δ=0.99 (d, 3H, *J*=6.2 Hz), 1.31 (dd, 1H, *J*=12.8, 3.4 Hz), 1.36 (dd, 1H, *J*=12.5, 3.1 Hz), 1.40 (dd, 1H, *J*=5.0, 1.8 Hz), 1.43 (dd, 1H, *J*=13.1, 3.1 Hz), 1.58–1.72 (m, 2H), 1.94 (dt, 1H, *J*=13.0, 3.0 Hz), 2.05–2.15 (m, 1H), 2.33 (sep, 1H, *J*=6.2 Hz), 2.46 (dddd, 1H, *J*=1.8, 1.8, 1.8, 2.5 Hz), 2.60 (t, 2H, *J*=7.8 Hz), 7.15 (dd, 3H, *J*=6.0, 6.9 Hz), 7.26 (ddd, 2H, *J*=4.0, 7.0, 5.0 Hz) ppm. ^{13}C NMR (125 MHz, $CDCl_3$): δ=14.35 (CH_3), 31.98 (CH_2), 32.98 (CH_2), 34.87 (CH_2), 39.86 (CH), 44.87 (CH_2), 48.23 (CH_2), 125.83 (CH), 128.25 (CH), 128.38 (CH), 142 (C), 212.80 (C=O) ppm. GC–MS (EI, 70 eV): *m/z* (%)=216 (M^+, 20), 131 (10), 115 (11), 111 (65), 104 (14), 92 (23), 91 (100), 79 (7), 77 (10), 65 (13), 56 (8), 55 (30).

4.6.6. (3*S*,3a*R*,8a*S*)-3-Methyloctahydroazulen-5(1*H*)-one (34).[21] Following general procedure D; the solution of cyclopropyl silyl ether **14** (150 mg, 0.63 mmol) and DCA (48 mg, 0.21 mmol) in 60 mL dry acetonitrile was filled into Pyrex irradiation tubes, flushed with argon for 20 min. and irradiated for 12 h using 420 nm lamps. The residue was purified by silica gel column chromatography (9% EtOAc in cyclohexane) to afford 35 (10 mg, 10%).

IR (KBr): υ=1653, 1507 cm^{-1}. NMR (^{1}H, ^{13}C, ^{13}C-DEPT); ^{1}H NMR (500 MHz, $CDCl_3$): δ=0.80 (d, 3H), 1.15–1.35 m, 4H), 1.50–1.55 and 1.85–1.95 (m, 2H), 1.60–1.70 and 2.45–2.58 (m, 2H), 1.75–1.88 (m, 2H), 1.09–1.95 (m, 1H), 2.02–2.10 (m, 1H), 2.10–2.20 (m, 1H), 2.35–2.45 (m, 2H). ^{13}C NMR (125 MHz, $CDCl_3$): δ=16.07 (CH_3), 24.86 (CH_2), 32.12 (CH_2), 32.53 (CH_2), 36.14 (CH_2), 37.64 (CH), 44.04 (CH_2), 44.28 (CH), 45.26 (CH_2), 45.88 (CH), 215.20 (C=O) ppm. NMR (^{1}H COSY, HMBC, HMQC and NOESY):

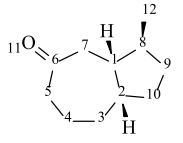

HMBC correlation of C-6 (215.20) to H-4 (1.50–1.55) and H-5; H-7 (1.75–1.95), and H-7 (2.30–2.50), C-12 (16.07) to H-9 and H-10 (1.15–1.35), H-1 and H-2 (1.75–1.85), H-8 (2.10–2.20). NOESY correlation between H-12 to H-1 and H-2 lead to the assignment of cis ring fusion. GC–MS (EI, 70 eV): *m/z* (%)=166 (M^+, 1), 165 (14), 123 (15), 121 (46), 110 (11), 107 (24), 94 (60), 80 (55), 78 (40), 67 (82), 55 (94), 41 (100).

4.6.7. (3a*S*,8a*S*)-3,3-Dimethyloctahydroazulen-5(1*H*)-one (35). Following general procedure D; the solution of cyclopropyl silyl ether **28** (120 mg, 0.476 mmol) and DCA (48 mg, 0.21 mmol) in 60 mL dry acetonitrile was filled into Pyrex irradiation tubes, flushed with argon for 20 min and irradiated for 12 h using 420 nm lamps. The residue was purified by silica column chromatography (9% EtOAc in cyclohexane) to afford **35** (12 mg, 14%). IR (KBr): υ=1690, 1540 cm^{-1}. NMR (^1H, ^{13}C, ^{13}C-DEPT); ^1H NMR (500 MHz, $CDCl_3$): δ=0.75 (s, 3H), 0.96 (s, 3H), 1.26–1.32 (m, 2H), 1.38–1.46 (m, 1H), 1.45–1.50 (2H, m), 1.57 and 2.50 (m, 2H), 1.60 and 2.40 (m, 1H), 1.68–1.78 (2H, m), 1.87–1.95 (m, 2H), 1.98–2.10 (m, 1H), 2.24 (dd, 1H, *J*=16.4, 12.0 Hz), 2.48–2.52 (m, 1H) ppm. ^{13}C NMR (125 MHz, $CDCl_3$): δ=22.31 (CH_3), 27.84 (CH_2), 27.93 (CH_3), 30.5 (CH_2), 37.02 (CH_2), 40.30 (CH_2), 43.65 (CH_2), 44.70 (C), 44.17 (CH_2), 46.69 (CH), 51.28 (CH), 215.18 (C=O) ppm. NMR (^1H COSY, HMBC, HMQC and NOESY):

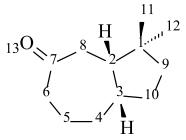

HMBC correlation of C-1 (217.18) to H-8 and H-6 (2.20–2.52), C-2 (51.28) to H-11 and H-12 (0.75, 0.96), H-3a (2.49); H-8 (2.20–2.48), C-3 (46.69) to H-11 and H-12; H-4 (1.42–1.50), H-10 (2.00), H-8. NOESY correlation between H-3 and H-2 and H-11 lead to the assignment of cis stereochemistry of the molecule. GC–MS (EI, 70 eV): *m/z* (%)=180 (M^+, 10), 165 (8), 152 (3), 147 (11), 136 (13), 124 (20), 120 (11), 109 (23), 94 (24), 90 (8), 79 (20), 70 (30), 66 (60), 40 (100), 38 (32). HRMS: Calcd for $C_{12}H_{20}O$ (M^+) 180.15142, found 180.15086.

4.6.8. 3a-Benzyl-hexahydropentalen-2-one (36).[24] Following general procedure D; the solution of cyclopropyl silyl ether **22** (160 mg, 0.56 mmol) and DCA (52 mg, 0.228 mmol) in 96 mL dry acetonitrile was filled into Pyrex irradiation tubes, flushed with argon for 20 min and irradiated for 17 h using 420 nm lamps. The residue was purified by silica gel column chromatography (9% EtOAc in cyclohexane) to afford **36** (36 mg, 31%). IR (KBr): υ= 2947, 2868, 1737, 1660, 1450, 1405, 1166 cm^{-1}. NMR (^1H, ^{13}C, ^{13}C-DEPT); ^1H NMR (500 MHz, $CDCl_3$): δ=1.38 (ddd, 1H, *J*=5.0, 11.7, 6.4 Hz), 1.50 (ddd, 1H, *J*=7.5, 12.5, 6.5 Hz), 1.65–1.80 (m, 4H), 1.90–2.10 (m, 2H), 2.25–2.45 (m, 3H), 2.65 (d, 1H, *J*=13.1 Hz), 2.69 (d, 1H, *J*= 13.1 Hz), 6.79 (dd, 2H, *J*=1.5, 6.9 Hz), 7.16 (dd, 1H, *J*= 7.2, 4.7 Hz), 7.22 (dd, 2H, *J*=1.9, 6.5 Hz) ppm. ^{13}C NMR (125 MHz, $CDCl_3$): δ=23.86 (CH_2), 32.52 (CH_2), 37.82 (CH_2), 44.44 (CH_2), 45.46 (CH_2), 48.95 (CH_2), 51.79 (C), 126.37 (CH), 128.20 (CH), 130.02 (CH), 138.62 (C), 219.87 (C=O) ppm. NMR (^1H COSY, HMBC, HMQC and NOESY):

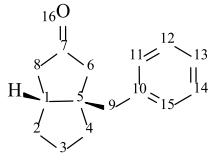

HMBC correlation of C-7 (219.87) to H-6 and H-8 (1.90–2.10; 2.25; 2.45), C-10 (138.62) to H-9 (2.65), C-1 (44.44) to H-3 and H-2 (1.70) and H-8 (1.90–2.09) and to H-9. NOESY correlation between H-9 and H-1a leads to the assignment of cis ring fusion. GC–MS (EI, 70 eV): *m/z* (%)=214 (M^+, 16), 149 (11), 123 (34), 117 (5), 95 (100), 81 (81), 67 (23), 65 (30).

4.6.9. 3,4,4a,5,8,8a-Hexahydro-1-(2*H*)-naphthalenone (38).[18] Following general procedure D; the solution of cyclopropyl silyl ether **12** (100 mg, 0.45 mmol) and DCA (25 mg, 0.109 mmol) in 60 mL dry acetonitrile was filled into Pyrex irradiation tubes, flushed with argon for 20 min and irradiated for 17 h using 420 nm lamps. The residue was purified by silica gel column chromatography (9% EtOAc in cyclohexane) to afford **38** (10 mg, 15%). IR (KBr): υ= 1720, 1666 cm^{-1}. ^1H NMR (500 MHz, $CDCl_3$): δ=1.40–2.45 (m, 10H), 2.55 (dd, 1H, *J*=6.9, 7.5 Hz), 2.75 (dd, 1H, *J*=4.3, 7.5 Hz), 4.87 (t, 2H, *J*=1.2 Hz) ppm. GC–MS (EI, 70 eV): *m/z* (%)=150 (M^+, 13), 134 (11.4), 121 (19.5), 106 (24), 91 (35), 79 (100), 77 (76), 52 (43), 40 (32).

5. Supplementary data

Supplementary data associated with 2D NMR experiments are available from the authors on request.

Acknowledgements

Financial support by the Deutsche Forschungsgemeinschaft (DFG), the Fonds der Chemischen Industrie, and the Innovationsfonds der Universität Bielefeld is gratefully acknowledged.

References and notes

1. Giese, B. *Angew. Chem.* **1983**, *95*, 771–782. *Angew. Chem., Int. Ed. Engl.* **1983**, *22*, 753.
2. Giese, B. *Angew. Chem.* **1985**, *97*, 555–567. *Angew. Chem., Int. Ed. Engl.* **1985**, *24*, 553.
3. Giese, B. *Radicals in Organic Synthesis: Formation of Carbon–Carbon Bonds*; Pergamon: Oxford, 1986.
4. Curran, D. P. *Synthesis* **1988**, 417–439.
5. (a) *Radicals in Organic Synthesis*; Renaud, P., Sibi, M., Eds.; Wiley-VCH: Weinheim, 2001. (b) Linker, T.; Schmittel, M. Radikale und Radikalionen in der Organischen Synthese; Wiley-VCH: Weinheim, 1998.
6. (a) Balzani, V., Ed.; Electron Transfer in Chemistry;

Wiley-VCH: Weinheim, 2001; Vol. 1–5. (b) Mattay, J., Ed.; Topics in Current Chemistry; Springer: Berlin, 1994–1996; Vol. 169. (c) Eberson, L. Electron Transfer Reactions in Organic Chemistry; Springer: Heidelberg, 1987.

7. (a) Mattay, J., Ed.; Topics in Current Chemistry; Springer: Berlin, 1990–1993; Vol. 156, 158, 159, 163, 168. (b) Fox, M.; Chanon, A. M. Photoinduced Electron Transfer; Elsevier: Amsterdam, 1988; Part A–D. (c) Mattay, J. *Angew. Chem.* **1987**, *99*, 849–870. *Angew. Chem., Int. Ed. Engl.* **1987**, *26*, 825. (d) Mattay, J. *Synthesis* **1989**, 233–252. (e) Kavarnos, G. J. Fundamentals of Photoinduced Electron Transfer; VCH: Weinheim, 1993.
8. (a) Albini, A.; Fagnoni, M. *Green Chem.* **2004**, *6*, 1–6. (b) Oelgemöller, M.; Mattay, J. In *CRC Handbook of Organic Photochemistry and Photobiology*; Horspool, W., Lenci, F., Eds.; CRC: Boca Raton, 2004; pp 88-1–88-45. (c) Mattay, J. *Chem. Unserer Zeit* **2002**, *36*, 98–106. (d) Abe, M.; Oku, A. *J. Org. Chem.* **1995**, *60*, 3065–3073. (e) Oku, A.; Takahashi, H.; Asmus, S. M. *J. Am. Chem. Soc.* **2000**, *122*, 7388–7389. (f) Abe, M.; Nojima, M.; Oku, A. *Tetrahedron Lett.* **1996**, *37*, 1833–1836. (g) Oku, A.; Abe, M.; Iwamoto, M. *J. Org. Chem.* **1994**, *59*, 7445–7452.
9. (a) Rinderhagen, H.; Mattay, J. *Chem. Eur. J.* **2004**, *10*, 851–874. (b) A comprehensive investigation of the cleavage of bicyclic cyclopropyl silyl ethers by means of spectroscopic and theoretical methods will be published separately. (c) Rinderhagen, H. Ph.D. Thesis, University of Bielefeld, 2002.
10. (a) Bunte, J. O.; Rinne, S.; Mattay, J. *Synthesis* **2004**, 619–633. (b) Bunte, J. O.; Heilmann, E. K.; Hein, B.; Mattay, J. *Eur. J. Org. Chem.* **2004**, 3535–3550. (c) Tzvetkov, N.; Schmidtmann, M.; Müller, A.; Mattay, J. *Tetrahedron Lett.* **2003**, *44*, 5979–5982.
11. (a) Hintz, S.; Heidbreder, A.; Mattay, J. *Top. Curr. Chem.* **1996**, *177*, 77–124. (b) Schmoldt, P.; Rinderhagen, H.; Mattay, J. *Molecular and Supramolecular Photochemistry* **2003**, *9*, 185–225. (c) Oelgemöller, M.; Bunte, J. O.; Mattay, J. *Molecular and Supramolecular Chemistry* **2004**, *10*, 267–295.
12. (a) Lee, P. H.; Lee, K.; Kim, S. *Org. Lett.* **2001**, *3*, 3205–3207. (b) Iwasawa, N.; Miura, T.; Kiyota, K.; Kusama, H.; Lee, K.; Lee, P. H. *Org. Lett.* **2002**, *4*, 4463–4466.
13. Bailey, W. F.; Punzaklan, E. R. *J. Org. Chem.* **1990**, *55*, 5404–5406.
14. Wolf, S.; Agosta, W. C. *J. Am. Chem. Soc.* **1983**, *105*, 1292–1299.
15. (a) Roth, H. D.; Schilling, M. L. M.; Schilling, F. C. *J. Am. Chem. Soc.* **1985**, *107*, 4152–4158. (b) Delgado, J.; Espinós, A.; Jiménez, M. C.; Miranda, M. A.; Roth, H. D.; Tormos, R. *J. Org. Chem.* **1999**, *64*, 6541–6546.
16. Baldwin, J. E. *J. Chem. Soc., Chem. Commun.* **1976**, 734–736.
17. Beckwith, A. L. J.; Easton, C. J.; Serelis, A. K. *J. Chem. Soc., Perkin Trans. 2* **1985**, 443–450.
18. Fringuelli, F.; Pizzo, F.; Taticch, T. D. J.; Halls, A.; Wenkert, E. *J. Org. Chem.* **1982**, *47*, 5056–5065.
19. Booker-Millburn, K. I.; Thomson, D. F. *J. Chem. Soc., Perkin Trans. 1* **1995**, 2315–2321.
20. Booker-Millburn, K. I.; Thomson, D. F. *Tetrahedron* **1995**, *51*, 12955–12962.
21. Iwasawa, N.; Funahashi, M.; Hayakawa, S.; Ikeno, T.; Narasaka, K. *Bull. Chem. Soc. Jpn.* **1999**, *72*, 85–97.
22. Thompson, H. W.; Long, D. J. *J. Org. Chem.* **1988**, *53*, 4201–4209.
23. (a) MacDonald, M.; Vander Velde, D.; Aubé, J. *J. Org. Chem.* **2001**, *66*, 2636–2642. (b) Kinney, W. A.; Crouse, G. D.; Paquette, L. A. *J. Org. Chem.* **1983**, *48*, 4986–5000.
24. Curran, D. P.; Diederichsen, U.; Palovich, M. *J. Am. Chem. Soc.* **1997**, *119*, 4797–4804.

Available online at www.sciencedirect.com
SCIENCE DIRECT
Tetrahedron
Tetrahedron 61 (2005) 10331–10337

Dithionite adducts of pyridinium salts: regioselectivity of formation and mechanisms of decomposition

Vincenzo Carelli,* Felice Liberatore, Luigi Scipione, Barbara Di Rienzo and Silvano Tortorella

Department of 'Studi di Chimica e Tecnologia delle Sostanze Biologicamente Attive', Università 'La Sapienza', Piazzale Aldo Moro, 5, 00185 Rome, Italy

Received 27 April 2005; revised 12 July 2005; accepted 28 July 2005

Available online 13 September 2005

Abstract—^{1}H and ^{13}C NMR spectroscopy has been used to detect and to characterize the adducts formed, in alkaline solutions, by the attack of dithionite anion on 3-carbamoyl or 3-cyano substituted pyridinium salts. In all studied cases, only 1,4-dihydropyridine-4-sulfinates, formed by attack of dithionite oxyanion on the carbon 4 of pyridinium ring, were found. This absolute regioselectivity seems to suggest a very specific interaction between the pyridinium cation and the dithionite through the formation of a rigidly oriented ion pair, determining the position of attack. In weak alkaline solution, the adducts decompose according to two mechanisms S_Ni and S_Ni': the S_Ni path is operative in all studied cases and preserves the 1,4-dihydro structure yielding the corresponding 1,4-dihydropyridines, whereas the S_Ni' path involves the shift of 2,3 or 5,6 double bonds yielding 1,2- or 1,6-dihydropyridines, respectively. The formation of 1,2- or 1,6-dihydropyridines, in addition to 1,4-dihydro isomers, depends on their respective thermodynamic stabilities.

1. Introduction

Sodium dithionite reduction has been largely applied to pyridinium salts bearing, in the 3- or 3,5-positions, electron-withdrawing groups such as –CN, –$CONH_2$, –COOR, and chiefly affords the corresponding 1,4-dihydropyridines.[1–7] Thermodynamic factors accounted for this high regioselectivity, since theoretical studies such as, for example, the calculation of the heats of formation using AM1 molecular orbital methods,[8a,b] demonstrated the greater thermodynamic stability of the 1,4-dihydropyridines in comparison with the isomeric 1,2- and 1,6-dihydroderivatives.[9] Intermediate adducts, identified by some authors[1,5,7] as sulfinate anions (Scheme 1, A), are found in the dithionite reduction. These adducts are stable at alkaline pH, while in neutral or weakly alkaline medium they undergo fast protonation and conversion to 1,4-dihydropyridines.

In a recent work[10] we have shown, in accordance with ^{1}H, ^{13}C and ^{17}O NMR spectroscopic evidence, that dithionite adducts are *S*-anions of esters of sulfinic acid (Scheme 1, B), originated by attack of the dithionite oxyanion at the carbon 4 of the pyridinium salts. We have also proposed that the decomposition of these esters, after protonation, may occur according to an intramolecular hydrogen transfer mechanism associated with sulfur dioxide evolution, leading to the formation of 1,4-dihydropyridines with high regioselectivity.

However, it has been reported[7] that in the dithionite reduction of some 4- and 4,6-methyl substituted *N*-Benzyl and *N*-(2,6-dichlorobenzyl)-nicotinamide salts, 1,2- and 1,6-dihydropyridines were formed in addition to the isomeric 1,4-dihydro derivatives.

During our studies on the dithionite reduction of pyridinium salts, in some instances we also noticed the presence of variable amounts of 1,2- or 1,6-dihydropyridines besides the predominant 1,4-dihydropyridines.

These findings led us to perform a careful examination of the dithionite reduction of a significant number of pyridinium salts in order to ascertain: (a) if the formation

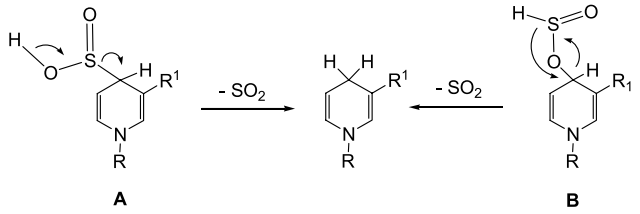

Scheme 1.

Keywords: Pyridinium salts; Dithionite adducts; Adduct decomposition; S_Ni and S_Ni' mechanisms; Dihydropyridines.
* Corresponding author. Tel.: +39 649913226; fax: +39 649913888; e-mail: vincenzo.carelli@uniroma1.it

0040–4020/$ - see front matter © 2005 Elsevier Ltd. All rights reserved.
doi:10.1016/j.tet.2005.07.096

of 1,2- and 1,6 -dihydropyridines, in addition to the 1, 4-dihydroderivatives, is a common occurrence and the extent of the phenomenon; (b) if the formation of 1,2- or 1, 6-dihydropyridines follows the decomposition of corresponding dithionite adducts at position 2 or 6 of the dihydropyridine system.

2. Results and discussion

Several pyridinium salts (**1a**–**m**, Scheme 2) have been used as model compounds for the present study.

The results of an accurate ^{1}H NMR analysis (Tables 1 and 5) performed directly on the chloroform extracts obtained from dithionite reduction of salts **1a**–**m**, were compared with the ^{1}H NMR data of known dihydroderivatives reported in the literature. In this way, it was possible to ascertain that the reduction sometimes led to a 1,4-dihydropyridine as unique product, in other cases to mixtures of 1,4- and 1,2- or 1,4- and 1,6-dihydropyridines. When not previously known, the dihydroderivatives obtained, such as the 1,4-dihydropyridines **3h**,**i**,**l** and the 1,2-dihydropyridines **4h**,**i**, were unambiguously identified and their relative abundances determined by means of HPLC, ^{1}H and ^{13}C NMR analyses (Tables 1 and 2).

The structure of the dithionite adducts **2a**–**m** has been determined from the ^{1}H and ^{13}C NMR analyses, directly carried out on the reduction mixtures (Tables 3 and 4). In order to prevent a possible decomposition of the adducts even in strongly alkaline medium, a particular procedure has been adopted for the preparation of the samples before their submission to NMR analyses (see Section 3). As stressed previously by us,[10] ^{1}H and ^{13}C NMR spectroscopies represent highly diagnostic techniques for identifying the position of attack of the dithionite on the pyridinium cation and in all the reactions studied have allowed us to establish, beyond doubt, that the unique intermediate adduct present was the sulfinic ester (*S*-anion) formed by attack of the dithionite oxyanion at carbon 4 of the pyridinium salt. The formation of this sole adduct was always observed even when the final reduction products were, besides the 1,4-dihydropyridines, also the isomeric 1,2- or 1,6-dihydro derivatives.

Similar examples of absolute regioselectivity in the reaction of a nucleophile with a pyridinium salt were previously reported and concerned the exclusive attack of nitroalkane carbanions at the 4 position of the pyridinium rings.[11]

As we have already reported,[10] carbons 4 of the dithionite adducts are strongly deshielded with respect to the carbons in the 4 position of the corresponding 1,4-dihydropyridines. Indeed, the chemical shifts of carbons in the 4 position in adducts **2a**,**b**,**c**,**d**,**h**–**m** (Scheme 2, Table 4) are all comprised in the 62–68 ppm range, and display, in comparison with the chemical shifts of 4-position carbons in corresponding 1,4-dihydropyridines (Table 2, Ref. 12–14), a downfield shift effect variable from ca. 32 to 46 ppm. Such a downfield shift suggests that carbon atoms are directly bonded to an oxygen atom. Indeed, the downfield effect of an oxygen atom on the ^{13}C chemical shift of the carbon to which is bonded, ranges in alkane and cycloalkanes from 49 to 42 ppm ca., respectively.[15,16]

Similarly, the H4 in the adducts are significantly deshielded as well (downfield shift 0.5–0.8 ppm, Table 3) with respect to H4 in the corresponding 1,4-dihydropyridines (Table 5).

The presence of adducts deriving from the dithionite attack to carbons 2 or 6 of the pyridinium ions would give rise in

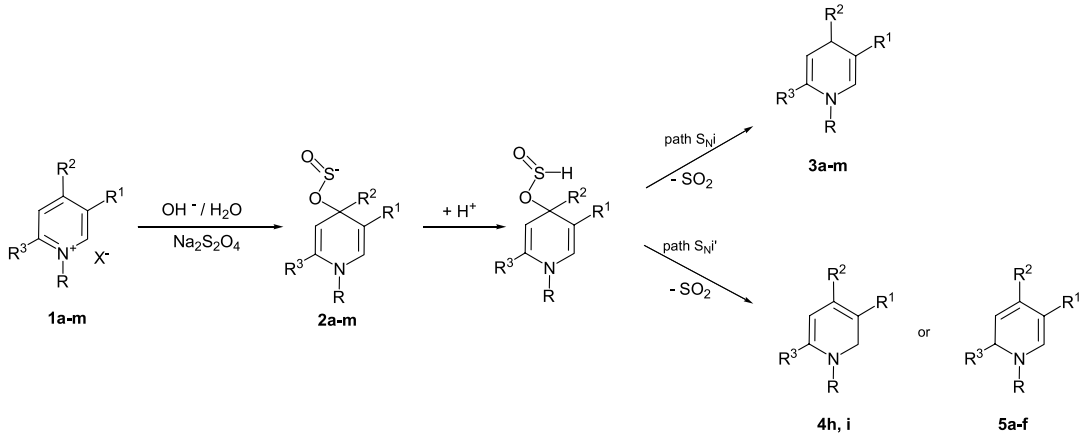

	R	R^1	R^2	R^3	X^-		R	R^1	R^2	R^3	X^-
a	Me	CN	H	H	I^-	**g**	Bn	$CONH_2$	H	Me	Br^-
b	Bn	CN	H	H	Br^-	**h**	Me	CN	Me	Me	I^-
c	Me	$CONH_2$	H	H	I^-	**i**	Bn	CN	Me	Me	Br^-
d	Bn	$CONH_2$	H	H	Br^-	**l**	Bn	$CONH_2$	Me	Me	Br^-
e	Bn;	$CONH_2$	Me	H	Br^-	**m**	2,6-DCB	$CONH_2$	Me	Me	Br^-
f	2,6-DCB	$CONH_2$	Me	H	Br^-						

Scheme 2.

Table 1. ^{1}H NMR chemical shifts of the 1,2-dihydropyridines **4h**,**i** and 1,6-dihydropyridines **5a–f**

	H2	H4	H5	H6	N–CH_3	N–CH_2	4-CH_3	6-CH_3	$J_{2,4}$	$J_{2,5}$	$J_{4,5}$	$J_{4,6}$	$J_{5,6}$
4h[a]	3.92 2Hs		4.73s		2.86s		1.59s	1.95s					
4i[a, b]	3.99 2Hs		4.93s			4.51s	2.00s	2.08s					
5a[a]	6.68dd	5.79m	5.01m	4.11 2Hdd	2.80s				1.2	0.8	10.0	1.6	3.2
5b[a, b]	6.86dd	5.80m	5.00m	4.03 2Hdd		4.15s			1.6	0.8	10.0	1.6	3.2
5c[a]	7.08s	6.13m	4.99dt	4.03 2Hdd	2.84s						10.0	1.6	3.2
5d[a, b]	[c]	6.09m	4.94dt	3.93 2Hdd		4.16s			1.2	0.8	9.8	1.6	3.2
5e[b, d, e]	7.16d		4.74m	3.85m		4.20s	1.98s						5.0
5f[b, d, f]	7.17s		4.74m	3.93d		4.49s	1.96s						4.5

[a] $CDCl_3$.
[b] Aromatic proton signals are in the range 7.20–7.50 ppm.
[c] Overlapped with aromatic signals.
[d] DMSO-d_6.
[e] $CONH_2$ 5.46s, $J_{2,6}=1.5$.
[f] $CONH_2$ 5.20s.

Table 2. ^{13}C NMR chemical shifts of the 1,4-dihydropyridines **3h–m** and 1,2-dihydropyridines **4h**,**i**

	C2	C3	C4	C5	C6	N–CH_3	N–CH_2	4-CH_3	6-CH_3	CN	$CONH_2$
3h[a]	145.4d	82.1s	30.4s	105.4d	133.4s	38.6q		20.6q	20.6q	123.1s	
3i[a,b]	144.1d	80.7s	30.1s	105.2d	140.9s		53.6t	20.3q	20.3q	121.2s	
3l[b,c]	139.4d	102.4s	26.2s	105.3d	138.3s		52.6t	20.0q	20.0q		169.1s
3m[b,c]	136.1d	104.3s	27.0s	107.6d	135.4s		47.8t	18.3q	24.6q		168.8s
4h[a]	52.3d	80.6s	151.2s	100.2d	153.6s	38.1q		20.6q	20.6q	121.3s	
4i[a,b]	47.3d	80.2s	151.1s	100.9d	152.4s		52.9t	20.1q	20.1q	121.5s	

^{13}C NMR spectra were obtained with Gate decoupled pulse sequence.
[a] $CDCl_3$.
[b] Aromatic carbon signals are in the range 125–140 ppm.
[c] DMSO-d_6.

Table 3. ^{1}H NMR chemical shifts of the adducts **2a–m**

	H2	H4	H5	H6	N–CH_3	N–CH_2		4-CH_3	6-CH_3	$J_{2,6}$	$J_{4,5}$	$J_{5,6}$
						Ha	Hb					
2a[a]	7.08s	3.68d	4.92dd	6.22d	3.07s	—		—	—	—	5.7	7.6
2b[b, c]	7.16d	3.59d	4.90dd	6.23dd	—	4.42s		—	—	1.1	5.3	8.1
2c[a]	[d]	3.98d	4.93dd	6.27d	3.08s	—		—	—	—	5.6	7.7
2d[a, c]	[d]	3.85 br s	4.75m	6.05d	—	4.39s		—	—	—	[e]	[e]
2e[b, c]	7.18d	—	4.49d	6.19dd	—	4.40s		1.30s	—	1.6	—	7.9
2f[b, c]	7.24s	—	4.46d	6.26d	—	4.70s		1.35s	—	—	—	7.9
2g[b, c]	7.02s	3.99d	4.53d	—	—	4.49s		—	1.66s	—	5.4	—
2h[b]	7.15s	—	4.49s		3.15s	—		1.30s	1.90s		—	—
2i[b, c]	7.23s	—	4.56s	—	—	4.70s		1.43s	1.91s	—	—	—
2l[b, c]	7.21s	—	4.37s	—	—	4.59d[f]	4.66d	1.41s	2.65s	—	—	—
2m[b, c]	6.87s	—	4.38s	—		[g]		1.34s	2.73s	—	—	—

[a] D_2O.
[b] D_2O/DMSO-d_6 1:1.
[c] Aromatic proton signals are in the range 7.30–7.50 ppm.
[d] Exchange with D_2O.
[e] Broad signals.
[f] $J_{a,b}$ 17.0 Hz.
[g] Obscured by D_2O signal.

the ^{13}C NMR spectrum to signals in the 85–95 ppm range, with an analogous substituent downfield shift effect of ca. 30–45 ppm in comparison with the chemical shifts of carbon 2 or 6 of the corresponding 1,2- or 1,6-dihydropyridines.

In all cases examined no signals were ever observed in 85–95 ppm range of the ^{13}C NMR spectra.

Therefore, on the whole, the ^{1}H and ^{13}C NMR spectroscopic data clearly demonstrate the 1,4-dihydropyridine structure of the dithionite adducts.

The above findings leave some questions open: (a) how can it be explained the absolute regioselectivity of the dithionite attack, which, in all cases examined, leads to the formation of only 1,4-dihydro-4-pyridine sulfinates; (b) how can the

Table 4. ^{13}C NMR chemical shifts of the adducts **2a**,**c**,**d**,**h**–**m**

	C2	C3	C4	C5	C6	CN	$CONH_2$	$N–CH_2$	$N–CH_3$
2a[a]	149.5d	74.6s	66.7d	100.3d	135.0d	125.8s			43.2q
2b[b, c]	145.4d	72.9s	64.1d	98.0d	129.5d	120.2s		54.1t	
2c[b]	146.0d	96.9s	65.9d	99.4d	133.9d		174.2s		[d]
2d[a, c]	143.9d	99.6s	68.5d	101.2d	134.1d		175.4s	59.5t	
2h[b, c, e]	148.0d	80.5s	62.3s	103.2d	138.1s	123.0s			[d]
2i[b, c, e]	150.3d	82.2s	61.6s	105.1d	139.2s	121.0s		54.5t	
2l[b, c, e]	144.3d	108.1s	64.2s	109.2d	136.5s		168.7s	62.8t	
2m[b, c, e]	142.8d	105.6s	64.6s	107.8d	142.3s		173.5s	49.3t	

^{13}C NMR spectra were obtained with Gated decoupled pulse sequence.
[a] D_2O.
[b] D_2O/ DMSO-d_6 1:1.
[c] Aromatic carbon signals are in the range 128–137 ppm.
[d] Obscured by solvent signal (DMSO-d_6).
[e] The incomplete H/D exchange in 4 and 6-CH_3 gives rise to broad peaks at about 20 ppm.

Table 5. ^1H NMR chemicals shift of the 1,4-dihydropyridines **3a**–**m**

	H2	H4	H5	H6	$N–CH_3$	$N–CH_2$		$4\text{-}CH_3$	$6\text{-}CH_3$	$J_{2,4}$	$J_{2,6}$	$J_{4,5}$	$J_{4,6}$	$J_{5,6}$	$J_{a,b}$	J_{CH_3}, H4
						Ha	Hb									
3a[a]	6. 54dd	3.12 2Hdd	4.66m	5.70m	2.90s					0.6	1.6	3.6	1.6	8.20		
3b[a, b]	6. 41dd	3.08 2H dd	4.63m	5.61m		4.24s				0.8	1.6	3.2	1.6	8.0		
3c[a]	6.83d	3.03 2H dd	4.69m	5.73m	2.88s						1.2	3.2	1.5	8.0		
3d[a, b]	7.11d	3.12 2H dd	4.71m	5.70m		4.24s					1.6	3.4	1.6	8.0		
3e[a, b]	7.18d	3.28m	4. 85dd	5. 80dd		4.36s		1.13d			1.5	5.0		8.0		6.5
3f[b, c]	7.29	3.30m	4. 79dd	6. 05dd		4.77s		1.03d			1.5	5.0		7.7		6.0
3g[b, c]	7.15s	3.21 2Hm	4.57m			4.47s			1. 71m[d]			3.2				
3h[a]	6.48s	3.22m	4.42m		2.98s			1.18d	1.80s			3.2				6.3
3i[a, b]	6.85s	3.27m	4.91d			4.79d	4.83d	1.23d	1.75s			5.1			16.9	
3l[a, b]	7.08s	3.25m	4.52d			4.54d	4.58d	0.98d	1.70s			5.1			16.7	
3m[b, c]	6.66s	3.13m	4.54d			4.69d	4.78d	0.82d	1.92s			5.1			14.34	

[a] $CDCl_3$.
[b] Aromatic proton signals are in the range 7.20–7.60 ppm.
[c] DMSO-d_6.
[d] J_{CH_3},H5 = 2.8.

decomposition of a unique adduct also lead to the formation of 1,2- or 1,6-dihydropyridines, together with the isomeric 1,4-dihydroderivatives.

In our opinion, the absolute regioselectivity of the reaction between dithionite and pyridinium salts seems to suggest the idea of a particular orientation of the two reagents determining the position of attack. A very specific interaction between the reagents through the formation of a rigidly oriented ion pair (Fig. 1), before the nucleophilic dithionite attacks the electrophilic carbon 4, may be supposed.

In this connection, it should be born in mind that, as shown by the X-ray structure of the dithionite anion,[17] the distance between the two nucleophilic centres located on the two oxygen atoms measures 2.868 Å, which is structurally consistent with the occurrence of a strong interaction with both the ring N^+ cation and the C4 electrophilic site (calculated distance ca. 2.87 Å) but not with the analogous pairs C2-ring N^+(1.51 Å) or C6-ring N^+(1.51 Å).

The collapse of the ion pair (Fig. 1) would then give rise to the formation of the C4-sulfinate bound with elimination of SO_2.

An answer to the second question may be given bearing in mind the analogy existing between the decomposition of the dithionite adducts of the pyridinium salts and that of the allyl chlorosulfinates resulting from the reaction of allyl alcohols with thionyl chloride. Indeed, it is well known that two mechanisms, S_Ni[18,19] or S_Ni',[20] may be operative in

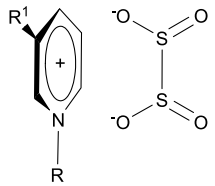

R = Alkyl or aralkyl
R^1 = $CONH_2$ or CN

Figure 1.

Table 6. Calculated heats of formation of all the dihydroderivatives, which could theoretically form in the dithionite reduction of salts **1a–m**; the table also lists the dihydropyridines actually formed and their relative abundances

Sale	1,2-DHP	ΔH_f (Kcal/mol)	1,4-DHP	ΔH_f (Kcal/mol)	1,6-DHP	ΔH_f (Kcal/mol)
1a	**4a** —	64.061	**3a** 92%	60.781	**5a** 8%	63.011
1b	**4b** —	91.137	**3b** 94%	87.770	**5b** 6%	90.466
1c	**4c** —	−5.022	**3c** 82%	−7.914	**5c** 18%	−5.829
1d	**4d** —	21.960	**3d** 95%	19.412	**5d** 5%	21.426
1e	**4e** —	16.026	**3e** 90%	15.973	**5e** 10%	16.345
1f	**4f** —	6.558	**3f** 50%	5.726	**5f** 50%	5.708
1g	**4g** —	17.200	**3g** 100%	14.225	**5g** —	18.560
1h	**4h** 70%	50.947	**3h** 30%	51.309	**5h** —	52.587
1i	**4i** 48%	79.869	**3i** 52%	79.782	**5i** —	80.513
1l	**4l**	9.583	**3l** 100%	8.778	**5l** —	11.634
1m	**4m**	2.031	**3m** 100%	0.432	**5m** —	1.176

such decompositions: the S_Ni mechanism leads to the preservation of the structure by the simple substitution of the sulfinate group with the chlorine atom, while the S_Ni' mechanism involves a structural rearrangement with migration of the double bond and shift of the chlorine atom to the carbon γ from the original position of the sulfinate. In both cases SO_2 is eliminated.

Path S_Ni R-CH=CH–CH_2–OSOCl → R-CH=CH–CH_2–Cl + SO_2

Path S_Ni' R-CH=CH–CH_2–OSOCl → R-CH(Cl)–CH=CH_2 + SO_2

Analogously, the decomposition of the 1,4-dihydropyridine-4-sulfinates may proceed according to the two mechanisms S_Ni or S_Ni'. In the first case, intramolecular hydrogen transfer occurs from the sulfinic SH group to the adjacent carbon atom 4 with SO_2 elimination and preservation of the 1,4-dihydropyridine structure, while the decomposition according to S_Ni' mechanism involves instead an intramolecular hydrogen transfer to atoms 2 or 6 with ensuing shift of the 2,3 or 5,6 double bonds to positions 3,4 or 4,5, respectively, and SO_2 elimination (Scheme 2). Thus, the possibility for the dithionite adducts of decomposing according to these mechanisms, may provide, in our opinion, a convincing explanation for the formation of all the three possible dihydroderivatives starting from an unique intermediate adduct. The occurrence of the decomposition mechanism S_Ni', which leads to 1,2- or 1,6-dihydropyridines, besides mechanism S_Ni, which affords 1,4-dihydropyridines, depends on the respective thermodynamic stability of the dihydroderivatives.

As may be seen from Table 6, in which the formation heats of dihydropyridines, calculated according to the AM1 molecular orbital methods,[8a,b] are summarized, 1,2- or 1,6-dihydropyridines are produced when their relative heats of formation are lower or very close to those of the corresponding 1,4-dihydro derivatives.

3. Experimental

3.1. Materials and methods

Chemical reagents and solvents were purchased from Aldrich Chemical Co. and were of analytical grade. Melting points were determined with a Tottoli apparatus and are uncorrected. IR spectra were registered with a Perkin Elmer mod. 281 spectrophotometer. ^1H and ^{13}C NMR were taken with a Bruker AVANCE 400 spectrometer, data were elaborated by using the WINNMR Bruker Daltonik GmbH, version 6.1.0.0 software. Chemical shifts are reported as ppm (δ) from TMS as internal standard when the solvent was DMSO-d_6 or $CDCl_3$ and from the D_2O signals (δ = 4.78 ppm) for D_2O solutions. Coupling constants are given in Hz. The HPLC analyses were performed with a Perkin Elmer Series 200 liquid chromatograph equipped with a Perkin Elmer series 200 diode array detector, HPLC data were elaborated by using TURBOCHROM NAVIGATOR, version 6.1.2.0.1 software. Preparative HPLC were performed on a Perkin Elmer series 3 apparatus equipped with a spectophotometric UV–vis Perkin Elmer LC55B detector and an analogic HP3390A integrator.

The column used were HPLC Lab Service Analytic Hypersil 5-NH_2 250/4.6 mm (5 μm) for the analytical determinations and 250/10 mm (5 μm) for the preparative determinations.

Formation enthalpies were calculated by AM1 molecular orbital methods[8a,b] making use of the Hyperchem version 7.0 software. Structure were minimised by using a Fletcher-Reeves algorithm with a convergence limit of 0.1 kcal/mol.

3.2. Pyridinium salts

3-Cyano-1-methylpyridinium iodide **1a**,[21] 1-benzyl-3-cyanopyridinium bromide **1b**,[22] 3-carbamoyl-1-methylpyridinium iodide **1c**,[23] 1-benzyl-3-carbamoylpyridinium bromide **1d**,[24] 1-benzyl-3-carbamoyl-4-metylpyridinium bromide **1e**,[25] 3-carbamoyl-1-(2,6-dichlorobenzyl)-4-methylpyridinium bromide **1f**,[7] 1-benzyl-3-carbamoyl-6-metylpyridinium bromide **1g**[26] and 3-carbamoyl-1-(2,6-dichlorobenzyl)-4,6-dimethylpyridinium bromide **1m**,[7] were prepared according to literature procedures and displayed the expected NMR properties.

3.3. General procedures for the preparation of pyridinium salts 1h–l

To a solution of 3-cyano-4,6-dimethylpyridine[27] (10.0 mmol) or 3-carbamoyl-4,6-dimetylpyridine[27] (10.0 mmol) in 20 ml of warm acetonitrile, 14.0 mmol of methyl iodide or 10.0 mmol of benzyl bromide was added and the mixture was refluxed for 12 h. To the cold solution,

Et_2O (50 ml) was then added: the precipitate was collected, washed with Et_2O and recrystallised from methanol.

3.3.1. 3-Cyano-1,4,6-trimethylpyridinium iodide 1h. Yield 70%, mp 228–9 °C; IR (nujol) cm^{-1}: 3175, 2245, 1650; ^1H NMR (DMSO-d_6), δ: 2.71 (3H, s, 4-CH_3), 3.31 (3H, s, 6-CH_3), 4.20 (3H, s, N-CH_3), 8.19 (1H, s, H5), 9.60 (1H, s, H2). Anal. Calcd for C_9 H_{11} N_2 I: C, 39.44; H, 4.05; N, 10.22. Found: C, 39.75; H, 3.86; N, 10.01.

3.3.2. 1-Benzyl-3-cyano-4,6-dimethylpyridinium bromide 1i. Yield 75%; mp 252–4 °C; IR (nujol) cm^{-1}: 3180, 2245, 1650; ^1H NMR (DMSO-d_6) δ: 2.74 (3H, s, 4-CH_3), 3.32 (3H, s, 6-CH_3), 5.92 (2H, s, N-CH_2), 7.30-7.45 (5H, m, Ar), 8.25 (1H, s, H5), 9.85 (1H, s, H2). Anal. Calcd for C_{15} H_{15} N_2 Br: C, 59.42; H, 4.99; N, 9.24. Found: C, 59.69; H, 5.10; N, 8.97.

3.3.3. 1-Benzyl-3-carbamoyl-4,6-dimethylpyridinium bromide 1l. Yield 95%; mp 225–7 °C; IR (nujol) cm^{-1}: 3200, 3030, 1690; ^1H NMR (DMSO-d_6) δ: 2.63 (3H, s, 4-CH_3), 2.67 (3H, s, 6-CH_3), 5.92 (2H, s, N–CH_2), 7.32-7.45 (5H, m, Ar), 8.43 (1H, s, H5), 9.30 (1H, s, H2). Anal. Calcd for C_{15} H_{17} N_2 O Br: C, 56.09; H, 5.33; N, 8.72. Found: C, 55.87; H, 5.65; N, 8.55.

3.4. General procedure for the dithionite reduction of pyridinium salts 1a–g,m

To a stirred solution of $NaHCO_3$ (2.5 mmol) and $Na_2S_2O_4$ (2.5 mmol) in H_2O (30 ml), chloroform (30 ml) and then slowly 0.5 mmol of the pyridinium salt were added at 4–5 °C and under argon flow. After 3 h, the organic phase was separated from the aqueous one, which was repeatedly extracted with chloroform (4×20 ml). The combined chloroform extracts were dried over anhydrous Na_2SO_4 and analyzed by ^1H NMR spectroscopy.

The spectral parameters listed in Tables 1 and 5, compared with the ^1H NMR data reported in literature, allowed to identify the dihydropyridine or the dihydropyridine mixture formed in every reduction run and to determine their relative abundances (Table 6).

The pyridinium salts **1a–g,m** were reduced according to the general procedure described above giving rise to the dihydropyridines listed below in the relative abundances near indicated:

Salt **1a** gave the 1,4-dihydropyridine **3a**[12] 92% and the 1,6-dihydropyridine **5a**[12] 8%. Salt **1b** afforded the 1,4-dihydropyridine **3b**[22] 94% and the 1,6-dihydropyridine **5b**[28] 6%. Salt **1c** yielded the 1,4-dihydropyridine **3c**[13] 82% and the 1,6-dihydropyridine **5c**[29] 18%. Salt **1d** gave the 1,4-dihydropyridine **3d**[25] 95% and the 1,6-dihydropyridine **5d**[25] 5%. Salt **1e** afforded the 1,4-dihydropyridine **3e**[30] 90% and the 1,6-dihydropyridine **5e**[30] 10%. Salt **1f** yielded the 1,4-dihydropyridine **3f**[7] 50% and the 1,6-dihydropyridine **5f**[7] 50%. Salt **1g** gave as unique product the 1,4-dihydropyridine **3g**.[26] Salt **1m** afforded as unique product the 1,4-dihydropyridine **3m**.[7]

3.5. Dithionite reduction of pyridinium salts 1h–l, identification of the dihydro derivatives obtained and determination of their relative abundances

3.5.1. Reduction of salt 1h. To a solution of $NaHCO_3$ (400 mg) and $Na_2S_2O_4$ (300 mg) in 40 ml of H_2O, 50 ml of $CHCl_3$ were added at 4–5 °C under argon flow and strong stirring, followed by addition of 150 mg of salt **1h**. After 3 h the chloroform layer was separated and the aqueous phase repeatedly extracted with $CHCl_3$ (4×20 ml). The combined organic extracts, after drying over Na_2SO_4, were brought to dryness and the residue was submitted to HPLC analysis employing a 90:10 hexane/CH_2Cl_2+2% MeOH mixture (flow 1 ml/min): the elution profile showed two major peaks. A preparative HPLC carried out on 20 mg of residue, adopting the same eluent (flow 5 ml/min), led to the separation of two fractions having retention time of 7.5 and 8.9 min, respectively, the purity, of which was determined as better than 97%. Both fractions were examined by ^1H and ^{13}C NMR and unambiguously identified. The first fraction (t_R=7–5 min) consisted of 3-cyano-1,4,6-trimethyl-1,2-dihydropyridine **4h** (Tables 1 and 2), while the second fraction (t_R=8.9 min) was identified as 3-cyano-1,4,6-trimethyl-1,4-dihydropyridine **3h** (Tables 5 and 2).

Anal. Calcd for C_9 H_{12} N_2: C, 72.94; H, 8.16; N, 18.90.

Compound **3h**. Found: C, 72.73; H, 7.87; N, 18.68.

Compound **4h**. Found: C, 73.41; H, 7.92; N, 18.53.

The relative abundance of dihydropyridines **3h** and **4h**, determined by ^1H NMR analysis of the crude $CHCl_3$ extract obtained directly from the reduction, resulted to be 30% and 70%, respectively (Table 6).

3.5.2. Reduction of salt 1i. From the reduction of **1i** carried out in the same conditions described above for **1h**, a crude residue was obtained, which, submitted to HPLC analysis (eluent: 90:10 hexane/CH_2Cl_2+2% MeOH, flow 1 ml/min) gave an elution profile characterized from two major peaks. A preparative HPLC carried out on 25 mg of residue using the same elution system (flow 5 ml/min), led to the separation of two fractions having retention times of 6.5 and 7.6 min, respectively, with an analytically controlled purity degree higher than 97%. Both fractions were examined by ^1H and ^{13}C NMR. The first fraction (t_R= 6.5 min) consisted of 1-benzyl-3-cyano-4,6-dimethyl-1,2-dihydropyridine **4i** (Tables 1 and 2), while the second fraction (t_R=7.6 min) was identified as the 1-benzyl-3-cyano-4,6-dimethyl-1,4-dihydropyridine **3i** (Tables 5 and 2).

Anal. Calcd for C_{15} H_{16} N_2: C, 80.32; H, 7.19; N, 12.49.

Compound **3i**. Found: C, 80.63; H, 6.97; N, 12.25.

Compound **4i**. Found: C, 80.06; H, 7.02; N, 12.18.

The relative abundance of dihydropyridines **3i** and **4i**, determined by ^1H NMR analysis of the crude $CHCl_3$ extract obtained directly from the reduction, resulted to be 30% and 48%, respectively (Table 6).

3.5.3. Reduction of salf 1l. From the reduction of salt **1l** carried out according the procedure described above for **1a**, a chloroform extract was obtained, the ^{1}H NMR analysis of which revealed the presence of a unique product, which was unambiguously identified, by ^{1}H and ^{13}C NMR spectroscopy, as 1-benzyl-3-carbamoyl-4,6-dimethyl-1,4-dihydropyridine **3l** (Tables 2 and 5).

Anal. Calcd for C_{15} H_{18} N_2 O: C, 74.35; H, 7.49; N, 11.56. Found: C, 74.48; H, 7.27; N, 11.34.

3.6. ^{1}H and ^{13}C NMR analysis of the dithionite adducts 2a–m

In a typical procedure for the preparation of an adduct sample for NMR examination, a solution of $Na_2S_2O_4$ (0.11 mmol) in 0.25 ml of 2 M NaOD (in D_2O) or 2 M Na_2CO_3 (in D_2O) was prepared in a NMR tube and subsequently cooled down to −20 °C. Over this frozen solution, kept at −20 °C, was then stratified the pyridinium salt solution (0.06 mmol of salt in 0.25 ml of D_2O or 0.25 ml of DMSO-d_6), which was afterwords frozen. The tube was finally sealed in vacuo always keeping the temperature at −20 °C. At the moment of performing the NMR analysis, the tube temperature was increased to 20 °C in order to cause the thawing of the solutions and their mixing.

The ^{1}H and ^{13}C NMR parameters of adducts **2** are summarized in Tables 3 and 4.

It was impossible to record ^{13}C NMR spectra on adducts **2e**–**g**, because of insufficient concentrations achievable both in NaOD and Na_2CO_3 solutions. Indeed, pyridinium salts **1e**–**g** displayed extreme reactivity towards aqueous NaOH, giving rise to mixtures of dihydropyridines and pyridones.[31] On the other hand, adducts **2e**–**g** rapidly decomposed, in aqueous Na_2CO_3, yielding 1,4-dihydropyridine and 1,4- and 1,6-dihydropyridine mixtures.

Acknowledgements

This work was financially supported by funds from 'Ministero dell'Istruzione, dell'Università e della Ricerca': 'Progetti di Ricerca di Interesse Nazionale'.

References and notes

1. Yarmolinsky, M. B.; Colowich, S. P. *Biochim. Biophys. Acta* **1956**, *20*, 177–189.
2. Sutter-Kostic, K.; Karrer, P. *Helv. Chim. Acta* **1956**, *39*, 677–681.
3. Wallenfels, K.; Schüly, H. *Justus Liebig Ann. Chem.* **1959**, *621*, 178–187.
4. Kosower, E. M.; Bauer, S. *J. Am. Chem. Soc.* **1960**, *82*, 2191–2194.
5. Caughey, W. S.; Shellenberg, K. *J. Org. Chem.* **1966**, *31*, 1978–1982.
6. Biellmann, J. F.; Callot, H. J. *Bull. Soc. Chim. Fr.* **1968**, 1154–1159.
7. Biellmann, J. F.; Callot, H. J. *Bull. Soc. Chim. Fr.* **1968**, 1159–1165.
8. (a) Dewar, M. J. S.; Stork, D. M. *J. Am. Chem. Soc.* **1985**, *107*, 3898–3902. (b) Dewar, M. J. S.; Zoebish, E. G.; Healy, E. I.; Stewart, J. J. P. *J. Am. Chem. Soc.* **1985**, *107*, 3902–3909.
9. Pop, E.; Brewster, M. E.; Bodor, N.; Huang, M. J. *J. Mol. Struct. (Theochem)* **1993**, *283*, 27–32.
10. Carelli, V.; Liberatore, F.; Scipione, L.; Musio, R.; Sciacovelli, O. *Tetrahedron Lett.* **2000**, *41*, 1235.
11. Damij, S. W. H.; Fyfe, C. A.; Smith, D.; Sharom, F. J. *J. Org. Chem.* **1979**, *44*, 1761–1765.
12. Butt, G. L.; Deady, L. W. *J. Heterocycl. Chem.* **1984**, *21*, 981–984.
13. Bossaerts, J. D.; Dommisse, R. A.; Alderweireldt, F. C.; Gerlings, P. *J. Chem. Res. (miniprint)* **1987**, *9*, 2360–2384.
14. Micheletti-Moracci, F.; Liberatore, F.; Carelli, V.; Arnone, A.; Carelli, I.; Cardinali, M. E. *J. Org. Chem.* **1978**, *43*, 3420–3422.
15. Breitmeir, E.; Bauer, G. ^{13}C NMR spectroscopie.; Georg Thieme: Struttgart, 1977; pp 52–54.
16. Schneider, H. J.; Hoppen, V. *J. Org. Chem.* **1978**, *43*, 3866–3873.
17. Dunitz, J. D. *Acta Crystallogr.* **1956**, *9*, 579–586.
18. Cowdrey, W. A.; Hughes, E. D.; Ingold, C. K.; Masterman, S.; Scott, A. D. *J. Chem. Soc.* **1937**, 1252–1271.
19. Sharman, S. H.; Caserio, F. F.; Nystrom, R. E.; Leak, J. C.; Young, W. G. *J. Am. Chem. Soc.* **1958**, *80*, 5965–5971.
20. Roberts, J. D.; Young, W. G.; Winstein, S. *J. Am. Chem. Soc.* **1942**, *64*, 2157–2164.
21. Schenker, K.; Druey, J. *Helv. Chim. Acta* **1959**, *42*, 1960–1970.
22. Brown, A.; Fisher, M. F. *J. Am. Chem. Soc.* **1976**, *98*, 5682–5688.
23. Kosower, E. M.; Klinedinst, P. E. *J. Am. Chem. Soc.* **1956**, *78*, 3493–3497.
24. Karrer, P.; Stare, F. J. *Helv. Chim. Acta* **1937**, *20*, 418–423.
25. Lovesey, A. C.; Ross, W. C. J. *J. Chem. Soc. (B)* **1969**, 192–195.
26. Takeda, J.; Ohta, S.; Hirobe, M. *Chem. Pharm. Bull.* **1987**, *35*, 2661–2667.
27. Wallenfels, K.; Schüly, H. *Justus Liebig Ann. Chem.* **1959**, *621*, 215–221.
28. Carelli, V.; Liberatore, F.; Tortorella, S.; Micheletti-Moracci, F. *Gazz. Chim. Ital.* **1983**, *113*, 569–571.
29. Acheson, R. M.; Paglietti, G. *J. Chem. Soc. Perkin Trans. 1* **1976**, 45–48.
30. Anne, A.; Moiroux, J. *Can. J. Chem.* **1995**, *73*, 531–538.
31. Micheletti-Moracci, F.; Casini, A.; Liberatore, F.; Carelli, V. *Tetrahedron Lett.* **1976**, *41*, 3723–3724.

Available online at www.sciencedirect.com
SCIENCE DIRECT
Tetrahedron
ELSEVIER
Tetrahedron 61 (2005) 10338–10348

Microwave-assisted organic synthesis: scale-up of palladium-catalyzed aminations using single-mode and multi-mode microwave equipment

Kristof T. J. Loones,[a] Bert U. W. Maes,[a,*] Geert Rombouts,[a] Steven Hostyn[a] and Gaston Diels[b]

[a]*Organic Synthesis, Department of Chemistry, University of Antwerp, Groenenborgerlaan 171, B-2020 Antwerp, Belgium*
[b]*Janssen Pharmaceutica, Johnson and Johnson Pharmaceutical Research & Development, Turnhoutseweg 30, B-2340 Beerse, Belgium*

Received 23 May 2005; revised 25 July 2005; accepted 27 July 2005

Available online 8 September 2005

Dedicated to the memory of Nancy Verhaert

Abstract—Batch wise scale-up of Buchwald–Hartwig aminations under microwave irradiation has been investigated for the first time. Multi-mode (microSYNTH and MARS) (several vessels irradiated in parallel per batch) as well as single-mode (Discover) (one vessel irradiated per batch) platforms can be successfully used for this purpose with trifluoromethylbenzene (benzotrifluoride: BTF) as amination solvent. The obtained yields indicate a direct scalability in BTF for all the studied aminations. The Voyager equipment (based on a Discover platform) is the most convenient system since it allows an automatic continuous batch wise production without the necessity to manually load and unload reaction vessels.

1. Introduction

Microwave-assisted organic synthesis (MAOS) is a rapidly growing subfield within the area of organic chemistry.[1] Since the first reports in the literature on MAOS in the mid eighties the number of annually published articles using microwave heating has increased continuously.[2] In the early days domestic microwaves were used, often giving only a poor reproducibility. Moreover, accidents were common due to the lack of control. This lack of control and reproducibility is partly responsible for the initial slow take up of microwave heating in organic syntheses. The introduction of dedicated equipment by Prolabo (closed down already), CEM, Milestone, Biotage (formerly Personal Chemistry), Plazmatronika and more recently by Anton Paar allowing the on-line monitoring of temperature, power and pressure had a large impact on the further development of this relatively young research field.[3] The latest trend is to use only microwave equipment designed for organic synthesis and to abandon scientific results for publication obtained using domestic microwaves. The organisation of annual workshops and conferences focusing on MAOS such as the 'MAOS meeting' in Graz and the 'International Microwaves in Chemistry Conference' in Orlando clearly support that microwave-assisted organic synthesis has now reached a mature scientific level. The growing interest, both from industry and academia, for such events indicates that the real impact of microwaves on the field of organic syntheses still has to come! Most of the chemistry hitherto performed in a dedicated microwave system has been executed on a small scale only. Single-mode microwaves are standardly used for this purpose, typically allowing the production of several hundred milligram quantities per run. One of the major current issues is the question whether microwave heating could be used to scale-up these reactions to gram and kilogram scale, preferentially without the requirement to reoptimize reaction parameters tuned for the small scale runs. For the scale-up purpose historically two different approaches, batch[4] and continuous-flow,[5] have been followed taking into account the physical limitations inherent to microwave equipment construction.[1h] Large batch reactors have been developed for a multi-mode or single-mode microwave platform. For these the most important drawback is the limited penetration depth of microwave irradiation. Alternatively, multi-mode equipment supplied with a rotor with several smaller vessels has been launched, which allows the use of a large total volume in one microwave run without the penetration depth issue. Besides batch approaches

Keywords: Palladium; Homogeneous catalysis; Buchwald–Hartwig amination; Aryl chlorides; Multi-mode cavity; Single-mode cavity; Microwave irradiation.
* Corresponding author. Tel.: +32 3 265 32 05; fax: +32 3 265 32 33; e-mail: bert.maes@ua.ac.be

0040–4020/$ - see front matter © 2005 Elsevier Ltd. All rights reserved.
doi:10.1016/j.tet.2005.07.105

continuous-flow systems based on single-mode and multi-mode cavities have been used as well. The major limitation of these continuous microwave reactors is that they are unsuitable for heterogeneous mixtures and viscous liquids. Interestingly, reports on scale-up using dedicated microwave equipment in peer reviewed journals is hitherto rather limited. In particular more complex chemistry, such as transition metal catalyzed reactions, is hardly studied.[6] Based on the limited availability of more complex examples and the background of our research group, we decided to investigate the scale-up of Buchwald–Hartwig aminations under microwave irradiation using dedicated multi-mode (MicroSYNTH, MARS) and single-mode (Voyager) batch reactors.[7,8]

2. Description of microwave equipment used

2.1. Voyager[3]

The Voyager system (stop/flow system) of CEM is based on the Discover single-mode platform equipped with an 80 mL glass vessel (borosilicate), a peristaltic pump and two valves (Fig. 1). The system has a continuous unpulsed microwave output ranging from 0 to 300 W. The temperature in the vessel is controlled internally by a fiber optic probe. On-line pressure monitoring is also provided. The Voyager microwave is designed to automatically fill the 80 mL vessel with reagents (two stock solutions), seal the vessel, perform a microwave experiment, release the vessel, remove the reaction mixture from the vessel and subsequently clean it with solvent (even under microwave irradiation if desired) (Fig. 2). The liquid of the cleaning step can be collected separately via a waste line or can be added to the product if desired. We always chose the latter. The contents of the closed vessel can be released after a microwave experiment at a pre-programmed temperature and pressure (in our experiments we used 95 °C and 10 psi as vessel release parameters), which allows a serious increase of the throughput (number of cycles in a given timeframe) of the system. Cooling to the set temperature value is done using a propelled air flow. When the Voyager platform is based on an older type of Discover microwave an enhanced stirring device is standardly used. This device fits in the small cavity located at the bottom of the microwave cavity (on top of the IR sensor). It consists of a magnet at both ends of the bar, which couples with the magnetic stirring plate located at the bottom of the Discover

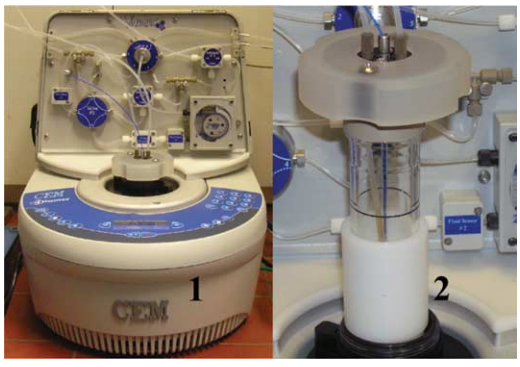

Figure 1. Voyager platform (**1**) and 80 mL glass vessel (**2**).

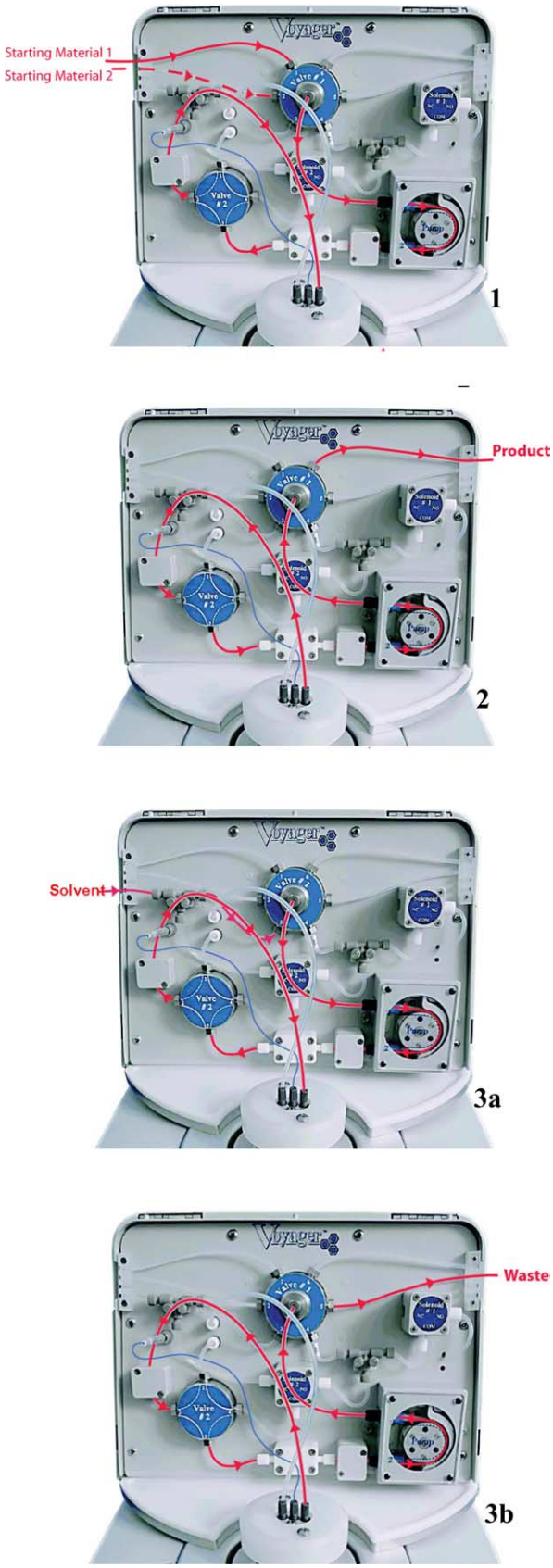

Figure 2. Add step (**1**), remove step (**2**) and clean vessel step (**3**) ((**3a**) fill with solvent, (**3b**) remove solvent to waste).

unit. Two more centrally located magnets couple with the stirring bar in the reaction vessel. The enhanced stirring device gives access to a microwave unit with a more powerful stirring capacity. All our experiments were done using this special device. Recent Discover units are equipped with electromagnetic stirring plates that deliver more stirring power in comparison with the older type of Discover unit. Therefore the enhanced stirring device is not used anymore in this newer unit.

2.2. MicroSYNTH[3]

The MicroSYNTH system of Milestone is a multi-mode platform equipped with a magnetic stirring plate and a rotor that allows parallel processing of several vessels per batch (Fig. 3). We used the high-pressure vessel assembly type based on a rotor with 10 vessel positions (teflon (TFM) inserts) (vessel volume 100 mL, max pressure 1450 psi, max temperature 300 °C). The system has two magnetrons that together deliver a maximum power output of 1000 W. The power supply of the magnetron is pulsed. Temperature is controlled internally by fiber optic probe in one control reference vessel. On-line pressure monitoring of the reference vessel is also provided. All rotor segments are protected by a reclosing (vent and reseal) relief valve mechanism. Additionally, the system is equipped with a solvent sensor detector safety feature. Cooling down of the rotor segments to room temperature is done by an air flow provided by the exhaust fan.

2.3. MARS[3]

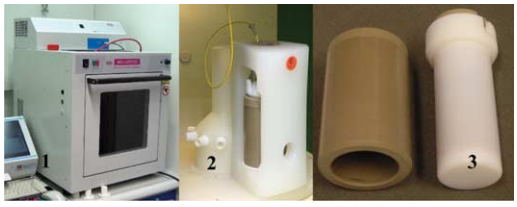

Figure 3. MicroSYNTH platform (**1**), control vessel rotor segment (**2**), high-pressure sleeve, insert and cap of a standard vessel assembly (**3**).

The MARS system of CEM is a multi-mode platform equipped with a magnetic stirring plate and a rotor that allows the parallel processing of several vessels per batch (Fig. 4). We used the HP-500 (teflon (TFA) insert) (vessel volume 80 mL, max pressure 350 psi, max temperature 210 °C) and Greenchem (glass (borosilicate) insert) (vessel volume 80 mL, max pressure 200 psi, max temperature 200 °C) vessel assembly types both based on a fourteen positions rotor. The system delivers a continuous power output between 0 and 1200 W. Temperature is controlled internally by fiber optic probe in one control reference vessel. On-line pressure monitoring of the reference vessel is also provided. All rotor segments are protected by a vent nut that contains a rupture membrane. Additionally, the system is equipped with a solvent sensor detector safety feature. Cooling down of the rotor segments to room temperature is done by an air flow provided by the exhaust fan.

3. Results

Recently our laboratory reported the rapid palladium-catalyzed amination of aryl chlorides under temperature controlled microwave heating using a CEM Discover single-mode microwave unit.[7c,71] In a reaction time of only 10 min using a relatively low catalyst loading (1 mol%) complete conversion of starting material and a good yield could be achieved for the coupling of both electron rich and electron neutral aryl chlorides with all types of amines (anilines, primary and secondary aliphatic amines). For the coupling of anilines and secondary cyclic aliphatic amines palladium precatalyst based on $Pd(OAc)_2$ and 2-(dicyclohexylphosphanyl)biphenyl[9] (DCPB) ligand worked smoothly while for the amination reactions using acyclic secondary and primary aliphatic amines $Pd(OAc)_2$ in combination with 2-(di-*t*-butylphospanyl)biphenyl[9] (DTPB) ligand was found to be optimal. All the reported examples were performed on a 1 mmol scale of aryl chloride allowing the production of hundred milligram quantities of *N*-substituted anilines.

First we investigated the direct scalability going from a 10 mL vessel to an 80 mL vessel in a Discover apparatus. We selected the coupling of electron rich 4-chloroanisole with morpholine, which we previously performed on a 1 mmol scale as a test case.[71] Unfortunately, running this reaction on a 20-fold scale (20 mmol 4-chloroanisole, 24 mmol morpholine, 28 mmol NaO*t*–Bu, 20 mL toluene) using the same microwave program (initial set power 300 W, 150 °C, 10 min (total reaction time including ramp time to set temperature)) as for the small scale reaction was unsuccessful. The reaction mixture heated up relatively slowly and the obtained final temperature after 10 min of microwave irradiation was only 128 °C, which is substantially lower than the desired set temperature of 150 °C. Consequently, an incomplete conversion of starting material and an isolated yield of 4-(4-methoxyphenyl)-morpholine of only 38% was obtained (Table 1). In contrast,

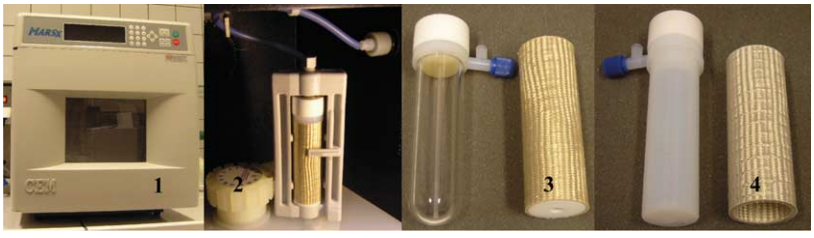

Figure 4. MARS platform (**1**), control vessel rotor segment (**2**), Greenchem insert, cap and sleeve of a standard vessel assembly (**3**) and HP-500 insert, cap and sleeve of a standard vessel assembly (**4**).

Table 1. Scale-up of the Pd-catalyzed amination of 4-chloroanisole with morpholine

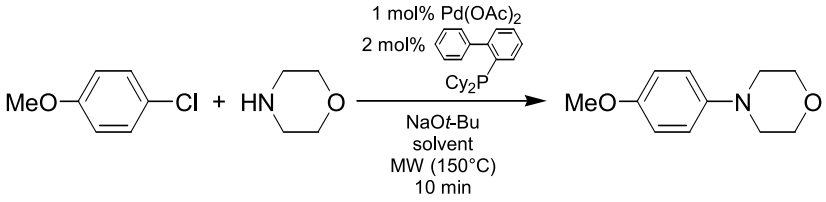

Microwave	4-Chloroanisole (mmol)	Vessel		Initial set power (W)	Solvent	Yield (%)[a]
		Volume (mL)	Type			
Discover	1	10	Glass	300	Toluene	76
Discover	20	80	Glass	300	Toluene	38[b]
Mars	20	80	Greenchem	1200	Toluene	78
Discover	1	10	Glass	300	BTF	78
Discover	20	80	Glass	300	BTF	85
Voyager	3×20	80	Glass	300	BTF	78[c]
microSYNTH	6×20	100	High-Pressure	600	BTF	77[c]
Mars	6×20	80	Greenchem	600	BTF	80[c]

[a] 4-Chloroanisole (y mmol), morpholine (1.2y mmol), NaOt-Bu (1.4y mmol), toluene or BTF (y mL).
[b] 150 °C could not be reached in 10 min.
[c] Average yield.

for the 1 mmol scale experiment in a 10 mL vessel the set temperature was reached in 2 min allowing a full conversion of starting material in 10 min.[71] Although polar reagents are present in the reaction mixture we realized the poor coupling characteristic of the solvent (tan δ toluene = 0.04) is responsible for the failure of the scale-up experiment.[10]

Due to this failure we became interested to investigate whether there is a substantial difference between single and multi-mode microwaves when solvents with low tan δ are used. Therefore, we performed power/time experiments (temperature is slave of the power) using 20 mL of pure toluene at full power in several commercial available microwave platforms (Discover, max power 300 W)[11] (MARS, max power 1200 W)[11] (microSYNTH, max power 1000 W)[11] (Fig. 5). The vessels used were either from glass (borosilicate) or teflon (PTFE or TFM). In all

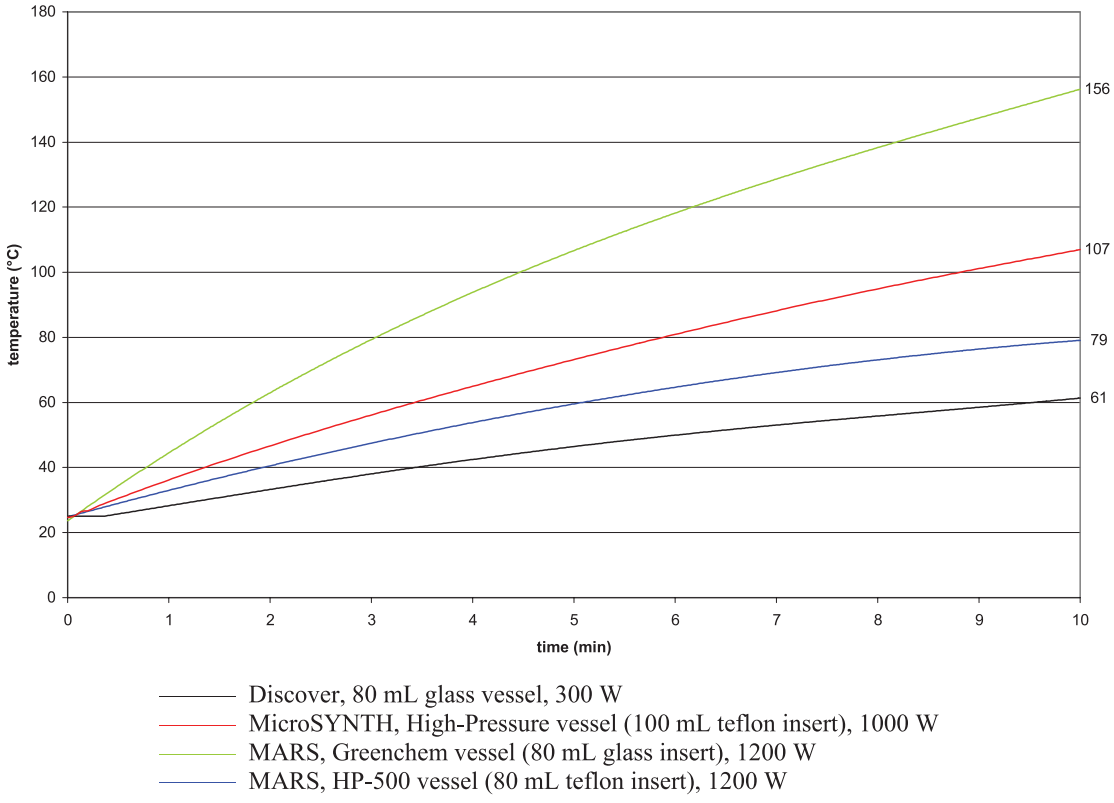

Figure 5. Heating profile of 20 mL of toluene in several commercial available microwave systems, irradiated in a power/time experiment at a constant maximum power output for 10 min.

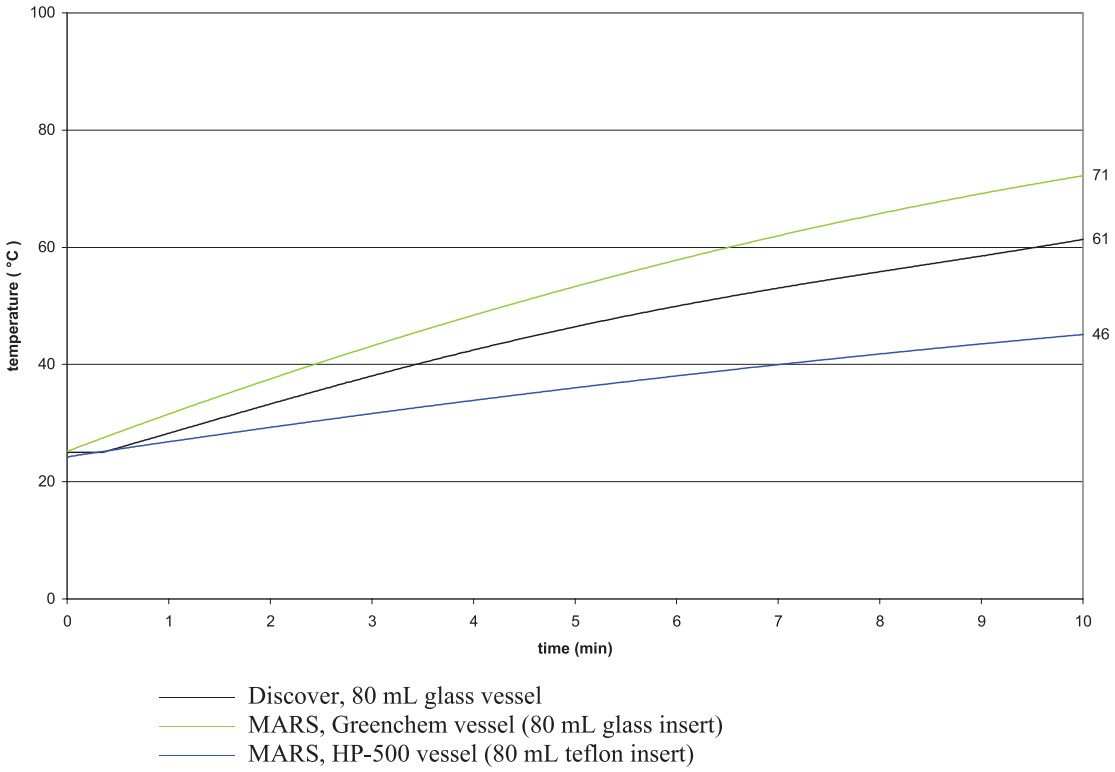

Figure 6. Heating profile of 20 mL of toluene in several commercial available microwave systems, irradiated in a power/time experiment at a constant power of 300 W for 10 min.

cases, the temperature was measured internally using a fiber optic probe. Interestingly, 20 mL of toluene could be heated to 156 °C in 10 min in a Greenchem vessel in the MARS platform. In contrast, 20 mL of toluene could only be heated to 61 °C in a similar 80 mL glass vessel in the Discover system. Important to mention is that even if the same

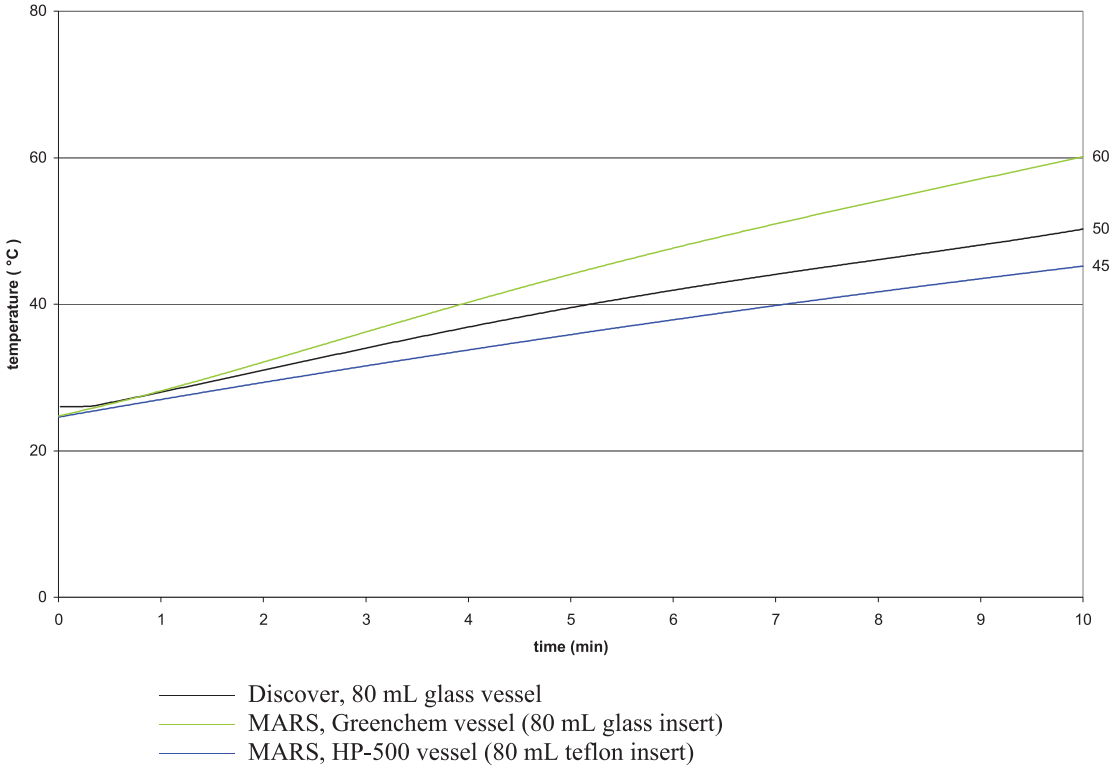

Figure 7. Heating profile of 20 mL of tetrachloromethane in several commercial available microwave systems, irradiated in a power/time experiment at a constant power of 300 W for 10 min.

constant power output is used in all microwave systems the final temperature of toluene is not the same (Fig. 6).[11] Heating the same volume of solvent in the three selected microwaves allows a direct comparison of the heating efficiency of these machines for that specific volume by simply comparing the obtained final temperatures of the heated solvent.[11] However, one should be very careful since the differences observed are also related to the specific material used for the vessel construction. This can be clearly deduced from a comparison of the heating profiles of toluene in the Greenchem and HP-500 vessel in the MARS at the same constant power (Fig. 6).[11] A simple heating experiment with 20 mL of microwave transparent tetrachloromethane clearly showed that the vessel material itself (sleeve and/or insert) is not completely microwave transparent and is at least partially responsible for the heating up of the irradiated solvent via conduction (Fig. 7).[12] This process becomes more and more important the more microwave transparent the irradiated solvent is. Remarkably, toluene and tetrachloromethane can not be heated in the high-pressure vessel of the microSYNTH at a constant power of 300 W since the system shuts down after a few minutes. The heating profiles of pure toluene confirm that our failure with the scale-up of the amination of 4-chloroanisole with morpholine is related to the use of toluene as solvent in that specific microwave platform. Importantly, the heating profiles also indicate that in the Greenchem vessel of the MARS multi-mode microwave, scale-up of the desired amination might be possible. Indeed, performing the amination on a 20 mmol scale of substrate at 150 °C using an initial set power of 1200 W and for a total reaction time of 10 min gave a complete conversion of starting material and an isolate yield of 4-(4-methoxyphenyl)morpholine of 78% (Table 1). This is similar to the result obtained on a 1 mmol scale in the 10 mL glass vessel of the Discover (76%). Although we were able to successfully perform scale-up in one glass vessel we realized that the further scale-up making use of the possibility to process multiple Greenchem vessels (rotor) in one microwave run would be problematic using toluene as solvent. Indeed, Figure 8 clearly shows that the final temperature of toluene in power/time experiments performed at 1200 W for 10 min drops each time a rotor segment that contains a glass vessel with 20 mL of toluene is added. This is obvious since the total volume to be heated increases each time a rotor segment is added. Therefore we looked for an alternative solvent for palladium-catalyzed aminations to allow scale-up in single-mode as well as multi-mode platforms. Possible candidates were screened by performing power/time experiments with 20 mL of solvent at 300 W for 10 min in each microwave system. 300 W was chosen as set power since it is the maximum power output of the Discover. First we looked at tetrahydrofurane (tan $\delta = 0.047$),[10] which has already been used frequently as solvent in Buchwald–Hartwig aminations (Fig. 9).[8f,8j] In comparison with toluene at the same power (Fig. 6), tetrahydrofurane significantly increased the obtained final temperatures in all microwave platforms (Fig. 9) although the tan δ is only slightly higher than that of toluene. Even though the heating profile of tetrahydrofurane is certainly a lot better, the solvent reaches a final temperature of only 94 °C upon heating at maximum power output for 10 min in the Discover. Therefore we looked for other alternatives. Inspired by a lecture where

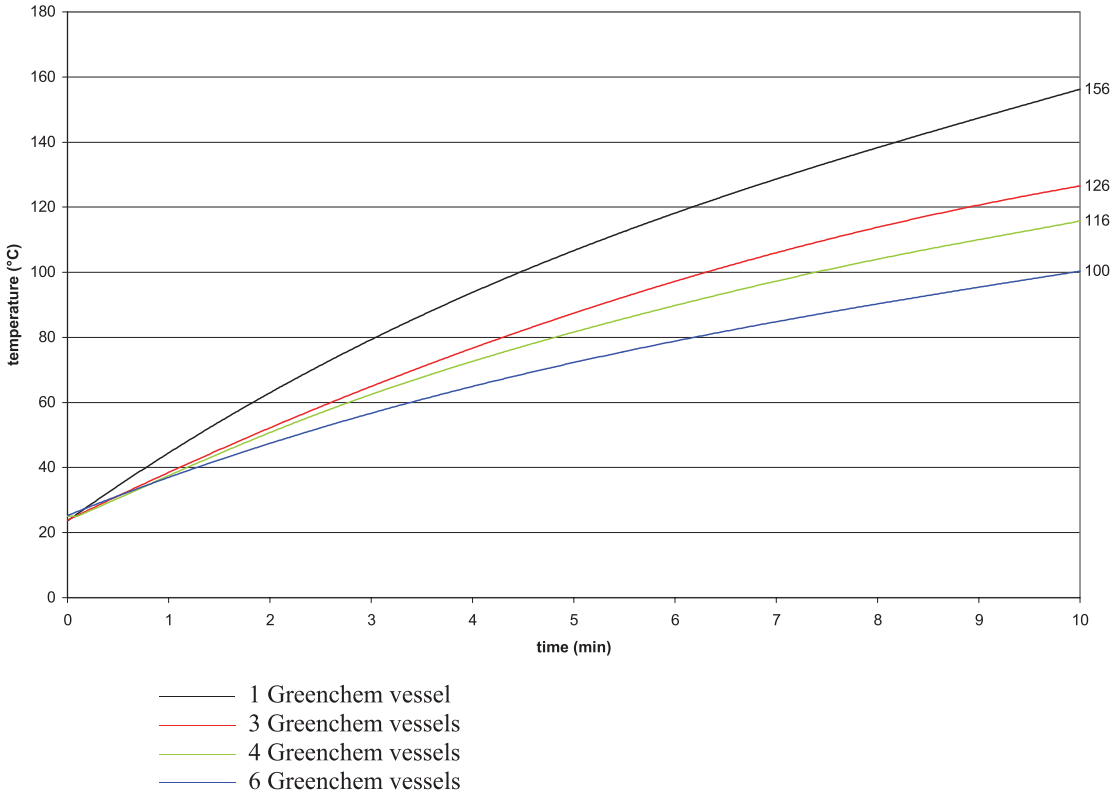

Figure 8. Heating profile of 1, 3, 4 and 6 Greenchem vessels, each filled with 20 mL of toluene, irradiated in the MARS system for 10 min in a power/time experiment at a constant power of 1200 W.

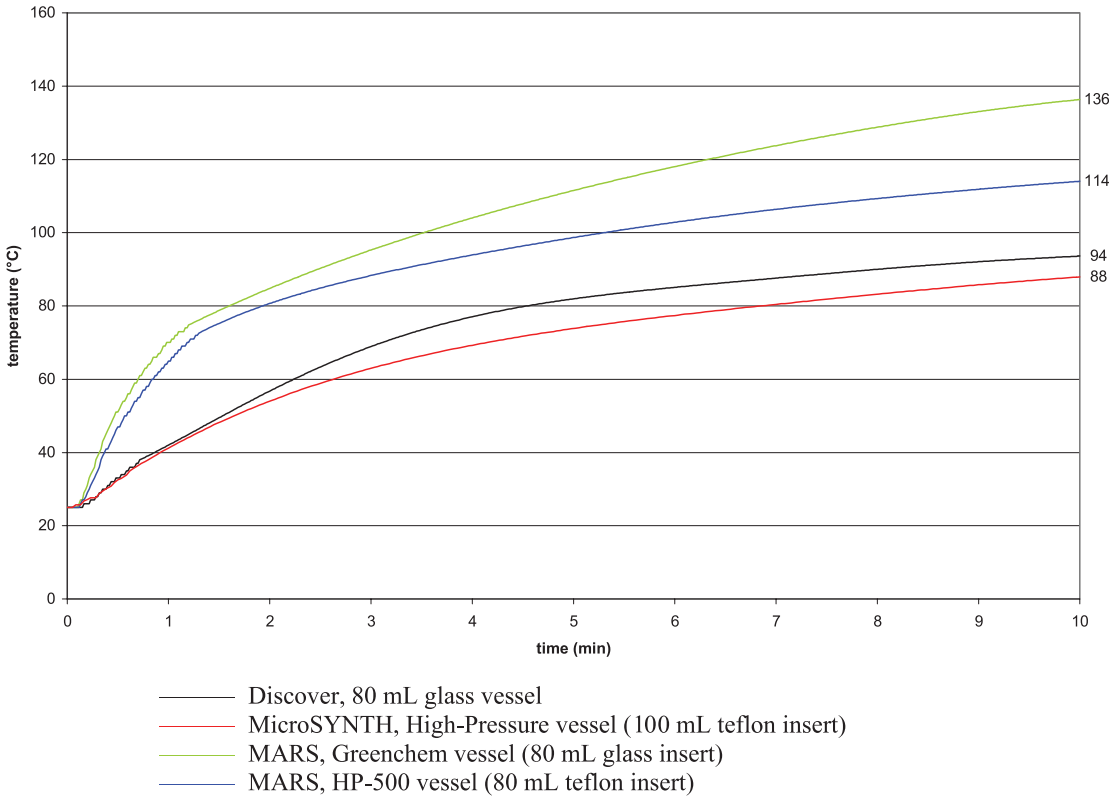

Figure 9. Heating profile of 20 mL of tetrahydrofurane in several commercial available microwave systems, irradiated in a power/time experiment at a constant power of 300 W for 10 min.

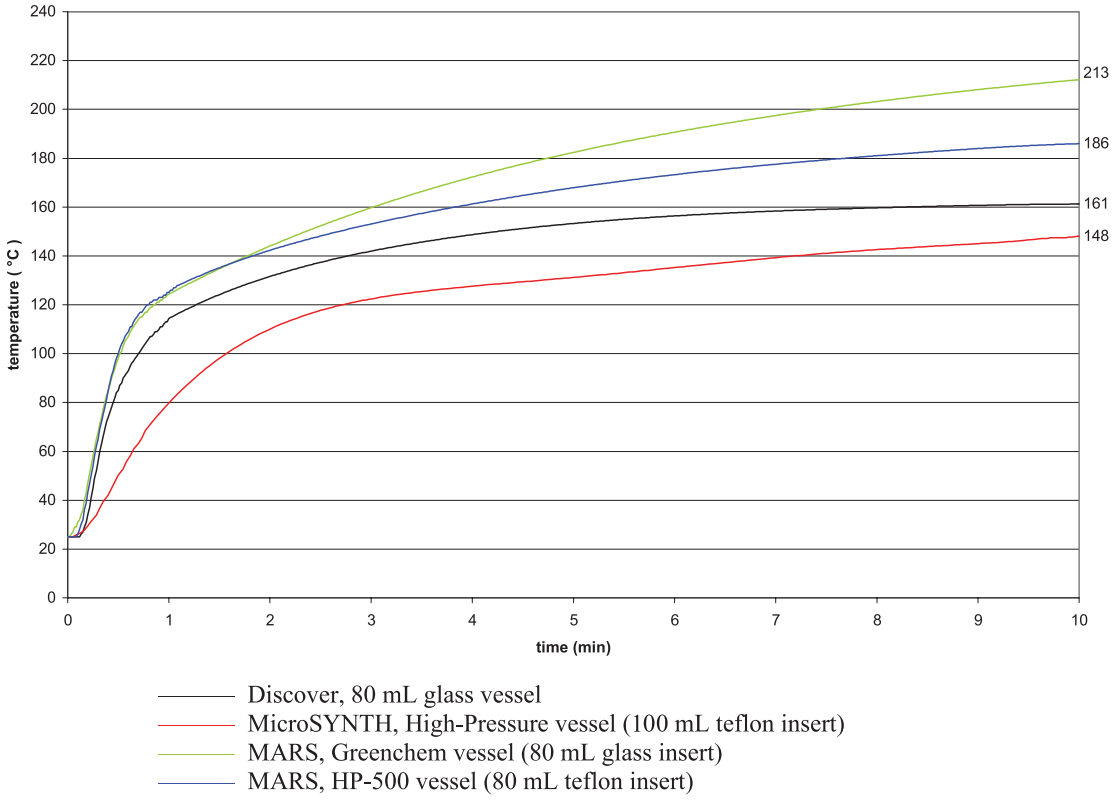

Figure 10. Heating profile of 20 mL of trifluoromethylbenzene (BTF) in several commercial available microwave systems, irradiated in a power/time experiment at a constant power of 300 W for 10 min.

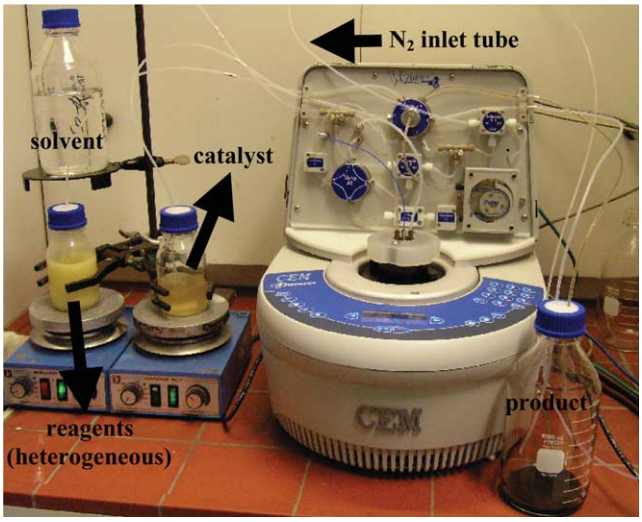

Figure 11. Experimental setup for the scale-up of Pd-catalyzed aminations using the Voyager platform.

Claisen rearrangements were executed using trifluoromethylbenzene (benzotrifluoride: BTF) as the solvent and a review stating the stability of this solvent under strongly basic conditions at high temperature we investigated the heating profile of 20 mL of this solvent at a constant power of 300 W.[13,14] Interestingly, we found that BTF heats up very rapidly, including in the Discover system at maximum power output, since all vessel-microwave combinations gave a final solvent temperature equal or higher than 148 °C (Fig. 10). Since in the real experiments our vessel contains in addition to solvent also polar reagents that will couple with microwaves we can expect that the required 150 °C will certainly be reached in one to two minutes as desired. Therefore we considered BTF as a good solvent candidate for scale-up of Buchwald–Hartwig aminations in single-mode as well as multi-mode platforms. Since BTF has hitherto never been used in palladium-catalyzed reactions we checked its potential as an amination solvent. Rewardingly, when we coupled 4-chloroanisole with morpholine at small scale in a 10 mL glass vessel in the Discover we found that in the same reaction time at the same final temperature a similar isolated yield was obtained using this solvent as a toluene substitute (Table 1).

For the scale-up experiments we first evaluated the Discover single-mode microwave of CEM. An attempt to scale-up our test case amination of 4-chloroanisole with morpholine with a factor 20 (20 mmol 4-chloroanisole, 24 mmol morpholine, 28 mmol NaO*t*-Bu, 20 mL BTF) in an 80 mL vessel proceeded smoothly since a complete conversion of starting material and an isolated yield of 85% of 4-(4-methoxyphenyl)morpholine could be achieved in the same reaction time (10 min) as when 1 mmol of the aryl chloride was used in BTF (Table 1).[15] Next we looked at the possibility to perform this experiment in a completely automized batch wise process. For this purpose we used the Voyager (stop/flow system) system of CEM. For our automized scale-up experiment we made a stock solution of catalyst ($Pd(OAc)_2$/2 DCPB) in BTF and a second solution containing 4-chloroanisole, morpholine and NaO*t*-Bu in BTF. The latter is a heterogeneous mixture due to the low solubility of NaO*t*–Bu in BTF. Therefore this stock solution was put on a magnetic stirring plate, which prevented precipitation of the base at the bottom of the bottle and, which allowed the creation of a more or less homogeneous suspension. The whole setup can be seen in Figure 11. When we programmed the Voyager for three cycles of 20 mmol aryl chloride the average yield was similar as the one obtained in the previously mentioned one batch experiment (Table 1). Even when we performed 12 cycles the yield did not drop significantly since an average yield of 76% for batches 10–12 was obtained. When one takes into account that a complete cycle takes only 16 min, the stop/flow system gives the opportunity to make 1.35 mol (around 261 g) of 4-(4-methoxyphenyl)morpholine in one day. Next we attempted to scale-up the most challenging coupling we previously published namely the amination of 4-chloroanisole with *N*,*N*-dibutylamine using DTPB as ligand for the palladium catalyst. Performing the experiment on a 20 mmol scale of 4-chloroanisole in an 80 mL glass vessel in the Discover gave the same yield as on a 1 mmol scale in a 10 mL glass vessel in toluene (Table 2). Further scale-up in the Voyager gave an average yield of 44% over three cycles and clearly illustrates the power of the Voyager system. Finally, we also tried to use a heteroaromatic substrate namely 3-chloropyridine. Pd-catalyzed amination of 3-chloropyridine (20 mmol) with benzylamine (30 mmol) using DTPB as ligand gave a 85% isolated yield in a one batch experiment in the 80 mL vessel

Table 2. Scale-up of the Pd-catalyzed amination of 4-chloroanisole with *N*,*N*-dibutylamine

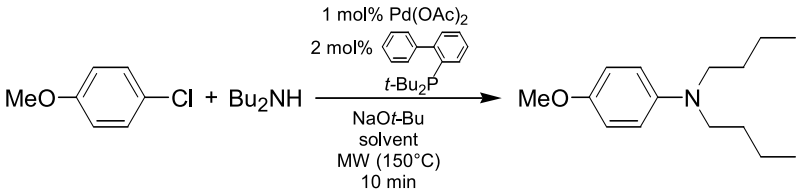

Microwave	4-Chloroanisole (mmol)	Vessel		Initial set power (W)	Solvent	Yield (%)[a]
		Volume (mL)	Type			
Discover	1	10	Glass	300	Toluene	50
Discover	20	80	Glass	300	BTF	45
Voyager	3×20	80	Glass	300	BTF	44[b]

[a] 4-Chloroanisole (*y* mmol), *N*,*N*-dibutylamine (1.2*y* mmol), NaO*t*–Bu (1.4*y* mmol), toluene or BTF (*y* mL).
[b] Average yield.

Table 3. Scale-up of the Pd-catalyzed amination of 3-chloropyridine with benzylamine

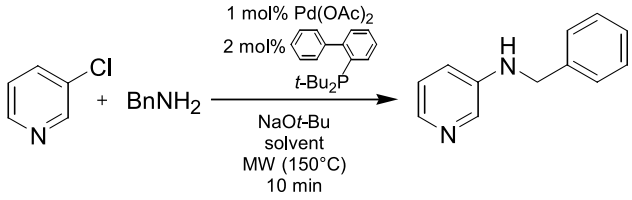

Microwave	3-Chloropyridine (mmol)	Vessel		Initial Set Power (W)	Solvent	Yield (%)[a]
		Volume (mL)	Type			
Discover	1	10	Glass	300	Toluene	87
Discover	20	80	Glass	300	BTF	85
Voyager	3×20	80	Glass	300	BTF	81[b]

[a] 3-Chloropyridine (*y* mmol), benzylamine (1.5*y* mmol), NaO*t*-Bu (1.4*y* mmol), toluene or BTF (*y* mL).
[b] Average yield.

in the Discover, which is essentially the same as the result obtained on a 1 mmol scale in toluene (Table 3). Running three cycles in the Voyager also gave a similar result (average yield of 81%) (Table 3).

Secondly, we looked at the scale-up possibilities (6× 20 mmol) of the MARS (Greenchem vessels) and microSYNTH (high-pressure vessels) multi-mode microwaves of the companies CEM and Milestone, respectively. To get an idea about the set power required to heat up multiple vessels we performed power/time experiments with 6 vessels each containing 20 mL of BTF. We decided to execute these power/time experiments in the microSYNTH (high-pressure vessels) since we already found that heating one Greenchem vessel with 20 mL of BTF at a constant power of 300 W for 10 min in the MARS system gives a higher final temperature than when a similar experiment is performed in a high-pressure vessel in the microSYNTH (Fig. 10). Heating 6 high-pressure vessels with 20 mL of BTF at a constant power of 300 W gave a final solvent temperature of 127 °C, which is 21 degrees lower than when one vessel is heated at the same constant power in the same time (Fig. 10). Increasing the power to 600 W increased the final temperature of the solvent for the 6 high-pressure vessels to a similar value as with one high-pressure vessel at 300 W and therefore 600 W was selected as the set power for the large scale amination experiments. Irradiating a rotor with 6 high-pressure vessels each containing 20 mmol 4-chloroanisole, 24 mmol morpholine, 28 mmol NaO*t*–Bu and 1 mol% $Pd(OAc)_2$/2 mol% DCPB catalyst in 20 mL BTF to 150 °C using an initial set power of 600 W gave a complete conversion of starting material in 10 min and an average isolated yield of 77% of 4-(4-methoxyphenyl)-morpholine (Table 1). A similar experiment with 6 Greenchem vessels in the MARS using the same microwave parameters gave 80% reaction product (Table 1). Both large scale (6×20 mmol) experiments performed in a microSYNTH and MARS multi-mode system gave a similar yield as the small scale (1 mmol) experiment in a 10 mL glass vessel in the Discover (Table 1).

4. Conclusion

Rapid Pd-catalyzed amination of aryl chlorides under microwave irradiation can be easily scaled-up without yield decrease if trifluoromethylbenzene (BTF) is used as solvent. Single-mode as well as multi-mode platforms can be used for this purpose. Although similar yields could be obtained in the Voyager, microSYNTH and MARS equipment, we prefer the Voyager since it is a completely automized unit that allows the continuous production of reaction product without the necessity to manually load and unload reaction vessels. Moreover, the Voyager allows pumping of heterogeneous mixtures, which is problematic in continuous-flow units.

5. Experimental

5.1. General

For column chromatography Kieselgel 60 (ROCC, 0.040–0.063 mm) was used. $Pd(OAc)_2$ (Acros), DCPB (Strem Chemicals or Acros), DTPB (Strem Chemicals or Acros), BTF (Acros) as well as all the amines and (hetero)aryl chlorides were obtained from commercial sources and used as such. The characterization data of 4-(4-methoxyphenyl) morpholine, *N*,*N*-dibutyl-4-methoxyaniline and *N*-benzyl-pyridin-3-amine were identical with those previously reported in the literature.[7l,16] For the microwave-assisted amination experiments in toluene extra dry (<30 ppm water) toluene of Acros was used. The toluene (Acros) used to determine the heating profiles was p.a. quality.

5.2. Scale-up of palladium-catalyzed aminations of (hetero)aryl chlorides using the Voyager platform

5.2.1. Preparation of the stock solutions. *Stock solution one*. A 250 mL bottle (Schott) was charged with (hetero)aryl chloride (70 mmol), amine (morpholine or *N*,*N*-dibutylamine: 84 mmol) (*N*-benzylamine: 105 mmol) and NaO*t*–Bu (9.42 g, 98 mmol) and BTF (35 mL) in air. Subsequently, the bottle was flushed with Ar for a few minutes under magnetic stirring. The stock solution of reagents (including base) is heterogeneous. Therefore it was placed on a magnetic stirring plate, which prevented precipitation of the base at the bottom of the bottle. This allowed the creation of a more or less homogeneous suspension.

Stock solution two. A 250 mL bottle (Schott) was charged with $Pd(OAc)_2$ (0.157 g, 0.70 mmol), 2-(dicyclohexylphosphanyl)biphenyl (DCPB) or 2-(di-*t*-butylphospanyl) biphenyl (DTPB) (1.4 mmol) and BTF (35 mL) in air. Subsequently, the bottle was flushed with Ar for 10 min under magnetic stirring. When DTPB was used as ligand for the catalyst the stock solution was stirred for 16 h before using it.[17]

5.3. Remarks

* The viscosity of the stock solutions influences the actual volume that will be pumped out of the stock solutions in the reaction vessel of the Voyager system in a certain timeframe. Therefore one needs to calibrate the system first by determining the pumping time necessary to pump in the desired volume (#mmol of reagents and base, catalyst).
* We coupled the Voyager platform to a nitrogen cylinder (Fig. 11). In this way flushing of the tubing during loading, unloading and cleaning of the reaction vessel is performed with N_2 gas instead of air.
* The set power for all amination experiments using the Voyager or Discover system was 300 W, the set temperature 150 °C. The total irradiation time (including the ramp time to the set temperature) was 10 min. Crude reaction mixture was filtered over Celite and rinsed well with dichloromethane. The filtrate was subsequently evaporated under reduced pressure and the residue purified by flash column chromatography on silica gel.

5.4. Scale-up of the palladium-catalyzed amination of 4-chloranisole with morpholine using the MARS and microSYNTH platform

A Greenchem or high-pressure vessel was charged with 4-chloranisole (20 mmol), morpholine (24 mmol) and NaO*t*–Bu (2.69 g, 28 mmol) in air. Subsequently the vial was flushed with Ar for one minute. Then, 20 mL of a stock solution of catalyst[†] was added via a syringe and the resulting mixture stirred and flushed with Ar for a few minutes. Next, the Greenchem or high-pressure vessel was sealed. 6 Greenchem or high-pressure vessels filled in this way were then heated to 150 °C in a MARS or microSYNTH platform, respectively. The set power was 600 W. The total irradiation time (including the ramp time to the set temperature) was 10 min. After the rotor was cooled down to room temperature the vessels were opened, the contents of the 6 vessels combined, filtered over Celite and rinsed well with dichloromethane. The filtrate was subsequently evaporated under reduced pressure and the residue purified by flash column chromatography on silica gel.

[†] Stock solution of catalyst, A 250 mL bottle (Schott) was charged with $Pd(OAc)_2$ (0.314 g, 1.40 mmol), 2-(dicyclohexylphosphanyl)biphenyl (DCPB) (0.981 g, 2.8 mmol) and BTF (70 mL) in air. Subsequently, the bottle was flushed with Ar for 10 min under magnetic stirring.

Acknowledgements

B. M. acknowledges the financial support by the 'Fund for Scientific Research-Flanders' (FWO-Vlaanderen) (research grant 1.5.088.04), the European Union and the University of Antwerp (RAFO-RUCA). The authors wish to thank the technical staff (ing. J. Aerts, J. Schrooten, W. Van Lierde and ing. J. Verreydt) and Gitte Van Baelen of the research group for their assistance. S. H. thanks the IWT-Vlaanderen ('Instituut voor de Aanmoediging van Innovatie door Wetenschap en Technologie in Vlaanderen') for a scholarship.

References and notes

1. For recent reviews and books on microwave-assisted organic synthesis: (a) Lidström, P.; Tierney, J.; Wathey, B.; Westman, J. *Tetrahedron* **2001**, *57*, 9225–9283. (b) Larhed, M.; Hallberg, A. *Drug Discovery Today* **2001**, *6*, 406–416. (c) Kappe, C. O. *Am. Lab.* **2001**, *33*, 13–19. (d) Larhed, M.; Moberg, C.; Hallberg, A. *Acc. Chem. Res.* **2002**, *35*, 717–727. (e) Lew, A.; Krutzik, P. O.; Hart, M. E.; Chamberlin, A. R. *J. Comb. Chem.* **2002**, *4*, 95–105. (f) Kappe, C. O. *Curr. Opin. Chem. Biol.* **2002**, *6*, 314–320. (g) Hayes, B. L. Microwave Synthesis: Chemistry at the Speed of Light; CEM: Matthews, 2002. (h) *Microwaves in Organic Synthesis*; Loupy, A., Ed.; Wiley-VCH: Weinheim, 2002. (i) Hayes, B. L. *Aldrichim. Acta* **2004**, *37*, 66–77. (j) *Microwave-Assisted Organic Synthesis*; Lindström, P., Tierney, J. P., Eds.; Blackwell: Oxford, 2004. (k) Kappe, C. O. *Angew. Chem., Int. Ed.* **2004**, *43*, 6250–6284.
2. (a) Gedye, R.; Smith, F.; Westaway, K.; Ali, H.; Baldisera, L.; Laberge, L.; Rousell, J. *Tetrahedron Lett.* **1986**, *27*, 279–282. (b) Giguere, R. J.; Bray, T. L.; Duncan, S. M.; Majetich, G. *Tetrahedron Lett.* **1986**, *27*, 4945–4958.
3. http://www.cem.com/; http://www.milestonesrl.com/; http://www.biotage.com/; http://www.plazmatronika.pl/eng/index.html; http://www.anton-paar.com/.
4. (a) Raner, K. D.; Strauss, C. R.; Trainor, R. W.; Thorn, J. S. *J. Org. Chem.* **1995**, *60*, 2456–2460. (b) Perio, B.; Dozias, M.-J.; Hamelin, J. *Org. Process Res. Dev.* **1998**, *2*, 428–430. (c) Cléophax, J.; Liagre, M.; Loupy, A.; Petit, A. *Org. Process Res. Dev.* **2000**, *4*, 498–504.
5. (a) Cablewski, T.; Faux, A. F.; Strauss, C. R. *J. Org. Chem.* **1994**, *59*, 3408–3412. (b) Kazba, K.; Chapados, B. R.; Gestwicki, J. E.; McGrath, J. L. *J. Org. Chem.* **2000**, *65*, 1210–1214. (c) Khadilkar, B. M.; Madyar, V. R. *Org. Process Res. Dev.* **2001**, *5*, 452–455. (d) Esveld, E.; Chemat, F.; van Haveren, J. *Chem. Eng. Technol.* **2000**, *23*, 279–283. (e) Esveld, E.; Chemat, F.; van Haveren, J. *Chem. Eng. Technol.* **2000**, *23*, 429–435. (f) Shieh, W.-C.; Dell, S.; Repi, O. *Tetrahedron Lett.* **2002**, *43*, 5607–5609.
6. For the scale-up of Heck and Negishi reactions in a prototype multi-mode microwave of Anton Paar GmbH see: Stadler, A.; Yousefi, B. H.; Dallinger, D.; Walla, P.; Van der Eycken, E.; Kaval, N.; Kappe, C. O. *Org. Process Res. Dev.* **2003**, *7*, 707–716. For the scale-up of Suzuki reactions in a single-mode microwave of CEM (Discover) using a 50 mL round-bottomed flask see: Leadbetter, N. E.; Marco, M. *J. Org. Chem.* **2003**, *68*, 888–892.

7. For small scale microwave-assisted Pd-catalyzed amination of aryl halides see: (a) Sharifi, A.; Hosseinzadeh, R.; Mirzaei, M. *Monatsh. Chem.* **2002**, *133*, 329–332. (b) Wan, Y.; Alterman, M.; Hallberg, A. *Synthesis* **2002**, 1597–1600. (c) Maes, B. U. W.; Loones, K. T. J.; Lemière, G. L. F.; Dommisse, R. A. *Synlett* **2003**, 1822–1824. (d) Wang, T.; Magnin, D. R.; Hamann, L. G. *Org. Lett.* **2003**, *5*, 897–900. (e) Antane, S. *Synth. Commun.* **2003**, *33*, 2145–2149. (f) Burton, G.; Cao, P.; Li, G.; Rivero, R. *Org. Lett.* **2003**, *5*, 4373–4376. (g) Weigand, K.; Pelka, S. *Mol. Divers.* **2003**, *7*, 181–184. (h) McCarroll, A. J.; Sandham, D. A.; Titcomb, L. R.; de K. Lewis, A. K.; Cloke, F. G. N.; Davies, B. P.; de Santana, A. P.; Hiller, W.; Caddick, S. *Mol. Divers.* **2003**, *7*, 115–123. (i) Brain, C. T.; Steer, J. T. *J. Org. Chem.* **2003**, *68*, 6814–6816. (j) Jensen, T. A.; Liang, X. F.; Tanner, D.; Skjaerbaek, N. *J. Org. Chem.* **2004**, *69*, 4936–4947. (k) Harmata, M.; Hong, X.; Ghosh, S. K. *Tetrahedron Lett.* **2004**, *45*, 5233–5236. (l) Maes, B. U. W.; Loones, K. T. J.; Hostyn, S.; Diels, G.; Rombouts, G. *Tetrahedron* **2004**, *60*, 11559–11564. (m) Poondra, R. R.; Turner, N. J. *Org. Lett.* **2005**, *7*, 863–866.
8. For reviews on palladium-catalyzed amination see: (a) Barañano, D.; Mann, G.; Hartwig, J. F. *Curr. Org. Chem.* **1997**, *1*, 287–305. (b) Frost, C. G.; Mendonça, P. *J. Chem. Soc., Perkin Trans. 1* **1998**, 2615–2623. (c) Hartwig, J. F. *Angew. Chem., Int. Ed.* **1998**, *37*, 2047–2067. (d) Yang, B. H.; Buchwald, S. L. *J. Organomet. Chem.* **1999**, *576*, 125–146. (e) Hartwig, J. F. In *Modern Amination Methods*; Ricci, A., Ed.; Wiley-VCH: Weinheim, 2000; pp 195–262. (f) Muci, A. R.; Buchwald, S. L. *Top. Curr. Chem.* **2002**, *219*, 131–209. For reviews containing a part on recent progress made in palladium-catalyzed amination see: (g) Littke, A. F.; Fu, G. C. *Angew. Chem., Int. Ed.* **2002**, *41*, 4176–4211. (h) Prim, D.; Campagne, J.-M.; Joseph, D.; Andrioletti, B. *Tetrahedron* **2002**, *58*, 2041–2075. (i) Wolfe, J. P.; Thomas, J. S. *Curr. Org. Chem.* **2005**, *9*, 625–655. For a review dealing with palladium-catalyzed aminations seen from an industrial point of view see: (j) Schlummer, B.; Scholz, U. *Adv. Synth. Catal.* **2004**, *346*, 1599–1626.
9. For pioneering literature on Buchwald's monodentate phosphine ligands based on a biphenyl backbone see: (a) Old, D. W.; Wolfe, J. P.; Buchwald, S. L. *J. Am. Chem. Soc.* **1998**, *120*, 9722–9723. (b) Wolfe, J. P.; Buchwald, S. L. *Angew. Chem., Int. Ed.* **1999**, *38*, 2413–2416. (c) Wolfe, J. P.; Tomori, H.; Sadighi, J. P.; Yin, J.; Buchwald, S. L. *J. Org. Chem.* **2000**, *65*, 1158–1174.
10. Gabriel, C.; Gabriel, S.; Grant, E. H.; Halstead, B. S. J.; Mingos, D. M. P. *Chem. Soc. Rev.* **1998**, *27*, 213–223.
11. The maximum power measurement method the manufacturers (CEM, Milestone) use to determine the power output of their multi-mode system (MARS, microSYNTH) is different. If the IEC method is used for the MARS platform it delivers a maximum power output of 1500 W instead of 1200 W. The microSYNTH platform delivers a maximum power output of 1000 W following the IEC method. This means one should take into account that the compared heating profiles, resulting from power/time experiments performed at the same constant power output in the MARS and microSYNTH platform, give only a rough indication of the difference in performance of both multi-modes. Working at the same set constant power output in both multi-mode platforms is in reality actually not working at the same power. The maximum power measurement method used to determine the power output of the single-mode Discover unit (CEM) is also different so comparing heating profiles, resulting from power/time experiments performed at the same constant power output in a multi-mode or single-mode platform, gives also only a rough indication of the difference in performance of the microwave systems. Working at the same set constant power output in both platforms is in reality actually not working at the same power. In addition, for all commercial microwaves (single-mode and multi-mode) there is a 'nominal' power. Not all units of a certain type produce exactly the same power so even comparison between two units can be tricky (MARS $\pm 15\%$, microSYNTH $\pm 10\%$, Discover $\pm 10\%$). Microwave power measurement: (1) MARS (1200 W): heat 1 L of water (T_{initial}: 18–22 °C) in a beaker for 2 min at the maximum power of the microwave and determine the temperature difference of the water; power in Watts $= 35\ (T_{\text{final}} - T_{\text{initial}})$; (2) microSYNTH (1000 W): heat 1 L of water (T_{initial}: around 10 °C) for 1 min in a beaker at the maximum power of the microwave and determine the temperature difference of the water; power in Watts $= 70\ (T_{\text{final}} - T_{\text{initial}})$; (3) Discover (300 W): heat 50 mL of water (T_{initial}: 18–22 °C) for 30 s in a 100 mL round-bottomed flask at the maximum power of the microwave and determine the temperature difference of the water; Power in Watts $= 7\ (T_{\text{final}} - T_{\text{initial}})$.
12. For the heating profiles (IR) of quartz and glass vessels filled with microwave transparent CCl_4 measured in a Smith Synthesizer (Personal Chemistry) see: Garbacia, S.; Desai, B.; Lavastre, O.; Kappe, C. O. *J. Org. Chem.* **2003**, *68*, 9136–9139.
13. Lecture of N. Moorcroft presented at the '2nd International Microwaves in Chemistry Conference', Orlando (USA), 4/3–7/3 2004.
14. Use of BTF as solvent in organic synthesis: Maul, J. J.; Ostrowski, P. J.; Ublacker, G. A.; Linclau, B.; Curran, D. P. *Top. Curr. Chem.* **1999**, *206*, 79–105.
15. For the amination of 4-chloroanisole with morpholine we also attempted to scale-up with a factor 36 (36 mmol 4-chloroanisole, 43.2 mmol morpholine, 50.4 mmol NaO*t*-Bu, 36 mL BTF) in the 80 mL vessel of the Discover apparatus. In the same reaction time as for the 1 mmol and 20 mmol experiments (10 min) an isolated yield of 73% of 4-(4-methoxyphenyl)morpholine could be obtained. This is similar to the yield obtained on a 1 mmol scale (78%) but lower than the isolated yield of the 20 mmol experiment (85%).
16. (a) Trifonov, L. S.; Orahovats, A. S. *Helv. Chim. Acta* **1987**, *70*, 1732–1736. (b) O'Connor, S. J.; Barr, K. J.; Wang, Le.; Sorensen, B. K.; Tasker, A. S.; Sham, H.; Ng, S.-C.; Cohen, J.; Devine, E.; Cherian, S.; Saeed, B.; Zhang, H.; Lee, J. Y.; Warner, R.; Tahir, S.; Kovar, P.; Ewing, P.; Alder, J.; Mitten, M.; Leal, J.; Marsh, K.; Bauch, J.; Hoffman, D. J.; Sebti, S. M.; Rosenberg, S. H. *J. Med. Chem.* **1999**, *42*, 3701–3710.
17. Recently, Buchwald and co-workers reported that by stirring a mixture of $Pd(OAc)_2$ and DTPB in toluene for 16 h at room temperature a palladacycle is formed. In consequence of this report, we always stirred our stock solution of $Pd(OAc)_2$ and DTPB for at least 16 h before using it: Zim, D.; Buchwald, S. L. *Org. Lett.* **2003**, *5*, 2413–2415.

Available online at www.sciencedirect.com
SCIENCE DIRECT
Tetrahedron
Tetrahedron 61 (2005) 10349–10362

Reactions of guaiazulene with 2-furaldehyde, thiophene-2-carbaldehyde and pyrrole-2-carbaldehyde in methanol in the presence of hexafluorophosphoric acid: comparative studies on molecular structures and spectroscopic, chemical and electrochemical properties of monocarbocations stabilized by 3-guaiazulenyl and 2-furyl (or 2-thienyl or 2-pyrrolyl) groups

Shin-ichi Takekuma,[a,*] Kenji Takahashi,[a] Akio Sakaguchi,[a] Yoshihiko Shibata,[a] Masato Sasaki,[a] Toshie Minematsu[b] and Hideko Takekuma[a]

[a]*Department of Applied Chemistry, Faculty of Science and Engineering, Kinki University, 3-4-1 Kowakae, Higashi-Osaka-shi, Osaka 577-8502, Japan*
[b]*School of Pharmaceutical Sciences, Kinki University, 3-4-1 Kowakae, Higashi-Osaka-shi, Osaka 577-8502, Japan*

Received 14 June 2005; accepted 26 July 2005

Available online 31 August 2005

Abstract—Reactions of guaiazulene (**1**) with heteroaromatic-carbaldehydes [i.e., 2-furaldehyde (**2**), thiophene-2-carbaldehyde (**3**) and pyrrole-2-carbaldehyde (**4**)] in methanol in the presence of hexafluorophosphoric acid at 25 °C for 30 min under aerobic conditions give (2-furyl)(3-guaiazulenyl)methylium hexafluorophosphate (**5**), (3-guaiazulenyl)(2-thienyl)methylium hexafluorophosphate (**6**) and (3-guaiazulenyl)(2-pyrrolyl)methylium hexafluorophosphate (**7**), respectively, in 93, 98 and 85% yields. Comparative studies on the molecular structures as well as the spectroscopic, chemical and electrochemical properties of the methylium hexafluorophosphates **5**–**7** stabilized by 3-guaiazulenyl and 2-furyl (or 2-thienyl or 2-pyrrolyl) groups are reported.

1. Introduction

In the previous papers,[1–9] we reported a facile preparation and the crystal structures as well as the spectroscopic, chemical and electrochemical properties of the mono- and dicarbocations stabilized by a 3-guaiazulenyl group. In relation to our basic studies, Ito et al. reported the synthesis, properties and redox behavior of a series of (1-azulenyl)-methylium and [9-(azuleno[1,2-*b*]thienyl)]methylium hexafluorophosphates.[10,11] Our interest has recently been focused on comparative studies on the molecular structures and characteristic properties of the mono-carbocations stabilized by 3-guaiazulenyl and 2-furyl (or 2-thienyl or 2-pyrrolyl) groups; namely, (2-furyl)(3-guaiazulenyl)methylium hexafluorophosphate (**5**), (3-guaiazulenyl)(2-thienyl)methylium hexafluorophosphate (**6**) and (3-guaiazulenyl)(2-pyrrolyl)methylium hexafluorophosphate (**7**), where the formation of the following two representative resonance forms [i.e., 3-guaiazulenylium **5′**–**7′** and 2-furanylium **5″** (or 2-thienylium **6″** or 2-pyrrolylium **7″**) structures] is possible (see Fig. 1). During the course of our investigations, we have quite recently found (i) that the reactions of naturally occurring guaiazulene (**1**) with 2-furaldehyde (**2**) and thiophene-2-carbaldehyde (**3**) in methanol in the presence of hexafluorophosphoric acid gave **5** and **6**, respectively, in 93 and 98% yields (see Fig. 1 and Table 1), (see Figs. 2–5, Tables 2–7), which upon reduction with zinc powder in acetonitrile afforded a mixture of a *meso* form and two enantiomeric forms of the molecular structures, 1,2-di(2-furyl)-1,2-di(3-guaiazulenyl)ethane (**11**) and 1,2-di(3-guaiazulenyl)-1,2-di(2-thienyl)ethane (**12**) (see Fig. 6 and Table 8), and (ii) that the reaction of **1** with pyrrole-2-carbaldehyde (**4**) under

Keywords: Carbenium ions; Electrochemistry; Furan; Guaiazulene; Pyrrole; Reduction; Thiophene; X-ray crystal structures.
* Corresponding author. Tel.: +81 6 6730 5880x4020; fax: +81 6 6727 4301; e-mail: takekuma@apch.kindai.ac.jp

0040–4020/$ - see front matter © 2005 Elsevier Ltd. All rights reserved.
doi:10.1016/j.tet.2005.07.104

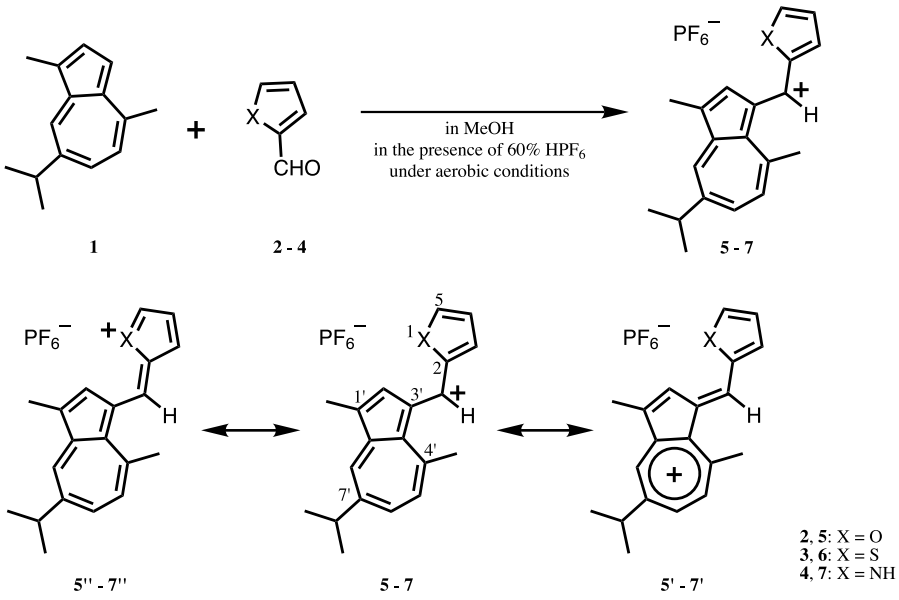

Figure 1. The reactions of **1** with **2–4** in CH_3OH with HPF_6 under aerobic conditions, affording the corresponding monocarbocation products **5–7** with the resonance forms of **5′–7′** and **5″–7″**.

Table 1. The yield/% of the products **5–7** obtained from the reactions of **1** with **2–4** in CH_3OH with HPF_6 under aerobic conditions

Entry	X	Temperature (°C)	Time (min)	Product	Yield (%)[a]
1	O	25	30	**5**	93
2	S	25	30	**6**	98
3	NH	25	30	**7**	85

[a] Isolated yield.

the same reaction conditions as **2** and **3** gave **7** in 85% yield (see Fig. 1 and Table 1). Similarly, as in the cases of **5** and **6**, the reduction of **7** with zinc powder in acetonitrile afforded a mixture of a *meso* form and two enantiomeric forms of the molecular structure, 1,2-di(3-guaiazulenyl)-1,2-di(2-pyrrolyl)ethane (**13**) (see Fig. 6 and Table 8). Although (2-furyl)(3-guaiazulenyl)methylium and (3-guaiazulenyl)(2-thienyl)methylium perchlorates[12] are known compounds, nothing has really been documented regarding the accurate spectral data, crystal structures and characteristic properties of those compounds. As a series of basic studies on the chemistry of the carbocations stabilized by a 3-guaiazulenyl group, we now wish to report the detailed studies on an efficient preparation and the molecular structures as well as the spectroscopic, chemical and electrochemical properties of the target compounds **5–7** compared with those of the previously-documented monocarbocation compound stabilized by 3-guaiazulenyl and phenyl groups, (3-guaiazulenyl)phenylmethylium hexafluorophosphate (**A**).[4–7]

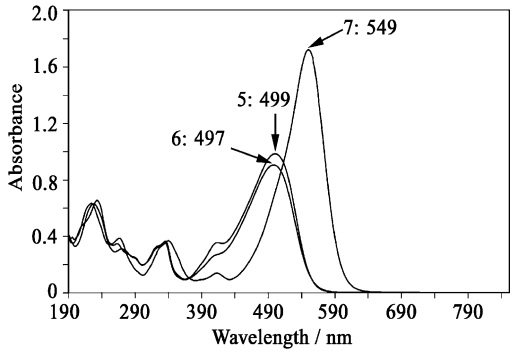

Figure 2. The UV–vis spectra of **5–7** in CH_3CN. Concentrations, **5**: 0.10 g/L (238 μmol/L), **6**: 0.10 g/L (228 μmol/L), **7**: 0.10 g/L (237 μmol/L). Length of the Cell, 0.1 cm each.

2. Results and discussion

2.1. Preparation and spectroscopic properties of (2-furyl)(3-guaiazulenyl)methylium hexafluorophosphate (5), (3-guaiazulenyl)(2-thienyl)methylium hexafluorophosphate (6) and (3-guaiazulenyl)(2-pyrrolyl)methylium hexafluorophosphate (7)

The monocarbocation compounds **5–7** were prepared using methanol as a solvent as shown in Figure 1, Table 1 and Sections 4.1.1–4.1.3, respectively, whose molecular structures were established on the basis of elemental analysis and spectroscopic data [UV–vis, IR, FAB-MS, ^1H and ^{13}C NMR including 2D NMR (i.e., H–H COSY, HMQC = ^1H detected hetero nuclear multiple quantum coherence and HMBC = ^1H detected hetero nuclear multiple bond connectivity)] and, further, chemical evidence (i.e., the reduction of **5–7** with $NaBH_4$).

Compound **5** (93% yield) was red prisms [mp > 150 °C, decomp., determined by the thermal analysis (TGA and DTA)]. The IR (KBr) spectrum showed two specific bands based on the counter anion (PF_6^-) at ν_{max} 840 and 559 cm^{-1}, whose wavenumbers coincided with those of (3-guaiazulenyl)phenylmethylium hexafluorophosphate (**A**) (ν_{max} 837 and 556 cm^{-1}).[5] The molecular formula $C_{20}H_{21}O$ for the carbocation unit was determined by the exact FAB-MS (3-nitrobenzyl alcohol matrix) spectrum. The elemental analysis confirmed the molecular formula $C_{20}H_{21}F_6OP$. A characteristic UV–vis (CH_3CN) absorption band based on the formation of the (2-furyl)(3-guaiazulenyl)methylium

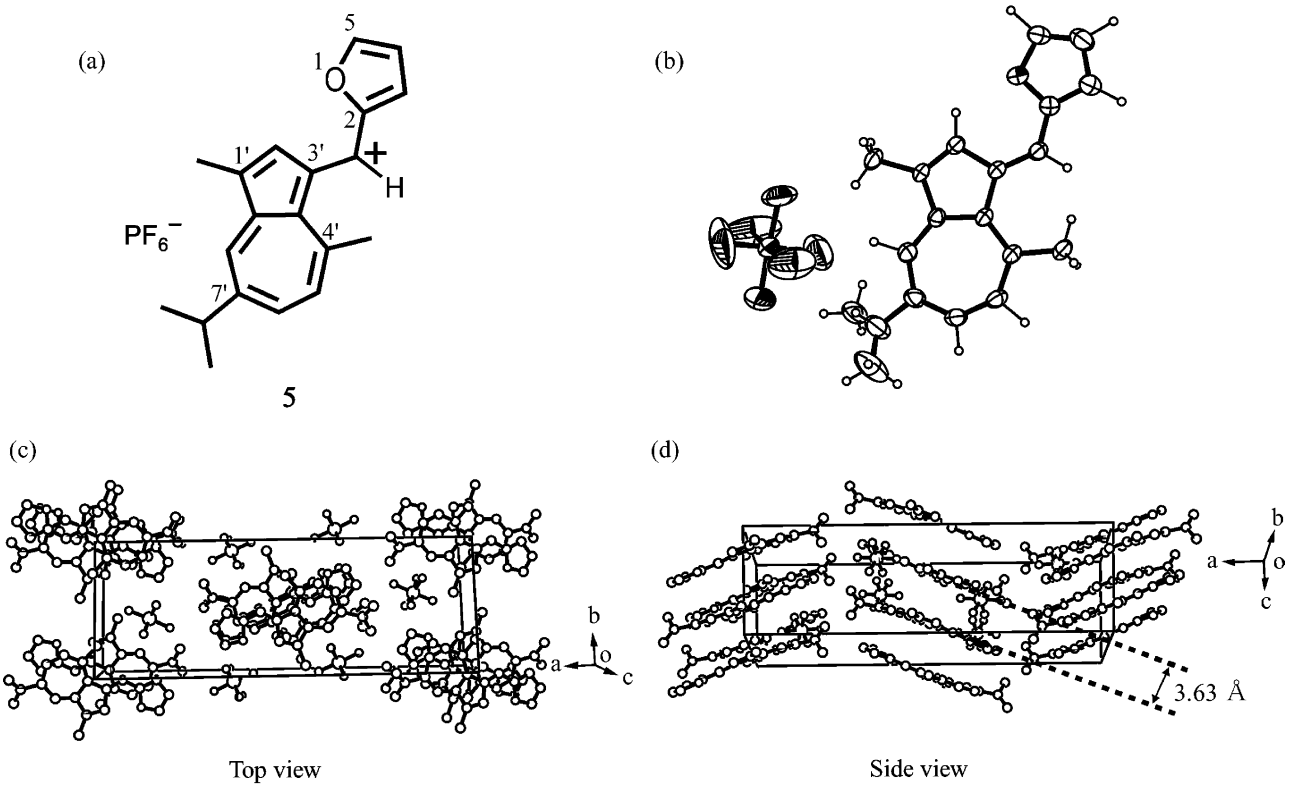

Figure 3. (a) The molecular structure of **5**. (b) The ORTEP drawing of **5** (30% probability thermal ellipsoids). The two different [top (c) and side (d)] views for the packing (molecular) structure of **5**; hydrogen atoms are omitted for reasons of clarity.

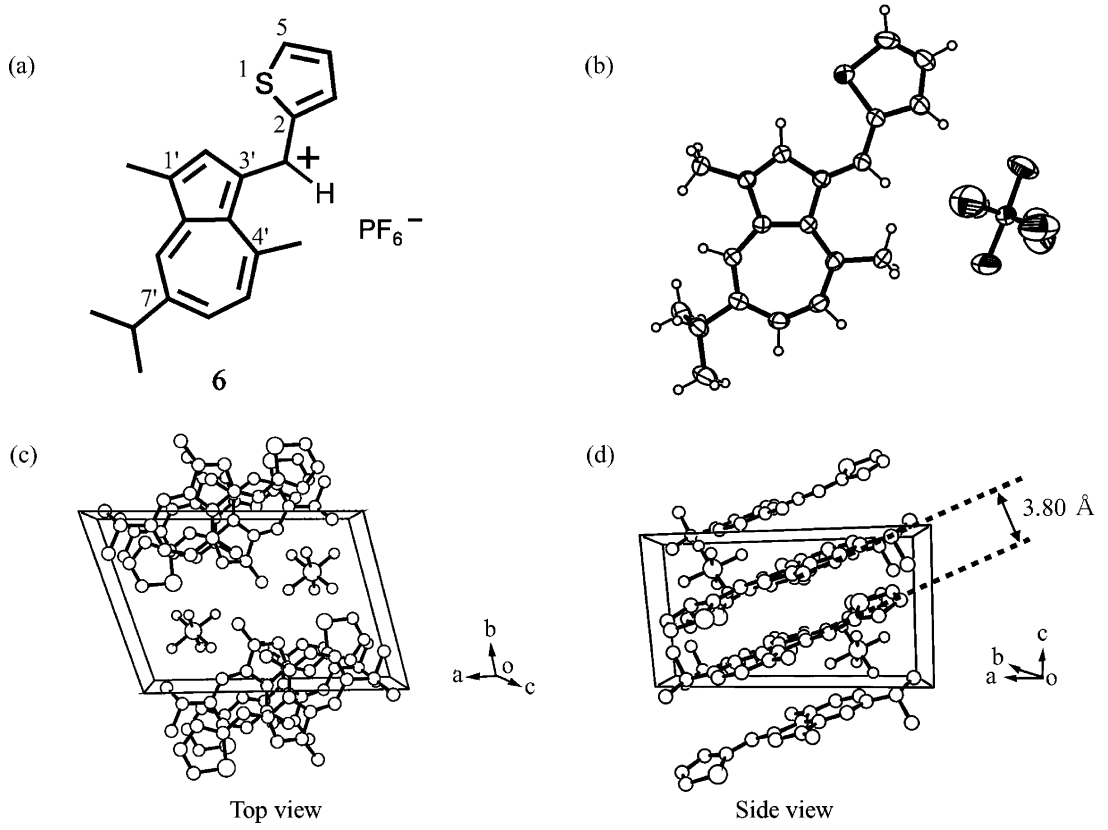

Figure 4. (a) The molecular structure of **6**. (b) The ORTEP drawing of **6** (30% probability thermal ellipsoids). The two different [top (c) and side (d)] views for the packing (molecular) structure of **6**; hydrogen atoms are omitted for reasons of clarity.

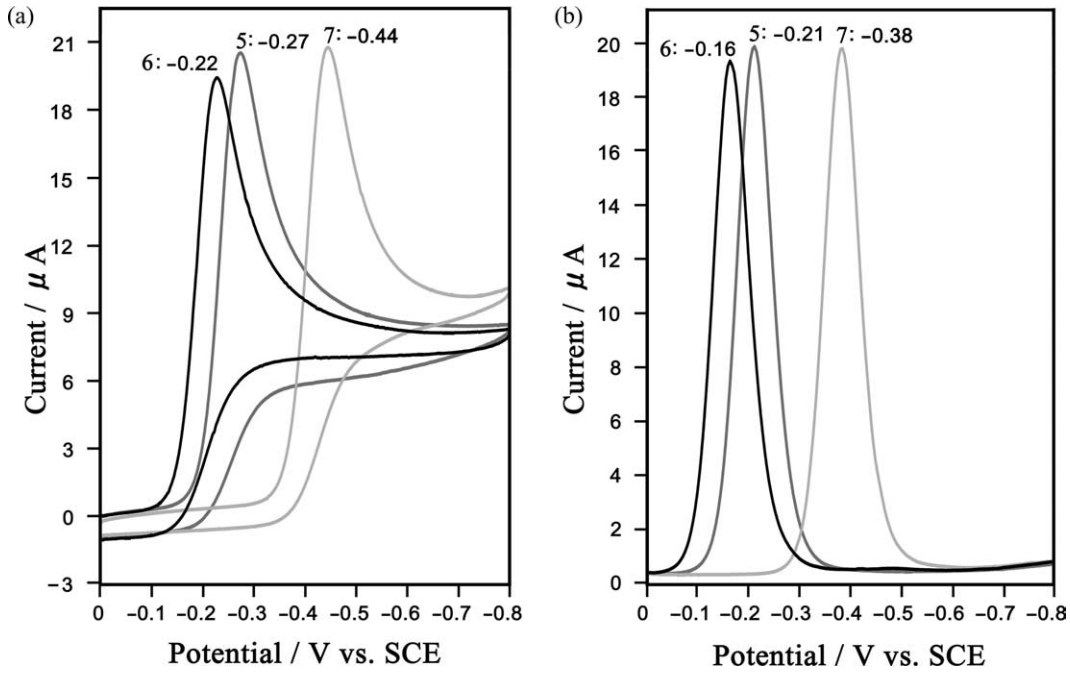

Figure 5. Cyclic (a) and differential pulse (b) voltammograms of **5** (3.0 mg, 7.1 μmol), **6** (3.0 mg, 6.8 μmol), **7** (3.0 mg, 7.1 μmol) in 0.1 M [*n*-Bu_4N]PF_6, CH_3CN (10 mL) at a glassy carbon (ID: 3 mm) and a platinum wire served as the working and auxiliary electrodes; scan rates 100 mVs^{-1} at 25 °C under argon, respectively. For comparative purposes, the oxidation potential using ferrocene as a standard material showed +0.42 (E_p) V by DPV and +0.40 ($E_{1/2}$) V by CV under the same electrochemical conditions as **5**–**7**.

Table 2. The selected ^{1}H NMR chemical shifts (δ, ppm) for the 3-guaiazulenylmethylium substituents (or the 3-guaiazulenylmethyl groups) of **5**–**10**

Compound	HC^+-α	H-2′	H-5′	H-6′	H-8′
5	8.52	8.31	8.39	8.35	8.55
6	8.81	8.24	8.43	8.36	8.56
7	8.56	8.20	8.18	8.19	8.51
8	4.99[a]	7.38	6.82	7.28	8.11
9	4.69[a]	7.48	6.85	7.33	8.13
10	4.47[a]	7.41	6.82	7.30	8.10

[a] 2-H_2C-3′.

Table 3. The ^{1}H NMR chemical shifts (δ, ppm) for the 2-furyl, 2-thienyl and 2-pyrrolyl groups of **5**–**10**

Compound	H-3	H-4	H-5	NH
5	7.54	6.85	8.01	—
6	7.94	7.34	8.13	—
7	7.50	6.67	7.62	10.62
8	5.72	6.25	7.35	—
9	6.64	6.88	7.14	—
10	5.95	5.58	6.56	8.69

moiety with a delocalized π-electron system appeared at the absorption maximum (λ_{max} 499 nm, log ε=4.61) (see Fig. 2), which showed a larger bathochromic shift (Δ 43 nm) and a hyperchromic effect in comparison with that of **A** (λ_{max} 456 nm, log ε=4.30).[5] The ^{1}H NMR (CD_3CN) spectrum showed signals based on the 3-guaiazulenylmethylium substituent and signals based on the 2-furyl group, which signals were carefully assigned using the H–H COSY technique and the computer simulation analysis (see Tables 2 and 3 and Section 4.1.1). The ^{13}C NMR (CD_3CN) spectrum exhibited nineteen carbon signals assigned by the HMQC and HMBC techniques (see Tables 4

Table 4. The selected ^{13}C NMR chemical shifts (δ, ppm) for the 3-guaiazulenylmethylium substituents (or the 3-guaiazulenylmethyl groups) of **5**–**10**

Compound	HC^+-α	C-1′	C-2′	C-3′	C-3a′	C-4′	C-5′	C-6′	C-7′	C-8′	C-8a′
5	141.0	143.5	131.0	152.46	152.51	155.8	148.4	143.9	168.5	138.7	158.8
6	140.7	144.5	139.1	135.1	152.9	156.3	148.8	143.8	168.9	139.7	159.0
7	137.7	140.4	139.7	129.8	150.4	153.9	144.8	142.0	163.0	138.2	154.9
8	30.8[a]	125.1	141.3	124.0	133.4	146.1	127.2	135.7	140.2	134.4	138.9
9	32.1[a]	124.7	140.4	126.6	133.4	146.3	127.3	135.9	140.4	134.5	138.9
10	30.3[a]	125.1	141.6	126.2	133.5	146.4	127.0	135.7	140.0	134.3	138.8

[a] 2-H_2C-3′.

Table 5. The ^{13}C NMR chemical shifts (δ, ppm) for the 2-furyl, 2-thienyl and 2-pyrrolyl groups of **5**–**10**

Compound	C-2	C-3	C-4	C-5
5	133.7	129.3	115.3	152.8
6	138.6	142.4	130.0	139.9
7	132.0	126.5	116.9	134.9
8	157.7	106.7	111.5	142.1
9	149.0	125.2	127.8	124.9
10	134.1	106.2	108.6	117.3

Table 6. The selected C–C bond distances (Å) for the 3-guaiazulenylmethylium substituents of **5** and **6**

Atom	**5**	**6**
C1′–C2′	1.333	1.352
C2′–C3′	1.456	1.447
C3′–C3a′	1.473	1.475
C3a′–C4′	1.397	1.409
C4′–C5′	1.421	1.406
C5′–C6′	1.370	1.372
C6′–C7′	1.398	1.402
C7′–C8′	1.393	1.392
C8′–C8a′	1.399	1.390
C8a′–C1′	1.444	1.452
C3a′–C8a′	1.444	1.445
C3′–Cα	1.360	1.363

Table 7. The bond distances (Å) for the 2-furyl and 2-thienyl groups of **5** and **6**

Atom	**5**	**6**
X[a]–C2	1.363	1.721
C2–C3	1.369	1.413
C3–C4	1.414	1.404
C4–C5	1.322	1.342
C5–X[a]	1.392	1.707
C2–Cα	1.419	1.433

[a] **5**: X=O, **6**: X=S.

and 5 and Section 4.1.1). Thus, the elemental analysis and these spectroscopic data for **5** led to the molecular structure, (2-furyl)(3-guaiazulenyl)methylium hexafluorophosphate.

Compound **6** (98% yield) was red prisms (mp > 160 °C, decomp., determined by the TGA and DTA). The IR (KBr) spectrum showed two specific bands based on the counter anion (PF_6^-) at ν_{max} 837 and 559 cm^{-1}, whose wavenumbers coincided with those of **5**. The molecular formula $C_{20}H_{21}S$ for the carbocation unit was determined by the exact FAB-MS (3-nitrobenzyl alcohol matrix) spectrum. The elemental analysis confirmed the molecular formula $C_{20}H_{21}F_6PS$. A characteristic UV–vis (CH_3CN) absorption band based on the formation of the (3-guaiazulenyl)(2-thienyl)methylium moiety with a delocalized π-electron system appeared at the absorption maximum (λ_{max} 497 nm, log ε=4.73) (see Fig. 2), whose spectral pattern and longest absorption wavelength resembled those of **5**. The ^1H NMR (CD_3CN) spectrum showed signals based on the 3-guaiazulenylmethylium substituent and signals based on the 2-thienyl group, which signals were assigned using similar techniques as in the case of **5** (see Tables 2 and 3 and Section 4.1.2). The ^{13}C NMR (CD_3CN) spectrum exhibited nineteen carbon signals assigned as shown in Tables 4 and 5 and Section 4.1.2. Thus, the elemental analysis and these spectroscopic data for **6** led to the molecular structure, (3-guaiazulenyl)(2-thienyl)methylium hexafluorophosphate.

Compound **7** (85% yield) was dark-green blocks (mp > 155 °C, decomp., determined by the TGA and DTA). The IR (KBr) spectrum showed two specific bands based on the counter anion (PF_6^-) at ν_{max} 840 and 555 cm^{-1}, whose wavenumbers coincided with those of **5** and **6**. The molecular formula $C_{20}H_{22}N$ for the carbocation unit was determined by the exact FAB-MS (3-nitrobenzyl alcohol matrix) spectrum. The elemental analysis confirmed the molecular formula $C_{20}H_{22}F_6NP$. A characteristic UV–vis

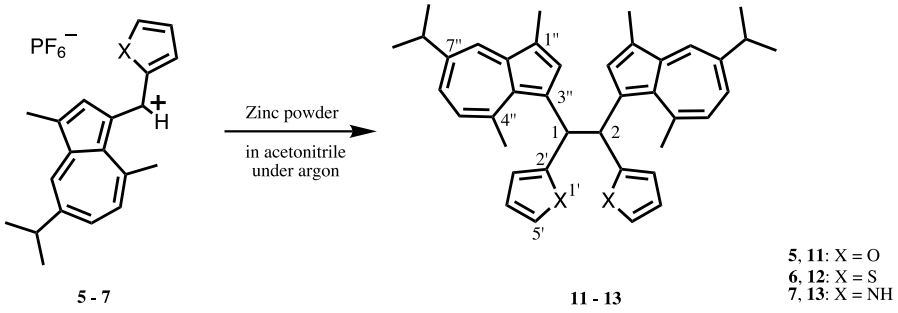

Figure 6. The reductions of **5**–**7** with zinc powder in acetonitrile under argon.

Table 8. The yield/% of the products **11a**,**b**–**13a**,**b** obtained from the reductions of **5**–**7** with zinc powder in acetonitrile under argon

Entry	X	Temperature (°C)	Time	Product		Yield (%)	
				meso	Enantiomers	*meso*	Enantiomers
1	O	25	1.5 h	**11a**	**11b**	36[a]	20[b]
2	S	25	1 h	**12a**	**12b**	23[a]	46[a]
3	NH	25	5 min[c]	**13a**	**13b**	5[a]	5[a]

[a] Isolated yield.
[b] The yield/% of **11b** was calculated based on a ratio of 700 MHz ^1H NMR signals for a mixture of a *meso* form and two enantiomeric forms of **11**.
[c] This reduction for 1 h gave a number of chromatographically inseparable products.

(CH_3CN) absorption band based on the formation of the (3-guaiazulenyl)(2-pyrrolyl)methylium moiety with a delocalized π-electron system appeared at the absorption maximum (λ_{max} 549 nm, log $\varepsilon = 4.86$) (see Fig. 2), which showed a larger bathochromic shift and a hyperchromic effect in comparison with those of **5** and **6**. The ^{1}H NMR (CD_3CN) spectrum showed signals based on the 3-guaiazulenylmethylium substituent and signals based on the 2-pyrrolyl group, which signals were assigned using similar techniques as in the cases of **5** and **6** (see Tables 2 and 3 and Section 4.1.3). The ^{13}C NMR (CD_3CN) spectrum exhibited nineteen carbon signals assigned as shown in Tables 4 and 5 and Section 4.1.3. Thus, the elemental analysis and these spectroscopic data for **7** led to the molecular structure, (3-guaiazulenyl)(2-pyrrolyl)methylium hexafluorophosphate.

2.2. Reduction of 5–7 with $NaBH_4$ and ^{1}H and ^{13}C NMR parameters of 5–10

The reduction of **5** with $NaBH_4$ in acetonitrile at 25 °C for 40 min under aerobic conditions gave as high as 91% yield of (2-furyl)(3-guaiazulenyl)methane (**8**) (see Section 4.1.4), in which a hydride-ion attached to the C-α position of **5**, selectively. Furthermore, a comparative study on the chemical shifts (δ, ppm) for the proton and carbon signals of **5** with those of **A** and **8** revealed (i) that the HC^+-α carbenium-ion center of **5** (8.52 for ^{1}H NMR; 141.0 for ^{13}C NMR) showed larger up-field shifts in comparison with those of **A** (8.78 for ^{1}H NMR; 149.6 for ^{13}C NMR),[13] (ii) that all the proton signals of **5** showed larger down-field shifts in comparison with those of **8** (see Tables 2 and 3), and (iii) that the carbon signals except at the C-2′ and C-2 positions of **5** showed larger down-field shifts in comparison with those of **8** (see Tables 4 and 5).

The reduction of **6** with $NaBH_4$ under the same reaction conditions as **5** afforded as high as 91% yield of (3-guaiazulenyl)(2-thienyl)methane (**9**) (see Section 4.1.5). A comparative study on the chemical shifts for the proton and carbon signals of **6** with those of **5** and **9** revealed (i) that, although the proton signal of the HC^+-α carbenium-ion center of **6** (δ 8.81) showed a larger down-field shift in comparison with that of **5**, it coincided with that of **A**,[13] and the carbon signal of the HC^+-α carbenium-ion center of **6** (δ 140.7) coincided with that of **5**, (ii) that all the proton signals of **6** showed larger down-field shifts in comparison with those of **9** (see Tables 2 and 3), and (iii) that the carbon signals except at the C-2′ and C-2 positions of **6** showed larger down-field shifts in comparison with those of **9** (see Tables 4 and 5).

The reduction of **7** with $NaBH_4$ under the same reaction conditions as **5** and **6** provided as high as 85% yield of (3-guaiazulenyl)(2-pyrrolyl)methane (**10**) (see Section 4.1.6). A comparative study on the chemical shifts for the proton and carbon signals of **7** with those of **5**, **6** and **10** revealed (i) that, although the proton signal of the HC^+-α carbenium-ion center of **7** (δ 8.56) coincided with that of **5**, the carbon signal of the HC^+-α carbenium-ion center of **7** (δ 137.7) showed a larger up-field shift in comparison with those of **5** and **6**, (ii) that all the proton signals of **7** showed larger down-field shifts in comparison with those of **10** (see Tables 2 and 3), and (iii) that the carbon signals except at the C-2′ and C-2 positions of **7** showed larger down-field shifts in comparison with those of **10** (see Tables 4 and 5).

From the $NaBH_4$-reduction of **5**–**7** and the comparative studies on the ^{1}H and ^{13}C NMR parameters of **A** and **5**–**10**, it can be inferred that, although each positive charge of **5**–**7** in acetonitrile is mainly localized at the C-α carbon atom, forming the 3-guaiazulenylmethylium-ion **5**–**7**, the positive charge apparently is transferred to the seven-membered ring and the furyl (or thienyl or pyrrolyl) group, forming the 3-guaiazulenylium **5′**–**7′** and 2-furanylium **5″** (or 2-thienylium **6″** or 2-pyrrolylium **7″**) structures (see Fig. 1).

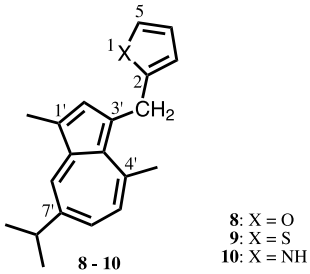

8 - 10

8: X = O
9: X = S
10: X = NH

2.3. X-ray crystal structures of 5 and 6

Although an X-ray crystallographic analysis of **7** has not yet been achieved because of difficulty in obtaining a single crystal suitable for this purpose, the crystal structures of **5** and **6** have been determined by means of the X-ray diffraction, producing accurate structural parameters (see Section 4.2 for **5** and Section 4.3 for **6**). The ORTEP drawings of **5** and **6**, indicating the molecular structures, (2-furyl)(3-guaiazulenyl)methylium and (3-guaiazulenyl)(2-thienyl)methylium hexafluorophosphates, are shown in Figures 3b and 4b. A comparative study on the selected bond distances for the 3-guaiazulenylmethylium substituents and the 2-furyl and 2-thienyl groups of **5** and **6** is shown in Tables 6 and 7. The structural parameters of **5** and **6** revealed (i) that, from the dihedral angle between the least-squares planes, it was found that the plane of the 2-furyl group of **5** twisted by 7.2° from the plane of the 3-guaiazulenyl group owing to the influence of a slight steric hindrance between the oxygen atom of the 2-furyl group and the hydrogen atom of the C2′ position of the 3-guaiazulenyl group, which was smaller than the dihedral angles between the planes of the 2-thienyl and 3-guaiazulenyl groups of **6** (13.7°) and between the planes of the phenyl and 3-guaiazulenyl groups of **A** (21.3°),[4,5] (ii) that, similarly as in the case of **A**, the 3-guaiazulenylmethylium substituents of **5** and **6** clearly underwent bond alternation between the single and double bonds, respectively, in comparison with the bond distances of the 3-guaiazulenyl group of 1,4-bis[(3-guaiazulenyl)methyl]benzene (**B**)[9] yielded from the reduction of 1,4-phenylenebis(3-guaiazulenylmethylium) bis(tetrafluoroborate) with $NaBH_4$,[4] (iii) that the average C–C bond distance for the seven-membered ring of the 3-guaiazulenyl group of **5** (1.403 Å) coincided with those of **6** (1.402 Å) and **A** (1.401 Å), (iv) that the C–C bond distances for the five-membered ring of the 3-guaiazulenyl group of **5** appreciably varied between 1.333 and 1.473 Å; in particular, the C1′–C2′ bond distance (1.333 Å)

was characteristically shorter than the average C–C bond distance for the five-membered ring (1.430 Å), whose bond alternation pattern resembled those of **6** and **A**, (v) that the C3′–Cα bond distance of **5** (1.360 Å) was also characteristically shorter than the C2–Cα bond distance (1.419 Å), and, although the C3′–Cα bond distance of **5** coincided with those of **6** (1.363 Å) and **A** (1.361 Å), the C2–Cα bond distance of **5** was shorter than those of **6** (1.433 Å) and **A** (1.461 Å), (vi) that the Cα–C2 bond distance (1.419 Å) for the (2-furyl)methylium unit of **5** was characteristically shorter than the Cα–C2 bond distance (1.517 Å) for the (2-furyl)methyl unit of tetrakis(2-furyl)methane (**C**),[14] and, further, although the C2–C3 (1.369 Å) and C5–O1 (1.392 Å) bond distances of the 2-furyl group of **5** were longer than those of **C** [C2–C3 (1.347 Å) and C5–O1 (1.375 Å)], the O1–C2 (1.363 Å), C3–C4 (1.414 Å) and C4–C5 (1.322 Å) bond distances of **5** were shorter than those of **C** [O1–C2 (1.370 Å), C3–C4 (1.431 Å) and C4–C5 (1.331 Å)], and (vii) that the Cα–C2 bond distance (1.433 Å) for the (2-thienyl)methylium unit of **6** was characteristically shorter than the C1–C2′ bond distance (1.511 Å) for the (2-thienyl)methyl unit of (1*R*,2*R*)- and (1*S*,2*S*)-1,2-di(3-guaiazulenyl)-1,2-di(2-thienyl)ethanes (**12b**) [see Fig. 7b caption] yielded by the reduction of **6** with zinc powder (see Sections 2.5 and 4.3.2), and, further, although the S1–C2 (1.721 Å), C2–C3 (1.413 Å), C4–C5 (1.342 Å) and C5–S1 (1.707 Å) bond distances of the 2-thienyl group of **6** were longer than those of **12b** [S1′–C2′ (1.716 Å), C2′–C3′ (1.402 Å), C4′–C5′ (1.334 Å) and C5′–S1′ (1.697 Å)], the C3–C4 (1.404 Å) bond distance of **6** was shorter than that of **12b** [C3′–C4′ (1.419 Å)]. Moreover, it can be inferred (i) that, from a comparative study on the bond distances of **5**, **6**, **A**, **C** and **12b**, although the positive charge of **5** in the single crystal is mainly localized at the Cα carbon atom, forming the 3-guaiazulenylmethylium-ion **5**, the positive charge apparently is transferred to the seven-membered ring and the furyl group, forming the 3-guaiazulenylium **5′** and 2-furanylium **5″** structures (see Fig. 1), and, further, the same result can be inferred about **6** (see Fig. 1), and (ii) that, from the result of the dihedral angle between the least-squares planes of the 3-guaiazulenyl and 2-furyl (or 2-thienyl) groups for **5** (or **6**), formation of a

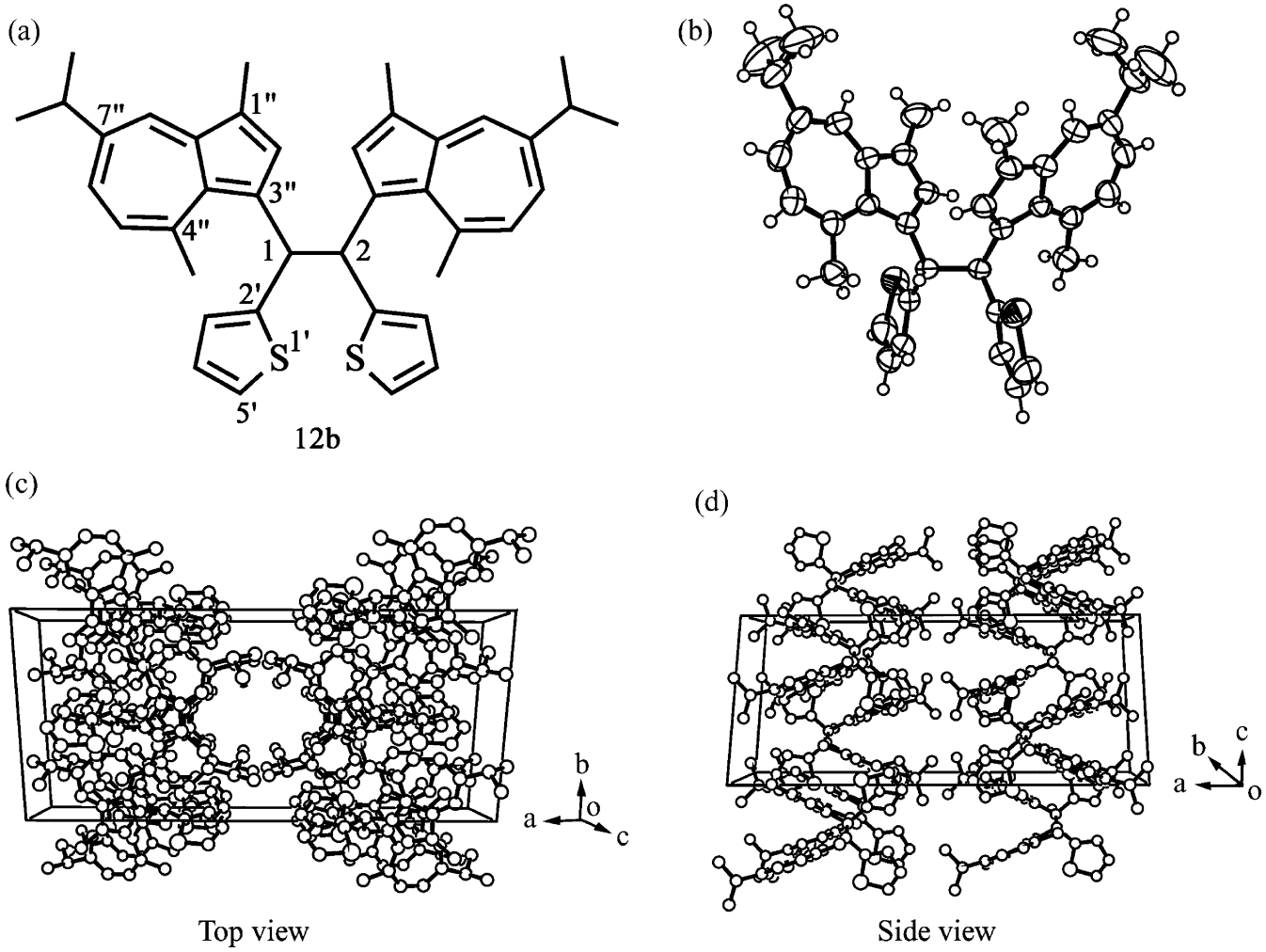

Figure 7. (a) The molecular structure of **12b**. (b) The ORTEP drawing of **12b** (30% probability thermal ellipsoids). The selected bond distances (Å) are as follows: S1′–C2′; 1.716(3), C2′–C3′; 1.402(4), C3′–C4′; 1.419(5), C4′–C5′; 1.334(6), C5′–S1′; 1.697(4), C2′–C1; 1.511(4), C1–C3″; 1.521(4), C1″–C2″; 1.389(4), C2″–C3″; 1.394(4), C3″–C3a″; 1.416(4), C3a″–C4″; 1.411(4), C4″–C5″; 1.405(4), C5″–C6″; 1.379(5), C6″–C7″; 1.381(5), C7″–C8″; 1.393(5), C8″–C8a″; 1.395(4), C8a″–C1″; 1.404(4), C8a″–C3a″; 1.507(4) and C1–C2; 1.596(5). The two different [top (c) and side (d)] views for the packing (molecular) structure of **12b**; hydrogen atoms are omitted for reasons of clarity.

conjugated π-electron system between them, which combined with the Cα carbon atom respectively, is possible.

Along with the crystal structures of **5** (and **6**), the two different (top and side) views for the packing (molecular) structures of **5** (and **6**) revealed that these molecules formed π-stacking structures in the single crystals, respectively, and that the average inter-plane distance between the overlapping molecules [i.e., the 3-guaiazulenylmethylium plane of a molecule and the 2-furyl (or 2-thienyl) plane of another molecule], which were overlapped so that those dipole moments might be negated mutually, was 3.63 Å for **5** [see Fig. 3c and d], and was 3.80 Å for **6** [see Fig. 4c and d].

2.4. Electrochemical behavior of 5–7

We have been interested further in the electrochemical properties of the monocarbenium hexafluorophosphates **5**, **6** and **7** with a view to a comparative study of them. The electrochemical behavior of **5**–**7** was, therefore, measured by means of the CV and DPV (Potential/V vs SCE) in CH_3CN containing 0.1 M $[n\text{-}Bu_4N]PF_6$ as a supporting electrolyte. From a comparative study on the reduction potentials of **5**–**7** with those of the previously-documented monocarbocation compounds stabilized by a 3-guaiazulenyl group,[3,5–7,9] it can be inferred that **5**, **6** and **7** undergo one-electron reduction, respectively, at the potentials of −0.27 (E_{pc}, irreversible) V by CV (−0.21 V by DPV) for **5**, −0.22 (E_{pc}, irreversible) V by CV (−0.16 V by DPV) for **6** and −0.44 (E_{pc}, irreversible) V by CV (−0.38 V by DPV) for **7** as shown in Figure 5, generating the corresponding (2-furyl)(3-guaiazulenyl)methyl, (3-guaiazulenyl)(2-thienyl)methyl and (3-guaiazulenyl)(2-pyrrolyl)methyl radical-species, which are rapidly converted into the radical homo-coupling products, respectively. Thus, **7** is less susceptible to reduction as compared with **5** and **6**, owing to the difference in electron affinity (corresponding to LUMO) based on those molecular structures and, further, the CV and DPV data of **7** resembled those of [4-(dimethylamino)phenyl](3-guaiazulenyl)methylium tetrafluoroborate (**D**) [−0.47 (E_{pc}, irreversible) V by CV (−0.39 V by DPV)].[5,9,15] The facility of one-electron reduction is in the order of **6**>**5**≫**7**; namely, the order of higher stability based on each reduction potential is **7**≫**5**>**6** and these different reduction potentials are obviously caused by the influence of a different heteroaromatic ring for **5**–**7**.

2.5. Reduction of 5–7 with zinc powder

In the previous papers,[5,9] we reported that the reductions of the four monocarbocation compounds stabilized by 3-guaiazulenyl and aryl groups with zinc powder in acetonitrile (or dichloromethane) at 25 °C for 20 min–2 h under argon gave a mixture of a *meso* form and two enantiomeric forms of the molecular structures, 1,2-diaryl-1,2-di(3-guaiazulenyl)ethanes, respectively. Furthermore, we clarified the crystal structure of the *meso* form, (1*R*,2*S*)-1,2-bis[4-(methoxycarbonyl)phenyl]-1,2-di(3-guaiazulenyl)ethane (**E**), by means of the X-ray diffraction.[9] We have been interested further in the reduction of **5**, **6** and **7** with zinc powder with a view to a comparative study with those of the monocarbocation compounds stabilized by 3-guaiazulenyl and aryl groups.

The reduction of **5** with zinc powder in acetonitrile at 25 °C for 1.5 h under argon gave 1,2-di(2-furyl)-1,2-di(3-guaiazulenyl)ethane (**11**) in 80% yield (see Section 4.3.1). A careful study of the 700 MHz ^{1}H NMR signals for **11** led us to a ca. 3:1, chromatographically inseparable mixture of a *meso* form, (1*R*,2*S*)-1,2-di(2-furyl)-1,2-di(3-guaiazulenyl)ethane (**11a**), and two enantiomeric forms, (1*R*,2*R*)- and (1*S*,2*S*)-1,2-di(2-furyl)-1,2-di(3-guaiazulenyl)ethanes (**11b**). Moreover, the product **11** was recrystallized from dichloromethane–methanol (1/5, vol/vol) (several times) to provide the crystals of only its *meso* form **11a**[16] in 36% isolated yield, whose molecular structure was established on the basis of elemental analysis and spectroscopic data [UV–vis, FAB-MS and ^{1}H and ^{13}C NMR including 2D NMR (i.e., H–H COSY, HMQC and HMBC)] (see Section 4.3.1).

The reduction of **6** with zinc powder in acetonitrile at 25 °C for 1 h under argon afforded a chromatographically separable mixture of the *meso* form, (1*R*,2*S*)-1,2-di(3-guaiazulenyl)-1,2-di(2-thienyl)ethane (**12a**),[16] in 23% isolated yield and the enantiomers, (1*R*,2*R*)- and (1*S*,2*S*)-1,2-di(3-guaiazulenyl)-1,2-di(2-thienyl)ethanes (**12b**),[16] in 46% isolated yield, whose molecular structures were established on the basis of similar analyses as **11a** (see Section 4.3.2). A careful study of the 500 MHz ^{1}H NMR signals for **12a** and **12b** led us to a *meso* form **12a** and two enantiomeric forms **12b** of the molecular structure, 1,2-di(3-guaiazulenyl)-1,2-di(2-thienyl)ethane (**12**). It is noteworthy that, although the product **11** was a ca. 3:1, chromatographically inseparable mixture of a *meso* form **11a** and two enantiomeric forms **11b**, the product **12** was a ca. 1:2, chromatographically separable mixture of a *meso* form **12a** and two enantiomeric forms **12b**.

Although the reduction of **7** with zinc powder in acetonitrile at 25 °C for 1 h under argon gave a number of chromatographically inseparable products, this reaction for 5 min afforded a separable mixture of the *meso* form, (1*R*,2*S*)-1,2-di(3-guaiazulenyl)-1,2-di(2-pyrrolyl)ethane (**13a**), in 5% isolated yield and the enantiomers, (1*R*,2*R*)- and (1*S*,2*S*)-1,2-di(3-guaiazulenyl)-1,2-di(2-pyrrolyl)-ethanes (**13b**), in 5% isolated yield, whose molecular structures were established on the basis of similar analyses as **11a** (see Section 4.3.3). A careful study of the 500 MHz ^{1}H NMR signals for **13a** and **13b** led us to a *meso* form **13a** and two enantiomeric forms **13b** of the molecular structure, 1,2-di(3-guaiazulenyl)-1,2-di(2-pyrrolyl)ethane (**13**).

2.6. ^{1}H NMR parameters of 11a,b–13a,b

An inspection of the molecular models of the most favorable conformations suggested that in the *meso* form **11a** an anisotropic effect exerted by the (2-furyl)(3-guaiazulenyl)-methyl region of the other moiety was likely to cause apparent up- and down-field shifts of the signals for the HC-1 (δ 6.17) of the ethane unit and the H-3′, 4′, 5′ (5.72, 5.93, 7.05) of the 2-furyl group and the Me-1″ (2.60), H-8″ (8.02) of the 3-guaiazulenyl group in comparison with those [the HC-1 (δ 6.10) of the ethane unit and the H-3′, 4′, 5′ (5.86, 6.17, 7.23) of the 2-furyl group and the Me-1″ (2.43), H-8″ (7.89) of the 3-guaiazulenyl group] of the enantiomers **11b**.

Table 9. The ^{1}H NMR chemical shifts (δ, ppm) for the 3-guaiazulenylmethyl groups of **11a**,**b**–**13a**,**b**

Compound	HC-1	Me-1″	H-2″	Me-4″	H-5″	H-6″	$(Me)_2CH$-7″	$(Me)_2CH$-7″	H-8″
11a	6.17	2.60	7.88	3.20	6.85	7.24	2.99	1.31	8.02
11b	6.10	2.43	7.83	3.18	6.83	7.20	2.94	1.259, 1.261	7.89
12a	6.30	2.65	7.94	3.10	6.84	7.26	3.02	1.34	8.07
12b	6.14	2.45	7.83	3.22	6.85	7.23	2.95	1.276, 1.283	7.93
13a	5.90	2.64	7.70	2.90	6.83	7.28	3.05	1.36	8.12
13b	5.78	2.46	7.70	3.02	6.81	7.23	2.97	1.287, 1.292	7.96

Similarly, as in the cases of the *meso* form **11a** and the two enantiomeric forms **11b**, an inspection of the molecular models of the most favorable conformations suggested that in the *meso* form **12a** an anisotropic effect exerted by the (3-guaiazulenyl)(2-thienyl)methyl region of the other moiety was likely to cause apparent up- and down-field shifts of the signals for the HC-1 (δ 6.30) of the ethane unit and the H-3′, 4′, 5′ (6.39, 6.56, 6.88) of the 2-thienyl group and the Me-1″ (2.65), H-2″ (7.94), Me-4″ (3.10), H-8″ (8.07) of the 3-guaiazulenyl group in comparison with those [the HC-1 (δ 6.14) of the ethane unit and the H-3′, 4′, 5′ (6.46, 6.75, 7.09) of the 2-thienyl group and the Me-1″ (2.45), H-2″ (7.83), Me-4″ (3.22), H-8″ (7.93) of the 3-guaiazulenyl group] of the enantiomers **12b**.

Similarly, as in the cases of the *meso* forms **11a**, **12a** and the enantiomers **11b**, **12b**, an inspection of the molecular models of the most favorable conformations suggested that in the *meso* form **13a** an anisotropic effect exerted by the (3-guaiazulenyl)(2-pyrrolyl)methyl region of the other moiety was likely to cause apparent up- and down-field shifts of the signals for the HC-1 (δ 5.90) of the ethane unit and the H-3′, 4′, 5′ (5.29, 5.75, 6.27) of the 2-pyrrolyl group and the Me-1″ (2.64), Me-4″ (2.90), H-8″ (8.12) of the 3-guaiazulenyl group in comparison with those [the HC-1 (δ 5.78) of the ethane unit and the H-3′, 4′, 5′ (5.47, 6.00, 6.53) of the 2-pyrrolyl group and the Me-1″ (2.46), Me-4″ (3.02), H-8″ (7.96) of the 3-guaiazulenyl group] of the enantiomers **13b**.

Furthermore, in the enantiomers **11b**, **12b** and **13b** an anisotropic effect would cause division of the methyl protons of the isopropyl-7″ group into two signals (a ratio of almost 1:1). These findings enabled us to make the most plausible assignment of all the ^{1}H NMR signals of these six compounds **11a**,**b**–**13a**,**b** (see Tables 9 and 10 and Sections 4.3.1–4.3.3).

2.7. X-ray crystal structure of the enantiomers 12b

Although the X-ray crystallographic analyses of **11a**,**b**, **12a** and **13a**,**b** have not yet been achieved because of difficulty in obtaining a single crystal suitable for this purpose, respectively, the crystal structure of the enantiomers **12b** has been determined by means of the X-ray diffraction, producing accurate structural parameters (see Section 4.4). The crystal structure of **12b**, indicating an enantiomeric form, (1*R*,2*R*)-1,2-di(3-guaiazulenyl)-1,2-di(2-thienyl)-ethane, is shown in Figure 7b together with the selected bond distances. A comparative study on the structural parameters of **12b** with those of (1*R*,2*S*)-1,2-bis[4-(methoxycarbonyl)phenyl]-1,2-di(3-guaiazulenyl)ethane (**E**)[9] revealed (i) that the C–C bond distance for the C1–C2 (1.596 Å) of the ethane unit was longer than that for the C1–C2 (1.529 Å) of the ethane unit of **E**, (ii) that the average C–C bond distance for the seven-membered ring of the 3″-guaiazulenyl group (1.410 Å) coincided with the C–C bond distance observed for that of the 3″-guaiazulenyl group of **E** (1.406 Å), (iii) that the C–C bond distances for the five-membered ring of the 3″-guaiazulenyl group appreciably varied between 1.389 and 1.507 Å; in particular, the C1″–C2″ bond distance (1.389 Å) was characteristically shorter than the average C–C bond distance (1.422 Å) for the five-membered ring of the 3″-guaiazulenyl group, whose bond alternation pattern resembled that of the 3″-guaiazulenyl group of **E**, and (iv) that the average C–C bond distance for the five-memberd ring of the 3″-guaiazulenyl group coincided with that of the 3″-guaiazulenyl group of **E** (1.424 Å). Along with the crystal structure of **12b**, the two different (top and side) views for the packing (molecular) structure of **12b** revealed that **12b** did not form a π-stacking structure in the single crystal [see Fig. 7c and d].

Table 10. The ^{1}H NMR chemical shifts (δ, ppm) for the 2-furyl, 2-thienyl and 2-pyrrolyl groups of **11a**,**b**–**13a**,**b**

Compound	H-3′	H-4′	H-5′
11a	5.72	5.93	7.05
11b	5.86	6.17	7.23
12a	6.39	6.56	6.88
12b	6.46	6.75	7.09
13a	5.29	5.75	6.27
13b	5.47	6.00	6.53

3. Conclusion

We have reported the following six points in this paper: (i) the reactions of guaiazulene (**1**) with 2-furaldehyde (**2**), thiophene-2-carbaldehyde (**3**) and pyrrole-2-carbaldehyde (**4**) in methanol in the presence of hexafluorophosphoric acid at 25 °C for 30 min under aerobic conditions gave the corresponding monocarbocation compounds, (2-furyl)(3-guaiazulenyl)methylium hexafluorophosphate (**5**), (3-guaiazulenyl)(2-thienyl)methylium hexafluorophosphate (**6**) and (3-guaiazulenyl)(2-pyrrolyl)methylium hexafluorophosphate (**7**), respectively, in 93, 98 and 85% yields; (ii) the spectroscopic data of the products **5**–**7** and, further, the chemical evidence (i.e., the reduction of **5**–**7** with $NaBH_4$) led to the molecular structures **5**–**7** with the two representative resonance forms [i.e., 3-guaiazulenylium **5**′–**7**′ and 2-furanylium **5**″ (or 2-thienylium **6**″ or 2-pyrrolylium **7**″) structures] in acetonitrile; (iii) along with the spectroscopic data for **5**–**7** in acetonitrile, the X-ray crystallographic analyses for **5** and **6** also led to the crystal structures **5** and **6** with the resonance forms of the 3-guaiazulenylium **5**′, **6**′ and 2-furanylium **5**″ (or

2-thienylium **6″**) structures; (iv) a comparative study on the reduction potentials of **5**–**7** based on their CV and DPV data indicated that the facility of one-electron reduction was in the order of **6** > **5** ≫ **7**; namely, the order of higher stability based on each reduction potential was **7** ≫ **5** > **6**; (v) the reduction of **5**–**7** with zinc powder in acetonitrile at 25 °C under argon afforded a mixture of a *meso* form (**a**) and two enantiomeric forms (**b**) of the molecular structures, 1,2-di(2-furyl)-1,2-di(3-guaiazulenyl)ethane (**11**), 1,2-di(3-guaiazulenyl)-1,2-di(2-thienyl)ethane (**12**) and 1,2-di(3-guaiazulenyl)-1,2-di(2-pyrrolyl)ethane (**13**), respectively, and, further, a careful study of the ^{1}H NMR signals for **11a**,**b**–**13a**,**b** led us to the *meso* forms **11a**, **12a**, **13a** and the two enantiomeric forms **11b**, **12b**, **13b**; and (vi) along with the spectroscopic data for **11a**,**b**–**13a**,**b**, the crystal structure of the enantiomers **12b** compared with that of the *meso* form, (1*R*,2*S*)-1,2-bis[4-(methoxycarbonyl)phenyl]-1,2-di(3-guaiazulenyl)ethane (**E**), was reported.

4. Experimental

4.1. General

Thermal (TGA/DTA) and elemental analyses were taken on a Shimadzu DTG-50H thermal analyzer and a Yanaco MT-3 CHN corder, respectively. MS spectra were taken on a JEOL The Tandem Mstation JMS-700 TKM data system. UV–vis and IR spectra were taken on a Beckman DU640 spectrophotometer and a Shimadzu FTIR-4200 Grating spectrometer, respectively. NMR spectra were recorded with a JEOL GX-500 (500 MHz for ^{1}H and 125 MHz for ^{13}C) and JNM-ECA700 (700 MHz for ^{1}H and 176 MHz for ^{13}C) cryospectrometers at 25 °C. The ^{1}H NMR spectra were assigned using the computer-assisted simulation analysis (the software: gNMR developed by Adept Scientific plc) on a DELL Dimension XPS T500 personal-computer with a Pentium III processor. Cyclic and differential pulse voltammograms were measured by an ALS Model 600 electrochemical analyzer.

4.1.1. Preparation of (2-furyl)(3-guaiazulenyl)methylium hexafluorophosphate (5). To a solution of hexafluorophosphoric acid (60% aqueous solution, 0.3 mL) was added a solution of guaiazulene (**1**) (85 mg, 0.43 mmol) in methanol (2.0 mL) containing 2-furaldehyde (**2**) (50 μL, 0.60 mmol). The mixture was stirred at 25 °C for 30 min under aerobic conditions, giving a precipitation of a red solid, and then was centrifuged at 2.5 krpm for 1 min. The crude product thus obtained was carefully washed with diethyl ether, and was recrystallized from acetonitrile–diethyl ether (1/5, vol/vol) (several times) to provide pure **5** as stable single crystals (168 mg, 0.40 mmol, 93% yield).

Compound **5**. Red prisms, mp > 150 °C [decomp., determined by thermal analysis (TGA and DTA)]. Found: C, 57.00; H, 4.90%. Calcd for $C_{20}H_{21}F_6OP$: C, 56.88; H, 5.01%; UV–vis λ_{max} (CH_3CN) nm (log ε), 224 (4.42), 262 (4.16), 321sh (4.12), 334 (4.18), 412 (4.17) and 499 (4.61); IR ν_{max} (KBr) cm^{-1}, 840 and 559 (PF_6^-); exact FAB-MS (3-nitorobenzyl alcohol matrix), found: *m*/*z* 277.1604; calcd for $C_{20}H_{21}O$: $[M-PF_6]^+$, 277.1592; 500 MHz ^{1}H NMR (CD_3CN), signals based on the 3-guaiazulenylmethyium substituent: δ 1.45 (6H, d, J=6.9 Hz, (CH_3)$_2$CH-7′), 2.55 (3H, s, Me-1′), 3.29 (3H, s, Me-4′), 3.47 (1H, sept, J=6.9 Hz, (CH_3)$_2$C*H*-7′), 8.31 (1H, s, H-2′), 8.35 (1H, dd, J=11.5, 2.0 Hz, H-6′), 8.39 (1H, d, J=11.5 Hz, H-5′), 8.52 (1H, s, HC$^+$-α) and 8.55 (1H, d, J=2.0 Hz, H-8′); signals based on the 2-furyl group: δ 6.85 (1H, dd, J=3.7, 1.7 Hz, H-4), 7.54 (1H, d, J=3.7 Hz, H-3) and 8.01 (1H, d, J=1.7 Hz, H-5); 125 MHz ^{13}C NMR (CD_3CN), δ 168.5 (C-7′), 158.8 (C-8a′), 155.8 (C-4′), 152.8 (C-5), 152.51 (C-3a′), 152.46 (C-3′), 148.4 (C-5′), 143.9 (C-6′), 143.5 (C-1′), 141.0 (HC$^+$-α), 138.7 (C-8′), 133.7 (C-2), 131.0 (C-2′), 129.3 (C-3), 115.3 (C-4), 39.1 ((CH_3)$_2$*C*H-7′), 28.6 (Me-4′), 22.9 ((CH$_3$)$_2$CH-7′) and 13.0 (Me-1′).

4.1.2. Preparation of (3-guaiazulenyl)(2-thienyl)methylium hexafluorophosphate (6). To a solution of guaiazulene (**1**) (120 mg, 0.61 mmol) in methanol (3.0 mL) was added a solution of thiophene-2-carbaldehyde (**3**) (80 μL, 0.88 mmol) in methanol (1.0 mL) containing hexafluorophosphoric acid (60% aqueous solution, 0.2 mL). The mixture was stirred at 25 °C for 30 min under aerobic conditions, giving a precipitation of a dark-red solid of **6**, and then was centrifuged at 2.5 krpm for 1 min. The crude product thus obtained was carefully washed with diethyl ether, and was recrystallized from acetonitrile–diethyl ether (1/5, vol/vol) (several times) to provide pure **6** as stable single crystals (263 mg, 0.59 mmol, 98% yield).

Compound **6**. Red prisms, mp > 160 °C [decomp., determined by thermal analysis (TGA and DTA)]. Found: C, 55.13; H, 4.74%. Calcd for $C_{20}H_{21}F_6PS$: C, 54.79; H, 4.83%; UV–vis λ_{max} (CH_3CN) nm (log ε), 227 (4.57), 269 (4.26), 290sh (4.15), 320sh (4.27), 334 (4.32), 408sh (4.19) and 497 (4.73); IR ν_{max} (KBr) cm^{-1}, 837 and 559 (PF_6^-); exact FAB-MS (3-nitrobenzyl alcohol matrix), found: *m*/*z* 293.1360; calcd for $C_{20}H_{21}S$: $[M-PF_6]^+$, 293.1364; 700 MHz ^{1}H NMR (CD_3CN), signals based on the 3-guaiazulenylmethylium substituent: δ 1.45 (6H, d, J=7.1 Hz, (CH_3)$_2$CH-7′), 2.56 (3H, d, J=1.0 Hz Me-1′), 3.32 (3H, s, Me-4′), 3.46 (1H, sept, J=7.1 Hz, (CH_3)$_2$C*H*-7′), 8.24 (1H, br d, s, H-2′), 8.36 (1H, dd, J=11.2, 2.2 Hz, H-6′), 8.43 (1H, d, J=11.2 Hz, H-5′), 8.56 (1H, d, J=2.2 Hz, H-8′) and 8.81 (1H, s, HC$^+$-α); signals based on the 2-thienyl group: δ 7.34 (1H, dd, J=4.8, 3.9 Hz, H-4), 7.94 (1H, d, J=4.8 Hz, H-3) and 8.13 (1H, d, J=3.9 Hz, H-5); 176 MHz ^{13}C NMR (CD_3CN), δ 168.9 (C-7′), 159.0 (C-8a′), 156.3 (C-4′), 152.9 (C-3a′), 148.8 (C-5′), 144.5 (C-1′), 143.8 (C-6′), 142.4 (C-3), 140.7 (HC$^+$-α), 139.9 (C-5), 139.7 (C-8′), 139.1 (C-2′), 138.6 (C-2), 135.1 (C-3′), 130.0 (C-4), 39.1 ((CH_3)$_2$*C*H-7′), 28.9 (Me-4′), 22.9 ((CH$_3$)$_2$CH-7′) and 13.0 (Me-1′).

4.1.3. Preparation of (3-guaiazulenyl)(2-pyrrolyl)-methylium hexafluorophosphate (7). To a solution of guaiazulene (**1**) (64 mg, 0.32 mmol) in methanol (1.5 mL) was added a solution of pyrrole-2-carbaldehyde (**4**) (20 mg, 0.21 mmol) in methanol (0.5 mL) containing hexafluorophosphoric acid (60% aqueous solution, 0.2 mL). The mixture was stirred at 25 °C for 30 min under aerobic conditions, giving a precipitation of a purple solid of **7**, and then was centrifuged at 2.5 kprm for 1 min. The crude product thus obtained was carefully washed with diethyl ether, and was recrystallized from acetonitorile–diethyl

ether (1/5, vol/vol) (several times) to provide pure **7** as stable single crystals (77 mg, 0.18 mmol, 85% yield).

Compound **7**. Dark-green blocks, mp>155 °C [decomp., determined by thermal analysis (TGA and DTA)]. Found: C, 57.01; H, 5.26; N, 3.33%. Calcd for $C_{20}H_{22}F_6NP$: C, 57.01; H, 5.26; N, 3.32%; UV–vis λ_{max} (CH_3CN) nm (log ε), 232 (4.44), 266 (4.21), 339 (4.19), 412 (3.77) and 549 (4.86); IR ν_{max} (KBr) cm^{-1}, 3390 (N–H), 1577 (C–N), 840 and 555 (PF_6^-); exact FAB-MS (3-nitrobenzyl alcohol matrix), found: *m/z* 276.1768; calcd for $C_{20}H_{22}N$: $[M-PF_6]^+$, *m/z* 276.1752; 500 MHz ^1H NMR (CD_3CN), signals based on the 3-guaiazulenylmethylium substituent: δ 1.44 (6H, d, $J=6.9$ Hz, $(CH_3)_2$CH-7′), 2.57 (3H, d, $J=1.0$ Hz, Me-1′), 3.26 (3H, s, Me-4′), 3.40 (1H, sept, $J=6.9$ Hz, $(CH_3)_2CH$-7′), 8.18 (1H, d, $J=11.2$ Hz, H-5′), 8.19 (1H, dd, $J=11.2$, 1.7 Hz, H-6′), 8.20 (1H, br d, s, H-2′), 8.51 (1H, d, $J=1.7$ Hz, H-8′) and 8.56 (1H, s, HC^+-α); signals based on the 2-pyrrolyl group: δ 6.67 (1H, dd, $J=4.0$, 2.5 Hz, H-4), 7.50 (1H, dd, $J=2.5$, 1.7 Hz, H-3), 7.62 (1H, br d, dd, $J=4.0$, 1.7 Hz, H-5) and 10.62 (1H, br d, s, N–H); 125 MHz ^{13}C NMR (CD_3CN), δ 163.0 (C-7′), 154.9 (C-8a′), 153.9 (C-4′), 150.4 (C-3a′), 144.8 (C-5′), 142.0 (C-6′), 140.4 (C-1′), 139.7 (C-2′), 138.2 (C-8′), 137.7 (HC^+-α), 134.9 (C-5), 132.0 (C-2), 129.8 (C-3′), 126.5 (C-3), 116.9 (C-4), 38.7 ($(CH_3)_2C$H-7′), 28.8 (Me-4′), 23.1 ($(CH_3)_2$CH-7′) and 12.7 (Me-1′).

4.1.4. Reduction of (2-furyl)(3-guaiazulenyl)methylium hexafluorophosphate (5) with $NaBH_4$. To a solution of $NaBH_4$ (9 mg, 238 μmol) in acetonitrile (2.0 mL) was added a solution of **5** (45 mg, 106 μmol) in acetonitrile (2.0 mL). The mixture was stirred at 25 °C for 40 min under aerobic conditions and then evaporated in vacuo. The residue thus obtained was dissolved in hexane and filtered. The hexane-filtrate was evaporated in vacuo, giving a pure (2-furanyl)(3-guaiazuleyl)methane (**8**) as a blue paste (27 mg, 97 μmol, 92% yield).

Compound **8**. Exact FAB-MS (3-nitorobenzyl alcohol matrix), found: *m/z* 278.1687; calcd for $C_{20}H_{22}O$: M^+, 278.1671; 500 MHz ^1H NMR (CD_3CN), signals based on the 3-guaiazuleneylmethyl group: δ 1.30 (6H, d, $J=6.8$ Hz, $(CH_3)_2$CH-7′), 2.56 (3H, s, Me-1′), 2.85 (3H, s, Me-4′), 3.00 (1H, sept, $J=6.8$ Hz, $(CH_3)_2CH$-7′), 4.99 (2H, s, 2-CH_2-3′), 6.82 (1H, d, $J=10.7$ Hz, H-5′), 7.28 (1H, dd, $J=10.7$, 2.0 Hz, H-6′), 7.38 (1H, s, H-2′) and 8.11 (1H, d, $J=2.0$ Hz, H-8′); signals based on the 2-furyl group: δ 5.72 (1H, dd, $J=3.2$, 0.9 Hz, H-3), 6.25 (1H, dd, $J=3.2$, 2.0 Hz, H-4) and 7.35 (1H, dd, $J=2.0$, 0.9 Hz, H-5); 125 MHz ^{13}C NMR (CD_3CN), δ 157.7 (C-2), 146.1 (C-4′), 142.1 (C-5), 141.3 (C-2′), 140.2 (C-7′), 138.9 (C-8a′), 135.7 (C-6′), 134.4 (C-8′), 133.4 (C-3a′), 127.2 (C-5′), 125.1 (C-1′), 124.0 (C-3′), 111.5 (C-4), 106.7 (C-3), 38.3 ($(CH_3)_2C$H-7′), 30.8 (2-CH_2-3′), 26.7 (Me-4′), 24.7 ($(CH_3)_2$CH-7′) and 12.9 (Me-1′).

4.1.5. Reduction of (3-guaiazulenyl)(2-thienyl)methylium hexafluorophosphate (6) with $NaBH_4$. To a solution of **6** (31 mg, 71 μmol) in acetonitrile (2.0 mL) was added a solution of $NaBH_4$ (4 mg, 106 μmol) in ethanol (1.0 mL). The mixture was stirred at 25 °C for 40 min under aerobic conditions and then evaporated in vacuo. The residue thus obtained was carefully separated by silica-gel column chromatography with hexane–diethyl ether (9/1, vol/vol) as an eluant, giving a pure (3-guaiazulenyl)(2-thienyl)-methane (**9**) as a blue paste (19 mg, 65 μmol, 92% yield).

Compound **9**. Exact FAB-MS (3-nitorobenzyl alcohol matrix), found: *m/z* 294.1460; calcd for $C_{20}H_{22}S$: M^+, 294.1442; 500 MHz ^1H NMR (CD_3CN), signals based on the 3-guaiazulenylmethyl group: δ 1.32 (6H, d, $J=6.9$ Hz, $(CH_3)_2$CH-7′), 2.58 (3H, s, Me-1′), 2.85 (3H, s, Me-4′), 3.03 (1H, sept, $J=6.9$ Hz, $(CH_3)_2CH$-7′), 4.69 (2H, s, 2-CH_2-3′), 6.85 (1H, d, $J=10.9$ Hz, H-5′), 7.33 (1H, dd, $J=10.9$, 2.3 Hz, H-6′), 7.48 (1H, s, H-2′) and 8.13 (1H, d, $J=2.3$ Hz, H-8′); signals based on the 2-thienyl group: δ 6.64 (1H, dd, $J=3.6$, 1.2 Hz, H-3), 6.88 (1H, dd, $J=5.2$, 3.6 Hz, H-4) and 7.14 (1H, dd, $J=5.2$, 1.2 Hz, H-5); 125 MHz ^{13}C NMR (CD_3CN), δ 149.0 (C-2), 146.3 (C-4′), 140.4 (C-2′), 140.4 (C-7′), 138.9 (C-8a′), 135.9 (C-6′), 134.5 (C-8′), 133.4 (C-3a′), 127.8 (C-4), 127.3 (C-5′), 126.6 (C-3′), 125.2 (C-3), 124.9 (C-5), 124.7 (C-1′), 38.3 ($(CH_3)_2C$H-7′), 32.1 (2-CH_2-3′), 26.7 (Me-4′), 24.7 ($(CH_3)_2$CH-7′) and 12.9 (Me-1′).

4.1.6. Reduction of (3-guaiazulenyl)(2-pyrrolyl)methylium hexafluorophosphate (7) with $NaBH_4$. To a solution of $NaBH_4$ (9 mg, 238 μmol) in ethanol (1.5 mL) was added a solution of **7** (45 mg, 110 μmol) in acetonitrile (2.0 mL). The mixture was stirred at 25 °C for 40 min under aerobic conditions and then evaporated in vacuo. The residue thus obtained was carefully separated by silica-gel column chromatography with hexane–diethyl ether (8/2, vol/vol) as an eluant, giving a pure (3-guaiazulenyl)(2-pyrrolyl)-methane (**10**) as a blue paste (26 mg, 94 μmol, 85% yield).

Compound **10**. Exact FAB-MS (3-nitrobenzyl alcohol matrix), found: *m/z* 277.1849; calcd for $C_{20}H_{23}N$: M^+, *m/z* 277.1830; 500 MHz ^1H NMR (CD_3CN), signals based on the 3-guaiazulenylmethyl group: δ 1.31 (6H, d, $J=6.9$ Hz, $(CH_3)_2$CH-7′), 2.57 (3H, d, $J=1.0$ Hz, Me-1′), 2.86 (3H, s, Me-4′), 3.02 (1H, sept, $J=6.9$ Hz, $(CH_3)_2CH$-7′), 4.47 (1H, s, 2-CH_2-3′), 6.82 (1H, d, $J=10.8$ Hz, H-5′), 7.30 (1H, dd, $J=10.8$, 2.3 Hz, H-6′), 7.41 (1H, s, H-2′) and 8.10 (1H, d, $J=2.3$ Hz, H-8′); signals based on the 2-pyrrolyl group: δ 5.58 (1H, dd, $J=5.0$, 2.6 Hz, H-4), 5.95 (1H, dd, $J=2.6$, 1.3 Hz, H-3), 6.56 (1H, dd, $J=5.0$, 1.3 Hz, H-5) and 8.69 (1H, br d, s, N–H); 125 MHz ^{13}C NMR (CD_3CN), δ 146.4 (C-4′), 141.6 (C-2′), 140.0 (C-7′), 138.8 (C-8a′), 135.7 (C-6′), 134.3 (C-8′), 134.1 (C-2), 133.5 (C-3a′), 127.0 (C-5′), 126.2 (C-3′), 125.1 (C-1′), 117.3 (C-5), 108.6 (C-4), 106.2 (C-3), 38.3 ($(CH_3)_2C$H-7′), 30.3 (2-CH_2-3′), 26.7 (Me-4′), 24.8 ($(CH_3)_2$CH-7′) and 12.9 (Me-1′).

4.2. X-ray crystal structure of (2-furyl)(3-guaiazulenyl) methylium hexafluorophosphate (5)

A total 4916 reflections with $2\theta_{max}=55.0°$ were collected on a Rigaku AFC-5R automated four-circle diffractometer with graphite monochromated Mo Kα radiation ($\lambda=$ 0.71069 Å, rotating anode: 50 kV, 180 mA) at 296 K. The structure was solved by direct methods (SIR97) and expanded using Fourier techniques (DIRDIF94). The non-hydrogen atoms were refined anisotropically. Hydrogen atoms were included but not refined. The final cycle of full-

matrix least-squares refinement was based on F^2. All calculations were performed using the teXsan crystallographic software package. Crystallographic data have been deposited at the CCDC, 12 Union Road, Cambridge CB2 1EZ, UK and copies can be obtained on request, free of charge, by quoting the publication citation and the deposition number CCDC 228481.

Crystallographic data for **5**: $C_{20}H_{21}F_6OP$ (FW=422.35), red prism (the crystal size, $0.20\times0.10\times0.30$ mm^3), monoclinic, $P2_1/n$ (#14), $a=7.788(6)$ Å, $b=26.609(4)$ Å, $c=9.862(5)$ Å, $\beta=106.94(4)°$, $V=1955(1)$ Å^3, $Z=4$, $D_{calcd}=1.435$ g/cm^3, μ(Mo Kα)=2.03 cm^{-1}, scan width=$(0.68+0.30\tan\theta)°$, scan mode=ω, scan rate=8.0°/min, measured reflections=4916, observed reflections=4211, no. of parameters=253, $R1=0.097$, $wR2=0.244$ and goodness of fit indicator=1.93.

4.3. X-ray crystal structure of (3-guaiazulenyl)(2-thienyl)methylium hexafluorophosphate (6)

A total 4780 reflections with $2\theta_{max}=55.0°$ were collected on a Rigaku AFC-5R automated four-circle diffractometer with graphite monochromated Mo Kα radiation ($\lambda=0.71069$ Å, rotating anode: 50 kV, 180 mA) at 296 K. The structure was solved by direct methods (SIR97) and expanded using Fourier techniques (DIRDIF94). The non-hydrogen atoms were refined anisotropically. Hydrogen atoms were included but not refined. The final cycle of full-matrix least-squares refinement was based on F^2. All calculations were performed using the teXsan crystallographic software package. The deposition number CCDC 203308.

Crystallographic data for **6**: $C_{20}H_{21}F_6PS$ (FW=438.41), red prism (the crystal size, $0.2\times0.3\times0.7$ mm^3), triclinic, P-1 (#2), $a=10.286(2)$ Å, $b=13.848(2)$ Å, $c=7.828$ Å, $\alpha=95.06(1)°$, $\beta=112.10(1)°$, $\gamma=72.51(1)°$, $V=985.0(3)$ Å^3, $Z=2$, $D_{calcd}=1.478$ g/cm^3, μ(Mo Kα)=3.03 cm^{-1}, scan width=$(1.15+0.30\tan\theta)°$, scan mode=$\omega-2\theta$, scan rate=8.0°/min, measured reflections=4780, observed reflections=4526, no. of parameters=253, $R1=0.074$, $wR2=0.247$ and goodness of fit indicator=2.22.

4.3.1. Reduction of (2-furyl)(3-guaiazuleyl)methylium hexafluorophosphate (5) with zinc powder. To a solution of **5** (168 mg, 0.40 mmol) in acetonitrile (2.0 mL) was added a zinc powder (300 mg, 4.59 mmol) under argon. The mixture was stirred at 25 °C for 1.5 h. After the reaction, the zinc powder was removed by using a centrifugal separator. The reaction solution was evaporated in vacuo, giving a bluish-green solid. The residue thus obtained was carefully separated by silica-gel column chromatography with hexane–ethyl acetate–dichloromethane (10/10/2, vol/vol/vol) as an eluant, giving a ca. 3:1, chromatographically inseparable mixture of a *meso* form and two enantiomeric forms of the molecular structure, 1,2-di(2-furyl)-1,2-di(3-guaiazulenyl)ethane (**11**), as a bluish-green solid (89 mg, 0.16 mmol, 80% yield) [$R_f=0.72$ on silica-gel TLC (hexane–AcOEt=9/1, vol/vol)]. The crude product **11** was recrystallized from dichloromethane–methanol (1/5, vol/vol) (several times) to provide the crystals of only its *meso* form, (1*R*,2*S*)-1,2-di(2-furyl)-1,2-di(3-guaiazulenyl)ethane (**11a**) (40 mg, 72 μmol, 36% yield).

Compound **11a**. Blue blocks, mp 170 °C [decomp., determined by thermal analysis (TGA and DTA)]. Found: C, 85.31; H, 7.73%. Calcd for $C_{80}H_{86}O_5$ [$2(C_{40}H_{42}O_2)\cdot H_2O$]: C, 85.22; H, 7.69%; UV–vis λ_{max} (CH_2Cl_2) nm (log ε), 248 (4.73), 294 (4.92), 309 (4.80), 357 (4.23), 373 (4.23), 616 (3.10), 674sh (3.01) and 750sh (2.64);exact FAB-MS (3-nitorobenzyl alcohol matrix), found: *m*/*z* 555.3264; calcd for $C_{40}H_{42}O_2$: $[M+H]^+$, *m*/*z* 555.3264; 700 MHz ^{1}H NMR (CD_2Cl_2), signals based on the 1,2-di(3-guaiazulenyl)ethane unit: δ 1.31 (12H, d, $J=6.8$ Hz, (CH_3)$_2$CH-7″,7‴), 2.60 (6H, s, Me-1″,1‴), 2.99 (2H, sept, $J=6.8$ Hz, (CH_3)$_2$C*H*-7″,7‴), 3.20 (6H, s, Me-4″,4‴), 6.17 (2H, s, HC-1,2), 6.85 (2H, d, $J=10.5$ Hz, H-5″,5‴), 7.24 (2H, dd, $J=10.5$, 1.9 Hz, H-6″,6‴), 7.88 (2H, s, H-2″,2‴) and 8.02 (2H, d, $J=1.9$ Hz, H-8″,8‴); signals based on the 1,2-di(2-furyl) groups: δ 5.72 (2H, dd, $J=3.2$, 0.7 Hz, H-3′,3‴), 5.93 (2H, dd, $J=3.2$, 1.6 Hz, H-4′,4‴) and 7.05 (2H, d, $J=1.6$, 0.7 Hz H-5′,5‴); 176 MHz ^{13}C NMR (CD_2Cl_2), δ 157.5 (C-2′,2‴), 144.4 (C-4″,4‴), 140.5 (C-5′,5‴), 139.7 (C-7″,7‴), 138.3 (C-8a″,8a‴), 137.7 (C-2″,2‴), 134.1 (C-6″,6‴), 133.4 (C-8″,8‴), 131.5 (C-3a″,3a‴), 127.1 (C-3″,3‴), 126.8 (C-5″,5‴), 124.8 (C-1″,1‴), 109.8 (C-4′,4‴), 105.7 (C-3′,3‴), 44.7 (C-1,2), 37.6 ((CH_3)$_2$*C*H-7″,7‴), 28.0 (Me-4″,4‴), 24.3 ((CH_3)$_2$CH-7″,7‴) and 12.8 (Me-1″,1‴).

Compound **11b**. 700 MHz ^{1}H NMR (CD_2Cl_2), signals based on the 1,2-di(3-guaiazulenyl)ethane unit: δ 1.259, 1.261 (6H each, d, $J=6.8$ Hz, (CH_3)$_2$CH-7″,7‴), 2.43 (6H, s, Me-1″,1‴), 2.94 (2H, sept, $J=6.8$ Hz, (CH_3)$_2$C*H*-7″,7‴), 3.18 (6H, s, Me-4″,4‴), 6.10 (2H, s, HC-1,2), 6.83 (2H, d, $J=10.5$ Hz, H-5″,5‴), 7.20 (2H, dd, $J=10.5$, 1.9 Hz, H-6″,6‴), 7.83 (2H, s, H-2″,2‴) and 7.89 (2H, d, $J=1.9$ Hz, H-8″,8‴); signals based on the 1,2-di(2-furyl) groups: δ 5.86 (2H, dd, $J=3.2$, 0.7 Hz, H-3′,3‴), 6.17 (2H, dd, $J=3.2$, 1.6 Hz, H-4′,4‴) and 7.23 (2H, dd, $J=1.6$, 0.7 Hz H-5′,5‴).

4.3.2. Reduction of (3-guaiazulenyl)(2-thienyl)methylium hexafluorophosphate (6) with zinc powder. To a solution of **6** (180 mg, 0.41 mmol) in acetonitrile (5.0 mL) was added a zinc powder (300 mg, 4.59 mmol) under argon. The mixture was stirred at 25 °C for 1 h. After the reaction, the zinc powder was removed by using a centrifugal separator. The reaction solution was evaporated in vacuo, giving a bluish-green solid. The residue thus obtained was carefully separated by silica-gel column chromatography with hexane–ethyl acetate (7/3, vol/vol) as an eluant, giving the two enantiomeric forms, (1*R*,2*R*)- and (1*S*,2*S*)-1,2-di(3-guaiazulenyl)-1,2-di(2-thienyl)ethane (**12b**), as a green solid, and, further, was carefully separated by silica-gel column chromatography with hexane–ethyl acetate–benzene (2/2/1, vol/vol/vol) as an eluant, giving the *meso* form, (1*R*,2*S*)-1,2-di(3-guaiazulenyl)-1,2-di(2-thienyl)-ethane (**12a**) as a blue solid. The crude product **12b** was recrystallized from ethyl acetate–methanol (1/5, vol/vol) (several times) to provide pure **12b** as stable single crystals (54 mg, 92 μmol, 46% yield). The crude product **12a** was recrystallized from dichloromethane–methanol (1/5, vol/

vol) (several times) to provide stable crystals **12a** (27 mg, 46 μmol, 23% yield).

Compound **12a**. Blue blocks, mp > 241 °C [decomp., determined by thermal analysis (TGA and DTA)]. Found: C, 81.83; H, 7.21%. Calcd for $C_{40}H_{42}S_2$, C: 81.86; H: 7.21%; R_f=0.63 on silica-gel TLC (hexane/AcOEt=7:3, vol/vol); UV–vis λ_{max} (CH_2Cl_2) nm (log ε), 246 (4.73), 293 (4.84), 312sh (4.55), 358sh (4.16), 372 (4.27), 623 (2.98), 680sh (2.87) and 754 (2.42); exact FAB-MS (3-nitrobenzyl alcohol matrix), found *m/z* 587.2780, calcd for $C_{40}H_{43}S_2$: $[M+H]^+$, *m/z* 587.2806; 500 MHz ^{1}H NMR (CD_2Cl_2), signals based on the 1,2-di(3-guaiazuleneyl)ethane unit: δ 1.34 (12H, d, J=6.8 Hz, $(CH_3)_2$CH-7″,7‴), 2.65 (6H, s, Me-1″,1‴), 3.02 (2H, sept, J=6.8 Hz, $(CH_3)_2CH$-7″,7‴), 3.10 (6H, s, Me-4″,4‴), 6.30 (2H, s, HC-1,2), 6.84 (2H, d, J=10.6 Hz, H-5″,5‴), 7.26 (2H, dd, J=10.6, 2.3 Hz, H-6″,6‴), 7.94 (2H, s, H-2″,2‴) and 8.07 (2H, d, J=2.3 Hz, H-8″,8‴); signals based on the 1,2-di(2-thienyl) groups: δ 6.39 (2H, dd, J=3.7, 1.1 Hz, H-3′,3‴), 6.56 (2H, dd, J=5.0, 3.7 Hz, H-4′,4‴), 6.88 (2H, dd, J=5.0, 1.1 Hz, H-5′,5‴); 125 MHz ^{13}C NMR (CD_2Cl_2), δ 150.2 (C-3″,3‴), 144.3 (C-4″,4‴), 139.5 (C-7″,7‴), 138.0 (C-8a″,8a‴), 137.0 (C-2″,2‴), 134.0 (C-6″,6‴), 133.3 (C-8″,8‴), 131.6 (C-3a″,3a‴), 129.2 (C-1″,1‴), 126.5 (C-5″,5‴), 125.4 (C-4′,4‴), 124.7 (C-3′,3‴), 124.3 (C-2′,2‴), 123.3 (C-5′,5‴), 47.5 (HC-1,2), 37.2 ($(CH_3)_2C$H-7″,7‴), 27.7 (Me-4″,4‴), 23.9 ($(CH_3)_2$CH-7″,7‴) and 12.6 (Me-1″,1‴).

Compound **12b**. Blue prisms, mp > 220 °C [decomp., determined by thermal analysis (TGA and DTA)]. Found: C, 81.74; H, 7.17%. Calcd for $C_{40}H_{42}S_2$: C, 81.86; H, 7.21%; R_f=0.63 on silica-gel TLC (hexane/AcOEt=7:3, vol/vol); UV–vis λ_{max} (CH_2Cl_2) nm (log ε), 246 (4.73), 293 (4.84), 312sh (4.55), 358sh (4.16), 372 (4.27), 623 (2.98), 680sh (2.87) and 754 (2.42); exact FAB-MS (3-nitrobenzyl alcohol matrix), found: *m/z* 587.2805; calcd for $C_{40}H_{43}S_2$: $[M+H]^+$, *m/z* 587.2806; 500 MHz ^{1}H NMR (CD_2Cl_2), signals based on the 1,2-di(3-guaiazuleneyl)ethane unit: δ 1.276, 1.283 (6H each, d, J=6.9 Hz, $(CH_3)_2$CH-7″,7‴), 2.45 (6H, s, Me-1″,1‴), 2.95 (2H, sept, J=6.9 Hz, $(CH_3)_2CH$-7″,7‴), 3.22 (6H, s, Me-4″,4‴), 6.14 (2H, s, HC-1,2), 6.85 (2H, d, J=10.6 Hz, H-5″,5‴), 7.23 (2H, dd, J=10.6, 2.3 Hz, H-6″,6‴), 7.83 (2H, s, H-2″,2‴) and 7.93 (2H, d, J=2.3 Hz, H-8″,8‴); signal based on the 1,2-di(2-thienyl) groups: δ 6.46 (2H, dd, J=3.7, 1.2 Hz, H-3′,3‴), 6.75 (2H, dd, J=4.9, 3.7 Hz, H-4′,4‴) and 7.09 (2H, dd, J=4.9, 1.2 Hz, H-5′,5‴); 125 MHz ^{13}C NMR (CD_2Cl_2), δ 151.2 (C-2′,2‴), 145.0 (C-4″,4‴), 139.8 (C-7″,7‴), 137.7 (C-3″,3‴), 137.1 (C-2″,2‴), 134.8 (C-6″,6‴), 133.7 (C-8″,8‴), 132.7 (C-3a″,3a‴), 129.8 (C-8a″,8a‴), 127.1 (C-5″,5‴), 126.2 (C-4′,4‴), 124.8 (C-1″,1‴ and 3′,3‴), 124.3 (C-5′,5‴), 49.7 (HC-1,2), 37.7 ($(CH_3)_2C$H-7″,7‴), 28.0 (Me-4″,4‴), 24.4 ($(CH_3)_2$CH-7″,7‴) and 13.1 (Me-1″,1‴).

4.3.3. Reduction of (3-guaiazulenyl)(2-pyrrolyl)methylium hexafluorophosphate (7) with zinc powder. To a solution of **7** (200 mg, 0.47 mmol) in acetonitrile (6.0 mL) was added a zinc powder (925 mg, 14.1 mmol) under argon. The mixture was stirred at 25 °C for 5 min. After reaction, the zinc powder was removed by using a centrifugal separator. The reaction solution was evaporated in vacuo, giving a bluish-green solid. The residue thus obtained was dissolved in hexane (80 mL) and filtered. The hexane filtrate was evaporated in vacuo, giving a blue paste. The blue paste residue thus obtained was recrystallized from ethanol (several times) and, further, from dichloromethane–ethanol (1/5 vol/vol) (several times) to provide the pure *meso* form, (1*R*,2*S*)-1,2-di(3-guaiazulenyl)-1,2-di(2-pyrrolyl)ethane (**13a**), as a blue solid (6.5 mg, 12 μmol, 5% yield). The crystallization solvent containing products was evaporated in vacuo, giving a green paste. The residue thus obtained was purified by silica-gel column chromatography with hexane–ethyl acetate (90/10, vol/vol) as an eluant, giving pure the two enantiomeric forms, (1*R*,2*R*)- and (1*S*,2*S*)-1,2-di(3-guaiazulenyl)-1,2-di(2-pyrrolyl)ethane (**13b**) as a green paste (6.5 mg, 12 μmol, 5% yield).

Compound **13a**. Blue solid. Found: C, 86.93; H, 8.03; N, 4.98%. Calcd for $C_{40}H_{44}N_2$: C, 86.91; H, 8.02; N, 5.07%; R_f=0.36 on silica-gel TLC (hexane/AcOEt=9:1, vol/vol); UV–vis λ_{max} (CH_2Cl_2) nm (log ε), 246 (4.73), 292 (4.92), 309 (4.76), 357 (4.27), 371 (4.21) and 618 (3.09); IR ν_{max} (KBr) cm^{-1}, 3436 (N–H); exact FAB-MS (3-nitrobenzyl alcohol matrix), found: *m/z* 551.3401; calcd for $C_{40}H_{43}N_2$: $[M-H]^+$, *m/z* 551.3426; 500 MHz ^{1}H NMR (CD_2Cl_2), signals based on the 1,2-di(3-guaiazulenyl)ethane unit: δ 1.36 (12H, d, J=6.9 Hz, $(CH_3)_2$CH-7″,7‴), 2.64 (6H, s, Me-1″,1‴), 2.90 (6H, s, Me-4″,4‴), 3.05 (2H, sept, J=6.9 Hz, $(CH_3)_2CH$-7″,7‴), 5.90 (2H, s, HC-1,2), 6.83 (2H, d, J=10.6 Hz, H-5″,5‴), 7.28 (2H, dd, J=10.6, 2.2 Hz, H-6″,6‴), 7.70 (2H, s, H-2″,2‴) and 8.12 (2H, d, J=2.2 Hz, H-8″,8‴); signals based on the 1,2-di(2-pyrrolyl) groups: δ 5.29 (2H, dd, J=2.6, 1.3 Hz, H-3′,3‴), 5.75 (2H, dd, J=5.0, 2.6 Hz, H-4′,4‴) and 6.27 (2H, dd, J=5.0, 1.3 Hz, H-5′,5‴); the two NH-proton signals based on the 1,2-di(2-pyrrolyl) groups were included in the moisture signal (δ 1.52) of the solvent; 125 MHz ^{13}C NMR (CD_2Cl_2): δ 144.8 (C-4″,4‴), 139.4 (C-7″,7‴), 138.0 (C-1″,1‴), 137.2 (C-2″,2‴), 135.4 (C-2′,2‴), 134.1 (C-6″,6‴), 133.3 (C-8″,8‴), 131.9 (C-3a″,3a‴), 128.6 (C-3″,3‴), 126.4 (C-5″,5‴), 124.7 (C-8a″,8a‴), 115.5 (C-5′,5‴), 107.1 (C-4′,4‴), 106.8 (C-3′,3‴), 44.6 (HC-1,2), 37.3 ($(CH_3)_2C$H-7″,7‴), 27.4 (Me-4″,4‴), 24.0 ($(CH_3)_2$CH-7″,7‴) and 12.6 (Me-1″,1‴).

Compound **13b**. Green paste; R_f=0.30 on silica-gel TLC (hexane/AcOEt=9:1, vol/vol); exact FAB-MS (3-nitrobenzyl alcohol matrix), found: *m/z* 551.3392; calcd for $C_{40}H_{43}N_2$: $[M-H]^+$, *m/z* 551.3426; UV–vis λ_{max} (CH_2Cl_2) nm (log ε), 246 (4.53), 291 (4.65), 357 (3.99), 372 (4.01) and 608 (2.87); 500 MHz ^{1}H NMR (CD_2Cl_2), signals based on the 1,2-di(3-guaiazulenyl)ethane unit: δ 1.287, 1.292 (6H each, d, J=6.9 Hz, $(CH_3)_2$CH-7″,7‴), 2.46 (6H, s, Me-1″,1‴), 2.97 (2H, sept, J=6.9 Hz, $(CH_3)_2CH$-7″,7‴), 3.02 (6H, s, Me-4″,4‴), 5.78 (2H, s, HC-1,2), 6.81 (2H, d, J=10.7 Hz, H-5″,5‴), 7.23 (2H, dd, J=10.7, 2.0 Hz, H-6″,6‴), 7.70 (2H, s, H-2″,2‴) and 7.96 (2H, d, J=2.0 Hz, H-8″,8‴); signals based on the 1,2-di(2-pyrrolyl) groups: δ 5.47 (2H, dd, J=2.6, 1.3 Hz, H-3′,3‴), 6.00 (2H, dd, J=5.2, 2.6 Hz, H-4′,4‴) and 6.53 (2H, dd, J=5.2, 1.3 Hz, H-5′,5‴); the two NH-proton signals based on the 1,2-di(2-pyrrolyl) groups were included in the moisture signal (δ 1.56) of the solvent; 125 MHz ^{13}C NMR (CD_2Cl_2): δ 144.7 (C-4″,4‴), 139.0 (C-7″,7‴), 137.047 (C-1″,1‴),

136.999 (C-2″,2‴), 135.7 (C-2′,2‴), 134.3 (C-6″,6‴), 133.1 (C-8″,8‴), 132.3 (C-3a″,3a‴), 128.3 (C-3″,3‴), 126.3 (C-5″,5‴), 124.0 (C-8a″,8a‴), 116.0 (C-5′,5‴), 107.6 (C-4′,4‴), 106.7 (C-3′,3‴), 46.1 (HC-1,2), 37.2 ($(CH_3)_2CH$-7″,7‴), 27.1 (Me-4″,4‴), 24.1, 23.9 ($(CH_3)_2CH$-7″,7‴) and 12.5 (Me-1″,1‴).

4.4. X-ray crystal structure of the two enantiomeric forms, (1*R*,2*R*)- and (1*S*,2*S*)-1,2-di(3-guaiazulenyl)-1,2-di(2-thienyl)ethane (12b)

A total 4107 reflections with $2\theta_{max}=55.0°$ were collected on a Rigaku AFC-5R automated four-circle diffract meter with graphite monochromatic Mo Kα radiation ($\lambda=0.71069$ Å, rotating anode: 50 kV, 180 mA) at 296 K. The structure was solved by direct methods (SIR92) and expanded using Fourier techniques (DIRDIF94). The non-hydrogen atoms were refined anisotropically. Hydrogen atoms were included but not refined. The final cycle of full-matrix least-squares refinement was based on F^2. All calculations were performed using the teXsan crystallographic software package. The deposition number CCDC 200074.

Crystallographic data for **12b**: $C_{40}H_{42}S_2$ (FW=586.89), blue prism [from ethyl acetate/methanol=1:5 (vol/vol), the crystal size, $0.5\times0.2\times0.2$ mm^3], monoclinic, *C*2/c (#15), $a=12.755(3)$ Å, $b=25.354(2)$ Å, $c=12.017(2)$ Å, $\beta=120.33(1)°$, $V=3354.0(10)$ Å^3, $Z=4$, $D_{calcd}=1.162$ g/cm^3, μ(Mo Kα)=1.85 cm^{-1}, scan width=$(1.31+0.30\tan\theta)°$, scan mode=$\omega-2\theta$, scan rate=8.0°/min, measured reflections=4107, observed reflections=3846, no. of parameters=190, $R1=0.056$, $wR2=0.155$ and goodness of fit indicator=1.90.

Acknowledgements

This work was partially supported by a Grant-in-Aid for Scientific Research from the Ministry of Education, Culture, Sports, Science, and Technology, Japan.

References and notes

1. Takekuma, S.; Sasaki, M.; Takekuma, H.; Yamamoto, H. *Chem. Lett.* **1999**, 999–1000.
2. Takekuma, S.; Takata, S.; Sasaki, M.; Takekuma, H. *Tetrahedron Lett.* **2001**, *42*, 5921–5924.
3. Takekuma, S.; Tanizawa, M.; Sasaki, M.; Matsumoto, T.; Takekuma, H. *Tetrahedron Lett.* **2002**, *43*, 2073–2078.
4. Sasaki, M.; Nakamura, M.; Hannita, G.; Takekuma, H.; Minematsu, T.; Yoshihara, M.; Takekuma, S. *Tetrahedron Lett.* **2003**, *44*, 275–279.
5. Sasaki, M.; Nakamura, M.; Uriu, T.; Takekuma, H.; Minematsu, T.; Yoshihara, M.; Takekuma, S. *Tetrahedron* **2003**, *59*, 505–516.
6. Nakamura, M.; Sasaki, M.; Takekuma, H.; Minematsu, T.; Takekuma, S. *Bull. Chem. Soc. Jpn.* **2003**, *76*, 2051–2052.
7. Takekuma, S.; Sasaki, K.; Nakatsuji, M.; Sasaki, M.; Minematsu, T.; Takekuma, H. *Bull. Chem. Soc. Jpn.* **2004**, *77*, 379–380.
8. Nakatsuji, M.; Hata, Y.; Fujihara, T.; Yamamoto, K.; Sasaki, M.; Takekuma, H.; Yoshihara, M.; Minematsu, T.; Takekuma, S. *Tetrahedron* **2004**, *60*, 5983–6000.
9. Takekuma, S.; Hata, Y.; Nishimoto, T.; Nomura, E.; Sasaki, M.; Minematsu, T.; Takekuma, H. *Tetrahedron* **2005**, *61*, 6892–6907.
10. Ito, S.; Kikuchi, S.; Okujima, T.; Morita, N.; Asao, T. *J. Org. Chem.* **2001**, *66*, 2470–2479.
11. Ito, S.; Kubo, T.; Kondo, M.; Kabuto, C.; Morita, N.; Asao, T.; Fujimori, K.; Watanabe, M.; Harada, N.; Yasunami, M. *Org. Biomol. Chem.* **2003**, *1*, 2572–2580.
12. Kirby, E. C.; Reid, D. H. *J. Chem. Soc.* **1960**, 494–501.
13. **A**: 700 MHz ^{1}H NMR (CD_3CN), signals based on the 3-guaiazulenylmethylium substituent: δ 1.46 (6H, d, $J=6.8$ Hz, $(CH_3)_2$CH-7′), 2.51 (3H, br d, s, Me-1′), 3.37 (3H, s, Me-4′), 3.50 (1H, sept, $J=6.8$ Hz, $(CH_3)_2CH$-7′), 7.99 (1H, br d, s, H-2′), 8.44 (1H, dd, $J=11.2$, 2.2 Hz, H-6′), 8.55 (1H, d, $J=11.2$ Hz, H-5′), 8.59 (1H, d, $J=2.2$ Hz, H-8′) and 8.78 (1H, s, HC^+-α); signals based on the phenyl group: δ 7.610 (2H, ddd, $J=8.0$, 7.5, 1.5 Hz, H-3,5), 7.616 (1H, dddd, $J=7.5$, 7.5, 1.0, 1.0 Hz, H-4) and 7.82 (2H, ddd, $J=8.0$, 1.5, 1.0 Hz, H-2,6); 176 MHz ^{13}C NMR (CD_3CN), δ 171.2 (C-7′), 160.9 (C-8a′), 157.3 (C-4′), 152.9 (C-3a′), 150.1 (C-5′), 149.6 (HC^+-α), 145.5 (C-1′), 144.3 (C-6′), 140.6 (C-2′), 139.6 (C-3′), 139.1 (C-8′), 135.6 (C-1), 132.8 (C-2,6), 132.1 (C-4), 129.5 (C-3,5), 39.4 ($(CH_3)_2CH$-7′), 28.9 (Me-4′), 22.9 ($(CH_3)_2$CH-7′) and 12.9 (Me-1′).
14. Kurata, H.; Oki, Y.; Matsumoto, K.; Kawase, T.; Oda, M. *Chem. Lett.* **2005**, *34*, 910–911.
15. For comparative purposes, the oxidation potential using ferrocene as a standard material showed +0.45 (E_p) V by DPV and +0.42 ($E_{1/2}$) V by CV in 0.1 M [*n*-Bu_4N]BF_4, CH_3CN under the same electrochemical conditions as C,[5] indicating that these values slightly shift +0.03 (E_p) V by DPV and +0.02 ($E_{1/2}$) V by CV from those in 0.1 M [*n*-Bu_4N]PF_6, CH_3CN (see Fig. 5).
16. Studies on chemical properties of **11a** and **12a**,**b** are currently under intensive investigation.

Available online at www.sciencedirect.com
SCIENCE DIRECT
Tetrahedron
ELSEVIER
Tetrahedron 61 (2005) 10363–10369

Synthesis of novel 1-(2,3-dihydro-5*H*-4,1-benzoxathiepin-3-yl)-uracil and -thymine, and their corresponding *S*-oxidized derivatives

M. del Carmen Núñez,[a] Antonio Entrena,[a] Fernando Rodríguez-Serrano,[b] Juan A. Marchal,[c] Antonia Aránega,[d] Miguel Á. Gallo,[a] Antonio Espinosa[a] and Joaquín M. Campos[a,*]

[a]*Departamento de Química Farmacéutica y Orgánica, Facultad de Farmacia, c/ Campus de Cartuja s/n, 18071 Granada, Spain*
[b]*Departamento de Biología Celular, Facultad de Ciencias, Avda. Severo Ochoa s/n, 18071 Granada, Spain*
[c]*Departamento de Ciencias de la Salud, Facultad de Ciencias Experimentales y de la Salud, Paraje de las Lagunillas s/n, 23071 Jaén, Spain*
[d]*Departamento de Ciencias Morfológicas, Facultad de Medicina, Avenida de Madrid s/n, 18071 Granada, Spain*

Received 18 May 2005; revised 12 July 2005; accepted 14 July 2005

Available online 26 August 2005

Abstract—On the basis of molecular variations on isosteric replacements from the prototype 1-(2,3-dihydro-5*H*-1,4-benzodioxepin-3-yl)-5-fluorouracil a series of 3-(2,3-dihydro-5*H*-4,1-benzoxathiepin-3-yl)-uracil or -thymine *O*,*N*-acetals was prepared. The nature of the *cis*- and *trans*-sulfoxide isomers was established by means of their conformational analyses carried out with Sybyl and after comparing the theoretical results with the ^{1}H NMR responses of the target molecules. (*RS*)-3-(1,1-Dioxo-2,3-dihydro-5*H*-4,1-benzoxathiepin-3-yl)thymine and (1*S**, 3*S**)-1-(1-oxo-3,5-dihydro-2*H*-4,1-benzoxathiepin-3-yl)thymine were found to be inhibitors of the MCF-7 cell growth.

1. Introduction

1-(2,3-Dihydro-5*H*-1,4-benzodioxepin-3-yl)-5-fluorouracils (**1**–**3**) have proved to be good antiproliferative agents against the MCF-7 human breast cancer cell line (Fig. 1).[1] Such compounds accumulate the cancerous cells in the G_0/G_1 phase. On the other hand, **4**[2] that shows an $IC_{50}=5.4$ μM against the MCF-7 cell line, acts in a similar way to Ftorafur, a known prodrug of 5-fluorouracil (5-FU) (Fig. 1), because both gather together the cancerous cells in the synthesis phase (S). In contrast to 5-FU,[3] the benzannelated 5-FU *O*,*N*-acetals[1] and corresponding open analogues[2] have proved to be non-toxic.

With all this background it seems that compounds **1**–**3** are drugs per se, whilst **4** is a prodrug of 5-FU. Therefore, following our ongoing Anticancer Drug Programme we have planned in this paper the synthesis of compounds **5**–**10** (Fig. 2) to be tested subsequently against the human breast cancer cell line MCF-7.

On the one hand, all these compounds bear a natural pyrimidine base (uracil for compounds **5**, **7** and **9** and thymine for **6**, **8** and **10**) and on the other, the oxygen atom at position 1 of the seven-membered cycle is replaced by its isosteric sulfur atom (**5** and **6**), and its oxidized states, that is sulfoxide (**7** and **8**) and sulfones (**9** and **10**). Should these compounds show antiproliferative activities, new avenues of anticancer research would be opened based on the non-toxic natural bases uracil and thymine and, very probably, with a mechanism of action different from that of 5-FU. *O*,*N*-Acetalic benzoxathiepins are compounds not referred to in bibliography, and with this paper we will try to fill the gap.

2. Results and discussion

2.1. Synthesis

The synthesis of the targets is depicted in Scheme 1. We have previously reported the preparation of the cyclic acetal (*RS*)-3-methoxy-2,3-dihydro-5*H*-1,4-benzodioxepin.[1] We applied the same procedure for the synthesis of **12**, starting from the commercially available *o*-(hydroxymethyl)thiophenol, that is selective alkylation using bromoacetaldehyde dimethyl acetal (1 mol in the presence of 1 mol of sodium hydride in dry dimethylformamide (DMF) under conditions published by Crombie et al.[4] gave **11** (79%). Subsequent cyclization of the resulting hydroxyacetal using catalytic amounts of *p*-toluenesulfonic acid in dry toluene for 3 h

Keywords: Antitumour compounds; Benzoxathiepins; Computer-assisted methods; Uracils.
* Corresponding author. Tel.: +34 958 243849; fax: +34 958 243845; e-mail: jmcampos@ugr.es

0040–4020/$ - see front matter © 2005 Elsevier Ltd. All rights reserved.
doi:10.1016/j.tet.2005.07.065

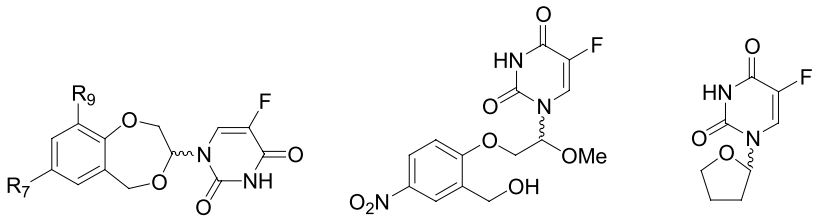

Figure 1.

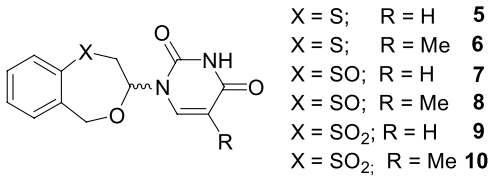

Figure 2. Novel benzo-fused seven-membered sulfur-containing *O,N*-acetals with natural pyrimidine nucleobases. In all the cases the aminalic bond between the C-3 atom of the seven-membered moiety and the nucleobase is through its *N*-1 atom.

produced the sulfur-containing acetal **12** (95%). The last step was the condensation reaction between the seven-membered acetal **12** and the natural pyrimidine bases uracil and thymine. For this procedure we used a 1.0 M solution of tin(IV) chloride in dichloromethane, trimethylchlorosilane (TCS) and 1,1,1,3,3,3-hexamethyldisilazane (HMDS) in dry acetonitrile, and the experimental conditions were optimised (unpublished results) by warming the reaction mixture up to 45 °C for 20–24 h. Under these conditions **5** and **6** were obtained with 73 and 58% yields, respectively.

The oxidation of sulfides is one of the most important and straightforward methods for the preparation of sulfones, which are utilized for biologically active substances and substrates for the synthesis of drugs.[5] Sulfoxides **7** and **8** were obtained using the procedure used by Matteucci et al.[6] who used catalytic scandium trifluoromethansulfonate that greatly increases the efficiency of hydrogen peroxide mediated monooxidation of alkyl–aryl sulfides and methyl cysteine-containing peptides. When applied to our sulfides a mixture of *cis*-**7** and *trans*-**7** (77%) was obtained, but after using the flash 40 equipment a fast-moving spot was isolated, that will be characterized as *cis*-**7** (vide infra). When the oxidation of **6** was carried out without catalyst, *trans*-**8** was the only product produced (50%). Finally, the oxidation of sulfide **5** (and **6**) with potassium peroxymonosulfate (OXONE™) under previously reported conditions[7] yielded **9** (and **10**) with 66 (and 55%) yields.

2.2. Spectroscopic analysis of 5

The ^{1}H and ^{13}C NMR spectra were recorded using DMSO-d_6 as solvent. Herein we will mention only the NMR spectroscopic data that explain the conformational preference for **5**. The hydrogen atoms of the seven-membered framework of **5** appear between δ 5.98 ppm and δ 3.18 ppm. The chemical shift found for the aminalic hydrogen H-3 is δ 5.98 ppm with a double doublet multiplicity (dd), and the respective couplings to the vicinal hydrogen atoms (H-2) are 9.1 and 2.2 Hz. In fact, the two H-2 atoms appear as two dd's with a $J_{gem}=14.1$ Hz and the two coupling constants observed at δ 5.98 ppm (9.6 and 1.8 Hz). Finally, each of the two benzylic H-5 atoms resonates as two doublets at δ 5.02 and δ 4.96 ppm with a $J_{gem}=13.6$ Hz, showing a diastereotopic character.

The most important consequence of the ^{1}H NMR study is that it unequivocally proves through the three following data that the linkage between the seven-membered moiety and uracil is through *N*-1′:

(a) At δ 5.60 ppm one hydrogen resonates as a dd ($J=8.0$ and 2.2 Hz), the former coupling constant being typical of an aromatic hydrogen atom, and this resonance could be assigned to H-5′[8] of the uracil base. H-6′ appears as a doublet (7.69 ppm, d, $J=8.0$ Hz) downfield in relation to H-5′. The coupling pattern for H-5′ is a dd due to its coupling with H-6′ ($J=8.0$ Hz) and a small one ($J_{H5'-NH_{3'}}=$ 2.2 Hz) through a 1–3 bond relationship, and a doublet for H-6′. Nevertheless, had the aminalic bond been established with N–$H_{3'}$ the coupling pattern would have been more

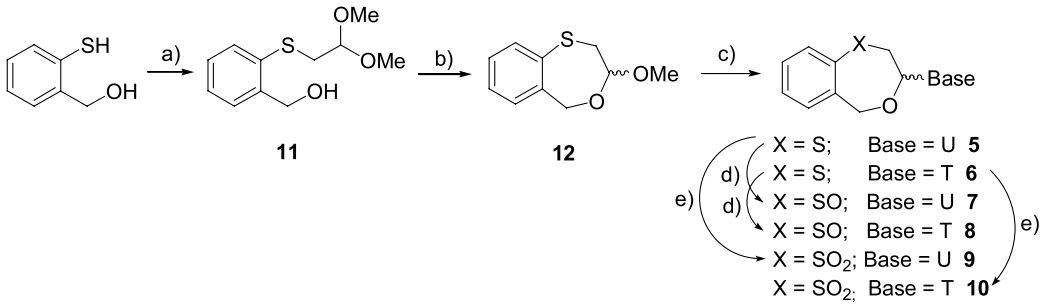

Scheme 1. Synthetic route for the preparation of the target molecules. Reagents and conditions: (a) $BrCH_2CH(OMe)_2$, NaH, anhydrous DMF; (b) *p*-TsOH, anhydrous toluene, 3 h; (c) pyrimidine base, HMDS, TCS, $SnCl_4$, MeCN, 45 °C; (d) H_2O_2, $Sc(OTf)_3$, CH_2Cl_2/10% EtOH; (e) OXONE™, MeOH, H_2O.

complicated due to the simultaneous coupling of H-6′ with H-5′ and N–$H_{1'}$ (a dd for each of the three hydrogen atoms involved, that is, N–$H_{1'}$, H-5′ and H-6′).

(b) H-3 exhibits connectivity through three bonds to C-6′ (HMBC[9]).

(c) The NOEDIFF effect observed between H-6′ and H-2β justifies the conformational preference of the uracil moiety in which H-6′ is near in space to H-2β. Accordingly, the carbonyl group C-2′ is far from the referred hydrogen atom and this obviously implies the linkage through N-1′. Had the aminalic bond been established through C-3 and N-3′, no NOEDIFF effect would have been detected between some hydrogen atoms of the seven-membered moiety and those of the uracil fragment. H-3 shows a NOEDIFF effect with the more deshielded H-5 atom (δ 5.02 ppm), and with the more shielded H-2 one (δ 3.18 ppm) and these facts strongly support a chair conformation of the seven-membered moiety in which the aminalic hydrogen atom adopts an axial disposition (as H-5 at δ 5.02 ppm). Hence, the uracil moiety occupies an equatorial position (Fig. 3).

2.3. Conformational analysis of *cis*-7 and *trans*-7, and *cis*-8 and *trans*-8

Compounds **7** and **8** can both exist as geometric isomers and accordingly, the question is immediately posed as to which are the *cis*- or the *trans*- ones. In the case of **7**, during the oxidation reaction of the sulfur atom, both isomers were obtained (in a ratio of 3:1) and the pure minor compound was isolated by flash chromatography. In the case of the mixture, the ^{1}H signals did not overlap and this fact allowed us the assignment of all the protons for both isomers. Nevertheless, the following question still remains to be answered: Which is the *cis*- and which is the *trans*- isomer?

In our case the seven-membered sulfoxides are scarcely reported in the literature and hence the support from bibliographic sources is null. To solve the identification of both isomers we decided to tackle the conformational analysis of the target molecules, trying to clarify the conformational differences between both isomers and their possible responses in their ^{1}H NMR spectra.

The conformational study of *cis*-**7** and *trans*-**7** was carried out in two well differentiated phases. In the first one, the study of the base ring, without the uracil moiety, was tackled to identify the most stable conformation of this compound. In the second one, starting from the less energetic conformations of this compound, the uracil fragment was added to give rise to the *cis*-**7** and the *trans*-**7** and the conformational analysis on both isomers was carried out. The whole process was accomplished as previously reported by us.[2]

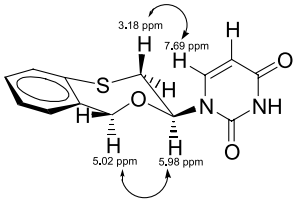

Figure 3. Preferred conformation of **5** showing the NOEDIFF effects by the double arrows.

Figure 4 shows the four most stable conformations of the *cis*-**7** isomer and Figure 5 shows the four most stable conformations of the *trans*-**7** isomer. In both isomers the energetic differences between the different conformations are important. These energy differences are sufficient to consider the upper left-handed conformation of *cis*-**7** in Figure 4, the only one existing in solution at 25 °C, its conformational population being calculated as 94.1%, considering a Boltzman distribution. For the *trans*-**7**, the most stable conformation represents 94.6% at 25 °C of the total population [upper left conformation in Figure 5 (*trans*-**7**)]. Therefore, it can be stated that the most stable conformations of both *cis*-**7** and *trans*-**7** are practically the only ones in the conformational equilibrium in solution, and the molecule properties could be explained from these conformers.

Figure 6 displays the most stable conformations of *cis*-**7** and *trans*-**7**. In both cases the uracil moiety adopts an equatorial disposition but the most interesting interactions are those established between the sulfinyl group (S═O) with the hydrogen atoms of the seven-membered fragment.

In the former case (*cis*-**7**) the equatorial S═O group bisects both H-2 atoms, whilst in *trans*-**7** the axial S═O group is antiperiplanar in relation to H-2α and accordingly, synperiplanar in relation to H-2β (see Fig. 6). Therefore, the H-2 atoms of both isomers must show a completely different behaviour in NMR. Moreover, the S═O group interacts with the axial H-3 atom and with the axial H-5 atom *trans*-**7**. Nevertheless such interactions are not observed in *cis*-**7** and, therefore, such interactions must result in different NMR responses of the hydrogen atoms of the seven-membered moieties of both isomers. In fact, the experimental data confirmed the conformational analysis data in the following way: in *trans*-**7**, the differences in chemical shifts of H-2 are higher than those of *cis*-**7** (3.62 ppm for H-2α and 3.30 ppm for H-2β for *trans*-**7**, whilst the chemical shifts are 3.47 ppm for H-2α and 3.34 ppm for H-2β for *cis*-**7**). The same holds true for H-5 of both isomers (4.84 ppm for H-5α and 5.61 ppm for H-5β for *trans*-**7**, being 4.67 ppm for H-5α and 4.83 ppm for H-5β for *cis*-**7**). Figure 6 shows that the distance between the sulfinyl group and the H-5α group (2.44 Å) adequately explains the chemical shift differences between H-5α and H-5β for *trans*-**7**. Moreover, H-3 is more deshielded in *trans*-**7** (δ 6.65 ppm) than in *cis*-**7** (δ 6.40 ppm). The whole ^{1}H NMR spectroscopic data are collected in the Section 4.

The conformational analysis of *cis*-**8** and *trans*-**8** was nearly identical to that of *cis*-**7** and *trans*-**7**, with only a slight variation in the energy of the several conformations (data not shown).

We have assigned the isomerism of the unique product in the reaction between **6** and H_2O_2 as being *trans*-**8**, based on the difference between the chemical shift of its H-2 atoms (0.36 ppm), which is closer to the 0.32 ppm difference

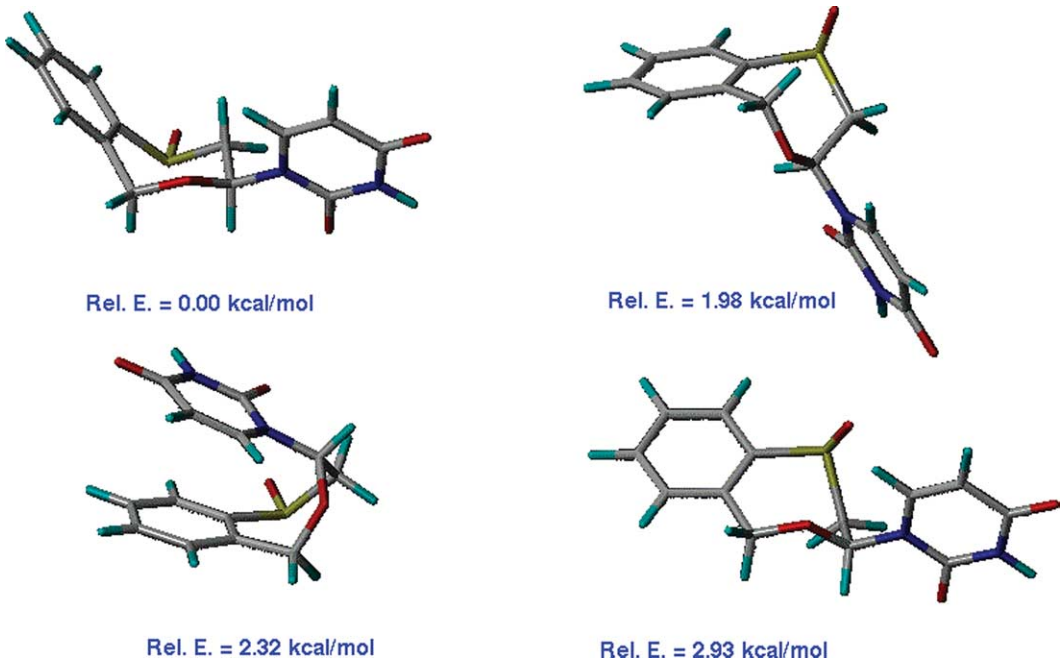

Figure 4. Representation of the four most stable conformations of compound *cis*-**7**. The relative energy values were calculated by means of molecular mechanics (tripos).

shown by *trans*-**7** and very different from the 0.13 ppm value of *cis*-**7**.

2.4. Antiproliferative activities

The MCF-7 human breast cancer cell line had been used as an excellent experimental model to improve the efficacy of different therapies before its use in patients.[10,11] Compounds **5**–**10** were assayed for their in vitro antiproliferative activity against the MCF-7 cell line.

The two antiproliferative compounds are **10** ($IC_{50}=12.74\pm4.79$ μM) and *trans*-**8** ($IC_{50}=30.05\pm0.71$ μM). The rest of the compounds are inactive ($IC_{50}>100$ μM). Therefore, it has to be pointed out that **10** and *trans*-**8** show an interesting antiproliferative activity with the natural base thymine in its structure. This is an outstanding fact that has not being previously reported in scientific bibliography, and this compound (or a related one) may serve as a prototype for the development of even more potent structures, probably endowed with a new mechanism of action. At present we are

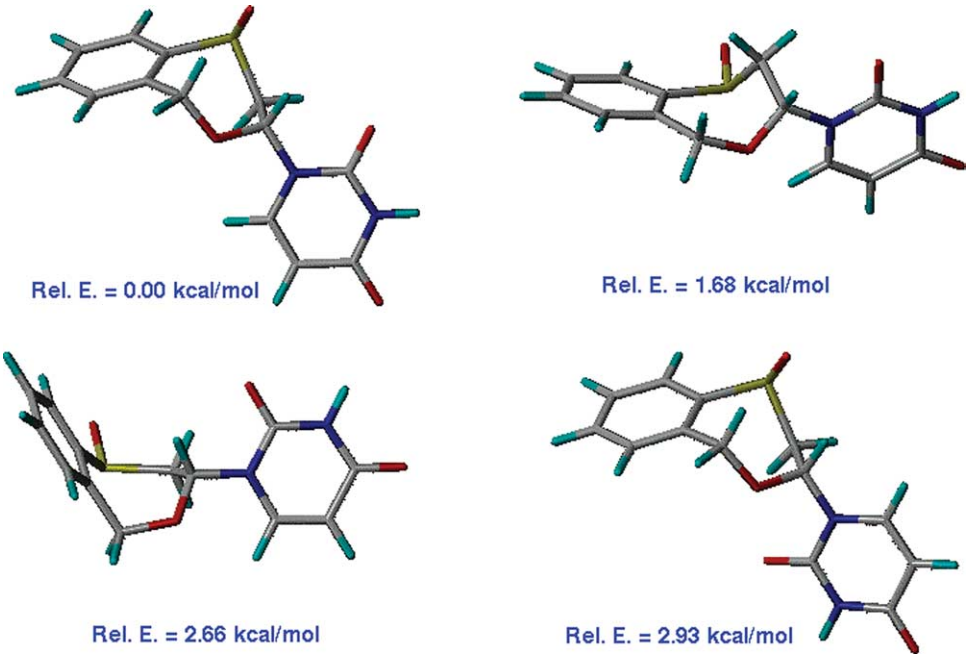

Figure 5. Representation of the four most stable conformations of compound *trans*-**7**. The relative energy values were calculated by means of molecular mechanics (tripos).

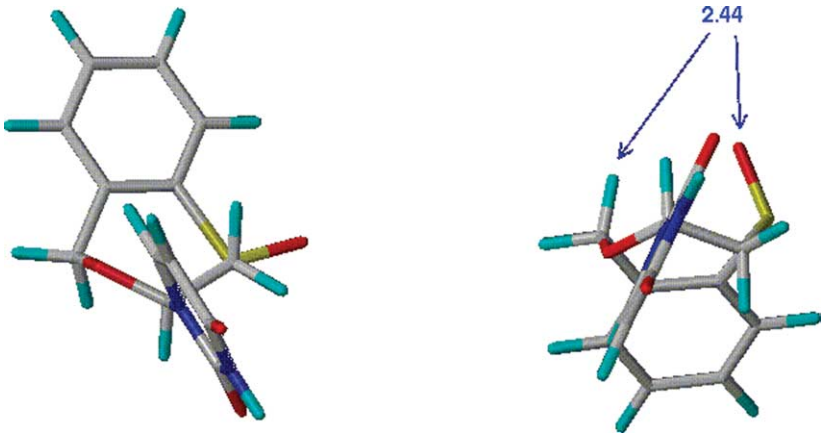

Figure 6. The most stable conformations of *cis*-**7** (left) and *trans*-**7** (right). The distance between the sulfinyl group and the H-5β group (2.44 Å) is shown for the *trans*-**7** conformer.

studying several antiproliferative markers in order to solve the mechanism of action at the molecular level of such a benzannelated seven-membered *O*,*N*-acetal.

3. Conclusions

Six final *O*,*N*-acetals have been obtained and screened for their anticancer activity. The modifications carried out affect two parts of the molecule: (a) on the one hand, the pyrimidine bases are always natural ones (uracil and thymine), and on the other (b) they affect the nature of the heteroatom of the seven-membered moiety that is linked directly to the benzene ring (sulfur, and several oxidation states of the sulfur atom: sulfinyl and sulfonyl). The NOEDIFF data for (*RS*)-3-(2,3-dihydro-5*H*-4,1-benzoxathiepin-3-yl)uracil **5** are compatible with a chair conformation for the seven-membered ring and an equatorial orientation of the uracil moiety on the C-3 position. The nature of the *cis*- and *trans*-sulfoxide isomers of **7** and **8** has been established by means of their conformational analyses and after comparing the theoretical results with the ^{1}H NMR responses of the target molecules. (*RS*)-3-(1,1-Dioxo-2,3-dihydro-5*H*-4,1-benzoxathiepin-3-yl)thymine **10** and (1*S**,3*S**)-1-(1-oxo-2,3-dihydro-5*H*-4,1-benzoxathiepin-3-yl)thymine (*trans*-**8**) were found to be inhibitors of the MCF-7 cell growth. To our knowledge, to date there have been no reports on nucleobase *O*,*N*-acetals with antitumour activities. At present, studies are being carried out to determine the mechanism of action at the molecular level of this compound.

4. Experimental

4.1. Chemistry

The general methods were the same as those previously described.[12,13]

4.1.1. Starting materials.

4.1.1.1. *o*-Hydroxymethylphenylthioacetaldehyde dimethyl acetal (11). 2-Mercaptobenzyl alcohol (1.62 mL, 14 mmol) was added dropwise to a stirred mixture of 547 mg (14 mmol) of a 60% (w/w) suspension of NaH in mineral oil and 40 mL of anhydrous DMF, under argon and at 0 °C; the resulting solution was left at rt until it became clear (45 min). To this clear solution was added dropwise 1.65 mL (14 mL) of bromoacetaldehyde dimethyl acetal and the resulting solution was left overnight at rt and then evaporated to dryness under vacuum. The residue was treated with water (20 mL), then extracted with dichloromethane (4×30 mL) and treated with brine: the combined organic phases were then dried (Na_2SO_4), filtered and evaporated under reduced pressure to yield a colourless oil, which after flash chromatography (EtOAc/hexane 1:4) gave pure **11** (2.9 g, 92% yield) as a clear dense liquid. The procedure previously reported used bromoacetaldehyde diethyl acetal[4] instead of bromoacetaldehyde dimethyl acetal. ^{1}H NMR (300 MHz, $CDCl_3$) δ 7.49 (m, 1H, H-arom); 7.38 (m, 1H, H-arom); 7.25 (m, 2H, H-arom); 4.77 (s, 2H, CH_2OH); 4.44 (t, J=5.6 Hz, 1H, CH(OMe)$_2$); 3.26 (s, 6H, O*Me*); 3.07 (d, J=5.6 Hz, 2H, SCH_2). ^{13}C NMR (75 MHz) δ 142.33 (C-1); 134.18 (C-2); 132.17, 129.12, 128.58, 127.62 (C-arom); 102.71 (*C*H(OMe)$_2$); 63.85 (*C*H_2OH); 53.04 (O*Me*); 37.09 (S*C*H_2). Anal. Calcd for $C_{11}H_{16}O_3S$: C, 57.87; H, 7.06; S, 14.05. Found: C, 57.90; H, 6.94; S, 14.26.

4.1.1.2. (*RS*)-3-Methoxy-2,3-dihydro-5*H*-4,1-benzoxathiepin (12). A mixture of 1.90 g (8.33 mmol) of **11**, 75 mg (0.436 mmol) of *p*-toluenesulfonic acid and 100 mL of anhydrous toluene was heated to reflux (110 °C) during 2 h; the solution was then brought back to rt and evaporated to dryness. The residue was taken up in diethyl ether (50 mL) and the resulting solution was dried (K_2CO_3): it was then filtered and evaporated to dryness, yielding an oil, which upon flash chromatography (EtOAc/hexane 1:2) gave 1.55 g of pure **12** (95% yield) as a clear oil. ^{1}H NMR (300 MHz, $CDCl_3$) δ 7.51 (m, 1H, H-arom); 7.23 (m, 3H, H-arom); 5.22 (d, J=13.5 Hz, 1H, H-5); 4.85 (t, J=4.1 Hz, 1H, H-3); 4.50 (d, J=13.5 Hz, 1H, H-5); 3.52 (s, 3H, O*Me*). ^{13}C NMR (75 MHz) δ 142.26 (C-9a); 136.61, 131.78, 129.59, 128.09, 127.58 (C-arom); 102.74 (C-3); 66.01 (C-5); 55.60 (O*Me*); 37.93 (C-2). HR LSIMS (NOBA matrix) calcd for $C_{10}H_{12}O_2S$: 196.0558; found: 196.0558. Anal. Calcd for $C_{10}H_{12}O_2S$: C, 61.20; H, 6.16; S, 16.34. Found: C, 61.56; H, 6.15; S, 16.68.

4.1.2. Final compounds.

4.1.2.1. (*RS*)-1-(2,3-Dihydro-5*H*-4,1-benzoxathiepin-3-yl)uracil (5). A 1.0 M solution of $SnCl_4/CH_2Cl_2$ (2.45 mL, 2.44 mmol) was added dropwise with stirring under argon to a suspension of **12** (400 mg, 2.04 mmol), uracil (250 mg, 2.23 mmol), which contained TCS (0.26 mL, 2.04 mmol) and HMDS (0.43 mL, 2.04 mmol) in dry acetonitrile (10 mL) at −25 °C. After 10 min at −20 °C, the suspension was left to reach rt and then warmed to 45 °C for 24 h. After cooling, the reaction was quenched by the addition of a concentrated aqueous solution of Na_2CO_3. The solvent was removed with a rotary evaporator and the residue was triturated with CH_2Cl_2 (5 mL), filtered and **5** was obtained as a creamy solid (410 mg, 73%); mp: 223–224 °C. ^{1}H NMR (300 MHz, DMSO-d_6) δ 11.48 (s, 1H, NH); 7.69 (d, 1H, J=8.0 Hz, H-6′); 7.66 (m, 1H, H-arom); 7.52 (m, 1H, H-arom); 7.39 (m, 1H, H-arom); 5.98 (dd, 1H, J=9.1, 2.2 Hz, H-3α); 5.60 (dd, 1H, J=8.0, 2.2 Hz, H-5′); 5.02 (d, 1H, J=13.6 Hz, H-5α); 4.96 (d, 1H, J=13.6 Hz, H-5β); 3.27 (dd, 1H, J=14.1, 9.1 Hz, H-2α); 3.18 (dd, 1H, J=14.1, 2.3 Hz, H-2β). ^{13}C NMR (75 MHz) δ 162.93 (C-4′); 149.85 (C-2′); 142.14; 141.07 (C-6′); 135.76, 132.12, 130.13, 128.73, 128.22 (C-arom); 101.66 (C-5′); 86.86 (C-3); 72.90 (C-5); 36.74 (C-2). Anal. Calcd for $C_{13}H_{12}N_2O_3S$ C, 56.51; H, 4.38; N, 10.14; S, 11.60. Found: C, 56.36; H, 4.20; N, 9.86; S, 11.72.

4.1.2.2. (*RS*)-1-(2,3-Dihydro-5*H*-4,1-benzoxathiepin-3-yl)thymine (6). A 1.0 M solution of $SnCl_4/CH_2Cl_2$ (1.22 mL, 1.22 mmol) was added dropwise with stirring under argon to a suspension of **12** (200 mg, 1.02 mmol), thymine (140 mg, 1.15 mmol), which contained TCS (0.13 mL, 1.02 mmol) and HMDS (0.22 mL, 1.02 mmol) in dry acetonitrile (6 mL) at −25 °C. After 10 min at −20 °C, the suspension was left to reach rt and then warmed to 45 °C for 40 h. After cooling, the reaction was quenched by the addition of a concentrated aqueous solution of Na_2CO_3. The solvent was removed with a rotary evaporator and the residue was purified by flash chromatography (CH_2Cl_2/MeOH 9.99:0.01) and **6** was obtained as a white solid (343 mg, 58%); mp: 203–204 °C. ^{1}H NMR (400 MHz, DMSO-d_6) δ 11.35 (s, 1H, NH); 7.59 (m, 1H, H-arom); 7.49 (s, 1H, H-6′); 7.44 (m, 1H, H-arom); 7.31 (m, 2H, H-arom); 5.89 (dd, J=9.7, 1.4 Hz, 1H, H-3); 4.89 (d, J=13.5 Hz, 1H, H-5β); 4.86 (d, J=13.5 Hz, 1H, H-5α); 3.20 (dd, J=14.1, 9.8 Hz, 1H, H-2α); 3.05 (dd, J=14.1, 1.4 Hz, 1H, H-2β); 1.68 (s, 3H, *Me*). ^{13}C NMR (100 MHz) δ 163.63 (C-4′); 149.84 (C-2′); 142.32 (C-arom); 136.59 (C-6′); 136.83, 132.18, 130.15, 128.72, 128.26 (C-arom); 109.40 (C-5′); 86.59 (C-3); 72.89 (C-5); 35.79 (C-2); 11.85 (*Me*). HR LSIMS (NOBA matrix) calcd for $C_{14}H_{14}N_2O_3SNa$ $(M+Na)^+$: 313.0623; found: 313.0624. Anal. Calcd for $C_{14}H_{14}N_2O_3S$: C, 57.92; H, 4.86; N, 9.65; S, 11.04. Found: C, 57.83; H, 5.10; N, 9.46; S, 11.32.

4.1.2.3. (1*R,3*S**)- and (1*S**,3*S**)-1-(2,3-Dihydro-5*H*-4,1-benzoxathiepin-3-yl)uracil (*cis*-7 and *trans*-7).** Hydrogen peroxide, 50 wt% solution in water (0.05 mL, 0.087 mmol) was added to a solution of $Sc(OTf)_3$ (71 mg, 0.145 mmol) in a mixture of 0.7 mL of EtOH and 6.3 mL of CH_2Cl_2. Compound **5** (200 mg, 0.724 mmol) was added after 5 min and the resulting solution was left at rt for 3.5 h. After this, more H_2O_2 was added (0.05 mL) and the reaction was left during 3.5 h more. The mixture was diluted with CH_2Cl_2 (20 mL) and washed with H_2O (2×15 mL), the organic layer was dried (Na_2SO_4), concentrated and purified by flash chromatography using a mixture of CH_2Cl_2/MeOH 9.5:0.5 to yield 164 mg, which were characterized as a mixture of *cis*-**7** and *trans*-**7** (164 mg, 77%). 130 mg of this mixture were purified by flash 40 chromatography using a gradient elution (EtOAc/hexane 3:2→EtOAc/hexane 4:1→EtOAc) and *cis*-**7** was obtained pure. *cis*-**7** ^{1}H NMR (300 MHz, $CDCl_3$ +2 drops of CD_3OD) δ 7.86 (dd, J=7.8, 1.3 Hz, 1H, H-arom); 7.63 (dt, J=7.7, 1.3 Hz, 1H, H-arom); 7.50 (dt, J=7.4, 1.4 Hz, 1H, H-arom); 7.32 (dd, J=7.4, 1.1 Hz, 1H, H-arom); 7.21 (d, J=8.2 Hz, 1H, H-6′); 6.40 (dd, J=10.6, 1.8 Hz, 1H, H-3); 5.67 (d, J=8.2 Hz, 1H, H-5′); 4.83 (d, J=14.3 Hz, 1H, H-5β); 4.67 (d, J=14.3 Hz, 1H, H-5α); 3.47 (dd, J=12.1, 1.8 Hz, 1H, H-2α); 3.34 (dd, J=12.0, 10.6 Hz, 1H, H-2β). *trans*-**7** ^{1}H NMR (300 MHz, $CDCl_3$ +2 drops of CD_3OD) δ 7.86 (dd, J=7.1, 1.8 Hz, 1H, H-arom); 7.50 (dt, J=7.6, 1.5 Hz, 1H, H-arom); 7.50 (dt, J=7.6, 1.5 Hz, 1H, H-arom); 7.40 (d, J=8.2 Hz, 1H, H-6′); 6.65 (dd, J=9.5, 2.4 Hz, 1H, H-3); 5.67 (d, J=8.2 Hz, 1H, H-5′); 5.61 (d, J=14.0 Hz, 1H, H-5β); 4.84 (d, J=14.0 Hz, 1H, H-5α); 4.84 (d, J=8.2 Hz, 1H, H-5′); 3.62 (dd, J=13.4, 2.4 Hz, 1H, H-2); 3.30 (dd, J=13.4, 6.7 Hz, 1H, H-2). Anal. Calcd for $C_{13}H_{12}N_2O_4S$: C, 53.42; H, 4.14; N, 9.58; S, 10.97. Found: C, 53.40; H, 4.20; N, 9.46; S, 10.72.

4.1.2.4. (1*S,3*S**)-1-(1-Oxo-2,3-dihydro-5*H*-4,1-benzoxathiepin-3-yl)thymine (*trans*-8).** Compound **6** (0.06 mL, 1.04 mmol) was dissolved in a H_2O_2 50 wt% solution in water, and the resulting solution was warmed under stirring for 2 h. After cooling, the mixture was diluted with H_2O (10 mL) and was extracted with EtOAc (3× 10 mL), the organic layer was dried (Na_2SO_4), concentrated and purified by flash chromatography using a gradient elution (CH_2Cl_2/MeOH 9.8:0.2→9.5:0.5→9:1) to yield *trans*-**8** (104 mg, 50%); mp: 271–273 °C. *trans*-**8** ^{1}H NMR (300 MHz, $CDCl_3$+DMSO-d_6) δ 10.85 (br s, 1H, N*H*); 7.66 (dd, J=7.6, 1.5 Hz, 1H, H-arom); 7.25 (dt, J=undet., 1.5 Hz, 1H, H-arom); 7.19 (dt, J=7.6, 1.5 Hz, 1H, H-arom); 7.06 (d, J=7.3, 1.3 Hz, 1H, H-arom); 6.88 (d, J=1.2 Hz, 1H, H-6′); 6.03 (dd, J=10.5, 1.6 Hz, 1H, H-3); 4.95 (d, J=14.0 Hz, 1H, H-5); 4.51 (d, J=14.0 Hz, 1H, H-5); 3.57 (dd, J=14.3, 10.4 Hz, 1H, H-2); 3.21 (dd, J=14.3, 1.6 Hz, 1H, H-2); 1.40 (d, J=1.2 Hz, 1H, *Me*). ^{13}C NMR (75 MHz) δ 165.02 (C-4′); 151.13 (C-2′); 140.71 (C-arom); 136.45, 135.31, 132.28, 130.25, 128.75 (C-arom+C-6′); 112.27 (C-5′); 83.58 (C-3); 72.59 (C-5); 60.66 (C-2); 13.38 (*Me*). LSIMS (NOBA matrix) calcd for $C_{14}H_{14}N_2O_4SNa$ $(M+Na)^+$: 329.0572; found: 329.0572. Anal. Calcd for $C_{14}H_{14}N_2O_5S$: C, 52.17; H, 4.38; N, 8.69; S, 9.95. Found: C, 52.40; H, 4.40; N, 8.36; S, 9.72.

4.1.2.5. (*RS*)-3-(1,1-Dioxo-2,3-dihydro-5*H*-4,1-benzoxathiepin-3-yl)uracil (9). Potassium peroxymonosulfate (OXONE™, 709 mg, 1.15 mmol) in H_2O (3 mL) was added to a solution of **5** in MeOH (10 mL) and the resulting suspension was left at rt for 2 h. After filtration and washing with H_2O and CH_2Cl_2, the residue was recrystallized from acetone to yield **9** (118 mg, 66%) as a white solid; mp: 245–247 °C. ^{1}H NMR (300 MHz, DMSO-d_6) δ 7.98 (d, J=7.6, 1.5 Hz, 1H, H-arom); 7.66 (d, J=8.2 Hz, 1H, H-6′); 7.61 (m, 3H, H-arom); 6.28 (d, J=10.6 Hz, 1H, H-5′); 5.58 (d,

$J=8.0$ Hz, 1H, H-3); 5.10 (d, $J=14.1$ Hz, 1H, H-5); 4.99 (d, $J=14.1$ Hz, 1H, H-5); 4.37 (dd, $J=14.3$, 10.7 Hz, 1H, H-2); 4.04 (d, $J=14.3$ Hz, 1H, H-2). ^{13}C NMR (75 MHz) δ 162.85 (C-4′); 149.90 (C-2′); 141.00 (C-6′); 139.60 (C-arom); 136.13, 136.29, 131.41, 129.29, 127.00 (C-arom); 102.20 (C-5′); 82.18 (C-3); 70.57 (C-5); 58.16 (C-2). Anal. Calcd for $C_{13}H_{12}N_2O_5S$: C, 50.64; H, 3.92; N, 9.09; S, 10.40. Found: C, 50.60; H, 3.80; N, 9.34; S, 10.75.

4.1.2.6. (*RS*)-3-(1,1-Dioxo-2,3-dihydro-5*H*-4,1-benzoxathiepin-3-yl)thymine (10). The procedure was similar to Section 4.1.2.5, but starting from **6**. Yield (58%) as a white solid; mp: 272–274 °C. ^{1}H NMR (300 MHz, DMSO-d_6) δ 11.55 (s, 1H, NH); 8.07 (dd, $J=7.6$, 1.4 Hz, 1H, H-6′); 7.74 (m, 1H, H-arom); 6.37 (dd, $J=10.6$, 1.4 Hz, 1H, H-3); 5.20 (d, $J=14.1$ Hz, 1H, H-5); 5.07 (d, $J=14.1$ Hz, 1H, H-5); 4.42 (dd, $J=14.5$, 10.7 Hz, 1H, H-2); 4.11 (dd, $J=14.5$, 1.4 Hz, 1H, H-2); 1.76 (s, 3H, *Me*). ^{13}C NMR (75 MHz) δ 163.34 (C-4′); 149.72 (C-2′); 139.48 (C-arom); 136.36, 136.02, 134.08, 131.22, 129.08, 126.79 (C-6′+C-arom); 109.66 (C-5′); 81.73 (C-3); 70.32 (C-5); 58.22 (C-2); 11.67 (*Me*). Anal. Calcd for $C_{14}H_{14}N_2O_5S$: C, 52.17; H, 4.38; N, 8.69; S, 9.95. Found: C, 52.40; H, 4.58; N, 8.44; S, 9.75.

4.2. Biological activity

The biological methods were the same as those previously described.[12]

Acknowledgements

This study was supported by the Instituto Carlos III (Fondo de Investigaciones Sanitarias, Projects PI03225 and PI041206).

References and notes

1. Saniger, E.; Campos, J.; Entrena, A.; Marchal, J. A.; Súarez, I.; Aránega, A.; Choquesillo, D.; Niclós, J.; Gallo, M. A.; Espinosa, A. *Tetrahedron* **2003**, *59*, 5457–5467.
2. Saniger, E.; Campos, J.; Entrena, A.; Marchal, J. A.; Houria, B.; Aránega, A.; Gallo, M. A.; Espinosa, A. *Tetrahedron* **2003**, *59*, 8017–8026.
3. Campos, J.; Domínguez, J. F.; Gallo, M. A.; Espinosa, A. *Curr. Pharm. Des.* **2000**, *6*, 1797–1810.
4. Crombie, L.; Josephs, J. L.; Larkin, J.; Weston, J. B. *Chem. Soc., Chem. Commun.* **1991**, *14*, 972–973.
5. For reviews, see: (a) Ward, R. S.; Diaper, R. *Sulfur Rep.* **2001**, *22*, 251. (b) Jackson, D. A.; Rawlinson, H.; Barba, O. *Spec. Publ.-R. Soc. Chem.* **2001**, *260*, 47–53. (c) Mashkina, A. V. *Sulfur Rep.* **1991**, *10*, 279–388.
6. Matteucci, M.; Bhalay, G.; Bradley, M. *Org. Lett.* **2003**, *5*, 235–237.
7. Khanapure, S. P.; Garvey, D. S.; Young, D. V.; Ezawa, M.; Earl, R. A.; Gaston, R. D.; Fang, X.; Murty, M.; Martino, A.; Shumway, M.; Trocha, M.; Marek, P.; Tam, S. W.; Janero, D. R.; Letts, L. G. *J. Med. Chem.* **2003**, *46*, 5484–5504.
8. From now on, the primes (′) will accompany the numbering of the pyrimidine bases.
9. Bax, A.; Summers, M. F. *J. Am. Chem. Soc.* **1986**, *108*, 2093–2094.
10. Matsuo, S.; Tanako, S.; Yamashita, J.; Ogawa, M. *Anticancer Res.* **2000**, *12*, 1575–1579.
11. Trouet, A.; Passioukov, A.; Derpooten, K. V.; Fernández, A. M.; Abarca-Quiñones, J.; Baurain, R.; Lobl, T. J.; Oliyai, C.; Dubois, V. *Cancer Res.* **2001**, *61*, 2843–2846.
12. Díaz-Gavilán, M.; Rodríguez-Serrano, F.; Gómez-Vidal, J. A.; Marchal, J. A.; Aránega, A.; Gallo, M. A.; Espinosa, A.; Campos, J. M. *Tetrahedron* **2004**, *60*, 11547–11557.
13. Saniger, E.; Díaz-Gavilán, M.; Delgado, B.; Choquesillo, D.; González-Pérez, J. M.; Aiello, S.; Gallo, M. A.; Espinosa, A.; Campos, J. M. *Tetrahedron* **2004**, *60*, 11453–11464.